

**Alma Mater Studiorum**  
**Università degli Studi di Bologna**

---

---

DIPARTIMENTO DI FISICA E ASTRONOMIA

Dottorato di ricerca in Astronomia  
Ciclo XXVII

**Improving the cosmic distance ladder.  
Distance and structure of the Large  
Magellanic Cloud.**

Dottoranda:  
**Tatiana Muraveva**

Relatore:  
**Prof. Bruno Marano**

Co-Relatori:  
**Dott.sa Gisella Clementini**

**Dott.sa Marcella Marconi**

**Dott. Enzo Brocato**

Coordinatore:  
**Prof. Lauro Moscardini**

Esame finale anno 2014

---

---



# Contents

<b>Introduction</b>	<b>1</b>
<b>1 The cosmological distance ladder</b>	<b>5</b>
1.1 Trigonometric parallax . . . . .	5
1.2 Gaia . . . . .	7
1.3 Variable stars as distance indicators . . . . .	10
1.4 Classical Cepheids . . . . .	12
1.5 RR Lyrae stars . . . . .	14
1.5.1 Metal abundance of RR Lyrae stars . . . . .	15
1.5.2 $M_V - [\text{Fe}/\text{H}]$ and $PL_KZ$ relations of RR Lyrae stars . . . . .	19
1.6 Eclipsing binaries . . . . .	24
1.6.1 Classification of eclipsing binaries . . . . .	24
1.6.2 Eclipsing binaries as distance indicators . . . . .	25
<b>2 The Large Magellanic Cloud</b>	<b>29</b>
2.1 Magellanic System . . . . .	29
2.2 Structure of the LMC . . . . .	30
2.3 Distance to the LMC . . . . .	32
2.4 LMC Surveys . . . . .	35
2.4.1 EROS-2 . . . . .	35
2.4.2 OGLE . . . . .	36
2.4.3 VMC . . . . .	38
<b>3 Classical Cepheids in the VMC tile LMC 8_3</b>	<b>41</b>
3.1 EROS-2 data for candidate Classical Cepheids . . . . .	41
3.2 Classification of candidate Classical Cepheids . . . . .	50

3.3	Strategy for extracting bona-fide Classical Cepheids . . . . .	52
<b>4</b>	<b>Eclipsing binaries in the LMC</b>	<b>57</b>
4.1	EROS-2 data for eclipsing binaries . . . . .	57
4.2	Cross-correlation with other catalogues of eclipsing binaries in the LMC . .	59
4.3	Characteristics of eclipsing binaries with existing spectroscopy . . . . .	63
4.3.1	Cross-matches with the VLT-FLAMES surveys . . . . .	63
4.3.2	AAOmega spectroscopy . . . . .	63
4.4	Classification of eclipsing binaries . . . . .	64
4.5	Period-Luminosity relation of eclipsing binaries . . . . .	67
4.5.1	$PL$ relation of eclipsing binaries from the EROS-2 sample . . . . .	67
4.5.2	$PL$ relation of eclipsing binaries from the OGLE III catalogue . . .	69
4.6	Structure of the LMC from “hot” eclipsing binaries and Classical Cepheids	74
<b>5</b>	<b>RR Lyrae stars in the VMC tile LMC 5_5</b>	<b>77</b>
5.1	Data for RR Lyrae stars in the bar of the LMC . . . . .	77
5.2	$PL_{K_s}Z$ relation of RR Lyrae stars in the LMC . . . . .	86
5.2.1	Method . . . . .	86
5.2.2	Zero-point of the $PL_{K_s}Z$ relation . . . . .	87
5.3	Gaia observation of RR Lyrae stars in the Milky Way . . . . .	90
5.3.1	Simulated Gaia data . . . . .	92
5.3.2	Simulation of the $M_V - [\text{Fe}/\text{H}]$ relation of RR Lyrae stars in the Milky Way . . . . .	95
<b>6</b>	<b>RR Lyrae stars in the VMC tile LMC 8_3</b>	<b>97</b>
6.1	Classification of EROS-2 candidate RR Lyrae stars . . . . .	97
6.2	Comparison with the OGLE III catalogue . . . . .	108
6.3	Fourier analysis of the RR Lyrae stars in tile LMC 8_3 . . . . .	112
6.4	Metallicity of the RR Lyrae stars in tile LMC 8_3 . . . . .	123
6.5	$K_s$ magnitude of the RR Lyrae stars in tile LMC 8_3 . . . . .	131
6.6	Distance to the tile LMC 8_3 from RR Lyrae stars . . . . .	140
	<b>Conclusions</b>	<b>145</b>
	<b>Appendix</b>	<b>151</b>

*CONTENTS*

---

<b>A Properties of the “hot” eclipsing binaries in the LMC</b>	<b>151</b>
--	------------



# Introduction

The knowledge of distances is crucially important to all branches of astronomy. In order to measure the distances astronomers have developed a number of different techniques. Some methods, such as the trigonometric parallax, are based on geometrical principals, others involve the concept of distance indicators. The successions of techniques used to measure distances to celestial objects, is called *cosmological distance ladder*.

The Large Magellanic Cloud (LMC) is widely considered as the first step of the cosmological distance ladder, since it contains many different distance indicators. An accurate determination of the distance to the LMC allows one to calibrate these distance indicators that are then used to measure the distance to far objects.

In standard cosmology the Universe expands uniformly according to the Hubble law  $v = H_0 d$ , where  $v$  is the recession velocity of a galaxy at a distance  $d$ , and  $H_0$  is the Hubble constant which measures the expansion rate at the current epoch.  $H_0$  sets the age of the Universe and the size of the observable Universe. Many of the methods that are used to measure  $H_0$  are calibrated by the distance to the LMC. The LMC is distant enough, and its main features lie close to the plane of the sky, hence, in first approximation it could be assumed that its stellar components are all at the same distance from us. However, the LMC has a rather complex internal structure, that must be taken into account when pushing for distance comparisons at a few percent level.

The main goal of this thesis is to study the distance and structure of the LMC, as traced by different distance indicators. For these purposes three types of distance indicators were chosen: Classical Cepheids, “hot” eclipsing binaries and RR Lyrae stars. These objects belong to different stellar populations tracing, in turn, different sub-structures of the LMC. The RR Lyrae stars (age  $\geq 10$  Gyr) are distributed smoothly and likely trace the halo of the LMC. Classical Cepheids are young objects (age  $\sim 50$ -200 Myr), mainly located in the bar and spiral arm of the galaxy, while “hot” eclipsing binaries mainly trace the star forming regions of the LMC. Furthermore, we have chosen these distance indicators for our study,

since the calibration of their zero-points is based on fundamental geometric methods. The ESA cornerstone mission Gaia, launched on 19 December 2013, will measure trigonometric parallaxes for one billion stars with an accuracy of 20 micro-arcsec ( $\mu\text{as}$ ) at  $V \sim 15$  mag, and 200  $\mu\text{as}$  at  $V \sim 20$  mag, thus will allow us to calibrate the zero-points of Classical Cepheids, eclipsing binaries and RR Lyrae stars with an unprecedented precision. One goal of this thesis was to check the impact of Gaia on the determination of distances with RR Lyrae stars, based on Gaia expected performances.

In this thesis we extensively use the data of the VISTA near-infrared ESO public survey of the Magellanic Clouds system (VMC, PI M.-R. Cioni, see Cioni et al. 2011). The determination of the distance to different tiles of the VMC survey by applying the Classical Cepheid's period-luminosity ( $PL_{K_s}$ ) and the RR Lyrae period-luminosity-metallicity ( $PL_{K_s}Z$ ) relations in the  $K_s$  passband allows us to study the structure of the LMC. We also use in our analysis visual data of the microlensing surveys EROS (Tisserand et al., 2007) and OGLE (Udalski et al., 1997).

Chapters 1 and 2 of the thesis provide the scientific concept of our study. In Chapter 1 we focus on the general description of the cosmological distance ladder with emphasis on the three types of distance indicators, which were specifically analysed in this study. Chapter 2 gives general information about the LMC. In Chapter 3 we provide the results of our analysis of Classical Cepheids in the LMC. We use the visual data from the EROS-2 survey in order to classify Classical Cepheids in the VMC tile LMC 8\_3 and determine their basic properties. These parameters will be used to derive the mean  $K_s$  magnitudes of Classical Cepheids and to estimate the distance to this tile by applying the Classical Cepheid's  $PL$  relation in the  $K_s$  passband. The general strategy developed to classify candidate Classical Cepheids from the EROS-2 survey, which will be applied to all the tiles covered only by the EROS-2 survey, is described.

Chapter 4 presents the results of our analysis of "hot" eclipsing binaries in the LMC observed by the EROS-2 survey. We classified them on the basis of the visual inspection and the Fourier analysis of their light curves. We then analyse the near-infrared light curves of the eclipsing binaries that have a counterpart in the VMC catalogue, in order to study their  $PL$  relation and the possibility of using the  $PL$  relation to determine the distance to the LMC.

Chapter 5 and 6 summarize the work done on the RR Lyrae stars in the VMC tiles LMC 5\_5 and 8\_3. By using the VMC data for a sample of RR Lyrae stars in tile LMC



## *INTRODUCTION*

---

5\_5 we derive our own  $PL_{K_s}Z$  relation. We then apply this relation in combination with the relations from the literature to determine the distance to tiles LMC 5\_5 and 8\_3. The derived distances allow us to make preliminary conclusions about the structure of the LMC. In order to check the impact of Gaia on the determination of the RR Lyrae  $PL_{K_s}Z$  and  $M_V - [\text{Fe}/\text{H}]$  relations we simulate Gaia parallaxes for 25 RR Lyrae stars in the Milky Way.

In the Conclusions section we summarize the work done, whereas the Appendix contains tables which are too long to be inserted in the main text of the thesis.



# Chapter 1

## The cosmological distance ladder

The cosmological distance ladder is a succession of different techniques by which astronomers measure the distances to celestial objects. The cosmic distance ladder is built by transferring geometrically measured distances to nearby stars to the far universe via multiple overlapping steps (Walker, 2012). In order to determine the distance to relatively close objects the method of *trigonometric parallax* is being used. However, this geometrical method is not applicable to derive accurate distance to the objects in other galaxies. In order to do this one needs to apply the so-called *primary* distance indicators which could be calibrated from observations in the Milky Way (MW) or from theoretical considerations (Rowan-Robinson, 1985). After establishing the distances to nearby galaxies with primary methods, one can apply them in order to calibrate the *secondary* distance indicators, which have to be used up to distances where the Hubble Law connecting the distance to the recession velocity can be applied and cosmological parameters can be estimated.

### 1.1 Trigonometric parallax

The most direct distance measurement technique is the method of trigonometric parallax. Due to the rotation of the Earth around the Sun, the position of the stars on the sky change with season in a way that depends on the distance to the star and on its direction on the sky. If the direction of the star lies in the plane of the Earth's orbit, the star will appear to move back and forth on a line in this plane by an amount of  $\pm\pi$ , where  $\pi = r_e/d$  rad. Here  $d$  is the distance of the star and  $r_e$  is the radius of the Earth's orbit around the Sun. If the star lies perpendicular to the plane of the Earth's orbit, at the ecliptic pole, the star will appear to move in a circle of angular radius  $\pi = r_e/d$ . If the star lies at ecliptic latitude  $b^e$ , it will move in an eclipse of semimajor axis  $\pi = r_e/d$  and of semiminor axis  $\pi \sin b^e$ . The quantity

$\pi$  is called trigonometric parallax of the star, and it is usually measured in arcseconds ( $''$ ).

The distance to stars is often expressed in terms of the parallax they would give. The unit 1 *parsec* ( $pc$ ) is defined as the distance at which the star would give a parallax of 1 arcsec. The distance  $d$  in parsecs is therefore  $d = 1/\pi('')$ .

Astronomers deal with enormous ranges of distances, so it is more convenient to use logarithmic measurements. For this reason the so-called *distance modulus* is widely used to describe the distance to the object. It is defined as:

$$\mu = m - M = 5\log(d) - 5, \quad (1.1)$$

where  $d$  is the distance in pc,  $m$  is the apparent magnitude of the star, and  $M$  is the *absolute magnitude*, which is the magnitude the object would have at a distance of 10 pc.

The first accurate measurements of the parallax of stars were made in 1838, when Friedrich Wilhelm Bessel at the Königsberg Observatory in Prussia estimated  $\pi = 0''.31 \pm 0''.02$  for the star 61 Cygni. In 1939 Thomas Henderson found  $1''.16 \pm 0''.11$  for  $\alpha$  Centauri. Work on measuring parallaxes proceeded slowly. In 1878 parallaxes of 17 stars were known, and by 1908 the number increased to 100. The *Yale Parallax Catalog* published in 1952 (Jenkins, 1952) gives parallaxes for 5822 stars. However, for the majority of stars the parallaxes were too small and not known accurately enough to give reliable distances. To measure the parallaxes with a good accuracy, space telescopes are needed. That's why the astronomers developed a space experiment, devoted specifically to precision astrometry, *Hipparcos*.

Hipparcos (High precision parallax collecting satellite) was a scientific mission of the European Space Agency (ESA), launched in 1989 and operated until 1993. The spacecraft was equipped with a single all-reflective, eccentric Schmidt telescope, with an aperture of 29 cm. The initial objectives of the mission were to determine parallaxes of  $\sim 120000$  stars to a precision of 2 milli-arcseconds (mas) for the core of the catalogue, along with the astrometry to 10-20 mas and two-colour photometry for additional 400000 stars (the Tycho experiment). An optimized scanning law allowed to cover the whole sky more or less regularly in such a way that every object was observed from 25 to 70 times depending on ecliptic latitude (Mignard, 1998). Regarding the photometry the number of individual observations per stars varied from 70 to 300. The resulting Hipparcos catalogue of  $\sim 120000$  stars with an astrometric accuracy of 1 mas or better for the brightest stars, was published in 1997. Additionally, the lower-precision Tycho Catalogue of more than a million stars

was published at the same time, while the enhanced Tycho-2 Catalogue of 2.5 million stars was published in 2000. A new reduction of the Hipparcos astrometric data was published by van Leeuwen (2007), who claims improvement of accuracies to a factor 4 for nearly all stars brighter than  $H_p=8$  mag<sup>1</sup>.

More accurate trigonometric parallaxes are being obtained with the Fine Guidance Sensor (FGS) instrument (Nelán, 2010) on board the *Hubble Space Telescope (HST)*. Unfortunately, the sample of objects, for which accurate *HST* parallaxes were obtained, is small. The determination of unprecedentedly accurate parallaxes of a huge sample of objects is expected with the ESA satellite Gaia (Perryman et al., 2001).

## 1.2 Gaia

Gaia is the ESA's cornerstone mission launched using the Soyuz ST-B rocket from Kourou in French Guiana on 19 December 2013. The satellite is designed to produce the most accurate three-dimensional (3D) map of the MW to date (Perryman et al., 2001). Gaia is located at the Lagrangian point L2 and scans the sky with two telescopes by continuously spinning around the axis perpendicular to the two lines of sight. Each celestial object will be observed on average 70 times during the five-year mission lifetime. Gaia will determine the position, distance, and annual proper motion of 1 billion stars with the unprecedented accuracy of about  $20 \mu\text{as}$  at  $V \sim 15$  mag, and  $200 \mu\text{as}$  at  $V \sim 20$  mag. The accuracy of the Gaia parallaxes in comparison with Hipparcos is shown in Figure 1.1. For the brightest objects the parallax errors are dominated by calibration errors and range from  $\sim 5$  to  $\sim 14 \mu\text{as}$ . At the faint end the behaviour of errors as a function of  $V$  magnitude is dictated by photon noise. As it could be seen in Fig. 1.1 at a given  $V$  magnitude, parallax accuracies are higher for red stars. Accuracy predictions include a rough estimate of the effects of radiation damage and a 20% margin (factor 1.2) to account for unmodelled effects. The standard errors in position and proper motions can be derived by applying factors  $\sim 0.7$  and  $\sim 0.5$ , respectively, to the parallax standard errors (Brown, 2013). Some millions of stars will be measured by Gaia with a distance accuracy of better than 1 per cent; some 100 millions or more to better than 10 per cent.

---

<sup>1</sup>Hipparcos magnitude is defined by the passband of the Hipparcos main detection chain which ranges from 340 to 850 nm.

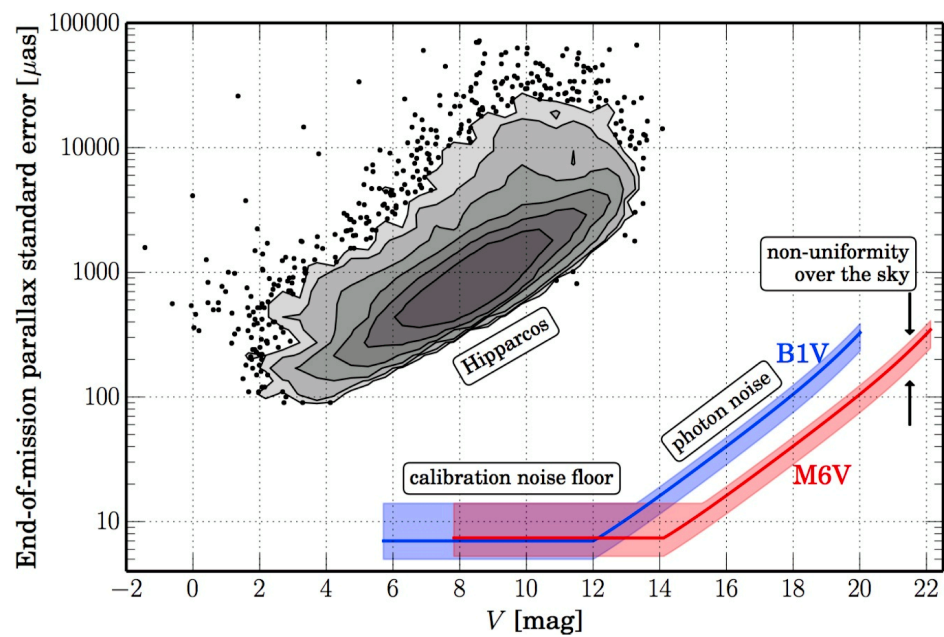


Figure 1.1 Accuracies of determination of parallaxes as a function of source brightness in the  $V$  band for Gaia and for Hipparcos. Contours and dots show the Hipparcos parallax errors from van Leeuwen (2007). The lines show the predicted Gaia sky averaged parallax standard errors for an early (blue) and a late (red) spectral type star. The bands around the average relations reflect uncertain calibration errors at the bright side and the variation in the sky coverage at the faint end. Figure is from Brown (2013).

The astrometric measurements are collected applying a wide photometric band (the Gaia G band) which covers the range 330-1000 nm. Multi-colour photometry will be obtained for all objects by means of low-resolution spectrophotometry. The photometric instrument consists of two prisms: one is called RP for Red Photometer and covers the wavelength range 640-1000 nm, the second one, called BP (Blue Photometer), operates in the wavelength range 330-680 nm.

Before the start of Gaia five-year science phase, the commissioning was performed. It revealed some unexpected anomalies. One problem detected during commissioning was associated with ice appeared on some parts of the optics, causing a temporary reduction in transmission of the telescopes. Heating the affected optics in order to remove the ice has largely solved this problem. Another issue is associated with “stray light”, which reaches Gaia’s focal plane at a level higher than it was predicted before launch. This light appears to be a mixture of light from the Sun finding its way past Gaia’s 10 m-diameter sunshield and light from other astronomical sources. The effect on the performance of Gaia is negligible for objects at magnitude  $V \sim 15$  mag and brighter, but a slight degradation in the positional accuracy is seen for fainter stars, reaching 50% for objects at Gaia’s nominal faint limit of  $V \sim 20$  mag. The phenomenon of stray light will also affect the accuracy to which stellar brightnesses will be measured. Moreover, the impact of the stray light should be more significant for faint stars seen by the Gaia’s Radial Velocity Spectrometer (RVS).

Further tests performed during commissioning have shown that it may be possible to extend Gaia’s reach to stars fainter than  $V \sim 20$  mag, while at the bright end, software changes make Gaia to be able to measure almost all of the brightest stars in the sky, previously considered too bright for such a sensitive system. Both of these extensions will need further analysis before being applied. Finally, Gaia laser device called the “basic angle monitor”, designed to measure the angle of separation between Gaia’s two telescopes to an extremely high level of accuracy, shows that the detected variations in the basic angle are larger than expected. These variations are caused by thermal changes in the payload as Gaia spins. Further efforts are being made to measure and accurately calibrate the variations. After extensive testing and analysis of the system both in space and on the ground, Gaia began scientific operations on the 25 of July 2014.

The first intermediate catalogue of science data is expected to be released to the public in 2017. However, in the case of detection of rapidly-changing objects such as supernovae and other transient events, open alerts are being issued as soon as possible. In fact, in September

2014 Gaia was announced to discover its first supernovae, Gaia14aaa in a distant galaxy.

Gaia is expected to provide a huge contribution to many fields of astronomy, such as the structure and dynamics of the MW, stellar astrophysics, physics of the Solar system, extragalactic astronomy and fundamental physics. Moreover, Gaia will provide valuable samples of variable stars of nearly all types, including detached eclipsing binaries (EBs), contact or semi-contact binaries, and pulsating stars (Paczynski, 1997). Among pulsating stars are key distance indicators such as the Cepheids, the RR Lyrae stars and the long-period variables (LPVs). A complete sample of objects will allow determination of the frequency of variable objects and accurate calibration of the basic relations that allow to use these variables as primary distance indicators (see Section 1.3). Estimated numbers are uncertain, but suggest some 18 million variables in total, including 5 million periodic variables, 2-3 million EBs, 2000-8000 Cepheids, 60000-240000  $\delta$  Scuti variables, 70000 RR Lyrae stars and 140000-170000 Miras (Eyer & Cuypers, 2000).

In order to investigate the performance of the Gaia satellite and the contents of the eventual end-of-mission catalogue, Gaia's Data Processing and Analysis Consortium (DPAC) has a group working on the simulation of several aspects of the Gaia mission. One major product of this work is the Gaia Object Generator (GOG, Luri et al. 2014), designed to simulate both individual Gaia observations and the full contents of the end-of-mission catalogue. GOG includes a full mathematical description of the nominal performance of the Gaia satellite, and is therefore capable of determining the expected precision in astrometric, photometric and spectroscopic observations. In general, the precision depends on the apparent magnitude of the star, its colour, and its sky position, which affects the number and type of observations made (due to the Gaia scanning law). In this thesis work we use GOG simulations in order to analyse the impact of Gaia on the determination of distances with the RR Lyrae stars.

### 1.3 Variable stars as distance indicators

The trigonometric parallax is a powerful tool which allows to derive the distance by using only geometrical principals. However, in order to determine the distance with some accuracy beyond  $\sim 10$  kpc one needs to apply indirect methods and use distance indicators. Objects which are widely used as primary distance indicators are *variable stars* of different types. A variable star is an object that shows a variation of luminosity (ranging from a



limit given by the instrument precision to magnitudes) within a time interval that is small compared with the evolution time of the star.

Variable stars play a fundamental role in the context of the distance scale, since they offer several advantages with respect to normal stars. The light variation makes the variable stars to be more easily recognised than normal stars in the same evolutionary phase, even when stellar crowding is significant. The most important observables of a variable star are the period and the amplitude of the luminosity variation, that can be determined with very high precision (the period in particular) and are both independent of uncertainties on distance and interstellar extinction.

There are two classes of variable stars: intrinsic and extrinsic variables. The variability of the former ones is connected with internal physical phenomena. This class of variables includes pulsating stars and supernovae. Extrinsic variables show variability connected to external causes and include EBs and pulsars. Among intrinsic periodic variable sources, an important role is played by the *radially pulsating variables*.

Radially pulsating variable stars undergo periodic changes in radius and temperature that are responsible for the change in luminosity. The pulsation period  $P$  is related to the natural oscillation period of a star, which can be shown to be proportional to  $\rho^{1/2}$ , where  $\rho$  is the mean density of the star. This natural oscillation period is essentially the time it would take for a star to collapse if the pressure support were suddenly removed. The pulsation mechanism is related to variations of the opacity (the so-called  $\kappa$  mechanism) and the adiabatic exponent in the ionization regions of the most abundant elements in the stellar envelopes, namely H, He and He+, the so-called  $\gamma$  mechanism (Eddington 1926, Zhevakin 1953, Cox & Whitney 1958). As the driving mechanisms of pulsation are active in external layers, the inner structure is not involved and can be neglected in pulsating models (King & Cox 1968 and references therein). Radially pulsating stars share this driving mechanism as demonstrated by the occurrence of the so-called instability strip, the almost vertical narrow region in the colour-magnitude diagram (CMD) where most of the pulsators are located. Stars in different evolutionary phases cross the instability strip at different luminosity levels so that their observations in Galactic and extra-galactic systems allow us to trace stellar populations of different ages. In particular: RR Lyrae stars and Type II Cepheids are the oldest stars (age > 10 Gyr); the Anomalous Cepheids are currently thought to trace the intermediate-age population ( $\sim 1$ -5 Gyr); the Classical Cepheids (CCs) and  $\delta$  Scuti stars are the youngest among radially pulsating variables (50-200 Myr).

In the following sections we will summarise the properties of some classes of variable stars which are widely being used as distance indicators: CCs, RR Lyrae stars and EBs.

## 1.4 Classical Cepheids

Classical Cepheids are primary distance indicators that allow to link the local distance scale to the cosmological distances needed to determine the Hubble constant (Clementini, 2009). CCs are high-luminosity ( $-2 > M_V > -7$ ), radially pulsating variable stars, with periods generally ranging from 1 to 100 days, and commonly associated with relatively young stellar populations, such as those found in open clusters, disks of spiral or irregular galaxies. From the stellar evolution point of view, these variables are intermediate-mass ( $3 - 12 M_{\odot}$ ) stars that cross the instability strip during the core-helium burning phase. The light curve of a CC in the LMC is presented in the left panel of Figure 1.2.

CCs are widely used as primary distance indicators because they follow a period-luminosity ( $PL$ ) relation, which is a two-dimensional projection of the higher-order period-luminosity-colour ( $PLC$ ) relation (Madore & Freedman, 2012). The  $PL$  relation was discovered by Henrietta Swan Leavitt (1868-1921), who studied 2400 CCs, mostly located in the Small Magellanic Cloud (SMC, Leavitt & Pickering 1912). The physical basis of the CC's  $PL$  relation is related to the above mentioned period-density relation coupled with the Stephan-Boltzman law, and the assumption of the mass-luminosity (ML) relation predicted by stellar evolution for intermediate-mass stars in the central He burning phase.

In order to estimate the slope of the  $PL$  relation, a statistically significant and homogeneous sample of CCs is needed. An extraordinary large amount of CCs was discovered in the two Magellanic Clouds (MCs) by the microlensing surveys MACHO and OGLE. Udalski et al. (1999) used fundamental mode pulsating CCs in the Large Magellanic and Small Magellanic Clouds to derive the following  $PL$  relations:

$$V_0(LMC) = -2.760 \log P - 17.042 \quad (1.2)$$

with  $\sigma=0.159$  mag

$$V_0(SMC) = -2.760 \log P - 17.611 \quad (1.3)$$

with  $\sigma=0.258$  mag.

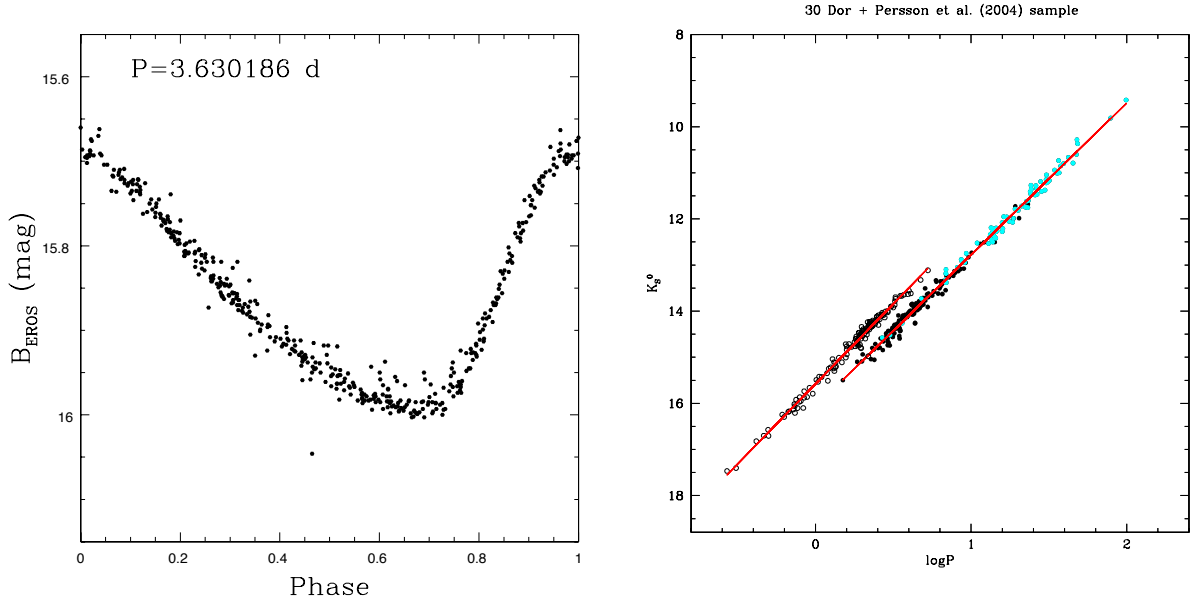


Figure 1.2 *Left panel*: Light curve of a CC in the LMC observed by the EROS-2 survey. Period, expressed in days, is from the EROS-2 catalogue. *Right panel*:  $K_s$ -band  $PL$  relation of CCs in the 30 Doradus field of the LMC from Ripepi et al. (2012). Black open and filled circles show fundamental mode and first-overtone mode Cepheids, respectively. Blue filled circles are fundamental mode CCs from Persson et al. (2004). The solid lines are least-squares fit to the data.

The derived slope is in good agreement with the slope of theoretical  $PL$  relations computed by Caputo et al. (2000) from nonlinear convective pulsation models of CCs ( $M_V = -2.75 \log P - 1.37$ ,  $\sigma = 0.18$  mag).

The zero-point of the  $PL$  relation can be calibrated either using Galactic CCs, for which absolute magnitudes are known from parallax measurements and/or Baade-Wesselink analyses (for a general review of the method see, for example, Gautschi 1987) or, by assuming a value for the distance to the LMC. In the latter case a robust distance determination for the LMC is necessary. The *HST* Key Project (Freedman et al., 2001) used the slope of the CC's  $PL$  relations from Udalski et al. (1999) and a zero-point consistent with an assumed distance modulus  $(m - M)_0 = 18.5$  mag for the LMC, to measure the distances to 31 galaxies in the range from 700 kpc to 20 Mpc. Estimated distances then served to calibrate other, more far-reaching secondary distance indicators and to determine the Hubble constant (Freedman et al., 2001).

Despite the fact that the CCs are successfully used to measure the distance up to 20 Mpc or more, a number of basic questions concerning the  $PL$  relation lack an answer (Fouqu 

et al. 2003, Marconi et al. 2010). The theoretical explanation of the observational evidence of a  $PL$  relation for CCs relies on the ML relation, which is significantly dependent on several physical and numerical assumptions (Marconi et al., 2010). Thus, the uncertainties of the ML relation reflect on the  $PLC$  relation's coefficients and zero-point. Another issue is a possible non-linearity of the  $PL$  relation and the existence of a break around 10 days (Tammann & Reindl 2002, Tammann et al. 2002, Kanbur & Ngeow 2004, Sandage et al. 2004, Ngeow et al. 2008). Moreover, it is not definitely established whether the  $PL$  relation is universal, and consequently, if the slope derived on the basis of LMC's and SMC's CCs can be safely applied to other galaxies. In the last decades, many studies were devoted to investigate the effect of metallicity on the coefficients of the  $PL$  relation. On the theoretical side, linear and adiabatic models mostly suggest a negligible dependence of the CC's  $PL$  relations on chemical composition (Chiosi et al. 1993, Alibert et al. 1999, Saio & Gautschy 1998, Sandage 1999), while nonlinear convective pulsation models predict a significant metallicity effect on the  $PL$  relations (Bono et al. 1999, Fiorentino et al. 2002, Marconi et al. 2005). Some empirical studies support the nonlinear theoretical scenario (Romaniello et al. 2005, 2008). Some of these issues can be resolved by using the  $PL$  relation in the infrared passbands. The  $PL$  relation in the  $K_s$  passband of CCs in the LMC observed with the near-infrared VMC survey (Cioni et al., 2011) is presented in the right panel of Figure 1.2. It is well known that the intrinsic width of the CC's  $PL$  relation decreases as a function of increasing wavelength (e. g. Madore & Freedman 1991; McGonegal et al. 1982; Caputo et al. 2000). The amplitude of pulsation in the infrared passbands is smaller than in the visual one, so the mean magnitude could be determined more precisely. Moreover, in the infrared bands the problem of reddening is less important and the effect of metallicity on the  $PL$  seems to be smaller (Groenewegen & Oudmaijer 2000; Caputo et al. 2000; Marconi et al. 2005). Therefore, the  $PL$  relation of CCs in the near-infrared passbands is a very powerful tool to determine the distances to the LMC and other galaxies.

## 1.5 RR Lyrae stars

RR Lyrae stars are primary distance indicators located mainly in the halos of galaxies and in globular clusters. RR Lyrae stars are old (age  $> 10$  Gyr), low-mass ( $\sim 0.6 - 0.8 M_{\odot}$ ) core-helium burning stars that lie within the instability strip on the horizontal branch (HB) of the CMD.

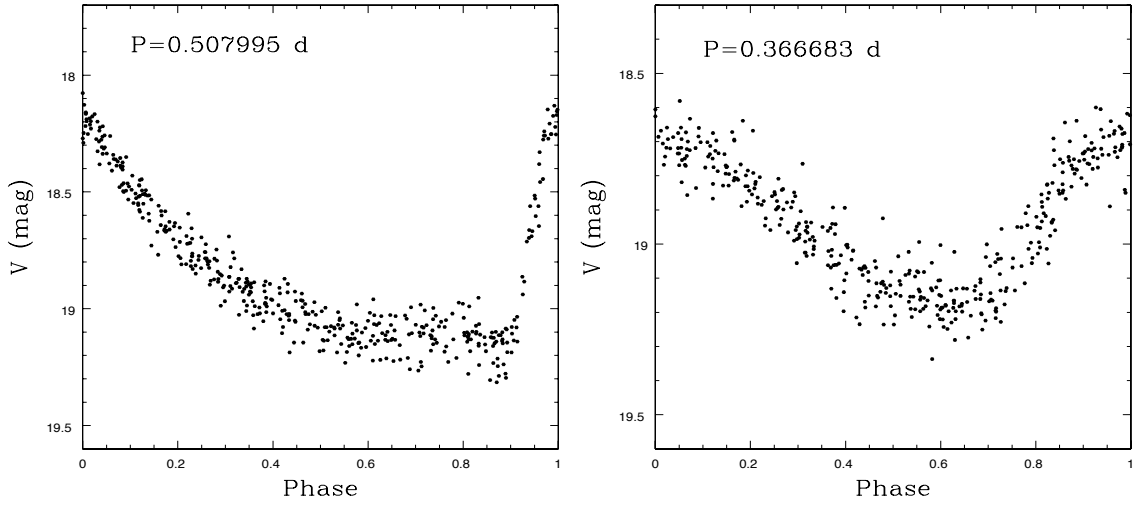


Figure 1.3 Light curves of *ab*-type (left panel) and *c*-type (right panel) RR Lyrae stars observed by the EROS-2 survey in the LMC. Periods expressed in days are from the EROS-2 catalogue.

The prototype star RR Lyrae in the constellation of Lyra was discovered in 1899 by Williamina Fleming. In the following years a significant number of these pulsators were observed in globular clusters by Bailey, who classified them on the basis of the period and shape of the light curve. In particular, RR Lyrae stars were divided into *ab*-type (RRab), which have asymmetric light curves, periods in the range from  $\sim 0.4$  to  $\sim 1$  day and amplitude in the visual band  $Amp(V)$  steadily decreasing as the period increases, and *c*-type (RRc) with amplitude ranging from 0.2 to 0.6 mag, sinusoidal shape of the light curves and period ranging from  $\sim 0.2$  to  $\sim 0.4$  day. Examples of light curves of RRab and RRc stars in the LMC are presented in Figure 1.3. According to the theory of stellar pulsation the two types of RR Lyrae stars undergo pulsation in different modes. RRab stars pulsate in the fundamental mode and RRc stars in the first-overtone mode. There is also a third type of RR Lyrae stars, called *double-mode* or RRd stars, who undergo pulsation in both modes. The RRd stars are particularly useful to obtain independent estimates of the stellar mass (Petersen 1973; Bono et al. 1996; Bragaglia et al. 2001).

### 1.5.1 Metal abundance of RR Lyrae stars

The RR Lyrae stars are relatively low-mass stars, so the nucleosynthesis of significant amount of elements heavier than carbon and oxygen is not expected during the lifetime of these stars (Smith, 1995). Thus, the abundance of heavy elements in the atmosphere of

the RR Lyrae stars reflects the abundance of heavy elements in the interstellar gas cloud from which the stars were formed. This fact makes the RR Lyrae stars useful tracers of the chemical history of the system they belong to.

In order to describe the iron (Fe) abundance of stars, the  $[\text{Fe}/\text{H}]$  notation is used. In this notation, the ratio of Fe over hydrogen (H) in the photosphere of a star is related to that ratio in the Sun:

$$[\text{Fe}/\text{H}] = \log(\text{Fe}/\text{H})_{star} - \log(\text{Fe}/\text{H})_{\odot} \quad (1.4)$$

The metallicity  $[\text{Fe}/\text{H}]$  of RR Lyrae stars ranges from  $\sim -2.5$  to  $\sim +0.2$  dex.

The metal abundance of RR Lyrae stars is often measured with the  $\Delta S$  index (Preston 1959). The spectral type of RR Lyrae stars as determined from the hydrogen Balmer lines is generally later than the spectral type determined from the CaII K-line, and the latter is generally weaker than expected on the basis of the Balmer line spectral classification. Preston (1959) defined the  $\Delta S$  index as the difference in tenths of spectral class between the spectral type of a RR Lyrae at minimum light estimated from the hydrogen lines  $[\text{Sp}(\text{H})]$  and that estimated from the intensity of the CaII  $K$  line  $[\text{Sp}(\text{K})]$ :

$$\Delta S = 10[\text{Sp}(\text{H}) - \text{Sp}(\text{K})]. \quad (1.5)$$

The  $[\text{Fe}/\text{H}]$  abundance is well correlated with the  $\Delta S$  index, and a number of different calibrations of the  $\Delta S$  index in terms of  $[\text{Fe}/\text{H}]$  abundance exist in the literature (e.g. Preston 1959; Jurcsik 1995; Gratton et al. 2004, etc.).

A few high resolution spectroscopic studies of elemental abundances of RR Lyrae stars are also found in the literature (Butler et al. 1976, 1979; Clementini et al. 1995; Lambert et al. 1996; Kolenberg et al. 2010; For et al. 2011; Kinman et al. 2012; Govea et al 2014, Pancino et al. 2014, submitted to MNRAS). For variables in globular clusters, individual metal abundances can be inferred from the accepted metallicities of the host clusters<sup>2</sup>.

Indeed, the most appropriate way to measure the metallicity of RR Lyrae stars is through spectroscopy. Gratton et al. (2004) derived metal abundances of 98 RR Lyrae stars in the

<sup>2</sup>A number of different metallicity scales exist in the literature. Among the most used ones are Zinn & West (1984) (hereafter referred as ZW) scale which is based on a variety of integrated photometric and spectroscopic indices calibrated from the few echelle photographic spectra existing at the time; Carretta & Gratton (1997) scale which was derived from the analysis of a large sample ( $\sim 160$ ) of bright giants in 24 globular clusters, whose chemical abundances were obtained from equivalent widths measured on high dispersion CCD spectra; and Carretta et al. (2009) scale (hereinafter, C09) that is based on the analysis of spectra of about 2000 red giant branch (RGB) stars in 19 Galactic globular clusters. Specifically used for RR Lyrae stars is Jurcsik (1995) metallicity scale (hereafter referred as J95) based on both spectroscopic cluster abundances and  $\Delta S$  measurements of cluster variables. J95 metallicity scale is valid both for globular clusters and field RR Lyrae

LMC from low resolution spectra by comparing the strength of the CaII K line with that of the H lines, the derived metallicities are on a metallicity scale which is, on average,  $\sim 0.06$  dex more metal-rich than the Zinn & West (1984) scale.

However, when spectroscopical observations are not available or feasible, an estimate of “photometric” metallicity could be inferred from the  $\phi_{31}$  parameter of the Fourier decomposition of RR Lyrae’s light curves. According to Simon & Teays (1982) the light curve of a RR Lyrae star can be fitted with a Fourier function of the form:

$$m(t) = A_0 + \sum_{i=1}^N A_i \cos[i\omega_0(t - t_0) + \phi_i] \quad (1.7)$$

where  $m(t)$  is the star apparent magnitude at time of observation  $t$ ,  $A_0$  is the average apparent magnitude,  $N$  is the number of fitted terms,  $\omega_0$  is the angular pulsation frequency of the star ( $\omega_0 = 2\pi/P_0$ ),  $t_0$  is the time of maximum light, and  $A_i$  and  $\phi_i$  are the amplitude and phase coefficients of the individual Fourier terms. The shape of the light curves can be quantified by the low order coefficients of the fit:  $R_{i1} = A_i/A_1$  and  $\phi_{i1} = \phi_i - i\phi_1$ . The  $A_1$ ,  $A_2$  and the  $\phi_{21}$ ,  $\phi_{31}$  parameters of the Fourier decomposition can be used to classify the RR Lyrae stars (see e.g., Simon & Teays 1982, Cacciari et al. 2005).

Jurcsik & Kovacs (1996) derived a relation between the Fourier parameter  $\phi_{31}$  of the V-band light curve of field *ab*-type RR Lyrae stars, the period and the star metallicity on the Jurcsik (1995) metallicity scale:

$$[\text{Fe}/\text{H}] = -5.038 - 5.394P + 1.345\phi_{31}. \quad (1.8)$$

Jurcsik & Kovacs (1996) introduced the so-called *compatibility condition* and defined a *deviation parameter*  $D_F$ :

$$D_F = |F_{obs} - F_{calc}|/\sigma_F, \quad (1.9)$$

where  $F_{obs}$  is the observed value of the given Fourier parameter,  $F_{calc}$  is its predicted value from the other observed parameters,  $\sigma_F$  is the corresponding standard deviation.  $D_m$  is the maximum of the deviation parameters  $\{D_F\}$  and measures the regularity of the light stars, and is related to the  $\Delta S$  index through the relation:

$$[\text{Fe}/\text{H}]_{J95} = -0.190(\pm 0.007)\Delta S + 0.027(\pm 0.052) \quad (1.6)$$

curve. According to Jurcsik & Kovacs (1996) only if the light curve of the RRab star satisfies the *compatibility condition*  $D_m < 3$  can Eq. 1.8 be used for a reliable estimate of the star metal abundance [Fe/H]. However, Cacciari et al. (2005) adopted a relaxed compatibility condition, and found that a maximum value of 5 for  $D_m$  allows to increase the statistic without affecting significantly the results. Kapakos et al. (2011) found that the criterion  $D_m < 3$  cannot lead to a robust sample of RRab stars without taking into consideration the  $\sigma_{D_m}$ . Thus they applied the criterion  $\sigma_{D_m} < 3$  and  $D_m - \sigma_{D_m} < 3$  in their analysis.

Morgan et al. (2007) found the relation between metallicity on the ZW metallicity scale,  $\phi_{31}$  and  $P$  for RRc stars:

$$[\text{Fe}/\text{H}]_{\text{ZW}} = 52.466P^2 - 30.075P + 0.131\phi_{31}^2 + 0.982\phi_{31} - 4.198\phi_{31}P + 2.424 \quad (1.10)$$

which has a standard deviation of 0.145 dex. Finally, Nemeč et al. (2013) have derived a new metallicity calibration of the  $\phi_{31}$  parameter based on spectroscopic and photometric properties of 41 RR Lyrae stars observed by the *Kepler* space telescope and derived  $P - \phi_{31} - [\text{Fe}/\text{H}]$  relations for RRab and RRc stars, separately. Since Nemeč et al. (2013) metallicity calibrations are derived using high dispersion spectra analysed with standard reduction procedures, the derived metallicities are on the high dispersion spectroscopy scale of Carretta et al. (2009).

For ab-type RR Lyrae stars the new calibration equation is:

$$[\text{Fe}/\text{H}] = b_0 + b_1P + b_2\phi_{31-kep}^s + b_3\phi_{31-kep}^sP + b_4(\phi_{31-kep}^s)^2 \quad (1.11)$$

The coefficients of equation (1.11) are:  $b_0 = -8.65 \pm 4.64$ ,  $b_1 = -40.12 \pm 5.18$ ,  $b_2 = 5.96 \pm 1.72$ ,  $b_3 = 6.27 \pm 0.96$ ,  $b_4 = -0.72 \pm 0.17$ , with rms of the fit of 0.084 dex. The  $\phi_{31-kep}^s$  is the parameter of the sine Fourier decomposition in Kepler magnitudes which can be derived from the  $\phi_{31}^s$  in the Johnson  $V$  band by applying the equation:

$$\phi_{31-kep}^s = \phi_{31}^s(V) + (0.151 \pm 0.026) \quad (1.12)$$

For c-type RR Lyrae stars Nemeč et al. (2013) derived the equation:

$$[\text{Fe}/\text{H}]_{\text{C09}} = b_0 + b_1P + b_2\phi_{31}^c + b_3\phi_{31}^cP + b_4P^2 + b_5(\phi_{31}^c)^2 \quad (1.13)$$

The coefficients of equation (1.13) are:  $b_0 = 1.70 \pm 0.82$ ,  $b_1 = -15.67 \pm 5.38$ ,  $b_2 = 0.20 \pm 0.21$ ,  $b_3 = -2.41 \pm 0.62$ ,  $b_4 = 18.00 \pm 8.70$ ,  $b_5 = 0.17 \pm 0.04$ , and the rms error of the fit was 0.13 dex. The  $\phi_{31}^c$  is the parameter of the cosine Fourier decomposition in the



$V$  band which could be derived from the  $V$  sine decomposition parameter by applying the equation:

$$\phi_{31}^c = \phi_{31}^s - \pi \quad (1.14)$$

We will use Nemec et al. (2013) relations in 6 to derive photometric metallicities for the RR Lyrae stars.

Di Fabrizio et al. (2005) measured photometric metallicities from the  $\phi_{31}$  Fourier parameter for 29 LMC RRab stars and compared their values with the spectroscopic metal abundances derived for these stars by Gratton et al. (2004). They found that the average difference between photometric and spectroscopic metallicities is  $0.30 \pm 0.07$  dex, with the photometric abundances being larger. This test provides an indication of the soundness of photometric metallicities of RR Lyrae stars.

### 1.5.2 $M_V - [\text{Fe}/\text{H}]$ and $PL_KZ$ relations of RR Lyrae stars

RR Lyrae stars make useful distance indicators because of the existence of an absolute magnitude-metallicity relation in the  $V$  band:  $M_V - [\text{Fe}/\text{H}]$  (Sandage 1981a,b) and of a period-luminosity-metallicity relation in the  $K$  band:  $PL_KZ$  (Longmore et al. 1986, Bono et al. 2003, Catelan et al. 2004, Sollima et al. 2008, and references therein).

In the past decades several authors studied the  $M_V - [\text{Fe}/\text{H}]$  relation for RR Lyrae stars using a number of methods, including synthetic Horizontal Branch models (Lee, 1994) and the Baade-Wesselink method (Fernley et al., 1998a). Gratton et al. (2004) combined spectroscopically determined metallicities with high accuracy photometry in the  $V$  band of  $\sim 100$  RR Lyrae stars in the LMC (Clementini et al., 2003) and derived the luminosity-metallicity relation:

$$V_0 = (0.214 \pm 0.047)([\text{Fe}/\text{H}] + 1.5) + (19.064 \pm 0.017), \quad (1.15)$$

where  $V_0$  is the apparent dereddened average magnitude.

The slope of this relation is in a good agreement with the slope derived for the luminosity-metallicity relation of RR Lyrae stars in the MW (Fernley et al., 1998a) and HB stars in the globular clusters of M31 (Rich et al., 2005). This fact supports the idea that the luminosity-metallicity relation of RR Lyrae stars is, in first approximation, linear and universal (Clementini, 2009).

The zero-point of the  $M_V - [\text{Fe}/\text{H}]$  relation can be determined with a number of different techniques among which are: (i) the parallaxes of RR Lyrae stars in the MW; (ii)

the calibration via globular clusters, whose distances are determined using absolute magnitudes of subdwarfs measured by the Hipparcos satellite; (iii) various theoretical and empirical assumptions, such as the adoption of the value for the distance to the LMC. Benedict et al. (2011) derived the zero-point  $M_V = 0.45 \pm 0.05$  mag for  $[\text{Fe}/\text{H}] = -1.5$  dex using *HST* parallaxes of five MW RR Lyrae stars and adopting the slope from Gratton et al. (2004). This value is about 0.2 mag brighter than the value of  $M_V = 0.66 \pm 0.14$  mag at  $[\text{Fe}/\text{H}] = -1.48 \pm 0.07$  derived by Catelan & Cortes (2008) for RR Lyrae itself, but has a significantly smaller error.

There are theoretical and empirical suggestions that the  $M_V - [\text{Fe}/\text{H}]$  relation is not linear over the whole metallicity range (Marconi, 2009). The relation may also be affected by a number of uncertain factors such as evolutionary effects,  $\alpha$ -element enhancement, etc. Finally, the determination of distances from analysis of field RR Lyrae stars observed in the optical passbands depends on the reddening; this is the strongest driver for moving to the infrared when at all possible. Three of the five galactic RR Lyrae stars with *HST* parallaxes (Benedict et al., 2011) have reddening  $E(B - V) \geq 0.1$  mag, so the zero-point is potentially more robust in the infrared (Walker, 2012). The near-infrared  $PL_KZ$  relation of RR Lyrae stars has a list of other advantages in comparison with the visual  $M_V - [\text{Fe}/\text{H}]$  relation. First of all, the luminosity in the  $K$  passband is less dependent on metallicity. Moreover, the light curves of RR Lyrae stars in the  $K$  band have smaller amplitudes and are more symmetrical, hence the determination of the mean  $K$  magnitudes is more precise.

The near-infrared  $PL_KZ$  relation of RR Lyrae stars was studied by several authors both from a theoretical and an observational point of view. Longmore et al. (1986) pioneering work was followed by Liu & Janes (1990), Skillen et al. (1993) and Jones et al. (1996). A comprehensive analysis of the IR properties of RR Lyrae stars was performed by Nemec et al. (1994).

Bono et al. (2003) derived the semi-theoretical relation:

$$M_K = -2.101 \log P + (0.231 \pm 0.012)[\text{Fe}/\text{H}] - (0.770 \pm 0.044), \quad (1.16)$$

Catelan et al. (2004) presented a theoretical calibration of the RR Lyrae  $PL_KZ$  relation based on synthetic horizontal branch models computed for several different metallicities, fully taking into account evolutionary effects besides the effect of chemical composition. They derived the relation:

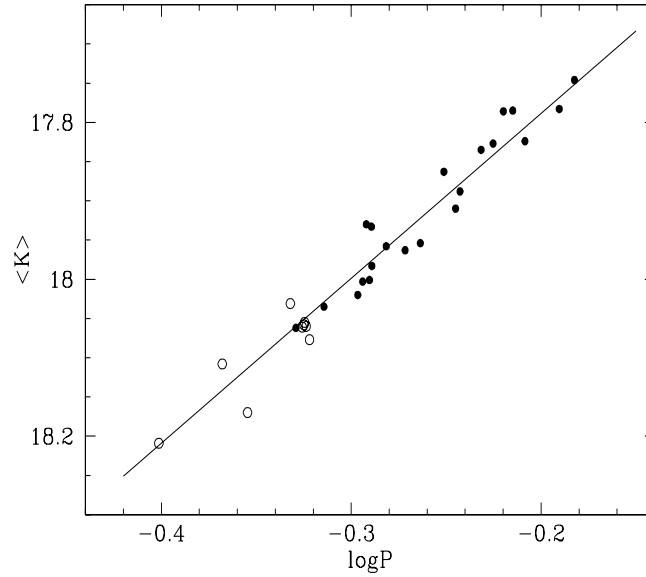


Figure 1.4  $PL_K$  relation for RR Lyrae stars in the LMC cluster Reticulum. Open symbols show RRC stars after their periods have been fundamentalized by adding 0.127 to the logarithm of the period. Filled symbols are RRab stars, the line shows the theoretical prediction from Bono et al. (2003). Figure is from Dall’Ora et al. (2004).

$$M_K = -2.353 \log P + 0.175 \log Z - 0.597 \quad (1.17)$$

By using Eqs. 9 and 10 in Catelan et al. (2004) and assuming  $[\alpha/\text{Fe}] \sim 0.3$  (e.g., Carney 1996) we transformed Eq. 1.17 into the form:

$$M_K = -2.353 \log P + 0.175 [\text{Fe}/\text{H}] - 0.869 \quad (1.18)$$

Dall’Ora et al. (2004) obtained the relation between apparent  $K$  magnitude and period for 21 RRab and 9 RRC stars in the LMC globular cluster Reticulum.:

$$\langle K \rangle = (-2.16 \pm 0.09) \log P + (17.352 \pm 0.025) \quad (1.19)$$

with standard deviation of 0.03 mag.

Figure 1.4 shows the  $PL_K$  relation derived by Dall’Ora et al. (2004). They used this relation in combination with Eq. 1.16 from Bono et al. (2003) to derive  $(m - M)_0 = 18.52 \pm 0.005(\text{random}) \pm 0.117(\text{systematic})$  mag for the distance modulus of Reticulum.

Del Principe et al. (2006) obtained the  $PL_KZ$  relation from the analysis of RR Lyrae stars of different metallicities in the globular cluster  $\omega$  Cen. Benedict et al. (2011) calibrated the zero-point of Del Principe et al.'s relation using the *HST* parallaxes of five RR Lyrae stars in the MW and obtained:

$$M_K = (-2.71 \pm 0.12)(\log P + 0.28) + (0.12 \pm 0.04)([\text{Fe}/\text{H}] + 1.58) - (0.57 \pm 0.02) \quad (1.20)$$

Sollima et al. (2008) derived the  $PL_KZ$  relation from the analysis of 544 RR Lyrae variables in 15 Galactic clusters and in the LMC globular cluster Reticulum. Mean  $K$  magnitudes were estimated by combining Two-Micron-All-Sky-Survey (2MASS, Cutri et al. 2003) photometry and literature data. The zero-point was calibrated on RR Lyrae itself, whose distance modulus was derived using the star trigonometric parallax by Benedict et al. (2002). Sollima et al. (2008) provide the relation:

$$M_K = (-2.38 \pm 0.04)\log P + (0.08 \pm 0.11)[\text{Fe}/\text{H}]_{\text{CG}} - (1.07 \pm 0.11), \quad (1.21)$$

where  $P$  is the fundamental-mode period, and the metallicity  $[\text{Fe}/\text{H}]_{\text{CG}}$  is in the Carretta & Gratton (1997) metallicity scale. By applying this relation to the  $K$  data from Dall'Ora et al. (2004) the distance modulus of Reticulum was determined to be:  $(m - M)_0 = 18.48 \pm 0.11$  mag (Sollima et al., 2008).

Szewczyk et al. (2008) obtained deep infrared  $J$  and  $K$  observations of five fields located in the LMC bar. Using different theoretical and empirical  $PL_KZ$  calibrations they found the distance modulus of the LMC to be  $18.58 \pm 0.03$  (*statistical*)  $\pm 0.11$  (*systematic*) mag.

Borissova et al. (2009) combined near-infrared photometry and spectroscopically measured metallicity for a sample of 50 field RR Lyrae stars in inner regions of the LMC, and derived the relation:

$$M_K = (-2.11 \pm 0.17)\log P + (0.05 \pm 0.07)[\text{Fe}/\text{H}] - 1.05 \quad (1.22)$$

Borissova et al. (2009) had 5 measurements in the  $K$  passband for most stars in their sample. Templates from Jones et al. (1996) were used to fit the light curves of the RR Lyrae stars and derive mean  $K$  magnitudes. The zero-point of the relation was calculated using

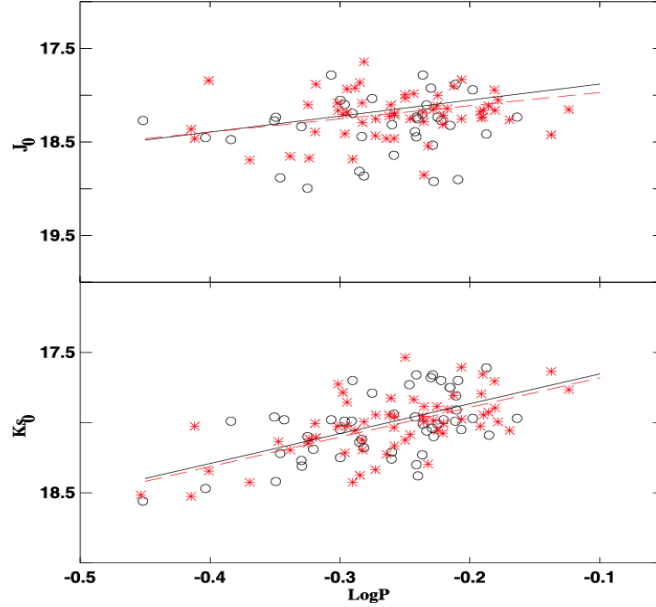


Figure 1.5 LogP vs.  $J_0$  and LogP vs  $K_0$  plots for field RR Lyrae stars in the LMC. Asterisks represent Szewczyk et al. (2008) data, open circles are data from Borissova et al. (2009). Solid lines show the best-fit relations obtained using only Borissova et al. (2009) data, dashed lines are for the combined samples. Figure is from Borissova et al. (2009).

the mean  $K$  magnitude, the reddening and the trigonometric parallax of RR Lyrae itself, from Sollima et al. (2008). By applying Eq. 1.22 Borissova et al. (2009) determined the LMC distance modulus to be:  $(m - M)_0 = 18.53 \pm 0.13$  mag.

Figure 1.5 shows the  $PL_K$  relation obtained by Borissova et al. (2009) combining their data with the data from Szewczyk et al. (2008). Comparing the  $PL_K$  relation derived for the RR Lyrae stars in the Reticulum cluster (Fig. 1.4) and to the relation for field LMC RR Lyrae stars (Fig. 1.5) one can see that the spread is significantly smaller for the objects in the cluster. It could be due to depth effects or, more likely, it could suggest that the metallicity effect should be taken into account.

Metallicities in all the above relations are on, or close to the Zinn & West metallicity scale, except for Eq. 1.21, which is on the Carretta & Gratton (1997) metallicity scale.

The  $PL_KZ$  relation is a very powerful tool to measure distances. However, the  $PL_KZ$

relations published in the literature often were derived from small samples of RR Lyrae stars. Additionally, the small number of observations in the  $K$  band limited the determination of accurate mean  $K$  magnitudes. A large sample of RR Lyrae stars in the LMC with 12 or more epochs in the  $K_s$  band light curves is provided by the VMC survey (Cioni et al., 2011). One goal of this thesis work was to derive a new  $PL_{K_s}Z$  relation based on the VMC photometry. Another fundamental issue is the derivation of the zero-point of the  $PL_KZ$  relation. This problem will be solved when unprecedentedly accurate trigonometric parallaxes for large numbers of RR Lyrae stars will be provided by Gaia. In this thesis we present simulated parallaxes for bright RR Lyrae stars in the MW and use them to establish the accuracy of the  $PL_KZ$  and  $M_V - [\text{Fe}/\text{H}]$  relations zero-points as it will be calibrated with Gaia.

## 1.6 Eclipsing binaries

EBs are binary stars in which the orbit plane of the two stars lies nearly in the line of the sight of the observer, so the components of the system undergo mutual eclipses. Examples of the light curves of EBs are presented in Figure 1.6.

### 1.6.1 Classification of eclipsing binaries

The classification of EBs is based on the distance between components, relative to their sizes. If the two components do not fill their Roche lobes, the system is considered to be a detached binary. In a semi-detached binary one of the two components fills its Roche lobe and mass transfer occurs. In contact EBs both stars fill their Roche lobes. To classify contact and detached/semi-detached binaries analysis of the Fourier parameters and visual inspection of the light curves are necessary.

Rucinski (1993) showed that a simple description of the light variation of binaries could be obtained through the cosine Fourier decomposition  $\sum a_i \cos(2\pi i\phi)$ . In this decomposition the coefficient  $a_0$  is the average magnitude of the model fit,  $a_1$  and  $a_3$  represent the difference in depth between the two eclipses,  $a_2$  reflects the total amplitude of the binary variability and  $a_4$  is related to the eclipse “peakedness” that goes to zero for the light curves of contact binaries. Hence, the combination of the two cosine coefficients  $a_2$  and  $a_4$  could serve as a separator of contact and non-contact (detached and semi-detached) binaries. Namely, the curve described by the relation  $a_4 = a_2(0.125 - a_2)$ , where both coefficients are negative, separates the regions of the contact and non-contact binaries on the  $a_2$  versus

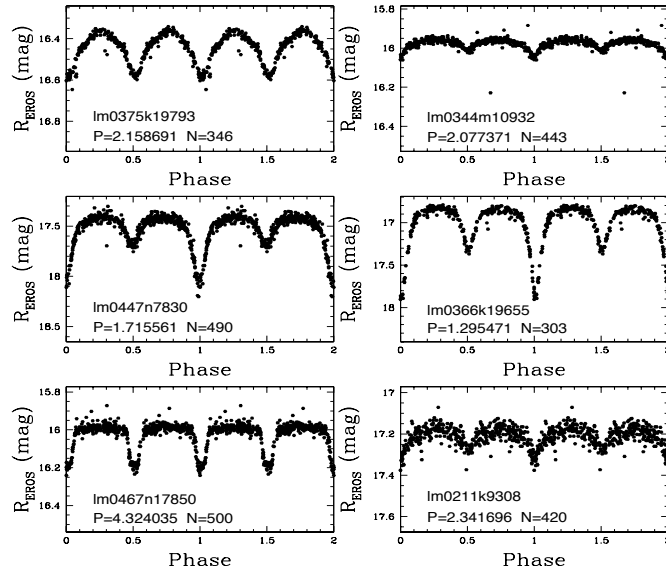


Figure 1.6 Light curves in the  $R_{EROS}$  band of EBs observed in the LMC by the EROS-2 survey. P - period (day), N - number of the observations. Figure is from Muraveva et al. (2014a).

$a_4$  plane (Rucinski, 1993). Rucinski (1997) performed the Fourier analysis of the  $I_C$ -band light curves to extract a sample of the contact binaries from OGLE EBs in nine fields in Baade’s Window.

However not only genuine contact binaries, but also variables with contact-like light curves such as the ellipsoidal variables may be misclassified as contact binaries. Ellipsoidal variability is observed in close binary systems when one or both components is (are) distorted by the tidal interaction with the companion. The main reason of the variability is the change of the projected areas on the sky because of the orbital motion of the components. Large samples of ellipsoidal variables were published by Soszyński et al. (2004), who used OGLE II and OGLE III photometry, and by Derekas et al. (2006), who used the MACHO database. Since the light curves of contact binaries and non-eclipsing ellipsoidal variables have similar shapes and could be easily mistaken, in the following analysis we adopt the term “contact-binary-like” systems for all objects passed by the Fourier filter.

## 1.6.2 Eclipsing binaries as distance indicators

EBs can be used as distance indicators, since some fundamental stellar parameters can be determined using geometrical constraints of the systems. Masses of components are esti-

mated dynamically via radial velocities, radii from the eclipse durations and the temperature ratio (strictly the surface-brightness ratio) from the eclipse depths. The radii and temperature together are used to measure the luminosity of the system. From the estimated luminosity and observed fluxes the distances to the EBs can be determined. This method requires photometric and spectroscopic data (see reviews by Andersen 1991; Torres et al. 2010) and is used to measure the distances to nearby galaxies. Recently, Pietrzyński et al. (2013) used EBs to measure a distance to the LMC which is considered to be accurate to 2 %.

EBs may serve as distance indicators even when spectroscopy is not available. W UMa type stars are contact binary systems with orbital periods typically less than 1 day, composed of main sequence turn-off stars (Rucinski, 1998). It was shown that this class of binaries could be used as distance indicators since the size of the two components could be determined from the orbital period, which in combination with the colour information allows one to derive absolute magnitudes (Rucinski 1997, and references therein). Indeed, Rucinski (1997) used the method to determine the distance to W UMa-type contact systems in the Galactic Bulge.

While W UMa type stars in the Galaxy seem to be limited to periods  $P < 1.3 - 1.5$  day, massive, young, blue systems of W UMa type with longer orbital periods of 2-3 day exist in the LMC (Rucinski, 1999). These objects may follow a  $PL$  relation. Rucinski (1999) suggested the existence of a  $PL$  relation at maximum light in the visual band (Figure 1.7), but with a large scatter, possibly due to unaccounted effects of the interstellar extinction. One goal of this thesis was to check the existence of the  $PL$  relation for young massive contact EBs in the LMC and the possibility of using this relation to determine the distance to this galaxy.



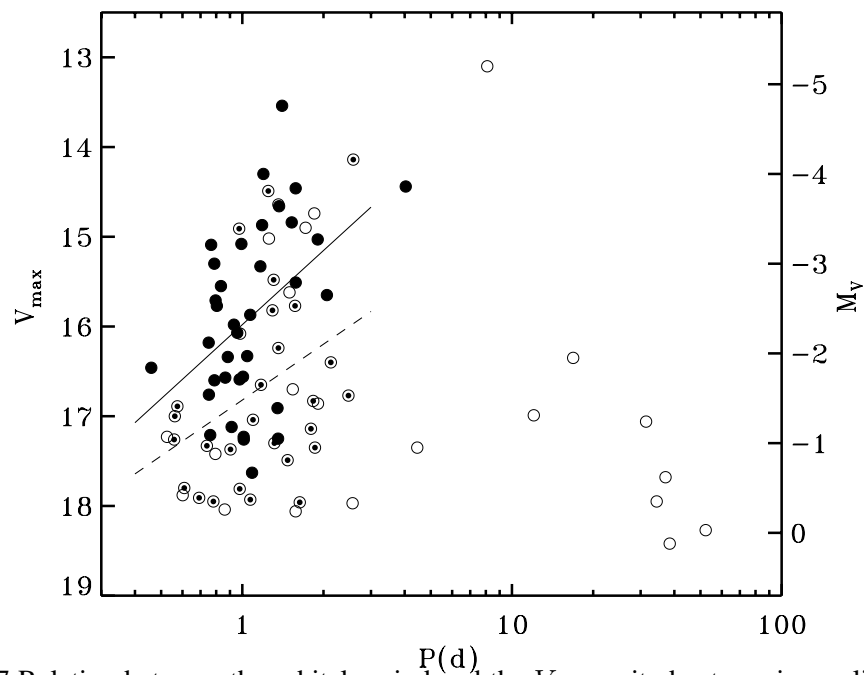


Figure 1.7 Relation between the orbital period and the  $V$ -magnitude at maximum light for EBs in the LMC. Different symbols mark three colour index ranges: filled circles represent extra-blue binaries, open circles - red binaries, semi-filled circles are moderately-blue systems (see Rucinski 1999 for details). Lines represent linear fits to the extra-blue (solid line) and moderately-blue (dashed line) subsamples. Figure is from Rucinski (1999).



## Chapter 2

# The Large Magellanic Cloud

### 2.1 Magellanic System

The Magellanic System (MS) is located at a distance of about 57 kpc (Cioni et al., 2000) from the MW and is formed by the LMC, the SMC, the Bridge connecting them and the Magellanic Stream, a trailing HI component. The LMC is a dwarf irregular galaxy, also considered as a late type spiral system. The SMC is a dwarf irregular galaxy sometimes referred to as a dwarf Spheroidal galaxy (dSph; Zaritsky 2000). The LMC has an inclination angle of  $\sim 35$  deg (Nikolaev et al. 2004, Olsen & Salyk 2002, van der Marel & Cioni 2001), but main structures of the galaxy lie reasonably close to the plane of the sky, while the SMC forms an extended structure almost along the line of sight (Cardwell & Coulson, 1986). Optical and infrared surveys of the MS show that the LMC and SMC are distinct objects separated in space by a projected distance of  $\sim 20$  kpc. However, the HI distribution shows a different picture. The MCs are connected by a low-metallicity bridge of gas and share a common gaseous envelope (Putman et al. 2003, Brüns et al. 2005). The existence of such features suggests that the LMC and the SMC are a binary interacting pair.

The Magellanic Stream is formed by HI gas and does not contain stars (Guhathakurta & Reitzel, 1998). It trails behind the Clouds at least 150 deg across the sky (Braun & Thilker 2004, Nidever et al. 2010). The Stream has historically been explained as the product of a tidal or hydrodynamical interaction between the MCs and the MW (Gardiner & Noguchi 1996, Mastrogiuseppe et al. 2005, Connors, Kawata & Gibson 2006). This picture is based on the assumption that the MCs have experienced multiple close passages near the MW. However, *HST* proper motion measurements of the MCs (Kallivayalil et al. 2006a; Kallivayalil et al. 2006b) have challenged this model. These studies suggest instead that the MCs have, at best, completed one orbit around the MW, or that they may even be still on

their first passage. Besla et al. (2010) introduced a model to explain the observed large-scale gas morphology of the MS, according to which the Magellanic Bridge and Stream could be explained through tidal interaction between the LMC and the SMC. Since the MW is not responsible for removing material from the system, this picture is consistent with the scenario of the first infall of the MS towards the MW. There is evidence that the tidal interactions of the MCs could also account for the internal structure of the LMC (Besla et al., 2012).

## 2.2 Structure of the LMC

The LMC has a diameter  $\sim 4.3$  kpc and contains one spiral arm and a bar. The LMC bar is a long-standing puzzle because it is off-centered relatively to the dynamical centre. Using relative distance measurements to Cepheids in the LMC, Nikolaev et al. (2004) showed that the bar is located  $\sim 0.5$  pc in front of the main disc. There are also evidences that the bar could be warped relatively to the disc plane, so the east and west ends are nearer the MW than the middle part (Subramaniam 2003, Lah et al. 2005, Koerwer 2009). The bar is not seen in the gas distribution (Kim et al., 1998) or as a site of ongoing star formation. Besla et al. (2012) showed that the internal structure and kinematics of the LMC strongly favour a scenario in which the MCs have recently (100-300 Myr ago) experienced a direct collision. The LMC contains large ( $\sim 1$  kpc in diameter) star-forming regions: 30 Doradus, located slightly above the bar, and Constellation III, located close to the LMC spiral arm (Dolphin & Hunter, 1998).

The structure of the LMC as traced by probes of different stellar populations was discussed in Moretti et al. (2014). In this paper we have compared the distribution of RR Lyrae stars, "hot" eclipsing binary stars (HEBs) and CCs from the OGLE III, OGLE IV and EROS-2 surveys (Figure 2.1). RR Lyrae stars (age  $\sim 10$  Gyr) have a larger density in the central region of the LMC, but in general they are distributed smoothly and likely trace the halo of the galaxy. On the contrary, CCs and HEBs are strongly concentrated towards the LMC bar and spiral arm, and almost disappear in the peripheral areas. Fig. 2.1 shows that distributions of CCs and HEBs are very similar, but HEBs (age  $\sim 12$  Myr) are more sharply concentrated toward recent star-forming regions (30 Doradus and Constellation III), while CCs (age  $\sim 50 - 200$  Myr) mostly follow the bar and spiral arm of the LMC. Since HEBs, RR Lyrae stars and CCs trace different stellar populations, they serve as perfect tools to study the internal structure of this galaxy.

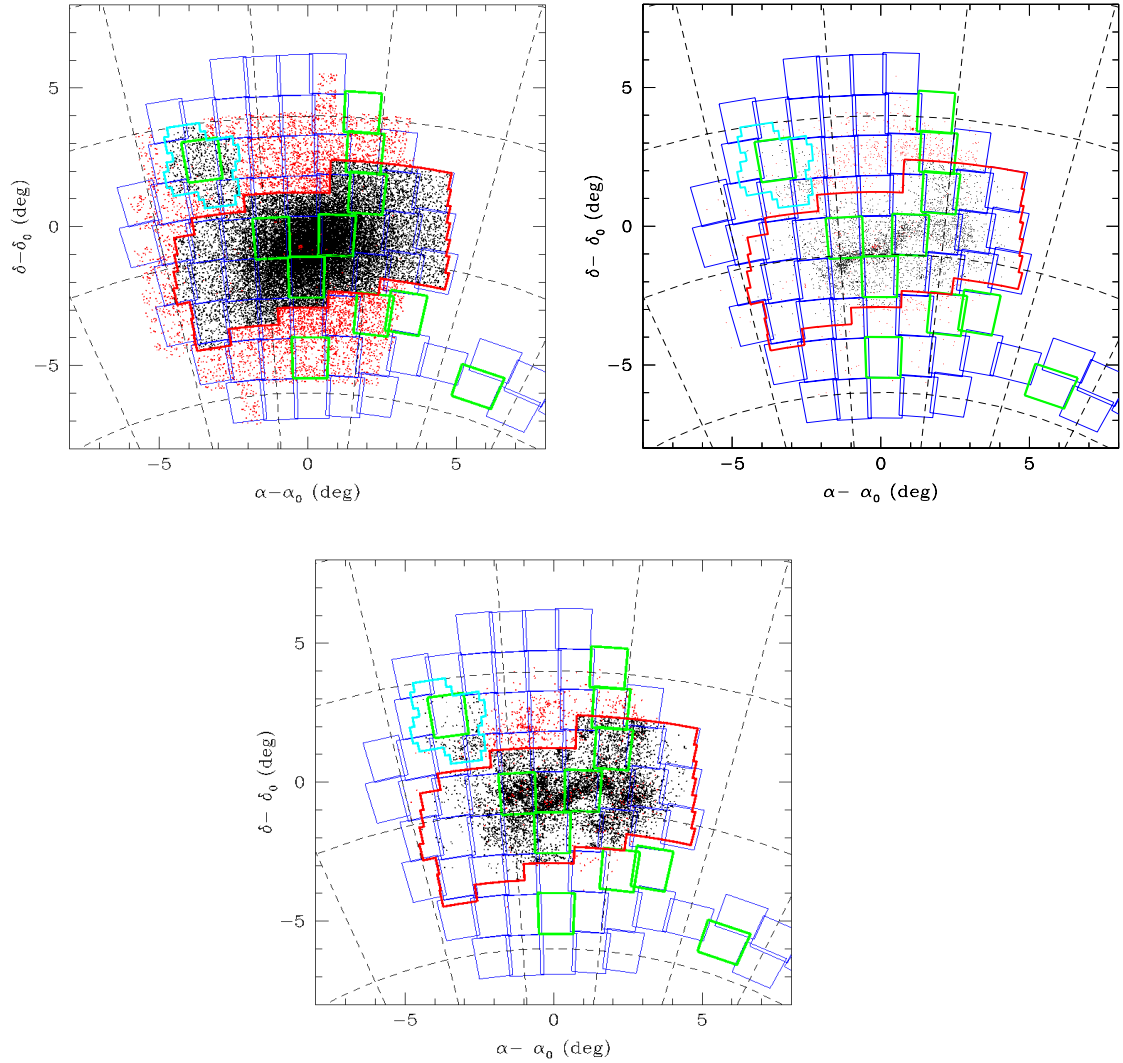


Figure 2.1 Distribution of RR Lyrae stars (upper-left), CCs (upper-right) and HEBs (central) in the LMC. Black points represent sources with OGLE data; red points are EROS-2 variables that do not have an OGLE counterpart within  $5''$ .  $\alpha_0 = 81^\circ.0$  and  $\delta_0 = 69^\circ.0$ . The sky coverage of the VMC survey (blue rectangles), OGLE III (red contour), OGLE IV (cyan contour) is shown. Green rectangles underline VMC tiles completely observed as of July 2013. Figure is from Moretti et al. (2014).

## 2.3 Distance to the LMC

The LMC is the closest large satellite of the MW and the first step of the cosmic distance ladder. The galaxy contains a large number of different distance indicators that allows its distance to be determined through many independent techniques. However, in spite of the large number of independent measurements of the last twenty years, a general consensus on the LMC distance has not been reached yet. Furthermore, when pushing distance uncertainties down to a few percent the effects of sample size, spatial distribution, depth and geometry become important and properly accounting for the LMC internal structure becomes necessary.

Figure 2.2 from Benedict et al. (2002) shows an impressive summary of the different values for the distance modulus of the LMC published during the ten years from 1992 to 2001. Values from 18.1 to 18.8 mag were reported in literature, with those less than 18.5 mag supporting the so-called “short” distance scale, and those larger than 18.5 mag, the “long” one. During the last decades dramatic progress in the calibration of the different distance indicators led the dispersion in the LMC distance modulus to shrink significantly, thus extreme values such as those listed in Benedict et al. (2002) are not very often seen in the recent literature (Clementini, 2009).

A number of analyses of the distances to the LMC as derived from different distance indicators have been performed (Gibson 2000; Benedict et al. 2002; Clementini et al. 2003; Schaefer 2008; De Grijs et al. 2014). Clementini et al. (2003) compared the LMC distances obtained from Population I and Population II indicators and showed that all distance determinations converge within  $1\sigma$  error on a distance modulus  $(m - M)_0 = 18.515 \pm 0.085$  mag. De Grijs et al. (2014) compiled 233 separate distance determinations, published from 1990 March to 2013 December, and concluded that the canonical modulus of  $(m - M)_0 = 18.49 \pm 0.09$  mag may be used for all practical purposes. These results are consistent with the recent determination of direct distances to eight long-period, late-type EBs in the LMC, which is claimed to be accurate to  $\sim 2\%$  (Pietrzyński et al., 2013). These authors found the distance to the LMC to be:  $D_{LMC} = 49.97 \pm 0.19(stat) \pm 1.11(syst)$  kpc, which corresponds to the distance modulus  $(m - M)_0 = 18.494 \pm 0.049$  mag. However, this result was called into question by Schaefer (2013) who, in addition to concerns on possible bandwagon effects, also pointed out that Pietrzyński et al. (2013) distance for the LMC differs significantly from the average distance to four hot, early-type EBs,  $D=47.1 \pm 1.4$  kpc,

published by Guinan et al. (1998), Fitzpatrick et al. (2002, 2003), and Ribas et al. (2002). Despite the large number of studies claiming to have determined independently the distance to the LMC, systematic uncertainties remain. Moreover, there were significant concerns about a possible "publication bias" affecting distances (Schaefer 2008, Rubele et al. 2012, Walker 2012). In particular, Schaefer (2008) noted that from 2002 to 2007, 31 independent papers reported new measurements of the distance of the LMC, and the new values clustered tightly around the value  $(m - M)_0 = 18.5 \pm 0.1$  mag, adopted by the *HST* Key Project on the extragalactic distance scale (Freedman et al. 2001). Schaefer (2008) considered the effects of "publication bias" to be the most likely cause of the clustering of LMC distance measurements. Improvements in the instrumentation over the past decade and a half have allowed the Cepheid distance scale to be extended well beyond the Local Group. Measurements with the *HST* FGS have provided a direct calibration via parallaxes of 10 Galactic CCs (Benedict et al., 2007). *HST* parallaxes of five RR Lyrae stars in the MW were obtained by Benedict et al. (2011). Gaia, the ESA cornerstone mission, successfully launched on December 2013, will measure parallaxes of one billion stars with unprecedented accuracy. All these facts will likely reduce the importance of the LMC as the first rung of the cosmic distance ladder. But the history shows that the systematic errors are inevitable. The famous phrase: "The Hubble Constant at any given time has always been known to 10 percent, despite having changed over the period by a factor of 10" should not be forgotten. For this reason the careful determination of the distance to the LMC is still crucially important, since this galaxy provides a sanity check of the validity of the lower rungs of the distance ladder (Walker, 2012).

This thesis work is focused on three types of distance indicators: CCs, HEBs and RR Lyrae stars. There are several reasons of this choice. Firstly, how it was discussed in Section 2.2, HEBs, CCs and RR Lyrae stars probe different stellar populations, hence, serve as perfect tools to study the internal structure of the LMC. Secondly, these three types of distance indicators follow relations which zero-points can be calibrated with fundamental geometric methods. These calibrations will be greatly improved when Gaia parallaxes will become available.

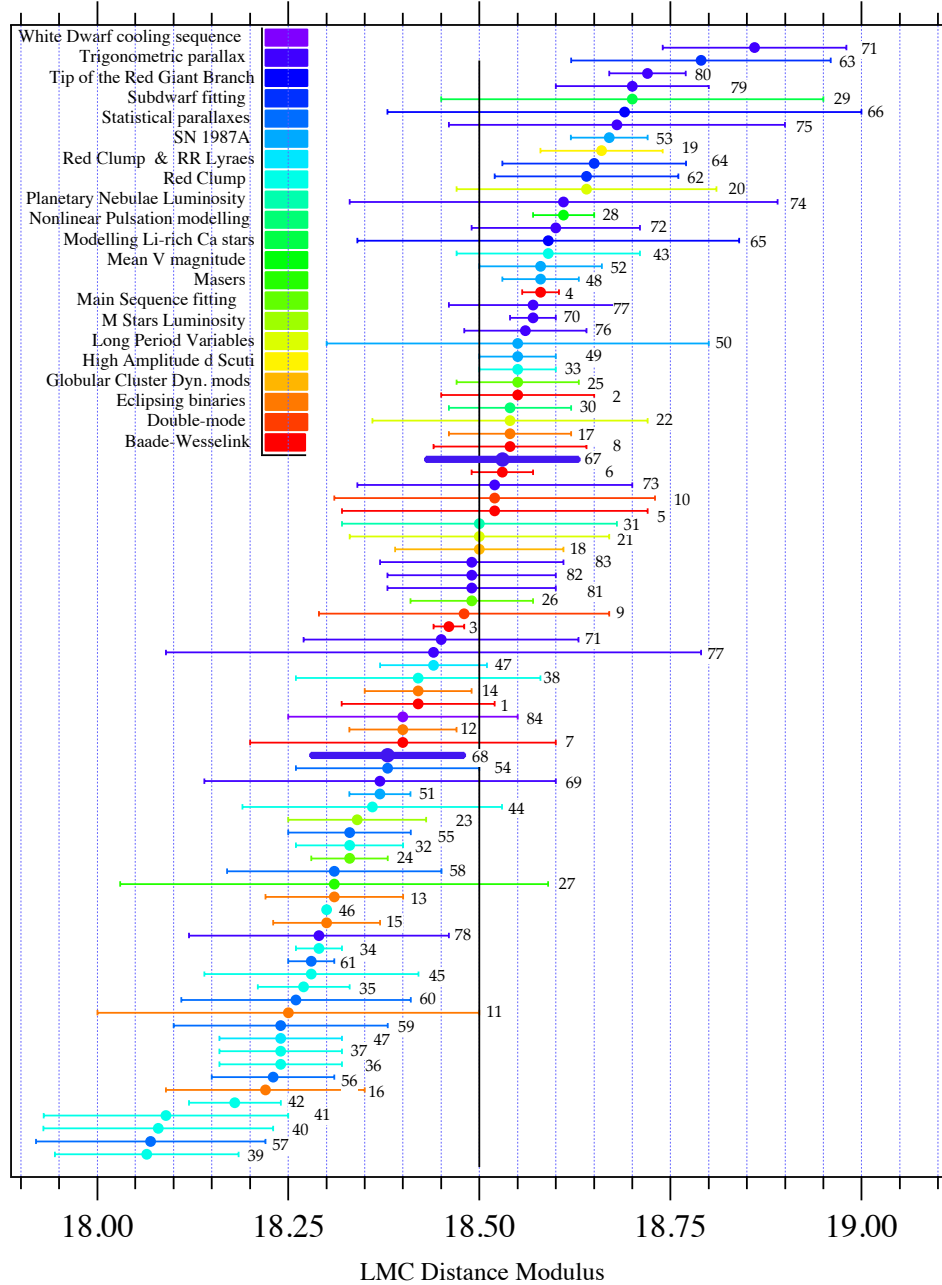


Figure 2.2 Determinations of the distance modulus of the LMC compiled by Benedict et al. (2002). Colors represent the various methods, numbers refer to individual investigations (see Table 10 in Benedict et al. 2002). The thick vertical line denotes the distance modulus adopted by the *HST* Distance Scale Key Project (Freedman et al., 2001) and the Type Ia Supernovae Calibration Team (Saha et al., 1999). Results for the distance modulus of the LMC from Benedict et al. (2002) are in bold.



## 2.4 LMC Surveys

In this thesis work we extensively use the near-infrared photometry being collected by the VMC survey (Cioni et al., 2011) and visual photometry obtained by the EROS-2, OGLE III and OGLE IV surveys.

### 2.4.1 EROS-2

EROS-2 (*Expérience pour la Recherche d'Objets Sombres*) is a microlensing survey (Tisserand et al., 2007) which monitored about 88 deg<sup>2</sup> of the LMC discovering a large number of CCs, RR Lyrae stars, binaries and LPVs, both in the centre and in the outer regions of the galaxy. The survey was carried out with the Marly 1-m telescope at ESO, La Silla, from July 1996 to February 2003. Observations were performed in two wide passbands, the so-called  $R_{EROS}$  band centered close to the  $I$  standard band, and the  $B_{EROS}$  band intermediate between the standard  $V$  and  $R$  bands. The  $B_{EROS}$  passband covers the wavelength interval from 420 to 720 nm, the  $R_{EROS}$  passband covers the interval from 620 to 920 nm. EROS magnitudes can be transformed to the Johnson-Cousins standard system to a precision of  $\sim 0.1$  mag, using the following equations from Tisserand et al. (2007):

$$R_{EROS} = I_C \quad (2.1)$$

$$B_{EROS} = V_J - 0.4(V_J - I_C) \quad (2.2)$$

The detection of variable stars and the determination of periods ( $P_{EROS}$ ) were performed by an automatic pipeline based on the Analysis of Variance (AoV) method and software developed by Beaulieu et al. (1997) and Schwarzenberg-Czerny (2003) (see Marquette et al. 2009 and references therein for further details). The left panel of Figure 2.3 shows the  $(B_{EROS}, B_{EROS} - R_{EROS})$  CMD obtained from the EROS-2 catalogue of the LMC candidate variables (red points). The candidate RR Lyrae stars were extracted by selecting in the CMD objects with  $18.46 < B_{EROS} < 20.03$  mag, and  $0.05 < B_{EROS} - R_{EROS} < 0.58$  mag (blue points).

Candidates CCs were visually selected in the  $B_{EROS}$  versus  $P_{EROS}$  diagram on the basis of the  $PL$  relation of CCs. The right panel of Fig. 2.3 shows how the selection was performed. The selected candidate CCs have EROS-2 periods in the range  $0.89 < P_{EROS} < 15.85$  days, and  $B_{EROS}$  magnitudes in the range  $13.39 < \langle B_{EROS} \rangle < 17.82$  mag. The faint magnitude/short period limit allows to reduce the contamination of the candidate CCs

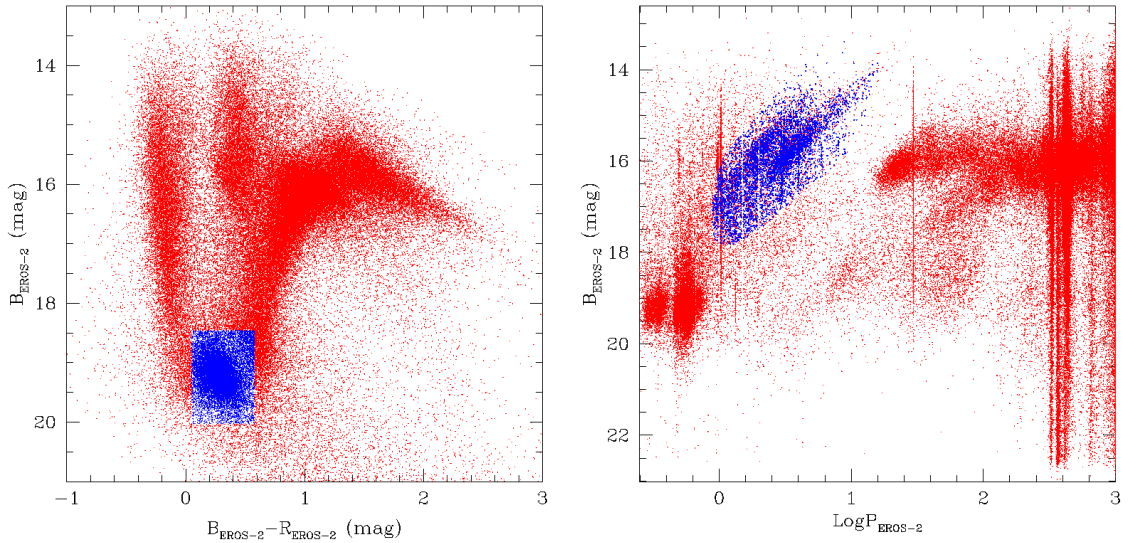


Figure 2.3 *Left panel:*  $B_{EROS}$  versus  $B_{EROS}-R_{EROS}$  CMD of LMC candidate variables from the EROS-2 data (red points). A blue box marks the region populated by the RR Lyrae candidates. *Right panel:* distribution of the EROS-2 candidate variables in the LMC (red points) in the  $\text{Log}P$  versus  $B_{EROS}$  plane. Blue points represent the candidate CCs. Figure is from Moretti et al. (2014).

by shorter period variables, such as the RR Lyrae stars, whereas the bright magnitude/long period limit reflects the bright cut of the EROS-2 data available to us.

As part of the collaboration between the VMC and EROS-2 teams,  $R_{EROS}$  and  $B_{EROS}$  time-series photometry (and related errors), periods and mean magnitudes for 5800 candidate CCs and 16337 candidate RR Lyrae stars were kindly made available to us by the EROS-2 team. We used these data in order to study the CCs (see Chapter 3) and the RR Lyrae stars (see Chapter 6) in the outer regions of the LMC. Moreover, visual inspection of the light curves of candidate CCs showed that the sample contains also a large fraction (1768) of EBs. These accidentally found EBs also became subject of this thesis research (see Chapter 4).

## 2.4.2 OGLE

The Optical Gravitational Lensing Experiment (OGLE) is a wide-field sky survey started in 1992. The main goal of this survey was to search for microlensing events (Soszyński et al. 2008, and references therein). The observing strategy of the project, originally proposed by Paczyński (1986), was the regular monitoring of brightness of about 200 million stars in the MCs and Galactic bulge, on time-scales of at least two years, in order to detect lensing

events connected with “dark halo” objects. As a byproduct, these observations provided an enormous database of photometric measurements. OGLE photometry is in the standard  $B_{Johnson}$ ,  $V_{Johnson}$  and  $I_{Cousins}$  filters.

The first phase of the project (OGLE I) started in 1992 and lasted till 1995. The 1 m Swope telescope at the Las Campanas Observatory, Chile, was used (Udalski et al., 1992). The project was very successful (Udalski et al., 1993) but it suffered from limited availability of telescope time. Therefore observations were performed only in the Galactic bulge, and the covered area on the sky was relatively small. The second phase of the project (OGLE II) was conducted between 1997 and 2000. The observations were performed with the new 1.3 m Warsaw Telescope dedicated to massive photometric surveys of dense stellar fields (Udalski et al., 1997). As a byproduct, catalogues of thousands of Cepheids, RR Lyrae stars, EBs and LPVs in the Galactic Bulge and the MCs were produced (Szymański, 2005).

The OGLE III phase started on June 2001 with the 1.3 m Warsaw telescope equipped with the new eight  $2048 \times 4096$  CCD detector mosaic camera at the Las Campanas Observatory, Chile (Udalski, 2003). OGLE III catalogues are publicly available at the OGLE website<sup>1</sup> and contain 3361 CCs (Soszyński et al., 2008), 24906 RR Lyrae stars (Soszyński et al., 2009), 26121 EBs (Graczyk et al., 2011) in the LMC and 4630 CCs (Soszyński et al., 2010a), 2475 RR Lyrae stars (Soszyński et al., 2010b) and 6138 EBs (Pawlak et al., 2013) in the SMC. For each object, the catalogues provide right ascension, declination, mean Johnson-Cousins  $V$ ,  $I$  magnitudes, period,  $I$ -band amplitude, along with the Fourier parameters  $R21$ ,  $\phi_{21}$ ,  $R31$  and  $\phi_{31}$  of the  $I$ -band light curves (Soszyński et al., 2009).

The most extended area coverage of the MS with OGLE was obtained during the third phase, however, a significant extension of the observed area is expected with OGLE IV. Nowadays, only a small region containing the LMC South Ecliptic Pole (SEP) field, observed with the OGLE IV, is publicly available. The so-called Gaia SEP (GSEP) is an area of about  $5.3 \text{ deg}^2$  around the SEP, of which a central rhombus-shaped portion of  $5 \times 0.7 \text{ deg}^2$  corresponds to the region that Gaia observed repeatedly during commissioning. The OGLE collaboration made the GSEP field data available after only two years of observations because this data could be potentially useful for the Gaia mission. The data set consists of photometry in the  $V$  and  $I$  bands for 6789 variables, with a number of data points between 338 and 351 in the  $I$  band, and about 29 epochs in the  $V$  band. The catalogue of variables in the GSEP field contains 132 CCs, 686 RR Lyrae stars, 2819 LPVs, 1377 EBs and 156

---

<sup>1</sup><http://ogle.astrouw.edu.pl/>

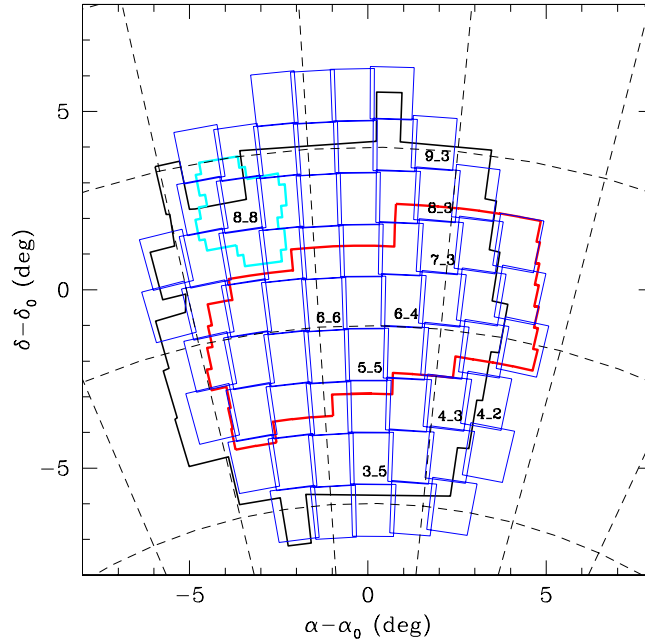


Figure 2.4 Sky coverage of the LMC for EROS-2 (black), OGLE III (red) and the first release of OGLE IV (cyan). VMC tiles are indicated in blue. Tiles already completed as of July 2013 are labelled.  $\alpha_0 = 81^\circ.0$  and  $\delta_0 = 69^\circ.0$ . Figure is from Moretti et al. (2014).

ellipsoidal variables.

The areas covered in the LMC by the EROS-2 (black), the OGLE III (red) and the first release of OGLE IV (cyan) surveys are shown in Figure 2.4. EROS-2 provided so far the largest coverage of the LMC, however, the EROS-2 team made available to us only catalogues of “candidate” CCs and RR Lyrae stars. Therefore, visual inspection of the light curves was necessary to validate the classification. Moreover, the EROS-2 observations are performed in non standard passbands. Therefore, in our study we used the OGLE III data whenever available (i.e. in the internal regions of the LMC), and the EROS-2 data in the outer regions of the galaxy.

### 2.4.3 VMC

The *VISTA for Magellanic Clouds* near-infrared survey (Cioni et al., 2011) started in November 2009 and is expected to extend beyond the originally planned  $\sim 5$  years time span. The main purpose of this survey is to study of the star formation history (SFH) and the 3D structure of the MS using both constant and variable stars. The strategy, main goals and first data were presented in Cioni et al. (2011), first results for pulsating variables, based on the VMC

$K_s$ -band light curves, were described in Ripepi et al. (2012) for CCs in the LMC, Ripepi et al. (2014a) for LMC Anomalous Cepheids (ACs), and Ripepi et al. (2014b, accepted to MNRAS) for Type II Cepheids in the LMC. In Moretti et al. (2014) we present the strategy of using CCs, RR Lyrae stars and EBs observed by VMC to study the LMC's structure. Muraveva et al. (2014a) used the VMC data to study the  $PL$  relations of the LMC EBs.

The VMC survey is observing  $\sim 200 \text{ deg}^2$  of the MS in the  $Y$ ,  $J$ ,  $K_s$  ( $\lambda = 1.02, 1.25$  and  $2.15 \mu\text{m}$ , respectively) passbands reaching a sensitivity limit on the stacked images close to Vega magnitudes  $Y = 21.1$  mag,  $J = 21.3$  and  $K_s = 20.7$  mag with a signal-to-noise ratio  $S/N = 10$ . The survey covers the LMC area ( $116 \text{ deg}^2$ ) with 68 tiles, the SMC ( $45 \text{ deg}^2$ ) with 27 tiles and the Bridge area ( $20 \text{ deg}^2$ ) with 13 tiles. Two additional tiles cover  $3 \text{ deg}^2$  in the Stream. The VMC  $K_s$ -band are taken over 12 separate epochs (Cioni et al., 2011), each epoch reaches a limiting magnitude of  $K_s \sim 19.3$  mag with a  $S/N \sim 5$ . This limit allows us to detect the minimum light of RR Lyrae stars in both the LMC and SMC. For bright stars, the VMC survey is limited by saturation at  $K_s \sim 11.4$  mag. The VMC images are processed by the Cambridge Astronomical Survey Unit (CASU) through the VISTA Data Flow System (VDFS) pipeline. The reduced data are then sent to the Wide Field Astronomy Unit (WFAU) in Edinburgh where the single epochs are stacked and catalogued by the VISTA Science Archive (VSA; Lewis et al. 2010, Cross et al. 2012).

The VMC coverage of the LMC is shown in Fig. 2.4 (blue) from Moretti et al. (2014). Tiles which were completely observed (12 epochs) as of July 2013, are labelled. One additional LMC tile (tile 6\_8) was completed after July 2013. The data for five LMC tiles (namely tiles 8\_8, 8\_3, 6\_6, 6\_4 and 5\_5) are now publicly available.

The time sampling of the VMC survey along with the significantly reduced amplitude of the light variation in the  $K_s$  band allows us to derive mean  $K_s$  magnitudes with a great precision (Ripepi et al. 2012, Ripepi et al. 2014a) but we have to rely in our research on variable star catalogues from the optical microlensing surveys for the identification, coordinates and pulsation properties, such as the period, epoch of maximum light and parameters of the Fourier decomposition of the visual light curves (Moretti et al., 2014).



## Chapter 3

# Classical Cepheids in the VMC tile LMC 8\_3

There are 11 tiles in the LMC that the VMC survey (Cioni et al., 2011) has completely observed (12 epochs in the  $K_s$  band) as of October 2014. In this thesis we have analysed the CCs in tile LMC 8\_3, the RR Lyrae stars in tiles LMC 8\_3 and 5\_5, and the HEBs in all LMC tiles, for which  $K_s$  data were available as of January 2014.

In this chapter we present results from the analysis of the EROS-2 candidate CCs located in the LMC outer tile 8\_3. The analysis of this tile was particularly useful to develop the methods for the classification of candidate CCs from the EROS-2 catalogue. The lower portion of tile LMC 8\_3 is covered also by the OGLE III survey (Fig. 2.4), making it possible a direct comparison between the EROS-2 and OGLE III results. Periods, epochs of maximum light, etc. derived in our analysis will be combined with the near-infrared data from the VMC survey to determine the distance to tile LMC 8\_3 from CCs.

### 3.1 EROS-2 data for candidate Classical Cepheids

The EROS-2 team provided us the catalogue and individual light curves in the  $B_{EROS}$  and the  $R_{EROS}$  passbands for 5800 candidate CCs in the LMC. Among them we selected objects which are located in tile LMC 8\_3. The coordinates of the center of the tile are: RA =  $05^h : 04^m : 53.952^s$ , DEC =  $-66^\circ : 15' : 29.880''$  (Cioni et al., 2011), the rotator angle is  $-97.2489$  deg. In order to extract objects located in this tile from the EROS-2 catalogue and study the completeness of the EROS-2 catalogue with respect to the VMC catalogue we performed the following steps:

- We selected on the VISTA Science Archive website<sup>1</sup> all sources located in tile LMC 8\_3 (1024384 objects). This procedure set the range of coordinates (RA and DEC) to use for extracting objects covering exactly the same area of the EROS-2 catalogue.
- We converted the RA and DEC coordinates of these objects to Cartesian (X and Y) coordinates using the center of the tile as a reference.
- We calculated new X1 and Y1 coordinates by rotating the reference system such as:

$$X1 = X \cos(90 - \alpha) - Y \sin(90 - \alpha) \quad (3.1)$$

$$Y1 = X \sin(90 - \alpha) + Y \cos(90 - \alpha) \quad (3.2)$$

where  $\alpha$  is the rotator angle

- By plotting the new X1 and Y1 coordinates we derived a straight-looking tile in which we were able to determine the range covered in each coordinate.
- We applied the same procedure to the EROS-2 catalogue. We converted the RA and DEC coordinates of the candidate CCs from the EROS-2 catalogue to the Cartesian (X and Y) coordinates using the center of tile LMC 8\_3 as a reference. Then we determined new X1 and Y1 coordinates of the objects by rotating the reference system (equation 3.1, 3.2). When both catalogues were in the same system we were able to extract objects from the EROS-2 catalogue which are located in the area of the VMC tile LMC 8\_3 by using the range of coordinates determined as described above.

By applying the described procedure we extracted 201 candidate CCs located in tile LMC 8\_3, 200 of them have counterparts in the VMC catalogue within a pairing radius of 1 arcsec. The counterpart of one object (EROS-2 id: lm0310k4094) was found within a pairing radius of 1.2 arcsec. The comparison of the  $K_s$  and EROS-2 optical light curves confirms the star counteridentification.

We analysed the EROS-2 light curves of the 201 candidate CCs with the GRaphical Analyser of TIme Series (GRATIS) software developed at the Bologna Observatory by P. Montegriffo (see, e.g., Clementini et al. 2000), and derived  $B_{EROS}$  and  $R_{EROS}$  mean magnitudes, amplitudes and epochs of maximum light in the  $B_{EROS}$  passband for each object. The results of our analysis are presented in Table 3.1. We corrected the period for 16 stars, since the EROS-2 catalogue provided aliases of the actual periods.

---

<sup>1</sup><http://horus.roe.ac.uk/vsa/>



EROS-2 id	RA (deg)	DEC (deg)	Period (day)	$\langle B_{EROS} \rangle$ (mag)	$Amp(B)$ (mag)	Epoch(max) $B_{EROS}$	$\langle R_{EROS} \rangle$ (mag)	$Amp(R)$ (mag)	Colour (mag)	Type
Im0444112369 <sup>a</sup>	77.70978	-65.78912	0.664995	17.27	0.27	2451189.6194	16.99	0.20	0.28	cAC
Im0435n13603 <sup>a</sup>	77.70995	-65.78915	0.664997	17.12	0.26	2451556.6837	16.88	0.18	0.24	cAC
Im0293126069	74.96489	-66.90412	0.897376	16.99	0.27	2452334.5608	16.71	0.18	0.28	cc
Im0301n2028	77.12442	-66.53385	0.904527	17.13	0.08	2452305.6537	17.30	0.08	-0.17	sm.am
Im0436n21036	76.81620	-66.20443	0.944593	17.01	0.57	2451126.7584	17.28	0.54	-0.27	bin
Im0300123623	75.51875	-66.56687	0.954923	16.55	0.30	2451901.7383	16.29	0.21	0.26	cc
Im0437k13766	77.15688	-65.99865	0.964389	16.97	0.25	2451533.6376	16.67	0.18	0.30	cc
Im0436m10069	76.66067	-65.98062	0.966700	16.49	0.42	2451476.6642	16.72	0.41	-0.22	bin
Im0437m21444	77.68774	-66.05287	0.985099	16.88	0.26	2450332.8638	16.61	0.19	0.27	cc
Im0312111935	77.43583	-66.83433	0.987896	16.55	0.28	2451100.6816	14.77	0.18	1.78	lpv
Im0427n12788	76.05393	-66.15369	1.024246	17.68	0.25	2451454.8722	17.80	0.22	-0.13	bin
Im030018578	75.76346	-66.45715	1.027220	16.13	0.03	2452551.6960	14.97	0.02	1.16	lpv
Im0424n14561	74.91334	-65.80545	1.047235	16.51	0.34	2450342.8891	16.79	0.34	-0.28	bin
Im0426n23242	75.02346	-66.21718	1.047365	16.42	0.36	2451482.6228	16.75	0.34	-0.33	bin
Im0303n15295	77.03270	-66.83695	1.069503	17.39	0.08	2451060.8754	17.71	0.07	-0.31	sm.am
Im0427k19766	75.27864	-66.05269	1.075378	16.68	0.47	2451182.6872	16.40	0.34	0.28	cc
Im0310k4550	77.55931	-66.27774	1.085795	16.68	0.33	2451889.6271	16.43	0.24	0.25	cc
Im0301m26336	76.87621	-66.41165	1.090782	17.63	0.12	2452239.5837	17.78	0.15	-0.15	bin
Im0425n26027	75.74082	-65.87874	1.090849	17.78	0.44	2451510.5912	17.92	0.44	-0.15	bin
Im0437k16072	77.24041	-66.01471	1.104245	15.95	0.07	2451830.7454	16.20	0.08	-0.24	sm.am
Im0293k19788	74.66297	-66.71494	1.117755	16.09	0.03	2451716.9260	16.32	0.03	-0.24	sm.am
Im0310k15114	77.52638	-66.35164	1.132918	17.56	0.50	2451645.5360	17.76	0.50	-0.20	bin
Im0301m13696	76.88649	-66.32851	1.160762	16.59	0.30	2451472.6559	16.30	0.21	0.29	cc
Im0426m23482 <sup>a</sup>	75.07795	-66.06284	1.172787	14.87	0.11	2450418.6526	15.22	0.10	-0.34	sm.am
Im0437n8267	77.38103	-66.11499	1.176646	17.39	0.24	2451623.5636	17.54	0.23	-0.16	bin
Im0303123428	76.80088	-66.88609	1.183669	17.50	0.73	2450855.6128	17.72	0.69	-0.22	bin
Im0312k15523	77.48035	-66.73194	1.188117	17.55	0.21	2451772.8507	17.53	0.18	0.02	bin
Im0310k4094	77.31567	-66.27462	1.212514	16.76	0.34	2451266.5345	16.44	0.24	0.32	cc
Im0302n12595	76.32740	-66.83223	1.213151	16.89	0.21	2452535.7713	17.18	0.15	-0.29	bin
Im0303n10523	77.20164	-66.80712	1.246321	17.54	0.44	2451502.6255	17.88	0.44	-0.34	bin

3.1. EROS-2 DATA FOR CANDIDATE CLASSICAL CEPHEIDS

lm0302113504	75.71178	-66.84312	1.261500	16.43	0.35	2451224.6080	16.16	0.25	0.27	cc
lm0436k8952	76.36602	-65.96754	1.275596	17.70	0.17	2450784.8308	17.83	0.14	-0.14	bin
lm0437n9267	77.58030	-66.12241	1.280097	16.48	0.21	2451497.7142	16.15	0.15	0.32	cc
lm0293114089	74.99618	-66.83478	1.292040	17.49	0.11	2450317.8596	17.74	0.11	-0.26	bin
lm0291m5905	75.36189	-66.27604	1.303899	16.32	0.40	2451252.5425	16.14	0.27	0.18	cc
lm0293n4438	75.10326	-66.77718	1.315011	17.56	0.09	2451156.7885	17.82	0.08	-0.26	sm.am
lm0426m6757	75.10942	-65.94266	1.372785	16.36	0.14	2451564.5990	16.60	0.12	-0.24	bin
lm0427k7569	75.48319	-65.95961	1.423526	16.32	0.58	2452008.5146	16.59	0.54	-0.27	bin
lm0436m20675 <sup>e</sup>	76.55530	-66.06799	122.445500	16.31	0.51	2450226.7490	14.13	0.28	2.18	lpv
lm0300k22331	75.89590	-66.40058	1.481380	17.66	0.34	2451353.9049	17.92	0.36	-0.26	bin
lm0300k23233	75.71698	-66.40716	1.528732	15.59	0.22	2450351.8972	15.52	0.18	0.08	cc
lm0426m22620	75.07370	-66.21255	1.529313	16.12	0.10	2450425.7808	16.44	0.10	-0.32	bin
lm0427m21459	75.79042	-66.06479	1.546547	16.67	0.30	2450372.7347	17.01	0.29	-0.33	bin
lm0301k12039	76.77238	-66.32046	1.550058	15.87	0.43	2451934.6566	15.61	0.29	0.26	cc
lm0424n15978 <sup>ab</sup>	75.18656	-65.81469	1.560930	16.64	0.27	2451479.6292	16.41	0.21	0.23	cc
lm0434m21038	76.54471	-65.69327	1.585547	16.08	0.12	2450404.7845	16.33	0.12	-0.25	bin
lm043515752	77.27269	-65.73683	1.597033	17.58	0.56	2451623.5636	17.75	0.54	-0.17	bin
lm0305k4072	76.49398	-66.97811	1.619923	17.16	0.05	2451149.6403	17.29	0.05	-0.13	sm.am
lm0425n15511	75.65717	-65.80273	1.623384	17.47	0.26	2451627.5233	17.69	0.25	-0.23	bin
lm0424n10133	74.97782	-65.77246	1.635390	16.06	0.13	2450498.6499	16.32	0.11	-0.25	bin
lm0427m4029	75.90082	-65.92882	1.636300	16.06	0.28	2451784.7345	15.77	0.19	0.29	cc
lm0302n26730	76.23651	-66.94132	1.663945	16.35	0.26	2451212.7016	16.04	0.19	0.31	cc
lm0291111728	74.96100	-66.46981	1.670662	16.88	0.30	2451895.7390	16.51	0.22	0.37	cc
lm0303m16963	77.03760	-66.69697	1.702557	16.08	0.20	2452604.7622	15.90	0.14	0.18	cc
lm0301m21301	76.94809	-66.37804	1.709915	16.04	0.18	2451511.6292	15.71	0.12	0.33	cc
lm0303k5608	76.52968	-66.63034	1.727237	16.67	0.63	2451642.4916	16.41	0.45	0.26	cc
lm0291k20831	74.80414	-66.37847	1.739627	16.13	0.34	2452245.6216	15.71	0.23	0.42	cc
lm0436114585	76.42263	-66.15917	1.756971	15.73	0.23	2451830.7454	16.11	0.26	-0.38	bin
lm0293k16840	74.64961	-66.69823	1.772508	15.86	0.36	2451553.6111	15.61	0.24	0.26	cc
lm0303k13861	76.76351	-66.67879	1.772845	17.01	0.10	2450351.8972	17.20	0.10	-0.19	bin
lm0291m21869	75.07896	-66.38380	1.774816	17.21	0.70	2452304.6717	17.40	0.68	-0.19	bin
lm0303119680	76.45461	-66.86658	1.793979	15.71	0.36	2451224.6080	15.51	0.25	0.19	cc
lm0291n7436 <sup>a</sup>	75.25535	-66.44051	1.794205	16.14	0.26	2450826.6293	15.77	0.18	0.36	cc

lm0300k5450	75.84331	-66.28245	1.801747	15.72	0.08	2452084.8991	16.05	0.07	-0.33	bin
lm0435n21894	77.62752	-65.84829	1.801802	15.92	0.32	2451878.6366	15.65	0.23	0.27	cc
lm0434n10152	76.50705	-65.77485	1.814666	15.79	0.37	2452609.6783	15.52	0.26	0.27	cc
lm0301m24570	76.85416	-66.39999	1.821526	15.75	0.37	2451577.6660	15.43	0.26	0.32	cc
lm0303n17856	76.92380	-66.85285	1.827710	16.23	0.12	2451257.5461	16.54	0.11	-0.31	bin
lm0424m15104	75.12583	-65.64843	1.861021	15.84	0.07	2451830.7142	16.11	0.07	-0.27	bin
lm0310k15527	77.59890	-66.40988	1.872873	15.70	0.26	2450424.8331	15.41	0.17	0.29	cc
lm0291i25349	74.75174	-66.55471	1.874248	16.86	0.12	2451826.7130	16.93	0.12	-0.07	bin
lm0310i18848	77.46563	-66.53873	1.894299	15.78	0.33	2450755.7254	15.44	0.23	0.34	cc
lm0293i23982	74.83080	-66.89299	1.898197	15.82	0.34	2451246.5900	15.56	0.24	0.26	cc
lm0312k16300 <sup>a</sup>	77.37623	-66.73736	1.906900	15.83	0.34	2451178.8033	15.46	0.25	0.37	cc
lm0424n24516	75.05272	-65.88275	1.915386	15.39	0.08	2451497.6153	15.71	0.11	-0.33	bin
lm0301i22532	76.46532	-66.54366	1.925101	15.93	0.54	2452265.6419	16.13	0.52	-0.20	bin
lm0291m14452	75.27195	-66.33402	1.928768	15.75	0.22	2451555.5911	15.48	0.15	0.26	cc
lm0300m12894	76.18996	-66.33030	1.944191	15.68	0.19	2451830.7320	15.48	0.14	0.20	cc
lm0437m15752 <sup>a</sup>	77.72249	-66.00990	1.966639	15.91	0.25	2450376.7445	15.60	0.16	0.31	cc
lm0446k15142 <sup>a</sup>	77.72235	-66.00991	1.966645	16.00	0.25	2451556.6964	15.62	0.17	0.38	cc
lm0303n13787	76.83778	-66.82972	1.966780	15.86	0.22	2452129.8190	15.66	0.15	0.21	cc
lm0302i5812 <sup>a</sup>	75.80726	-66.79176	1.988660	15.70	0.36	2450835.6299	15.42	0.25	0.28	cc
lm0301i21365	76.63322	-66.53518	2.066042	15.70	0.40	2452183.7002	15.37	0.28	0.33	cc
lm0303i22257 <sup>a</sup>	76.40139	-66.88160	2.078516	15.62	0.30	2451655.5189	15.43	0.21	0.19	cc
lm0302i16660	75.60709	-66.86448	2.085372	15.69	0.24	2451006.9442	15.53	0.17	0.16	cc
lm0293k2961	75.03127	-66.61400	2.095923	15.56	0.37	2451889.5940	15.32	0.26	0.24	cc
lm0435i25960	77.21729	-65.87469	2.190691	15.42	0.08	2450389.8044	15.70	0.07	-0.28	sm.am
lm0300m25571	76.14499	-66.41666	2.200747	15.61	0.20	2452257.6065	15.92	0.20	-0.31	bin
lm0310k10813	77.43635	-66.42755	2.211064	15.75	0.27	2450879.5695	15.37	0.19	0.37	cc
lm0303n12403	76.83486	-66.82148	2.234478	16.42	0.34	2451551.6410	16.69	0.35	-0.27	bin
lm0301n9832	76.87818	-66.45832	2.242879	15.96	0.11	2451169.7140	16.10	0.11	-0.14	bin
lm0300m17427	76.20188	-66.36094	2.280384	15.56	0.27	2452683.7579	15.31	0.19	0.25	cc
lm0305m2711	76.87207	-66.96614	2.357607	15.88	0.87	2452355.5595	15.64	0.61	0.23	cc
lm0303k12257	76.79103	-66.66880	2.368192	15.47	0.32	2450369.8289	15.28	0.22	0.19	cc
lm0310k19198	77.38119	-66.38092	2.382246	16.07	0.73	2451790.8087	15.72	0.51	0.35	cc
lm0427m16915	76.03440	-66.02195	2.382868	17.09	0.33	2451447.7508	17.41	0.31	-0.32	bin

3.1. EROS-2 DATA FOR CANDIDATE CLASSICAL CEPHEIDS

lm0437m9268	77.33703	-65.96636	2.392800	15.04	0.11	2451339.9372	15.29	0.10	-0.25	sm.am
lm0435k10984	76.95992	-65.62475	2.467624	16.05	0.66	2452304.7042	15.69	0.48	0.36	cc
lm0427l10110	75.28292	-66.13402	2.489254	16.49	0.28	2451467.6728	16.75	0.31	-0.26	bin
lm0303m21604	76.86080	-66.72639	2.507010	15.95	0.12	2451257.5461	16.29	0.13	-0.34	bin
lm0291k18618	74.73526	-66.36418	2.518067	16.19	0.72	2452297.6552	15.76	0.51	0.43	cc
lm0291k11979	74.84301	-66.31999	2.531380	15.70	0.18	2452337.5554	15.28	0.12	0.42	cc
lm0434l15605	76.10665	-65.82192	2.546594	15.51	0.28	2451627.5374	15.19	0.19	0.32	cc
lm0312k9715	77.36394	-66.66809	2.565057	15.49	0.33	2450788.8490	15.08	0.24	0.41	cc
lm0427m16528	75.77647	-66.02178	2.608226	16.01	0.26	2451793.7228	16.31	0.26	-0.30	bin
lm0425n8591	75.93291	-65.75266	2.615299	15.95	0.67	2450435.7555	15.67	0.48	0.28	cc
lm0303n16128	76.82415	-66.84364	2.621196	16.76	0.50	2450845.7351	17.02	0.49	-0.26	bin
lm0300m26009	76.26200	-66.41913	2.682304	15.87	0.95	2452242.5651	15.63	0.67	0.24	cc
lm0301k12078	76.60772	-66.32178	2.684560	15.68	0.42	2451078.7631	15.39	0.29	0.29	cc
lm0305m11940	77.00428	-67.02136	2.694819	15.82	0.93	2451948.6978	15.59	0.67	0.23	cc
lm0435l7382	76.91829	-65.75014	2.697293	15.81	0.97	2451124.7468	15.49	0.69	0.32	cc
lm0434k9723	76.26202	-65.61995	2.701297	15.95	0.72	2450410.8229	15.59	0.53	0.37	cc
lm0291l5438	74.86958	-66.43047	2.703680	15.75	0.60	2450781.6213	15.83	0.60	-0.07	bin
lm0310k17708	77.45565	-66.37042	2.736883	16.10	0.68	2451201.6079	15.70	0.49	0.40	cc
lm0427l9939	75.46303	-66.13154	2.771489	16.20	0.57	2451897.7396	15.88	0.46	0.32	cc
lm0427k15685	75.52656	-66.07629	2.791595	15.55	0.11	2451398.8270	15.87	0.12	-0.32	bin
lm0310l19242	77.47706	-66.54207	2.810024	16.05	0.64	2451886.6343	15.65	0.46	0.41	cc
lm0305k7040	76.52476	-66.99542	2.861740	15.98	0.51	2451571.6250	15.59	0.37	0.39	cc
lm0424n23353	75.09632	-65.86689	2.869312	14.65	0.28	2450396.7221	15.04	0.32	-0.38	bin
lm0303l6182	76.49645	-66.78740	2.894713	15.73	0.89	2450419.5964	15.49	0.59	0.24	cc
lm0427n7395	75.99907	-66.10706	2.899146	15.94	0.66	2451606.5799	15.62	0.46	0.32	cc
lm0300k8884	75.75457	-66.30696	2.921834	16.61	0.31	2450812.8682	16.89	0.26	-0.28	bin
lm0426n17949	75.10564	-66.17679	2.924628	16.23	0.11	2451872.6350	16.54	0.11	-0.31	bin
lm0303m5318	76.92088	-66.62704	2.926082	16.82	0.31	2451920.6912	17.10	0.29	-0.27	bin
lm0303k20577	76.65658	-66.71908	2.931312	15.93	0.61	2451082.8328	15.62	0.44	0.30	cc
lm0435n9522	77.67406	-65.76091	2.933944	15.85	0.52	2450410.8229	15.54	0.36	0.31	cc
lm0303m5774	76.98484	-66.62924	2.957616	15.71	0.63	2450776.7430	15.53	0.43	0.18	cc
lm0437l12785	77.28106	-66.15555	2.963888	15.96	0.66	2451625.5553	15.59	0.48	0.37	cc
lm0436n18193 <sup>a</sup>	76.75575	-66.18253	3.000081	15.81	0.81	2450321.5772	15.50	0.58	0.32	cc

lm0426m22458 <sup>a</sup>	74.99331	-66.21124	3.001172	15.87	0.72	2451786.7259	15.56	0.39	0.31	cc
lm0291k2974	74.83436	-66.32026	3.048863	16.01	0.71	2451455.7233	15.42	0.46	0.59	cc
lm043717188	76.93822	-66.10915	3.062278	15.94	0.63	2451317.4928	15.54	0.44	0.41	cc
lm031019678	77.44955	-66.59607	3.090273	15.03	0.22	2452247.8307	14.68	0.15	0.35	cc
lm0435k16509	77.18997	-65.66115	3.091422	15.79	0.54	2451329.4786	15.46	0.41	0.33	cc
lm0300m5551	76.01798	-66.27971	3.095440	15.87	0.60	2451595.6926	15.60	0.43	0.26	cc
lm0303k8191	76.57712	-66.64572	3.113387	15.83	0.69	2451905.7471	15.56	0.49	0.27	cc
lm030118214	76.58141	-66.59655	3.123158	15.91	0.66	2450800.6827	15.47	0.47	0.43	cc
lm0291m22215	75.07876	-66.42292	3.127545	15.81	0.65	2452495.8137	15.43	0.46	0.39	cc
lm043617972	76.30773	-66.10797	3.128903	15.73	0.79	2452001.5552	15.36	0.56	0.36	cc
lm0436120924	76.07118	-66.20891	3.140133	16.11	0.45	2452681.7447	15.70	0.30	0.41	cc
lm0300k13081	75.73368	-66.33645	3.148857	15.87	0.32	2451577.6660	15.53	0.23	0.34	cc
lm0427n17676	75.68183	-66.19575	3.167981	15.76	0.82	2452466.8817	15.45	0.58	0.31	cc
lm0301n16049	76.80537	-66.49814	3.186794	15.29	0.31	2451075.8463	14.92	0.23	0.37	cc
lm030019883	75.66061	-66.46650	3.188358	16.00	0.33	2451110.7609	15.58	0.24	0.42	cc
lm0303k19341	76.73629	-66.71116	3.193448	15.70	0.75	2451756.8603	15.47	0.54	0.23	cc
lm0434k24315	76.44897	-65.72779	3.207143	15.75	0.75	2451342.9380	15.38	0.54	0.37	cc
lm0444k21188	77.72476	-65.69096	3.245950	15.94	0.62	2451583.6756	15.56	0.45	0.38	cc
lm0301n14422	76.95364	-66.48692	3.264528	15.70	0.77	2451125.6284	15.34	0.54	0.36	cc
lm0435k20023	77.25556	-65.68476	3.281595	16.68	0.19	2450372.7607	16.90	0.22	-0.22	bin
lm0435n13778	77.56030	-65.79180	3.286657	15.70	0.69	2452582.6299	15.39	0.48	0.31	cc
lm0436119007	76.28093	-66.19386	3.301123	14.96	0.05	2452240.5754	15.26	0.05	-0.30	bin
lm0437k16586	76.91184	-66.02031	3.327489	16.01	0.48	2451901.7472	15.59	0.34	0.42	cc
lm0301k17513	76.71701	-66.35814	3.328361	16.01	0.57	2451763.8941	15.66	0.42	0.35	cc
lm0300m8010	76.02162	-66.29691	3.377967	15.87	0.45	2451575.6628	15.55	0.32	0.32	cc
lm0301m6025	76.83190	-66.27650	3.412130	15.75	0.80	2451491.6430	15.43	0.56	0.32	cc
lm0424m26545	75.06331	-65.72738	3.509444	15.69	0.83	2451908.7288	15.35	0.59	0.34	cc
lm0310118849	77.55575	-66.58347	3.518785	15.75	0.68	2451067.7701	15.33	0.49	0.41	cc
lm0435124878	76.91970	-65.86900	3.540739	15.76	0.66	2452605.7595	15.37	0.47	0.39	cc
lm0436k11123	76.42184	-65.98504	3.599299	15.69	0.61	2451951.6654	15.35	0.43	0.34	cc
lm0435111832	77.26535	-65.77816	3.630186	15.85	0.30	2452096.8743	15.45	0.22	0.41	cc
lm0303124720	76.71642	-66.89406	3.630665	16.40	0.05	2451920.6912	16.62	0.05	-0.22	sm.am
lm0425n18874	75.93826	-65.82298	3.649476	15.65	0.83	2452315.6312	15.35	0.59	0.30	cc

3.1. EROS-2 DATA FOR CANDIDATE CLASSICAL CEPHEIDS

lm0303m26388 <sup>b</sup>	77.09012	-66.75258	3.700482	15.38	0.31	2451116.8084	15.23	0.23	0.15	cc
lm0300k15119	75.64848	-66.35089	3.705800	15.73	0.42	2451153.6115	15.35	0.31	0.38	cc
lm0427l7011	75.43113	-66.10621	3.735044	15.53	0.79	2452259.5869	15.19	0.55	0.35	cc
lm0291l4891	75.00036	-66.42614	3.751829	15.15	0.51	2450838.6385	15.43	0.50	-0.27	bin
lm0303m3523	76.86127	-66.61622	3.756494	15.62	0.54	2450879.5630	15.37	0.38	0.25	cc
lm0302k15867	75.65471	-66.74975	3.832809	15.50	0.73	2451255.5600	15.13	0.53	0.38	cc
lm0437m3722	77.52490	-65.92443	3.893687	15.69	0.32	2451595.7028	15.31	0.23	0.38	cc
lm0436k13349	76.23076	-66.00337	3.916362	15.67	0.61	2451761.8185	15.27	0.44	0.40	cc
lm0437l14075	77.20916	-66.16578	3.965000	15.70	0.47	2451306.5146	15.28	0.33	0.41	cc
lm0303n19840	77.19733	-66.86188	3.968168	15.53	0.72	2450532.5716	15.31	0.51	0.22	cc
lm0437n18565	77.68727	-66.20216	3.972664	15.76	0.66	2450763.7960	15.42	0.47	0.35	cc
lm0300m22019	75.95469	-66.39246	3.986529	16.34	0.44	2451468.6174	16.62	0.46	-0.28	bin
lm0303n11462 <sup>a</sup>	76.84417	-66.81567	4.003414	15.55	0.53	2452582.6163	15.26	0.37	0.29	cc
lm0435m21088	77.42768	-65.68669	4.050212	15.60	0.42	2451833.7398	15.20	0.31	0.40	cc
lm0303n14110	76.82339	-66.83168	4.240275	15.54	0.60	2451125.6284	15.26	0.42	0.28	cc
lm0436n21775	76.61175	-66.21120	4.325470	15.45	0.33	2451246.6277	15.15	0.28	0.30	cc
lm0436l17465	76.05097	-66.23806	4.377315	14.71	0.12	2452327.6169	15.00	0.13	-0.29	sm.am
lm0310k19077	77.57698	-66.37977	4.390880	15.48	0.47	2450369.8365	15.06	0.34	0.41	cc
lm0303n19424	77.05204	-66.86078	4.460733	15.46	0.65	2451844.7158	15.20	0.45	0.26	cc
lm0300n18729	76.09649	-66.52527	4.484193	15.63	0.38	2451563.6306	15.24	0.27	0.40	cc
lm0301n21884	76.82732	-66.58124	4.508161	15.43	0.66	2450855.6128	14.99	0.47	0.44	cc
lm0300k14043	75.59119	-66.34340	4.605099	15.49	0.55	2452207.5989	15.13	0.39	0.36	cc
lm0436n22963	76.56901	-66.22040	4.662191	15.44	0.71	2451899.7779	15.06	0.49	0.38	cc
lm0436k16816	76.18391	-66.03049	4.751419	15.46	0.25	2450756.7592	15.03	0.18	0.42	cc
lm0427l12767	75.27200	-66.15544	4.805932	15.88	0.13	2451815.7447	16.15	0.13	-0.27	bin
lm0425n14050	76.03249	-65.78951	4.819204	15.36	0.39	2450846.7634	15.03	0.28	0.33	cc
lm0436n23124	76.82989	-66.22073	4.871080	15.47	0.67	2451492.6289	15.10	0.48	0.37	cc
lm0426n23478	75.18067	-66.21849	4.936644	16.27	0.10	2451751.9015	16.24	0.09	0.04	sm.am
lm0427k13855	75.55629	-66.00605	5.016469	15.64	0.45	2451948.6800	15.89	0.43	-0.25	bin
lm0427k7505	75.42766	-65.95939	5.122964	15.17	0.11	2452355.5460	15.44	0.13	-0.27	bin
lm0427m13697	75.89942	-66.07558	5.606188	15.08	0.59	2451510.5912	14.76	0.41	0.33	cc
lm0427n16272 <sup>a</sup>	76.03168	-66.18205	6.003740	14.97	0.12	2451564.5990	15.27	0.12	-0.30	bin
lm0303k23599	76.57203	-66.73731	6.463085	15.36	0.43	2451038.8223	15.59	0.41	-0.23	bin

lm0427n12122	75.86553	-66.14977	7.194033	15.48	0.18	2452123.8419	15.77	0.20	-0.29	bin
lm0435m12381	77.55651	-65.62774	7.696551	15.87	0.62	2451888.6354	16.04	0.57	-0.17	bin
lm0434k8023	76.23518	-65.60718	8.126396	14.54	0.70	2451341.9322	14.11	0.51	0.43	cc
lm0436k11112	76.38695	-65.98500	11.331810	14.39	0.08	2452562.6772	14.11	0.06	0.27	sm.am
lm0436m12100 <sup>e</sup>	76.75148	-65.99706	109.899010	16.17	0.51	2450262.4836	14.29	0.21	1.88	lpv
lm0304m5953	75.94165	-66.99012	2.712221	16.03	0.67	2450800.6827	15.66	0.49	0.36	cc

Table 3.1: Properties of candidate CCs in tile LMC 8\_3 (Column 1:

EROS-2 identification number; Column 2: Right ascension from the EROS-2 catalogue; Column 3: Declination from the EROS-2 catalogue; Column 4: Period from the EROS-2 catalogue (<sup>a</sup> - Stars for which a new period estimate was derived. See text for details;<sup>b</sup>-Double-mode CCs, the first period, derived with GRATIS, is given. See text and Table 3.2 for details); Column 5: Mean magnitude in the  $B_{EROS}$  band; Column 6: Amplitude in the  $B_{EROS}$  band; Column 7: Epoch of maximum light in the  $B_{EROS}$  band; Column 8: Mean magnitude in the  $R_{EROS}$  band; Column 9: Amplitude in the  $R_{EROS}$  band; Column 10: Colour  $B_{EROS} - R_{EROS}$ ; Column 11: Classification: cc - confirmed Classical Cepheids, cAC - candidate Anomalous Cepheids, bin - binary stars, sm.am - small amplitude variables, lpv - long period variables).

### 3.2. CLASSIFICATION OF CANDIDATE CLASSICAL CEPHEIDS

EROS-2 id	$P_{1,GRATIS}$ (day)	$P_{2,GRATIS}$ (day)	$P_2/P_{1,GRATIS}$	$P_{1,OGLE III}$ (day)	$P_{2,OGLE III}$ (day)	$P_2/P_{1,OGLE III}$
lm0424n15978	1.560930	1.135416	0.7274	-	-	-
lm0303m26388	3.700482	2.653466	0.7171	3.700349	2.653591	0.7171

Table 3.2 Double-mode CCs in tile LMC 8\_3. (Column 1: EROS-2 identification of the star; Column 2: First period derived with GRATIS; Column 3: Second period derived with GRATIS; Column 4: Ratio of the periods; Column 5: First period from the OGLE III catalogue; Column 6: Second period from the OGLE III catalogue; Column 7: Ratio of the periods from OGLE III).

By analysing the light curves with GRATIS we discovered two double-mode pulsators, namely lm0303m26388 and lm0424n15978. For lm0303m26388 our second periodicity is also confirmed by the OGLE III survey, while for lm0424n15978 there is no OGLE III counterpart. Information about these two objects is presented in Table 3.2.

### 3.2 Classification of candidate Classical Cepheids

The visual inspection of the light curves of the 201 candidate CCs returned a sample of 126 bona-fide CCs, 58 EBs, 13 variables with small amplitudes (generally around 0.1 mag or lower) and 4 LPVs. The latter accidentally fall in the sample of the candidate CCs, based on the  $P_{EROS}$  and  $B_{EROS}$  values, because their EROS periods are aliases of the actual periods, which are usually in the range from tens to thousands of days for LPVs. In the sample of confirmed Cepheids we have also found two candidate Anomalous Cepheids: lm0435n13603 ( $P=0.664997$  days) and lm0444112369 ( $P=0.664995$  days). These objects have shorter periods, than CCs, and are relatively fainter being located in the lower part of the Cepheid's region on the CMD (1.2-1.4 mag brighter than HB stars). Results of our classification for the 201 candidate CCs in tile LMC 8\_3 are presented in Table 3.1.

OGLE III covers the lower 1/4 of tile LMC 8\_3 and identified 52 CCs in this region, of which 36 are in common with EROS-2 and 16 do not have a counterpart in the EROS-2 catalogue of CC candidates. Four of these 16 objects have a counterpart in the general catalogue of EROS-2 stars but they were not classified as CC candidates. Information about the 36 CCs in common between the EROS-2 and OGLE III catalogues is presented in Table 3.3. There are a total number of 142 CCs in this tile, of which 141 have a counterpart in the VMC catalogue within a pairing radius of  $1''$ . This corresponds to a 99 % completeness of the VMC survey with respect to the number of CCs identified by both EROS-2 and



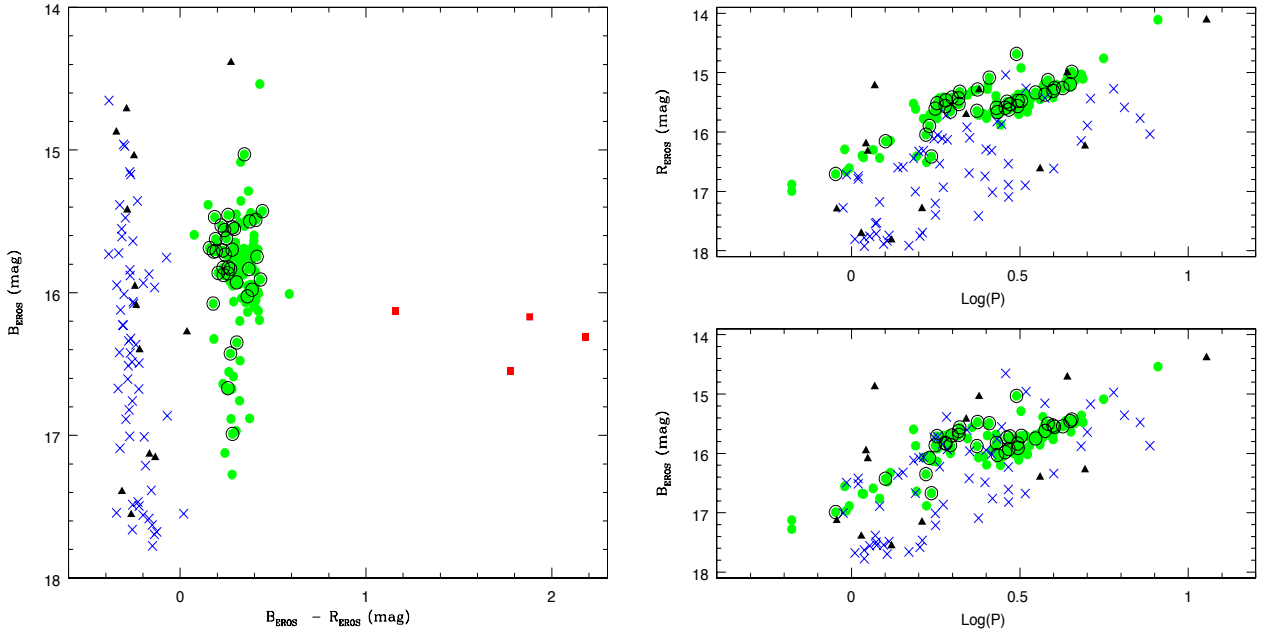


Figure 3.1 *Left panel:*  $B_{EROS}$ ,  $B_{EROS} - R_{EROS}$  CMD of EROS-2 candidate CCs in the VMC tile LMC 8\_3. Blue crosses, green filled circles and black filled triangles represent EBs, bona-fide CCs and small amplitude variables, respectively. Red filled squares are LPVs. Black empty circles are 36 CCs observed also by the OGLE III survey, confirming their classification as CCs. *Right panel:*  $PL$  relations in the  $R_{EROS}$  (upper-right) and  $B_{EROS}$  (lower-right) bands of the EROS-2 candidate CCs in tile LMC 8\_3. Symbols and colours coding are as in the left panel. The LPVs were omitted. Figure is from Moretti et al. (2014).

### OGLE III.

The results of the classification show that the candidates CCs selected by the EROS-2 on the basis of the  $PL$  distribution (right panel of Fig. 2.3) are mainly contaminated by EBs. We have investigated whether we could find methods to clean the candidate CCs without checking visually all the light curves, and found that the EROS-2 CMD is well suited for this purpose, as also was pointed out by Spano et al. (2011) in their Fig. 8. The left panel of Fig. 3.1 shows the  $B_{EROS}$ ,  $B_{EROS} - R_{EROS}$  CMD of the EROS-2 candidate CCs in tile LMC 8\_3. In the CMD objects classified as EBs (blue crosses) after visual inspection of the light curves are very well separated and definitely bluer ( $B_{EROS} - R_{EROS} < 0.1$  mag) than sources confirmed to be CCs (green circles). Furthermore, both binaries and CCs appear to be constrained in small  $B_{EROS} - R_{EROS}$  colour ranges. A number of small amplitude

variables (black triangles in Fig. 3.1) also fall in the region of EBs. As suggested by the amplitude smaller than 0.1 mag, the typical periods and the blue colours, they likely are main sequence variables such as  $\beta$  Cepheids, Be stars, slowly pulsating B variables (see, e.g. Baldacci et al. (2005) and reference therein, for characteristics of these types of variables). Four LPVs (red squares in Fig. 3.1) lie at colours redder than  $B_{EROS} - R_{EROS} \sim 1$  mag. Spano et al. (2011) analysed light curves of 856864 variables in the EROS-2 data obtaining a final list of 43551 LPVs in the LMC. The catalogue of 5800 EROS-2 candidate CCs has 296 objects in common with the LPV catalogue from Spano et al. (2011). The 4 LPVs found in tile LMC 8\_3 are all included in the catalogue of LPVs published by Spano et al. (2011).

The right panel of Fig. 3.1 shows the  $PL$  relations in the  $R_{EROS}$  (upper panel) and  $B_{EROS}$  (lower panel) passbands of the EROS-2 candidate CCs (the LPVs were omitted). The bona-fide CCs are distributed along the two loci occupied by first-overtone and fundamental mode CCs, respectively. EBs significantly contaminate the Cepheid's  $B_{EROS}$   $PL$ , while seem to be more separated from bona-fide CCs in the  $R_{EROS}$   $PL$ . To summarize, by combining  $B_{EROS}$ ,  $B_{EROS} - R_{EROS}$  CMD and the  $B_{EROS}$ ,  $R_{EROS}$   $PL$ s it should be possible to separate quite easily bona-fide CCs from binaries and small amplitude variables.

### 3.3 Strategy for extracting bona-fide Classical Cepheids

In the analysis of the VMC tiles for which information on the variable stars is available only from the EROS-2 survey, we will use the following strategy to extract bona-fide CCs from the EROS-2 sample of candidate CCs. As a general rule we expect that sources with  $0.1 < (B_{EROS} - R_{EROS}) < 1$  mag are likely to be bona-fide CCs, sources with  $(B_{EROS} - R_{EROS}) < 0.1$  mag are likely to be EBs, and objects with  $(B_{EROS} - R_{EROS}) \geq 1$  mag are likely LPVs (Moretti et al., 2014). According to this method out of the 5800 EROS-2 candidate CCs in the LMC, 3484 (60.1 %) are bona-fide CCs, 2003 (34.5 %) are EBs and 313 (5.4 %) are likely LPVs. However, we are aware that the above colour separations may sometimes be too crude. Especially for tiles where reddening is large and patchy (internal regions of the LMC), there may be sources with colours between the two main distributions that may belong to one or the other group, and thus will need to be checked visually.

In order to check the robustness of the described procedure and verify that bona-fide CCs selected on the basis of the colour-cuts in the CMD are no longer contaminated by

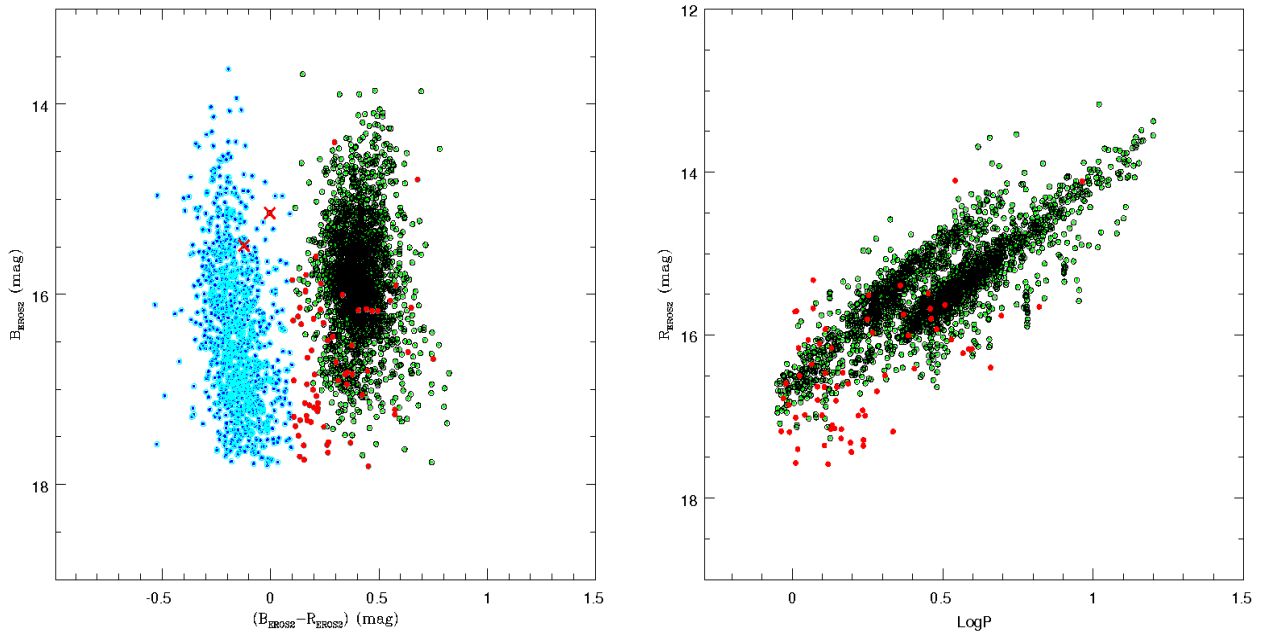


Figure 3.2 *Left panel*: CMD of the 3488 candidate CCs that have a counterpart in the OGLE III catalogue of EBs or CCs. Blue points represent EROS-2 candidate CCs with colour  $B_{EROS} - R_{EROS} < 0.1$  mag. Cyan circles represent EROS-2 candidate CCs with an OGLE III counterpart classified as EBs. Green points are EROS-2 candidate CCs with colour  $0.1 < (B_{EROS} - R_{EROS}) < 1.0$  mag. Black circles are EROS-2 candidate CCs with an OGLE III counterpart classified as CCs. Red crosses mark two CCs, that fall in the region of the CMD mainly occupied by EBs. Red filled circles are EBs falling in the region of the CMD occupied by bona-fide CCs (67 objects). *Right panel*:  $PL$  in the  $R_{EROS}$  passband of the objects with  $0.1 < (B_{EROS} - R_{EROS}) < 1.0$  mag. Figure is from Moretti et al. (2014).

### 3.3. STRATEGY FOR EXTRACTING BONA-FIDE CLASSICAL CEPHEIDS

---

spurious sources, we have compared our selection of the EROS-2 candidate CCs with the OGLE III catalogues of CCs and EBs. The EROS-2 catalogue of candidate CCs contains a total number of 5800 sources, this number reduces to 5487 if only objects with colour bluer than 1.0 mag are selected (i.e after discarding the LPVs). Of these 5487 objects, 3488 have a counterpart in the OGLE III catalogues of CCs and EBs within a pairing radius of 1 arcsec.

The left panel of Figure 3.2 shows the CMD of the 3488 stars with a counterpart in the OGLE III catalogue. This sample contains 2357 CCs and 1062 EBs according to the colour-cut criteria and the OGLE III classification. There are only two objects (red crosses in Fig. 3.2) that we would classify as EBs based on their colours and are instead CCs according to the OGLE III classification and the visual inspection of the light curves. These are stars with EROS-2 identification *lm0551n20500* and *lm0036k8214*, corresponding to OGLE-LMC-CEP-0962 and OGLE-LMC-CEP-2595, respectively. The latter has a clean light curve, while OGLE-LMC-CEP-0962 has variable mean luminosity. According to the OGLE III remarks its classification as CC is uncertain. On the other hand, there are 67 objects (red filled circles in Fig. 3.2) that we would classify as CCs based on their colours and are instead EBs both according to OGLE III and the visual inspection of the EROS-2 light curves. This corresponds to a 3 % contamination of the bona-fide CCs sample. Thirty-three of these binaries have colour in the range [0.1;0.2] mag, suggesting that stars with these colours need visual inspection to be properly classified.

The right panel of Fig. 3.2 shows the  $PL$  distributions in the  $R_{EROS}$  passband of the sources with  $0.1 < (B_{EROS} - R_{EROS}) < 1.0$  mag. There are two separate sequences formed by the fundamental and the first-overtone mode pulsators. Part of EBs that still contaminate the CCs sample (red points in Fig. 3.2) deviate significantly from the CCs sequences and could be eliminated with a sigma-clipping procedure. This will allow us to further reduce the 3 % contamination of the sample of bona-fide CCs. In summary, the application of colour-cuts in the CMD is a robust criterion that combined with the analysis of the scatter in the  $PL$  relations allows one to extract a sample of bona-fide CCs more than 97 % clean from contaminating sources (Moretti et al., 2014). In any case, a 3 % contamination is not expected to affect significantly the  $PL_{K_s}$  relations of CCs in regions where only the EROS-2 data are available.

OGLE III id	EROS-2 id	RA (HH:MM:SS)	DEC (DD:MM:SS)	Type	I (mag)	V (mag)	P (day)
OGLE-LMC-CEP-0598	lm0293i26069	4:59:51.63	-66:54:15.2	I	16.568	17.215	0.897332
OGLE-LMC-CEP-0769	lm0302i13504	5:02:50.85	-66:50:35.5	I	16.019	16.572	1.261291
OGLE-LMC-CEP-0876	lm0302n26730	5:04:56.83	-66:56:29.1	I	15.825	16.540	1.664000
OGLE-LMC-CEP-1050	lm0303m16963	5:08:09.07	-66:41:49.2	I	15.662	16.378	1.702563
OGLE-LMC-CEP-0941	lm0303k5608	5:06:07.13	-66:37:49.3	F	16.228	16.847	1.727254
OGLE-LMC-CEP-0534	lm0293k16840	4:58:35.95	-66:41:53.8	I	15.444	15.995	1.772482
OGLE-LMC-CEP-0921	lm0303i19680	5:05:49.15	-66:52:00.0	I	15.345	15.933	1.793972
OGLE-LMC-CEP-0574	lm0293i23982	4:59:19.44	-66:53:35.2	I	15.382	16.007	1.898245
OGLE-LMC-CEP-1126	lm0312k16300	5:09:30.30	-66:44:14.7	I	15.312	15.898	1.906954
OGLE-LMC-CEP-1000	lm0303n13787	5:07:21.10	-66:49:47.4	I	15.467	16.182	1.966774
OGLE-LMC-CEP-0792	lm0302i5812	5:03:13.78	-66:47:30.6	I	15.242	15.827	1.988642
OGLE-LMC-CEP-0911	lm0303i22257	5:05:36.39	-66:52:54.0	I	15.210	-99.99	2.078685
OGLE-LMC-CEP-0746	lm0302i16660	5:02:25.73	-66:51:52.4	I	15.381	16.061	2.085401
OGLE-LMC-CEP-0618	lm0293k2961	5:00:07.52	-66:36:50.7	I	15.124	15.638	2.095957
OGLE-LMC-CEP-1018	lm0305m2711	5:07:29.33	-66:57:58.3	F	15.525	16.128	2.357619
OGLE-LMC-CEP-0988	lm0303k12257	5:07:09.87	-66:40:07.7	I	15.041	15.595	2.368493
OGLE-LMC-CEP-1121	lm0312k9715	5:09:27.37	-66:40:05.4	I	14.913	15.535	2.564991
OGLE-LMC-CEP-1039	lm0305m11940	5:08:01.06	-67:01:17.1	F	15.448	16.096	2.694834
OGLE-LMC-CEP-0818	lm0304m5953	5:03:46.02	-66:59:24.6	F	15.489	16.182	2.712216
OGLE-LMC-CEP-0939	lm0305k7040	5:06:05.98	-66:59:43.9	F	15.483	16.202	2.861735
OGLE-LMC-CEP-0933	lm0303i6182	5:05:59.19	-66:47:15.0	F	15.341	15.977	2.894750
OGLE-LMC-CEP-0960	lm0303k20577	5:06:37.62	-66:43:08.8	F	15.432	16.141	2.931299
OGLE-LMC-CEP-1035	lm0303m5774	5:07:56.39	-66:37:45.4	F	15.271	15.913	2.957635
OGLE-LMC-CEP-1134	lm0310i9678	5:09:47.91	-66:35:46.1	I	14.575	15.162	3.090031
OGLE-LMC-CEP-0951	lm0303k8191	5:06:18.53	-66:38:44.7	F	15.375	15.992	3.113395
OGLE-LMC-CEP-0952	lm0301i8214	5:06:19.60	-66:35:47.8	F	15.384	16.075	3.123234
OGLE-LMC-CEP-0974	lm0303k19341	5:06:56.76	-66:42:40.3	F	15.256	15.907	3.193414
OGLE-LMC-CEP-1150	lm0310i18849	5:10:13.39	-66:35:00.7	F	15.323	16.125	3.518752
OGLE-LMC-CEP-1064	lm0303m26388	5:08:21.68	-66:45:09.5	F1	15.014	15.689	3.700349
OGLE-LMC-CEP-1013	lm0303m3523	5:07:26.73	-66:36:58.5	F	15.136	15.890	3.756495

OGLE-LMC-CEP-0762	lm0302k15867	5:02:37.14	-66:44:59.4	F	14.961	15.632	3.832815
OGLE-LMC-CEP-1085	lm0303n19840	5:08:47.38	-66:51:43.0	F	15.063	15.827	3.968188
OGLE-LMC-CEP-1003	lm0303n11462	5:07:22.63	-66:48:56.8	F	15.081	15.847	4.003405
OGLE-LMC-CEP-0994	lm0303n14110	5:07:17.64	-66:49:54.5	F	15.054	15.848	4.240270
OGLE-LMC-CEP-1056	lm0303n19424	5:08:12.53	-66:51:39.2	F	14.977	15.774	4.460721
OGLE-LMC-CEP-0997	lm0301n21884	5:07:18.60	-66:34:52.7	F	14.805	15.579	4.508196

Table 3.3: Properties of CCs in tile LMC 8\_3, which have a counterpart in the OGLE III catalogue (Column 1: OGLE III identification of the star; Column 2: Identification of the star from the EROS-2 catalogue; Column 3: Right ascension from the OGLE III catalogue; Column 4: Declination from the OGLE III catalogue; Column 5: Type according to the OGLE III classification: F - Fundamental mode CCs, 1 - First-overtone mode CCs, F1 - Double-mode CCs; Column 6: OGLE III  $I$  mean magnitude; Column 7: OGLE III  $V$  mean magnitude; Column 8: Period from the OGLE III catalogue).

## Chapter 4

# Eclipsing binaries in the LMC

The EROS-2 sample of candidate CCs is significantly contaminated by EBs. These objects have blue colours, hence, we classed them as “hot” eclipsing binaries (HEBs; Muraveva et al. 2014a). In this chapter we describe the results of our analysis of these HEBs.

### 4.1 EROS-2 data for eclipsing binaries

As it was described in Section 3.3 a large number of objects with colour  $(B_{EROS} - R_{EROS}) < 0.1$  mag are EBs. It was also noted that sources with colour  $0.1 < (B_{EROS} - R_{EROS}) < 0.2$  mag are located in the CMD between the distributions of CCs and EBs and may belong to one or the other group. Thus, stars with these colour need visual inspection of the light curves to be properly classified. In order to characterise the EROS-2 EBs that contaminate the sample of LMC bona-fide CCs we extract from the EROS-2 catalogue of candidate CCs all objects with colour  $(B_{EROS} - R_{EROS}) < 0.2$  mag (2085 sources). We explicitly note that the EROS-2 catalogue of candidate variables contains a much larger number of EBs. Recently, Kim et al. (2014) identified new EBs in the LMC based on the full EROS-2 dataset by applying a machine learning approach. However, in this thesis work we focused only on the objects contaminating the CC sample.

The analysis of these sources was performed running GRATIS on the  $R_{EROS}$  light curves and showed that 83 objects from the sample are bona-fide CCs, 225 are small amplitude variables, nine objects have light curves which are too noisy to be classified, and 1768 stars are EBs. Information on these EBs is presented in Table A.1 (Appendix).

We transformed the  $B_{EROS}$ ,  $R_{EROS}$  average magnitudes of the sources to  $V$ ,  $I$  standard magnitudes by applying equations 2.1 and 2.2 (Subsection 2.4.1). The left panel of Figure 4.1 shows the distributions of mean  $V$ ,  $I$  magnitudes and  $V - I$  colours for our sam-

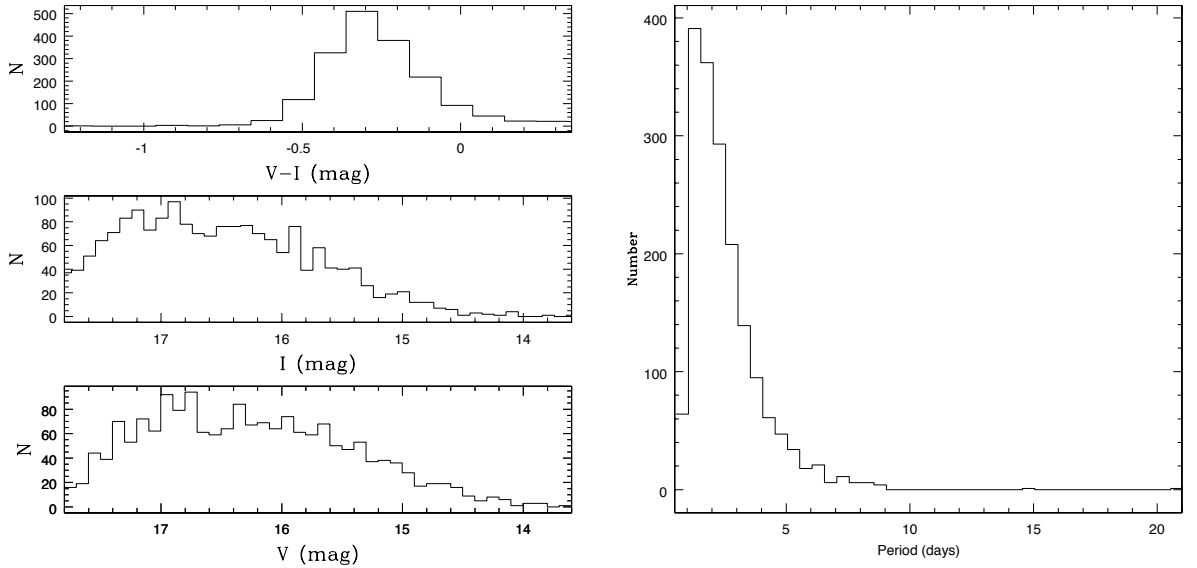


Figure 4.1 Distributions of mean  $V$ ,  $I$  magnitudes and  $V - I$  colours (left panels), and period (right panel) of the LMC EBs in our sample. Figure is from Muraveva et al. (2014a).

ple of EBs. The mean  $V$  and  $I$  magnitudes range from  $\sim 17.8$  to  $\sim 13.2$  mag (which reflects the initial cuts in magnitude used to extract the sample of candidate CCs from the EROS-2 catalogue) and from  $\sim 18.1$  to  $\sim 13$  mag, respectively, with a peak around 17.1-17.2 mag in both bands. The  $V - I$  colours range from  $\sim -1.3$  to 0.33 mag and peak at  $V - I = -0.3$  mag, which reflects instead the colour selection we applied to separate binaries from bona-fide CCs. According to their blue colours the EBs in our sample are mainly composed by hot components: main sequence stars or blue giants, hence, we classified them as HEBs.

We have compared the periods provided by the EROS-2 survey for the HEBs with those determined by the visual inspection of light curves with GRATIS ( $P_{GRATIS}$ ). For the majority of binaries  $P_{GRATIS}$  is in good agreement with  $P_{EROS}$ . However, in some cases,  $P_{EROS}$  was a harmonic or a subharmonic of the actual period. We corrected the period of 225 objects in the sample by multiplying  $P_{EROS}$  by different constants until the shape of the light curve was consistent with that of an EB. The same technique was used by Derekas et al. (2007) as part of the redetermination of periods for 3031 EBs in the MACHO catalogue. Examples of the light curves before and after the period correction are presented in Figure 4.2. The systems in the middle and bottom panels of Figure 4.2 have rather eccentric orbits which hinders the automatic determination of the period. In some cases it was not clear if EROS-2 determined aliases of the true period or if the binary star had only one



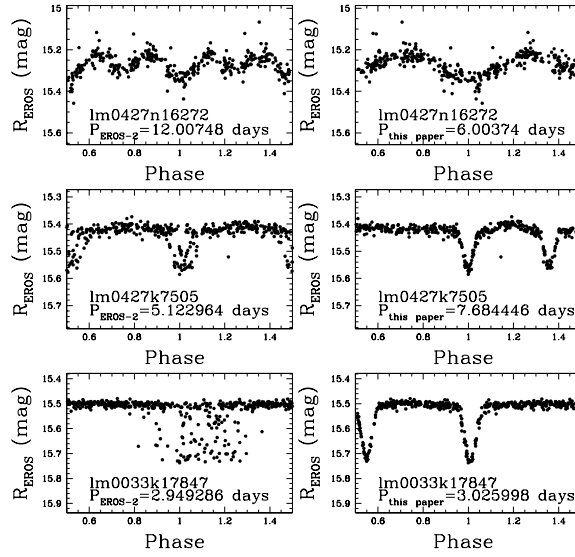


Figure 4.2 Light curves of EBs before (left panels) and after (right panels) correction of the period (see text for details). Figure is from Muraveva et al. (2014a).

strong expressed minimum. For these objects we decided to use the periods provided by EROS-2.

We studied the period distribution of our sample of HEBs even though the true periods of these objects cover a relatively narrow range (from  $\sim 0.89$  to  $\sim 20$  day). The distribution of periods is shown on the right panel of Fig. 4.1. Most of our HEBs are short-period systems. The distribution sharply peaks between 1 and 2 days and the majority of HEBs in our sample (94 %) have periods shorter than 5 days.

## 4.2 Cross-correlation with other catalogues of eclipsing binaries in the LMC

Nine different catalogues of EBs detected in the LMC by the microlensing surveys have been published. During the first stage of the EROS survey, 79 candidate EBs were identified in the bar of the LMC (Grison et al., 1995). The MACHO survey identified an initial sample of 611 LMC EBs (Alcock et al., 1997). Subsequently, Derekas et al. (2007) reanalysed the eclipsing variables in the MACHO database, corrected their periods and presented a “clean” sample of 3031 EBs. Faccioli et al. (2007) provided a new sample of 4634 EBs in the LMC from the MACHO catalogue, expanding the previous sample of 611 objects from Alcock et

#### 4.2. CROSS-CORRELATION WITH OTHER CATALOGUES OF ECLIPSING BINARIES IN THE LMC

---

al. (1997). Using the OGLE II data, 3332 EBs were identified in the LMC (Wyrzykowski et al. 2003, Groenewegen 2005, Graczyk & Eyer 2010). Graczyk et al. (2011) provided a sample of 26121 LMC EBs detected by the OGLE III survey. Finally, Soszyński et al. (2012) identified 1377 EBs and 156 ellipsoidal variables in the GSEP area based on the OGLE IV survey.

We cross-correlated our sample of 1768 HEBs with the catalogues of EBs identified in the LMC by the various microlensing surveys. Specifically, we considered: the first stage of the EROS survey (Grison et al. 1995), the MACHO survey (Alcock et al. 1997; Derekas et al. 2007; Faccioli et al. 2007), the OGLE III (Graczyk et al. 2011) and IV (Soszyński et al. 2012) surveys. Objects in the various catalogues were cross-identified when their right ascension and declination differed by less than  $10''$ , and the periods differed by less than 1%. We also considered objects located within less than  $10''$  and with the ratio of the periods approximately equal to integer numbers, in case one of the surveys had picked harmonics or subharmonics of the true period. We used a rather large pairing radius in order to avoid missing counterparts of our EBs in other catalogues, however, we note that the vast majority of the counterparts were found to be within a pairing radius of  $1''$  (OGLE III: 99%; MACHO from Faccioli et al. 2007: 57%; MACHO from Derekas et al. 2007: 63%; EROS: 100%).

Twenty-five out of seventy-nine EBs detected in the LMC bar by the first stage of the EROS microlensing survey (Grison et al. 1995) have a counterpart in our sample of HEBs. Panel (a) of Figure 4.3 shows the position of those 25 EBs (green dots) on the map of our 1768 HEBs (black dots). The cross-correlation with Derekas et al. (2007) and Faccioli et al. (2007) catalogues of EBs detected in the LMC by the MACHO survey shows that 797 objects were already known (panel (b) of Fig. 4.3). The cross-correlation with the sample of 26121 EBs from the OGLE III catalogue (Graczyk et al. 2011), the 1377 EBs and the 156 ellipsoidal stars in the OGLE IV catalogue (Soszyński et al. 2012) showed that 1074 objects were already known (panel (c) of Fig. 4.3). We also cross-matched our sample with the spectroscopy of massive stars available from the VLT-FLAMES surveys of Evans et al. (2006,2011), in the NGC 2004, N11 and 30 Doradus regions of the LMC. Eight objects from our sample have been observed by these surveys: four stars in 30 Doradus by the VLT-Flames Tarantula Survey (VFTS), two in NGC 2004 and two in N11, as summarized in Table 4.1. Four of these eight objects have a counterpart in the OGLE III catalogue, one was observed by the MACHO project, three objects have not been detected before. Optical

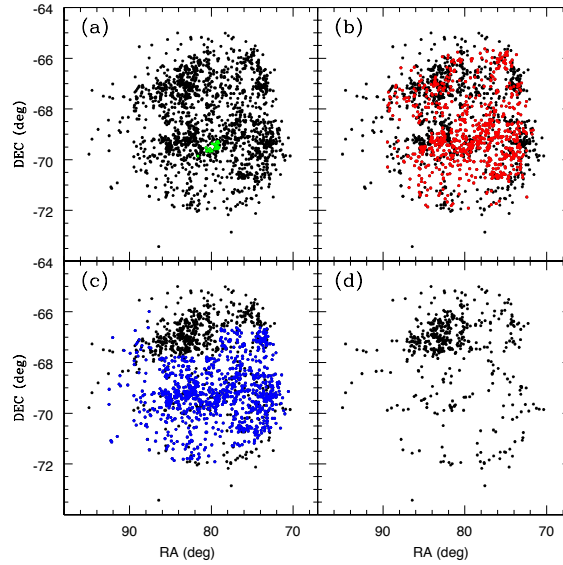


Figure 4.3 Panels (a)-(c): spatial distribution of the 1768 HEBs analysed in this study (black dots) compared with those detected from previous surveys; (a) the first stage of the EROS survey (green dots), (b) the MACHO project (red dots), (c) the OGLE III/IV surveys (blue dots). Panel (d) shows the location of the 493 EBs detected only by the EROS-2 survey. Figure is from Muraveva et al. (2014a).

spectroscopy is available for a further five of our detected EBs, from observations with the AAOmega multi-object spectrograph on the Anglo-Australian Telescope, one of these objects has not been detected by previous surveys.

To summarize, a total number of 1275 sources in our EROS-2 HEBs sample had previously been detected by other surveys (OGLE III, OGLE IV, MACHO, EROS, with the FLAMES and AAOmega spectrographs), whereas 493 were observed only by the EROS-2 survey. The positions of these objects in the LMC are shown in panel (d) of Figure 4.3. As expected they are mainly located in the outer regions of the LMC.

We also compared our corrected periods with the periods from other catalogues of EBs (MACHO, OGLE III, OGLE IV). Among the 225 objects for which we corrected the period 163 were also detected by the OGLE III survey, and our corrected periods are in good agreement (to within 1%) for all but one system. Other 6 and 19 objects with corrected periods were observed by the OGLE IV and MACHO (Faccioli et al. 2007, Derekas et al. 2007) surveys, respectively. The corrected periods for all of these are in good agreement with the published values (to within 1%). In conclusion, of the 225 objects for which we

## 4.2. CROSS-CORRELATION WITH OTHER CATALOGUES OF ECLIPSING BINARIES IN THE LMC

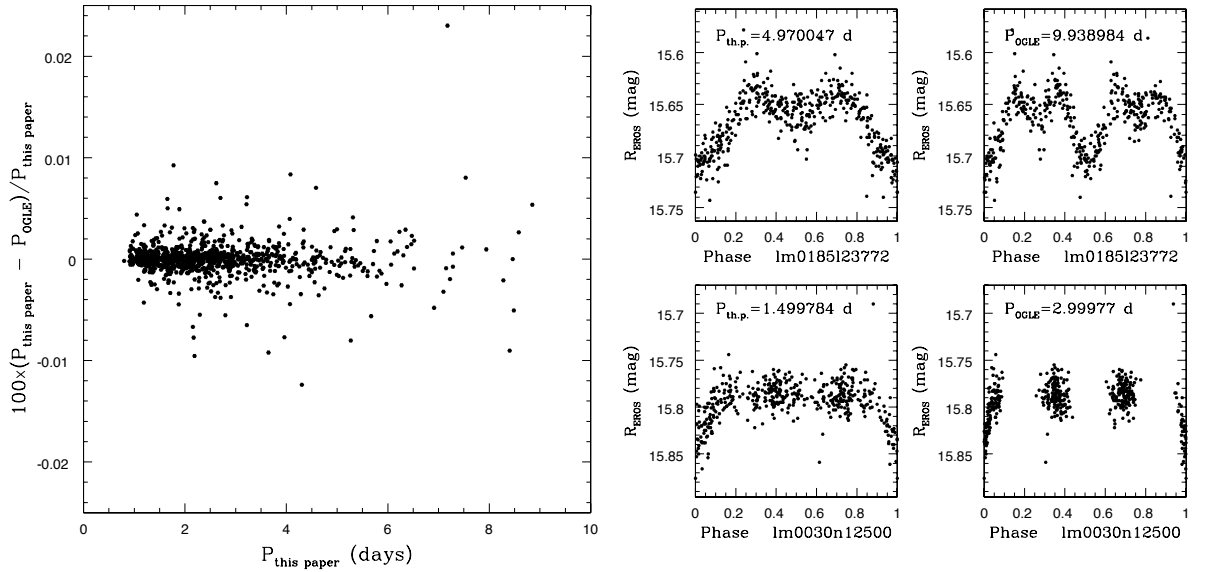


Figure 4.4 *Left panel*: comparison between periods adopted in this study and those in the OGLE III and OGLE IV catalogues for the 1072 EBs in common. Two objects, namely *lm0185123772* and *lm0030n12500*, were not included because their OGLE periods differ significantly from our values. *Right panels*: light curves of *lm0185123772* and *lm0030n12500* with the periods used in this thesis work (on the left) and provided by the OGLE III catalogue (on the right). Figure is from Muraveva et al. (2014a).

corrected the periods, 188 were detected by other surveys and our estimates are confirmed in all but one of these cases (i.e.  $> 99\%$ ).

The left panel of Figure 4.4 shows the comparison of the periods adopted in this thesis work with those provided by the OGLE III and OGLE IV catalogues for the 1072 objects in common. Two objects, namely *lm0185123772* and *lm0030n12500* are not shown in the plot because their OGLE III periods are harmonics of the periods derived in this study so they differ significantly. We checked the light curves of these objects with GRATIS and could not confirm the periods in the OGLE III catalogue. In particular, for *lm0185123772* (OGLE-LMC-ECL-09445) we confirmed the period provided by the EROS-2 catalogue ( $P=4.97$  days), whereas for *lm0030n12500* (OGLE-LMC-ECL-20762) we determined a new period ( $P=1.4998$  days) which is one third of the period provided by EROS-2, while OGLE III determined a period approximately equal to two thirds of the EROS-2 period. The light curves of these objects are presented on the right panel of Figure 4.4. Apart from these two objects, the periods adopted in this thesis work and those in the OGLE III catalogue generally differ by less than 0.03% (left panel of Fig. 4.4).

## 4.3 Characteristics of eclipsing binaries with existing spectroscopy

### 4.3.1 Cross-matches with the VLT-FLAMES surveys

As already mentioned in Section 4.2, eight HEB systems in our sample have existing optical spectroscopy from surveys with FLAMES at the VLT (Evans et al. 2006, Evans et al. 2011), as summarized in Table 4.1. All were detected as binaries in the multi-epoch spectroscopy, except for VFTS 462 (Dunstall et al. in prep). In addition to the EROS-2 periods, estimates are also available from the OGLE III data for the four VFTS systems (Graczyk et al., 2011), with excellent agreement in all cases; the other four systems (in NGC 2004 and the N11 region) are beyond the OGLE III survey area.

Quantitative analysis of the VFTS spectra is still underway, but evolutionary mass estimates (of the primaries) of the other systems are available from Hunter et al. (2008);  $M = 13 M_{\odot}$  for both N11-107 and N11-119, and  $M = 11$  and  $10 M_{\odot}$  for NGC 2004-079 and NGC 2004-094, respectively<sup>1</sup>. Photospheric chemical abundances were presented for the two systems in NGC 2004 by Hunter et al. (2009), with seemingly unremarkable nitrogen abundances. The spectroscopy from the FLAMES surveys was effective in detecting spectroscopic binaries, but further monitoring is generally required to characterize the orbital parameters (e.g., Ritchie et al. 2012). Indeed, spectroscopic monitoring of a subset of the O-type binaries discovered by the VFTS is now underway (P.I. Sana), and includes VFTS 061 among its targets.

### 4.3.2 AAOmega spectroscopy

Optical spectroscopy is available for a further five of our detected EBs, from observations with the AAOmega multi-object spectrograph on the Anglo-Australian Telescope, obtained during 2006 February 22-24 (P.I. van Loon). The five targets discussed here were obtained as part of two fields centred on N11 and 30 Dor. AAOmega is a twin-arm spectrograph (providing simultaneous blue/red coverage), but only the blue data are discussed here. Both fields were observed on the first night with the 1700B grating and two central wavelengths (4100 and 4700 Å), giving coverage of 3765-5015 Å, at a resolution of 1 Å. The 30 Doradus field was also observed on the second night with the 1500V grating, at a central wavelength of 4375 Å, providing coverage of 3975-4755 Å, at a resolution of 1.25 Å. These data were reduced using the AAOmega reduction pipeline and the relevant spectra were rectified and

---

<sup>1</sup>However, note that these estimates were on the basis of effective temperatures adopted from the spectral classifications, and the expected uncertainties on these masses is typically 30% (Hunter et al., 2008).

#### 4.4. CLASSIFICATION OF ECLIPSING BINARIES

EROS-2 id	RA(J2000) (deg)	DEC(J2000) (deg)	Period EROS-2	Period OGLE III	Alternative id	Spectral type	Notes	Ref.
lm0290l18998	73.88709	-66.54208	3.224805	—	N11-107	B1-2 + Early B	SB2	E06
lm0290l5213	73.95604	-66.43437	1.791025	—	N11-119	B1.5 V	SB2	E06
lm0344l12773	82.6699	-67.19545	4.952487	—	NGC 2004-079	B2 III	SB1	E06
lm034l21656	82.78869	-67.25619	4.164156	—	NGC 2004-094	B2.5 III	Binary	E06
lm0030m4163	84.37804	-69.08817	2.333416	2.333427	VFTS 061	ON8.5III: + O9.7: V:	SB2	W14
lm0030m3468	84.42029	-69.07812	1.674098	1.674119	VFTS 112	Early B + Early B	SB2	E14
lm0030m9744	84.46997	-69.16274	1.434738	1.434745	VFTS 189	B0.7: V	Binary	E14
lm0226n24168	84.66296	-69.02808	1.176008	1.176008	VFTS 462	B0.5-0.7 V	—	E14
lm0426m23482	75.07795	-66.06284	2.345573	—	—	B1: V	SB2?	...
lm0294m4825	74.53203	-66.98277	2.97779	2.9778	—	B0-0.5 V	SB?	...
lm0436l19007	76.28093	-66.19386	3.301123	—	—	B2 V	—	...
lm0020n19615	82.67397	-69.32445	4.585353	4.585031	—	B1.5 Ib	SB1?	...
lm0031l22987	85.19681	-69.34126	5.413977	5.414011	—	B1 III	SB2	...

Table 4.1 EROS-2 HEBs with existing optical spectroscopy; E06 (Evans et al., 2006); W14 (Walborn et al., 2014); E14 (Evans et al. in prep). OGLE III periods are from Graczyk et al. (2011). SB1 and SB2 stand for single- and double-lined spectroscopic binaries, respectively.

co-added.

Spectral classifications for the five systems are presented in Table 4.1, in which we have employed the same framework as that used by Evans et al. 2014 (in prep.). All five systems have early B-type spectra (in line with the expectation of these as HEBs), with morphological evidence for binarity (double-lined and/or asymmetric profiles) in all but one.

#### 4.4 Classification of eclipsing binaries

Our classification of the EBs was based on both the Fourier analysis (Rucinski 1993,1997 and Maceroni & Rucinski 1999) and the visual inspection of the light curves. As it was shown in Subsection 1.6.1 the combination of two cosine coefficients of the Fourier decomposition of EB’s light curves,  $a_2$  and  $a_4$ , could serve as a separator of contact and non-contact binaries. Namely, the curve described by the relation  $a_4 = a_2(0.125 - a_2)$ , where both coefficients are negative, separates the regions of the contact and non-contact binaries on the  $a_2$  versus  $a_4$  plane (Rucinski, 1993). We adopt the term “contact-binary-like” systems for all objects passed by the Fourier filter (see Subsection 1.6.1).

By analysis of the Fourier decomposition of the light curves in the  $R_{EROS}$  passband we identified the contact-like binaries in our sample. The light curves were not expressed in magnitudes but in intensity units, relative to the maxima at phases in the range [0.24, 0.26]. Columns from 8 to 13 of Table A.1 (Appendix) present the 6 Fourier coefficients  $a_0$  to  $a_5$  of the Fourier analysis for the 1768 EBs in our sample.

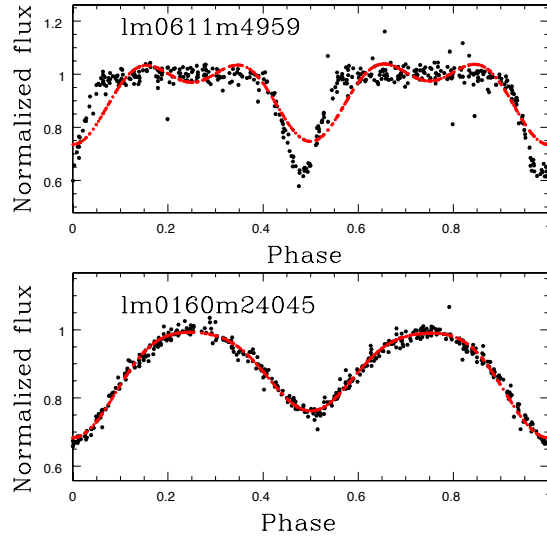


Figure 4.5 Examples of the Fourier fit obtained using 6 harmonics to model the light curve of detached (upper panel) and contact-like (bottom panel) binaries in our sample. Black dots represent the observational data, red solid lines show the resultant Fourier fits. Six harmonics are clearly not sufficient to reproduce detached systems. Figure is from Muraveva et al. (2014a).

Figure 4.5 shows examples of the resultant fits for both contact-like (lower panel) and non-contact (upper panel) binary systems. It should be noticed that six harmonics generally allow very satisfactory fits for contact-like systems, whereas some noticeable differences arose between the observations and the fitted curves for non-contact binaries, which would indeed require a much larger number of harmonics (8-10 or more) to be modelled. This is often due to elliptical orbits, yielding a shift of the secondary minimum from phase 0.5 of the non-contact systems.

Figure 4.6 shows the position of 1768 EBs in our sample on the  $a_2$  versus  $a_4$  plane. The solid line in the figure is the contact locus line defined by Rucinski (1993). We classified objects located below the line as contact-like binaries (324 sources) and those above as non-contact binaries (1444 sources). However, being aware that detached and semi-detached systems could accidentally appear below the locus line due to a bad fit of the light curve, we visually inspected the light curves of all the objects (324 stars) located below the line; we discovered eight objects which have light curves without the characteristic form of contact binaries, so we discarded them. In conclusion, in our analysis a system is classified as contact-like if it is located below the locus line from Rucinski (1993) on the  $a_2$  versus  $a_4$

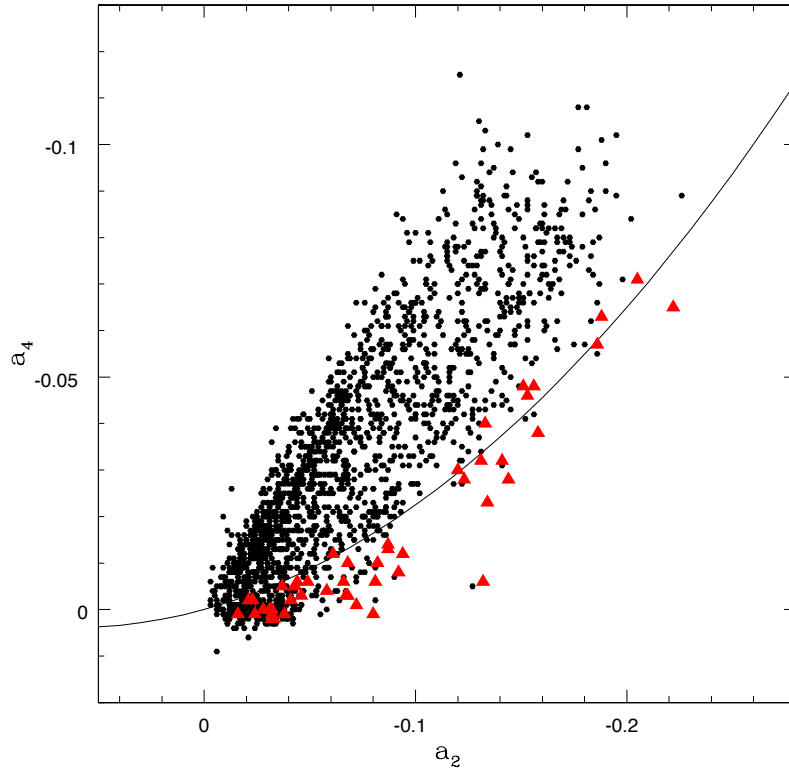


Figure 4.6 Fourier coefficients  $a_2$  and  $a_4$  of the 1768 HEBS in our sample. The solid curve is described by the relation  $a_4 = a_2(0.125 - a_2)$  which, according to Rucinski (1993), separates the regions of contact and non-contact binaries. Objects located below the line are considered to be contact systems. Red filled triangles identify objects classified as contact binaries in the OGLE III catalogue (see text for details). Figure is from Muraveva et al. (2014a).



plane and its light curve has the characteristic shape of a contact system.

We compared our classifications with those from the OGLE III catalogue. Out of 1055 objects in common, 48 stars were classified as contact systems in the OGLE III catalogue (red filled triangles in Figure 4.6). Figure 4.6 shows that the majority of these objects are in fact located below the locus line traced by Rucinski (1993), while the majority of the systems classified as non-contact variables by OGLE III are above the curve. However, eight objects located marginally above the locus line were classified as contact binaries by OGLE III. We checked their light curves and confirmed that these binaries are indeed contact-like systems. When including these, the final number of contact-like binaries in our sample is 324. In contrast, 50 of 1055 objects in common were classified as contact-like systems by us, but as detached, semi-detached or ellipsoidal systems by OGLE III. We double checked their light curves, and found that our classification is in disagreement with OGLE III in some cases. The majority of these objects have low amplitudes so it is difficult to provide an exact classification by visual inspection of light curves. In the following analysis we use our classification for those objects, thus our final sample consists of 324 contact-like binaries and 1444 non-contact systems.

## 4.5 Period-Luminosity relation of eclipsing binaries

### 4.5.1 $PL$ relation of eclipsing binaries from the EROS-2 sample

The  $PL$  relation of blue, luminous contact systems, observed in the LMC by the MACHO project, was studied by Rucinski (1999). He suggested the existence of a  $PL$  relation at maximum light in the visual band, but with a large scatter, possibly due to unaccounted effects of the interstellar extinction (see Section 1.6). Following Rucinski (1999) we have investigated whether our sample of HEBs follows a  $PL$  relation at maximum light using the red passband photometry of EROS-2 ( $R_{EROS}$ ) and near-infrared photometry in the  $K_s$ -band obtained as part of the VMC survey (Cioni et al. 2011). The latter was used in order to minimize possible extinction effects.

When this study was performed, the complete multi-epoch dataset was available for ten LMC tiles, whereas further seven tiles had been observed at least once. These 17 tiles sample different regions of the LMC from the inner bar to the outer regions.

We have cross-matched our catalogue of 1768 HEBs against the VMC catalogue available at VSA (observations completed until the 1st of April 2013) for the 17 tiles and found

4.5. PERIOD-LUMINOSITY RELATION OF ECLIPSING BINARIES

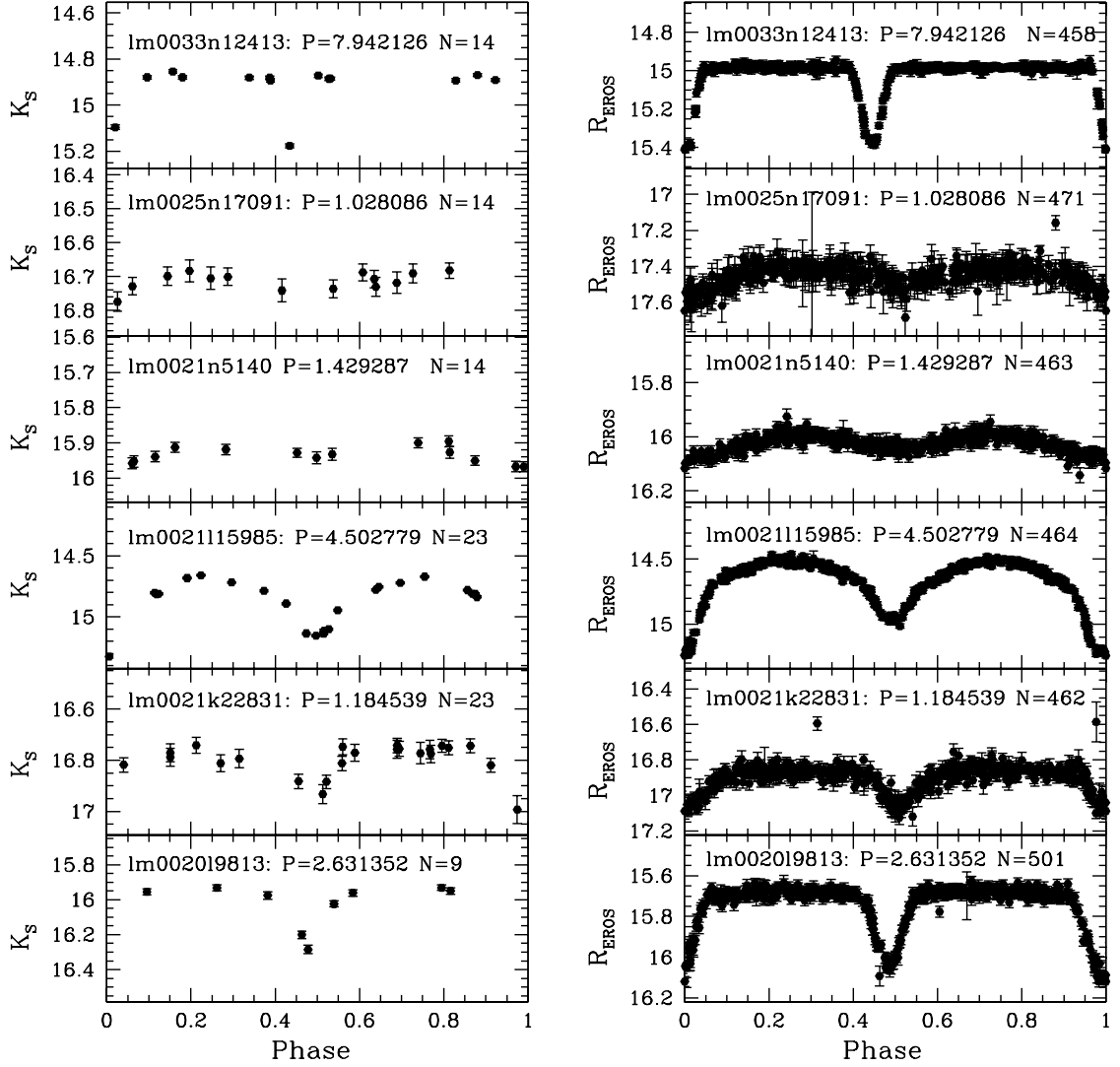


Figure 4.7 Light curves in the  $K_s$  (left panels) and  $R_{EROS}$  (right panels) passbands of example HEBs with a counterpart in the VMC catalogue.  $P$  - period (day),  $N$  - number of observations in the corresponding passband. Figure is from Muraveva et al. (2014a).

999 binaries in common using a pairing radius of  $1''$ . Examples of the  $K_s$  and  $R_{EROS}$  light curves for some of these binaries are shown in Figure 4.7. The number of phase-points of the  $K_s$ -band light curves varied from a minimum of one for EBs located in tiles with incomplete observations to a maximum of over 30 phase points for EBs located in regions where different tiles overlap. Furthermore, the EBs in our sample are relatively bright sources. Therefore the shallow VMC epochs, for which the integration time of observation is half that for deep epochs, or epochs not meeting the original quality criteria (e.g., seeing, etc.) were enough to measure the EBs thus increasing the number of available phase-points.

The  $R_{EROS}$  and  $K_s$  magnitudes at maximum light of the binaries that have a VMC counterpart are presented in Table A.2 (Appendix). In order to better determine the  $K_s$ -band magnitudes at maximum light, we performed an additional analysis of the light curves with GRATIS, for those HEBs which have 13 or more good-quality observations. The left panel of Figure 4.8 shows the  $PL$  distribution in the  $R_{EROS}$  band of the 999 EBs with a VMC counterpart, whereas the right panel shows their  $PL$  distribution in the  $K_s$  band. In both figures red open circles identify the sources which we classified as contact-like systems. The contact binaries for which we have 13 or more  $K_s$ -band epochs (and for which maximum magnitudes were determined with GRATIS) are highlighted in green. Unfortunately, the use of a more robust method to determine the  $K_s$  magnitude at maximum light does not decrease the scatter. Both the optical and near-infrared  $PL$  distributions exhibit a very large dispersion, which is of the same order of the scatter observed in the  $PL$  relation originally used by the EROS-2 team to extract the candidate CCs from the EROS-2 general catalogue of LMC variables (see right panel of Fig. 2.3). Thus, a  $PL$  relation for HEBs doesn't seem to exist.

#### 4.5.2 $PL$ relation of eclipsing binaries from the OGLE III catalogue

In order to study the  $PL$  relation of contact binaries in a more general sample and over a larger range of periods we have used the OGLE III catalogue of EB stars published by Graczyk et al. (2011). We extracted all the objects which were classified as contact binaries in the Graczyk et al. (2011) catalogue. Among them we selected objects with VMC counterparts and, with both  $V$  and  $I$  magnitudes from OGLE III, giving 563 objects in total. Twenty-five of these sources have their counterparts in our sample of HEBs from the EROS-2 catalogue and were already discussed in Section 4.5.1. To account for extinction we used the LMC reddening maps derived by Haschke et al. (2011) on the basis of OGLE III

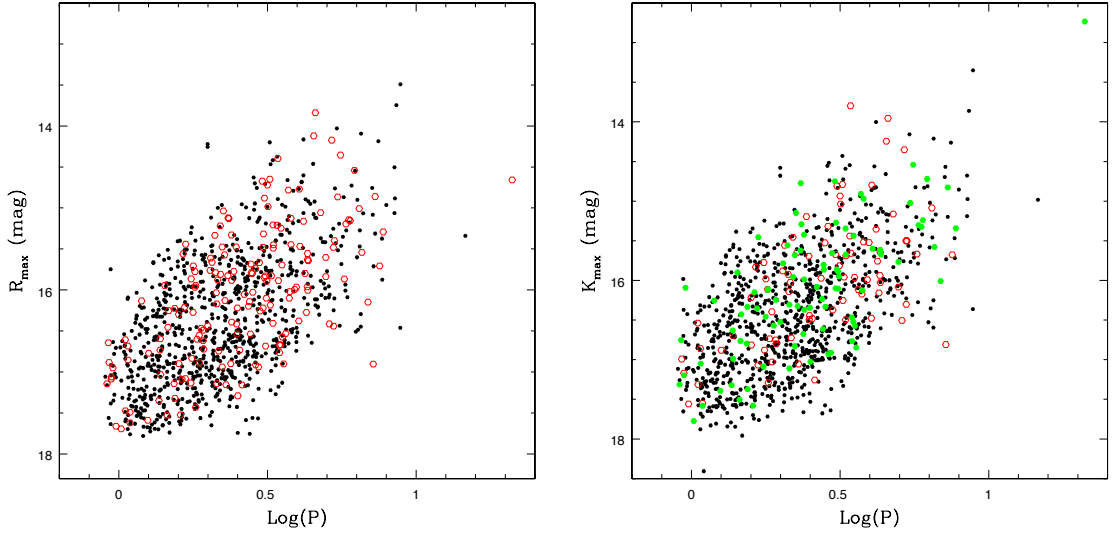


Figure 4.8  $PL$  distribution in the  $R_{EROS}$  (left panel) and  $K_s$  (right panel) passbands of 999 HEBS that have a counterpart in the VMC catalogue (black dots). Red open circles are objects which we classified as contact binaries. Green filled circles are 90 contact EBs for which we have 13 or more epochs in the  $K_s$  light curves. Figure is from Muraveva et al. (2014a).

data. To compute extinction values in the various bands we used the relations from Schlegel et al. (1998) and Cardelli et al. (1989), these were then applied to correct each source.

The reddening corrected  $V_0, (V - I)_0$  CMD of contact binaries from the OGLE III catalogue is shown in Figure 4.9. Contact binaries are located in two regions in the CMD: HEBS which contain MS stars or blue giants have  $(V - I)_0 < 0.3$  mag, whereas EBs with a red giant component have  $(V - I)_0 \geq 0.3$  mag. The corresponding  $PL$  distributions in the  $I_0$  and  $K_{s,0}$  bands are presented in Figure 4.10. In the figures HEBS are indicated with black dots and binary systems containing red giants are indicated with red triangles. For 164 EBs with a red giant component, which have 13 or more good-quality epochs from the VMC survey, we analysed the light curves with GRATIS in order to determine the  $K_s$  magnitude at maximum light with a good accuracy. On the right panel of Fig. 4.10 we have highlighted these objects with green triangles. While contact HEBS from the OGLE III sample do not distribute along a  $PL$  sequence, contact binaries containing red giant components seem to follow at least one, maybe two, different  $PL$  sequences.

To further investigate this point we restricted our analysis to 164 objects with carefully determined  $K_s$  maximum magnitudes (green triangles on the right panel of Fig. 4.10). Their  $PL$  distribution is shown in Figure 4.11. As it could be seen, there are 11 objects with short

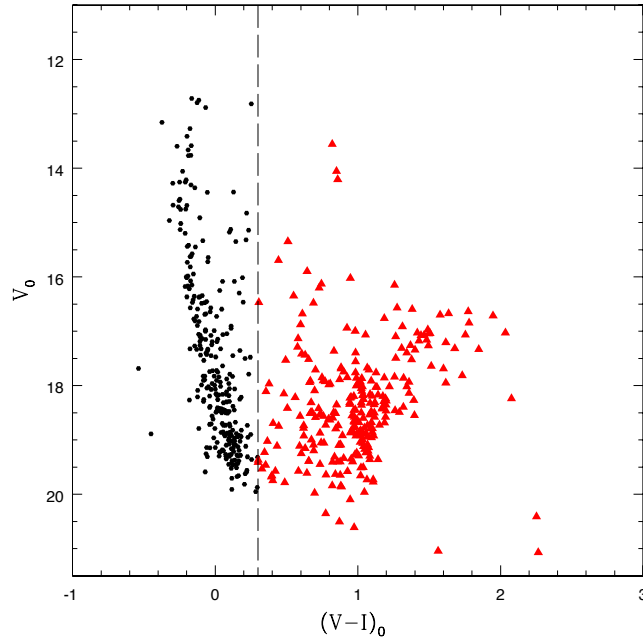


Figure 4.9 CMD of 563 contact binary stars which have  $V$  and  $I$  (OGLE III) and  $K_s$  (VMC) magnitudes. Black dots are objects with  $(V - I)_0 < 0.3$  mag and red triangles are objects with  $(V - I)_0 \geq 0.3$  mag. The dashed line corresponds to  $(V - I)_0 = 0.3$  mag. Figure is from Muraveva et al. (2014a).

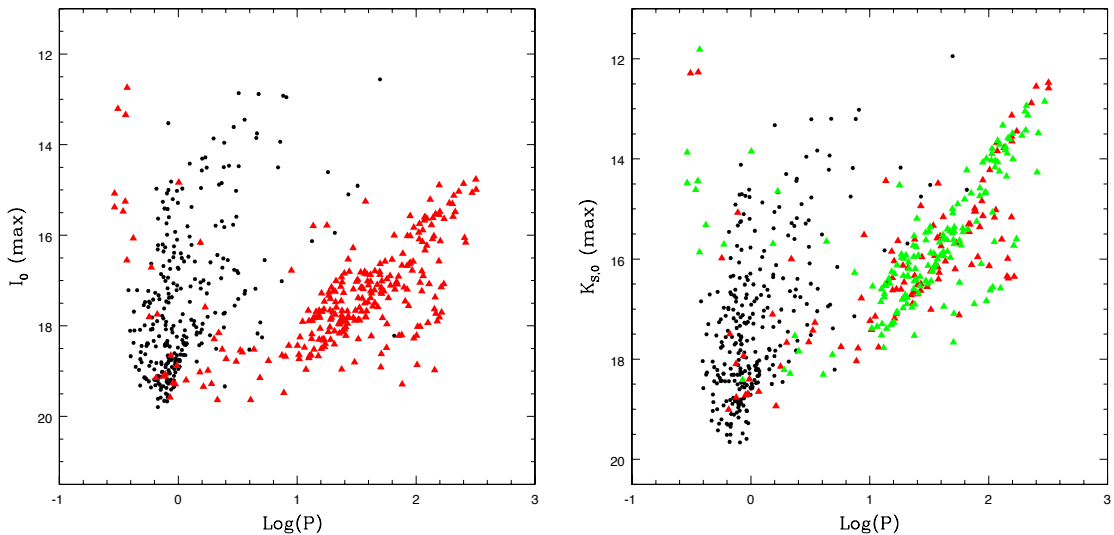


Figure 4.10  $PL$  distribution at  $I_0$  maximum (left panel) and at  $K_{s,0}$  maximum (right panel) of the 563 contact binaries shown in Fig. 4.9. Black dots are objects with  $(V - I)_0 < 0.3$  mag, red triangles are objects with  $(V - I)_0 \geq 0.3$  mag of which those with 13 or more epochs in the  $K_s$ -band are marked in green. Figures are from Muraveva et al. (2014a).

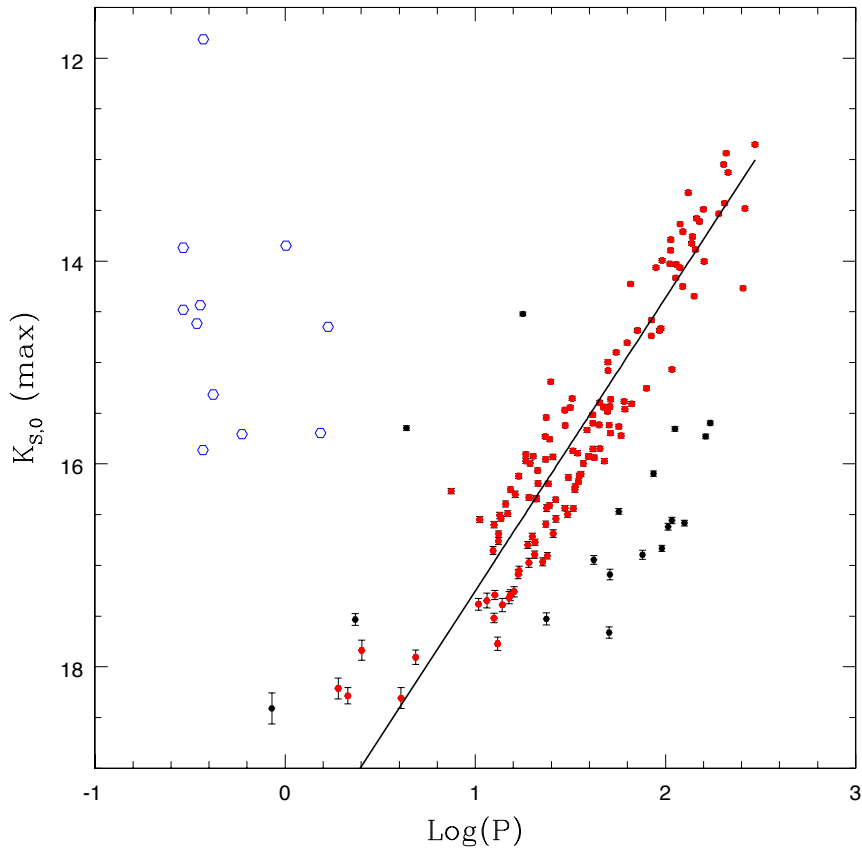


Figure 4.11  $PL$  distribution of contact binaries containing red giant components. Blue open circles are candidate HEBs falling in the region of binaries with red giant components (their errors are smaller than the size of the circles), red and black dots represent EBs which deviate less (red) and more (black) than  $3\sigma$  from a linear regression, respectively. The line is the weighted linear fit obtained from the objects marked in red. Figure is from Muraveva et al. (2014a).

periods which do not follow any  $PL$  sequence (blue open circles in Fig. 4.11). We checked the position of these objects in the CMD (Fig. 4.9) and found that they are located in the border region between HEBs and binaries with red giant components. Since these objects do not follow the  $PL$  sequence and could be HEBs, we discarded them from the following analysis.

For other 153 EBs we computed a weighted linear regression through the data by progressively discarding objects which deviate more than  $3\sigma$  from the linear regression. The majority of contact systems with carefully determined  $K_s$  maximum magnitudes (red dots in Figure 4.11) appear to follow the relation :

$$K_{s,0} = (-2.888 \pm 0.096)\log(P) + (20.139 \pm 0.171) \quad (4.1)$$

with rms=0.406 mag.

In Figure 4.11 we have highlighted objects located more than  $3\sigma$  from the  $PL$  distribution with black dots. Some of them seem to follow a  $PL$  sequence parallel to the one described by Eq. 4.1 and located  $\sim 1$  mag fainter than the previous one.

To summarize, HEBs do not follow any  $PL$  relation while the existence of red giant  $PL$  sequence(s) (at least, one) seems quite clear and, as shown by Fig. 4.10, this relation appears to be narrower in the  $K_s$  passband. However, the large scatter makes it impossible to use these sequences any further. On the other hand, that red giants follow multiple  $PL$  relations was already reported in many studies (Wood et al. 1999, Soszyński et al. 2004, Derekas et al. 2006). Wood et al. (1999) were the first to recognize five different  $PL$ -sequences: A, B and C, occupied by pulsating red giants, D composed by stars that have long secondary periods (LSPs), and sequence E, containing red giants in contact EBs and ellipsoidal variables. Soszyński et al. (2004) showed that a  $PL$  relation of ellipsoidal variables could be well described by a simple model using the Roche-lobe geometry and that sequences E and D merge at specific luminosities. Derekas et al. (2006) presented a period-luminosity-amplitude analysis of 5899 red giant and binary stars in the LMC from the MACHO database and discovered that the  $PL$  sequence of binaries is composed only by contact EBs, while detached and semi-detached systems are spread everywhere in the  $PL$  plane. Moreover, they concluded that sequence E, is located at periods a factor two greater and overlaps with the sequence of LSPs (sequence D). In our study we confirm the existence of a  $PL$  sequence containing contact binaries with red giant components (Eq. 4.1) and find evidence for a possible additional  $PL$  sequence of contact binaries located  $\sim 1$  mag fainter.

Furthermore, thanks to the depth achieved by the VMC data, we are able to extend the  $PL$  relation of contact binaries, containing red giants, to  $K_s \sim 18$  mag, roughly two magnitudes fainter than in Derekas et al. (2006). The existence of  $PL$  relation(s) for red giant EBs and its absence for HEBs could be explained by intrinsic differences occurring between the two samples. In the case of contact systems with red giants the total luminosity of the binary system is dominated by one component - the red giant star, the luminosity of the second component being negligible. On the contrary, for HEBs the ratio of luminosities of the two O-B components could vary significantly. Therefore, the scatter of the  $PL$  relation of binaries with O-B components is expected to be much larger than the scatter of the  $PL_{K_s}$  relation of contact systems with a red giant component.

#### 4.6 Structure of the LMC from “hot” eclipsing binaries and Classical Cepheids

The distribution of the LMC CCs and HEBs is presented in Figure 4.12. As it was discussed in the previous sections, we suggested that the EROS-2 candidate CCs with colour  $0.2 \leq (B_{EROS} - R_{EROS}) \leq 1$  mag are bona-fide CCs. The upper-left panel of Figure 4.12 shows the distribution of CCs in the LMC. CCs are relatively young objects (50-200 Myr), so they trace the bar of the galaxy and the spiral arm. In the upper-right panel of Figure 4.12 the distribution of 1768 HEBs from our sample is shown. It differs from the distribution of CCs as it could be seen on the bottom-left panel of Figure 4.12. HEBs are more clustered, do not follow the entire bar and locate in the regions of recent star formation activity, such as 30 Doradus and Constellation III, and supergiant shells (SGS 11, SGS 7, SGS 3, SGS 12 and others). On the bottom-right panel of Figure 4.12 the distribution of objects which were classified as contact-like binary stars is shown. It is similar to the distribution of the whole sample of EBs. These results are in agreement with the Star Formation History of the LMC. Harris & Zaritsky (2009) found that the bar of the LMC had partially active episodes of star formation 5 Gyr, 500 Myr and 100 Myr ago. CCs in the bar were formed during the last episode of star formation activity 100 Myr years ago, while the activity at 12 Myr is dominated by 30 Doradus and the Constellation III regions, which are not related to the bar and where the majority of binary stars from our sample is concentrated.



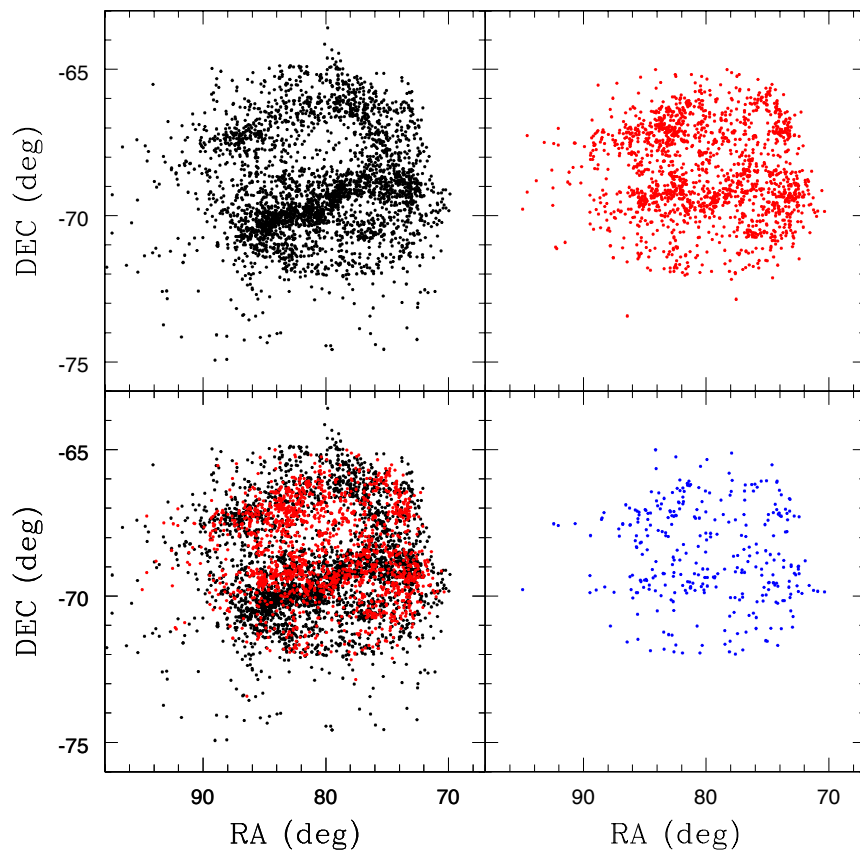


Figure 4.12 Distribution of CCs (black dots), HEBs (red dots) and contact-like binaries (blue dots) in the LMC.



## Chapter 5

# RR Lyrae stars in the VMC tile LMC 5\_5

RR Lyrae stars make useful distance indicators because of the existence of a  $M_V - [\text{Fe}/\text{H}]$  relation in the visual band and of a  $PLZ$  relation in the infrared passbands (see Subsection 1.5.2). In this chapter we present results of the analysis of 71 RR Lyrae stars located in tile LMC 5\_5, close to the bar of the galaxy, for which individual spectroscopically determined  $[\text{Fe}/\text{H}]$  abundances exist in the literature (Gratton et al., 2004). Combining the metallicities of these stars, precise periods from the OGLE III catalogue and multi-epoch  $K_s$  photometry from the near-infrared VISTA survey of the Magellanic Clouds system (Cioni et al., 2011) we derive a new near-infrared  $PL_{K_s}Z$  relation for RR Lyrae variables. In order to check the impact of Gaia (Section 1.2) on the determination of the zero-points of the RR Lyrae  $PL_{K_s}Z$  and  $M_V - [\text{Fe}/\text{H}]$  relations, we simulate Gaia parallaxes for 25 RR Lyrae stars in the Milky Way.

### 5.1 Data for RR Lyrae stars in the bar of the LMC

Optical photometry for the LMC RR Lyrae stars discussed in this chapter was obtained using the Danish 1.54 meter telescope, the 3.6 m, and the VLT ESO telescopes, at two different sky positions, hereafter called fields A and B. Both are located in tile LMC 5\_5, close to the bar of the galaxy (Clementini et al. 2003, Di Fabrizio et al. 2005). As a result, accurate  $B$ ,  $V$  and  $I$  light curves tied to the Johnson-Cousins standard system and pulsation characteristics (period, epoch of maximum light, amplitudes and mean magnitudes; Di Fabrizio et al. 2005) for 125 RR Lyrae stars were obtained. Low-resolution spectra for 98 of these RR Lyrae stars were collected by Gratton et al. (2004) using the FORS1 (FOcal Reducer/low dispersion Spectrograph) instrument mounted at the ESO VLT. They were used

to derive metal abundances by comparing the strength of the Ca II K line with that of the H lines (Preston, 1959). For the calibration of the method, four Galactic globular clusters with metallicities in the range  $[-2.06; -1.26]$  dex were used. The obtained metallicities are tied to a scale, which is, on average, 0.06 dex more metal-rich than the Zinn & West (1984) metallicity scale.

We cross-matched the sample of 98 RR Lyrae variables with known metallicities against the catalogue of RR Lyrae stars observed by the OGLE III survey (Soszyński et al., 2009). The OGLE III catalogue contains information about the position, photometric and pulsation properties of 24906 RR Lyrae stars in the LMC (see Subsection 2.4.2). We found that, respectively, 94, 2 and 2 objects are cross-identified with sources in the OGLE III catalogue within a pairing radius of  $1''$ ,  $3''$  and  $7''$ . The 2 stars with a counterpart at more than  $5''$  are OGLE-LMC-RRLYR-10345 and OGLE-LMC-RRLYR-10509; for these two stars we checked both the OGLE III finding charts and Gratton et al. (2004) Figure 5 (field B1) in order to understand if they are affected by any problem. Star OGLE-LMC-RRLYR-10345 is an isolated lightly elongated star without any clear blending problem, while star OGLE-LMC-RRLYR-10509 is very close to another source possibly making more difficult to accurately locate the star center. Considering that Gratton et al. (2004) and OGLE III periods for these 2 stars agree within 0.5%, we kept these stars in our sample.

We compared the periods of the 98 RR Lyrae stars provided by Di Fabrizio et al. (2005) and those in the OGLE III catalogue (Soszyński et al., 2009). For 96 objects the periods agree within  $\sim 2\%$ , while for two objects periods differ significantly. For star A6332 the difference is  $\sim 25\%$  and for star A5148 it is  $\sim 37\%$  (star identifications are from Di Fabrizio et al. 2005). Moreover, star A5148 has been classified as a first-overtone RR Lyrae star in the OGLE III catalogue, and as a fundamental-mode RR Lyrae by Di Fabrizio et al. (2005). Since accurately estimated periods and classifications play a key role in the current study, we decided to discard these two objects from the following analysis.

Seven objects (B2811, B4008, B3625, B2517, A2623, A2119, A10360) in our sample are classified as RRc by Di Fabrizio et al. (2005) and as RRe in the OGLE III catalogue. We removed them from our analysis because of the uncertain classification. Furthermore, since one of the main purposes of the current research is to study the  $PL_{K_s}Z$  relation of RR Lyrae stars of ab- and c-types we also discarded seven objects, which were classified as double-mode RR Lyrae stars (RRd) by Di Fabrizio et al. (2005): A7137, A8654, A3155, A4420, B7467, B6470 and B3347. This left us with a final sample of 61 RRab and 21

RRc stars, which have counterparts in the OGLE III catalogue. The period search for the RR Lyrae stars in the OGLE III catalogue was performed using an algorithm based on the Fourier analysis of the light curves (Soszyński et al., 2009). The uncertainties in the OGLE III periods for the 82 RR Lyrae stars in our sample are declared to be less than  $5 \times 10^{-6}$  days. Therefore we used the periods provided by the OGLE III catalogue in order to fit the  $PL_{K_s}Z$  relation, and do not consider errors in the periods since they are negligible in comparison to the other uncertainties.

In order to derive mean  $K_s$  magnitudes for the RR Lyrae stars in our sample we used data from the VMC survey (Cioni et al. 2011, see Subsection 2.4.3). The majority of RR Lyrae stars in our sample are located within the VMC tile LMC 5\_5. PSF photometry of the time-series data for this tile was performed on the homogenised epoch-tile images (Rubele et al., 2012) using the IRAF Daophot (Stetson et al., 1990) packages. On each epoch-tile image the PSF model was created using 2500 stars uniformly distributed, finally the Daophot ALLSTAR routine was used to perform the PSF photometry on all epoch images and time-series catalogues were correlated within a tolerance of one arcsec. We have cross-matched our sample of 82 RR Lyrae stars against the PSF photometry catalogue of tile LMC 5\_5. VMC counterparts for 71 objects were found within a pairing radius of  $1''$ . For 70 of them we have 13 epochs in the  $K_s$ -band, and for one object (B4749) we have observations only in 6 epochs.

We determined mean  $K_s$  magnitudes using  $K_s$ -band light curve templates for RR Lyrae stars from Jones et al. (1996) to fit the 13 different epochs (6 for B4749) available for the 71 stars. All available epochs were used in the present analysis. However, checks are in progress to verify that photometric errors and varying observing conditions of the individual epochs do not affect the derived  $PL_{K_s}Z$  relation. Jones et al. (1996) developed one  $K_s$ -band light curve template for RRc variables and four different templates for RRab stars, the latter vary depending on the Johnson  $V$  amplitude of pulsation ( $V_J$ ). Di Fabrizio et al. (2005) provides amplitudes in the  $V$  passband (hereinafter,  $Amp(V)$ ) for the majority but not all the 71 RR Lyrae stars in our sample. Specifically,  $Amp(V)$  of star A26715 is missing and for five other objects (B6798, A16249, B1907, A28066, B24089) Di Fabrizio et al. (2005) provided more than one value of amplitude, likely because these objects have photometric problems, e.g. blends. On the other hand, the OGLE III catalogue provides Cousins  $I$  band ( $I_C$ ) amplitudes [ $Amp(I)$ ] for all the variables in our list. We have transformed them to  $V_J$

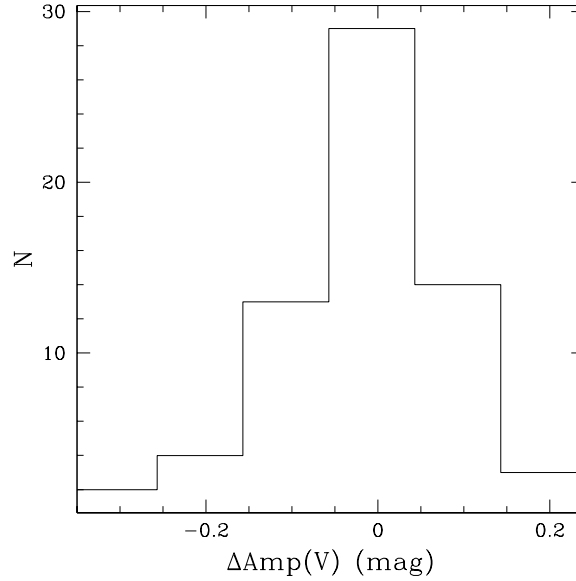


Figure 5.1 Distribution of the differences between the  $V$ -band amplitudes provided by Di Fabrizio et al. (2005) and those derived by transforming to  $Amp(V)$  the  $Amp(I)$  values in the OGLE III catalogue.

amplitudes using the relation by Di Criscienzo et al. (2011):

$$Amp(V) = 1.58 \times Amp(I) \quad (5.1)$$

and have compared the derived  $Amp(V)$  values with those published by Di Fabrizio et al. (2005). This comparison is shown in Fig.5.1. The distribution of amplitude differences is symmetric around the value zero and for the vast majority of sources is smaller than 0.1 mag. Only in a few extreme cases this difference is as large as 0.31 mag. Given the higher completeness of OGLE III dataset, in order to fit templates to the light curves of the 71 RR Lyrae stars in our sample we have thus adopted OGLE III epochs of maximum light and the  $I_C$  amplitudes transformed to  $V_J$  as discussed above. We also corrected for any phase shift between template and data points when necessary. Examples of the  $K_s$ -band light curves of RR Lyrae stars in our sample and their fitting templates are presented in Fig. 5.2.

In order to test the robustness of our determination of the  $K_s$  mean magnitudes using templates, for a number of RR Lyrae stars with evenly sampled light curves mean  $K_s$  magnitudes were also derived by Fourier fitting the light curves with GRATIS period search package. This analysis showed that the  $K_s$  mean magnitudes derived with the GRATIS are consistent within the errors with those obtained by applying templates, thus supporting our

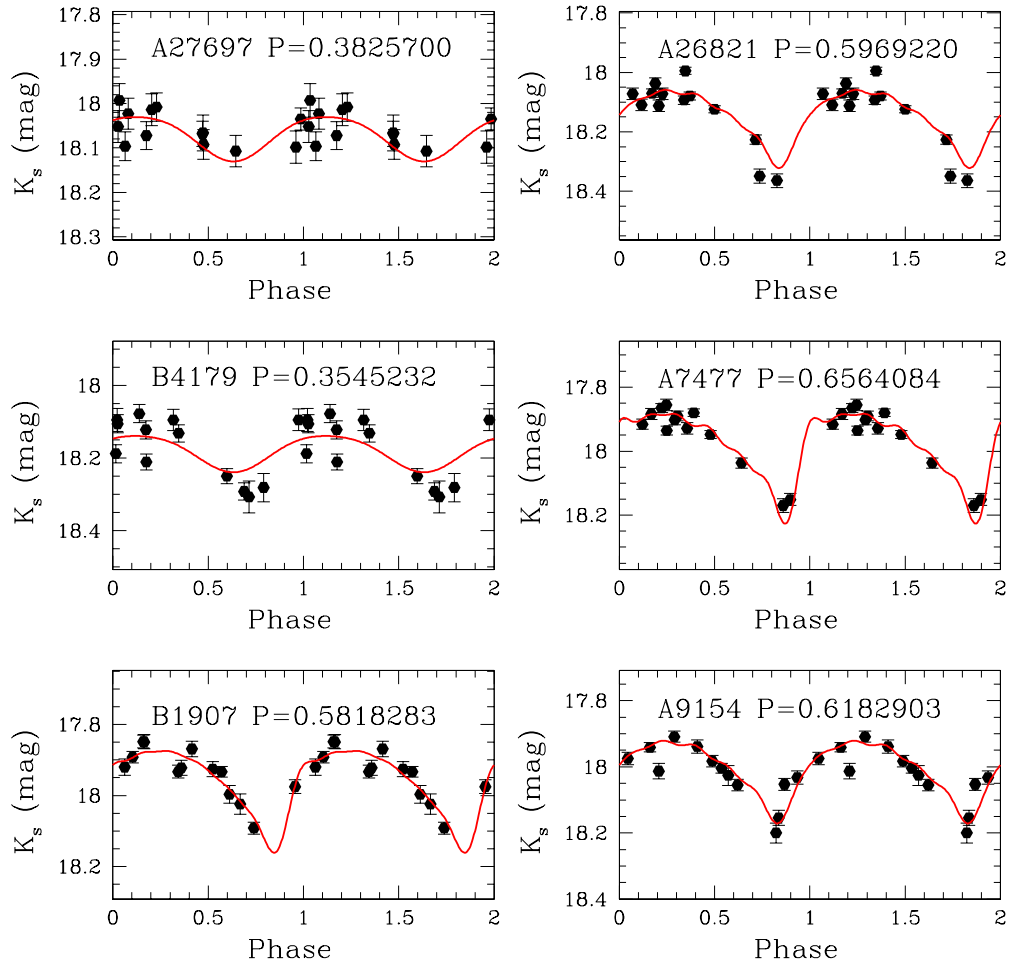


Figure 5.2 Examples of the  $K_s$ -band light curves of RR Lyrae stars in our sample. Identification numbers are from Di Fabrizio et al. (2005), periods are from the OGLE III catalogue (Soszyński et al., 2009) and are given in days. Solid (red) lines are best fitting templates.

estimates of mean  $K_s$  magnitudes via template fitting.

After deriving the  $K_s$  mean magnitudes we performed the dereddening procedure. Clementini et al. (2003) estimated reddening values of  $E(B - V) = 0.116 \pm 0.017$  and  $0.086 \pm 0.017$  mag in fields A and B, respectively, using the method from Sturch (1966) and the colours of the edges of the instability strip defined by the RR Lyrae variables. Applying the coefficients from Cardelli et al. (1989) of  $A_K/A_V = 0.114$  and assuming a ratio of total to selective absorption of  $R_V = 3.1$ , we estimated the extinction in the  $K_s$ -band as:

$$A_{K_s} = 0.35 \times E(B - V) \quad (5.2)$$

Table 5.1 summarizes the properties of the sample of 71 RR Lyrae stars. The first two columns of the table give the identification of the stars in Di Fabrizio et al. (2005) and in the OGLE III catalogue, respectively. The table also shows coordinates and classification of the stars from the OGLE III catalogue, metallicity with errors from Gratton et al. (2004) and dereddened mean  $K_s$  magnitudes, determined by template fitting, along with their errors.



Star	OGLE ID	RA (J2000)	DEC (J2000)	Type	[Fe/H] (dex)	$\sigma_{[\text{Fe}/\text{H}]}$ (dex)	P (days)	$\langle K_{s,0} \rangle$ (mag)	$\sigma_{\langle K_{s,0} \rangle}$ (mag)
A28665	OGLE-LMC-RR1YR-12944	5:22:06.55	-70:27:55.6	c	-0.63	0.24	0.3008299	18.469	0.014
A7864	OGLE-LMC-RR1YR-13857	5:23:39.25	-70:31:38.1	c	-1.36	0.22	0.3129458	18.504	0.014
B4946	OGLE-LMC-RR1YR-10621	5:18:11.08	-70:59:35.6	c	-1.11	0.25	0.3130142	18.369	0.008
A2636	OGLE-LMC-RR1YR-13548	5:23:09.09	-70:39:08.1	c	-1.61	0.29	0.3154437	18.558	0.013
A8837	OGLE-LMC-RR1YR-13326	5:22:45.70	-70:30:14.3	c	-1.52	0.22	0.3165579	18.584	0.011
A8622	OGLE-LMC-RR1YR-13164	5:22:28.93	-70:30:35.9	c	-1.44	0.28	0.3212334	18.405	0.010
A7231	OGLE-LMC-RR1YR-13680	5:23:22.42	-70:32:35.4	c	-1.46	0.26	0.3228047	18.225	0.011
A2234	OGLE-LMC-RR1YR-13479	5:23:01.47	-70:39:44.4	c	-1.53	0.18	0.3228060	18.323	0.009
B4749	OGLE-LMC-RR1YR-10406	5:17:49.73	-71:00:01.4	c	-1.45	0.16	0.3267353	18.364	0.014
A4388	OGLE-LMC-RR1YR-12614	5:21:31.67	-70:36:46.3	c	-1.33	0.27	0.3417737	18.395	0.012
A10113	OGLE-LMC-RR1YR-14046	5:24:00.38	-70:28:06.1	c	-1.52	0.25	0.3506618	18.237	0.012
B6255	OGLE-LMC-RR1YR-10111	5:17:17.88	-70:57:26.4	c	-1.52	0.16	0.3535596	18.297	0.010
B4179	OGLE-LMC-RR1YR-10142	5:17:19.95	-71:01:02.1	c	-1.53	0.27	0.3545232	18.150	0.009
A8812	OGLE-LMC-RR1YR-13150	5:22:26.44	-70:30:19.1	c	-1.23	0.24	0.3549660	18.254	0.013
A26715	OGLE-LMC-RR1YR-12593	5:21:29.33	-70:29:23.4	c	-1.39	0.18	0.3569006	18.291	0.012
A2024	OGLE-LMC-RR1YR-13572	5:23:11.02	-70:40:03.3	c	-1.62	0.26	0.3590534	18.244	0.008
B6164	OGLE-LMC-RR1YR-10612	5:18:10.17	-70:57:30.7	c	-1.88	0.22	0.3744821	18.027	0.008
A27697	OGLE-LMC-RR1YR-13012	5:22:14.03	-70:28:35.0	c	-1.33	0.25	0.3825700	18.030	0.011
A19450	OGLE-LMC-RR1YR-13841	5:23:37.95	-70:34:06.7	ab	-0.76	0.13	0.3979182	18.550	0.011
B7064	OGLE-LMC-RR1YR-10708	5:18:18.63	-70:55:58.7	c	-2.03	0.20	0.4004744	17.997	0.009
B6957	OGLE-LMC-RR1YR-10702	5:18:18.08	-70:56:08.7	c	-1.48	0.18	0.4047399	18.050	0.008
B23502	OGLE-LMC-RR1YR-10509	5:18:00.25	-70:54:31.0	ab	-1.55	0.14	0.4724681	18.249	0.008
A3061	OGLE-LMC-RR1YR-13704	5:23:25.18	-70:38:28.9	ab	-1.26	0.12	0.4744410	18.324	0.009
B10811	OGLE-LMC-RR1YR-10684	5:18:16.01	-71:04:27.0	ab	-1.42	0.20	0.4760753	18.238	0.009
B3400	OGLE-LMC-RR1YR-10072	5:17:14.51	-71:02:26.6	ab	-1.45	0.24	0.4852148	18.344	0.011
A7325	OGLE-LMC-RR1YR-13855	5:23:39.13	-70:32:24.8	ab	-1.18	0.26	0.4864544	18.234	0.009
B3033	OGLE-LMC-RR1YR-10659	5:18:14.04	-71:03:00.5	ab	-1.26	0.21	0.4986975	18.082	0.008
B2055	OGLE-LMC-RR1YR-10108	5:17:17.44	-71:04:50.2	ab	-1.70	0.23	0.5207746	18.253	0.010
A26525	OGLE-LMC-RR1YR-12811	5:21:52.50	-70:29:28.7	ab	-1.41	0.22	0.5225029	18.140	0.008
A7211	OGLE-LMC-RR1YR-13092	5:22:21.17	-70:32:43.9	ab	-1.33	0.19	0.5226857	18.170	0.008

5.1. DATA FOR RR LYRAE STARS IN THE BAR OF THE LMC

A2767	OGLE-LMC-RRLYR-13634	5:23:17.75	-70:38:55.9	ab	-1.37	0.08	0.5325871	18.069	0.012
B24089	OGLE-LMC-RRLYR-10345	5:17:43.51	-70:54:02.7	ab	-1.48	0.16	0.5580613	18.042	0.009
A8788	OGLE-LMC-RRLYR-13678	5:23:22.41	-70:30:14.6	ab	-1.61	0.21	0.5591710	18.177	0.011
A6398	OGLE-LMC-RRLYR-13294	5:22:40.76	-70:33:50.2	ab	-1.40	0.30	0.5619466	17.955	0.008
A7247	OGLE-LMC-RRLYR-13708	5:23:25.58	-70:32:33.4	ab	-1.38	0.21	0.5621512	18.025	0.008
A25301	OGLE-LMC-RRLYR-12638	5:21:34.00	-70:30:24.5	ab	-1.58	0.27	0.5631146	18.279	0.009
A15387	OGLE-LMC-RRLYR-12603	5:21:30.43	-70:37:11.3	ab	-1.81	0.12	0.5635914	18.037	0.009
B22917	OGLE-LMC-RRLYR-10713	5:18:19.10	-70:54:56.1	ab	-1.29	0.16	0.5646803	18.159	0.008
A9245	OGLE-LMC-RRLYR-13536	5:23:07.67	-70:29:36.5	ab	-1.27	0.18	0.5678763	18.043	0.009
A12896	OGLE-LMC-RRLYR-13330	5:22:46.15	-70:38:54.9	ab	-1.53	0.10	0.5719281	18.147	0.008
A7609	OGLE-LMC-RRLYR-13941	5:23:48.39	-70:32:00.3	ab	-1.63	0.11	0.5724984	18.079	0.008
B7442	OGLE-LMC-RRLYR-10082	5:17:15.73	-70:55:26.8	ab	-1.58	0.11	0.5740274	18.017	0.008
A25362	OGLE-LMC-RRLYR-13848	5:23:38.53	-70:30:08.5	ab	-1.39	0.15	0.5787944	18.027	0.008
B1907	OGLE-LMC-RRLYR-10638	5:18:12.36	-71:04:59.5	ab	-1.70	0.26	0.5818283	17.930	0.008
A4974	OGLE-LMC-RRLYR-13372	5:22:51.26	-70:35:47.7	ab	-1.36	0.10	0.5820430	17.996	0.009
B6798	OGLE-LMC-RRLYR-10044	5:17:11.37	-70:56:32.6	ab	-1.40	0.23	0.5822610	17.926	0.011
B14449	OGLE-LMC-RRLYR-09999	5:17:05.37	-71:01:40.9	ab	-1.70	0.13	0.5822854	18.122	0.010
A9494	OGLE-LMC-RRLYR-13354	5:22:49.26	-70:29:13.5	ab	-1.69	0.28	0.5844615	17.908	0.008
A18314	OGLE-LMC-RRLYR-13353	5:22:49.13	-70:34:59.2	ab	-1.42	0.18	0.5875708	18.086	0.010
A10487	OGLE-LMC-RRLYR-13126	5:22:24.61	-70:27:40.6	ab	-1.49	0.11	0.5909585	18.045	0.009
A10214	OGLE-LMC-RRLYR-12609	5:21:31.14	-70:28:12.0	ab	-1.48	0.12	0.5918196	17.913	0.008
A28066	OGLE-LMC-RRLYR-13765	5:23:30.10	-70:28:11.0	ab	-1.44	0.17	0.5959296	17.985	0.009
A26821	OGLE-LMC-RRLYR-12831	5:21:53.95	-70:29:17.5	ab	-1.37	0.13	0.5969220	18.103	0.007
B2249	OGLE-LMC-RRLYR-10061	5:17:13.06	-71:04:27.1	ab	-1.56	0.15	0.6030630	17.983	0.008
A16249	OGLE-LMC-RRLYR-12960	5:22:08.27	-70:36:31.0	ab	-1.87	0.12	0.6067385	18.038	0.007
A4933	OGLE-LMC-RRLYR-13175	5:22:30.05	-70:35:53.7	ab	-1.48	0.12	0.6134920	17.752	0.009
A7734	OGLE-LMC-RRLYR-12956	5:22:07.86	-70:31:59.8	ab	-1.40	0.15	0.6149615	17.891	0.008
A2525	OGLE-LMC-RRLYR-13788	5:23:32.45	-70:39:15.3	ab	-2.06	0.14	0.6161452	17.987	0.008
A9154	OGLE-LMC-RRLYR-13494	5:23:02.93	-70:29:44.6	ab	-1.66	0.14	0.6182903	17.961	0.008
B1408	OGLE-LMC-RRLYR-10067	5:17:13.84	-71:06:06.9	ab	-1.70	0.11	0.6297088	18.002	0.009
A5589	OGLE-LMC-RRLYR-12968	5:22:09.60	-70:35:02.5	ab	-1.60	0.13	0.6375745	17.950	0.008
A7468	OGLE-LMC-RRLYR-13176	5:22:30.06	-70:32:20.6	ab	-1.55	0.11	0.6386908	18.041	0.009
A25510	OGLE-LMC-RRLYR-13002	5:22:13.43	-70:30:11.4	ab	-1.72	0.11	0.6495506	17.718	0.010

A8720	OGLE-LMC-RRLYR-13956	5:23:50.19	-70:30:16.7	ab	-1.88	0.34	0.6508174	17.866	0.008
B7063	OGLE-LMC-RRLYR-10973	5:18:44.05	-70:55:55.8	ab	-1.49	0.14	0.6548698	17.857	0.010
B7620	OGLE-LMC-RRLYR-10541	5:18:03.58	-70:55:03.1	ab	-2.05	0.12	0.6561602	17.734	0.007
A7477	OGLE-LMC-RRLYR-14068	5:24:02.97	-70:32:08.6	ab	-1.67	0.28	0.6564084	17.938	0.007
A28293	OGLE-LMC-RRLYR-12758	5:21:46.13	-70:28:13.3	ab	-1.74	0.10	0.6602890	17.955	0.008
A6426	OGLE-LMC-RRLYR-13196	5:22:32.51	-70:33:48.7	ab	-1.59	0.09	0.6622400	17.841	0.008
A3948	OGLE-LMC-RRLYR-13285	5:22:40.40	-70:37:17.0	ab	-1.46	0.12	0.6623845	17.956	0.008
A8094	OGLE-LMC-RRLYR-13306	5:22:43.06	-70:31:23.7	ab	-1.83	0.12	0.7420663	17.870	0.008

Table 5.1: Properties of the 71 RR Lyrae stars in the VMC tile LMC

5\_5 used to derive a new  $PL_{K_s}$   $Z$  relation (Column 1: Identification of the star from Di Fabrizio et al. (2005); Column 2: Identification from the OGLE III catalogue (Soszyński et al., 2009); Column 3: Right ascension (OGLE); Column 4: Declination (OGLE); Column 5: RR Lyrae type; Column 6: Metallicity from Gratton et al. (2004); Column 7: Error of metallicity from Gratton et al. (2004); Column 8: Period (OGLE); Column 9: Dereddened mean  $K_s$  magnitude from the VMC survey; Column 10: Error of the mean  $K_s$  magnitude).

## 5.2 $PL_{K_s}Z$ relation of RR Lyrae stars in the LMC

### 5.2.1 Method

Using the dereddened mean  $K_s$  magnitudes of the 71 RR Lyrae stars derived as described in Section 5.1, spectroscopically determined metallicities from Gratton et al. (2004) and accurately estimated periods from the OGLE III catalogue (with RRC stars "fundamentalized" by adding 0.127 to the logarithm of the period) we can now fit the  $PL_{K_s}Z$  relation. The fit was performed using a Bayesian fitting approach developed by Max Palmer, PhD student of the University of Barcelona. This method takes into account potentially significant intrinsic dispersion of the data, not-negligible errors in two dimensions ( $K_s$  and [Fe/H]) and the possibility of inaccuracy in the formal error estimates (e.g. in the determination of the precision metallicity estimates). The detailed description of the method is presented in Muraveva et al. (2014b, submitted to AJ).

By applying this method we found the following relation between periods of pulsation, metallicities and mean apparent  $K_s$  magnitudes determined with templates:

$$\begin{aligned}
 K_{s,0} &= (-2.70 \pm 0.22)\log P + (0.03 \pm 0.06)[\text{Fe}/\text{H}] \\
 &+ (17.44 \pm 0.05)
 \end{aligned}
 \tag{5.3}$$

The intrinsic dispersion of the relation is found to be 0.09 mag.

The projections of the  $PL_{K_s}Z$  relation (Eq. 5.3) on the  $\text{Log}(P) - K_s$  and  $K_s - [\text{Fe}/\text{H}]$  planes is shown in Figure 5.3. The grey lines in the figure are lines of equal metallicity (top) or equal period (bottom). The method finds the relation (values of A, B, and C for the relation  $K_s = A \log P + B [\text{Fe}/\text{H}] + C$ ) in three dimensions ( $\log P$ ,  $K_s$ , and  $[\text{Fe}/\text{H}]$ ). So each of the grey lines in the top plot are  $K_s = A \log P + B [\text{Fe}/\text{H}] + C$  for the full range of periods, at the metallicity of each star (one line per star). Thus, by following the line up and down it is seen how  $K_s$  changes with period at some specific metallicity. The lines do not always cross the points on the diagram because the line is the result of the fit, and the points are affected by errors and intrinsic dispersion so may be above or below the fit. In the bottom plot the lines are  $K_s = A \log P + B [\text{Fe}/\text{H}] + C$  for the full range of metallicity with  $\log P$  taken from each star.

It is worth noting that we find a very small dependence of the  $K_s$  magnitude on the metallicity. However, the metal abundance range spanned by our RR Lyrae stars does not

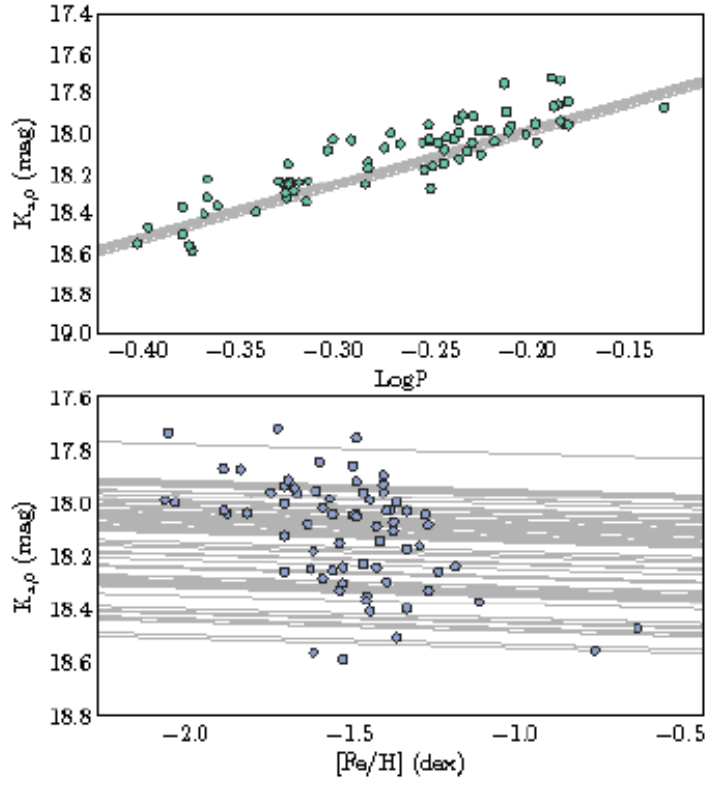


Figure 5.3 Projections of the  $PL_{K_s}Z$  relation (given in Eq. 5.3) on the  $\text{Log}(P)$  versus  $K_s$  (top panel) and  $K_s$  versus  $[\text{Fe}/\text{H}]$  (bottom panel) planes. Grey lines represent lines of equal metallicities (top panel) and periods (bottom panel).

reach the highest values (up to solar and supersolar) observed in the MW bulge and disk RR Lyrae populations.

### 5.2.2 Zero-point of the $PL_{K_s}Z$ relation

To use the derived  $PL_{K_s}Z$  relation for determining distances it is necessary to calibrate its zero-point. This can be done in a number of different ways. In this study we follow two different approaches: the first one is based on adopting a value for the distance of the LMC; in the second approach we use the absolute magnitudes of Galactic RR Lyrae stars for which trigonometric parallaxes have been measured with the *HST*/FGS (Benedict et al., 2011). Both approaches have their advantages and disadvantages, we discuss them in the following sections.

### Zero-point based on the LMC distance

The measure of the distance to the LMC has been the subject of many studies (see Section 2.3). A recent determination of direct distances to eight long-period EBs in the LMC was presented by Pietrzyński et al. (2013) and claimed to be accurate to  $\sim 2\%$ :  $D_{LMC} = 49.97 \pm 0.19$  (stat)  $\pm 1.11$  (syst) kpc, corresponding to the distance modulus  $(m - M)_0 = 18.494 \pm 0.049$  mag.

The RR Lyrae stars in our sample are located in a relatively small area close to the center of the LMC bar. Neglecting depth/projection effects they can be considered as being all at the same distance from us and close to late-type EBs (Pietrzyński et al., 2013), which are all located relatively close to the barycentre of the LMC. In the following analysis we adopted for the distance modulus of the LMC the value published by Pietrzyński et al. (2013) and subtracted this value from the dereddened mean  $K_s$  apparent magnitudes of our 71 RR Lyrae stars to derive absolute  $K_s$  magnitudes ( $M_K$ ). Then by applying the technique described in Section 5.2.1 we derived the relation between absolute magnitudes, periods and metallicities obtaining for the zero-point the value of:  $-1.05 \pm 0.05$  mag (see column 2 of Table 5.2). In using the late-type EBs to calibrate the RR Lyrae  $PL_{K_s}Z$  relation we have implicitly assumed that RR Lyrae stars and EBs are at same distance from us. However, when pushing for distance comparisons at a few percent level the effects of sample size, spatial distribution, depth and geometric projection become important and properly accounting for the internal structure of the LMC may become necessary (see e.g. Fig. 2.1 for different features of the LMC structure traced by CCs, RR Lyrae stars and HEBs).

### Zero-point based on trigonometric parallaxes of Galactic RR Lyrae stars

In order to obtain an estimate of the  $PL_{K_s}Z$  relation zero-point which is independent from the distance to the LMC and, in turn, be able to measure the distance to this galaxy from the  $PL_{K_s}Z$  relation, it is necessary to know the RR Lyrae absolute magnitude with reasonable accuracy. Trigonometric parallaxes remain the only direct method to measure distances and hence derive absolute magnitudes (see Section 1.1). Benedict et al. (2011) derived absolute trigonometric parallaxes for five Galactic RR Lyrae stars (RZ Cep, XZ Cyg, SU Dra, RR Lyr and UV Oct) with the *HST*/FGS. With these parallaxes the authors estimated absolute magnitudes in the  $K$  and  $V$  passbands, corrected for interstellar extinction and Lutz-Kelker-Hanson bias (hereinafter LKH, Lutz & Kelker 1973, Hanson 1979). Absolute magnitudes

Relation	ZP from $D_{LMC}$	ZP from Benedict et al. (2011)
$M_K = (-2.70 \pm 0.22)\log P + (0.03 \pm 0.06)[\text{Fe}/\text{H}]_{\text{Har}} + ZP$	$(-1.05 \pm 0.05)$	$(-1.27 \pm 0.08)$

Table 5.2 Absolute calibration of the new  $PL_{K_s}Z$  relation.

in the  $K_s$ -band, periods and metallicities from Benedict et al. (2011), and the slopes of the relation derived in Eq. 5.3 were used in order to determine a zero-point from each of these five MW RR Lyrae stars. The metallicities in Benedict et al. (2011) are in the Zinn & West metallicity scale and were converted to the metallicity scale in Gratton et al. (2004) by adding 0.06 dex. The logarithm of the period of the RRc star RZ Cep was "fundamentalized" by adding 0.127. Then we calculated the weighted mean of the five zero-points, this corresponds to:  $-1.27 \pm 0.08$  mag (see column 3 of Table 5.2).

There is a difference of  $\sim 0.2$  mag between the two zero-points. In fact, if we apply our  $PL_{K_s}Z$  relation with zero-point calibrated on Benedict et al. (2011) parallaxes to determine the absolute magnitudes of the 71 RR Lyrae stars in our sample, we obtain a distance modulus for the LMC, determined as the weighted average of the distance moduli of these 71 RR Lyrae stars, of  $(m - M)_0 = 18.71 \pm 0.01$  mag with  $\sigma = 0.09$ . This distance modulus is about 0.2 mag longer than the widely adopted value of  $(m - M)_0 = 18.5$  mag.

There are a number of possible explanations for this discrepancy. First of all, we assumed that all RR Lyrae stars in our sample are located at the same distance from us, equal to the distance derived from the LMC EBs analysed by Pietrzyński et al. (2013). However, the RR Lyrae stars could in fact be distributed along the whole depth of the LMC. Furthermore, RR Lyrae stars and EBs from Pietrzyński et al. (2013) could reside in different sub-structures of the LMC, which could be the reason for the systematic error in the determination of the zero-point. On the other hand, when calibrating the zero-point by applying the parallaxes of the MW RR Lyrae stars by Benedict et al. (2011) we implicitly assume that the  $PL_{K_s}Z$  relation is the same in the MW and in the LMC, which may not be true. It is well known, in fact, that the LMC is in general more metal-poor than our Galaxy. The difference in metal abundances could affect the  $PL_{K_s}Z$  relation of RR Lyrae stars. Indeed, as mentioned above, the derived low metallicity dependence of our  $PL_{K_s}Z$  relation could be due to the smaller metallicity range covered by the LMC RR Lyrae stars, that does not reach the highest values of the Galactic variables.

We may also wonder whether there might be unknown systematic errors affecting Benedict et al.'s parallaxes. These come from *HST* fields, which provide relative and not absolute

trigonometric parallaxes. Absolute parallaxes of the reference stars in each field are estimated via a complex procedure of fitting the spectral type and luminosity class of each star. A general formal error of 0.5 mas is applied to the absolute parallax of the reference stars, equal for all stars in all fields, and without justification. This could result in miscalculated estimates of the precision of the final absolute parallax measurements of the five RR Lyrae stars. The Lutz-Kelker bias is corrected a posteriori. In this respect it is worth of notice that, according to van Leeuwen (2007), Hipparcos parallax of RR Lyrae itself, the only RR Lyrae variable for which the satellite could measure the parallax with some precision ( $\pm 0.64$  mas), is about 0.31 mas smaller than (Benedict et al., 2011)'s parallax for this star, although consistent with it within the errors, hence, the corresponding distance modulus is about 0.17 mag longer. In any case, a great contribution to the determination of the zero-point of the RR Lyrae  $PL_{K_s}Z$  relation is expected from the ESA astrometric satellite Gaia. We discuss this topic in Section 5.3.

We compared our new  $PL_{K_s}Z$  relation (Table 5.2) with the relations in the literature (see Section 1.5.2). The slope in period of the RR Lyrae  $PL_{K_s}Z$  relation differs significantly in different studies. The value derived in the present study is in excellent agreement with that derived by Del Principe et al. (2006). Metallicities in all studies, but Sollima et al. (2008) one, are on the Zinn & West scale, while in the current study are on a scale, which is systematically 0.06 dex higher than the Zinn & West one. Since the difference between two scales is small, this should not affect significantly the results of this comparison. The dependence on metallicity of the  $PL_{K_s}Z$  relation also varies significantly among the different studies. Our slope in metallicity is the smallest among all previous studies and it is closer to that found by Borissova et al. (2009).

### 5.3 Gaia observation of RR Lyrae stars in the Milky Way

The Gaia astrometric satellite will revolutionise many fields of astronomy (Perryman et al., 2001). Of particular importance will be its catalogue of trigonometric parallaxes for more than one billion stars, with astrometric precision to the  $\mu\text{as}$  level (see Section 1.2). Due to Gaia's constant observation of the sky over the five-year nominal mission, the satellite will repeatedly observe all stars brighter than its limiting magnitude, with an average of 80 observations per star. This will also make it possible for Gaia to discover and characterise many types of variables, including RR Lyrae stars and Cepheids.



Gaia is observing in the broad visual band  $G$  (Jordi et al., 2010) for its astrometric measurements, and is therefore not ideal for characterising the RR Lyrae  $PLZ$  relation, which exists only in the infrared passbands. However, since Gaia will provide accurate parallaxes for an expected tens of thousands of MW RR Lyrae stars, it could serve as a perfect tool for the determination of the zero-point of the  $PL_{K_s}Z$  relation through the combination with external datasets. Moreover, Gaia will contribute significantly to the determination of the luminosity-metallicity relation of RR Lyrae stars in the visual passband. The current largest limiting factor in the zero-point calibration of the  $PL_{K_s}Z$  and  $M_V - [\text{Fe}/\text{H}]$  relations is the lack of a reliable and statistically significant sample of parallax measurements. The current state of the art is the sample of five RR Lyrae parallaxes from Benedict et al. (2011) using the *HST*. Gaia will improve this situation by several orders of magnitude in both precision and numbers of objects.

In order to study the impact of Gaia in the determination of the  $PM_{K_s}Z$  and  $M_V - [\text{Fe}/\text{H}]$  relations we have selected a sample of 25 bright Galactic fundamental-mode RR Lyrae stars with known metallicities and photometry in the  $K_s$  and  $V$  bands. We estimated distances to the selected variables by comparing apparent and absolute magnitudes determined on the basis of the  $PM_{K_s}Z$  relation derived in this thesis work (Table 5.2) and the  $M_V - [\text{Fe}/\text{H}]$  relation (Eq. 14) in Benedict et al. (2011). Then we simulated parallaxes along with their errors for the selected RR Lyrae stars, assuming nominal Gaia mission performance. The simulation of Gaia parallaxes was performed by M. Palmer, using the Gaia Object Generator (GOG; Luri et al. 2014, see Subsection 5.3.1). By using simulated parallaxes including observational errors we recalculated the  $PM_{K_s}Z$  and  $M_V - [\text{Fe}/\text{H}]$  relations and compare them with those used for the estimate of parallaxes. This exercise is designed to show if parallaxes determined with Gaia will allow us to derive the "true"  $PM_{K_s}Z$  and  $M_V - [\text{Fe}/\text{H}]$  relations.

Information about the 25 RRab stars in the MW, for which we simulate Gaia parallaxes, is presented in Table 5.3. Stars listed in this table were selected because they are close and bright enough ( $V < 11.5$  mag) to have Gaia parallaxes determined better than 2-3%. Moreover, these objects have spectroscopically derived metallicities and are the least reddened of the nearby RR Lyrae stars. Many of them have been analysed in radial velocities and Baade-Wesselink studies, and they do not exhibit a strong Blazko effect (Blazko, 1907). Three of these stars are part of the sample used in this thesis work to calibrate the zero-point of the  $PL_{K_s}Z$  relation (see Subsection 5.2.2).

Feast et al. (2008) derived mean  $K_s$  magnitudes of these RR Lyrae stars, by using single-epoch  $K_s$  photometry from 2MASS (Cutri et al. 2003), ephemerides of the stars, amplitudes in the visual passband and template fitting of the  $K_s$  light curves. Feast et al. (2008) compared the derived mean  $K_s$  magnitudes with those obtained by Fernley et al. (1993), and declare that the difference is  $0.008 \pm 0.0015$  mag. For comparison, the average error of the dereddened mean  $K_s$  magnitudes of our sample of 71 RR Lyrae stars in the LMC (Table 5.1), derived by applying templates, is 0.009 mag. Since Feast et al. (2008) did not provide the errors for the mean  $K_s$  magnitudes of the individual RR Lyrae stars in their sample, we assumed a worse case scenario with an error of  $\sim 0.01$  mag and consider this value in the determination of absolute magnitudes in the  $K_s$  passband. Feast et al. (2008) also provided information about the reddening of the 25 RR Lyrae stars. We used these values of reddening, but since these RR Lyrae stars have small values of reddening, especially in the  $K_s$  passband, we consider the errors in the reddening to be negligible.

We performed the transformation from the 2MASS system to the VISTA system, by using mean  $K_s$  and J magnitudes (Feast et al., 2008) and applying the empirical relations provided by the Cambridge Astronomy Survey Unit (CASU)<sup>1</sup>:

$$K_s(VISTA) = K_s(2MASS) + 0.010 \times (J - K_s)(2MASS) \quad (5.4)$$

Metallicities for the 25 RR Lyrae stars, calibrated to the Zinn & West metallicity scale, were determined spectroscopically by Layden (1994). We converted them to the metallicity scale of our sample of 71 RR Lyrae stars by adding 0.06 dex (Gratton et al., 2004). The periods of the RR Lyrae variables are taken from Feast et al. (2008), and coordinates are from the SIMBAD database.

### 5.3.1 Simulated Gaia data

GOG (Luri et al., 2014) is designed to simulate both individual Gaia observations and the full contents of the end-of-mission catalogue (see Section 1.2). GOG is capable of determining the expected precision in astrometric, photometric and spectroscopic observations of Gaia. In general, the precision depends on the apparent magnitude of the star, its colour, and its sky position, which affects the number and type of observations made (due to the Gaia scanning law).

---

<sup>1</sup><http://casu.ast.cam.ac.uk/surveys-projects/vista/technical/photometric-properties>

To obtain an absolute magnitude for each RR Lyrae star in our sample of 25 bright MW variables, we used:

$$M_{K_s} = -2.70 \log P + 0.03[\text{Fe}/\text{H}] - 1.05 \quad (5.5)$$

as determined in Table 5.2 and the zero-point fixed by the distance to the LMC. We then obtained a distance by combining this absolute magnitude with the apparent magnitude and extinction as defined above. Colour information as (V-I) was obtained from the Hipparcos catalogue (Perryman and ESA, 1997) where available. The apparent magnitude, position, colour, period, and metallicity data form the basis of a synthetic catalogue of RR Lyrae stars, along with the distance obtained from the  $PM_{K_s}Z$  relation, and is used as the input catalogue of ‘true’ parameters for GOG. GOG then creates simulated Gaia observations for our sample. We take the  $PM_{K_s}Z$  relation (Eq. 5.5) as true, as a study of the possible precision in  $PL_{K_s}Z$  calibration after the Gaia data will become available. Table 5.3 gives the  $M_{K_s}$  magnitudes and parallaxes of the 25 MW RR Lyrae stars.

Using the fitting method described in Sect. 5.2.1 to the data including the simulated parallax observations and simulated errors applied to parallax, metallicity and apparent magnitude, we find a  $PM_{K_s}Z$  relation of:

$$\begin{aligned} M_{K_s} = & (-2.70 \pm 0.07) \log P + (0.028 \pm 0.008)[\text{Fe}/\text{H}] \\ & + (-1.01 \pm 0.03) \end{aligned} \quad (5.6)$$

Comparison of these results to the input  $PL_{K_s}Z$  relation shows very good agreement. This shows that the capabilities of fitting the absolute  $PL_{K_s}Z$  relation using Gaia parallaxes for the 25 selected MW RR Lyrae stars will allow a precision in the zero-point of around 0.03 mag. Moreover, this is an additional test that the fitting procedure given in Sect. 5.2.1 is accurate and unbiased.

5.3. GAIA OBSERVATION OF RR LYRAE STARS IN THE MILKY WAY

Star	RA (deg)	DEC (deg)	$\pi_{Hipparcos}$ (mas)	$\sigma_{Hipparcos}$ (mas)	$\pi_{Gaia}$ (mas)	$\sigma_{Gaia}$ (mas)	E(B-V) (mag)	P (day)	[Fe/H] (dex)	$\sigma_{[Fe/H]}$ (dex)	$K_s,VISTA$ (mag)	$M_K$ (mag)	$\sigma_{M_K}$ (mag)	$M_V$ (mag)	$\sigma_{M_V}$ (mag)
RR Lyr	291.36630	42.78436	3.46	0.64	4.151	0.007	0.030	0.566839	-1.31	0.08	6.492	-0.428	0.011	0.494	0.011
X Ari	47.12869	10.44590	0.88	1.32	1.961	0.019	0.180	0.651154	-2.34	0.09	7.945	-0.655	0.023	0.308	0.027
RX Eri	72.43455	-15.74118	1.50	1.12	1.685	0.020	0.058	0.587246	-1.24	0.16	8.432	-0.455	0.027	0.502	0.013
SW And	5.92954	29.40101	1.48	1.21	1.907	0.021	0.038	0.442262	-0.32	0.17	8.508	-0.103	0.026	0.709	0.013
SV Eri	47.96711	-11.35391	1.48	1.67	1.370	0.006	0.085	0.713865	-1.98	0.07	8.645	-0.701	0.014	0.339	0.014
RR Cet	23.03405	1.34173	-1.29	1.35	1.627	0.023	0.022	0.553030	-1.46	0.12	8.523	-0.428	0.032	0.473	0.014
DX Del	311.86815	12.46408	0.77	1.38	1.695	0.005	0.092	0.472618	-0.50	0.12	8.689	-0.198	0.012	0.657	0.012
SU Dra	174.48586	67.32974	0.20	1.13	1.425	0.005	0.010	0.660418	-1.68	0.14	8.622	-0.613	0.012	0.413	0.013
XZ Cyg	293.12211	56.38819	2.29	0.84	1.670	0.021	0.096	0.466610	-1.46	0.11	8.725	-0.195	0.029	0.456	0.012
VY Ser	232.75803	1.68382	-1.28	1.57	1.235	0.007	0.040	0.714101	-1.76	0.23	8.830	-0.725	0.016	0.408	0.017
V Ind	317.87460	-45.07455	1.57	1.47	1.440	0.007	0.043	0.479604	-1.44	0.11	8.988	-0.235	0.014	0.469	0.015
XZ Dra	287.42754	64.85893	2.26	0.88	1.361	0.007	0.062	0.476497	-0.81	0.09	9.150	-0.202	0.015	0.590	0.016
BH Peg	343.25432	15.78794	0.31	1.82	1.194	0.008	0.077	0.640991	-1.32	0.21	9.070	-0.572	0.018	0.498	0.016
SW Dra	184.44429	69.51062	-0.46	1.29	1.131	0.007	0.014	0.569671	-1.18	0.07	9.322	-0.416	0.016	0.512	0.015
SV Hya	187.62710	-26.04754	4.49	1.76	1.226	0.008	0.080	0.478542	-1.64	0.27	9.369	-0.216	0.018	0.423	0.017
RU Scl	0.70046	-24.94530	-0.11	1.42	1.275	0.007	0.018	0.493347	-1.19	0.13	9.231	-0.247	0.016	0.522	0.017
AV Peg	328.01164	22.57483	2.28	1.72	1.397	0.006	0.067	0.390378	-0.08	0.22	9.349	0.051	0.014	0.755	0.014
XX And	19.36423	38.95056	2.54	1.90	0.953	0.006	0.039	0.722755	-1.95	0.07	9.412	-0.705	0.016	0.372	0.017
RV Oct	206.63230	-84.40177	1.32	1.32	1.057	0.006	0.180	0.571169	-1.28	0.25	9.530	-0.413	0.016	0.507	0.017
RS Boo	218.38839	31.75462	0.11	1.40	1.298	0.005	0.012	0.377339	-0.26	0.31	9.509	0.071	0.013	0.716	0.012
WY Ant	154.02061	-29.72845	-0.24	1.61	0.956	0.006	0.059	0.574341	-1.60	0.20	9.677	-0.441	0.017	0.423	0.018
UY Boo	209.69307	12.95179	1.00	1.80	0.866	0.006	0.033	0.650889	-2.43	0.16	9.726	-0.597	0.018	0.270	0.022
RY Col	78.78242	-41.62824	1.36	1.34	1.053	0.006	0.026	0.478832	-1.05	0.17	9.705	-0.193	0.016	0.536	0.019
DN Aqr	349.82168	-24.21633	1.82	2.11	0.809	0.008	0.025	0.633757	-1.57	0.15	9.903	-0.566	0.024	0.431	0.022
AN Ser	238.37938	12.96115	-1.71	2.93	0.949	0.007	0.040	0.522069	0.02	0.21	9.845	-0.283	0.019	0.788	0.018

Table 5.3: Properties of 25 bright fundamental-mode RR Lyrae stars in the MW (Column 1: Name of the star; Column 2: Right Ascension (J2000) from SIMBAD database; Column 3: Declination (J2000) from SIMBAD database; Column 4: Parallaxes from the revised *Hipparcos* catalogue (van Leeuwen, 2007); Column 5: Errors of parallaxes from *Hipparcos* catalogue (van Leeuwen, 2007); Column 6: Gaia parallaxes simulated using Eq. 5.5; Column 7: Simulated errors of Gaia parallaxes; Column 8: Reddening from Feast et al. (2008); Column 9: Periods from Feast et al. (2008); Column 10: Metallicity from Layden (1994) calibrated to the metallicity scale of the 71 LMC RR Lyrae stars by adding 0.06 dex; Column 11: Errors in metallicity from Layden (1994); Column 12:  $K_s$  apparent magnitude in the VISTA system; Column 13: Calculated absolute magnitude in the  $K_s$  passband; Column 14: Errors in the absolute  $K_s$  magnitude; Column 15: Calculated absolute magnitude in the  $V_J$  passband; Column 16: Errors in the absolute  $V_J$  magnitude).

### 5.3.2 Simulation of the $M_V - [\text{Fe}/\text{H}]$ relation of RR Lyrae stars in the Milky Way

We applied the same approach in order to check if it will be possible to derive the  $M_V - [\text{Fe}/\text{H}]$  relation of RR Lyrae stars by using Gaia data. We used metallicities from Layden (1994) and apparent  $V$  magnitudes from Fernley et al. (1998b). Fernley et al. (1998b) mean  $V$  magnitudes were derived from the Hipparcos photometry and compared with mean  $V$  magnitudes for 11 RRab and 2 RRC stars from Liu & Janes (1990). The mean difference was found to be 0.003 mag with an rms scatter of 0.007 mag (Fernley et al., 1998b). We assume a conservative error on the apparent mean magnitudes of  $\sim 0.01$  mag and consider this value in the determination of absolute magnitudes in the  $V$  passband. We applied the values of reddening  $E(B-V)$  from Feast et al. (2008) and determined the extinction using the relation:

$$A_V = 3.1E(B - V) \quad (5.7)$$

In order to obtain absolute  $M_V$  magnitudes for the 25 RR Lyrae stars we applied the relation in Benedict et al. (2011):

$$M_V = (0.214 \pm 0.047)([\text{Fe}/\text{H}] + 1.5) + (0.45 \pm 0.05), \quad (5.8)$$

where the metallicity is in the Zinn & West scale. Eq. 5.8 was derived using the slope obtained by Gratton et al. (2004) and the zero-point determined from the *HST* parallaxes of the five MW RR Lyrae stars measured by Benedict et al. (2011). Applying the procedure described in Section 5.3.1 we simulated Gaia parallaxes and related errors of the 25 RR Lyrae stars. To fit the relation we used the method developed by M. Palmer for two dimensions and determined a new  $M_V - [\text{Fe}/\text{H}]$  relation:

$$M_V = (0.208 \pm 0.003)([\text{Fe}/\text{H}] + (0.779 \pm 0.005)) \quad (5.9)$$

As it could be seen using Gaia parallaxes for only 25 RR Lyrae variables will allow us to recover the slope of the relation within 3%, and to recover the zero-point to within 1%. Obviously a larger sample of RR Lyrae stars with Gaia parallaxes will allow us to determine the  $M_V - [\text{Fe}/\text{H}]$  and  $PL_{K_s}Z$  relations with much greater precision. The main issues in

### 5.3. GAIA OBSERVATION OF RR LYRAE STARS IN THE MILKY WAY

the future will be concerned with the accurate estimate of metallicities, mean  $K_s$  and  $V$  magnitudes, and reddening.

## Chapter 6

# RR Lyrae stars in the VMC tile LMC 8\_3

### 6.1 Classification of EROS-2 candidate RR Lyrae stars

The EROS-2 survey provided light curves in the  $B_{EROS}$  and  $R_{EROS}$  passbands for 16337 candidate RR Lyrae stars in the LMC, selected from EROS-2 catalogue of candidate variables on the basis of the  $B_{EROS}$ ,  $B_{EROS} - R_{EROS}$  CMD (see left panel of Figure 2.3). We crossmatched the EROS-2 catalogue of candidate RR Lyrae stars against the VMC catalogue (internal VMC release from 5 August 2013) and found 5570 sources in common. Among them we selected objects which are located in the tile LMC 8\_3 (291 stars in total). After discarding objects with periods longer than 4.1 days<sup>1</sup>, we obtained a sample of 268 candidate RR Lyrae stars which have a counterpart in the VMC catalogue. This sample includes also star Im0303n13977 which according to EROS-2 should have a period  $P_{EROS} = 918.06335$  days. However, in the OGLE III catalogue this star is listed among the RR Lyrae stars with a period around half a day. We visually inspected the EROS-2 light curve of the star with GRATIS and derived a new period  $P = 0.499556$  days which in excellent agreement with OGLE III's. By applying Eqs. 2.1 and 2.2 we transformed the  $B_{EROS}$  and the  $R_{EROS}$  magnitudes to Johnson  $V$  magnitudes and analysed the light curves of the 268 candidate RR Lyrae stars in the  $B_{EROS}$  and  $V$  passbands with GRATIS. We corrected the period provided by the EROS-2 survey for four stars, namely: Im0303n13977, Im0434120435, Im0301125140 and Im0291126545. Through the visual inspection of the light curves we performed a preliminary classification of RRab, RRc, RRd stars and misclassified objects, which light curves do not have the characteristic shape of a RR Lyrae star. According to the

---

<sup>1</sup>This limit in period was chosen as to include typical periods of RR Lyrae stars and their most frequent aliases.

visual inspection of the light curves, our sample includes 252 confirmed RR Lyrae stars and 16 misclassified sources which mainly are EBs.

To classify the 268 candidate RR Lyrae stars we also plotted them on the  $\text{Log}P$  versus  $\text{Amp}V$  diagram, (see Fig. 6.1). In this figure one can distinguish three main groups of objects:

- $\text{Log}P < -0.7$  and  $\text{Log}P > -0.05$ : misclassified objects
- $-0.7 \leq \text{Log}P \leq -0.3$  and  $\text{Amp}(V) \leq 0.8$  mag: RRc stars
- $-0.4 \leq \text{Log}P \leq -0.3$  and  $\text{Amp}(V) > 0.8$  mag or  $-0.3 \leq \text{Log}P \leq 0.05$ : RRab stars

Twelve sources lie outside both the RRab and the RRc regions. All of them but one were classified as non-RR Lyrae stars by the visual inspection of the light curves with GRATIS. One object among these 12 stars (lm0291n13464) was classified as RRc after analysis of the light curve. However, the star is located outside the regions of RR Lyrae stars in the period-amplitude diagram (Figure 6.1), hence, we discarded it. Five objects (lm0434m21890, lm0300n19430, lm0303k15709, lm0303n10802, lm0303l25724) were classified as RRab with the period-amplitude diagram, but after the analysis with GRATIS they all were discarded, since they are misclassified sources. Similarly, ten stars were classified as c-type RR Lyrae stars with the period-amplitude diagram, but the analysis with GRATIS showed that they are in fact RRd stars. Information about these RRd stars and the comparison with the OGLE III catalogue, for those which were observed also by the OGLE III survey, is presented in Table 6.1.

The final catalogue of confirmed RR Lyrae stars in tile LMC 8\_3, for which EROS-2 and VMC data are available contains 251 sources. The sample includes 167 RRab, 74 RRc and 10 RRd stars. For each star we derived mean magnitudes, amplitudes, epochs of maximum light in the  $B_{EROS}$  and  $V$  passbands. Some of these parameters and the classification in type of the 251 RR Lyrae stars are presented in Table 6.2.



EROS-2 id	$P_1$	$P_0$	$P_1/P_0$	OGLE III $P_1$	OGLE III $P_0$	OGLE III $P_1/P_0$
lm0293k.30764	0.353758	0.475592	0.7438	0.3537438	0.4755950	0.7438
lm0435k.8479	0.365147	0.490433	0.7445	-	-	-
lm0444l.8138	0.354920	0.476967	0.7441	-	-	-
lm0293n.14230	0.362863	0.487836	0.7438	0.3629116	0.4878202	0.7440
lm0310l.12653	0.362132	0.486196	0.7448	0.3621078	0.4861951	0.7448
lm0303m.23391	0.385532	0.516902	0.7459	0.3855124	0.5168991	0.7458
lm0303k.24363	0.391872	0.524815	0.7467	0.3918820	0.5247920	0.7467
lm0301n.13911	0.357182	0.479980	0.7442	-	-	-
lm0291n.25922	0.365509	0.490849	0.7446	-	-	-
lm0301l.26933	0.360587	0.484494	0.7443	0.3605884	0.4844985	0.7443

Table 6.1 RRd stars in tile LMC 8\_3. (Column 1: EROS-2 identification number; Column 2: First-overtone period derived with GRATIS; Column 3: Fundamental mode period derived with GRATIS; Column 4: Ratio of the periods; Column 5: First-overtone period from the OGLE III catalogue; Column 6: Fundamental mode period from the OGLE III catalogue ; Column 7: Ratio of the periods from the OGLE III catalogue).

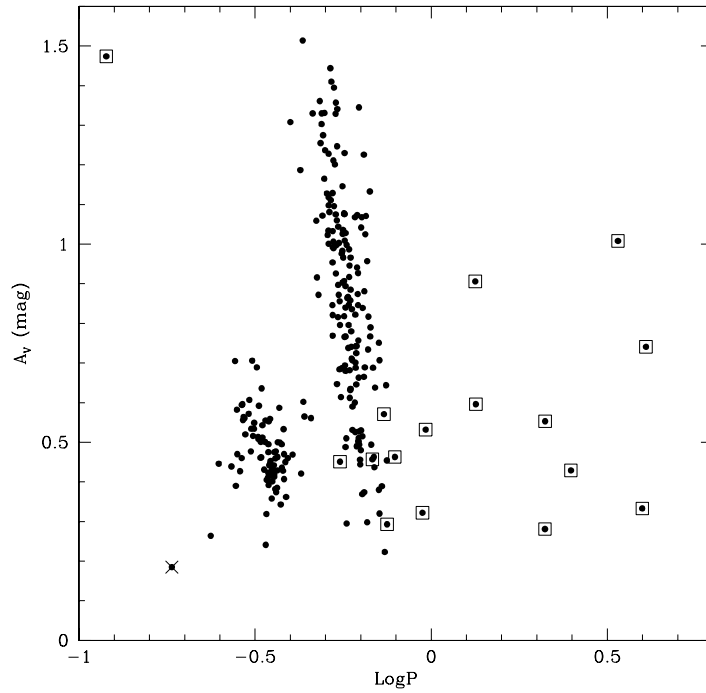


Figure 6.1 Period-amplitude diagram of the 268 candidate RR Lyrae stars in tile LMC 8\_3. Misclassified objects discarded from the following analysis include: short period variables (crosses) and EBs (squares).

6.1. CLASSIFICATION OF EROS-2 CANDIDATE RR LYRAE STARS

EROS-2 id	RA (deg)	DEC (deg)	Period (days)	$\langle B_{EROS} \rangle$ (mag)	$Amp(B)$ (mag)	$\langle V \rangle$ (mag)	$Amp(V)$ (mag)	Epoch(max) V	Type
lm0301n16576	77.03389	-66.49982	0.236645	18.75	0.21	18.87	0.26	2452164.7465	c
lm0305m3332	76.89820	-66.96981	0.249311	19.51	0.36	19.67	0.45	2451193.5867	c
lm0300l15247	75.80446	-66.50370	0.270920	19.35	0.35	19.45	0.44	2451589.6512	c
lm0436l17456	76.22323	-66.18169	0.277319	19.55	0.61	19.60	0.71	2451922.6709	c
lm0293l18421	74.79358	-66.86072	0.278759	19.07	0.33	19.16	0.39	2452298.6545	c
lm0437m22126	77.39874	-66.06973	0.280684	19.42	0.47	19.52	0.58	2451745.8545	c
lm0425l24389	75.46457	-65.86768	0.281388	19.05	0.39	19.12	0.47	2451593.6165	c
lm0427m19332	75.92683	-66.04073	0.286546	19.11	0.36	19.16	0.43	2451906.9071	c
lm0435m10888	77.48819	-65.61824	0.289555	19.16	0.37	19.24	0.46	2451927.6789	c
lm0425l20513	75.50109	-65.84096	0.289973	18.82	0.47	18.87	0.59	2450508.6286	c
lm0423l20069	75.59747	-65.49339	0.291086	19.08	0.51	19.13	0.60	2451467.6728	c
lm0302n4858	76.13749	-66.78444	0.292002	19.00	0.45	19.05	0.56	2451493.6596	c
lm0291k24862	75.00092	-66.40342	0.293334	19.68	0.42	20.02	0.56	2451128.6539	c
lm0435m9109	77.32164	-65.60798	0.295152	18.92	0.48	19.02	0.56	2450706.7920	c
lm0434n14310	76.70655	-65.80327	0.296573	19.20	0.40	19.28	0.52	2451905.5749	c
lm0291l11940	74.89917	-66.47166	0.303318	19.20	0.48	19.31	0.57	2451886.5948	c
lm0424m19442	75.10627	-65.67820	0.304605	19.29	0.44	19.41	0.61	2451182.6872	c
lm0425n15519	75.78383	-65.80184	0.307507	19.00	0.43	19.08	0.48	2451830.7142	c
lm0291n25551	75.11817	-66.55566	0.308322	18.90	0.45	19.03	0.53	2451885.6054	c
lm0425n18680	75.92700	-65.82173	0.310366	19.24	0.54	19.27	0.71	2451591.6272	c
lm0304m2952	75.94720	-66.97185	0.311944	19.08	0.41	19.21	0.52	2451207.6161	c
lm0303n31583	77.14986	-66.93050	0.314180	19.15	0.45	19.19	0.53	2452307.6381	c
lm0301n7929	76.89016	-66.44610	0.314271	19.14	0.47	19.24	0.55	2450871.5779	c
lm0425k9319	75.47239	-65.60967	0.319697	19.55	0.55	19.75	0.69	2451478.6192	c
lm0434l23190	76.23528	-65.87827	0.322595	19.27	0.46	19.33	0.51	2452020.5110	c
lm0303m22504	77.15498	-66.72917	0.323404	19.45	0.44	19.46	0.51	2452204.7726	c
lm0425n13753	75.73800	-65.79020	0.324285	19.51	0.46	19.56	0.59	2451125.6205	c
lm0303n16841	77.10276	-66.84558	0.327493	19.23	0.38	19.33	0.46	2451078.7631	c
lm0291n15412	75.41471	-66.49017	0.328223	19.31	0.41	19.46	0.50	2451124.7292	c
lm0300m6808	76.00554	-66.28864	0.329139	19.18	0.37	19.26	0.46	2451491.6430	c

lm0301m15847	77.12213	-66.34112	0.330077	19.11	0.54	19.21	0.64	2451199.5639	c
lm0436m8308	76.72609	-65.96599	0.331619	19.11	0.45	19.39	0.54	2451774.8316	c
lm0312115193	77.42594	-66.85716	0.331780	19.36	0.47	19.51	0.51	2451565.6391	c
lm0425k4625	75.55453	-65.57518	0.335537	19.18	0.36	19.30	0.43	2451623.5479	c
lm0423117670	75.34933	-65.50210	0.337594	19.05	0.42	19.18	0.50	2452249.8013	c
lm0293m19803	75.41086	-66.71085	0.338538	19.16	0.46	19.21	0.56	2451838.7084	c
lm030318655	76.69337	-66.80070	0.339125	18.48	0.21	18.54	0.24	2451563.6306	c
lm0310n11585	77.66864	-66.49466	0.340596	19.06	0.18	19.23	0.32	2451271.5430	c
lm030016753	75.82456	-66.44405	0.340936	18.77	0.35	18.89	0.41	2451383.8448	c
lm0436115993	76.37296	-66.17058	0.343821	19.21	0.37	19.31	0.41	2451886.6258	c
lm0302116395	75.66204	-66.86281	0.344601	19.14	0.38	19.28	0.42	2452239.5837	c
lm0303m10773	76.94934	-66.66027	0.344942	19.09	0.42	19.14	0.50	2451067.7597	c
lm042516481	75.31167	-65.74371	0.344997	18.95	0.41	19.07	0.48	2452237.5730	c
lm0435m18280	77.56386	-65.66690	0.345305	19.08	0.31	19.20	0.39	2450840.7622	c
lm0425110656	75.55837	-65.77181	0.345737	19.29	0.46	19.39	0.55	2450383.7849	c
lm0436n10024	76.58557	-66.12169	0.346597	19.47	0.38	19.65	0.44	2451556.6837	c
lm030018890	75.81890	-66.45933	0.348701	18.89	0.52	18.99	0.56	2452345.5449	c
lm0310112440	77.32674	-66.48791	0.348783	19.24	0.39	19.36	0.45	2451997.5510	c
lm0436n14285	76.66342	-66.15315	0.349850	19.29	0.34	19.47	0.45	2452018.5169	c
lm0302k3782	75.73802	-66.63133	0.352431	19.27	0.32	19.46	0.36	2451117.6421	c
lm0434120168	76.33503	-65.85612	0.353452	19.47	0.39	19.66	0.43	2451575.6684	c
lm0293k30764	74.95375	-66.77676	0.353740	19.36	0.31	19.52	0.40	2451424.8113	d
lm029119716	74.90131	-66.45757	0.354199	19.73	0.39	19.94	0.44	2451190.6306	c
lm0435m13533	77.33903	-65.63724	0.354274	19.01	0.35	19.15	0.43	2451504.6454	c
lm044418138	77.76094	-65.75855	0.354926	19.04	0.35	19.18	0.42	2451226.6081	d
lm0301n13911	77.03367	-66.48302	0.357188	19.10	0.38	19.26	0.44	2451750.9205	d
lm0291123359	74.60627	-66.54347	0.358093	19.22	0.36	19.40	0.42	2451947.6718	c
lm0427k10785	75.29491	-65.98454	0.358370	19.06	0.36	19.19	0.41	2452242.7908	c
lm0425m3355	75.94157	-65.56209	0.358864	19.12	0.40	19.23	0.48	2451462.6646	c
lm0301126933	76.39115	-66.57905	0.360584	19.06	0.32	19.26	0.38	2451599.6039	d
lm0422n16993	75.07383	-65.46963	0.360726	19.12	0.38	19.28	0.46	2451469.6348	c
lm0310112653	77.42654	-66.59188	0.362102	19.17	0.35	19.32	0.48	2450731.8795	d
lm0293n14230	75.45233	-66.83197	0.362897	18.91	0.32	18.95	0.37	2451791.7370	d

6.1. CLASSIFICATION OF EROS-2 CANDIDATE RR LYRAE STARS

lm0435k8479	77.11971	-65.60672	0.365160	19.01	0.29	19.15	0.39	2451886.6258	d
lm0291n25922	75.17050	-66.55760	0.365493	19.13	0.35	19.30	0.43	2451920.6770	d
lm0293m10988	75.07649	-66.66119	0.366121	19.15	0.40	19.27	0.46	2452496.8002	c
lm0305m6294	76.97324	-66.98749	0.366683	18.84	0.40	18.93	0.50	2451482.6407	c
lm0310k9300	77.61115	-66.31121	0.370288	19.15	0.52	19.23	0.59	2451982.5726	c
lm0434m22078	76.47651	-65.70050	0.372157	19.38	0.41	19.58	0.50	2450379.8638	c
lm0444i9270	77.74804	-65.76665	0.374023	19.03	0.31	19.13	0.34	2451997.5565	c
lm0425m8144	75.79879	-65.59725	0.376376	19.06	0.40	19.17	0.50	2451653.5187	c
lm0300n24904	76.12396	-66.56460	0.376841	18.99	0.38	19.16	0.44	2451388.9318	c
lm0434i19810	76.38578	-65.88519	0.379506	18.75	0.37	18.85	0.43	2451768.8205	c
lm0427i17346	75.48775	-66.18771	0.380922	19.31	0.46	19.42	0.53	2451966.5759	c
lm0436m11977	76.65728	-65.99637	0.382103	19.24	0.37	19.43	0.41	2451460.6605	c
lm0425k8207	75.39793	-65.60249	0.382111	18.80	0.40	18.94	0.47	2452183.6822	c
lm0303m23391	76.80510	-66.73721	0.385510	19.25	0.40	19.39	0.45	2451173.6461	d
lm0427i4507	75.53004	-66.08408	0.387359	18.66	0.31	18.74	0.36	2451659.4931	c
lm0303k24363	76.73134	-66.74087	0.391884	18.81	0.42	18.91	0.46	2451872.6528	d
lm0424m22887	75.13167	-65.70164	0.398125	19.49	1.09	19.60	1.31	2451183.6480	ab
lm0302k5022	75.75683	-66.64249	0.404202	19.28	0.41	19.41	0.47	2451860.5816	c
lm0302i12678	75.85530	-66.83750	0.424945	19.09	1.03	19.17	1.19	2450432.7573	ab
lm0303m22989	77.03243	-66.73305	0.427324	18.53	0.37	18.53	0.42	2451253.5588	c
lm0436n11172	76.75415	-66.12991	0.431733	19.34	1.26	19.46	1.51	2451618.5691	ab
lm0300i14647	75.54689	-66.59292	0.433620	19.38	0.48	19.48	0.60	2451383.8448	c
lm0293n31080	75.15616	-66.93208	0.436530	19.22	0.50	19.24	0.57	2451090.6690	c
lm0434i7912	76.43811	-65.76134	0.455709	19.53	0.38	19.68	0.56	2451581.6628	c
lm0293k3928	77.39336	-66.76995	0.460600	19.18	1.09	19.36	1.33	2451595.7083	ab
lm0293n30795	74.84921	-66.62125	0.471742	19.29	0.91	19.41	1.06	2451629.5964	ab
lm0432i12420	75.45401	-66.92786	0.474027	18.98	0.74	19.07	0.92	2451828.6830	ab
lm0427n7741	76.18633	-65.53826	0.478439	19.46	0.68	19.63	0.87	2452021.5603	ab
lm0300m9935	75.78808	-66.11239	0.482840	19.02	1.14	19.13	1.36	2451393.8494	ab
lm0437k15772	76.00253	-66.31022	0.485127	19.21	1.05	19.33	1.26	2451300.5041	ab
lm0434i20435 <sup>a</sup>	77.00170	-66.01396	0.488322	19.22	1.13	19.36	1.30	2451620.5741	ab
lm0437k22654	76.33615	-65.85811	0.488810	19.11	1.06	19.27	1.33	2450476.72360	ab
	77.01247	-66.06322	0.491312	19.21	0.87	19.36	1.07	2451349.9377	ab

lm0436n20628	76.77019	-66.20120	0.493107	19.10	1.08	19.20	1.28	2452191.6897	ab
lm0302n23523	76.21095	-66.89987	0.497153	18.99	0.88	19.06	1.17	2452388.4745	ab
lm0293k28352	74.72341	-66.76451	0.497779	19.11	1.14	19.25	1.33	2451875.5967	ab
lm0303n13977 <sup>a</sup>	76.93426	-66.83012	0.499556	19.20	1.07	19.32	1.24	2451756.8603	ab
lm0303n15322	76.82352	-66.83882	0.505733	18.97	0.97	19.05	1.13	2451246.6159	ab
lm0293m14375	75.19999	-66.68054	0.507995	18.76	0.86	18.83	1.02	2451653.5100	ab
lm0301124255	76.59798	-66.55346	0.510580	19.05	0.87	19.25	1.03	2451203.5589	ab
lm0436120450	76.40491	-66.20527	0.511395	19.02	0.92	19.13	1.12	2451966.6073	ab
lm0437m20444	77.70208	-66.04521	0.511423	19.38	0.77	19.53	1.00	2451870.6193	ab
lm0302123297	75.87528	-66.90811	0.511473	19.21	1.04	19.36	1.23	2451579.6640	ab
lm0291m8710	75.29738	-66.29542	0.511745	19.52	0.98	19.68	1.10	2450776.7363	ab
lm0435k20062	77.08979	-65.68616	0.514125	19.25	0.95	19.40	1.08	2451556.6837	ab
lm0291n20101	75.41745	-66.52001	0.517254	19.17	1.13	19.39	1.44	2451577.6393	ab
lm0300m17178	76.02068	-66.35996	0.518967	19.35	0.91	19.56	1.11	2451960.6609	ab
lm0302m22487	76.30911	-66.76329	0.520562	19.73	0.99	19.93	1.41	2452219.5892	ab
lm0303m17152	76.98350	-66.69861	0.524201	18.87	0.73	18.92	0.85	2451353.9049	ab
lm0300k12184	75.78071	-66.32998	0.524813	19.04	0.69	19.18	0.95	2451918.6675	ab
lm0303k25210	76.70220	-66.74596	0.524918	19.39	0.62	19.54	0.77	2451563.6306	ab
lm0435m17793	77.44960	-65.66472	0.524956	19.04	0.94	19.19	1.13	2451934.6702	ab
lm0435m23563	77.51267	-65.70218	0.525048	19.04	0.70	19.14	0.82	2451868.6062	ab
lm0425n23250	76.04345	-65.87922	0.525312	19.33	0.94	19.43	0.99	2452214.8489	ab
lm0300m19324	76.27787	-66.42927	0.525312	19.15	0.88	19.23	1.03	2451233.7163	ab
lm0300113312	75.76052	-66.59446	0.527452	18.85	0.90	18.99	1.01	2451833.7264	ab
lm0291n6040	75.20907	-66.43175	0.527619	19.27	1.03	19.39	1.21	2451888.5997	ab
lm0301n16814	77.11029	-66.50065	0.528262	19.05	0.80	19.19	0.99	2451589.6512	ab
lm0426n12018	75.09864	-66.13259	0.529460	19.63	1.16	19.87	1.40	2451804.7660	ab
lm0291n20061	75.06329	-66.52272	0.529756	19.51	0.92	19.69	1.10	2451973.5702	ab
lm0301n21605	76.87595	-66.53319	0.532545	19.26	1.05	19.43	1.20	2451175.6907	ab
lm0301m22780	77.19099	-66.38563	0.535459	18.95	1.10	19.16	1.33	2451459.7352	ab
lm0301k17554	76.37739	-66.36031	0.535567	19.45	0.94	19.64	1.08	2451573.6131	ab
lm0425114852	75.33257	-65.80227	0.536054	19.37	1.18	19.53	1.36	2451892.8354	ab
lm0437m17477	77.59584	-66.07382	0.536134	19.47	0.73	19.55	0.93	2452200.6693	ab
lm0310k11253	77.25582	-66.32523	0.537149	19.04	0.84	19.16	1.00	2451191.6807	ab

6.1. CLASSIFICATION OF EROS-2 CANDIDATE RR LYRAE STARS

lm0434k22095	76.39710	-65.73215	0.539682	19.11	0.87	19.30	1.06	2450736.7900	ab
lm0425k11500	75.33082	-65.62627	0.540233	18.72	0.47	18.84	0.65	2450880.5798	ab
lm0434m6139	76.65853	-65.58909	0.540358	19.14	1.07	19.27	1.25	2451602.5686	ab
lm0301m15584	76.96520	-66.34056	0.541340	19.43	1.09	19.60	1.34	2451502.6255	ab
lm0446k20706	77.74377	-66.05372	0.543569	19.36	0.55	19.56	0.82	2451589.6790	ab
lm0427m14753	75.89361	-66.00800	0.544010	18.87	0.74	18.99	0.90	2451573.6030	ab
lm0437n14794	77.71665	-66.16543	0.544769	19.24	0.99	19.33	1.04	2450806.8093	ab
lm0300m23701	75.96552	-66.40392	0.546102	19.00	0.75	19.16	0.87	2452297.6731	ab
lm0425m12624	75.71720	-65.62945	0.547065	18.89	0.80	19.00	1.00	2451587.6229	ab
lm0300m23266	76.32789	-66.39973	0.548868	18.92	0.55	19.02	0.68	2450864.7109	ab
lm0301n14847	76.93447	-66.48958	0.549535	19.21	0.60	19.38	0.86	2451945.6803	ab
lm0435m9334	77.37913	-65.60896	0.550850	18.87	0.67	19.04	0.80	2451854.6176	ab
lm0423111740	75.40143	-65.51925	0.554337	19.15	0.49	19.29	0.61	2451912.6947	ab
lm0291k10561	74.77965	-66.31058	0.557100	18.96	0.82	19.16	0.98	2452038.4930	ab
lm0291m11933	75.41718	-66.31573	0.558102	18.96	0.58	19.09	0.69	2452190.6718	ab
lm0423n26224	75.75980	-65.52229	0.559366	19.40	0.82	19.55	0.98	2452210.7725	ab
lm0302k14796	75.62213	-66.74150	0.559635	19.23	0.78	19.40	0.90	2451997.5382	ab
lm0300m11839	75.92208	-66.32392	0.559733	19.10	0.93	19.26	1.15	2451317.4864	ab
lm0303117671	76.73167	-66.85344	0.560588	18.95	0.87	19.08	1.03	2450820.6003	ab
lm042317926	75.54610	-65.53056	0.561818	19.28	0.89	19.43	1.04	2451813.7576	ab
lm0427118856	75.64163	-66.19734	0.562698	19.17	0.78	19.38	0.97	2451625.5332	ab
lm0303m17812	77.06791	-66.70197	0.565556	19.20	0.89	19.28	1.08	2450398.7132	ab
lm0302n12351	75.94097	-66.83188	0.566134	19.63	0.58	19.80	0.82	2452516.7872	ab
lm0300k14335	75.65971	-66.34538	0.566157	19.02	0.73	19.18	0.91	2451870.6089	ab
lm0300n27286	75.94449	-66.58057	0.566301	18.92	0.91	19.07	1.08	2451623.5582	ab
lm0302112960	75.73262	-66.83949	0.567341	18.98	0.75	19.14	0.77	2452223.8058	ab
lm0300n21091	76.32909	-66.53946	0.567460	19.39	1.01	19.57	1.23	2451253.5588	ab
lm0434k9008	76.39164	-65.61437	0.567635	18.92	0.92	19.08	1.08	2451927.6789	ab
lm0301111630	76.57024	-66.47409	0.568156	19.12	0.82	19.29	1.01	2451791.7477	ab
lm0300k17665	75.74862	-66.36812	0.568997	18.86	0.55	19.07	0.69	2452232.8191	ab
lm0291110775	74.69280	-66.46539	0.570992	19.87	0.43	20.17	0.49	2451623.5424	ab
lm0300m11600	76.14728	-66.32166	0.570995	18.69	0.58	18.77	0.68	2452185.6485	ab
lm0437n15049	77.49507	-66.16951	0.571014	19.24	0.77	19.42	0.89	2451440.8455	ab

lm0434n13704	76.72655	-65.79908	0.571166	19.40	0.82	19.57	1.03	2451745.8545	ab
lm0427112462	75.38109	-66.15291	0.571194	19.10	0.64	19.28	0.84	2451961.7336	ab
lm043515247	76.92213	-65.73542	0.571823	18.95	0.60	19.12	0.77	2452227.6073	ab
lm0434m21424	76.75130	-65.69519	0.573820	19.36	0.40	19.57	0.51	2451943.7360	ab
lm0437n8455	77.73625	-66.11333	0.574999	19.10	0.90	19.23	1.00	2450763.7960	ab
lm0444120033	77.76182	-65.89427	0.575092	18.57	0.26	18.62	0.30	2451490.6919	ab
lm0293n20870	75.36086	-66.87147	0.578190	18.52	0.73	18.68	0.86	2451830.7052	ab
lm0437m20883	77.60790	-66.04953	0.580287	19.33	0.72	19.52	0.87	2451821.7638	ab
lm0293m19628	75.29061	-66.71099	0.581141	19.06	0.73	19.20	0.87	2451589.6291	ab
lm0303n12799	76.91560	-66.82310	0.581848	19.06	0.64	19.21	0.74	2452199.8086	ab
lm0434117031	76.34705	-65.83271	0.582937	19.29	0.68	19.53	0.80	2452028.5012	ab
lm0293m19003	75.26169	-66.70727	0.583546	19.28	0.68	19.44	0.85	2450820.6936	ab
lm0437k15328	76.98154	-66.01065	0.584568	19.28	0.76	19.53	0.99	2451870.8183	ab
lm0291k10047	74.82401	-66.30667	0.585024	19.43	0.79	19.66	0.92	2451894.5925	ab
lm0293k25226	74.87683	-66.74562	0.586479	19.13	0.79	19.31	0.95	2451976.5671	ab
lm0303n27302	77.21128	-66.90501	0.586637	19.24	0.57	19.34	0.68	2452471.9041	ab
lm0435n11321	77.35012	-65.77656	0.587183	18.89	0.49	19.18	0.61	2451530.6598	ab
lm0437k8681	76.96496	-65.96417	0.589055	19.04	0.47	19.21	0.63	2450440.8116	ab
lm0300120739	75.68550	-66.54657	0.589066	18.91	0.73	19.13	0.86	2451478.6339	ab
lm0310118147	77.45244	-66.53289	0.590217	18.75	0.56	18.91	0.64	2451623.5755	ab
lm0302126417	75.70471	-66.93057	0.590296	19.34	0.69	19.54	0.89	2451953.6490	ab
lm0310k18010	77.55657	-66.40282	0.590299	19.27	0.88	19.42	0.97	2452316.6514	ab
lm0300k16563	75.87714	-66.36044	0.592704	19.18	0.65	19.38	0.78	2451120.6248	ab
lm0303m21245	77.01340	-66.72311	0.593551	18.85	0.64	18.93	0.74	2452305.6537	ab
lm0437k13906	77.30504	-65.99851	0.594332	19.15	0.63	19.32	0.71	2451885.6314	ab
lm0293m17000	75.18543	-66.69597	0.595224	19.11	0.70	19.27	0.84	2452231.7729	ab
lm0435m7058	77.57013	-65.59222	0.597486	19.03	0.45	19.19	0.53	2450404.7845	ab
lm0425m4288	75.85896	-65.56967	0.597504	19.04	0.57	19.17	0.71	2451929.6322	ab
lm0435n13913	77.44001	-65.79393	0.597578	19.33	0.45	19.54	0.59	2451746.6642	ab
lm0426m24414	74.85054	-66.07064	0.606869	19.21	0.55	19.40	0.60	2451938.6425	ab
lm0425110247	75.26573	-65.77068	0.607461	18.92	0.85	19.07	1.07	2451587.6229	ab
lm0310k15738	77.42775	-66.40958	0.608534	19.16	0.42	19.37	0.53	2452201.7970	ab
lm0435k12309	77.10144	-65.63307	0.608992	19.15	0.70	19.35	0.82	2451502.6358	ab

6.1. CLASSIFICATION OF EROS-2 CANDIDATE RR LYRAE STARS

lm043519858	76.91847	-65.76707	0.609462	19.15	0.58	19.34	0.70	2451890.6303	ab
lm0434k7302	76.14762	-65.60166	0.610192	19.30	0.59	19.53	0.69	2451994.5443	ab
lm0293112631	74.80625	-66.82752	0.610866	19.24	0.60	19.46	0.74	2452177.6975	ab
lm0435k17589	77.22723	-65.66834	0.612635	19.28	0.57	19.46	0.65	2451861.6691	ab
lm029315252	74.96458	-66.78360	0.612908	19.23	0.60	19.43	0.73	2451220.6303	ab
lm0312k4503	77.38073	-66.62996	0.613847	19.49	0.50	19.79	0.74	2450430.6813	ab
lm0436k15855	76.16415	-66.02233	0.614185	18.98	0.43	19.17	0.49	2451764.8463	ab
lm0425121048	75.43903	-65.84525	0.615813	18.80	0.79	18.99	0.94	2451861.6474	ab
lm0427m20466	75.99099	-66.04834	0.616626	19.63	0.82	19.82	1.07	2451577.6481	ab
lm0435k12002	76.96857	-65.63167	0.618774	19.37	0.74	19.59	0.87	2452202.6519	ab
lm0424n5227	75.11837	-65.73591	0.619983	18.58	0.65	18.74	0.85	2450907.5366	ab
lm0437m9713	77.53209	-65.96782	0.620011	18.93	0.75	19.07	0.93	2451830.7454	ab
lm0303126148	76.45407	-66.90387	0.620647	18.83	0.45	18.97	0.50	2452240.5697	ab
lm0302k13534	75.90035	-66.73166	0.620880	19.03	0.64	19.20	0.76	2452229.5983	ab
lm0305k5704	76.53880	-66.98748	0.621600	19.26	0.45	19.49	0.50	2451482.6407	ab
lm0437115735	77.06524	-66.17934	0.622553	19.29	0.42	19.51	0.51	2450503.6541	ab
lm0434m19648	76.56045	-65.68376	0.622604	19.09	0.56	19.30	0.66	2451183.6623	ab
lm0300n13961	76.23893	-66.49314	0.623548	18.91	1.14	19.04	1.35	2452297.6731	ab
lm0303127610	76.59394	-66.91158	0.623747	18.96	0.44	19.13	0.53	2452257.6065	ab
lm0292n22612	74.51012	-66.89940	0.624068	19.10	0.39	19.24	0.49	2452206.5991	ab
lm0293n18229	75.16869	-66.85795	0.628127	19.01	0.39	19.16	0.46	2452231.7729	ab
lm0303n9745	77.01868	-66.80425	0.628757	19.21	0.34	19.35	0.44	2451266.5201	ab
lm0435m18273	77.66155	-65.66592	0.631476	18.98	0.39	19.15	0.48	2451571.6385	ab
lm0423121178	75.59644	-65.48937	0.632125	18.95	0.47	19.14	0.53	2452684.6900	ab
lm0303n16102	76.88992	-66.84296	0.632428	18.85	0.89	18.96	1.04	2452301.6523	ab
lm0424n12543	74.90326	-65.79083	0.635316	18.99	0.89	19.16	1.07	2452259.5869	ab
lm0300n19927	76.24113	-66.53242	0.637129	19.16	0.32	19.33	0.37	2451939.7443	ab
lm0300125566	75.67367	-66.57969	0.638155	18.98	0.46	19.18	0.52	2450532.5716	ab
lm0435k15816	76.92775	-65.65774	0.638794	18.86	0.68	19.05	0.84	2451943.7360	ab
lm0300k11860	75.51738	-66.32796	0.643757	19.05	0.53	19.17	0.67	2451259.5591	ab
lm0303m11005	77.14924	-66.65987	0.643770	19.12	1.06	19.15	1.23	2451177.8395	ab
lm0301n14943	76.88253	-66.49069	0.645196	19.10	0.31	19.32	0.37	2451233.7163	ab
lm0436m17011	76.56619	-66.03765	0.645996	19.13	0.72	19.35	0.88	2452051.4810	ab



lm0301122786	76.44374	-66.54541	0.648027	19.02	0.60	19.24	0.69	2451815.7624	ab
lm0436n8236	76.82037	-66.10734	0.650192	18.73	0.84	18.88	1.03	2451447.7726	ab
lm0300m25109	76.25662	-66.41288	0.652891	19.05	0.94	19.09	1.07	2450430.5753	ab
lm0310116334	77.43882	-66.51749	0.657788	18.99	0.25	19.26	0.30	2450445.7695	ab
lm0293125506	74.82889	-66.90170	0.657982	18.98	0.82	19.17	0.96	2452172.7236	ab
lm0310114484	77.32418	-66.50280	0.661652	18.74	0.62	19.01	0.73	2451939.7506	ab
lm0301125140 <sup>e</sup>	76.51123	-66.55949	0.663184	18.57	0.70	18.70	0.82	2451296.5118	ab
lm0291126545 <sup>e</sup>	74.66819	-66.56263	0.669488	19.06	0.94	19.32	1.13	2451623.5424	ab
lm0434n8413	76.74585	-65.76182	0.670871	18.94	0.64	19.09	0.77	2452183.7135	ab
lm0300n12088	76.16779	-66.48111	0.672356	19.30	0.65	19.50	0.79	2452326.5740	ab
lm0427k17452	75.35321	-66.07494	0.675498	19.13	0.43	19.32	0.49	2451538.5761	ab
lm0300n12109	76.11925	-66.48140	0.683459	18.88	0.60	19.04	0.69	2451951.6517	ab
lm0426n9666	75.17663	-66.11497	0.687625	19.09	0.42	19.28	0.46	2452030.4939	ab
lm0434n22292	76.48691	-65.85960	0.689693	19.21	0.34	19.39	0.44	2452032.4950	ab
lm0303m5651	77.13918	-66.62705	0.692547	19.04	0.52	19.14	0.64	2451870.6089	ab
lm0301m15788	77.01923	-66.34154	0.710038	18.70	0.34	18.85	0.38	2451866.6022	ab
lm0305m3882	76.85877	-66.97363	0.710488	19.03	0.65	19.19	0.75	2451533.6272	ab
lm0305m7850	77.22390	-66.99474	0.713324	18.76	0.27	18.88	0.32	2451502.6255	ab
lm0427m6338	75.99025	-65.94538	0.713501	19.16	0.63	19.28	0.71	2452395.4980	ab
lm0434n17383	76.51344	-65.89259	0.724152	18.83	0.31	19.04	0.39	2452254.5884	ab
lm0301116487	76.55635	-66.50519	0.738143	18.98	0.18	19.24	0.22	2452008.5249	ab
lm0300123462	75.60295	-66.58330	0.744314	18.76	0.55	18.97	0.64	2451886.6168	ab
lm0310118911	77.52338	-66.53928	0.748431	19.04	0.38	19.29	0.45	2452213.7774	ab

Table 6.2: Properties of the 251 confirmed RR Lyrae stars in tile LMC

8\_3 (Column 1: EROS-2 identification of the star; Column 2: Right ascension from the EROS-2 catalogue; Column 3: Declination from the EROS-2 catalogue; Column 4: Period from the EROS-2 catalogue (<sup>a</sup>-Stars for which a new period was estimated in this study); Column 5: Mean magnitude in the  $B_{EROS}$  band; Column 6: Amplitude in the  $B_{EROS}$  band; Column 7: Mean magnitude in the  $V$  band; Column 8: Amplitude in the  $V$  band; Column 9: Epoch of maximum light in the  $V$  band; Column 10: Classification in type).

## 6.2 Comparison with the OGLE III catalogue

We compared our classification of the RR Lyrae stars in tile LMC 8\_3 with the classification provided in the OGLE III catalogue. The OGLE III survey covered only part of the tile LMC 8\_3. We were able to make a comparison for 72 RR Lyrae stars which are in common between the two catalogues. Information about these 72 objects is presented in Table 6.3. For the majority of the RR Lyrae stars our classification is in agreement with the classification provided by OGLE III, but there are some discrepancies.

According to the OGLE III classification the source *lm0305m3332* is an RRab star, but we classified it as RRc star. Also the period of this star, determined by the EROS-2 survey ( $P=0.249311$  day), differs from the period provided by the OGLE III survey ( $P=0.4986339$  day). After analysis of the light curve with GRATIS we concluded that OGLE III provided an alias of the actual period. Star *lm0293l18421* was classified as RRc by us and as RRe by the OGLE III. Star *lm0300l14647* is an RRd star according to the OGLE III classification, but we analysed the light curve with GRATIS and did not confirm the existence of a second periodicity, therefore, we classified the star as c-type RR Lyrae. Star *lm0293n31080* is RRab in the OGLE III classification and RRc in our classification.

OGLE III id	EROS-2 id	RA (HH:MM:SS)	DEC (DD:MM:SS)	Type	I (mag)	V (mag)	P (day)	Epoch(max) (HJD-2450000)
OGLE-LMC-RRLYR-02465	lm0292n22612	4:58:02.47	-66:53:58.2	RRab	18.836	19.411	0.6240672	2166.64831
OGLE-LMC-RRLYR-02630	lm0293k28352	4:58:53.66	-66:45:52.4	RRab	18.752	19.215	0.4977800	2166.80015
OGLE-LMC-RRLYR-02740	lm0293l18421	4:59:10.51	-66:51:39.0	RRe	18.778	19.143	0.2787614	2166.79715
OGLE-LMC-RRLYR-02767	lm0293l12631	4:59:13.54	-66:49:39.4	RRab	18.750	19.396	0.6108660	2166.72786
OGLE-LMC-RRLYR-02795	lm0293l25506	4:59:18.97	-66:54:06.6	RRab	18.582	19.181	0.6579816	2166.79864
OGLE-LMC-RRLYR-02814	lm0293k3928	4:59:23.82	-66:37:16.8	RRab	18.811	19.292	0.4717423	2172.56258
OGLE-LMC-RRLYR-02841	lm0293k25226	4:59:30.49	-66:44:44.4	RRab	18.707	19.290	0.5864819	2166.59334
OGLE-LMC-RRLYR-02913	lm0293k30764	4:59:48.97	-66:46:36.5	RRd	19.123	19.625	0.3537438	2166.58727
OGLE-LMC-RRLYR-02928	lm0293l5252	4:59:51.57	-66:47:01.2	RRab	18.826	19.449	0.6129133	2166.36864
OGLE-LMC-RRLYR-03045	lm0293m10988	5:00:18.38	-66:39:40.5	RRC	18.852	19.355	0.3661132	2166.54533
OGLE-LMC-RRLYR-03129	lm0293n31080	5:00:37.50	-66:55:55.6	RRab	19.184	19.610	0.4365123	2166.73257
OGLE-LMC-RRLYR-03144	lm0293n18229	5:00:40.54	-66:51:28.8	RRab	18.718	19.322	0.6281261	2166.46907
OGLE-LMC-RRLYR-03159	lm0293m17000	5:00:44.55	-66:41:45.6	RRab	18.754	19.342	0.5952245	2166.30304
OGLE-LMC-RRLYR-03174	lm0293m14375	5:00:48.01	-66:40:50.0	RRab	18.712	19.212	0.5079962	2166.58739
OGLE-LMC-RRLYR-03227	lm0293m19003	5:01:02.85	-66:42:26.3	RRab	18.853	19.449	0.5835871	2166.30463
OGLE-LMC-RRLYR-03255	lm0293m19628	5:01:09.79	-66:42:39.7	RRab	18.681	19.244	0.5811319	2166.72346
OGLE-LMC-RRLYR-03330	lm0293n20870	5:01:26.59	-66:52:17.4	RRab	18.573	19.099	0.5781914	2166.63326
OGLE-LMC-RRLYR-03382	lm0293m19803	5:01:38.65	-66:42:39.2	RRC	18.938	19.371	0.3385449	2166.73510
OGLE-LMC-RRLYR-03423	lm0293n14230	5:01:48.55	-66:49:54.7	RRd	18.774	19.228	0.3629116	2166.60785
OGLE-LMC-RRLYR-03425	lm0293n30795	5:01:48.98	-66:55:40.0	RRab	18.821	19.338	0.4740098	2166.69079
OGLE-LMC-RRLYR-03524	lm0300l14647	5:02:11.22	-66:35:34.9	RRd	18.543	19.047	0.4336058	2166.57704
OGLE-LMC-RRLYR-03580	lm0300l23462	5:02:24.69	-66:35:00.3	RRab	18.412	18.995	0.7443101	2166.49600
OGLE-LMC-RRLYR-03602	lm0302k14796	5:02:29.31	-66:44:29.6	RRab	18.831	19.410	0.5596368	2166.54348
OGLE-LMC-RRLYR-03637	lm0302l16395	5:02:38.91	-66:51:46.4	RRC	18.838	19.278	0.3445963	2166.53368
OGLE-LMC-RRLYR-03654	lm0300l25566	5:02:41.69	-66:34:47.2	RRab	18.716	19.283	0.6381508	2172.62908
OGLE-LMC-RRLYR-03689	lm0302l26417	5:02:49.15	-66:55:50.3	RRab	19.036	19.687	0.5903018	2166.75562
OGLE-LMC-RRLYR-03717	lm0302l12960	5:02:55.86	-66:50:22.4	RRab	18.646	19.196	0.5673193	2166.52992
OGLE-LMC-RRLYR-03722	lm0302k3782	5:02:57.11	-66:37:52.8	RRC	18.941	19.431	0.3524353	2166.82662
OGLE-LMC-RRLYR-03749	lm0302k5022	5:03:01.62	-66:38:33.1	RRC	18.843	19.356	0.4042293	2166.55134
OGLE-LMC-RRLYR-03757	lm0300l13312	5:03:02.53	-66:35:40.6	RRab	18.730	19.244	0.5274506	2166.55412

6.2. COMPARISON WITH THE OGLE III CATALOGUE

OGLE-LMC-RRLYR-03858	Im0302112678	5:03:25.28	-66:50:15.2	RRab	19.040	19.470	0.4249448	2166.52539
OGLE-LMC-RRLYR-03881	Im0302123297	5:03:30.11	-66:54:29.5	RRab	18.909	19.491	0.5114616	2166.33240
OGLE-LMC-RRLYR-03902	Im0302k13534	5:03:36.12	-66:43:54.3	RRab	18.622	19.256	0.6208809	2166.25905
OGLE-LMC-RRLYR-03956	Im0302n12351	5:03:45.85	-66:49:55.3	RRab	19.107	19.797	0.5661573	2166.29086
OGLE-LMC-RRLYR-03960	Im0300n27286	5:03:46.69	-66:34:50.3	RRab	18.649	19.185	0.5663033	2166.64361
OGLE-LMC-RRLYR-03965	Im0304m2952	5:03:47.34	-66:58:18.9	RRc	18.835	19.221	0.3119118	2166.72170
OGLE-LMC-RRLYR-04196	Im0302n4858	5:04:33.01	-66:47:04.3	RRc	18.857	19.200	0.2920038	2166.73196
OGLE-LMC-RRLYR-04299	Im0302n23523	5:04:50.69	-66:53:59.9	RRab	18.710	19.131	0.4971214	2166.76838
OGLE-LMC-RRLYR-04522	Im0302m22487	5:05:14.23	-66:45:48.0	RRab	19.106	19.642	0.5204521	2166.59996
OGLE-LMC-RRLYR-04643	Im0301126933	5:05:33.87	-66:34:44.9	RRd	18.702	-99.990	0.3605884	2166.80471
OGLE-LMC-RRLYR-04736	Im0303126148	5:05:49.03	-66:54:14.3	RRab	18.642	19.235	0.6206484	2166.70892
OGLE-LMC-RRLYR-04853	Im0305k5704	5:06:09.35	-66:59:15.3	RRab	18.861	19.520	0.6215964	2166.41611
OGLE-LMC-RRLYR-04942	Im0303127610	5:06:22.59	-66:54:42.0	RRab	18.610	19.211	0.6237479	2166.56503
OGLE-LMC-RRLYR-05088	Im0303186655	5:06:46.46	-66:48:02.7	RRc	18.608	18.980	0.3391250	2166.60545
OGLE-LMC-RRLYR-05094	Im0303k25210	5:06:48.56	-66:44:45.7	RRab	18.954	19.530	0.5249210	2166.76883
OGLE-LMC-RRLYR-05143	Im0303k24363	5:06:55.56	-66:44:27.3	RRd	18.507	18.982	0.3918820	2166.54281
OGLE-LMC-RRLYR-05144	Im0303117671	5:06:55.64	-66:51:12.7	RRab	18.663	19.150	0.5605849	2166.56231
OGLE-LMC-RRLYR-05238	Im0303m23391	5:07:13.26	-66:44:14.2	RRd	18.877	19.533	0.3855124	2166.74170
OGLE-LMC-RRLYR-05263	Im0303n15322	5:07:17.67	-66:50:20.1	RRab	18.844	19.369	0.5057311	2166.55255
OGLE-LMC-RRLYR-05317	Im0305m3882	5:07:26.13	-66:58:25.3	RRab	18.629	19.242	0.7104875	2166.66993
OGLE-LMC-RRLYR-05360	Im0303n16102	5:07:33.62	-66:50:35.1	RRab	18.609	19.121	0.6324295	2166.32994
OGLE-LMC-RRLYR-05375	Im0305m3332	5:07:35.60	-66:58:11.5	RRab	19.177	19.677	0.4986339	2166.87261
OGLE-LMC-RRLYR-05405	Im0303n12799	5:07:39.77	-66:49:23.6	RRab	18.816	19.423	0.5818589	2166.63784
OGLE-LMC-RRLYR-05426	Im0303n13977	5:07:44.26	-66:49:48.9	RRab	18.978	19.472	0.4995655	2166.50195
OGLE-LMC-RRLYR-05446	Im0303m10773	5:07:47.87	-66:39:37.1	RRc	18.740	19.213	0.3449414	2166.78490
OGLE-LMC-RRLYR-05476	Im0305m6294	5:07:53.60	-66:59:15.2	RRc	18.650	19.095	0.3666785	2166.87690
OGLE-LMC-RRLYR-05490	Im0303m17152	5:07:56.06	-66:41:55.2	RRab	18.735	19.240	0.5242037	2166.41207
OGLE-LMC-RRLYR-05539	Im0303m21245	5:08:03.26	-66:43:23.3	RRab	18.659	19.237	0.5935504	2166.76882
OGLE-LMC-RRLYR-05551	Im0303n9745	5:08:04.51	-66:48:15.8	RRab	18.824	19.455	0.6287787	2166.32230
OGLE-LMC-RRLYR-05576	Im0303m22989	5:08:07.85	-66:43:59.3	RRc	18.435	18.937	0.4273778	2166.67659
OGLE-LMC-RRLYR-05617	Im0303m17812	5:08:16.34	-66:42:07.3	RRab	18.803	19.414	0.5655545	2166.64750
OGLE-LMC-RRLYR-05672	Im0303n16841	5:08:24.70	-66:50:44.4	RRc	19.013	19.520	0.3274989	2166.70472
OGLE-LMC-RRLYR-05721	Im0303m5651	5:08:33.42	-66:37:37.5	RRab	18.702	19.331	0.6925355	2166.33100

OGLE-LMC-RRLYR-05732	lm0303m11005	5:08:35.84	-66:39:35.7	RRab	18.641	19.252	0.6437728	2166.67716
OGLE-LMC-RRLYR-05734	lm0303n31583	5:08:36.01	-66:55:50.0	RRc	18.975	19.395	0.3141783	2166.87421
OGLE-LMC-RRLYR-05740	lm0303m22504	5:08:37.25	-66:43:45.2	RRc	19.077	-99.990	0.3234019	2223.82337
OGLE-LMC-RRLYR-05815	lm0303n27302	5:08:50.73	-66:54:18.2	RRab	18.878	19.513	0.5866399	2166.85939
OGLE-LMC-RRLYR-05842	lm0305m7850	5:08:53.76	-66:59:41.2	RRab	18.620	19.286	0.7133254	2166.73515
OGLE-LMC-RRLYR-06089	lm0312k4503	5:09:31.40	-66:37:48.1	RRab	18.841	19.474	0.6138503	2166.66862
OGLE-LMC-RRLYR-06113	lm0312k21111	5:09:34.39	-66:46:12.1	RRab	18.920	19.355	0.4605988	2166.85945
OGLE-LMC-RRLYR-06171	lm0312l15193	5:09:42.24	-66:51:26.1	RRc	19.048	19.534	0.3317823	2166.83342
OGLE-LMC-RRLYR-06173	lm0310l12653	5:09:42.36	-66:35:31.1	RRd	18.935	19.424	0.3621078	2166.55986

Table 6.3: Properties of RR Lyrae stars in tile LMC 8\_3, which have a counterpart in the OGLE III catalogue (Column 1: OGLE III identification of the star; Column 2: EROS-2 identification of the star; Column 3: Right ascension from the OGLE III catalogue; Column 4: Declination from the OGLE III catalogue; Column 5: Type according to the OGLE III classification; Column 6: OGLE III  $I$  mean magnitude; Column 7: OGLE III  $V$  mean magnitude; Column 8: Period from the OGLE III catalogue; Column 9: Epoch of maximum light from the OGLE III catalogue).

### 6.3 Fourier analysis of the RR Lyrae stars in tile LMC 8\_3

The Fourier decomposition of the light curves was also used to check the classification of the RR Lyrae stars in tile LMC 8\_3 and to infer their metallicity (see Section 1.5.1). In order to perform the Fourier analysis we first transformed the light curves in the EROS passbands to the  $V$ -band using Eqs. 2.1 and 2.2, and then cleaned the  $V$ -band light curves of the 251 confirmed RR Lyrae stars from the possible outliers, according to the following iterative procedure:

- we discarded all data-points with residuals  $> 0.200$  mag from GRATIS best fit model of the light curve;
- we checked the standard deviation  $\sigma$  of the distribution of residuals:
  - if  $\sigma < 0.070$  mag we stopped the cleaning procedure;
  - if  $\sigma > 0.070$  mag we discarded also data points with residual  $\in (0.150, 0.200)$  mag from the best fit model.
- we again checked the standard deviation  $\sigma$  of the distribution of residuals:
  - if  $\sigma < 0.070$  mag we stopped the cleaning procedure;
  - if  $\sigma > 0.070$  mag we discarded also data points with residual  $\in (0.100, 0.150)$  mag from the best fit model.

Note that all light curves still have more than 73 data points after this cleaning procedure. We performed the sine Fourier decomposition of the light curves and derived normalized Fourier parameters  $A_{21}$ ,  $A_{31}$ ,  $\phi_{21}$ ,  $\phi_{31}$  and the  $D_m$  values (see Section 1.5.1). Some of these parameters are listed in Table 6.4.

Figure 6.2 shows the distribution of the 251 RR Lyrae stars in our sample on the  $A_{21}$  versus  $\phi_{21}$  plane. The vast majority of the RR Lyrae stars are located in two well separated regions which correspond to the RRab (upper-left region) and RRc (bottom-right region) stars. Thus, the Fourier analysis generally confirms our classification based on the visual inspection of the light curves and the period-amplitude diagram. A few deviating objects in Figure 6.2 deserve further discussion. Star Im0427117346 lies rather separated from both groups. We visually inspected its light curve and analysed its position on the period-amplitude diagram (Fig. 6.1), but did not find any peculiarities. Stars Im0293n31080 and

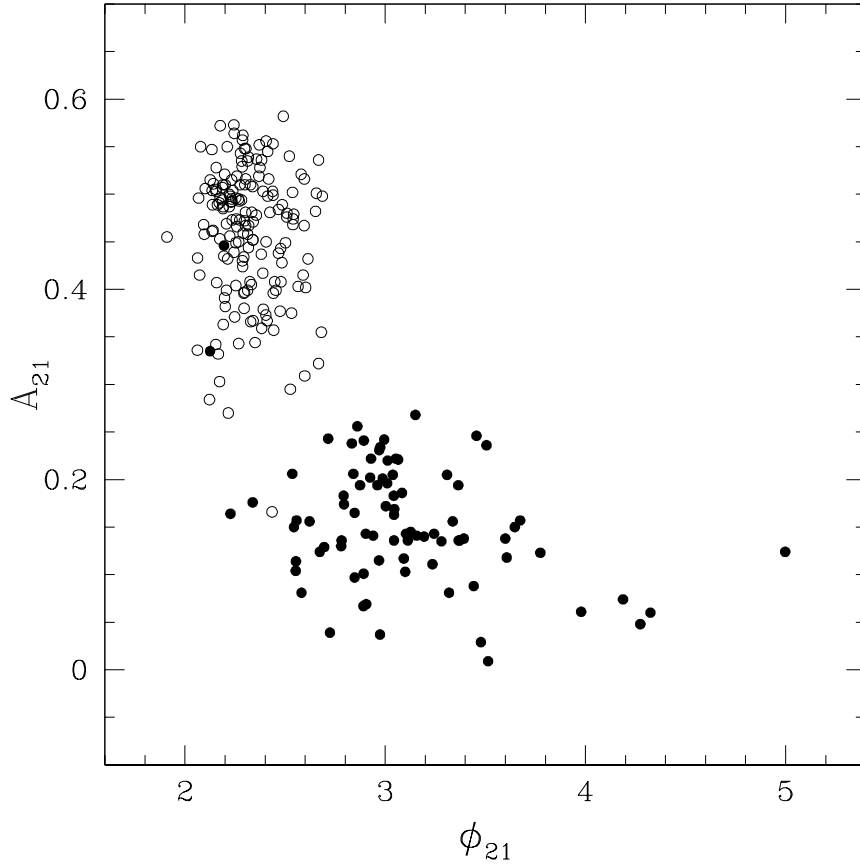


Figure 6.2  $A_{21}$  Fourier parameter versus  $\phi_{21}$ . Empty circles are RRab stars, filled circles are RRc variables. Errors are omitted for clarity, but they are provided in Table 6.4.

Im0434l7912 were classified as RRc, however they are both located in the region of the fundamental-mode RR Lyrae stars in Figure 6.2. It should be noted that one of them (star Im0293n31080) was classified as RRab also by the OGLE III survey. On the contrary, star Im0426n9666, which we classified as RRab, is located in the region of the first-overtone mode RR Lyrae stars. In the following, for these few objects we adopted the classification based on the visual inspection of the light curves and the period-amplitude diagram.

Figure 6.3 shows the distribution of RR Lyrae stars on the  $\phi_{31}$  versus logarithm of period plane. There is a clear separation between RRab and RRc stars. Furthermore, for the RRab stars there is a quite clear linear correlation of the  $\phi_{31}$  parameter with  $\text{Log}(P)$ , whereas the correlation is definitely worse and errors are much larger for the RRc stars.

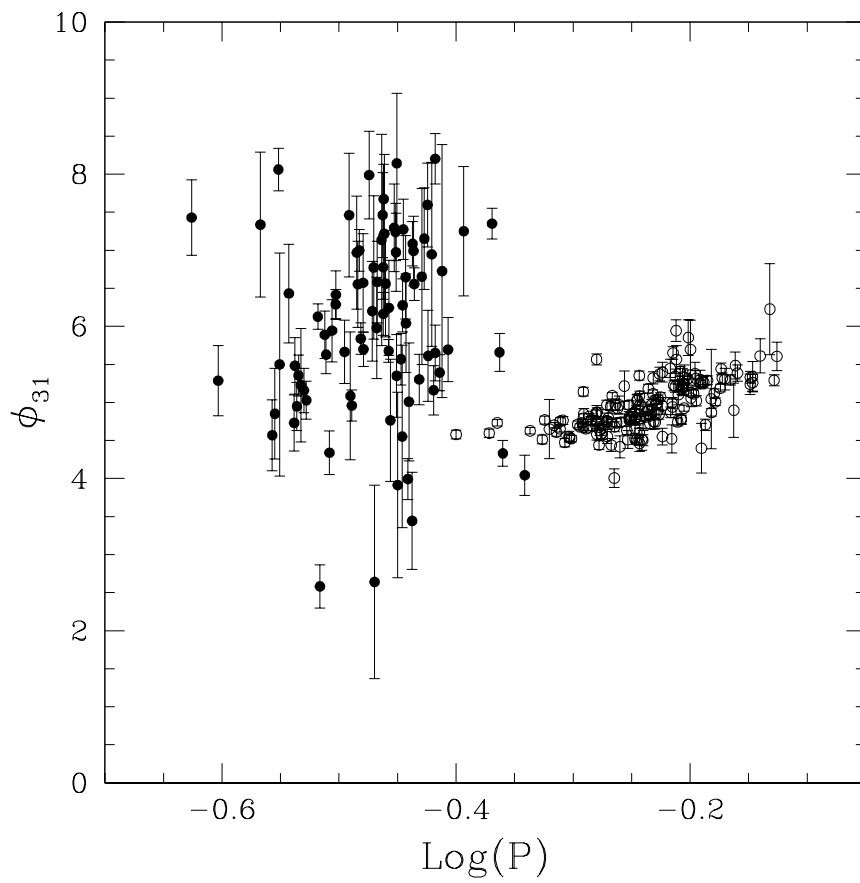


Figure 6.3  $\phi_{31}$  parameter *versus* logarithm of the period. Empty circles are RRab stars, filled circles are RRc stars.



EROS-2 id	Type	$\phi_{21}$	$\sigma_{\phi_{21}}$	$\phi_{31}$	$\sigma_{\phi_{31}}$	$A_{21}$	$\sigma_{A_{21}}$	$A_{31}$	$\sigma_{A_{31}}$	$D_m$
lm030ln16576	c	2.582	0.448	7.43	0.497	0.081	0.03	0.067	0.028	55.02
lm0305m3332	c	2.929	0.137	5.286	0.463	0.222	0.029	0.07	0.026	12.24
lm0300l15247	c	2.974	0.821	7.337	0.954	0.037	0.02	0.027	0.018	77.58
lm0436l17456	c	2.78	0.182	4.569	0.467	0.13	0.023	0.057	0.021	23.75
lm0293l18421	c	2.794	0.149	4.851	0.595	0.174	0.025	0.051	0.022	7.55
lm0437m22126	c	3.084	0.095	8.061	0.277	0.186	0.018	0.065	0.016	80.42
lm0425l24389	c	2.97	0.133	5.499	1.467	0.231	0.029	0.015	0.019	29.77
lm0427m19332	c	2.987	0.126	6.432	0.648	0.201	0.024	0.046	0.021	36.99
lm0435m10888	c	3.281	0.179	4.731	0.368	0.135	0.024	0.073	0.021	16.17
lm0425l20513	c	2.995	0.08	5.482	0.372	0.242	0.019	0.057	0.017	9.81
lm0423l20069	c	3.053	0.083	4.949	0.316	0.222	0.018	0.06	0.017	9.68
lm0302n4858	c	2.841	0.108	5.354	0.27	0.206	0.021	0.084	0.02	5.17
lm0291k24862	c	2.553	0.193	5.227	0.747	0.104	0.019	0.032	0.016	28.52
lm0435m9109	c	3.012	0.09	5.158	0.291	0.22	0.019	0.071	0.017	22.31
lm0434n14310	c	2.715	0.096	5.029	0.25	0.243	0.022	0.096	0.02	15.58
lm0291l11940	c	2.975	0.072	6.127	0.167	0.234	0.016	0.101	0.015	8.36
lm0424m19442	c	3.365	0.12	2.582	0.284	0.194	0.023	0.082	0.02	34.97
lm0425n15519	c	3.01	0.111	5.889	0.311	0.196	0.021	0.075	0.019	10.65
lm0291n2551	c	2.861	0.07	5.628	0.249	0.256	0.017	0.073	0.016	5.39
lm0425n18680	c	2.338	0.099	4.339	0.285	0.176	0.017	0.064	0.015	16.94
lm0304m2952	c	2.925	0.114	5.944	0.409	0.202	0.023	0.063	0.021	7.39
lm0303n31583	c	3.038	0.087	6.288	0.198	0.205	0.018	0.087	0.017	9.31
lm0301n7929	c	3.065	0.088	6.415	0.314	0.221	0.019	0.066	0.017	33.81
lm0425k9319	c	3.151	0.063	5.664	0.415	0.268	0.017	0.044	0.015	14.45
lm0434l23190	c	2.673	0.172	7.462	0.811	0.124	0.02	0.029	0.018	60.67
lm0303m22504	c	2.892	0.189	5.086	0.841	0.101	0.019	0.027	0.015	6.07
lm0425n13753	c	3.478	0.909	4.959	0.204	0.029	0.017	0.111	0.02	35.26
lm0303n16841	c	3.1	0.203	6.969	0.744	0.103	0.02	0.034	0.018	64.11
lm0291n15412	c	3.093	0.177	6.553	0.566	0.117	0.02	0.042	0.019	11.61
lm0300m6808	c	2.557	0.117	6.998	0.274	0.157	0.018	0.063	0.018	15.81

6.3. FOURIER ANALYSIS OF THE RR LYRAE STARS IN TILE LMC 8\_3

lm0301m15847	c	2.893	0.074	5.838	0.206	0.241	0.017	0.088	0.016	12.31
lm0436m8308	c	3.514	1.477	6.572	0.646	0.0090	0.013	0.034	0.018	17.32
lm0312115193	c	2.536	0.112	5.699	0.224	0.206	0.022	0.104	0.021	8.3
lm0425k4625	c	3.442	0.41	7.988	0.576	0.088	0.028	0.055	0.026	71.25
lm0423117670	c	3.157	0.143	6.2	0.656	0.141	0.02	0.037	0.018	9.7
lm0293m19803	c	2.782	0.132	6.773	0.943	0.136	0.018	0.022	0.015	58.37
lm030318655	c	3.6	0.238	2.641	1.271	0.138	0.031	0.023	0.023	39.71
lm0310n11585	c	3.506	0.157	5.978	0.666	0.236	0.036	0.067	0.03	10.46
lm030016753	c	3.104	0.155	6.582	0.535	0.143	0.022	0.048	0.02	9.62
lm0436115993	c	2.905	0.512	7.136	1.39	0.069	0.028	0.017	0.021	24.53
lm0302116395	c	3.607	0.253	7.463	0.558	0.118	0.028	0.056	0.026	63.49
lm0303m10773	c	3.372	0.136	6.777	0.42	0.136	0.018	0.049	0.017	12.45
lm042516481	c	3.113	0.169	6.163	0.281	0.136	0.022	0.077	0.022	9.2
lm0435m18280	c	4.274	0.629	7.673	0.458	0.048	0.022	0.056	0.022	21.7
lm0425110656	c	3.045	0.111	7.217	1.041	0.169	0.019	0.019	0.014	52.65
lm0436n10024	c	3.367	0.197	6.56	0.697	0.136	0.026	0.045	0.023	49.23
lm030018890	c	2.554	0.146	5.677	0.149	0.114	0.016	0.112	0.016	12.2
lm0310112440	c	2.969	0.179	6.243	0.626	0.115	0.02	0.038	0.018	25.65
lm0436n14285	c	2.227	0.154	4.765	0.802	0.164	0.024	0.037	0.02	9.08
lm0302k3782	c	2.544	0.251	7.295	0.576	0.15	0.035	0.067	0.031	55.75
lm0434120168	c	4.188	0.346	7.239	0.376	0.074	0.023	0.068	0.022	39.83
lm0293k30764	d	2.961	0.145	6.973	0.512	0.194	0.027	0.058	0.025	63.28
lm029119716	c	3.674	0.178	5.35	0.544	0.157	0.027	0.059	0.024	17.31
lm0435m13533	c	3.244	0.174	8.143	0.918	0.143	0.024	0.029	0.02	46.47
lm044418138	d	3.647	0.185	3.914	1.218	0.15	0.027	0.023	0.019	28.72
lm0301n13911	d	3.127	0.132	5.568	0.34	0.145	0.018	0.061	0.017	15.51
lm0291123359	c	3.319	0.503	4.551	1.199	0.081	0.029	0.028	0.023	44.47
lm0427k10785	c	2.695	0.175	6.277	0.349	0.129	0.022	0.075	0.02	14.2
lm0425m3355	c	2.622	0.255	7.274	0.397	0.156	0.037	0.097	0.034	72.29
lm0301126933	d	3.393	0.203	6.646	0.549	0.138	0.027	0.057	0.026	27.71
lm0422n16993	c	2.874	0.124	6.04	0.649	0.194	0.023	0.042	0.019	7.54
lm0310112653	d	3.043	0.135	3.993	0.268	0.183	0.024	0.089	0.025	18.5
lm0293m14230	d	2.847	0.174	5.008	0.774	0.165	0.028	0.044	0.023	22.6

lm0435k8479	d	2.891	0.72	3.443	0.637	0.067	0.032	0.072	0.032	0.032	0.032	26.59
lm0291n25922	d	3.194	0.154	7.085	0.293	0.14	0.021	0.075	0.021	0.021	0.021	32.76
lm0293m10988	c	3.236	0.188	6.991	0.458	0.111	0.02	0.044	0.018	0.018	0.018	14.58
lm0305m6294	c	3.003	0.107	6.555	0.216	0.172	0.018	0.083	0.018	0.018	0.018	27.47
lm0310k9300	c	3.337	0.108	5.302	0.332	0.156	0.017	0.057	0.015	0.015	0.015	18.14
lm0434m22078	c	2.903	0.166	6.653	1.156	0.143	0.023	0.02	0.017	0.017	0.017	22.48
lm0444i9270	c	2.94	0.221	7.152	0.669	0.141	0.029	0.053	0.027	0.027	0.027	62.54
lm0425m8144	c	3.775	0.178	7.596	0.551	0.123	0.021	0.042	0.019	0.019	0.019	77.87
lm0300n24904	c	3.044	0.137	5.612	0.6	0.163	0.022	0.045	0.019	0.019	0.019	34.31
lm0434i19810	c	2.847	0.252	6.946	1.211	0.097	0.023	0.018	0.017	0.017	0.017	12.67
lm0427i17346	c	4.998	0.174	5.159	0.326	0.124	0.021	0.074	0.02	0.02	0.02	39.84
lm0436m11977	c	3.309	0.162	5.651	0.365	0.205	0.032	0.097	0.029	0.029	0.029	9.5
lm0425k8207	c	3.044	0.176	8.203	0.332	0.136	0.023	0.072	0.023	0.023	0.023	18.38
lm0303m23391	d	2.833	0.102	5.392	0.238	0.238	0.023	0.105	0.021	0.021	0.021	6.93
lm0427i4507	c	3.979	0.635	6.726	1.664	0.061	0.028	0.0040	0.021	0.021	0.021	17.88
lm0303k24363	d	2.792	0.114	5.694	0.42	0.183	0.02	0.056	0.019	0.019	0.019	13.77
lm0424m22887	ab	2.19	0.04	4.578	0.058	0.485	0.017	0.295	0.017	0.017	0.017	2.21
lm0302k5022	c	4.325	0.509	7.25	0.85	0.06	0.023	0.034	0.021	0.021	0.021	15.12
lm0302i12678	ab	2.068	0.039	4.596	0.055	0.496	0.017	0.312	0.017	0.017	0.017	2.41
lm0303m22989	c	2.724	0.703	7.35	0.204	0.039	0.018	0.106	0.021	0.021	0.021	47.98
lm0436n11172	ab	2.136	0.031	4.731	0.042	0.504	0.014	0.333	0.014	0.014	0.014	1.93
lm0300i14647	c	3.456	0.112	5.659	0.249	0.246	0.027	0.115	0.024	0.024	0.024	10.81
lm0293n31080	c	2.125	0.062	4.331	0.17	0.335	0.019	0.119	0.018	0.018	0.018	23.27
lm0434i7912	c	2.195	0.084	4.043	0.264	0.446	0.034	0.131	0.029	0.029	0.029	37.59
lm0312k21111	ab	2.101	0.032	4.626	0.043	0.506	0.014	0.325	0.014	0.014	0.014	2.16
lm0293k3928	ab	2.073	0.035	4.514	0.058	0.415	0.013	0.234	0.012	0.012	0.012	9.58
lm0293n30795	ab	2.222	0.036	4.769	0.052	0.5	0.016	0.308	0.016	0.016	0.016	2.31
lm0432i12420	ab	2.122	0.083	4.65	0.39	0.284	0.022	0.063	0.019	0.019	0.019	42.88
lm0427n7741	ab	2.256	0.026	4.699	0.036	0.474	0.011	0.305	0.011	0.011	0.011	1.2
lm0300m9935	ab	2.297	0.039	4.61	0.053	0.397	0.014	0.264	0.014	0.014	0.014	9.15
lm0437k15772	ab	2.233	0.031	4.654	0.043	0.495	0.014	0.317	0.014	0.014	0.014	1.88
lm0434i20435	ab	2.171	0.034	4.754	0.046	0.491	0.015	0.318	0.015	0.015	0.015	1.49
lm0437k22654	ab	2.275	0.036	4.764	0.053	0.51	0.017	0.308	0.017	0.017	0.017	2.39

6.3. FOURIER ANALYSIS OF THE RR LYRAE STARS IN TILE LMC 8\_3

lm0436n20628	ab	2.213	0.041	4.473	0.055	0.432	0.016	0.289	0.016	4.37
lm0302n23523	ab	2.34	0.043	4.55	0.069	0.367	0.014	0.211	0.014	10.81
lm0293k28352	ab	2.254	0.033	4.534	0.042	0.404	0.012	0.291	0.012	6.65
lm0303n13977	ab	2.254	0.031	4.524	0.042	0.449	0.013	0.301	0.013	1.53
lm0303n15322	ab	2.162	0.032	4.71	0.044	0.489	0.014	0.315	0.014	1.76
lm0293m14375	ab	2.189	0.029	4.678	0.04	0.51	0.014	0.328	0.013	2.55
lm0301l24255	ab	2.201	0.034	4.732	0.047	0.51	0.016	0.325	0.015	2.32
lm0436l20450	ab	2.246	0.043	4.792	0.059	0.564	0.022	0.366	0.021	3.12
lm0437m20444	ab	2.439	0.036	5.141	0.057	0.553	0.018	0.312	0.016	2.07
lm0302l23297	ab	2.134	0.036	4.676	0.05	0.547	0.017	0.341	0.017	3.26
lm0291m8710	ab	2.294	0.045	4.849	0.073	0.434	0.018	0.239	0.017	1.8
lm0435k20062	ab	2.142	0.039	4.654	0.053	0.511	0.018	0.332	0.018	2.55
lm0291n20101	ab	2.302	0.028	4.814	0.039	0.467	0.012	0.303	0.012	1.67
lm0300m17178	ab	2.259	0.035	4.765	0.048	0.519	0.016	0.339	0.016	2.19
lm0302m22487	ab	2.443	0.052	4.689	0.06	0.357	0.018	0.297	0.018	6.57
lm0303m17152	ab	2.312	0.039	4.844	0.056	0.535	0.019	0.332	0.018	2.93
lm0300k12184	ab	2.294	0.038	4.76	0.056	0.396	0.014	0.245	0.014	1.69
lm0303k25210	ab	2.596	0.045	5.566	0.073	0.516	0.021	0.276	0.019	0.87
lm0435m17793	ab	2.235	0.034	4.744	0.048	0.473	0.015	0.298	0.014	1.3
lm0435m23563	ab	2.383	0.047	4.867	0.091	0.359	0.016	0.175	0.015	4.13
lm0425n23250	ab	2.093	0.045	4.581	0.075	0.468	0.019	0.258	0.018	2.73
lm0300m19324	ab	2.41	0.033	4.871	0.058	0.367	0.011	0.193	0.011	3.92
lm0300l13312	ab	2.174	0.039	4.439	0.056	0.453	0.016	0.281	0.016	2.59
lm0291n6040	ab	2.324	0.034	4.677	0.048	0.408	0.013	0.266	0.013	2.65
lm0301n16814	ab	2.245	0.034	4.629	0.064	0.439	0.014	0.21	0.013	6.98
lm0426n12018	ab	2.096	0.053	4.59	0.073	0.458	0.022	0.297	0.022	1.86
lm0291n20061	ab	2.207	0.042	4.582	0.07	0.399	0.015	0.222	0.015	6.67
lm0301n21605	ab	2.063	0.033	4.703	0.04	0.433	0.013	0.337	0.013	5.24
lm0301m22780	ab	2.267	0.037	4.759	0.05	0.495	0.016	0.325	0.016	1.26
lm0301k17554	ab	2.299	0.041	4.967	0.06	0.51	0.019	0.304	0.018	1.58
lm0425l14852	ab	2.126	0.032	4.753	0.044	0.515	0.015	0.325	0.015	2.29
lm0437m17477	ab	2.062	0.059	4.552	0.091	0.336	0.018	0.213	0.017	19.77
lm0310k11253	ab	2.233	0.045	4.797	0.063	0.515	0.021	0.331	0.02	2.19

lm0434k22095	ab	2.283	0.034	4.945	0.05	0.535	0.016	0.327	0.016	2.1
lm0425k11500	ab	2.154	0.064	4.441	0.086	0.342	0.02	0.245	0.02	3.99
lm0434m6139	ab	2.156	0.037	4.728	0.049	0.528	0.017	0.348	0.017	2.26
lm0301m15584	ab	2.317	0.03	5.088	0.043	0.539	0.015	0.331	0.014	1.67
lm0446k20706	ab	1.91	0.068	4.006	0.122	0.455	0.028	0.23	0.026	5.62
lm0427m14753	ab	2.155	0.047	4.681	0.064	0.505	0.022	0.33	0.021	2.95
lm0437n14794	ab	2.282	0.047	4.968	0.075	0.494	0.021	0.271	0.019	1.81
lm0300m23701	ab	2.187	0.041	4.731	0.057	0.507	0.019	0.318	0.018	2.72
lm0425m12624	ab	2.302	0.042	4.922	0.07	0.481	0.018	0.267	0.017	1.57
lm0300m23266	ab	2.176	0.075	4.967	0.116	0.572	0.038	0.327	0.034	3.57
lm0301n14847	ab	2.295	0.053	4.417	0.145	0.38	0.018	0.128	0.017	12.91
lm0435m9334	ab	2.198	0.043	4.741	0.058	0.521	0.02	0.335	0.019	3.34
lm0423l11740	ab	2.681	0.087	5.214	0.199	0.355	0.029	0.151	0.026	3.04
lm0291k10561	ab	2.136	0.041	4.631	0.055	0.461	0.017	0.314	0.017	1.62
lm0291m11933	ab	2.197	0.051	4.512	0.118	0.391	0.018	0.152	0.018	21.22
lm0423n26224	ab	2.297	0.039	4.966	0.058	0.548	0.019	0.332	0.018	2.39
lm0302k14796	ab	2.405	0.05	4.811	0.069	0.45	0.02	0.29	0.02	2.7
lm0300m11839	ab	2.191	0.034	4.777	0.048	0.487	0.015	0.311	0.014	1.46
lm0303l17671	ab	2.225	0.032	4.801	0.046	0.498	0.014	0.317	0.013	1.85
lm0423l7926	ab	2.224	0.035	4.773	0.055	0.456	0.014	0.26	0.014	1.41
lm0427l18856	ab	2.259	0.046	4.812	0.064	0.466	0.02	0.303	0.019	1.15
lm0303m17812	ab	2.318	0.038	4.868	0.052	0.467	0.016	0.301	0.016	1.24
lm0302n12351	ab	2.448	0.067	4.655	0.122	0.408	0.025	0.199	0.024	3.26
lm0300k14335	ab	2.191	0.04	4.529	0.054	0.363	0.013	0.253	0.013	1.51
lm0300n27286	ab	2.238	0.028	4.782	0.039	0.504	0.013	0.314	0.012	2.06
lm0302l12960	ab	2.313	0.06	4.803	0.103	0.399	0.022	0.222	0.02	7.43
lm0300n21091	ab	2.244	0.048	4.895	0.069	0.573	0.024	0.35	0.023	3.05
lm0434k9008	ab	2.35	0.038	4.505	0.06	0.344	0.012	0.19	0.012	2.78
lm0301l11630	ab	2.441	0.041	5.023	0.075	0.396	0.015	0.2	0.014	3.16
lm0300k17665	ab	2.357	0.048	5.037	0.07	0.537	0.023	0.325	0.022	2.69
lm0291l10775	ab	2.491	0.041	5.352	0.061	0.582	0.021	0.346	0.02	1.43
lm0300m11600	ab	2.14	0.044	4.6	0.059	0.462	0.019	0.307	0.018	3.5
lm0437n15049	ab	2.137	0.044	4.786	0.065	0.489	0.019	0.297	0.018	2.07

6.3. FOURIER ANALYSIS OF THE RR LYRAE STARS IN TILE LMC 8\_3

lm0434n13704	ab	2.277	0.044	5.084	0.064	0.543	0.021	0.336	0.02	1.7
lm0427l12462	ab	2.173	0.072	4.462	0.108	0.303	0.02	0.197	0.019	24.7
lm0435l5247	ab	2.332	0.062	4.969	0.15	0.405	0.023	0.155	0.021	3.35
lm0434m21424	ab	2.526	0.099	4.515	0.145	0.295	0.028	0.202	0.026	11.26
lm0437n8455	ab	2.248	0.065	4.503	0.073	0.371	0.022	0.309	0.023	9.94
lm0444l20033	ab	2.268	0.131	4.818	0.187	0.343	0.041	0.241	0.039	18.27
lm0293n20870	ab	2.268	0.039	4.81	0.049	0.45	0.016	0.331	0.016	2.43
lm0437m20883	ab	2.271	0.039	4.893	0.057	0.493	0.017	0.297	0.017	1.82
lm0293m19628	ab	2.338	0.039	5.182	0.059	0.508	0.018	0.293	0.017	1.86
lm0303n12799	ab	2.288	0.047	4.902	0.077	0.424	0.018	0.235	0.017	0.97
lm0434l17031	ab	2.078	0.051	4.721	0.071	0.55	0.025	0.343	0.025	3.95
lm0293m19003	ab	2.328	0.046	4.826	0.052	0.366	0.015	0.315	0.016	8.53
lm0437k15328	ab	2.289	0.042	4.894	0.061	0.562	0.021	0.336	0.02	3.01
lm0291k10047	ab	2.287	0.046	4.971	0.067	0.557	0.022	0.333	0.021	2.61
lm0293k25226	ab	2.438	0.037	5.113	0.053	0.503	0.017	0.31	0.016	0.87
lm0303m27302	ab	2.539	0.048	5.322	0.08	0.468	0.02	0.254	0.019	1.74
lm0435n11321	ab	2.201	0.057	4.748	0.095	0.382	0.02	0.211	0.019	3.81
lm0437k8681	ab	2.158	0.053	4.742	0.092	0.407	0.02	0.215	0.019	1.86
lm0300l20739	ab	2.274	0.038	5.03	0.056	0.473	0.016	0.281	0.016	1.76
lm0310l18147	ab	2.189	0.055	4.85	0.08	0.494	0.024	0.307	0.024	3.06
lm0302l26417	ab	2.304	0.053	4.974	0.072	0.548	0.026	0.353	0.025	2.64
lm0310k18010	ab	2.286	0.034	4.978	0.05	0.529	0.016	0.311	0.015	2.12
lm0300k16563	ab	2.303	0.037	5.041	0.057	0.516	0.017	0.292	0.016	1.91
lm0303m21245	ab	2.176	0.044	4.843	0.065	0.496	0.02	0.301	0.019	2.53
lm0437k13906	ab	2.508	0.054	5.372	0.09	0.476	0.023	0.264	0.021	0.62
lm0293m17000	ab	2.356	0.039	5.07	0.058	0.478	0.017	0.29	0.016	0.86
lm0435m7058	ab	2.166	0.069	4.551	0.11	0.332	0.021	0.184	0.022	7.92
lm0425m4288	ab	2.334	0.061	4.955	0.109	0.481	0.026	0.245	0.024	2.13
lm0435n13913	ab	2.475	0.061	5.398	0.128	0.377	0.021	0.171	0.019	21.96
lm0426m24414	ab	2.502	0.071	5.447	0.121	0.449	0.029	0.251	0.026	1.19
lm0425l10247	ab	2.221	0.046	4.869	0.069	0.487	0.02	0.292	0.019	1.63
lm0310k15738	ab	2.216	0.081	4.521	0.184	0.27	0.02	0.117	0.02	17.13
lm0435k12309	ab	2.291	0.046	4.993	0.069	0.459	0.019	0.283	0.019	1.05

lm043519858	ab	2.253	0.068	4.941	0.103	0.496	0.03	0.292	0.029	2.21
lm0434k7302	ab	2.667	0.055	5.65	0.084	0.536	0.027	0.295	0.026	0.59
lm0293112631	ab	2.413	0.044	5.224	0.069	0.498	0.02	0.29	0.019	0.84
lm0435k17589	ab	2.509	0.061	5.342	0.098	0.48	0.026	0.278	0.024	0.76
lm029315252	ab	2.34	0.047	5.21	0.074	0.471	0.02	0.272	0.019	1.94
lm0312k4503	ab	2.686	0.074	5.942	0.142	0.498	0.033	0.238	0.029	9.81
lm0436k15855	ab	2.155	0.074	5.566	0.182	0.503	0.033	0.179	0.028	7.97
lm0425121048	ab	2.228	0.039	4.743	0.054	0.492	0.017	0.316	0.017	2.05
lm0427m20466	ab	2.339	0.064	5.102	0.135	0.452	0.026	0.195	0.023	4.15
lm0435k12002	ab	2.521	0.046	5.409	0.066	0.54	0.022	0.326	0.021	0.7
lm0424n5227	ab	2.211	0.048	4.781	0.067	0.55	0.023	0.349	0.022	3.64
lm0437m9713	ab	2.234	0.039	4.772	0.058	0.492	0.017	0.294	0.017	2.27
lm0303126148	ab	2.467	0.056	5.202	0.095	0.438	0.022	0.24	0.021	1.01
lm0302k13534	ab	2.424	0.05	5.179	0.082	0.481	0.021	0.266	0.02	0.87
lm0305k5704	ab	2.478	0.065	5.334	0.112	0.443	0.026	0.234	0.024	0.87
lm0437115735	ab	2.287	0.062	5.199	0.108	0.43	0.025	0.211	0.024	2.76
lm0434m19648	ab	2.479	0.054	5.248	0.095	0.408	0.02	0.214	0.019	0.98
lm0300n13961	ab	2.327	0.029	4.925	0.041	0.51	0.013	0.325	0.013	1.03
lm0303127610	ab	2.389	0.061	5.249	0.101	0.417	0.023	0.234	0.022	1.37
lm0292n22612	ab	2.614	0.082	5.327	0.165	0.432	0.032	0.204	0.029	1.71
lm0293n18229	ab	2.381	0.065	5.31	0.116	0.437	0.026	0.222	0.025	1.85
lm0303n9745	ab	2.652	0.074	5.852	0.233	0.482	0.032	0.138	0.028	37.03
lm0435m18273	ab	2.603	0.078	5.695	0.386	0.402	0.029	0.08	0.025	12.43
lm0423121178	ab	2.194	0.067	5.057	0.112	0.435	0.026	0.245	0.024	2.9
lm0303n16102	ab	2.418	0.032	5.128	0.045	0.516	0.015	0.315	0.014	0.97
lm0424n12543	ab	2.39	0.035	5.115	0.051	0.503	0.016	0.306	0.016	0.71
lm0300n19927	ab	2.565	0.083	5.378	0.149	0.403	0.031	0.198	0.031	1.03
lm0300125566	ab	2.454	0.06	5.316	0.1	0.399	0.022	0.226	0.021	1.11
lm0435k15816	ab	2.297	0.045	5.023	0.067	0.472	0.019	0.289	0.018	1.21
lm0300k11860	ab	2.484	0.057	5.302	0.121	0.428	0.022	0.184	0.02	1.94
lm0303m11005	ab	2.374	0.03	5.249	0.044	0.528	0.014	0.32	0.013	2.12
lm0301n14943	ab	2.391	0.098	4.398	0.326	0.379	0.034	0.111	0.03	8.01
lm0436m17011	ab	2.537	0.046	5.278	0.078	0.502	0.021	0.271	0.019	1.03

6.3. FOURIER ANALYSIS OF THE RR LYRAE STARS IN TILE LMC 8\_3

lm0301122786	ab	2.467	0.048	5.266	0.075	0.484	0.021	0.277	0.019	0.7
lm0436n8236	ab	2.313	0.057	4.707	0.074	0.458	0.024	0.314	0.024	3.22
lm0300m25109	ab	2.382	0.035	5.29	0.056	0.536	0.017	0.291	0.016	2.43
lm0310l16334	ab	2.532	0.109	5.045	0.654	0.375	0.037	0.066	0.031	19.71
lm0293l25506	ab	2.207	0.035	4.869	0.049	0.469	0.015	0.3	0.015	1.47
lm0310l14484	ab	2.369	0.045	5.118	0.063	0.519	0.021	0.321	0.02	1.76
lm0301l25140	ab	2.371	0.034	5.009	0.048	0.552	0.017	0.34	0.016	2.65
lm0291l26545	ab	2.413	0.033	5.188	0.049	0.545	0.016	0.324	0.015	1.38
lm0434n8413	ab	2.58	0.048	5.441	0.076	0.521	0.022	0.293	0.021	0.64
lm0300n12088	ab	2.405	0.041	5.32	0.07	0.556	0.02	0.287	0.018	1.74
lm0427k17452	ab	2.317	0.075	5.306	0.142	0.444	0.03	0.221	0.027	4.07
lm0300n12109	ab	2.486	0.043	5.297	0.066	0.489	0.019	0.275	0.018	0.63
lm0426n9666	ab	2.435	0.19	4.897	0.355	0.166	0.03	0.096	0.027	48.54
lm0434n22292	ab	2.656	0.086	5.484	0.178	0.501	0.039	0.218	0.034	5.84
lm0303m5651	ab	2.595	0.055	5.386	0.107	0.467	0.023	0.221	0.02	2.12
lm0301m15788	ab	2.339	0.086	5.239	0.133	0.452	0.035	0.279	0.033	6.1
lm0305m3882	ab	2.54	0.05	5.33	0.078	0.474	0.021	0.277	0.02	0.78
lm0305m7850	ab	2.598	0.099	5.338	0.199	0.309	0.029	0.151	0.026	16.23
lm0427m6338	ab	2.543	0.052	5.259	0.111	0.479	0.023	0.204	0.019	12.2
lm0434n17383	ab	2.404	0.086	5.611	0.224	0.373	0.029	0.136	0.026	5.61
lm0301l16487	ab	2.667	0.149	6.226	0.599	0.322	0.044	0.087	0.038	44.37
lm0300l23462	ab	2.44	0.047	5.291	0.073	0.499	0.021	0.286	0.02	0.88
lm0310l18911	ab	2.59	0.071	5.605	0.188	0.415	0.027	0.145	0.024	4.97

Table 6.4: Fourier parameters of the 251 confirmed RR Lyrae stars in tile LMC 8\_3.



## 6.4 Metallicity of the RR Lyrae stars in tile LMC 8\_3

Spectroscopically determined metallicities are not available for the RR Lyrae stars in tile LMC 8\_3, so we estimated individual photometric metal abundances from the Fourier parameters of the light curves (see Subsection 1.5.1). In particular, we applied Eqs. 1.11 and 1.13 to derive the metallicity of RRab and RRC stars, respectively, and Eq. 1.12 to obtain the  $\phi_{31}$  Fourier parameters in the *Kepler* magnitudes.

Following Cacciari et al. (2005) and Kapakos et al. (2011) we only considered RRab stars for which  $D_m < 5$  (132 RRab stars) and RRC stars for which  $\sigma(\phi_{31}) < 0.3$  (20 RRC stars). Among the RRC stars we also discarded:

- Im0437m22126, since it has a positive value of metallicity ( $[Fe/H] = 0.490 \pm 0.368$  dex), out of the range of typical metallicities of RR Lyrae stars in the LMC;
- Im0300114647. This star was classified as RRC by us, and as RRd by OGLE III.
- Im0293n31080 - RRC according to our classification, but RRab according to the OGLE III catalogue. Since the classification of this star is doubtful we discarded this star from the following analysis. However, it should be noted that if the star were considered as an RRab its  $D_m$  value would be larger than 5, hence, its photometric metallicity would not be reliable.

Individual photometric metallicities for the 132 RRab stars and 17 RRC stars are presented in Tables 6.5 and 6.6, respectively. They are all on the Carretta et al. (2009) metallicity scale. The weighted mean metallicity of the RRab stars in tile LMC 8\_3 is:  $\langle [Fe/H]_{C09} \rangle = (-1.58 \pm 0.01)$  dex,  $\sigma = 0.5$ , average on 132 stars. The weighted mean metallicity mean of the RRC stars is:  $\langle [Fe/H]_{C09} \rangle = (-1.82 \pm 0.04)$  dex,  $\sigma = 0.3$ , average on 17 stars. There is a systematic difference of  $\sim 0.25$  dex between the two mean metallicities, with the RRab stars being more metal rich. Nemeč et al. (2013) calibrated Eq. 1.11 using accurate pulsation periods, Fourier light curve parameters and spectroscopic metal abundances of 37 field RRab stars observed by the *Kepler* satellite. Instead the sample of *Kepler*-field RRC stars contained only four objects, so it was not possible to derive independently a relation similar to Eq. 1.11 for the RRC stars. Nemeč et al. (2013) added the four *Kepler*-RRC stars to the sample of 106 RRC stars in 12 globular clusters analysed by Morgan et al. (2007), who derived the  $P - \phi_{31} - [Fe/H]$  relation on the range of metallicities from -2.2 to -1.0

#### 6.4. METALLICITY OF THE RR LYRAE STARS IN TILE LMC 8\_3

---

dex. Nemeč et al. (2013) obtained Eq. 1.13 by recalibrating Morgan et al. (2007)'s relation. Some systematics in the calibration of the two different relations used to estimate the metallicity of the RRab and RRc stars could be the cause of the systematic offset of  $\sim 0.25$  dex we find between the metallicity of RRab and RRc stars in tile LMC 8\_3.

EROS-2 id	Period (days)	$\phi_{31}$ (V)	$\phi_{31\_kep}$	Error $\phi_{31\_kep}$	$[Fe/H]_{C09}$ (dex)	Error $[Fe/H]_{C09}$ dex	$D_m$
lm0436n8236	0.650192	4.707	4.858	0.078	-2.97	0.249	3.22
lm0434k9008	0.567635	4.505	4.656	0.065	-2.711	0.2	2.78
lm0300k14335	0.566157	4.529	4.68	0.06	-2.628	0.184	1.51
lm0425k11500	0.540233	4.441	4.592	0.09	-2.584	0.254	3.99
lm0293i25506	0.657982	4.869	5.02	0.055	-2.563	0.177	1.47
lm0425i21048	0.615813	4.743	4.894	0.06	-2.537	0.184	2.05
lm0437m9713	0.620011	4.772	4.923	0.064	-2.496	0.192	2.27
lm0300m11600	0.570995	4.6	4.751	0.064	-2.485	0.191	3.5
lm0424n5227	0.619983	4.781	4.932	0.072	-2.471	0.211	3.64
lm0300i13312	0.527452	4.439	4.59	0.062	-2.444	0.182	2.59
lm0302n12351	0.566134	4.655	4.806	0.125	-2.29	0.323	3.26
lm0437k8681	0.589055	4.742	4.893	0.096	-2.287	0.257	1.86
lm0434i17031	0.582937	4.721	4.872	0.076	-2.283	0.21	3.95
lm0291k10561	0.5571	4.631	4.782	0.061	-2.261	0.175	1.62
lm0435n11321	0.587183	4.748	4.899	0.098	-2.254	0.262	3.81
lm0301i25140	0.663184	5.009	5.16	0.055	-2.218	0.167	2.65
lm0425i10247	0.607461	4.869	5.02	0.074	-2.126	0.202	1.63
lm0300n13961	0.623548	4.925	5.076	0.049	-2.12	0.149	1.03
lm0426n12018	0.52946	4.59	4.741	0.077	-2.08	0.204	1.86
lm0303m21245	0.593551	4.843	4.994	0.07	-2.07	0.19	2.53
lm0425n23250	0.525191	4.581	4.732	0.079	-2.058	0.207	2.73
lm0310i18147	0.590217	4.85	5.001	0.084	-2.024	0.219	3.06
lm0293n20870	0.57819	4.81	4.961	0.055	-2.015	0.157	2.43
lm0437n15049	0.571014	4.786	4.937	0.07	-2.008	0.187	2.07
lm0427m14753	0.54401	4.681	4.832	0.069	-2.006	0.184	2.95
lm0300i23462	0.744314	5.291	5.442	0.077	-2.004	0.228	0.88
lm0435k15816	0.638794	5.023	5.174	0.072	-1.993	0.196	1.21
lm0300n27286	0.566301	4.782	4.933	0.047	-1.975	0.139	2.06
lm0436n20628	0.493107	4.473	4.624	0.061	-1.973	0.166	4.37
lm0435i9858	0.609462	4.941	5.092	0.106	-1.964	0.266	2.21

6.4. METALLICITY OF THE RR LYRAE STARS IN TILE LMC 8\_3

lm0423l7926	4.773	4.924	0.061	-1.955	0.166	1.41
lm0435m9334	4.741	4.892	0.064	-1.928	0.17	3.34
lm0300m11839	4.777	4.928	0.055	-1.926	0.153	1.46
lm0303n13977	4.524	4.675	0.049	-1.922	0.142	1.53
lm0310l14484	5.118	5.269	0.068	-1.922	0.188	1.76
lm0300m23701	4.731	4.882	0.063	-1.907	0.167	2.72
lm0303l17671	4.801	4.952	0.053	-1.877	0.148	1.85
lm0427l18856	4.812	4.963	0.069	-1.871	0.179	1.15
lm0437k15328	4.894	5.045	0.066	-1.869	0.175	3.01
lm0434m6139	4.728	4.879	0.055	-1.859	0.152	2.26
lm0423l21178	5.057	5.208	0.115	-1.858	0.282	2.9
lm0291n6040	4.677	4.828	0.055	-1.854	0.15	2.65
lm0302k14796	4.811	4.962	0.074	-1.845	0.187	2.7
lm0435k12309	4.993	5.144	0.074	-1.835	0.19	1.05
lm0437m20883	4.893	5.044	0.063	-1.835	0.166	1.82
lm0425m4288	4.955	5.106	0.112	-1.833	0.268	2.13
lm0303n12799	4.902	5.053	0.081	-1.827	0.203	0.97
lm0291l26545	5.188	5.339	0.055	-1.801	0.159	1.38
lm0435k20062	4.654	4.805	0.059	-1.773	0.156	2.55
lm0303m17812	4.868	5.019	0.058	-1.766	0.155	1.24
lm0425l14852	4.753	4.904	0.051	-1.761	0.141	2.29
lm0424n12543	5.115	5.266	0.057	-1.743	0.157	0.71
lm0301m22780	4.759	4.91	0.056	-1.742	0.15	1.26
lm0302l26417	4.974	5.125	0.077	-1.731	0.19	2.64
lm0300n21091	4.895	5.046	0.074	-1.722	0.183	3.05
lm0310k18010	4.978	5.129	0.056	-1.721	0.151	2.12
lm0305m3882	5.33	5.481	0.082	-1.701	0.219	0.78
lm0302l23297	4.676	4.827	0.056	-1.697	0.149	3.26
lm0291k10047	4.971	5.122	0.072	-1.695	0.179	2.61
lm0303n16102	5.128	5.279	0.052	-1.692	0.146	0.97
lm0435m17793	4.744	4.895	0.055	-1.677	0.145	1.3
lm0310k11253	4.797	4.948	0.068	-1.673	0.169	2.19
lm0293m14375	4.678	4.829	0.048	-1.659	0.133	2.55

lm0300k12184	0.524813	4.76	4.911	0.062	-1.641	0.156	1.69
lm0427m20466	0.616626	5.102	5.253	0.137	-1.639	0.309	4.15
lm0300n12109	0.683459	5.297	5.448	0.071	-1.624	0.187	0.63
lm0300k16563	0.592704	5.041	5.192	0.063	-1.599	0.159	1.91
lm0300l20739	0.589066	5.03	5.181	0.062	-1.596	0.157	1.76
lm0435l5247	0.571823	4.969	5.12	0.152	-1.594	0.325	3.35
lm0300m17178	0.518967	4.765	4.916	0.055	-1.576	0.142	2.19
lm0303n15322	0.505733	4.71	4.861	0.051	-1.568	0.136	1.76
lm0301l24255	0.51058	4.732	4.883	0.054	-1.567	0.14	2.32
lm0427k17452	0.675498	5.306	5.457	0.144	-1.556	0.333	4.07
lm0293m17000	0.595224	5.07	5.221	0.064	-1.555	0.159	0.86
lm0437k15772	0.488322	4.654	4.805	0.05	-1.515	0.134	1.88
lm0300n12088	0.672356	5.32	5.471	0.075	-1.505	0.187	1.74
lm0423n26224	0.559366	4.966	5.117	0.064	-1.5	0.155	2.39
lm0302k13534	0.62088	5.179	5.33	0.086	-1.498	0.2	0.87
lm0303m11005	0.64377	5.249	5.4	0.051	-1.492	0.14	2.12
lm0425m12624	0.547065	4.922	5.073	0.075	-1.492	0.173	1.57
lm0301l22786	0.648027	5.266	5.417	0.079	-1.481	0.191	0.7
lm0437l15735	0.622553	5.199	5.35	0.111	-1.466	0.246	2.76
lm0303m5651	0.692547	5.386	5.537	0.11	-1.465	0.262	2.12
lm0291n20101	0.517254	4.814	4.965	0.047	-1.457	0.127	1.67
lm0300m25109	0.652891	5.29	5.441	0.062	-1.457	0.158	2.43
lm0303m17152	0.524201	4.844	4.995	0.062	-1.457	0.15	2.93
lm0301l11630	0.568156	5.023	5.174	0.079	-1.45	0.181	3.16
lm0436l20450	0.511395	4.792	4.943	0.064	-1.449	0.154	3.12
lm0303l26148	0.620647	5.202	5.353	0.098	-1.447	0.221	1.01
lm0436m17011	0.645996	5.278	5.429	0.082	-1.442	0.194	1.03
lm0300k17665	0.568997	5.037	5.188	0.075	-1.428	0.172	2.69
lm0435m23563	0.525048	4.867	5.018	0.095	-1.418	0.203	4.13
lm0300m23266	0.548868	4.967	5.118	0.119	-1.414	0.246	3.57
lm0300m19324	0.525312	4.871	5.022	0.064	-1.412	0.151	3.92
lm0293k25226	0.586479	5.113	5.264	0.059	-1.4	0.146	0.87
lm0434k22095	0.539682	4.945	5.096	0.056	-1.384	0.139	2.1

6.4. METALLICITY OF THE RR LYRAE STARS IN TILE LMC 8\_3

lm0293l5252	0.612908	5.21	5.361	0.078	-1.379	0.18	1.94
lm0437n14794	0.544769	4.968	5.119	0.079	-1.379	0.176	1.81
lm0300k11860	0.643757	5.302	5.453	0.124	-1.377	0.268	1.94
lm0427n7741	0.48284	4.699	4.85	0.044	-1.369	0.121	1.2
lm0303l27610	0.623747	5.249	5.4	0.104	-1.367	0.227	1.37
lm0434m19648	0.622604	5.248	5.399	0.098	-1.362	0.216	0.98
lm0434n13704	0.571166	5.084	5.235	0.069	-1.349	0.159	1.7
lm0291m8710	0.511745	4.849	5.0	0.077	-1.338	0.17	1.8
lm0293l12631	0.610866	5.224	5.375	0.074	-1.337	0.17	0.84
lm0437k22654	0.491312	4.764	4.915	0.059	-1.32	0.141	2.39
lm0434l20435	0.48881	4.754	4.905	0.053	-1.317	0.132	1.49
lm0300l25566	0.638155	5.316	5.467	0.103	-1.314	0.224	1.11
lm0301k17554	0.535567	4.967	5.118	0.065	-1.307	0.15	1.58
lm0312k21111	0.4606	4.626	4.777	0.05	-1.293	0.128	2.16
lm0293n18229	0.628127	5.31	5.461	0.119	-1.268	0.246	1.85
lm0434n8413	0.670871	5.441	5.592	0.08	-1.23	0.185	0.64
lm0293m19628	0.581141	5.182	5.333	0.064	-1.226	0.147	1.86
lm0310l18911	0.748431	5.605	5.756	0.19	-1.215	0.431	4.97
lm0292n22612	0.624068	5.327	5.478	0.167	-1.21	0.323	1.71
lm0300n19927	0.637129	5.378	5.529	0.151	-1.182	0.297	1.03
lm0305k5704	0.6216	5.334	5.485	0.115	-1.182	0.232	0.87
lm0293n30795	0.474027	4.769	4.92	0.058	-1.15	0.134	2.31
lm0301m15584	0.54134	5.088	5.239	0.05	-1.124	0.122	1.67
lm0435k17589	0.612635	5.342	5.493	0.101	-1.115	0.203	0.76
lm0435k12002	0.618774	5.409	5.56	0.071	-1.024	0.152	0.7
lm0303n27302	0.586637	5.322	5.473	0.084	-1.003	0.166	1.74
lm0423l1740	0.554337	5.214	5.365	0.201	-0.991	0.325	3.04
lm0302l12678	0.424945	4.596	4.747	0.061	-0.983	0.135	2.41
lm0437k13906	0.594332	5.372	5.523	0.094	-0.959	0.177	0.62
lm0426m24414	0.606869	5.447	5.598	0.124	-0.896	0.217	1.19
lm0291l10775	0.570992	5.352	5.503	0.066	-0.863	0.134	1.43
lm0437m20444	0.511423	5.141	5.292	0.063	-0.822	0.126	2.07
lm0436n11172	0.431733	4.731	4.882	0.049	-0.819	0.115	1.93

lm0424m22887	0.398125	4.578	4.729	0.064	-0.735	0.132	2.21
lm0434k7302	0.610192	5.65	5.801	0.088	-0.592	0.147	0.59
lm0303k25210	0.524918	5.566	5.717	0.077	-0.353	0.112	0.87

Table 6.5: Photometric metallicity of 132 RRab stars in tile LMC 8\_3 for which  $D_m < 5$  (Column 1: EROS-2 identification of the star; Column 2: Period of the star from the EROS-2 catalogue; Column 3: Fourier parameter  $\phi_{31}$  of the sine Fourier decomposition of light curves in the  $V_I$  passband; Column 4: Fourier parameter  $\phi_{31}$  of the sine Fourier decomposition in the Kepler magnitudes derived with Eq. 1.12; Column 5: Error of  $\phi_{31}$  in the Kepler magnitudes; Column 6: Metallicity on the C09 metallicity scale derived with Eq. 1.11; Column 7: Error of metallicity on the C09 metallicity scale; Column 8:  $D_m$  value).

6.4. METALLICITY OF THE RR LYRAE STARS IN TILE LMC 8\_3

EROS-2 id	Period (days)	$\phi_{31}^c$	err $\phi_{31}^c$	$[Fe/H]_{C09}$ (dex)	err $[Fe/H]_{C09}$ (dex)
lm0300l14647	0.43362	2.517	0.249	-2.76	0.131
lm0293n31080	0.43653	1.189	0.17	-2.483	0.148
lm0434l7912	0.45709	0.901	0.264	-2.374	0.194
lm0303m22989	0.427324	4.208	0.204	-2.191	0.184
lm0300l8890	0.348701	2.535	0.149	-2.106	0.135
lm0425n13753	0.324285	1.817	0.204	-1.984	0.131
lm0305m6294	0.366683	3.413	0.216	-1.979	0.171
lm0312l15193	0.33178	2.557	0.224	-1.939	0.147
lm0425l6481	0.344997	3.021	0.281	-1.92	0.18
lm0301m15847	0.330077	2.696	0.206	-1.881	0.149
lm0425n18680	0.310366	1.197	0.285	-1.842	0.133
lm0434n14310	0.296573	1.887	0.25	-1.73	0.137
lm0291n2551	0.308322	2.486	0.249	-1.72	0.156
lm0435m9109	0.295152	2.016	0.291	-1.697	0.145
lm0302n4858	0.292002	2.212	0.27	-1.623	0.152
lm0303n31583	0.31418	3.146	0.198	-1.517	0.169
lm0291l11940	0.303318	2.985	0.167	-1.467	0.156
lm0300m6808	0.329139	3.856	0.274	-1.267	0.247
lm0424m19442	0.304605	-0.56	0.284	-1.051	0.232
lm0437m22126	0.280684	4.919	0.277	0.49	0.368

Table 6.6: Photometric metallicity of 20 RRc stars in tile LMC 8\_3 (Column 1: EROS-2 identification of the star; Column 2: Period; Column 3: Fourier parameter  $\phi_{31}^c$  of the cosine Fourier decomposition; Column 4: Error of  $\phi_{31}^c$ ; Column 5: Metallicity in the C09 metallicity scale derived with Eq. 1.13; Column 6: Error of metallicity in the C09 metallicity scale).



## 6.5 $K_s$ magnitude of the RR Lyrae stars in tile LMC 8\_3

We built the  $K_s$ -band light curves of the 251 confirmed RR Lyrae stars in tile LMC 8\_3, using the  $K_s$  aperture photometry of the VMC data provided by the VSA internal release of 5 August 2013. In order to derive the mean  $\langle K_s \rangle$  magnitudes we fitted the light curves of the RR Lyrae stars with the templates from Jones et al. (1996). This method requires a precise knowledge of the ephemerides and amplitudes in the  $V_J$  band, for which we used the values derived in our analysis of the EROS-2 light curves with GRATIS (see Table 6.2). We also corrected for any phase shift between templates and data points.

To correct the mean magnitudes for reddening we adopted the mean value of the extinction in the  $V$  band for tile LMC 8\_3 derived by Rubele et al. (2012) and applied the relation  $A_K/A_V = 0.114$  from Cardelli et al. (1989). The absorption the  $K$  band is then  $A_K = 0.038 \pm 0.006$  mag. Dereddened mean  $K_s$  magnitudes of the 251 RR Lyrae stars are presented in Table 6.7.

6.5.  $K_S$  MAGNITUDE OF THE RR LYRAE STARS IN TILE LMC 8\_3

VMC id	EROS-2 id	RA (deg)	DEC (deg)	RR type	Period (days)	$K_{s,0}$ (mag)	$\sigma_{K_{s,0}}$ (mag)
VMC J050223.44-652936.47	lm0423l20069	75.59747	-65.49339	c	0.291086	18.406	0.019
VMC J050017.74-652810.85	lm0422n16993	75.07383	-65.46963	c	0.360726	18.06	0.021
VMC J050123.87-653007.76	lm0423l17670	75.34933	-65.5021	c	0.337594	18.201	0.023
VMC J050917.20-653628.82	lm0435m9109	77.32164	-65.60798	c	0.295152	18.245	0.023
VMC J050957.20-653705.78	lm0435m10888	77.48819	-65.61824	c	0.289555	18.506	0.029
VMC J050346.01-653343.72	lm0425m3355	75.94157	-65.56209	c	0.358864	18.207	0.023
VMC J050921.39-653814.14	lm0435m13533	77.33903	-65.63724	c	0.354274	18.118	0.021
VMC J051015.38-654000.96	lm0435m18280	77.56386	-65.6669	c	0.345305	18.149	0.021
VMC J050213.12-653430.92	lm0425k4625	75.55453	-65.57518	c	0.335537	18.285	0.024
VMC J050311.74-653550.23	lm0425m8144	75.79879	-65.59725	c	0.376376	18.124	0.021
VMC J050135.53-653609.22	lm0425k8207	75.39793	-65.60249	c	0.382111	17.834	0.017
VMC J050153.40-653635.13	lm0425k9319	75.47239	-65.60967	c	0.319697	18.418	0.027
VMC J050554.38-654202.05	lm0434m22078	76.47651	-65.7005	c	0.372157	18.17	0.021
VMC J051059.57-654600.06	lm0444l9270	77.74804	-65.76665	c	0.374023	18.092	0.02
VMC J050025.52-654041.56	lm0424m19442	75.10627	-65.6782	c	0.304605	18.414	0.028
VMC J050545.16-654541.03	lm0434l7912	76.43811	-65.76134	c	0.455709	18.421	0.027
VMC J050649.59-654811.93	lm0434n14310	76.70655	-65.80327	c	0.296573	18.43	0.027
VMC J050114.82-654437.48	lm0425l6481	75.31167	-65.74371	c	0.344997	18.149	0.022
VMC J050214.04-654618.69	lm0425l10656	75.55837	-65.77181	c	0.345737	18.251	0.024
VMC J050257.13-654724.98	lm0425n13753	75.738	-65.7902	c	0.324285	18.365	0.026
VMC J050308.15-654806.87	lm0425n15519	75.78383	-65.80184	c	0.307507	18.319	0.024
VMC J050342.51-654918.48	lm0425n18680	75.927	-65.82173	c	0.310366	18.396	0.026
VMC J050520.41-655122.21	lm0434l20168	76.33503	-65.85612	c	0.353452	18.322	0.025
VMC J050532.60-655306.83	lm0434l19810	76.38578	-65.88519	c	0.379506	17.568	0.013
VMC J050200.28-655027.73	lm0425l20513	75.50109	-65.84096	c	0.289973	18.142	0.022
VMC J050456.47-655241.83	lm0434l23190	76.23528	-65.87827	c	0.322595	18.241	0.024
VMC J050151.53-655203.97	lm0425l24389	75.46457	-65.86768	c	0.281388	18.327	0.024
VMC J050654.27-655757.68	lm0436m8308	76.72609	-65.96599	c	0.331619	18.253	0.023
VMC J050637.75-655947.19	lm0436m11977	76.65728	-65.99637	c	0.382103	18.192	0.022
VMC J050935.73-660411.25	lm0437m22126	77.39874	-66.06973	c	0.280684	18.533	0.03

VMC J050110.80-655904.57	lm0427k10785	75.29491	-65.98454	c	0.35837	18.099	0.02
VMC J050342.45-660226.85	lm0427m19332	75.92683	-66.04073	c	0.286546	18.347	0.025
VMC J050620.52-660718.45	lm0436n10024	76.58557	-66.12169	c	0.346597	18.401	0.026
VMC J050207.24-660502.83	lm0427l4507	75.53004	-66.08408	c	0.387359	17.919	0.017
VMC J050639.22-660911.85	lm0436n14285	76.66342	-66.15315	c	0.34985	18.181	0.022
VMC J050529.49-661014.55	lm0436l15993	76.37296	-66.17058	c	0.343821	18.274	0.024
VMC J050453.54-661054.45	lm0436l17456	76.22323	-66.18169	c	0.277319	18.514	0.029
VMC J050157.09-661115.87	lm0427l17346	75.48775	-66.18771	c	0.380922	18.116	0.02
VMC J051026.70-661840.19	lm0310k9300	77.61115	-66.31121	c	0.370288	18.083	0.02
VMC J050401.37-661719.33	lm0300m6808	76.00554	-66.28864	c	0.329139	18.335	0.024
VMC J050829.34-662027.95	lm0301m15847	77.12213	-66.34112	c	0.330077	18.137	0.021
VMC J050733.67-662645.94	lm0301n7929	76.89016	-66.4461	c	0.314271	18.272	0.024
VMC J051040.41-662940.91	lm0310n11585	77.66864	-66.49466	c	0.340596	18.294	0.053
VMC J050918.46-662916.88	lm0310l12440	77.32674	-66.48791	c	0.348783	18.139	0.021
VMC J050808.19-662959.33	lm0301n16576	77.03389	-66.49982	c	0.236645	17.81	0.016
VMC J050317.90-662638.48	lm0300l6753	75.82456	-66.44405	c	0.340936	18.017	0.019
VMC J050000.27-662412.25	lm0291k24862	75.00092	-66.40342	c	0.293334	18.588	0.031
VMC J050316.54-662733.42	lm0300l8890	75.8189	-66.45933	c	0.348701	17.786	0.016
VMC J050313.07-663013.26	lm0300l15247	75.80446	-66.5037	c	0.27092	18.628	0.031
VMC J045936.35-662727.30	lm0291l9716	74.90131	-66.45757	c	0.354199	18.299	0.024
VMC J050139.58-662924.71	lm0291n15412	75.41471	-66.49017	c	0.328223	18.239	0.022
VMC J045935.83-662818.01	lm0291l1940	74.89917	-66.47166	c	0.303318	18.378	0.026
VMC J050429.77-663352.58	lm0300n24904	76.12396	-66.5646	c	0.376841	17.929	0.018
VMC J050028.40-663320.76	lm0291n25551	75.11817	-66.55566	c	0.308322	18.151	0.021
VMC J050747.88-663937.12	lm0303m10773	76.94934	-66.66027	c	0.344942	18.216	0.023
VMC J050211.22-663534.89	lm0300l14647	75.54689	-66.59292	c	0.43362	17.807	0.017
VMC J045825.50-663236.72	lm0291l23359	74.60627	-66.54347	c	0.358093	18.234	0.024
VMC J050257.12-663753.02	lm0302k3782	75.73802	-66.63133	c	0.352431	18.023	0.019
VMC J050301.63-663833.15	lm0302k5022	75.75683	-66.64249	c	0.404202	18.191	0.022
VMC J050837.23-664345.17	lm0303m22504	77.15498	-66.72917	c	0.323404	18.471	0.028
VMC J050807.83-664359.20	lm0303m22989	77.03243	-66.73305	c	0.427324	17.811	0.017
VMC J050018.38-663940.46	lm0293m10988	75.07649	-66.66119	c	0.366121	18.212	0.023
VMC J050138.64-664239.19	lm0293m19803	75.41086	-66.71085	c	0.338538	18.358	0.026

6.5.  $K_S$  MAGNITUDE OF THE RR LYRAE STARS IN TILE LMC 8\_3

VMC J050646.44-664802.84	lm030318655	76.69337	-66.8007	c	0.339125	17.994	0.02
VMC J050433.03-664704.30	lm0302n4858	76.13749	-66.78444	c	0.292002	18.357	0.025
VMC J050942.23-665126.02	lm0312115193	77.42594	-66.85716	c	0.33178	18.386	0.027
VMC J050824.66-665044.50	lm0303n16841	77.10276	-66.84558	c	0.327493	18.178	0.036
VMC J050836.01-665550.04	lm0303n31583	77.14986	-66.9305	c	0.31418	18.412	0.027
VMC J050238.91-665146.42	lm0302116395	75.66204	-66.86281	c	0.344601	18.164	0.022
VMC J045910.51-665138.98	lm0293118421	74.79358	-66.86072	c	0.278759	18.33	0.025
VMC J050735.59-665811.53	lm0305m3332	76.8982	-66.96981	c	0.249311	18.141	0.022
VMC J050753.60-665915.19	lm0305m6294	76.97324	-66.98749	c	0.366683	18.028	0.02
VMC J050037.51-665555.71	lm0293n31080	75.15616	-66.93208	c	0.43653	18.527	0.024
VMC J050347.33-665819.01	lm0304m2952	75.9472	-66.97185	c	0.311944	18.304	0.018
VMC J051016.85-653532.02	lm0435m7058	77.57013	-65.59222	ab	0.597486	17.908	0.013
VMC J050302.40-653120.51	lm0423n26224	75.7598	-65.52229	ab	0.559366	18.174	0.022
VMC J050931.00-653632.31	lm0435m9334	77.37913	-65.60896	ab	0.55085	17.895	0.017
VMC J050136.39-653109.44	lm0423111740	75.40143	-65.51925	ab	0.554337	17.959	0.021
VMC J050211.10-653150.27	lm042317926	75.5461	-65.53056	ab	0.561818	18.082	0.021
VMC J050638.07-653520.91	lm0434m6139	76.65853	-65.58909	ab	0.540358	18.059	0.02
VMC J050326.18-653410.97	lm0425m4288	75.85896	-65.56967	ab	0.597504	17.973	0.019
VMC J050824.37-653759.21	lm0435k12309	77.10144	-65.63307	ab	0.608992	17.965	0.019
VMC J050752.49-653754.29	lm0435k12002	76.96857	-65.63167	ab	0.618774	18.117	0.021
VMC J051038.81-653957.41	lm0435m18273	77.66155	-65.66592	ab	0.631476	17.756	0.015
VMC J050435.44-653606.07	lm0434k7302	76.14762	-65.60166	ab	0.610192	17.978	0.018
VMC J050534.00-653651.80	lm0434k9008	76.39164	-65.61437	ab	0.567635	17.77	0.016
VMC J050947.94-653953.14	lm0435m17793	77.4496	-65.66472	ab	0.524956	18.071	0.021
VMC J050854.55-654006.09	lm0435k17589	77.22723	-65.66834	ab	0.612635	18.045	0.02
VMC J050742.69-653928.17	lm0435k15816	76.92775	-65.65774	ab	0.638794	17.69	0.014
VMC J051003.09-654208.05	lm0435m23563	77.51267	-65.70218	ab	0.525048	17.972	0.018
VMC J050821.58-654110.34	lm0435k20062	77.08979	-65.68616	ab	0.514125	18.195	0.022
VMC J050252.15-653746.20	lm0425m12624	75.7172	-65.62945	ab	0.547065	17.967	0.019
VMC J050614.54-654101.80	lm0434m19648	76.56045	-65.68376	ab	0.622604	17.838	0.017
VMC J050700.34-654142.90	lm0434m21424	76.7513	-65.69519	ab	0.57382	18.069	0.02
VMC J050119.43-653734.91	lm0425k11500	75.33082	-65.62627	ab	0.540233	17.858	0.017
VMC J050741.32-654407.60	lm043515247	76.92213	-65.73542	ab	0.571823	17.953	0.019

VMC J050535.32-654355.85	lm0434k22095	76.3971	-65.73215	ab	0.539682	18.088	0.02
VMC J050924.06-654635.78	lm0435n11321	77.35012	-65.77656	ab	0.587183	17.491	0.013
VMC J050740.45-654601.59	lm0435l9858	76.91847	-65.76707	ab	0.609462	18.026	0.02
VMC J050659.03-654542.60	lm0434n8413	76.74585	-65.76182	ab	0.670871	17.786	0.016
VMC J050945.64-654738.28	lm0435n13913	77.44001	-65.79393	ab	0.597578	18.14	0.021
VMC J050031.62-654206.12	lm0424m22887	75.13167	-65.70164	ab	0.398125	18.632	0.034
VMC J050654.39-654756.81	lm0434n13704	76.72655	-65.79908	ab	0.571166	18.165	0.022
VMC J050028.44-654409.42	lm0424n5227	75.11837	-65.73591	ab	0.619983	17.34	0.012
VMC J050103.78-654614.63	lm0425l10247	75.26573	-65.77068	ab	0.607461	17.9	0.018
VMC J051102.96-655339.53	lm0444l20033	77.76182	-65.89427	ab	0.575092	17.793	0.016
VMC J050523.30-654957.92	lm0434l17031	76.34705	-65.83271	ab	0.582937	17.979	0.019
VMC J050556.87-655134.75	lm0434n22292	76.48691	-65.8596	ab	0.689693	17.886	0.017
VMC J050119.83-654808.40	lm0425l14852	75.33257	-65.80227	ab	0.536054	18.191	0.022
VMC J050520.68-655129.43	lm0434l20435	76.33615	-65.85811	ab	0.4888095	18.024	0.019
VMC J045936.81-654727.16	lm0424n12543	74.90326	-65.79083	ab	0.635316	17.821	0.017
VMC J050603.24-655333.47	lm0434n17383	76.51344	-65.89259	ab	0.724152	17.55	0.013
VMC J050145.38-655042.88	lm0425l21048	75.43903	-65.84525	ab	0.615813	17.576	0.014
VMC J050410.43-655245.19	lm0425n23250	76.04345	-65.87922	ab	0.525191	18.056	0.019
VMC J051007.73-655804.30	lm0437m9713	77.53209	-65.96782	ab	0.620011	17.806	0.016
VMC J050751.59-655751.27	lm0437k8681	76.96496	-65.96417	ab	0.589055	17.949	0.018
VMC J050913.23-655954.52	lm0437k13906	77.30504	-65.99851	ab	0.594332	17.938	0.018
VMC J050357.69-655643.65	lm0427m6338	75.99025	-65.94538	ab	0.713501	17.778	0.016
VMC J050755.57-660038.96	lm0437k15328	76.98154	-66.01065	ab	0.584568	17.992	0.019
VMC J050800.42-660050.63	lm0437k15772	77.0017	-66.01396	ab	0.488322	18.153	0.021
VMC J051048.50-660242.86	lm0437m20444	77.70208	-66.04521	ab	0.511423	18.349	0.025
VMC J051058.57-660313.36	lm0446k20706	77.74377	-66.05372	ab	0.543569	18.076	0.019
VMC J051025.89-660258.51	lm0437m20883	77.6079	-66.04953	ab	0.580287	18.188	0.022
VMC J051023.01-660425.80	lm0437m17477	77.59584	-66.07382	ab	0.536134	18.054	0.02
VMC J050615.88-660215.95	lm0436m17011	76.56619	-66.03765	ab	0.645996	17.914	0.017
VMC J050334.48-660029.23	lm0427m14753	75.89361	-66.008	ab	0.54401	17.953	0.018
VMC J050803.01-660347.82	lm0437k22654	77.01247	-66.06322	ab	0.491312	18.203	0.022
VMC J050439.43-660120.57	lm0436k15855	76.16415	-66.02233	ab	0.614185	17.838	0.016
VMC J051056.74-660648.08	lm0437n8455	77.73625	-66.11333	ab	0.574999	18.042	0.019

6.5.  $K_S$  MAGNITUDE OF THE RR LYRAE STARS IN TILE LMC 8\_3

VMC J050357.85-660254.64	lm0427m20466	75.99099	-66.04834	ab	0.616626	17.914	0.017
VMC J050716.92-660626.56	lm0436n8236	76.82037	-66.10734	ab	0.650192	17.602	0.013
VMC J051052.01-660955.34	lm0437n14794	77.71665	-66.16543	ab	0.544769	17.883	0.017
VMC J050701.01-660748.02	lm0436n11172	76.75415	-66.12991	ab	0.431733	18.385	0.026
VMC J050958.87-661010.55	lm0437n15049	77.49507	-66.16951	ab	0.571014	17.991	0.019
VMC J050124.80-660429.92	lm0427k17452	75.35321	-66.07494	ab	0.675498	17.847	0.017
VMC J050309.18-660645.01	lm0427n7741	75.78808	-66.11239	ab	0.48284	18.191	0.022
VMC J050815.71-661046.07	lm0437l15735	77.06524	-66.17934	ab	0.622553	17.912	0.018
VMC J045924.15-660414.72	lm0426m24414	74.85054	-66.07064	ab	0.606869	18.021	0.019
VMC J050042.40-660654.21	lm0426n9666	75.17663	-66.11497	ab	0.687625	17.859	0.017
VMC J050704.87-661204.64	lm0436n20628	76.77019	-66.2012	ab	0.493107	18.032	0.019
VMC J050023.70-660757.58	lm0426n12018	75.09864	-66.13259	ab	0.52946	18.177	0.022
VMC J050131.48-660910.93	lm0427l12462	75.38109	-66.15291	ab	0.571194	17.851	0.017
VMC J050537.17-661219.31	lm0436l20450	76.40491	-66.20527	ab	0.511395	17.843	0.016
VMC J050233.99-661150.13	lm0427l18856	75.64163	-66.19734	ab	0.562698	18.059	0.019
VMC J050901.51-661931.25	lm0310k11253	77.25582	-66.32523	ab	0.537149	17.937	0.018
VMC J050751.68-662025.78	lm0301m15584	76.9652	-66.34056	ab	0.54134	18.258	0.023
VMC J050804.65-662029.19	lm0301m15788	77.01923	-66.34154	ab	0.710038	17.662	0.016
VMC J050400.65-661836.81	lm0300m9935	76.00253	-66.31022	ab	0.485127	18.118	0.02
VMC J050435.36-661917.95	lm0300m11600	76.14728	-66.32166	ab	0.570995	17.765	0.015
VMC J050341.33-661926.07	lm0300m11839	75.92208	-66.32392	ab	0.559733	17.958	0.018
VMC J050845.88-662308.37	lm0301m22780	77.19099	-66.38563	ab	0.535459	18.104	0.027
VMC J051013.61-662410.19	lm0310k18010	77.55657	-66.40282	ab	0.590299	18.048	0.02
VMC J050111.42-661743.68	lm0291m8710	75.29738	-66.29542	ab	0.511745	18.336	0.024
VMC J050530.59-662137.18	lm0301k17554	76.37739	-66.36031	ab	0.535567	18.223	0.023
VMC J050307.36-661947.80	lm0300k12184	75.78071	-66.32998	ab	0.524813	18.068	0.02
VMC J050942.68-662434.51	lm0310k15738	77.42775	-66.40958	ab	0.608534	17.988	0.018
VMC J050140.14-661856.66	lm0291m11933	75.41718	-66.31573	ab	0.558102	17.893	0.017
VMC J050204.20-661940.86	lm0300k11860	75.51738	-66.32796	ab	0.643757	17.792	0.016
VMC J050405.00-662135.69	lm0300m17178	76.02068	-66.35996	ab	0.518967	17.99	0.018
VMC J050238.30-662042.97	lm0300k14335	75.65971	-66.34538	ab	0.566157	17.941	0.018
VMC J050330.54-662137.49	lm0300k16563	75.87714	-66.36044	ab	0.592704	18.08	0.02
VMC J045917.82-661824.09	lm0291k10047	74.82401	-66.30667	ab	0.585024	18.121	0.021

VMC J045907.17-661838.18	lm0291k10561	74.77965	-66.31058	ab	0.5571	17.909	0.018
VMC J050518.74-662359.17	lm0300m23266	76.32789	-66.39973	ab	0.548868	17.899	0.018
VMC J050259.67-662204.90	lm0300k17665	75.74862	-66.36812	ab	0.568997	17.72	0.016
VMC J050501.62-662446.46	lm0300m25109	76.25662	-66.41288	ab	0.652891	17.646	0.014
VMC J050351.73-662414.02	lm0300m23701	75.96552	-66.40392	ab	0.546102	18.075	0.019
VMC J050506.73-662545.68	lm0300m19324	76.27787	-66.42927	ab	0.525312	18.111	0.02
VMC J050917.87-663010.23	lm0310l14484	77.32418	-66.5028	ab	0.661652	17.239	0.011
VMC J050744.32-662922.45	lm0301m14847	76.93447	-66.48958	ab	0.549535	18.116	0.02
VMC J050616.88-662826.74	lm0301l1630	76.57024	-66.47409	ab	0.568156	18.028	0.019
VMC J050826.52-663002.34	lm0301m16814	77.11029	-66.50065	ab	0.528262	18.126	0.023
VMC J050731.84-662926.36	lm0301m14943	76.88253	-66.49069	ab	0.645196	17.885	0.017
VMC J050945.32-663103.00	lm0310l16334	77.43882	-66.51749	ab	0.657788	17.804	0.016
VMC J050948.61-663158.65	lm0310l18147	77.45244	-66.53289	ab	0.590217	17.846	0.017
VMC J051005.62-663221.50	lm0310l18911	77.52338	-66.53928	ab	0.748431	17.728	0.015
VMC J050440.29-662851.85	lm0300m12088	76.16779	-66.48111	ab	0.672356	17.972	0.018
VMC J050050.21-662554.35	lm0291m6040	75.20907	-66.43175	ab	0.527619	18.092	0.02
VMC J050428.64-662852.88	lm0300m12109	76.11925	-66.4814	ab	0.683459	17.787	0.015
VMC J050613.56-663018.70	lm0301l16487	76.55635	-66.50519	ab	0.738143	17.412	0.013
VMC J050457.37-662935.19	lm0300m13961	76.23893	-66.49314	ab	0.623548	17.8	0.016
VMC J050730.28-663159.48	lm0301m21605	76.87595	-66.53319	ab	0.532545	18.125	0.021
VMC J050457.89-663156.79	lm0300m19927	76.24113	-66.53242	ab	0.637129	18.012	0.019
VMC J050546.52-663243.58	lm0301l22786	76.44374	-66.54541	ab	0.648027	17.892	0.017
VMC J050623.56-663312.53	lm0301l24255	76.59798	-66.55346	ab	0.51058	17.799	0.015
VMC J050519.02-663222.23	lm0300m21091	76.32909	-66.53946	ab	0.56746	18.064	0.019
VMC J050602.75-663334.37	lm0301l25140	76.51123	-66.55949	ab	0.6631835	17.755	0.016
VMC J045846.28-662755.50	lm0291l10775	74.6928	-66.46539	ab	0.570992	18.345	0.025
VMC J050140.25-663112.05	lm0291m20101	75.41745	-66.52001	ab	0.517254	17.975	0.019
VMC J050244.52-663247.81	lm0300l20739	75.6855	-66.54657	ab	0.589066	17.789	0.016
VMC J050931.40-663748.14	lm0312k4503	77.38073	-66.62996	ab	0.613847	18.058	0.02
VMC J050015.23-663121.94	lm0291m20061	75.06329	-66.52272	ab	0.529756	18.266	0.023
VMC J050833.42-663737.55	lm0303m5651	77.13918	-66.62705	ab	0.692547	17.883	0.017
VMC J050346.69-663450.22	lm0300m27286	75.94449	-66.58057	ab	0.566301	17.936	0.017
VMC J050241.69-663447.20	lm0300l25566	75.67367	-66.57969	ab	0.638155	17.898	0.017

6.5.  $K_S$  MAGNITUDE OF THE RR LYRAE STARS IN TILE LMC 8\_3

VMC J050224.70-663500.23	lm0300l23462	75.60295	-66.5833	ab	0.744314	17.637	0.014
VMC J050835.85-663935.74	lm0303m11005	77.14924	-66.65987	ab	0.64377	17.907	0.017
VMC J050302.54-663540.49	lm0300l13312	75.76052	-66.59446	ab	0.527452	18.067	0.019
VMC J045840.37-663345.71	lm0291l26545	74.66819	-66.56263	ab	0.6694875	17.724	0.016
VMC J050756.07-664155.19	lm0303m17152	76.9835	-66.69861	ab	0.524201	17.999	0.02
VMC J050816.34-664207.26	lm0303m17812	77.06791	-66.70197	ab	0.565556	18.005	0.02
VMC J050803.26-664323.35	lm0303m21245	77.0134	-66.72311	ab	0.593551	17.865	0.018
VMC J045923.84-663716.72	lm0293k3928	74.84921	-66.62125	ab	0.471742	18.15	0.023
VMC J050934.40-664612.11	lm0312k21111	77.39336	-66.76995	ab	0.4606	18.26	0.023
VMC J050648.56-664445.67	lm0303k25210	76.7022	-66.74596	ab	0.524918	18.274	0.023
VMC J050048.02-664050.02	lm0293m14375	75.19999	-66.68054	ab	0.507995	17.969	0.019
VMC J050336.11-664354.24	lm0302k13534	75.90035	-66.73166	ab	0.62088	17.904	0.017
VMC J050044.55-664145.65	lm0293m17000	75.18543	-66.69597	ab	0.595224	18.0	0.018
VMC J050102.85-664226.34	lm0293m19003	75.26169	-66.70727	ab	0.583546	18.167	0.022
VMC J050514.22-664547.98	lm0302m22487	76.30911	-66.76329	ab	0.520562	18.332	0.025
VMC J050109.79-664239.69	lm0293m19628	75.29061	-66.71099	ab	0.581141	17.97	0.019
VMC J050229.32-664429.58	lm0302k14796	75.62213	-66.7415	ab	0.559635	18.081	0.02
VMC J050804.51-664815.72	lm0303n9745	77.01868	-66.80425	ab	0.628757	17.868	0.018
VMC J050744.26-664948.84	lm0303n13977	76.93426	-66.83012	ab	0.4995561	18.236	0.024
VMC J050739.78-664923.56	lm0303n12799	76.9156	-66.8231	ab	0.581848	17.987	0.019
VMC J050717.67-665020.16	lm0303n15322	76.82352	-66.83882	ab	0.505733	18.042	0.019
VMC J050733.61-665035.07	lm0303n16102	76.88992	-66.84296	ab	0.632428	17.892	0.017
VMC J045930.50-664444.46	lm0293k25226	74.87683	-66.74562	ab	0.586479	17.936	0.018
VMC J050655.64-665112.73	lm0303l17671	76.73167	-66.85344	ab	0.560588	17.935	0.018
VMC J045853.67-664552.45	lm0293k28352	74.72341	-66.76451	ab	0.497779	17.932	0.019
VMC J050345.85-664955.21	lm0302n12351	75.94097	-66.83188	ab	0.566134	18.172	0.022
VMC J045951.56-664701.22	lm0293l5252	74.96458	-66.7836	ab	0.612908	18.009	0.02
VMC J050325.29-665015.18	lm0302l12678	75.8553	-66.8375	ab	0.424945	18.401	0.026
VMC J050850.74-665418.25	lm0303n27302	77.21128	-66.90501	ab	0.586637	18.115	0.021
VMC J050255.86-665022.40	lm0302l12960	75.73262	-66.83949	ab	0.567341	17.929	0.018
VMC J050622.59-665442.03	lm0303l27610	76.59394	-66.91158	ab	0.623747	17.887	0.017
VMC J050549.03-665414.23	lm0303l26148	76.45407	-66.90387	ab	0.620647	17.87	0.017
VMC J050450.69-665359.87	lm0302n23523	76.21095	-66.89987	ab	0.497153	18.104	0.021



VMC J045913.55-664939.41	lm0293n12631	74.80625	-66.82752	ab	0.610866	18.016	0.02
VMC J050040.53-665128.79	lm0293n18229	75.16869	-66.85795	ab	0.628127	17.882	0.018
VMC J050126.66-665217.05	lm0293n20870	75.36086	-66.87147	ab	0.57819	17.201	0.011
VMC J050330.10-665429.42	lm0302i23297	75.87528	-66.90811	ab	0.511473	18.225	0.023
VMC J050726.13-665825.30	lm0305m3882	76.85877	-66.97363	ab	0.710488	17.861	0.017
VMC J050853.74-665941.23	lm0305m7850	77.2239	-66.99474	ab	0.713324	17.66	0.015
VMC J050249.16-665550.35	lm0302i26417	75.70471	-66.93057	ab	0.590296	18.113	0.022
VMC J050148.97-665540.11	lm0293n30795	75.45401	-66.92786	ab	0.474027	17.985	0.019
VMC J045918.98-665406.56	lm0293i25506	74.82889	-66.9017	ab	0.657982	17.83	0.017
VMC J050609.35-665915.29	lm0305k5704	76.5388	-66.98748	ab	0.6216	18.038	0.02
VMC J045802.46-665358.25	lm0292n22612	74.51012	-66.8994	ab	0.624068	18.086	0.016
VMC J050223.18-652921.68	lm0423i21178	75.59644	-65.48937	ab	0.632125	17.405	0.013
VMC J050444.73-653217.60	lm0432i12420	76.18633	-65.53826	ab	0.478439	18.277	0.033
VMC J050828.76-653624.37	lm0435k8479	77.11971	-65.60672	d	0.36516	18.023	0.019
VMC J051102.67-654530.93	lm0444i8138	77.76094	-65.75855	d	0.354926	18.081	0.02
VMC J050808.12-662858.86	lm0301n13911	77.03367	-66.48302	d	0.357188	18.141	0.022
VMC J050942.36-663531.04	lm0310i12653	77.42654	-66.59188	d	0.362102	18.203	0.022
VMC J050533.89-663444.89	lm0301i26933	76.39115	-66.57905	d	0.360584	17.969	0.018
VMC J050040.98-663327.65	lm0291n25922	75.1705	-66.5576	d	0.365493	18.191	0.022
VMC J050713.26-664414.20	lm0303m23391	76.8051	-66.73721	d	0.38551	18.176	0.022
VMC J050655.56-664427.31	lm0303k24363	76.73134	-66.74087	d	0.391884	17.868	0.017
VMC J045948.97-664636.55	lm0293k30764	74.95375	-66.77676	d	0.35374	18.457	0.028
VMC J050148.56-664954.79	lm0293n14230	75.45233	-66.83197	d	0.362897	18.077	0.02

Table 6.7: Properties of the RR Lyrae stars in tile LMC 8\_3 (Column 1:

VMC identification of the star; Column 2: EROS-2 identification of the star; Column 3: Right ascension from the EROS-2 catalogue; Column 4: Declination from the EROS-2 catalogue; Column 5: RR Lyrae type; Column 6: Period from the EROS-2 catalogue; Column 7: Dereddened mean magnitude in the  $K_s$  passband; Column 8: Error of the dereddened  $K_s$  mean magnitudes).

## 6.6 Distance to the tile LMC 8\_3 from RR Lyrae stars

In Chapter 5 we derived a new  $PL_{K_s}Z$  relation based on a sample of the 71 RR Lyrae stars in tile LMC 5\_5. We can apply the new relation, as well as other  $PL_{K_s}Z$  relations in the literature, to estimate the distance to each VMC tile, separately. This will, in turn, allow us to study the structure of the LMC.

In this section we describe preliminary results we have obtained from the application of the  $PL_{K_s}Z$  relations to the RR Lyrae stars in the VMC tile LMC 8\_3. Once we have period and dereddened mean  $K_s$  magnitude for each RR Lyrae star (Table 6.7), we can immediately plot the  $PL$  relation. This is shown in Figure 6.4, where filled and open circles are RRab and RRC stars, respectively. We computed a weighted  $PL_{K_s}$  relation through the data by progressively discarding objects which deviate more than  $3\sigma$  from the linear regression:

$$K_{s,0} = (-2.40 \pm 0.13)\log P + (17.38 \pm 0.03) \quad (6.1)$$

Figure 6.4 shows only objects that are located within  $3\sigma$  from the best fit line. The slope of Eq. 6.1 differs from the slope in  $\log P$  derived for the 71 RR Lyrae stars in tile LMC 5\_5 (Eq. 5.3), but is still consistent with it within the errors. The zero-points of Eqs. 6.1 and 5.3 are consistent within the errors, even if Eq. 6.1 does not take into account the metallicity.

A number of different  $PL_{K_s}Z$  relations exist in the literature (see Section 1.5.2): Bono et al. (2003) (see Eq. 6.4), Dall’Ora et al. (2004) (see Eq. 6.5), Sollima et al. (2006) (see Eq. 6.3), Sollima et al. (2008) (see Eq. 6.2), Del Principe et al. (2006) (see Eq. 6.6), Borissova et al. (2009) (see Eq. 6.7). Benedict et al. (2011) have estimated zero-points for all these  $PL_{K_s}Z$  relations, based on their *HST* trigonometric parallaxes for five Galactic field RR Lyrae stars:

$$M_K = (-2.38 \pm 0.04)(\log P + 0.28) + (0.08 \pm 0.11)([Fe/H] + 1.58) + a_1, \quad (6.2)$$

$$M_K = (-2.38 \pm 0.04)(\log P + 0.28) + a_2, \quad (6.3)$$

$$M_K = -2.101(\log P + 0.28) + (0.231 \pm 0.012)([Fe/H] + 1.58) + a_3, \quad (6.4)$$

$$M_K = (-2.16 \pm 0.09)(\log P + 0.28) + a_4, \quad (6.5)$$

$$M_K = (-2.71 \pm 0.12)(\log P + 0.28) + (0.12 \pm 0.04)([Fe/H] + 1.58) + a_5 \quad (6.6)$$

$$M_K = (-2.11 \pm 0.17)(\log P + 0.28) + (0.05 \pm 0.07)([Fe/H] + 1.58) + a_6 \quad (6.7)$$

where the  $a_1 - a_6$  values are:  $-0.56 \pm 0.02$ ,  $-0.57 \pm 0.03$ ,  $-0.58 \pm 0.04$ ,  $-0.56 \pm 0.02$ ,  $-0.57 \pm 0.02$ , and  $-0.56 \pm 0.03$ , respectively. They were derived by fitting the Lutz-Kelker-Hanson-corrected absolute magnitudes to the equations (Benedict et al., 2011). The different  $PL_{K_s}Z$  relations are based on a number of different metallicity scales. In particular, Bono et al. (2003) and Del Principe et al. (2006) use the Zinn & West metallicity scale. Sollima et al. (2008) use the Carretta & Gratton (1997) metallicity scale. The relations from Dall’Ora et al. (2004) and Sollima et al. (2006) do not have metallicity terms. Finally, Borissova et al. (2009) use the same metallicity scale adopted by Gratton et al. (2004).

We add to the above literature relations (Eqs. 6.2-6.7) our own  $PL_{K_s}Z$  relation derived using the dereddened mean  $K_s$  magnitudes of the 71 RR Lyrae stars in tile LMC 5\_5, spectroscopically determined metallicities from Gratton et al. (2004) and accurately estimated periods from the OGLE III catalogue (see Chapter 5):

$$M_K = (-2.70 \pm 0.22)\log P + (0.03 \pm 0.06)[Fe/H] + (-1.27 \pm 0.08) \quad (6.8)$$

The zero-point of our relation is also calibrated on the Benedict et al. (2011)’s *HST* trigonometric parallaxes for RR Lyrae stars and the metallicity is on Gratton et al. (2004) scale, hence, on average, 0.06 dex higher than Zinn & West’s. To derive the distance to tile LMC 8\_3 we entered the above relations using: periods for the RR Lyrae stars taken from the EROS-2 catalogue, mean  $\langle K_s \rangle$  dereddened magnitudes estimated as described in Section 6.5, and metallicities obtained by the Fourier analysis of the  $V$  band light curves (see Section 6.4).

In order to take into account the systematic difference of  $\sim 0.25$  dex between the mean metallicities of RRab and RRC stars, we used three different approaches:

- We used the mean metallicity derived by averaging the photometric metallicities of both RRab and RRC stars. We associated to the mean value obtained in this way an error corresponding to the standard deviation of the distribution  $\langle [Fe/H]_{C09} \rangle = -1.61$ ;  $\sigma_{[Fe/H]_{C09}} = 0.4$ . Then we used the whole sample of 241 RRab and RRC stars in tile LMC 8\_3 to estimate the distance.
- We used the mean metallicities determined by averaging the photometric metallicities obtained only for RRab stars. We associate to this mean value an error corresponding to the standard deviation of the average:  $\langle [Fe/H]_{C09ab} \rangle = -1.58$ ;  $\sigma_{[Fe/H]_{C09ab}} = 0.5$ ,

and inferred distance moduli from the above  $PL_{K_s}Z$  relations for each of the 167 ab-type RR Lyrae stars.

- We used the mean metallicity derived by averaging the photometric metallicities obtained only from the RRc stars. We associated to this mean value an error corresponding to the standard deviation of the average:  $\langle [Fe/H]_{C09c} \rangle = -1.82$ ;  $\sigma_{[Fe/H]_{C09c}} = 0.3$ , and inferred distance moduli from the above  $PL_{K_s}Z$  relations for each of the 74 c-type RR Lyrae stars.

The derived mean metallicities are on the Carretta et al. (2009) metallicity scale. To transform them to the Zinn & West metallicity scale, used in the majority of the  $PL_{K_s}Z$  relations listed above we applied the transformation equation provided by Carretta et al. (2009):

$$[Fe/H]_{C09} = (1.105 \pm 0.061)[Fe/H]_{ZW} + 0.160 \quad (6.9)$$

To transform the mean metallicities on the Zinn & West scale to the metallicity scale of Eq. 6.8, we simply added 0.06 dex (Gratton et al., 2004). In order to determine the mean metallicities on the Carretta & Gratton (1997) metallicity scale we applied the relation from Carretta et al. (2009):

$$[Fe/H]_{C09} = (1.137 \pm 0.060)[Fe/H]_{G97} - 0.003 \quad (6.10)$$

Each of the above  $PL_{K_s}Z$  relations (Eqs. 6.2-6.8) was used to infer the  $M_K$  absolute magnitude for each RR Lyrae star in tile LMC 8\_3. The  $M_K$  values were combined with the dereddened apparent  $K$  magnitude providing a distance modulus estimate  $\mu_0$  for each individual star. Average  $\mu_0$  values and related standard errors inferred from the different  $PL_{K_s}Z$  relations are summarized in Table 6.8.

In Chapter 5 we applied our  $PL_{K_s}Z$  relation with zero-point based on the *HST* parallaxes for RR Lyrae stars by Benedict et al. (2011) to 71 RR Lyrae stars in tile LMC 5\_5 and determined the mean distance  $\mu_0 = 18.71 \pm 0.01$  mag, which can now be compared with the average distance to tile LMC 8\_3 :  $\mu_0 = 18.615 \pm 0.006$  mag. Taken at face value these results indicate that the external tile LMC 8\_3 is located 0.1 mag closer to us than the central tile LMC 5\_5. These results are preliminary and need to be further confirmed, still they are promising. Combining them with results obtained from the RR Lyrae stars in other

$PL_K$ -relation	$\mu_0(< ab >)$ mag	$\mu_0(< c >)$ mag	$\mu_0(< ab + c >)$ mag
Bono et al 2003	$18.623 \pm 0.164$	$18.696 \pm 0.192$	$18.636 \pm 0.173$
Dall'Ora et al. 2004	$18.596 \pm 0.170$	$18.610 \pm 0.193$	$18.600 \pm 0.176$
Sollima et al. 2008	$18.596 \pm 0.165$	$18.596 \pm 0.200$	$18.594 \pm 0.174$
Sollima et al. 2006	$18.622 \pm 0.164$	$18.612 \pm 0.197$	$18.619 \pm 0.174$
Del Principe et al. 2006	$18.632 \pm 0.165$	$18.618 \pm 0.195$	$18.624 \pm 0.174$
Borissova et al. 2009	$18.600 \pm 0.165$	$18.632 \pm 0.186$	$18.607 \pm 0.171$
Relation from this study	$18.634 \pm 0.159$	$18.605 \pm 0.195$	$18.625 \pm 0.170$
average	$18.615 \pm 0.006$	$18.625 \pm 0.013$	$18.615 \pm 0.006$

Table 6.8 Distance moduli of tile LMC 8\_3 obtained applying different  $PL_{K_s}Z$  relations to the RR Lyrae stars in this tile (Column 1: References for the  $PL_{K_s}Z$  relations; Column 2: Distance modulus obtained using only RRab stars; Column 3: Distance modulus obtained using only RRC stars; Column 4: Distance modulus obtained using all the ab and c-type RR Lyrae stars in tile LMC 8\_3. See text for details).

VMC tiles we will be able to map the internal structure of the LMC as traced by the old population stars.

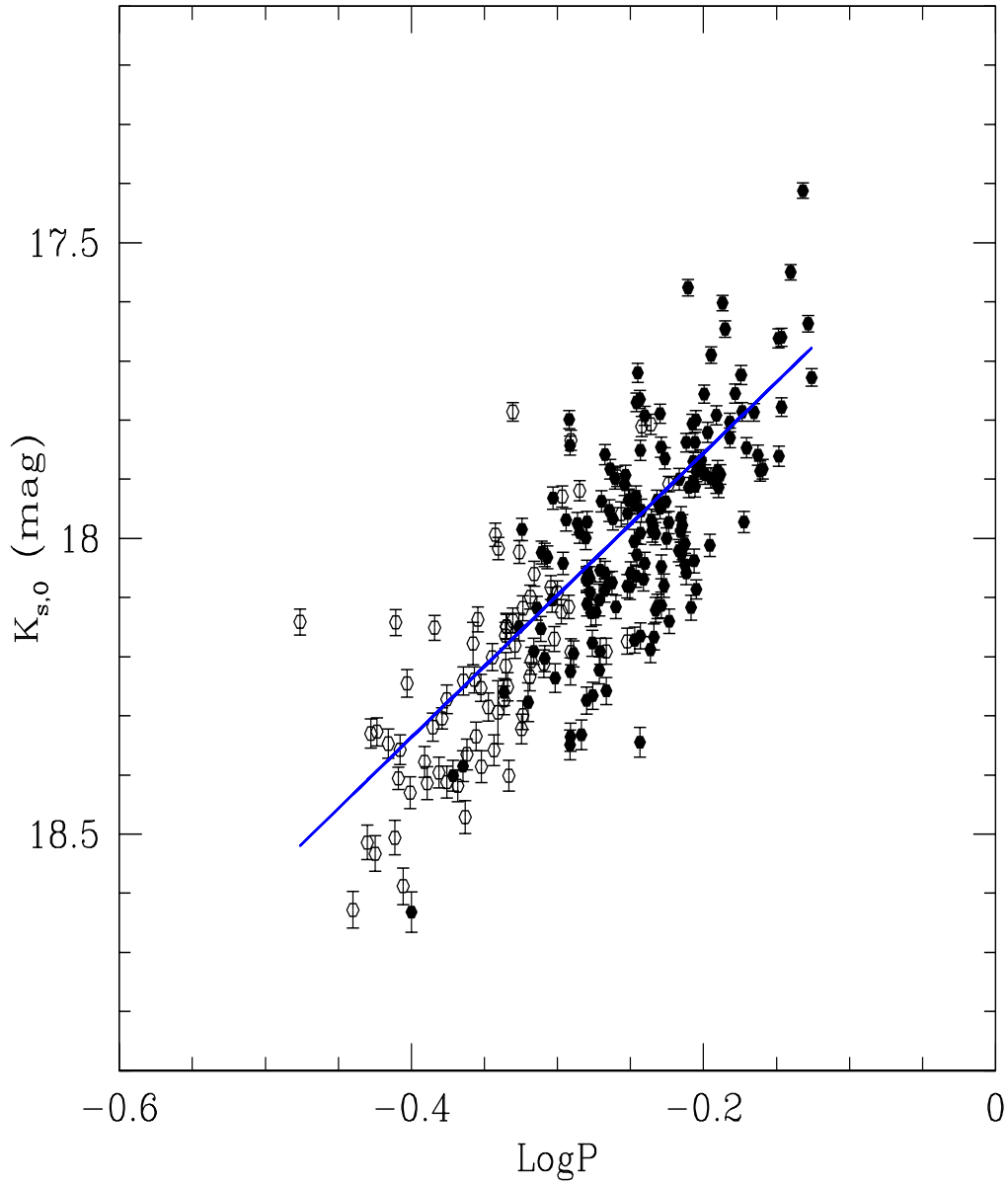


Figure 6.4 Dereddened mean  $K_s$  magnitudes versus  $\text{LogP}$  for RR Lyrae stars in tile LMC 8\_3. Empty and filled circles represent RRc and RRab stars, respectively. The periods of RRc stars were fundamentalized by adding 0.127 to the  $\text{LogP}$ .

# Conclusions

The main goal of this thesis was to study the geometric structure and the distance to the Large Magellanic Cloud (LMC). To this purpose we have analysed three different types of distance indicators: Classical Cepheids (CCs), “hot” eclipsing binaries (HEBs) and RR Lyrae stars, which trace different sub-structures of the LMC.

Main results which we derived for the CCs are:

- We analysed 201 candidate CCs observed by the EROS-2 survey in the VMC tile LMC 8\_3. We classified the candidate CCs through visual inspection of the light curves. The sample was found to contain 124 bona-fide CCs, 2 candidate Anomalous Cepheids, 58 eclipsing binaries, 13 small amplitude variables and 4 long period variables. Furthermore, in the sample of bona-fide CCs we found two double-mode CCs and derived second periods for both of them.
- We determined main parameters (mean magnitudes, amplitudes and epochs of maximum light in the  $B_{EROS}$  and  $R_{EROS}$  passbands) for all the 201 objects, checked the periods provided by the EROS-2 survey and derived new periods for 16 of them. The main parameters of the bona-fide CCs will be used in the future along with near-infrared data from the VMC survey to measure the distance to the genuine CCs in this tile.
- We developed a strategy for extracting bona-fide CCs from the EROS-2 sample of candidate CCs which is based on the combination of colour-cuts in the CMD and analysis of the scatter in the  $PL$  relations. This approach allowed us to extract a sample of bona-fide CCs more than 97 % clean from contaminating sources. This strategy will be applied in the analysis of all the external tiles of the LMC, for which only the EROS-2 data are available.

The main results for HEBs are:

- We identified in the whole sample of the EROS-2 candidate CCs, 1768 EBs by combining the colour-cut criterion and the visual inspection of the light curves. They are composed by hot main sequence stars or blue giants, hence we classed them HEBs.
- We analysed the light curves of the 1768 HEBs and re-determined the previously defined periods for 225 of them.
- We divided the sample of 1768 HEBs into contact-like (324) and non-contact (1444) systems by visual inspection of their light curves and by analysis of the Fourier decomposition parameters.
- We analysed the  $PL$  relation in the optical ( $R_{EROS}$  and  $I$ ) and  $K_s$  passbands of the contact-like HEBs in the EROS-2 sample. We did not confirm the existence of a  $PL$  relation for contact-like HEBs.
- We found that contact EBs containing a red giant component from the OGLE III catalogue do follow  $PL$  sequences in the  $I$  and  $K_s$  passbands. We computed the weighted linear regression of the  $PL$  relation in the  $K_s$  passband:

$$K_{s,0} = (-2.888 \pm 0.096)\log(P) + (20.139 \pm 0.171) \quad (6.11)$$

with rms=0.406 mag.

There is a possible additional  $PL$  sequence located  $\sim 1$  mag fainter, but the number of objects following it, is too small to allow a reliable fit.

Main results for the RR Lyrae stars in tile LMC 5\_5 are:

- We analysed a sample of 71 RR Lyrae stars in this tile close to the bar of the LMC, for which multi-epoch  $K_s$  photometry from the VMC survey, precise periods from the OGLE III catalogue and spectroscopically determined metallicity are available. We derived the mean  $K_s$  magnitudes of these stars by fitting templates from Jones et al. (1996) to the VMC data.
- We derived a new  $PL_{K_s}Z$  relation for RR Lyrae stars by using a Bayesian fitting approach. The new  $PL_{K_s}Z$  relation has a number of advantages: (i) it uses multi-epoch  $K_s$  photometry from the VMC survey to derive light curves and estimate mean  $K_s$  magnitudes of the RR Lyrae stars, while in most studies single-epoch photometry is



## CONCLUSIONS

---

used; (ii) it uses precisely determined periods from the OGLE III survey; (iii) the relation is based on a relatively large sample of the RR Lyrae stars with spectroscopically determined metallicities in the range  $-2.06 < [\text{Fe}/\text{H}] < -0.63$  dex (Gratton et al., 2004); (iv) it is derived based on a Bayesian fitting approach developed specifically for this study. This method takes into account: 1) the potentially significant intrinsic dispersion of the data; 2) non-negligible errors in two dimensions; 3) the possibility of inaccuracy in the formal error estimates.

- We calibrated the zero-point of our new  $PL_{K_s}Z$  relation by applying two different techniques: (i) by using the distance to the LMC determined by Pietrzyński et al. (2013); (ii) by applying the *HST* parallaxes of five MW RR Lyrae stars from Benedict et al. (2011).
- We applied our  $PL_{K_s}Z$  relation with the zero-point calibrated from the *HST* parallaxes and derived the distance to tile LMC 5\_5:  $(m - M)_0 = 18.71 \pm 0.09$  mag. This distance modulus is about 0.2 mag longer than the widely adopted value of  $(m - M)_0 = 18.5$  mag. In future studies we suggest to use the relation with the zero-point based on the precise distance to the LMC:

$$M_K = (-2.70 \pm 0.22)\log P + (0.03 \pm 0.06)[\text{Fe}/\text{H}]_{\text{Har}} + (-1.05 \pm 0.05) \quad (6.12)$$

- We estimated the impact of Gaia on definition of the zero-point of the RR Lyrae  $PL_{K_s}Z$  and  $M_V - [\text{Fe}/\text{H}]$  relations. We selected 25 bright MW RR Lyrae stars and simulated their Gaia parallaxes with observational errors. We applied a Bayesian fitting approach specifically developed for this study to derive  $PL_{K_s}Z$  and  $M_V - [\text{Fe}/\text{H}]$  relations based on the simulated parallaxes. The final relations are very close to those which were considered as "true" in the input and their zero-points have respectively precisions of 0.03 mag and 0.005 mag.

Main results for the RR Lyrae stars in tile LMC 8\_3 are:

- We analysed the sample of EROS-2 candidate RR Lyrae stars in tile LMC 8\_3 and extracted 251 bona-fide RR Lyrae variables that have a counterpart in the VMC catalogue.
- We classified the 251 bona-fide RR Lyrae stars based on both, the visual inspection of the light curves and the analysis of the period-amplitude diagram. The sample

contains 167 RRab, 74 RRC and 10 RRd stars. For each star we derived mean magnitudes, amplitudes, epochs of maximum light in the  $B_{EROS}$  and  $V$  passbands.

- We checked the periods provided by the EROS-survey and corrected them for four objects. We determined the second periods for the 10 RRd stars.
- We performed the Fourier decomposition of the light curves of the 241 bona-fide RRab and RRC variables and determined photometric metallicities from the Fourier parameters of the light curves for 132 RRab stars and 17 RRC stars. The mean metallicity on the Carretta et al. (2009) metallicity scale, of the RRab stars in tile LMC 8\_3 is  $\langle [Fe/H]_{C09ab} \rangle = -1.58$ ;  $\sigma_{[Fe/H]_{C09ab}} = 0.5$ , whereas the mean metallicity of the RRC stars is  $\langle [Fe/H]_{C09c} \rangle = -1.82$ ;  $\sigma_{[Fe/H]_{C09c}} = 0.3$ . The mean metallicity derived by averaging the photometric metallicities of both RRab and RRC stars is  $\langle [Fe/H]_{C09} \rangle = -1.61$ ;  $\sigma_{[Fe/H]_{C09}} = 0.4$ . There is a shift of about 0.25 dex between mean metallicities of RRab and RRC stars, the reason of which could be some systematics in the calibration of the relations used to derive the photometric metallicities.
- We fitted the  $K_s$  band light curves obtained by the VMC survey with templates from Jones et al. (1996) and derived mean  $K_s$  magnitudes for 241 RR Lyrae stars. We computed a weighted  $PL_{K_s}$  relation through the data:

$$K_{s,0} = (-2.40 \pm 0.13) \log P + (17.38 \pm 0.03) \quad (6.13)$$

- We used the  $PL_{K_s}Z$  relations in the literature and our new  $PL_{K_s}Z$  relation computed from 71 RR Lyrae stars in tile LMC 5\_5 to determine individual distances to the 251 RR Lyrae stars in tile LMC 8\_3 and derived the mean distance modulus:  $(m - M)_0 = 18.615 \pm 0.006$  mag. These results show that the external tile LMC 8\_3 seems to be located 0.1 mag closer to us than the central tile LMC 5\_5.

The comparison of the spatial distribution of the three different distance indicators revealed the internal structure of the LMC. The RR Lyrae stars have a larger density in the central region of the LMC, but in general they are distributed smoothly and likely trace the halo of the galaxy. On the contrary, CCs and HEBs are strongly concentrated towards the LMC bar and spiral arm, and almost disappear in the peripheral areas. HEBs are more sharply concentrated toward regions of recent star formation such as 30 Doradus and Constellation III, while CCs mostly follow the bar and spiral arm of the LMC.

## CONCLUSIONS

---

From the analysis of the EBs we confirmed the existence of  $PL$  relations only for contact EBs that contain a red giant component, while did not confirm the existence of a  $PL$  relation for contact HEBs. The luminosity ratio of the components of the HEBs (main sequence stars and blue giants) can vary significantly. In contrast, in contact systems with a red giant component, the giant dominates the luminosity while the contribution from the secondary is usually negligible. As a consequence the  $PL$  relation of contact HEBs can be much more scattered than the  $PL$  of contact EBs with a red giant component. In any case, the scatter of the  $PL$  relation for EBs with a red giant component is too large to be used for the determination of the distance.

The results from the RR Lyrae stars in tiles LMC 8\_3 and 5\_5 are puzzling and need further investigation. The zero-point of the  $PL_{K_s}Z$  relation of RR Lyrae stars still remains a controversial issue that cannot be solved with the present data. While this is not going to affect our study of the structure of the LMC through the VMC data, for which we will use differential distances, the absolute distance to the LMC from RR Lyrae stars can be derived only when the RR Lyrae zero-point issue will be settled. A huge improvement in this topic is expected with the astrometric mission Gaia which will measure the parallaxes of thousands MW RR Lyrae stars. In this thesis we simulated Gaia parallaxes of only 25 bright Galactic RR Lyrae stars and showed that using even a small sample of RR Lyrae stars with precisely determined parallaxes we will be able to estimate the  $PL_{K_s}Z$  and  $M_V - [\text{Fe}/\text{H}]$  relations with a great precision, when combined with metallicity and photometry from other sources. The zero-points of the CCs and EBs will also be recalibrated with Gaia, thus allowing a direct and robust comparison of the the distance to the LMC as derived from independent distance indicators.



## Appendix A

# Properties of the “hot” eclipsing binaries in the LMC

Main properties and Fourier parameters of the light curves of 1768 HEBs in our sample are presented in Table A.1. The table provides the EROS-2 identification numbers (column 1) and coordinates (RA and DEC at J2000; columns 2 and 3) of the HEBs. Periods (column 4) for the majority of stars are from the EROS-2 catalogue, while for 225 sources marked by an asterisk, periods were recalculated in this study. Number of digits in the periods are the same as originally listed in the EROS-2 catalogue. Mean  $\langle B_{EROS} \rangle$  and  $\langle R_{EROS} \rangle$  magnitudes are listed in columns 5 and 6, respectively. The EROS-2 team provided us values with three digits as computed using all observations involved in the period determination (e.g. after excluding outliers), however we rounded them to two digits to account for the typical errors of the individual data-points which vary from 0.02 to 0.08 mag depending on magnitude. Column 7 lists the epochs of minimum light in the  $R_{EROS}$  passband we calculated in this study, they are listed with four digits, in agreement with the actual precision of EROS-2 HJDs (see below). Columns from 8 to 13 of Table A.1 present the parameters of the Fourier decomposition in the  $R_{EROS}$  passband calculated in this study. HJDs provided by the EROS-2 catalogue are accurate to within 10 s, hence, epochs of minimum light have four digit accuracy.

Finally, Table A.2 provides information about the cross-identifications (EROS-2 and VMC IDs) for 999 HEBs in common between the two catalogues, their periods and the  $K_s$  and  $R_{EROS}$  magnitudes at maximum light.

EROS-2 id	RA (J2000) (deg)	DEC (J2000) (deg)	Period (day)	$\langle R_{EROS} \rangle$ (mag)	$\langle B_{EROS} \rangle$ (mag)	Epoch(min) (HJD-2,450,000)	$\alpha_0$	$\alpha_1$	$\alpha_2$	$\alpha_3$	$\alpha_4$	$\alpha_5$
Im0555k12721*	76.2287	-71.23919	0.8010095	17.26	17.08	2184.7009	0.957	-0.037	-0.055	-0.0070	-0.016	0.0030
Im0322n20546	80.4206	-66.8744	0.900708	17.24	17.06	1851.6263	0.879	-0.028	-0.167	-0.014	-0.062	-0.0030
Im0354n8770	85.11371	-67.16454	0.904003	17.64	17.40	1185.7298	0.913	-0.03	-0.127	-0.0080	-0.041	0.0020
Im0193k19182	79.73758	-68.10716	0.905358	17.05	16.99	2213.7821	0.958	-0.01	-0.047	-0.0060	-0.024	0.0060
Im0341k8979	83.66655	-66.30307	0.911721	17.00	16.75	1173.7244	0.882	-0.032	-0.173	-0.011	-0.074	0.0
Im0285n10229	73.41711	-67.17722	0.911792	17.07	16.85	1532.5773	0.973	-0.015	-0.02	-0.0010	0.0010	-0.0020
Im0344m26510	83.0365	-67.12818	0.912445	17.32	17.18	1751.8628	0.917	-0.01	-0.117	0.0020	-0.052	0.0060
Im0023n11843	83.3321	-69.62209	0.912568	17.46	17.39	1701.4807	0.854	-0.033	-0.141	-0.01	-0.032	0.017
Im0123m11836	73.49311	-69.46511	0.919332	17.18	17.29	2519.7319	0.97	-0.014	-0.037	-0.0050	-0.013	-0.0010
Im0122n13303	72.46236	-69.64522	0.922604	17.17	16.94	438.8273	0.947	-0.023	-0.08	-0.01	-0.018	0.0040
Im0030m21391	84.32319	-69.38179	0.922672	16.88	16.77	2304.7686	0.883	-0.043	-0.153	-0.018	-0.046	-0.0010
Im0226m20767	84.60396	-69.00125	0.923941	17.65	17.45	1975.6799	0.913	-0.013	-0.12	-0.0050	-0.056	-0.0
Im0106n13876	76.54384	-70.34353	0.925344	17.51	17.36	498.6062	0.892	-0.033	-0.133	-0.021	-0.043	-0.0010
Im0231k9063	87.12851	-67.70653	0.927999	17.07	16.84	1072.8079	0.88	-0.02	-0.141	-0.0050	-0.031	0.0020
Im0114k6489	74.04547	-69.78932	0.932097	17.54	17.43	952.4663	0.882	-0.028	-0.025	0.0	-0.011	0.0040
Im0283n8062	73.68666	-66.79684	0.938923	17.10	16.81	2255.5680	0.855	-0.034	-0.198	-0.014	-0.071	-0.0050
Im0214m10459	82.86371	-68.5704	0.938971	17.76	17.72	1659.5486	0.95	-0.013	-0.084	-0.0020	-0.05	0.0050
Im0171m16733*	76.18353	-67.74663	0.939001	15.91	15.61	1915.7516	0.948	-0.010	-0.071	-0.0020	-0.028	-0.0010
Im0127k12134	73.26783	-70.18084	0.939454	17.47	17.51	2225.5710	0.981	-0.030	-0.046	-0.0	-0.029	-0.0
Im0215115004	83.63246	-68.59249	0.940678	17.24	17.06	2200.7849	0.912	-0.050	-0.141	-0.0030	-0.08	-0.0010
Im0043k23371	86.99351	-69.5312	0.941374	17.45	17.43	1478.7717	0.902	-0.031	-0.114	-0.011	-0.043	-0.0010
Im0342k18196	82.89531	-66.75002	0.941447	17.03	16.82	434.8095	0.911	-0.060	-0.111	-0.0010	-0.045	-0.0050
Im0346114981	82.79685	-67.5609	0.941548	17.04	17.07	1657.5184	0.985	-0.025	-0.035	-0.011	-0.017	-0.0
Im0466k23468	81.40389	-66.07126	0.943032	17.24	17.04	1140.6191	0.867	-0.04	-0.186	-0.018	-0.055	-0.0070
Im0167m21114	74.75322	-68.83467	0.943189	17.76	17.59	336.8708	0.956	-0.02	-0.055	-0.0060	-0.032	-0.0020
Im0436m21036	76.8162	-66.20443	0.944593	17.19	16.93	1866.6125	0.874	-0.031	-0.156	-0.012	-0.042	-0.0040
Im0341k18581	83.73331	-66.3684	0.947627	17.37	17.22	1981.6242	0.985	-0.033	-0.060	-0.0050	-0.0050	0.0030
Im0341k4660	83.61982	-66.27231	0.953374	17.34	17.09	1869.6179	0.932	-0.070	-0.107	-0.011	-0.069	-0.0050
Im0217m19208	84.09004	-68.82472	0.954486	16.98	17.01	2338.6617	0.976	-0.024	-0.031	-0.0040	-0.0030	0.0
Im0030n19548	84.47044	-69.33711	0.955261	17.09	16.93	2167.8026	0.942	-0.050	-0.077	-0.0010	-0.031	-0.0010
Im0090n16243	78.41769	-69.30601	0.956439	16.92	16.90	2198.6689	0.953	-0.0080	-0.07	-0.0050	-0.04	-0.0020
Im0340m15852	83.06971	-66.35575	0.958465	17.46	17.28	2310.7127	0.979	-0.062	-0.109	-0.017	-0.0060	0.0070
Im0072n12336	92.50478	-69.65075	0.9593	17.61	17.47	1784.8682	0.91	-0.042	-0.128	-0.019	-0.058	0.0010
Im0102m10441	76.45363	-69.46743	0.960451	17.26	16.96	2496.8222	0.859	-0.01	-0.226	0.0050	-0.089	0.0040
Im0015k6383	80.93404	-69.7931	0.964159	17.16	16.97	772.8383	0.879	-0.0090	-0.166	-0.0070	-0.073	-0.0010
Im0542k20454	72.90434	-70.96458	0.963838	17.37	17.32	1659.4784	0.975	-0.048	-0.039	-0.032	-0.02	-0.0040
Im0034k10238	83.79916	-69.8204	0.968988	17.19	17.28	2160.7476	0.92	-0.03	-0.122	-0.01	-0.056	0.0010
Im0160m26440	73.52748	-67.81702	0.969158	17.74	17.73	1493.6251	0.961	-0.014	-0.036	0.0020	-0.0030	0.0

APPENDIX A. PROPERTIES OF THE "HOT" ECLIPSING BINARIES IN THE LMC

Im0355n11866	86.03532	-67.17845	0.969348	17.22	17.08	1774.9203	0.98	-0.056	-0.03	-0.02	-0.01	-0.0080
Im0604l15733	85.46777	-71.41346	0.976899	17.82	17.67	1179.8447	0.957	-0.026	-0.065	-0.017	-0.027	-0.0090
Im0093k16356	79.09752	-69.48908	0.977186	17.00	16.95	554.5324	0.926	-0.017	-0.105	-0.060	-0.032	-0.0010
Im0321l27158	80.22724	-66.57613	0.977509	17.28	17.14	1236.6025	0.937	-0.125	-0.086	-0.054	-0.025	0.0010
Im0352m18009	85.08721	-66.74919	0.978963	17.81	17.61	1142.7253	0.966	-0.010	-0.05	-0.0040	-0.032	0.0020
Im0223n26953	85.68687	-68.31242	0.979034	17.68	17.56	1636.5279	0.982	-0.017	-0.025	-0.0010	-0.0020	-0.0
Im0023k20021	83.11516	-69.51038	1.011662	16.90	16.89	1482.7311	0.942	-0.012	-0.083	-0.0050	-0.039	-0.0020
Im0594k12700	83.46081	-71.23035	1.019228	17.52	17.56	2201.6443	0.973	-0.012	-0.027	0.0	-0.0040	0.0020
Im0033m10429	85.35668	-69.46249	1.019232	17.86	17.78	2169.8024	0.962	-0.02	-0.047	-0.0030	-0.0070	0.0030
Im0117l9906	75.04975	-70.32301	1.020034	17.26	17.10	1388.8013	0.932	-0.019	-0.084	-0.0090	-0.031	-0.0060
Im0030n22649	84.33989	-69.35789	1.026528	16.76	16.64	1255.6286	0.951	-0.0070	-0.076	-0.0020	-0.035	0.0020
Im0323l27434	79.93833	-66.91902	1.027206	17.34	17.22	1776.8380	0.909	-0.016	-0.121	-0.0080	-0.055	0.0020
Im0025n17091	83.55948	-69.99927	1.028086	17.57	17.71	1763.8121	0.968	-0.015	-0.048	-0.011	-0.015	-0.0010
Im0166m24423	73.69688	-69.01934	1.033285	17.41	17.09	864.6976	0.952	-0.022	-0.038	-0.0010	-0.0	0.0
Im0415m21902	74.36223	-65.69419	1.033457	17.62	17.35	2241.6069	0.957	-0.010	-0.073	-0.0010	-0.048	-0.0030
Im0165n14065	74.77506	-68.58243	1.038072	17.52	17.34	480.7638	0.974	-0.023	-0.028	-0.0010	-0.0040	0.0010
Im0157l17821	72.4731	-68.98049	1.04055	17.63	17.47	2229.5660	0.889	-0.046	-0.144	-0.023	-0.028	-0.0010
Im0091m27064	79.32571	-69.20378	1.041214	17.32	16.97	333.8872	0.826	-0.048	-0.183	-0.013	-0.076	0.0060
Im0093m5032	79.586	-69.58177	1.042603	16.84	16.65	1549.6498	0.918	-0.023	-0.09	-0.0040	-0.022	-0.0010
Im0405n23786	94.58284	-67.26861	1.046324	16.39	16.48	865.7215	0.995	-0.02	-0.0040	-0.0040	-0.0040	-0.0020
Im0173m9757	76.23218	-68.05139	1.04688	16.83	16.78	748.7953	0.94	-0.013	-0.083	-0.0060	-0.037	-0.0020
Im0424n14561	74.91334	-65.80545	1.047235	16.78	16.53	2057.4711	0.933	-0.030	-0.093	-0.0060	-0.051	0.0010
Im0317m24351	78.60369	-67.46527	1.049265	17.24	17.12	2185.6581	0.987	-0.042	-0.03	-0.025	-0.018	-0.0050
Im0112n5096	74.4563	-69.58371	1.050223	17.77	17.65	2327.5878	0.878	-0.050	-0.195	0.0040	-0.089	0.0010
Im0493n18692	87.28121	-65.47855	1.050931	17.63	17.74	830.8104	0.914	-0.041	-0.115	-0.018	-0.039	-0.0030
Im0031m9651	85.60344	-69.10275	1.051009	17.06	17.15	2174.8031	0.938	-0.060	-0.095	-0.010	-0.056	-0.0020
Im0011l15712	80.95532	-69.23951	1.051238	17.18	16.89	2214.6057	0.845	-0.028	-0.186	-0.017	-0.057	-0.0020
Im0244k10748	87.99523	-68.4218	1.051608	17.82	17.80	1576.7872	0.871	-0.039	-0.149	-0.018	-0.048	0.0070
Im0356m24069	84.9963	-67.46769	1.051643	17.26	17.11	1263.6234	0.977	-0.083	-0.035	-0.023	-0.0080	-0.012
Im0540l15552	72.91439	-70.70636	1.052165	17.83	17.64	2296.6801	0.806	-0.046	-0.222	-0.022	-0.065	-0.0070
Im0020l8553	81.83968	-69.26417	1.054358	17.15	16.92	1835.7998	0.893	-0.010	-0.161	-0.0040	-0.087	0.0010
Im0367n18805	87.43252	-67.60061	1.055955	17.66	17.47	2353.6709	0.962	-0.035	-0.07	-0.018	-0.039	0.0050
Im0311l9606	78.42094	-66.46266	1.059117	16.53	16.32	1858.8409	0.93	-0.021	-0.098	-0.0080	-0.027	-0.0
Im0356m10264	84.89458	-67.37154	1.059355	17.17	17.05	405.8067	0.965	0.0	-0.075	0.0010	-0.052	-0.0060
Im0463m8760	82.47922	-65.24737	1.059483	17.87	17.68	1934.7227	0.956	-0.02	-0.04	0.0020	-0.0040	0.0050
Im0355k17216	85.56442	-67.06382	1.060366	16.99	16.83	1248.6155	0.883	-0.045	-0.163	-0.02	-0.07	0.0
Im0551m9243	76.43002	-70.50588	1.064649	16.53	16.19	1856.6163	0.946	-0.014	-0.064	-0.0020	-0.016	0.0020
Im0184n14844	77.14324	-68.59311	1.067386	17.02	16.85	2020.5151	0.968	-0.011	-0.051	-0.0020	-0.027	0.0
Im0585m29810	83.06159	-71.3173	1.06795	17.24	17.05	1923.6854	0.925	-0.023	-0.088	-0.0080	-0.018	0.0030
Im0290k18569	74.02612	-66.38129	1.068392	16.21	16.01	1925.5978	0.948	-0.013	-0.058	-0.0	-0.0090	-0.0020
Im0341n1901	84.04694	-66.42796	1.069987	16.73	16.43	1616.5871	0.93	-0.022	-0.111	-0.01	-0.061	-0.0

lm0570m20301	1.070216	16.24	16.03	875.6007	0.935	-0.021	-0.082	-0.0050	-0.02	-0.0020
lm0336i21294	1.070847	17.81	17.55	353.8358	0.925	-0.0060	-0.139	0.0	-0.1	0.0030
lm0334i20690	1.071333	17.05	16.88	1495.8507	0.953	-0.101	-0.07	-0.053	-0.026	-0.012
lm0116m17752	1.071932	16.90	16.68	1608.5570	0.859	-0.04	-0.188	-0.019	-0.063	-0.0020
lm0123m3222	1.072633	16.94	16.85	1618.5335	0.931	-0.017	-0.086	-0.0050	-0.028	-0.0
lm0335i16808	1.073703	16.19	15.96	1867.6534	0.955	-0.0070	-0.061	-0.0020	-0.025	0.0
lm0337k16442	1.07405	17.61	17.48	2463.8803	0.963	-0.0090	-0.061	-0.0040	-0.041	-0.0030
lm0295i19334	1.074702	16.93	16.71	2080.9085	0.974	-0.011	-0.024	-0.0020	0.0010	0.0010
lm0207n19761	1.074897	17.24	17.07	2337.6175	0.943	-0.019	-0.097	-0.013	-0.045	0.0010
lm0335n6422	1.076161	17.28	17.00	802.8039	0.976	-0.023	-0.027	-0.0080	-0.012	-0.0010
lm0022k2100	1.079389	16.35	16.12	1881.6874	0.924	-0.021	-0.082	-0.0010	-0.02	0.0050
lm0184k20015	1.079741	17.45	17.36	1224.6259	0.965	-0.043	-0.045	-0.015	-0.027	-0.0020
lm0157n9803	1.080202	17.43	17.25	429.7768	0.926	-0.035	-0.115	-0.016	-0.046	0.0030
lm0314n10220	1.080563	16.37	16.15	2234.5971	0.948	-0.0040	-0.066	-0.0020	-0.028	-0.0
lm0326i7561	1.081099	16.91	16.86	440.5993	0.977	-0.0	-0.034	0.0020	-0.03	0.0070
lm0120n26206	1.081433	16.78	16.70	1531.5736	0.964	-0.012	-0.054	-0.0030	-0.021	-0.0020
lm0040k16225	1.087516	17.45	17.27	1900.6187	0.92	0.0010	-0.1	0.0	-0.042	-0.0030
lm0044m4203	1.087685	16.34	16.22	1585.7240	0.917	-0.012	-0.131	-0.0030	-0.077	-0.0010
lm0311i24725	1.090105	17.92	17.74	2234.5971	0.9	-0.047	-0.143	-0.022	-0.067	-0.0030
lm0374n6047	1.090677	17.53	17.37	1939.7827	0.97	-0.012	-0.018	-0.0020	0.0	0.0060
lm0301m26336	1.090782	17.84	17.66	1438.8198	0.971	-0.03	-0.019	-0.016	-0.0010	0.014
lm0425n26027	1.090849	17.95	17.82	1609.5550	0.937	0.045	-0.098	0.022	-0.041	0.0010
lm0584i11571	1.091989	17.78	17.77	1828.7310	0.934	-0.016	-0.08	-0.01	-0.02	0.0030
lm0466m12019	1.092537	16.92	16.69	2142.8398	0.972	-0.01	-0.029	-0.0030	-0.013	0.0020
lm0343k8884	1.092644	16.74	16.54	1764.8820	0.911	-0.0080	-0.117	-0.0060	-0.04	0.0010
lm0593i24799	1.093375	17.49	17.45	1915.6440	0.936	-0.0040	-0.109	-0.0	-0.052	-0.0040
lm0207i9965	1.094904	16.84	16.63	1966.6365	0.929	-0.026	-0.09	-0.0040	-0.02	-0.0020
lm0360n11911	1.095179	17.76	17.64	1925.8028	0.966	-0.033	-0.041	-0.0050	-0.011	-0.0020
lm0207i11656	1.095419	17.74	17.74	2327.6642	0.981	-0.037	-0.031	-0.011	-0.012	-0.0010
lm0021m12890	1.095632	17.44	17.39	537.5088	0.856	-0.012	-0.161	-0.0040	-0.06	-0.0030
lm0344m10458	1.098211	16.26	16.04	1300.5634	0.992	-0.01	-0.012	-0.0020	-0.0020	0.0040
lm0095n12350	1.100478	17.72	17.67	1463.7176	0.983	-0.014	-0.066	-0.0060	-0.042	-0.0
lm0550k13137	1.10302	17.13	16.94	1591.6349	0.967	-0.01	-0.055	0.0	-0.027	-0.0030
lm0121i5053	1.104991	16.37	16.07	1888.5707	0.94	-0.0050	-0.083	-0.0010	-0.036	0.0
lm0366k17409	1.105186	16.49	16.38	1627.6123	0.979	-0.069	-0.039	-0.025	-0.01	-0.0010
lm0364i13690	1.105617	17.08	16.87	1579.7251	0.977	-0.013	-0.047	-0.011	-0.031	0.0030
lm0343i24033	1.107295	17.08	17.03	1607.6250	0.963	-0.074	-0.066	-0.049	-0.038	0.0040
lm0346i8111	1.112761	17.17	16.99	780.8348	0.931	0.0080	-0.109	0.0020	-0.07	0.0
lm0243i16058	1.112807	17.48	17.51	1116.8745	0.951	-0.025	-0.06	-0.0010	-0.013	0.0
lm0156n21172	1.11399	17.80	17.59	1603.5730	0.947	-0.021	-0.073	-0.016	-0.039	0.0040
lm0283k11461	1.114622	16.97	16.84	1848.7862	0.92	-0.022	-0.08	-0.01	0.0010	0.0020



APPENDIX A. PROPERTIES OF THE “HOT” ECLIPSING BINARIES IN THE LMC

lm023217259	1.120751	17.33	17.21	1660.5418	0.879	-0.051	-0.179	-0.026	-0.085	0.0040
lm0265k11680	1.121349	17.67	17.58	1660.5844	0.922	-0.0	-0.109	-0.0010	-0.055	-0.0010
lm0457k18380	1.127347	17.50	17.34	1257.5744	0.906	-0.036	-0.128	-0.015	-0.045	-0.0010
lm017216626	1.13021	17.10	16.90	1848.8070	0.895	-0.0050	-0.152	-0.0020	-0.078	-0.0030
lm010215415	1.131352	16.44	16.31	1956.6302	0.913	-0.027	-0.1	-0.014	-0.037	0.0040
lm048616605	1.131517	17.21	16.99	537.5438	0.941	-0.02	-0.075	-0.0040	-0.035	-0.0010
lm0310k15114	1.132918	17.74	17.56	1147.8079	0.966	-0.089	-0.071	-0.056	-0.034	-0.0010
lm0690124400	1.13369	17.31	17.18	2124.8448	0.989	-0.017	-0.03	-0.0070	-0.015	0.0020
lm0325127285	1.135758	16.48	16.19	2262.6074	0.993	-0.012	-0.0080	-0.0060	-0.0050	-0.0
lm0010k15429	1.136931	16.89	16.57	1253.5933	0.966	-0.067	-0.051	-0.015	-0.035	-0.014
lm0347119578	1.138713	17.23	17.14	2140.8425	0.91	0.0050	-0.128	0.0050	-0.082	0.0020
lm0292k21101	1.139525	16.63	16.40	2554.6585	0.932	0.0050	-0.081	-0.0	-0.033	-0.0
lm0556m19867	1.139527	17.52	17.36	481.6831	0.967	-0.021	-0.046	-0.0060	-0.012	-0.0010
lm0214n9616	1.143016	17.44	17.42	1538.6564	0.918	-0.0020	-0.143	-0.0030	-0.091	0.0010
lm0245k7908	1.143467	17.54	17.45	781.7629	0.933	-0.0050	-0.088	0.0010	-0.045	0.0040
lm045515567	1.143775	16.48	16.23	1290.5307	0.992	0.0030	-0.079	0.0040	-0.054	-0.0030
lm0561n18106	1.143839	16.36	16.09	1126.6240	0.967	-0.01	-0.063	-0.0080	-0.039	-0.0020
lm0217n14277*	1.147572	16.33	16.20	2320.6728	0.957	-0.039	-0.059	-0.01	-0.018	-0.0010
lm0467m6802	1.147802	16.09	15.85	789.6918	0.929	-0.152	-0.102	-0.063	-0.031	0.0070
lm0417n9358	1.14811	17.30	17.03	2311.6124	0.948	-0.017	-0.053	-0.0	-0.070	-0.0020
lm0571124463	1.148628	17.77	17.55	1150.6653	0.973	-0.01	-0.053	-0.0050	-0.029	0.0020
lm0031n17224	1.14893	16.51	16.32	342.8286	0.928	-0.016	-0.09	-0.0060	-0.033	-0.0010
lm0225112189	1.157422	17.33	17.23	1532.6827	0.978	-0.011	-0.019	-0.0030	0.0010	0.0
lm0033m26708	1.158284	17.16	17.10	1997.5843	0.982	-0.018	-0.047	-0.0070	-0.028	-0.0
lm0575n11053	1.16016	17.35	17.16	1819.7524	0.965	-0.014	-0.046	-0.0040	-0.029	-0.0010
lm0014120054	1.160262	17.84	17.65	1272.5921	0.93	-0.041	-0.07	-0.0040	-0.025	0.0020
lm0466119242	1.163589	17.46	17.37	2016.5482	0.975	-0.016	-0.026	-0.0080	-0.011	0.0020
lm0283n14097	1.164051	17.07	16.95	1948.6386	0.928	0.011	-0.131	0.0	-0.091	-0.0010
lm0535n11277	1.168449	17.09	17.03	1563.5932	0.979	-0.017	-0.031	-0.0080	-0.014	-0.0020
lm0121116803	1.170021	16.85	16.92	1276.4939	0.981	-0.0060	-0.038	-0.0020	-0.021	-0.0010
lm0356n9591	1.173114	17.38	17.26	2018.5699	0.889	-0.0030	-0.147	-0.0060	-0.059	0.0020
lm0103113951	1.174507	16.78	16.66	388.8527	0.912	-0.027	-0.12	-0.012	-0.044	-0.0030
lm0226n24168	1.176008	16.20	15.99	1453.8637	0.944	0.0090	-0.086	0.0020	-0.047	-0.0060
lm0457119060	1.176108	17.40	17.22	1479.6849	0.961	-0.0060	-0.052	-0.0	-0.034	0.0020
lm0211k19128	1.178264	17.67	17.36	1117.6979	0.944	-0.029	-0.079	-0.0080	-0.042	-0.0030
lm0214m29033	1.178663	16.54	16.60	2072.4587	0.925	-0.040	-0.1	-0.0040	-0.066	0.0050
lm0540122424	1.181881	17.14	16.99	1464.6401	0.921	-0.0020	-0.12	0.0010	-0.07	0.0
lm0303123428	1.183669	17.71	17.61	1383.8448	0.883	-0.054	-0.163	-0.025	-0.067	0.0030
lm0021k22831	1.184539	17.05	17.03	931.4717	0.967	0.0050	-0.062	0.0030	-0.036	-0.0030
lm0201k10778	1.187596	17.74	17.71	780.8087	0.97	-0.0090	-0.04	-0.0020	-0.03	-0.0010
lm0312k15523	1.188117	17.51	17.52	1764.8517	0.956	-0.023	-0.051	-0.0070	-0.012	-0.0

lm0114m27899	74.30206	-69.91214	1.191167	16.89	16.81	2009.5409	0.942	0.0020	-0.078	-0.0030	-0.048	0.0020
lm0200k19885	80.42683	-67.83092	1.191483	17.40	17.41	2193.7733	0.94	-0.032	-0.065	-0.0040	-0.014	-0.0050
lm0120m6124	72.41807	-69.23849	1.191658	16.47	16.31	1071.7427	0.958	-0.012	-0.036	0.0	-0.0050	0.0
lm0366k10436	86.23861	-67.37474	1.193346	16.52	16.28	1941.7860	0.914	-0.012	-0.153	-0.01	-0.087	-0.0030
lm0165m30398	74.76377	-68.52016	1.19364	17.37	17.08	442.8182	0.965	-0.014	-0.044	-0.0070	-0.024	0.0050
lm0044k3974	86.12024	-69.77893	1.19368	16.19	16.09	1941.6268	0.961	-0.013	-0.046	-0.0030	-0.0030	0.0
lm0344m1850	83.06417	-66.96759	1.193709	16.30	16.11	1129.7481	0.946	-0.0060	-0.065	-0.0030	-0.038	0.0010
lm0121k24922	72.80762	-69.22294	1.195194	15.90	15.79	1281.5149	0.941	-0.017	-0.061	-0.0040	-0.012	-0.0020
lm0471m3631	84.12683	-65.00347	1.195592	17.68	17.44	1751.9244	0.862	-0.052	-0.127	-0.0090	-0.0050	0.013
lm0210m25568	83.09413	-67.96484	1.196126	17.32	17.12	2000.5638	0.961	-0.024	-0.043	-0.0020	-0.0050	0.0030
lm0193110262	79.73984	-68.212	1.20099	17.30	17.11	1750.8674	0.971	-0.065	-0.059	-0.02	-0.044	0.0070
lm0115m19779	73.33247	-69.51175	1.202701	17.11	17.13	2187.6492	0.978	-0.012	-0.045	-0.0080	-0.028	-0.0
lm0214m25393	82.79608	-68.66299	1.205505	17.38	17.37	494.5888	0.969	-0.01	-0.051	-0.0010	-0.031	-0.0010
lm0100m7540	76.27001	-69.09826	1.206217	17.43	17.33	2003.5390	0.936	-0.041	-0.097	-0.013	-0.031	-0.0060
lm0115m14463	75.73343	-69.98184	1.2068	17.13	16.94	1962.6879	0.959	-0.0070	-0.071	0.0020	-0.034	0.0
lm0290m12236	74.27758	-66.33021	1.206866	16.80	16.84	949.4763	0.966	-0.017	-0.045	-0.0020	-0.017	0.0010
lm0286m23081	72.09821	-67.61777	1.207038	17.49	17.21	1899.7279	0.879	-0.042	-0.125	-0.016	-0.048	0.0
lm0373m20395	89.298	-66.73849	1.207672	17.88	17.77	1606.6476	0.936	-0.043	-0.088	-0.016	-0.02	-0.0010
lm0230m9259	86.43074	-67.71334	1.207767	17.67	17.49	1620.6740	0.871	-0.06	-0.116	-0.02	-0.072	-0.0010
lm0193m5944	80.25679	-68.18293	1.207775	17.54	17.45	1929.6674	0.867	-0.054	-0.169	-0.021	-0.068	-0.0
lm0316k13597	77.61099	-67.39053	1.209809	16.48	16.25	1874.6235	0.981	-0.0080	-0.016	-0.0010	-0.0	0.0010
lm0540k22686	72.95889	-70.60238	1.210708	17.84	17.64	1627.5133	0.98	-0.017	-0.046	-0.0090	-0.035	0.0010
lm0302m12595	76.3274	-66.83223	1.213151	17.18	16.89	1531.6134	0.926	-0.01	-0.03	-0.0020	-0.017	0.0090
lm0030m6815	84.47005	-69.39718	1.213239	16.40	16.27	818.8345	0.937	-0.025	-0.071	-0.0060	-0.015	0.0030
lm0167120879	74.06404	-69.00567	1.213472	17.05	16.83	760.7172	0.937	-0.0050	-0.117	-0.0030	-0.073	-0.0020
lm0290m7651	74.33292	-66.29643	1.213756	17.46	17.64	459.7105	0.896	-0.0030	-0.14	-0.0010	-0.073	-0.0030
lm0255m21132	91.17064	-68.51592	1.213994	17.74	17.57	1828.8639	0.899	-0.0020	-0.132	-0.0010	-0.069	-0.0010
lm0352124112	84.5875	-66.92691	1.214317	17.63	17.43	1812.7679	0.901	-0.0010	-0.14	0.0020	-0.063	0.0040
lm003318069	84.98061	-69.60168	1.215039	16.80	16.91	1883.7074	0.949	-0.011	-0.071	-0.0040	-0.038	0.0040
lm0423m21313	75.77782	-65.34184	1.21574	17.68	17.52	1279.5999	0.974	0.03	-0.0060	-0.0060	0.0090	0.024
lm0553126427	75.93462	-71.10917	1.216011	16.23	16.11	1284.5120	0.952	-0.015	-0.045	-0.0010	-0.0	0.0010
lm0240113940	87.98811	-67.89771	1.220005	17.38	17.26	2256.6495	0.984	-0.028	-0.023	-0.0070	-0.011	-0.0020
lm0352111634	84.54092	-66.83952	1.221534	17.64	17.46	2346.6610	0.955	-0.019	-0.047	-0.0070	-0.014	-0.0010
lm0343m24594	84.0397	-66.75127	1.222063	17.60	17.42	1774.9006	0.956	-0.016	-0.036	-0.0010	-0.0010	0.0010
lm0343127142	83.74179	-66.92211	1.22436	17.46	17.34	1271.5780	0.955	0.0080	-0.063	0.0020	-0.028	-0.0010
lm0552m28102	75.40852	-71.12939	1.224882	17.61	17.44	1836.6810	0.973	-0.012	-0.064	-0.0060	-0.034	-0.0040
lm0025119940	83.13371	-70.01572	1.225202	17.64	17.61	1305.5497	0.976	-0.018	-0.036	-0.0070	-0.017	0.0050
lm0346113640	82.56262	-67.54979	1.225316	16.41	16.17	1953.7492	0.935	-0.0090	-0.113	-0.0060	-0.059	-0.0020
lm0200120561	80.50397	-67.9453	1.225852	16.01	15.79	1259.5936	0.935	-0.02	-0.081	-0.0090	-0.03	0.0040
lm0191k12306	79.849	-67.71351	1.226024	17.34	17.06	828.6758	1.006	-0.028	-0.06	-0.0040	-0.039	-0.0070
lm0184m22563	77.17364	-68.63574	1.226475	17.45	17.30	2185.8582	0.929	-0.045	-0.1	-0.011	-0.042	-0.0060

APPENDIX A. PROPERTIES OF THE “HOT” ECLIPSING BINARIES IN THE LMC

lm0304n29842	76.16502	-67.29102	1.229024	16.64	16.32	1476.6539	0.902	-0.016	-0.148	-0.0090	-0.087	0.0060
lm0100l22131	75.96004	-69.35493	1.229371	17.53	17.40	1945.6895	0.894	-0.061	-0.145	-0.023	-0.064	-0.0
lm0452ml6067	79.92772	-65.338	1.229623	16.50	16.31	826.7593	0.949	-0.015	-0.053	-0.0020	-0.0030	0.0030
lm0344m8364	83.34386	-67.0099	1.231791	17.66	17.58	1184.6913	0.96	-0.018	-0.058	-0.013	-0.039	-0.0010
lm0347k20628	83.76059	-67.44287	1.231871	16.57	16.38	2255.6691	0.992	-0.0040	-0.012	-0.0	-0.0080	0.0010
lm0090m26466	78.63557	-69.20741	1.232396	17.23	16.97	1881.6416	0.877	0.010	-0.19	-0.0030	-0.096	0.0010
lm0252l22660	90.15279	-68.32599	1.233638	17.15	16.97	835.8110	0.877	-0.0070	-0.182	-0.0060	-0.073	0.0080
lm0336m21470	81.59424	-67.44576	1.236096	17.43	17.22	1974.6066	0.944	-0.011	-0.09	-0.0050	-0.068	0.0070
lm0343ml8540	84.17664	-66.71152	1.237336	16.56	16.25	1940.7662	0.951	-0.0070	-0.071	-0.0020	-0.051	-0.0040
lm0157n7217	72.68138	-68.89908	1.237435	16.39	16.15	435.8342	0.89	-0.026	-0.145	-0.01	-0.043	-0.0030
lm0222n4768	84.59285	-68.18699	1.238392	17.19	17.12	1578.6544	0.924	0.011	-0.127	0.0070	-0.074	-0.0080
lm0344l5959	82.6187	-67.14957	1.240057	17.30	17.09	1187.6999	0.947	-0.010	-0.107	-0.0090	-0.076	-0.0040
lm0090ml3647	78.28454	-69.13381	1.240532	16.87	16.73	1503.6563	0.922	-0.0050	-0.123	-0.0030	-0.078	-0.0020
lm0095l32222	78.88433	-70.08634	1.242849	17.75	17.61	1224.6295	0.948	-0.0030	-0.109	-0.0050	-0.068	0.0050
lm0110l8980	73.88764	-69.26169	1.24406	16.78	16.54	1210.6036	0.898	-0.021	-0.149	-0.0070	-0.067	0.0060
lm0175ml7458	76.53673	-68.44791	1.244897	16.47	16.22	1150.6119	0.953	-0.014	-0.053	-0.0030	-0.011	-0.0
lm0303ml0523	77.20164	-66.80712	1.246321	17.89	17.65	1936.6491	0.907	-0.0060	-0.143	-0.0050	-0.045	-0.0
lm0276kl3982	93.83765	-68.80429	1.247657	17.15	16.93	1786.9127	0.855	-0.049	-0.145	-0.02	-0.05	0.0020
lm0294l7825	74.04649	-67.15764	1.248422	16.53	16.33	1775.7783	0.969	-0.016	-0.024	0.0020	0.0010	0.0020
lm0342n24002	82.99553	-66.92396	1.24847	17.49	17.24	1114.7613	0.984	-0.04	-0.027	-0.022	-0.016	-0.0020
lm0551ml8330	76.57531	-70.71054	1.249127	16.58	16.28	1761.8763	0.964	0.0030	-0.055	0.0010	-0.036	0.0070
lm0343ml25612	83.84745	-66.91102	1.249653	17.38	17.24	792.7570	0.991	-0.021	-0.018	-0.0070	-0.012	0.0020
lm0304n24921	75.99117	-67.26056	1.249985	16.56	16.29	1628.5280	0.963	-0.0060	-0.052	0.0	-0.032	0.0030
lm0214n7884	82.80062	-68.55439	1.250305	17.07	16.88	1937.7049	0.927	-0.02	-0.105	-0.0070	-0.056	0.01
lm0044l24715	85.98352	-70.06185	1.251463	17.73	17.77	1388.8593	0.94	-0.03	-0.068	-0.011	-0.01	0.011
lm0322m4386	79.71801	-66.62687	1.254285	17.83	17.68	2018.5400	0.989	-0.037	-0.017	-0.017	-0.014	0.0050
lm0020ml4007	82.44224	-69.14128	1.256518	16.99	17.15	1448.7009	0.93	-0.0060	-0.086	-0.0060	-0.053	0.0020
lm0182l13191	76.98715	-68.23504	1.256523	17.14	16.88	2198.6547	0.871	-0.048	-0.19	-0.031	-0.09	-0.0020
lm0290ml19111	74.20515	-66.38201	1.257556	16.14	15.85	2199.7976	0.971	-0.015	-0.04	-0.0040	-0.015	0.0010
lm0325ml5768	80.75234	-67.04384	1.260551	16.89	16.59	434.7552	0.971	-0.014	-0.028	0.0020	0.0010	-0.0020
lm0283m24518	73.52331	-66.7657	1.260717	16.17	15.93	1777.7739	0.935	-0.025	-0.094	-0.0090	-0.057	0.0020
lm0054l5210	87.76585	-69.93961	1.261836	16.38	16.18	1317.5507	0.951	-0.018	-0.06	-0.0060	-0.017	0.0030
lm0343l25912	83.71114	-66.91478	1.264852	16.03	15.85	1266.6094	0.985	-0.016	-0.024	-0.0060	-0.011	0.0
lm0110l13288	73.8525	-69.29033	1.271404	16.17	15.96	1306.5003	0.972	-0.02	-0.052	-0.0060	-0.031	-0.0
lm067l15056	74.58004	-72.12418	1.271916	17.83	17.76	1856.6083	0.969	-0.039	-0.057	-0.019	-0.036	0.0030
lm0253l8355	90.8511	-68.34826	1.274284	17.47	17.39	1759.9022	0.935	-0.051	-0.088	-0.018	-0.032	-0.0050
lm0436k8952	76.36602	-65.96754	1.275596	17.75	17.60	2021.5603	0.99	-0.059	-0.02	-0.012	-0.0050	-0.01
lm0214m29858	82.79206	-68.53141	1.279218	17.36	17.35	2008.5639	0.953	-0.0080	-0.066	-0.0030	-0.042	0.0020
lm0555ml2064	76.75923	-71.23615	1.279848	16.15	15.86	2186.6970	0.88	-0.017	-0.073	-0.0030	-0.013	0.0050
lm0583m25712	82.93324	-70.93984	1.280423	17.05	17.09	2183.7762	0.951	-0.026	-0.06	-0.011	-0.026	0.0040
lm0595n9126	85.45416	-71.35427	1.282031	16.31	16.18	1388.8560	0.984	-0.020	-0.034	-0.0020	-0.02	0.0

lm005019127	88.16042	1.283015	17.94	17.76	1862.7808	0.951	-0.049	-0.11	-0.014	-0.05	-0.0030
lm0012m20602	80.64068	1.284101	17.65	17.29	1138.8386	0.941	-0.020	-0.146	-0.0030	-0.094	-0.0030
lm0197n19534	80.18187	1.284845	17.62	17.26	1933.7380	0.896	0.030	-0.188	0.0060	-0.101	-0.0070
lm0354117529	84.64993	1.288998	17.94	17.82	1181.7935	0.906	-0.076	-0.162	-0.038	-0.081	0.0010
lm0017m17883	81.75557	1.289967	17.21	17.30	1480.8179	0.982	-0.016	-0.031	-0.0060	-0.012	0.0020
lm0343k10539	83.43929	1.291479	17.81	17.75	1597.6622	0.901	-0.027	-0.09	-0.012	-0.0070	0.0030
lm0293l14089	74.99618	1.29204	17.72	17.54	1842.8031	0.981	0.050	-0.026	0.0	-0.019	-0.0010
lm0030k6634	84.02922	1.293848	16.18	16.06	1808.8535	0.879	-0.03	-0.137	-0.0080	-0.044	0.0010
lm0366k19655	86.14187	1.295471	16.85	16.67	1443.7901	0.867	-0.058	-0.183	-0.036	-0.09	0.0050
lm0351m7030	85.95719	1.296153	16.49	16.27	556.5973	0.976	0.010	-0.038	-0.0020	-0.025	0.0010
lm0184k11257	76.96216	1.297875	16.95	16.84	1455.7438	0.978	-0.012	-0.022	-0.0070	-0.013	0.0010
lm0134m16531	70.36211	1.298416	16.83	16.75	1874.5483	0.966	-0.015	-0.035	-0.0020	0.0010	-0.0030
lm0220n20494	84.7732	1.299183	17.16	17.01	1262.5922	0.946	-0.022	-0.06	-0.0050	-0.0070	0.0040
lm0345k2244	83.68146	1.301085	16.48	16.33	1511.7218	0.946	-0.016	-0.08	-0.0090	-0.039	-0.0030
lm0207l9702	81.62493	1.302753	16.36	16.29	1444.7445	0.97	-0.011	-0.038	-0.0040	-0.02	-0.0040
lm0200l20952	80.52018	1.304803	16.39	16.16	2029.4867	0.917	-0.022	-0.122	-0.0070	-0.064	-0.0020
lm0313k26622	78.36045	1.305016	17.44	17.29	2310.6596	0.934	-0.0050	-0.129	-0.0030	-0.09	0.0020
lm0122n21809	72.58673	1.305534	16.49	16.25	2356.5619	0.946	0.020	-0.077	0.0010	-0.038	-0.0
lm0033k16643	84.83539	1.305743	15.79	15.73	1629.6272	0.945	-0.024	-0.082	-0.0090	-0.044	0.0
lm0033k28357	84.92359	1.306841	15.88	15.77	2350.6233	0.881	-0.017	-0.151	-0.0090	-0.066	0.0020
lm0313k25371	78.46932	1.307306	17.71	17.60	539.5305	0.955	0.020	-0.076	-0.0	-0.055	0.0010
lm0221m26418	85.52184	1.30898	17.45	17.34	1538.6834	0.941	0.020	-0.07	-0.0040	-0.043	-0.0010
lm0632l19736	92.18	1.30977	16.95	16.79	1493.8556	0.925	-0.038	-0.104	-0.013	-0.053	-0.0
lm0344k4525	82.80274	1.310804	16.68	16.51	802.8137	0.939	-0.015	-0.081	-0.0080	-0.041	-0.0010
lm0345k7107	83.7232	1.311042	16.12	15.91	1152.8469	0.944	-0.030	-0.09	0.0020	-0.046	-0.0040
lm0190n14623	79.11976	1.311657	15.87	15.63	1195.6954	0.847	-0.02	-0.205	-0.0080	-0.071	-0.0
lm0551m16504	76.62832	1.312793	17.08	16.90	489.6383	0.932	-0.0070	-0.115	0.0020	-0.077	0.0010
lm0570l6310	79.15194	1.314737	17.66	17.50	423.6287	0.944	-0.025	-0.079	-0.012	-0.04	0.0020
lm0323l7738	80.2597	1.315224	16.99	16.89	1870.6559	0.937	-0.0040	-0.064	-0.0060	-0.043	-0.0010
lm0595m25154	85.29765	1.317016	17.59	17.74	1304.4933	0.984	-0.011	-0.043	-0.0020	-0.036	0.0
lm0321m13358	80.34625	1.31821	17.46	17.16	2227.6596	0.972	-0.020	-0.067	-0.0020	-0.046	0.0020
lm0551k19078	76.01596	1.318882	17.34	17.16	1959.6417	0.935	-0.0050	-0.1	-0.0020	-0.05	0.0010
lm0466m23585	81.44584	1.318958	16.68	16.51	1278.5415	0.978	-0.017	-0.026	-0.0060	-0.011	-0.0010
lm0340n22383	83.09296	1.319689	17.76	17.62	2250.6023	0.904	-0.039	-0.142	-0.012	-0.051	-0.0010
lm0366n14593	86.89847	1.321337	17.78	17.55	1476.7417	0.934	-0.017	-0.078	-0.0020	-0.037	0.0020
lm0032k20313	84.14494	1.323792	17.14	17.07	450.8444	0.93	-0.017	-0.091	-0.0050	-0.051	-0.0030
lm0012l17935	79.96302	1.323984	16.59	16.44	802.7603	0.97	-0.0040	-0.063	-0.0070	-0.051	0.0
lm0210m22011	83.11026	1.324956	17.02	16.86	1622.5521	0.929	-0.030	-0.106	-0.0060	-0.051	0.0010
lm0033m6850	85.37087	1.32799	17.17	17.03	1179.7954	0.87	-0.056	-0.184	-0.027	-0.079	0.0010
lm0343l5977*	83.64748	1.329154	15.82	15.64	2009.5248	0.933	-0.0090	-0.105	-0.0050	-0.07	0.0010
					760.6928	0.965	-0.014	-0.039	-0.0010	-0.0070	0.0010

APPENDIX A. PROPERTIES OF THE “HOT” ECLIPSING BINARIES IN THE LMC

lm0175n26107	76.52785	-68.64711	1.329774	17.56	17.07	1866.5926	0.972	0.0060	-0.078	-0.0070	-0.043	-0.0020
lm0330118021	81.08209	-66.52792	1.330011	16.54	16.42	1219.6459	0.962	0.0040	-0.052	0.0010	-0.023	0.0
lm0364f6843	86.31096	-67.15385	1.331375	16.87	16.69	1150.7712	0.899	-0.039	-0.127	-0.013	-0.042	0.0070
lm0324n11221	79.50773	-67.17439	1.334227	16.89	16.77	1842.8412	0.995	-0.025	-0.0030	-0.0060	-0.0020	0.0020
lm0701k23779	81.55107	-71.99519	1.334253	17.02	16.86	1496.6813	0.962	-0.0010	-0.065	0.0	-0.046	-0.0010
lm0175k18907	75.80158	-68.4579	1.335629	16.02	15.96	1447.7545	0.98	-0.0040	-0.02	-0.0030	-0.0050	0.0040
lm0110m24838	74.60204	-69.19898	1.337458	16.65	16.11	1198.6206	0.881	-0.043	-0.161	-0.016	-0.074	0.0030
lm0210k24451	82.3372	-67.82148	1.337468	16.71	16.53	2324.6279	0.898	-0.02	-0.108	-0.0080	-0.033	0.0010
lm0587n19385	82.93165	-71.78783	1.339509	16.72	16.65	792.6937	0.939	-0.032	-0.094	-0.011	-0.045	0.0
lm0056n22735	88.60805	-70.40959	1.341028	16.83	16.65	2240.8556	0.941	0.0050	-0.09	0.0	-0.047	-0.0010
lm0012119396	80.17763	-69.67576	1.342001	16.58	16.17	1528.6604	0.923	-0.02	-0.082	-0.0040	-0.018	0.0010
lm0045n27451	87.48414	-70.06132	1.34273	16.22	15.90	1478.7717	0.954	-0.021	-0.067	-0.013	-0.037	-0.0040
lm0125m17447	73.73964	-69.84709	1.343061	17.76	17.68	2184.6421	0.926	-0.046	-0.091	-0.012	-0.039	-0.0010
lm0032m19079	84.23338	-69.55235	1.344214	16.41	16.25	833.7956	0.952	-0.0080	-0.057	-0.0040	-0.022	-0.0010
lm0090k15522	77.83539	-69.15415	1.345239	17.16	17.33	596.4683	0.931	-0.0090	-0.098	-0.0050	-0.058	-0.0
lm0424k12950	74.77183	-65.63993	1.345498	16.39	16.19	2184.6886	0.979	-0.01	-0.021	-0.0050	-0.0070	0.0010
lm0557n16353	76.78602	-71.77228	1.346996	17.01	16.80	1196.5924	0.931	-0.026	-0.082	-0.0070	-0.017	0.0020
lm0091113141	79.18465	-69.27812	1.347207	16.91	16.91	1903.5899	0.925	-0.01	-0.1	-0.0090	-0.052	-0.0010
lm0040k25840	85.88344	-69.22795	1.352819	17.77	17.60	2228.8571	0.945	-0.016	-0.099	-0.0080	-0.062	-0.0010
lm0095n21786	79.35908	-70.02443	1.355226	17.39	17.34	2263.6459	0.883	-0.048	-0.141	-0.023	-0.046	-0.0030
lm0033112538	85.18187	-69.62848	1.356261	17.03	17.10	663.9331	0.977	-0.0010	-0.041	-0.0010	-0.031	-0.0010
lm0162111792	73.15868	-68.22971	1.356383	17.47	17.42	1763.7818	0.977	-0.014	-0.035	-0.0090	-0.0090	0.0
lm0020m2675	82.41469	-69.06903	1.356457	17.21	17.00	1439.7768	0.932	-0.0040	-0.131	0.0010	-0.088	-0.0040
lm0225k23166	85.09911	-68.495	1.357519	16.52	16.39	1211.7171	0.871	-0.020	-0.167	-0.0010	-0.056	0.0020
lm0541n10909	74.41288	-70.69434	1.357818	17.91	17.70	1476.6226	0.968	-0.013	-0.05	-0.0080	-0.038	0.0020
lm0122n14730	72.59675	-69.65419	1.359095	17.44	17.26	2227.5645	0.971	-0.018	-0.041	0.0010	-0.0040	0.0020
lm0033120481	85.12016	-69.67734	1.359961	17.11	17.28	1888.7095	0.948	-0.017	-0.046	-0.0020	-0.0080	0.0020
lm0225m4465	85.93241	-68.37478	1.360634	16.37	16.15	1952.6404	0.958	-0.0010	-0.073	-0.0070	-0.046	-0.0020
lm0325k8184	80.16287	-67.00164	1.361238	16.25	16.09	2223.8295	0.959	-0.012	-0.044	-0.0010	-0.0090	0.0010
lm0164n10943	73.5325	-68.57395	1.362005	16.58	16.38	1851.5868	0.972	-0.029	-0.035	-0.0070	-0.017	0.0020
lm0306m11218	76.16053	-67.36918	1.36289	16.87	16.65	2233.8258	0.935	-0.017	-0.071	-0.0050	-0.017	-0.0
lm0167n6619	74.39294	-68.90038	1.363124	17.50	17.26	434.7245	0.935	-0.0050	-0.077	0.0030	-0.048	-0.0050
lm0331n11495	82.33892	-66.56266	1.363165	15.84	15.54	2168.7479	0.856	-0.037	-0.186	-0.012	-0.066	0.0
lm0055m20627	89.47672	-69.88236	1.365312	17.43	17.26	2020.6020	0.978	-0.02	-0.022	-0.0020	-0.0010	0.0010
lm0326k15236	79.27837	-67.39888	1.365702	17.77	17.72	2236.5552	0.964	-0.024	-0.024	0.0010	-0.0020	0.011
lm0292k4705	74.0262	-66.63217	1.366304	17.67	17.53	1973.5702	0.956	-0.012	-0.06	-0.0060	-0.042	-0.0
lm0610k1228	88.04573	-70.49025	1.36879	17.48	17.34	452.7291	0.976	-0.022	-0.023	-0.0	-0.0080	0.0050
lm0551k21201	76.17855	-70.61236	1.37035	15.97	15.74	1769.8058	0.952	0.0010	-0.06	0.0040	-0.025	0.0010
lm021617335	82.63094	-68.90996	1.370367	17.28	17.18	1547.6934	0.939	-0.025	-0.064	-0.0030	-0.015	-0.0
lm0331112991	81.69989	-66.48707	1.370492	17.56	17.42	1774.8883	0.927	-0.044	-0.108	-0.019	-0.046	-0.0020
lm0587k6387	82.40128	-71.54306	1.372249	17.00	16.78	1761.8865	0.985	-0.015	-0.024	0.0	-0.0060	-0.0020

lm0584k14035	81.31538	-71.23568	1.372777	16.40	16.24	670.8905	0.966	-0.024	-0.025	-0.0040	-0.012	0.0030
lm0426m6757	75.10942	-65.94266	1.372785	16.54	16.32	325.9102	0.99	-0.029	-0.016	-0.0040	-0.013	0.0010
lm0194j20512	78.55626	-68.63336	1.373732	16.92	16.76	2009.5506	0.977	-0.02	-0.036	-0.0060	-0.013	0.0040
lm0485l16305	85.51608	-65.81286	1.374021	17.56	17.39	1398.8692	0.889	-0.072	-0.167	-0.022	-0.08	-0.0
lm0031m12282	85.26232	-69.38275	1.375196	16.14	16.07	1498.7112	0.901	-0.0060	-0.124	-0.0010	-0.061	-0.0010
lm0295k27975	74.85443	-67.11972	1.375483	16.96	16.83	1147.7847	0.876	-0.034	-0.116	-0.0080	-0.044	0.0040
lm0575n3947	80.7159	-71.35661	1.375523	16.40	16.19	825.8252	0.975	-0.0060	-0.036	-0.0020	-0.023	-0.0020
lm0186m25699	77.46551	-69.03439	1.376787	16.94	16.72	2187.7215	0.856	-0.043	-0.156	-0.019	-0.048	0.0010
lm0285k3972	73.07218	-66.9733	1.377486	16.90	16.90	2130.7948	0.98	-0.011	-0.031	-0.0040	-0.02	0.0
lm0315n6821	78.88115	-67.13714	1.378079	17.02	16.75	2240.8052	0.979	0.0030	-0.033	0.0020	-0.013	0.0010
lm0601l27234	86.71128	-70.76364	1.378285	17.76	17.72	1388.8630	0.907	-0.063	-0.123	-0.028	-0.062	0.0050
lm0010n9981	80.63701	-69.27116	1.379098	16.86	16.61	2202.6855	0.979	-0.013	-0.034	-0.0010	-0.0050	0.0050
lm0123k25550	73.25735	-69.54389	1.379496	17.75	17.75	424.8026	0.945	-0.0050	-0.083	-0.0020	-0.057	-0.0020
lm0010k3563	79.88856	-69.07681	1.380453	17.53	17.36	1306.5393	0.866	-0.055	-0.132	-0.0030	-0.060	0.016
lm0161l22253	74.14008	-67.93355	1.380684	17.29	17.12	1755.9068	0.946	0.0060	-0.073	0.0020	-0.024	-0.0040
lm0033k16425	84.81241	-69.50067	1.381841	15.95	15.84	1549.7162	0.928	-0.0030	-0.104	0.0030	-0.064	-0.0030
lm0187k25395	77.81155	-68.85996	1.384476	16.89	16.89	884.5797	0.943	-0.0050	-0.091	-0.0030	-0.038	0.0010
lm0033l8982	85.15985	-69.60625	1.384664	17.46	17.36	2347.5957	0.959	-0.0090	-0.074	-0.0030	-0.056	-0.0020
lm0121n10952	73.64131	-69.26381	1.389631	16.94	16.77	1503.6168	0.963	-0.01	-0.034	-0.0070	-0.017	-0.0010
lm0037n15636	85.47739	-70.36678	1.389987	17.71	17.63	1465.7833	0.936	-0.04	-0.11	-0.0080	-0.038	-0.0070
lm0453n18119	80.8885	-65.46498	1.392487	17.53	17.40	2160.7252	0.906	-0.027	-0.050	-0.0040	-0.030	0.0040
lm0346m15709	83.1288	-67.40781	1.396164	15.72	15.53	1910.7349	0.993	-0.019	-0.060	-0.0050	-0.020	0.0040
lm0337k24187	81.78841	-67.4714	1.397227	16.60	16.39	2020.5398	0.98	-0.011	-0.04	-0.0070	-0.017	0.0020
lm0217n12376	83.96639	-68.94279	1.398198	16.30	16.08	2327.6841	0.989	-0.0080	-0.011	-0.0	-0.0020	0.0010
lm0110n11270	74.41183	-69.27154	1.398457	16.52	16.36	2005.5927	0.877	-0.05	-0.174	-0.026	-0.078	0.0070
lm00127l20498	73.21769	-70.39849	1.398538	16.88	16.64	2234.7856	0.887	-0.044	-0.162	-0.022	-0.072	0.0010
lm0040l12070	86.00517	-69.28234	1.399558	16.81	17.00	1965.6435	0.948	-0.0010	-0.064	-0.0020	-0.039	0.0010
lm0597l19272	84.77925	-71.78888	1.402455	16.03	15.75	1259.6094	0.861	-0.041	-0.183	-0.018	-0.062	-0.0010
lm0200k21051	80.56212	-67.78808	1.403365	17.88	17.63	1237.6677	0.961	-0.029	-0.076	-0.024	-0.048	0.0080
lm0457k24395	80.28756	-66.07303	1.40671	17.81	17.72	1506.6956	0.887	-0.01	-0.16	0.0030	-0.083	0.0010
lm0306l18659	75.83359	-67.57889	1.407038	17.58	17.47	1893.6378	0.97	-0.038	-0.04	-0.0090	-0.019	0.0010
lm0166l12641	73.17995	-68.94171	1.408868	17.56	17.22	1526.6080	0.982	-0.063	-0.044	-0.019	-0.041	-0.0040
lm0343n25594	84.13251	-66.9085	1.409684	15.79	15.50	1885.7015	0.88	-0.027	-0.157	-0.01	-0.054	-0.0020
lm0174l19373	74.79143	-68.64692	1.410559	17.87	17.73	1971.6428	0.93	-0.058	-0.104	-0.025	-0.04	0.01
lm0165n25052	74.79152	-68.64701	1.410581	17.88	17.68	2208.5815	0.913	-0.06	-0.119	-0.034	-0.057	-0.0010
lm0433m7146	77.48491	-65.23679	1.413646	16.31	16.20	2259.6061	0.931	-0.03	-0.101	-0.012	-0.049	-0.0020
lm0440m22885	78.28887	-65.01113	1.415373	17.24	17.08	1805.8437	0.915	-0.032	-0.092	-0.0080	-0.026	0.0050
lm0332l24989	80.93409	-66.92286	1.415919	17.55	17.44	2160.7344	0.957	-0.0030	-0.063	0.0040	-0.04	0.0080
lm0332n21956	81.49459	-66.89928	1.416264	17.05	16.92	1086.8833	0.938	-0.047	-0.076	-0.012	-0.026	-0.0020
lm0191l10165	79.64741	-67.85672	1.418043	16.30	16.04	1433.8104	0.884	-0.031	-0.151	-0.013	-0.048	0.0010
lm0226k21375	84.3577	-68.8611	1.418055	17.47	17.37	1875.7102	0.924	0.0020	-0.132	0.0010	-0.088	0.0060

APPENDIX A. PROPERTIES OF THE “HOT” ECLIPSING BINARIES IN THE LMC

lm0033m14746	85.31466	69.48864	1.420343	15.73	15.64	2053.5057	0.948	-0.017	-0.058	-0.0050	-0.011	0.0
lm0186m6732	77.46315	-68.90315	1.420433	16.24	16.20	418.8373	0.969	-0.022	-0.061	-0.0050	-0.043	0.0010
lm0123n23584	73.5269	-69.69047	1.421185	16.50	16.28	2161.7151	0.981	-0.0070	-0.032	-0.0020	-0.015	-0.0
lm0331k22319	81.79609	-66.3964	1.421485	16.26	16.09	1764.8726	0.881	-0.048	-0.162	-0.018	-0.061	-0.0010
lm0427k7569	75.48319	-65.95961	1.423526	16.56	16.30	1920.6071	0.9	0.0050	-0.153	0.0010	-0.086	0.0010
lm0090l7821	78.22237	-69.25835	1.425433	17.63	17.50	1481.6316	0.9	-0.06	-0.154	-0.024	-0.068	0.0050
lm0454n5409	80.13029	-65.77294	1.426147	16.01	15.73	760.8097	0.976	-0.0060	-0.033	-0.0020	-0.01	0.0
lm0021n5140	83.50823	-69.22983	1.429287	16.17	15.98	1977.6517	0.967	-0.015	-0.03	-0.0	0.0010	-0.0
lm0467l1196	82.14063	-66.14551	1.429906	16.33	16.09	1630.5178	0.937	0.0	-0.097	-0.0010	-0.043	-0.0
lm0475m15984	84.08721	-65.64972	1.43014	17.30	17.11	2244.8131	0.969	-0.02	-0.03	-0.0030	-0.0040	0.0010
lm0225l18523	85.44312	-68.6193	1.432481	16.68	16.51	1093.8515	0.895	-0.0	-0.148	-0.0010	-0.065	0.0040
lm0050m1668	88.44083	-69.12669	1.432856	16.74	16.47	2211.7860	0.981	-0.0040	-0.024	0.0020	-0.013	-0.0030
lm0030m9744	84.46997	-69.16274	1.434738	16.31	16.38	2320.6911	0.955	-0.023	-0.067	-0.0080	-0.041	-0.0020
lm0216m6805	82.71499	-68.74527	1.436319	16.03	15.91	1253.6164	0.973	-0.0020	-0.036	-0.0	-0.024	0.0
lm0080m5139	94.59422	-69.19273	1.436427	17.89	17.66	2294.8690	0.944	-0.02	-0.115	-0.017	-0.076	-0.0020
lm036m6255	81.5183	-67.48752	1.438008	16.32	16.03	1904.7623	0.923	-0.03	-0.136	-0.013	-0.087	-0.0080
lm0030m5266	84.28567	-69.24086	1.438845	16.32	16.36	2183.7966	0.946	-0.01	-0.094	-0.0030	-0.056	-0.0010
lm0327m23717	80.53188	-67.45696	1.439496	15.98	15.69	1764.8625	0.968	0.0010	-0.024	-0.0	-0.015	0.0010
lm0111m6204	75.48886	-69.07911	1.439999	16.97	16.72	821.8173	0.955	-0.022	-0.037	-0.0010	-0.0050	0.0050
lm0048k10155	84.42319	-69.33551	1.441502	17.79	17.65	431.7545	1.006	-0.06	-0.12	-0.012	-0.025	0.0040
lm0030m19275	85.34155	-65.2635	1.443148	17.78	17.68	530.5960	0.908	0.0	-0.02	-0.0040	-0.045	-0.0010
lm0365k19917	87.05624	-67.08298	1.443952	17.68	17.58	2211.7715	0.908	-0.014	-0.132	0.0010	-0.089	0.01
lm0223l20472	85.27026	-68.27476	1.446918	17.25	17.17	1860.6640	0.953	-0.010	-0.056	-0.0020	-0.017	-0.0
lm0101l4898	76.79501	-69.2365	1.447797	17.36	17.18	1591.6497	0.948	-0.052	-0.044	-0.025	-0.0090	-0.0070
lm0105l4144	76.92017	-69.94938	1.44808	16.14	15.99	1468.6220	0.948	-0.03	-0.069	-0.0070	-0.024	0.0030
lm0424n17758	74.85874	-65.82873	1.448589	16.52	16.28	1623.5479	0.973	-0.0090	-0.039	-0.0050	-0.028	-0.0020
lm0364k11532	86.37889	-67.03275	1.448958	16.88	16.80	2240.6680	0.96	-0.025	-0.056	-0.0050	-0.016	0.0
lm0023m4635*	83.6221	-69.4251	1.450334	17.16	16.92	1506.7163	0.924	-0.047	-0.11	-0.014	-0.046	-0.0020
lm0030k13920	84.05815	-69.15323	1.450827	16.22	16.17	2305.7311	0.943	-0.015	-0.069	-0.0070	-0.016	0.0040
lm0040k25978	85.98418	-69.22539	1.451215	16.41	16.32	2202.8033	0.934	-0.013	-0.099	-0.0070	-0.06	0.0040
lm0165m18311	74.45511	-68.4546	1.452122	16.60	16.39	835.6115	0.898	-0.027	-0.141	-0.0090	-0.044	0.0
lm0280l8851	72.27003	-66.45684	1.45283	17.61	17.45	2304.6395	0.944	0.0030	-0.083	0.0	-0.041	0.0030
lm0440l7192	77.91995	-65.11383	1.453087	17.63	17.57	1133.6887	0.98	-0.017	-0.017	0.0010	-0.0	0.0080
lm0151n14381	72.5678	-67.88503	1.453122	17.49	17.34	2226.7864	0.937	-0.01	-0.079	-0.0050	-0.021	-0.0040
lm0010m3763	80.26873	-69.07534	1.453338	16.23	15.50	555.5407	0.859	-0.031	-0.122	-0.01	-0.027	-0.0030
lm0337k19646	81.9815	-67.43854	1.453921	17.55	17.39	705.7539	0.972	-0.02	-0.052	-0.011	-0.037	-0.0020
lm0095m18525	79.43239	-69.85274	1.454941	17.27	17.39	589.4691	0.976	-0.024	-0.036	-0.0070	-0.013	-0.0020
lm0180n14087	77.27753	-67.98465	1.455871	16.36	16.18	2243.6109	0.911	-0.034	-0.119	-0.012	-0.041	0.0
lm0090k11333	77.98484	-69.12846	1.456551	17.52	17.61	870.6308	0.955	0.0060	-0.084	-0.0010	-0.061	-0.0030
lm0156m14534	71.88183	-68.94286	1.4571	17.82	17.67	2237.5526	0.978	-0.011	-0.047	-0.0060	-0.023	-0.0060
lm0335m23184	82.24436	-67.09144	1.457715	16.60	16.34	443.6144	0.982	-0.026	-0.031	-0.0090	-0.018	0.0

lm0605n23731	87.57283	-71.44329	1.458149	17.02	17.21	1580.6986	0.976	-0.04	-0.025	-0.022	-0.0080	0.0060
lm0315n19202	78.6093	-67.21954	1.460027	15.84	15.56	800.6893	0.978	-0.014	-0.026	0.0	-0.0	0.0
lm0021114650	83.19818	-69.28828	1.462272	15.73	15.47	1475.7387	0.978	-0.01	-0.03	-0.0010	-0.0050	-0.0010
lm0344m20086	83.02973	-67.08729	1.462707	17.24	17.08	1576.6962	0.944	0.0020	-0.076	-0.0040	-0.051	0.0040
lm0034k9201	84.1425	-69.81442	1.463902	16.55	16.40	1381.9065	0.968	-0.021	-0.037	-0.0010	-0.0050	0.0020
lm0035k26831	81.7029	-67.11759	1.464774	17.45	17.34	388.7234	0.964	-0.013	-0.057	-0.0060	-0.033	-0.0010
lm0121m27778	73.53912	-69.21625	1.465146	17.26	17.04	488.6762	0.963	-0.028	-0.062	-0.017	-0.045	-0.0020
lm0164k26049	72.9875	-68.51413	1.467167	17.00	16.79	1750.8564	0.948	-0.014	-0.079	-0.0050	-0.061	0.0030
lm0165n17378	74.57454	-68.60381	1.46948	17.21	17.16	795.6563	0.962	-0.033	-0.049	-0.0060	-0.017	-0.0
lm0033k9023	85.02569	-69.45353	1.469976	16.33	16.22	2174.8031	0.984	-0.013	-0.024	-0.0010	0.0010	-0.0020
lm0455k3349	80.45913	-65.57179	1.470166	17.16	17.13	1529.6556	0.922	-0.027	-0.081	-0.0080	-0.0090	0.0050
lm0092n16033	78.64	-69.65524	1.47342	15.82	15.61	811.8528	0.962	0.0010	-0.045	-0.0010	-0.02	-0.0010
lm0290k16764	74.06053	-66.36717	1.475127	16.34	16.17	2297.6552	0.981	0.0030	-0.035	0.0020	-0.023	0.0020
lm0121n27034	73.74454	-69.35929	1.475848	16.96	16.70	797.6586	0.974	0.0030	-0.035	0.0010	-0.022	-0.0010
lm0214k25540	82.55892	-68.5152	1.476843	17.60	17.54	2240.6240	0.965	-0.011	-0.044	-0.0040	-0.026	-0.0040
lm0364m9855	86.49504	-67.17615	1.477007	17.69	17.53	2223.6470	0.947	-0.0060	-0.078	0.0010	-0.054	-0.0020
lm0294k13944	73.96427	-67.04175	1.478161	17.00	16.88	1402.8898	0.93	-0.0070	-0.119	-0.0040	-0.077	-0.0
lm0020m14812	82.52879	-69.14608	1.478725	16.14	15.91	1917.8257	0.937	-0.025	-0.075	-0.0060	-0.02	0.0050
lm0173m22752	76.36809	-68.12565	1.479232	16.81	16.55	1888.6122	0.937	-0.011	-0.099	-0.0090	-0.063	0.0020
lm0173i29233	75.89828	-68.3149	1.480115	16.88	16.77	2496.8050	0.982	-0.0060	-0.022	-0.0080	-0.046	-0.0010
lm0300k22331	75.8959	-66.40038	1.48138	17.93	17.69	1987.5560	0.945	-0.023	-0.065	-0.015	-0.046	0.0050
lm0041k25162	86.98972	-69.204	1.481594	17.64	17.60	1965.6435	0.914	0.0020	-0.125	0.0040	-0.06	-0.0
lm0347i5780	83.52995	-67.49362	1.481679	16.06	15.85	1495.7041	0.966	-0.0070	-0.053	-0.0040	-0.036	-0.0010
lm0346k12896	82.93704	-67.39484	1.481784	16.90	16.95	558.5593	0.975	-0.01	-0.049	-0.01	-0.031	0.0050
lm0333m10861	82.0787	-66.6627	1.482148	16.03	15.78	388.7234	0.989	-0.02	-0.080	-0.0080	-0.0050	0.0050
lm0556m6525*	75.68396	-71.53566	1.4934938	16.10	15.94	864.5988	0.961	-0.076	-0.052	-0.035	-0.02	-0.0040
lm0030m12500*	84.29712	-69.39052	1.499784	15.82	15.66	1197.6811	0.995	-0.011	-0.01	-0.0090	-0.0050	-0.0
lm0346m23398	83.07818	-67.46183	1.519681	16.45	16.26	467.6031	0.941	-0.024	-0.072	-0.0060	-0.022	-0.0030
lm0056k8196	88.08715	-70.15366	1.523926	16.95	16.76	420.7308	0.949	-0.0080	-0.065	0.0010	-0.028	0.0040
lm0350i5717	84.30406	-66.44258	1.524372	16.18	15.99	1835.8272	0.954	-0.021	-0.068	-0.0020	-0.039	-0.0030
lm0125i9302	73.27849	-69.95682	1.526312	16.98	17.00	1311.4914	0.999	-0.023	-0.01	-0.0030	-0.0070	-0.0020
lm0103m23150	77.28643	-69.52645	1.527199	17.23	17.07	1482.6498	0.985	-0.025	-0.027	0.0030	-0.0060	0.0020
lm0184i11316	76.83495	-68.57777	1.529922	17.48	17.27	327.8375	0.993	-0.02	-0.032	-0.0090	-0.016	-0.0020
lm0551k17670	76.15162	-70.58525	1.532272	17.22	16.99	1236.5848	0.979	-0.018	-0.033	-0.0020	-0.0	-0.0020
lm0123m9848	73.42535	-69.45393	1.534145	17.27	17.16	2516.7341	0.985	-0.050	-0.022	-0.0030	-0.011	0.0030
lm0040i13585	86.0081	-69.29276	1.534167	17.25	17.40	1207.7430	0.969	-0.021	-0.031	0.0010	-0.0	0.0020
lm0020k13620	81.88991	-69.15231	1.534702	16.55	16.36	762.6655	0.915	-0.0060	-0.128	-0.01	-0.072	0.0020
lm0196k26764	78.83527	-68.88038	1.538051	16.68	16.38	1901.8365	0.888	-0.03	-0.161	-0.013	-0.085	-0.0030
lm0290i17409	74.07302	-66.52894	1.539003	16.34	16.21	2236.7852	0.98	-0.0020	-0.033	-0.0010	-0.021	-0.0040
lm0090m4818	78.4994	-69.08215	1.541924	16.49	16.18	1310.5084	0.962	-0.027	-0.043	-0.0010	-0.0050	0.0020
lm0016m17269	80.51855	-70.20887	1.542338	17.37	17.24	1957.6685	0.915	-0.057	-0.125	-0.012	-0.051	-0.0020



APPENDIX A. PROPERTIES OF THE “HOT” ECLIPSING BINARIES IN THE LMC

Im0422121894	74.63795	-65.51208	1.545397	15.61	15.38	1794.7992	0.947	-0.021	-0.047	-0.0	-0.0040	0.0010
Im0573n13173	80.74914	-71.02406	1.545989	17.48	17.44	1854.8646	0.926	-0.031	-0.082	-0.015	-0.01	-0.0030
Im034018577	82.71093	-66.46405	1.546361	16.64	16.39	1977.6605	0.952	-0.011	-0.068	-0.0040	-0.031	0.0
Im0427m21459	75.79042	-66.06479	1.546547	16.97	16.65	2257.5932	0.945	-0.0020	-0.077	-0.0020	-0.038	0.0010
Im0026k10665	81.82562	-70.17208	1.548267	16.98	16.98	2025.5258	0.947	-0.04	-0.074	-0.016	-0.036	-0.0020
Im0214k24604	82.55082	-68.509	1.548706	15.87	15.81	1933.7564	0.975	-0.0080	-0.034	-0.0040	-0.024	-0.0010
Im0281n7749	73.40284	-66.44262	1.549061	17.20	16.95	1844.6662	0.956	0.0030	-0.05	0.0040	-0.034	0.0020
Im0340n7354	83.22525	-66.45093	1.553586	16.48	16.17	800.6454	0.984	-0.0070	-0.034	-0.0050	-0.024	0.0010
Im0375l16164	88.90677	-67.14641	1.553943	16.67	16.55	801.7426	0.978	-0.0080	-0.029	-0.0020	-0.0080	-0.0
Im0090n11730	78.43501	-69.27997	1.554973	17.00	16.92	1152.8088	0.905	-0.0	-0.137	-0.0050	-0.0040	0.0040
Im0114l16671	74.03483	-69.94284	1.555878	16.54	16.46	1804.7621	0.962	-0.0020	-0.052	-0.0050	-0.02	-0.0030
Im0586l23592	81.65496	-71.80958	1.55705	17.54	17.28	2242.6071	0.939	-0.021	-0.085	-0.0050	-0.038	-0.0050
Im0040l19766	86.20322	-69.33944	1.557666	17.25	17.20	1196.7048	0.946	-0.015	-0.034	-0.0020	0.0020	0.0030
Im0285n5241	73.70857	-67.13632	1.557745	15.93	15.64	1902.7300	0.937	-0.0010	-0.076	0.0	-0.023	0.0010
Im0341m14670	83.81784	-66.34805	1.558747	15.92	15.66	1819.6920	0.985	-0.011	-0.022	-0.0050	-0.011	-0.0
Im0285m12790	73.53067	-67.03147	1.55907	16.69	16.47	815.8174	0.949	-0.013	-0.039	0.0020	-0.0040	0.0080
Im0285l26585	73.15896	-67.28642	1.559802	17.32	17.10	1145.6945	0.982	-0.012	-0.028	-0.0040	-0.021	-0.0010
Im0315m10164	78.76589	-67.00723	1.560277	16.94	16.68	1145.6945	0.975	-0.0010	-0.034	0.0010	-0.02	0.0
Im0110n25668	74.28218	-69.35849	1.564822	16.31	16.13	2031.4803	0.963	-0.02	-0.051	-0.0090	-0.028	-0.0
Im0184l9660	76.88569	-68.56789	1.568984	16.21	16.05	1591.6576	0.955	0.0010	-0.066	-0.0010	-0.031	-0.0020
Im0167l5740	73.9332	-68.89664	1.572604	17.56	17.36	2183.6625	0.907	-0.0	-0.129	-0.0020	-0.076	-0.0050
Im0214l25109	82.37873	-68.6702	1.575578	17.44	17.59	1492.6950	0.995	-0.0040	-0.029	-0.0080	-0.017	0.0010
Im0032l22874	83.87382	-69.70626	1.576927	15.61	15.43	1108.8457	0.867	-0.03	-0.147	-0.013	-0.057	0.0020
Im0337k23492	81.83501	-67.46624	1.578628	17.35	17.18	1459.7822	0.963	-0.012	-0.07	-0.015	-0.041	0.0040
Im0207k15472	81.65377	-68.8002	1.579423	15.73	15.67	1317.5052	0.938	-0.024	-0.077	-0.011	-0.045	-0.0020
Im0166l16390	73.29455	-68.96988	1.579747	16.09	15.81	2245.7783	0.97	-0.019	-0.048	-0.01	-0.033	0.0030
Im0023m7584	83.58765	-69.44209	1.579887	16.13	15.90	2235.6280	0.864	-0.044	-0.185	-0.024	-0.086	0.0020
Im0115ms231	75.35313	-69.77872	1.580373	17.73	17.66	1862.5755	0.949	-0.0020	-0.097	-0.0040	-0.064	0.0010
Im0341n6753	84.07502	-66.49064	1.580968	16.67	16.42	2014.5633	0.965	-0.011	-0.044	-0.0030	-0.023	0.0010
Im0593m12530	85.29938	-70.86681	1.581396	17.34	17.22	2199.6400	0.934	-0.055	-0.09	-0.027	-0.037	0.0090
Im0192n30512	79.22526	-68.33805	1.583547	16.95	16.84	2232.6252	0.946	-0.04	-0.125	-0.052	-0.079	0.01
Im0434m21038	76.54471	-65.69327	1.585547	16.29	16.06	1415.8778	0.988	-0.014	-0.029	-0.0040	-0.015	-0.0020
Im0503l15319	88.80091	-65.5445	1.586779	17.27	17.19	1931.7332	0.964	-0.07	-0.061	-0.044	-0.033	-0.0010
Im0172l15709	75.0954	-68.33731	1.588034	17.55	17.46	2099.8753	0.95	0.0070	-0.096	-0.0050	-0.062	-0.0010
Im0540k9199	73.10941	-70.50689	1.588396	16.40	16.15	1813.7314	0.953	-0.016	-0.046	-0.0020	-0.0030	0.0030
Im0335n5747	82.24693	-67.13654	1.588518	17.22	17.04	1149.7113	0.947	0.0080	-0.087	-0.0060	-0.053	0.0010
Im0123m22700	73.5523	-69.52692	1.588994	16.49	16.31	556.5427	0.878	-0.048	-0.168	-0.019	-0.077	0.0040
Im0121m25422	73.30901	-69.38155	1.590681	17.37	17.23	1815.6981	0.902	-0.108	-0.16	-0.046	-0.092	-0.0030
Im0370m12338	88.53671	-67.38796	1.591615	16.88	16.70	503.6912	0.95	-0.015	-0.053	-0.0040	-0.0040	0.0
Im0100k13660	75.90439	-69.14193	1.591895	16.78	16.67	1305.5094	0.944	-0.0080	-0.093	-0.0030	-0.045	-0.0030
Im0387l7856	90.74458	-67.51762	1.592243	16.65	16.44	1919.7987	0.935	-0.135	-0.097	-0.068	-0.043	0.0020

lm0330m10876	81.26355	-66.47367	1.593612	16.74	16.83	1150.6932	0.974	-0.015	-0.037	-0.0060	-0.013	-0.0
lm0120i24125	72.06416	-69.37028	1.59448	17.42	17.41	1115.6637	0.908	0.020	-0.153	-0.0	-0.088	-0.0010
lm0210i20271	82.43808	-67.93822	1.594599	16.62	16.42	2028.5189	0.887	-0.046	-0.156	-0.02	-0.066	-0.0040
lm0453k8106	80.37816	-65.24698	1.595613	17.48	17.34	1840.7251	0.99	-0.031	-0.02	-0.016	-0.0070	-0.0040
lm0550m7880	75.80149	-70.65441	1.596858	17.14	16.86	2258.5811	0.979	-0.021	-0.029	-0.011	-0.017	0.0020
lm0435i5752	77.27269	-65.73683	1.597033	17.74	17.59	2224.5803	0.955	-0.072	-0.102	-0.036	-0.057	-0.0030
lm0344m8291	83.09827	-67.01023	1.597243	16.54	16.36	825.8571	0.883	-0.04	-0.159	-0.019	-0.071	0.0
lm0292n11621	74.27999	-66.82953	1.599642	16.80	16.59	1860.5672	0.973	0.030	-0.042	-0.020	-0.028	-0.0060
lm0126k13758	72.26426	-70.20293	1.601905	17.03	16.85	1918.6018	0.981	-0.022	-0.038	-0.01	-0.019	-0.0040
lm0154k21118	71.39661	-68.4872	1.60291	17.39	17.25	1750.8511	0.964	-0.013	-0.052	-0.0060	-0.034	0.0030
lm0175n23496	76.59228	-68.6319	1.604598	17.43	17.32	1878.6166	0.907	-0.072	-0.125	-0.031	-0.069	-0.0010
lm0111m16092	75.53049	-69.13855	1.604599	16.33	16.05	1890.6056	0.94	-0.024	-0.067	-0.0050	-0.019	-0.0030
lm0031m7414	85.61249	-69.08713	1.605989	15.61	15.46	1591.7013	0.94	-0.018	-0.1	-0.012	-0.044	0.0010
lm0175k18167	76.06658	-68.45256	1.606206	16.47	16.33	1402.8984	0.938	-0.023	-0.076	-0.0050	-0.016	0.0
lm0044i23659	85.83336	-70.0552	1.607072	16.39	16.20	1481.7363	0.876	-0.075	-0.169	-0.026	-0.082	0.0010
lm0197k23467	79.84263	-68.84883	1.608347	16.32	16.07	1918.7104	0.975	-0.011	-0.028	-0.0070	-0.011	0.0020
lm0325n23385	80.4343	-67.24883	1.60901	17.10	16.88	2058.4899	0.953	-0.0	-0.057	-0.0020	-0.025	0.0010
lm0052m18926	88.6084	-69.55504	1.611031	16.05	15.77	1566.7203	0.964	-0.025	-0.056	-0.0070	-0.026	0.0010
lm0161m24107	74.51188	-67.94182	1.611475	17.76	17.56	1564.5855	0.978	-0.03	-0.025	0.0020	-0.0030	0.0070
lm0367n6835	87.45523	-68.40499	1.61154	17.73	17.52	2033.5447	0.971	-0.030	-0.068	-0.0010	-0.061	-0.0040
lm0215m22585	83.79433	-68.48498	1.613457	17.45	17.22	2155.8047	0.969	-0.02	-0.059	-0.013	-0.046	-0.0010
lm0603i24970	86.8177	-71.09986	1.614227	17.27	17.24	1087.8655	0.887	-0.079	-0.195	-0.042	-0.102	0.0030
lm0030k13205	83.98549	-69.14764	1.615205	16.09	16.11	1808.8535	0.906	-0.03	-0.113	-0.011	-0.037	0.0030
lm0550m20196	75.55269	-70.58644	1.616823	17.31	17.09	1126.6152	0.979	-0.018	-0.05	-0.0080	-0.035	-0.0
lm0294k3195	74.15299	-66.97358	1.620032	17.18	17.08	1173.6244	0.981	-0.016	-0.033	-0.0070	-0.02	-0.0020
lm0156m4262	71.91081	-68.8573	1.620264	15.97	15.78	2257.5616	0.933	-0.019	-0.078	-0.0040	-0.021	-0.0
lm0425n15511	75.65717	-65.80273	1.623384	17.71	17.51	1603.5934	0.972	-0.016	-0.05	0.0080	-0.041	-0.0070
lm0426i15702	74.42631	-66.16279	1.624957	15.72	15.46	508.6286	0.897	-0.03	-0.11	-0.01	-0.031	0.0070
lm0210i18828	82.52517	-67.92671	1.625897	17.63	17.54	2302.7223	0.91	-0.047	-0.074	-0.016	-0.025	0.0080
lm0710k10285	82.93166	-71.92374	1.627842	17.71	17.66	1593.6823	0.969	-0.050	-0.045	0.0010	-0.03	0.0010
lm0090n29958	78.5351	-69.38331	1.628407	17.44	17.35	2164.7591	0.938	-0.0090	-0.097	-0.0070	-0.057	-0.0020
lm0344k10601	82.55039	-67.02696	1.628604	16.66	16.51	1441.7890	0.912	-0.034	-0.107	-0.015	-0.039	0.0020
lm0711m4218	84.53837	-71.86447	1.630559	17.34	17.24	488.7207	0.891	-0.035	-0.094	-0.0070	-0.012	0.026
lm0236i25640	86.2682	-69.0344	1.631312	17.32	17.10	941.5417	0.842	-0.05	-0.202	-0.0050	-0.084	0.015
lm0584i6042	81.67559	-71.34087	1.632344	17.07	15.58	1957.6888	0.939	-0.039	-0.078	-0.01	-0.03	-0.0010
lm0151m4128	72.46664	-67.70253	1.633059	15.95	15.58	1465.6564	0.906	0.0040	-0.155	0.0030	-0.093	0.0030
lm0424n10133	74.97782	-65.77246	1.63539	16.30	16.08	706.7728	0.985	-0.016	-0.029	-0.0060	-0.016	0.0
lm0093n24281	79.27628	-69.68239	1.635799	17.49	17.35	556.5191	0.925	-0.0070	-0.141	-0.0	-0.078	-0.0020
lm0204m18679	81.1552	-68.45898	1.636472	17.44	17.36	1455.7692	0.963	-0.019	-0.04	-0.0080	-0.027	0.0010
lm0201n26407	82.14915	-67.95391	1.63867	17.71	17.47	1093.8296	0.941	-0.015	-0.05	-0.0090	-0.021	0.0010
lm0333k9915	81.69675	-66.65927	1.639068	16.58	16.40	2245.6773	0.955	-0.0090	-0.059	-0.0050	-0.025	-0.0020

APPENDIX A. PROPERTIES OF THE “HOT” ECLIPSING BINARIES IN THE LMC

lm0090m4321	78.60131	-69.07897	1.641272	17.19	17.04	1231.6101	0.906	-0.057	-0.118	-0.025	-0.052	0.0040
lm0032m22261	84.35161	-69.57203	1.644146	15.70	15.48	2345.5978	0.974	-0.070	-0.038	-0.0090	-0.03	-0.0030
lm0551i21081	75.92228	-70.73455	1.645211	15.68	15.48	1903.7453	0.963	-0.016	-0.037	0.0	-0.0010	-0.0010
lm0354m13875	84.96551	-67.04351	1.645882	17.36	17.22	819.8363	0.983	-0.012	-0.023	0.0030	-0.0020	-0.0050
lm0314k24373	77.64572	-67.11118	1.649179	16.35	16.30	2186.7216	0.879	-0.057	-0.166	-0.028	-0.075	0.0020
lm00524698	88.10094	-69.58579	1.650979	17.20	17.05	1549.7634	0.936	-0.01	-0.099	-0.0090	-0.058	0.0040
lm0551i15365	76.0721	-70.6985	1.652083	16.25	15.98	1266.5146	0.988	-0.0080	-0.028	-0.0050	-0.021	-0.0010
lm0101i22900	76.92021	-69.34193	1.653449	16.26	16.14	1139.8452	0.891	-0.026	-0.122	-0.01	-0.032	0.0030
lm0310m15759	77.9497	-66.42246	1.653658	17.30	17.10	1257.5597	0.982	-0.024	-0.019	-0.0010	0.0010	-0.0040
lm0315n14721	78.62626	-67.19175	1.654997	16.87	16.57	1786.7429	0.977	-0.020	-0.037	0.0010	-0.02	0.0030
lm0317k4869	78.57766	-67.33758	1.65617	17.71	17.50	776.7495	0.984	-0.060	-0.059	-0.0090	-0.054	0.0060
lm0304n25535	76.06779	-67.2643	1.657245	15.76	15.46	2248.7779	0.999	-0.0020	-0.017	-0.0060	-0.011	0.0010
lm0033k15395	85.06121	-69.49326	1.65801	15.92	15.85	2257.6709	0.908	-0.04	-0.116	-0.013	-0.044	0.0020
lm00304662	84.09164	-69.23679	1.660651	16.99	17.17	1468.6786	0.928	0.0040	-0.12	-0.0010	-0.078	0.0040
lm0325k9805	82.64183	-67.27292	1.662852	16.30	16.12	1447.8349	0.933	-0.022	-0.077	-0.0020	-0.011	-0.0
lm0207n18537	80.31871	-67.0104	1.664351	16.19	15.95	1166.6467	0.949	-0.0070	-0.073	-0.0010	-0.039	0.0030
lm0583i22712	82.02376	-68.98467	1.664777	15.60	15.36	2318.6740	0.959	-0.018	-0.051	0.0	-0.0090	0.0040
lm0351m12773	85.82224	-71.08236	1.665565	15.60	15.44	1253.6088	0.948	-0.015	-0.087	-0.0080	-0.048	-0.0010
lm0364m5107	86.61851	-66.32968	1.666009	16.42	16.15	1865.6943	0.976	-0.054	-0.049	-0.019	-0.041	-0.0010
lm0377n7000	89.18435	-66.98545	1.666231	17.45	17.28	1439.8010	0.929	-0.010	-0.132	0.0010	-0.082	0.0020
lm0212n20573	83.02989	-67.51179	1.667075	17.21	16.93	1625.6667	0.952	-0.012	-0.066	-0.0090	-0.026	0.0020
lm0347i17494	83.75017	-68.28504	1.668092	16.91	16.94	1953.7398	0.929	-0.011	-0.115	-0.0080	-0.085	0.0
lm0216i8793	82.57622	-67.59003	1.668901	16.46	16.31	1093.8434	0.983	-0.012	-0.026	-0.0060	-0.01	0.0010
lm0174k23286	73.55984	-70.29475	1.669043	15.86	15.68	1997.5803	0.928	-0.031	-0.103	-0.0020	-0.034	-0.0060
lm0174k23286	74.93274	-68.49368	1.669262	16.32	16.07	1958.5996	0.887	-0.05	-0.161	-0.022	-0.062	0.0010
lm0155k17320	72.16521	-68.45851	1.669782	17.56	17.47	2206.7780	0.949	-0.034	-0.065	-0.014	-0.019	0.0050
lm0460i23118	81.2029	-65.17684	1.670786	17.40	17.37	1980.5256	0.968	-0.083	-0.06	-0.028	-0.05	-0.0020
lm0473i15309	83.70999	-65.44981	1.670908	17.67	17.59	1424.8901	0.924	-0.015	-0.13	-0.0050	-0.068	-0.0040
lm0184k22807	76.85244	-68.49225	1.671121	17.39	17.32	1885.7063	0.962	-0.07	-0.059	-0.047	-0.035	0.0020
lm0030m3468	84.42029	-69.07812	1.672505	16.85	16.66	1583.6601	0.964	-0.027	-0.082	-0.015	-0.062	0.0010
lm0127m8589	73.76225	-70.15474	1.674098	16.18	16.11	2264.7604	0.927	-0.01	-0.118	-0.0090	-0.08	0.0040
lm0035m23233	85.69645	-69.88486	1.676613	17.14	16.98	2297.6318	0.959	-0.022	-0.032	0.0	0.0020	0.0050
lm0156m1619	71.73244	-68.76539	1.677625	15.58	15.34	797.5962	0.951	-0.014	-0.042	0.0	0.0	0.0
lm0113k25259	74.86216	-69.53946	1.681305	17.15	17.03	1864.5613	0.993	0.0020	-0.02	-0.0	-0.015	-0.0020
lm0356i7100	84.6971	-67.50193	1.681418	17.45	17.39	858.7184	0.977	-0.019	-0.032	-0.010	0.0010	0.0030
lm0344i13598	82.62982	-67.20105	1.682072	16.96	16.81	2185.7040	0.923	-0.029	-0.08	-0.012	-0.026	0.0
lm0376m11230	88.29172	-67.53606	1.683395	16.39	16.15	450.8185	0.919	0.0010	-0.129	-0.0020	-0.089	-0.0010
lm0106i16000	76.19455	-70.3658	1.686368	17.59	17.41	1664.5486	0.965	-0.0060	-0.115	-0.017	-0.076	0.0090
lm0377i92	89.09938	-67.60036	1.686602	17.45	17.29	1779.7788	0.936	0.0040	-0.088	-0.0050	-0.052	-0.0010
lm0055i7331	88.76966	-69.94608	1.687677	17.60	17.37	761.7583	0.956	-0.045	-0.074	-0.022	-0.041	-0.0040
			1.688479	17.40	17.39	1911.8249	0.977	-0.0040	-0.02	-0.0020	-0.019	-0.0030

lm0424m17990	74.79369	-65.8914	1.690344	17.02	16.79	2198.6336	0.96	-0.018	-0.078	-0.01	-0.059	0.0030
lm0340m5950	83.04071	-66.44099	1.692577	15.68	15.47	1607.6250	0.916	-0.0010	-0.143	0.0	-0.089	0.0040
lm0021m15207	83.3337	-69.13687	1.695205	17.50	17.39	1145.7030	0.874	-0.075	-0.177	-0.041	-0.099	0.014
lm0186m18764	77.37196	-68.82633	1.697031	15.73	15.55	2257.6156	0.965	0.0030	-0.05	0.0030	-0.032	-0.0020
lm0344k4409	82.52554	-66.98509	1.697053	16.28	16.09	1616.5871	0.95	0.0010	-0.089	-0.0	-0.053	-0.0010
lm0121115224	72.80434	-69.29254	1.699708	16.64	16.51	1090.6622	0.974	-0.023	-0.036	0.0010	-0.013	0.0010
lm0221n12398	85.79938	-67.87471	1.700592	17.39	17.20	1889.6969	0.908	-0.0030	-0.123	0.0010	-0.059	0.0020
lm0160m24045	73.42043	-67.80215	1.702329	16.25	16.01	1898.7369	0.88	-0.028	-0.134	-0.011	-0.023	0.0010
lm0215k25234	83.54176	-68.50065	1.702711	16.67	16.57	1375.8974	0.956	-0.031	-0.061	-0.0050	-0.021	-0.0030
lm0214m4693	82.90646	-68.53389	1.702754	17.44	17.52	2178.7367	0.975	0.0010	-0.066	-0.0020	-0.049	-0.0090
lm0604k19867	85.55982	-71.28186	1.702836	16.50	16.50	445.7279	0.962	-0.012	-0.069	-0.011	-0.048	-0.0030
lm0315k19071	78.23229	-67.06729	1.702953	17.17	17.06	401.7588	0.988	-0.01	-0.019	-0.0030	-0.01	0.0020
lm0085k5094	94.95248	-69.7825	1.705211	16.48	16.33	2223.6899	0.98	-0.016	-0.02	0.0010	0.0	0.0010
lm0167n6064	74.66638	-68.894	1.70812	16.65	16.44	1888.5883	0.986	-0.011	-0.033	-0.0060	-0.023	-0.0020
lm0160k15778	73.30671	-67.75401	1.709211	16.65	16.37	1811.7418	0.888	-0.039	-0.155	-0.019	-0.053	0.0010
lm0155k22815	72.37866	-68.49162	1.710128	16.93	17.00	1907.7234	0.972	-0.061	-0.042	-0.015	-0.027	0.0030
lm0131112846	71.28977	-69.39025	1.710566	16.23	16.09	870.5622	0.966	-0.024	-0.051	-0.0080	-0.021	0.0040
lm0587k27742	82.46904	-71.67718	1.711556	16.43	16.19	1208.7473	0.975	-0.015	-0.025	0.0	-0.0020	0.0
lm0111m7486	75.329	-69.08815	1.713146	17.40	17.16	2171.7004	0.932	0.0	-0.11	-0.0020	-0.063	0.0030
lm0207m26339	81.84312	-68.86879	1.715015	16.11	15.89	1803.8386	0.847	-0.051	-0.167	-0.027	-0.079	0.0040
lm0447n7830	79.20754	-66.10822	1.715561	17.47	17.27	2225.6609	0.892	-0.063	-0.134	-0.024	-0.06	0.0040
lm0326k23448	79.16561	-67.45773	1.716036	16.92	16.81	2028.5100	0.942	-0.014	-0.098	-0.0080	-0.054	0.0030
lm0292n16483	74.36928	-66.86049	1.71682	15.67	15.42	2471.8868	0.972	-0.011	-0.03	-0.0020	0.0010	-0.0020
lm0050n20280	88.64721	-69.38678	1.71811	17.57	17.45	871.6393	0.962	0.0010	-0.059	0.0010	-0.036	0.0010
lm0344n5050	83.00607	-67.14045	1.71895	16.62	16.45	1364.9387	0.981	-0.02	-0.022	-0.0060	-0.011	0.0050
lm0347k17722	83.53896	-67.42469	1.724282	16.89	16.78	1768.8560	0.957	0.0070	-0.072	-0.0010	-0.054	0.0020
lm0320n19241	79.72365	-66.52775	1.724774	17.04	16.91	1258.5611	0.993	-0.036	-0.080	-0.0090	-0.0070	-0.0020
lm0117k26536	75.07509	-70.28025	1.725788	16.89	16.63	797.5999	0.972	-0.015	-0.047	-0.0070	-0.027	-0.0030
lm0366m3543	86.48229	-67.32311	1.727942	17.08	16.97	1828.8028	0.895	-0.056	-0.137	-0.022	-0.054	0.0030
lm0285117543	73.29965	-67.21674	1.728627	16.25	15.98	1838.6761	0.977	-0.013	-0.036	-0.0030	-0.0090	-0.0010
lm0126120410	72.08139	-70.39526	1.729185	16.94	16.90	1860.5466	0.939	-0.05	-0.111	-0.026	-0.064	-0.0020
lm0333k27925	81.90691	-66.76681	1.731749	17.55	17.49	1883.6645	0.893	-0.066	-0.144	-0.03	-0.07	-0.0040
lm0110k23246	74.04754	-69.19853	1.732018	15.94	15.74	1755.8812	0.899	-0.032	-0.127	-0.013	-0.043	-0.0010
lm0354n9564	84.74262	-67.17105	1.735055	16.94	16.80	1305.5632	0.982	-0.016	-0.02	0.0	0.0	-0.0
lm0125k22446	72.99053	-69.88508	1.735186	16.64	16.56	1600.5591	0.906	-0.038	-0.126	-0.017	-0.055	0.0040
lm0114m15151	74.59423	-69.83697	1.741331	17.20	17.09	1605.5445	0.945	-0.012	-0.1	-0.0090	-0.081	-0.0020
lm0623m17431	91.49637	-70.91431	1.74138	17.59	17.43	2307.7738	0.976	-0.052	-0.052	-0.01	-0.029	-0.0010
lm0345k3891	83.71194	-66.97972	1.742486	15.98	15.79	507.5786	0.881	-0.057	-0.17	-0.027	-0.08	0.0030
lm0317k17162	78.18883	-67.42939	1.744914	16.35	16.18	1529.6295	0.953	-0.0070	-0.073	-0.0040	-0.043	-0.0020
lm0700k13942	80.50345	-71.94293	1.746361	17.33	17.12	190.7323	0.979	-0.028	-0.029	-0.0010	-0.0010	0.0060
lm0710k7222	82.61599	-71.90232	1.746476	17.28	17.07	1889.8399	0.966	-0.024	-0.034	-0.0010	-0.0020	0.0030

APPENDIX A. PROPERTIES OF THE “HOT” ECLIPSING BINARIES IN THE LMC

lm012716731	73.2126	-70.29473	1.748158	15.49	15.21	1992.5178	0.896	-0.041	-0.133	-0.015	-0.045	-0.0020
lm0127m9330	73.63977	-70.16074	1.751161	15.87	15.67	2555.6741	0.987	-0.011	-0.014	0.0010	-0.0010	0.0030
lm0181m21196	78.02705	-67.77272	1.751491	16.77	16.74	1271.5380	0.99	-0.043	-0.012	-0.0090	-0.011	0.0010
lm0205n15591	81.83723	-68.58954	1.753697	16.30	16.00	377.8122	0.98	-0.012	-0.03	-0.0050	-0.016	0.0030
lm0356k5526	84.67436	-67.33731	1.754305	17.51	17.53	1842.8603	0.925	-0.0020	-0.098	-0.011	-0.061	0.0040
lm0564f1600	77.32867	-71.33535	1.754488	16.79	16.54	1844.7313	0.971	0.040	-0.065	0.0010	-0.045	-0.0010
lm0285n7322	73.69427	-67.15244	1.754575	16.47	16.16	1091.6638	0.963	0.0030	-0.041	-0.0030	-0.022	0.0030
lm0112n12775	74.60744	-69.62906	1.756539	15.83	15.66	2231.5677	0.987	-0.010	-0.026	-0.0020	-0.017	0.0
lm0436l14585	76.42263	-66.15917	1.756971	16.04	15.65	1864.6055	0.964	-0.023	-0.057	-0.012	-0.034	-0.0020
lm0184n9824	77.50189	-68.56479	1.757143	16.14	15.97	2084.9119	0.965	0.0010	-0.057	0.0020	-0.038	-0.0010
lm0020m10621	82.48696	-69.1202	1.758876	15.39	15.25	1875.6794	0.986	0.0010	-0.026	-0.0010	-0.01	0.0010
lm0223m18449	85.77103	-68.1128	1.759816	16.87	16.66	1101.8784	0.94	-0.027	-0.052	-0.0030	-0.0080	0.0
lm0090l21236	77.96417	-69.34711	1.7601	17.35	17.26	530.5569	0.964	-0.012	-0.069	-0.0080	-0.046	-0.0020
lm0030m22278	84.361	-69.3554	1.760563	16.78	16.69	2226.8657	0.956	-0.0	-0.052	-0.0010	-0.023	0.0
lm0095l30693	78.92326	-70.07762	1.761016	16.00	15.82	1579.7005	0.895	-0.0010	-0.14	0.0010	-0.066	0.0020
lm0217n24885	84.03969	-68.92426	1.762408	16.27	16.18	802.8084	0.937	0.0	-0.108	-0.0020	-0.075	0.0050
lm0343m9142	83.83843	-66.65304	1.763556	16.69	16.58	468.6578	0.917	-0.053	-0.109	-0.02	-0.05	0.0040
lm0045n24754	87.40513	-70.09581	1.76449	16.81	16.51	819.7090	0.983	-0.011	-0.028	-0.0040	-0.018	0.0040
lm0206k18004	80.53653	-68.81668	1.765559	16.82	16.71	1595.7398	0.894	-0.059	-0.156	-0.022	-0.074	-0.0050
lm0446k12751	77.94	-65.99113	1.766655	17.10	16.95	1904.7499	0.965	-0.02	-0.069	-0.01	-0.05	0.0040
lm0304n29084	75.99117	-67.28674	1.772755	15.80	15.52	1628.5280	0.981	-0.012	-0.024	-0.0060	-0.0080	0.0
lm0223n19445	85.65399	-68.342	1.773336	17.30	17.17	1122.6356	0.983	-0.021	-0.018	0.0010	0.0010	0.0010
lm0283k13755	73.1644	-66.6928	1.774409	16.51	16.34	414.7384	0.965	-0.019	-0.035	0.0	0.0	0.0010
lm0550k19577	75.29269	-70.58692	1.774651	16.04	15.74	2304.6848	0.99	-0.0030	-0.03	0.0	-0.023	-0.0010
lm0291m21869	75.07896	-66.3838	1.774816	17.40	17.17	1820.6752	0.931	-0.09	-0.112	-0.039	-0.062	0.0010
lm0101k8669	77.07802	-69.10507	1.775599	16.49	16.23	1305.5094	0.987	-0.018	-0.024	-0.0020	-0.0030	-0.0050
lm0107k18605	77.0512	-70.22121	1.776644	16.94	16.73	2259.6017	0.953	-0.012	-0.062	-0.0060	-0.029	-0.0020
lm0241m18034	89.22676	-67.77295	1.777518	17.44	17.25	1255.6486	0.972	-0.01	-0.034	-0.0050	-0.018	0.0010
lm0347m22080	83.96817	-67.45279	1.777695	15.66	15.38	428.7524	0.961	-0.011	-0.057	-0.0070	-0.029	-0.0010
lm0012116381	79.91597	-69.65842	1.77902	15.96	15.68	376.8729	0.949	-0.028	-0.08	-0.0090	-0.015	-0.0020
lm0031m22434	85.61171	-69.19466	1.779049	17.32	17.21	1181.7833	0.978	-0.014	-0.061	-0.0050	-0.035	-0.0030
lm0543k12503	74.17109	-70.86893	1.780468	17.12	16.99	1567.6014	0.972	-0.01	-0.031	-0.0030	-0.0070	-0.0020
lm0110n11015	74.56563	-69.2696	1.781704	16.04	15.82	1139.8417	0.978	-0.012	-0.016	-0.0010	0.0	0.0010
lm0217117550	83.38491	-68.98159	1.784201	16.77	16.70	2556.7273	0.973	-0.01	-0.028	-0.0050	-0.017	-0.0
lm0014m14940*	80.45421	-69.8381	1.785634	17.27	17.15	1711.9362	0.976	-0.0080	-0.044	-0.0040	-0.018	-0.0030
lm0120m6840	72.47689	-69.08672	1.785889	17.13	16.96	1777.7684	0.958	-0.026	-0.041	-0.0010	-0.0020	0.0040
lm0313k19939	78.39902	-66.71775	1.787155	17.26	17.17	1097.6547	0.879	-0.067	-0.163	-0.031	-0.082	0.0040
lm0031m11024	85.62526	-69.22031	1.788741	17.59	17.54	2230.6328	0.925	-0.0050	-0.12	-0.0030	-0.062	-0.0050
lm0167m10826	74.47513	-68.77391	1.788779	16.05	15.85	1181.6320	0.986	-0.012	-0.015	-0.0010	-0.0010	-0.0
lm0290l5213	73.95604	-66.43437	1.791025	15.47	15.28	2201.5927	0.932	-0.028	-0.089	-0.011	-0.025	-0.0
lm0285n12253*	73.37758	-67.1925	1.791998	17.11	16.93	1524.5967	0.923	-0.020	-0.13	-0.0080	-0.105	0.0020

lm0344116103	82.63064	-67.21831	1.79294	15.60	15.36	1576.6962	0.983	-0.0090	-0.049	-0.0050	-0.03	0.0010
lm0122m19436	72.56834	-69.55117	1.796151	16.25	16.15	1825.6591	0.945	-0.0010	-0.069	-0.0050	-0.021	-0.0
lm0121k17851	73.25922	-69.09305	1.797637	16.56	16.29	2265.5959	0.961	-0.01	-0.088	-0.0030	-0.052	0.0020
lm0284m22583	72.81971	-67.26464	1.798432	16.90	16.71	1579.6087	0.958	-0.02	-0.044	-0.0	-0.0060	0.0010
lm0053k11941	89.14892	-69.47271	1.799736	17.55	17.53	800.7358	0.913	-0.072	-0.124	-0.033	-0.062	0.0040
lm0300k5450	75.84331	-66.28245	1.801747	16.08	15.75	419.5964	0.969	-0.014	-0.025	0.0010	-0.0	0.0050
lm0164m28010	73.58927	-68.5165	1.801762	17.38	17.23	733.7068	0.978	-0.01	-0.024	0.0020	-0.018	0.0
lm0467k11376	82.08206	-65.98337	1.802175	15.57	15.34	2215.8423	0.925	-0.036	-0.109	-0.013	-0.043	-0.0010
lm0497m3294	87.59641	-65.98825	1.802402	17.01	16.77	1828.7983	0.944	-0.034	-0.075	-0.0070	-0.02	-0.0010
lm0173m15001	76.39634	-68.08	1.803035	17.54	17.30	1880.5939	0.973	-0.017	-0.031	-0.012	-0.026	0.0010
lm0010124269	80.10633	-69.36683	1.803838	15.97	15.74	1197.6493	0.992	-0.070	-0.012	-0.0	-0.0	-0.0020
lm0455m9465	80.88538	-65.75858	1.804726	17.27	17.02	1447.8054	0.961	-0.012	-0.065	-0.011	-0.053	-0.0030
lm0336120011	81.16875	-67.63918	1.807377	17.15	16.84	533.5488	0.94	0.0010	-0.095	-0.0020	-0.063	0.0
lm0342k4708	82.88024	-66.63464	1.807389	16.97	16.78	1952.6230	0.952	-0.048	-0.071	-0.014	-0.03	0.0030
lm0340119594	82.80536	-66.58521	1.809525	15.58	15.36	1388.9012	0.875	-0.055	-0.173	-0.026	-0.08	0.0010
lm055118608	76.25012	-70.6546	1.809783	16.84	16.57	1183.6547	0.985	-0.021	-0.106	0.0030	-0.081	-0.011
lm0112n12177	74.39924	-69.62607	1.812665	15.44	15.27	2256.5889	0.962	-0.01	-0.039	-0.0	-0.0010	0.0030
lm0334120839	80.94674	-67.29686	1.813255	16.02	15.77	1059.8849	0.958	-0.019	-0.047	-0.0020	-0.0040	-0.0010
lm0323m29284	80.33912	-66.77685	1.814879	17.56	17.42	1701.4666	0.953	-0.032	-0.042	-0.0	-0.0020	0.0050
lm0046k17569	86.16095	-70.23705	1.815216	16.94	16.78	1939.6243	0.908	-0.05	-0.107	-0.018	-0.044	0.0090
lm0257m20281*	91.27433	-68.85292	1.821306	17.30	17.08	1506.8157	0.951	0.0030	-0.053	0.0020	-0.018	0.0010
lm0555m8415	76.75804	-71.20828	1.821561	16.47	16.20	1093.6251	0.978	-0.0080	-0.027	-0.0030	-0.012	0.0
lm0583119373	82.45484	-71.06311	1.822309	16.04	15.89	1906.5891	0.969	-0.017	-0.058	-0.01	-0.035	0.0010
lm0353116176	85.31671	-66.86048	1.823357	17.26	17.19	1960.7184	0.909	-0.055	-0.117	-0.021	-0.052	0.0060
lm0135119824	71.00415	-70.02456	1.823883	17.02	16.92	2234.5602	0.897	-0.047	-0.153	-0.016	-0.061	-0.0020
lm0340m6792	83.04816	-66.29128	1.825479	16.52	16.22	2240.6288	0.981	-0.011	-0.028	-0.0060	-0.0080	-0.0020
lm0045k18341	86.97064	-69.86122	1.825661	16.26	16.15	741.8133	0.991	-0.0090	-0.023	-0.0030	-0.014	-0.0080
lm0186m11896	77.3649	-68.93847	1.82799	17.18	16.97	1830.7491	0.949	-0.0090	-0.067	-0.014	-0.045	0.013
lm0131m10839*	71.63107	-69.26347	1.829012	18.10	17.58	1920.6538	0.918	0.0080	-0.121	-0.0090	-0.115	0.01
lm0415123100	73.70022	-65.86156	1.83048	16.43	16.24	1599.5827	0.961	-0.0050	-0.065	-0.0090	-0.047	0.0090
lm0166m13077	73.67342	-68.78261	1.832137	16.96	17.03	838.6081	0.89	0.0030	-0.133	-0.0010	-0.04	-0.0010
lm0231124501	87.07148	-67.95773	1.833426	16.68	16.49	891.6922	0.978	-0.02	-0.014	0.0040	0.0040	0.0
lm0305117796	76.78645	-67.2086	1.833544	17.40	17.27	2137.8799	0.967	-0.028	-0.031	-0.0020	-0.0050	0.0050
lm0193m13361	80.32984	-68.22558	1.834589	17.61	17.41	1862.6168	0.975	-0.013	-0.06	-0.0070	-0.049	-0.0020
lm0121m24865	73.64449	-69.19693	1.835103	16.05	15.85	1640.4899	0.899	-0.031	-0.147	-0.015	-0.057	-0.0050
lm0294k24995	73.99868	-67.11078	1.838354	15.98	15.81	317.8596	0.886	-0.057	-0.159	-0.029	-0.068	-0.0030
lm0321k20265	80.06634	-66.41474	1.839855	17.24	17.11	1975.6187	0.968	-0.029	-0.04	-0.0010	-0.0030	0.0020
lm0114k17880	74.08566	-69.86228	1.842075	17.02	16.85	2192.6912	0.974	-0.017	-0.031	-0.0070	-0.015	0.0010
lm0033k2872	84.96754	-69.41477	1.842642	17.23	17.08	1838.8431	0.945	-0.011	-0.113	-0.0050	-0.09	0.0010
lm0213k25910	83.49101	-68.14804	1.843778	17.30	17.29	1885.6921	0.967	-0.0080	-0.034	-0.0050	-0.015	-0.0010
lm0211122519	83.28888	-67.9377	1.844761	16.59	16.47	1918.7507	0.968	-0.026	-0.034	-0.0010	-0.0020	0.0030

APPENDIX A. PROPERTIES OF THE “HOT” ECLIPSING BINARIES IN THE LMC

lm0587110491	82.5171	-71.72761	1.848852	17.22	17.08	1264.6099	0.93	-0.072	-0.116	-0.038	-0.074	-0.0030
lm0195m11246	79.98669	-68.41411	1.853886	17.54	17.46	2213.7821	0.943	-0.050	-0.081	-0.0050	-0.045	-0.0030
lm0345m8739	83.84796	-67.0051	1.854807	16.14	15.86	404.6316	0.949	-0.060	-0.086	-0.0020	-0.064	0.0050
lm0057m6525	89.44652	-70.29132	1.855932	15.94	15.62	1240.7207	0.895	-0.032	-0.126	-0.0080	-0.038	-0.0
lm0317m6804*	78.70661	-67.34242	1.858256	17.21	16.98	1768.8260	0.955	-0.070	-0.076	-0.0010	-0.066	-0.0010
lm0551m8091	76.52553	-70.49753	1.859092	15.52	15.12	2187.7080	0.892	-0.039	-0.164	-0.014	-0.069	0.0030
lm0095m2603*	79.7062	-69.76787	1.859576	17.75	17.66	1951.6915	0.907	-0.020	-0.083	-0.0080	-0.021	0.0050
lm0093m10002	79.25987	-69.45666	1.860486	16.59	16.38	554.5324	0.934	-0.040	-0.099	-0.0010	-0.046	-0.0030
lm0424m15104	75.12583	-65.64843	1.861021	16.09	15.86	781.8019	0.99	-0.011	-0.012	-0.0060	-0.0090	0.0010
lm0340m12083	83.2381	-66.32889	1.861203	17.22	17.01	1820.7202	0.976	0.0010	-0.036	0.0010	-0.025	0.0
lm0241m8563	89.39576	-67.85644	1.861482	16.16	15.93	1582.7486	0.901	-0.052	-0.127	-0.023	-0.058	-0.0010
lm0022113631	81.91629	-69.64278	1.863346	16.83	16.77	2216.6431	0.879	-0.053	-0.131	-0.023	-0.032	0.0040
lm0100k6156	76.10384	-69.09203	1.863582	16.74	16.55	1154.8129	0.969	-0.0010	-0.036	-0.011	-0.02	-0.0060
lm0455117462	80.37103	-65.8268	1.866168	16.97	16.85	1947.7648	0.953	-0.0010	-0.07	-0.0030	-0.039	0.0
lm01159321	75.11513	-69.95691	1.867104	16.99	16.85	1890.6056	0.96	-0.023	-0.028	0.0040	0.0020	0.0030
lm0027m12372*	83.59952	-70.1811	1.871012	16.78	16.95	2311.7005	0.985	0.0030	-0.027	0.0030	-0.01	-0.0010
lm0291125349	74.75174	-66.55471	1.874248	16.97	16.84	2177.6975	0.987	-0.012	-0.022	0.0020	-0.016	-0.0030
lm0173m20587	76.25369	-68.11408	1.874478	17.07	16.83	851.7610	0.985	-0.021	-0.018	-0.0060	-0.01	-0.0
lm0107k3631	77.27077	-70.12601	1.876618	17.44	17.27	1278.5456	0.95	-0.023	-0.051	0.0030	-0.0030	-0.0090
lm0540m22710	73.45325	-70.59575	1.876681	16.75	16.55	1983.5465	0.947	-0.020	-0.098	-0.0010	-0.065	0.0030
lm0171m18834	76.49656	-67.96039	1.877095	17.29	17.29	390.7627	0.926	-0.068	-0.122	-0.035	-0.066	0.0030
lm0226k6378	84.44984	-68.74611	1.877873	16.91	16.94	1661.5381	0.913	-0.057	-0.103	-0.026	-0.048	0.0060
lm0550k19385	75.06188	-70.58553	1.878439	16.16	15.91	1154.8434	0.93	-0.029	-0.076	-0.0040	-0.02	0.0020
lm0375m24137	89.19523	-67.2793	1.879778	17.11	17.10	1590.6778	0.98	-0.0030	-0.017	0.0	-0.012	0.0010
lm0195m9279	80.30964	-68.39999	1.880086	16.69	16.47	1600.6298	0.943	0.0040	-0.104	0.0060	-0.05	-0.0010
lm0125m29599	73.43014	-69.92033	1.881055	17.70	17.49	1815.6981	0.959	-0.0	-0.075	0.0	-0.054	0.014
lm0161121830	73.9687	-67.98756	1.88166	17.08	16.89	1491.6080	0.957	-0.0090	-0.054	-0.0040	-0.029	-0.0010
lm0341m6056	84.20983	-66.48003	1.883617	15.51	15.19	2241.8182	0.965	-0.016	-0.057	-0.0070	-0.042	0.0
lm0335122611	81.73184	-67.24997	1.886389	15.86	15.65	2020.5398	0.989	-0.0060	-0.019	-0.0040	-0.014	0.0
lm0015124985	80.86542	-70.04807	1.886947	16.14	15.91	1200.6796	0.971	-0.0080	-0.037	-0.0060	-0.019	-0.0
lm0012n19000	80.55954	-69.66548	1.887943	16.00	15.71	1135.7745	0.932	-0.024	-0.078	-0.0070	-0.019	0.0
lm0545n19142	74.50541	-71.41391	1.888095	16.81	16.59	480.7577	0.963	-0.0010	-0.054	0.0010	-0.035	-0.0030
lm0175m26832*	76.45506	-68.50123	1.88968	17.01	16.89	1234.6289	0.973	-0.0080	-0.026	-0.0020	-0.0090	0.0
lm0184n18118	77.42301	-68.61054	1.890723	16.61	16.33	2057.4846	0.938	-0.034	-0.057	0.0010	-0.0090	0.0040
lm0030110277	84.17894	-69.27775	1.890838	17.28	17.22	1869.6248	0.974	-0.019	-0.04	-0.0010	-0.011	-0.0060
lm0347112982	83.77751	-67.55415	1.891817	15.58	15.49	2027.5739	0.907	-0.026	-0.126	-0.012	-0.051	0.0020
lm0011n17783	81.62521	-69.30326	1.90002	17.56	17.20	562.5280	0.973	-0.026	-0.047	-0.01	-0.042	0.0040
lm0212m19169	82.75026	-68.15107	1.900405	15.68	15.60	1599.6421	0.899	-0.026	-0.13	-0.01	-0.037	0.0
lm0466m20073	81.58242	-66.19818	1.900502	17.08	16.89	1912.7399	0.958	-0.041	-0.048	-0.0050	-0.0090	0.0
lm0013m7466	81.51409	-69.44365	1.903719	15.63	15.31	342.7785	0.923	-0.018	-0.092	-0.0060	-0.027	0.0010
lm0217n17433	83.92103	-68.98272	1.906896	16.32	16.29	2228.6537	0.973	-0.0040	-0.049	-0.0010	-0.033	0.0040

lm0093m28032	79.54609	-69.54877	1.908406	17.25	17.14	401.6675	0.99	-0.037	-0.024	-0.03	-0.018	-0.0040
lm045518958	80.51532	-65.76372	1.909773	16.78	16.57	1272.5857	0.988	-0.0020	-0.015	-0.0020	-0.0040	0.0010
lm0164n28849	73.4462	-68.68422	1.91087	17.35	17.24	1610.5590	0.965	-0.031	-0.045	-0.0030	-0.011	0.0
lm0355n1731	85.98205	-67.29131	1.914858	17.46	17.28	1533.7298	0.922	-0.058	-0.116	-0.023	-0.052	0.0020
lm0424n24516	75.05272	-65.88275	1.915386	15.69	15.41	1529.6083	0.986	-0.011	-0.027	-0.0060	-0.012	-0.0010
lm0447m19131	79.23011	-66.0312	1.915947	16.43	16.15	2164.7552	0.978	-0.021	-0.037	-0.0090	-0.019	-0.0010
lm0220m11743	84.88121	-67.72826	1.917261	17.11	16.90	1745.8922	0.966	-0.027	-0.02	0.0	0.0010	0.0090
lm0333n16187	82.20617	-66.84772	1.91737	15.96	15.71	1495.8508	0.962	-0.0080	-0.053	-0.0050	-0.022	0.0
lm0354k2785	84.45844	-66.97058	1.918015	17.61	17.44	1972.6113	0.975	-0.014	-0.03	-0.0070	-0.0090	-0.0010
lm0194k17002	78.71717	-68.44985	1.918376	17.10	16.99	792.7186	0.97	-0.014	-0.034	-0.0020	-0.017	0.0010
lm0355118117	85.46136	-67.2273	1.918576	17.54	17.41	1297.5746	0.97	-0.019	-0.028	0.0	0.0020	0.0040
lm0014k22435	80.15328	-69.88395	1.918806	16.71	16.57	1945.7460	0.969	-0.022	-0.029	0.0020	-0.0010	0.0040
lm0111k26219*	74.92394	-69.20579	1.919088	17.32	17.24	1913.6862	0.95	0.0010	-0.089	-0.0040	-0.044	-0.0020
lm0211122349	83.20144	-67.93699	1.91982	16.58	16.49	2258.6050	0.869	-0.057	-0.187	-0.034	-0.08	0.0040
lm0586m26185	82.15901	-71.66707	1.920948	15.86	15.57	456.8295	0.957	-0.021	-0.044	-0.0040	-0.011	0.0070
lm0100m15042*	76.34099	-69.1476	1.92189	17.21	17.17	1842.8203	0.946	-0.030	-0.042	0.0050	-0.012	0.0040
lm0595118614	84.68188	-71.41471	1.923223	16.89	16.78	2048.4974	0.97	-0.022	-0.032	-0.0030	-0.0070	0.0
lm009115423	79.05376	-69.2368	1.923877	16.90	16.97	2259.6207	0.979	-0.021	-0.011	-0.0010	0.0030	0.0050
lm0590m5052	84.3154	-70.63626	1.925012	17.42	17.32	2297.7623	0.887	-0.073	-0.149	-0.026	-0.061	0.0090
lm0301122532	76.46532	-66.54366	1.925101	16.21	15.97	1731.9349	0.924	-0.049	-0.122	-0.019	-0.047	0.0020
lm0187k17340	77.8906	-68.81097	1.925776	17.04	16.86	1870.6228	0.904	-0.065	-0.145	-0.029	-0.071	-0.0070
lm0113k26292	74.91511	-69.54491	1.927036	16.44	16.41	2027.5238	0.97	-0.021	-0.033	-0.0050	-0.0050	0.0030
lm0306m3943	75.94557	-67.32225	1.927241	16.77	16.71	1842.8157	0.955	0.0010	-0.074	-0.0030	-0.049	-0.0060
lm035119504	85.33408	-66.46349	1.928336	17.56	17.41	1236.6965	0.918	-0.010	-0.131	0.0020	-0.096	-0.0030
lm0355m16251	85.7856	-67.05684	1.929207	17.31	17.15	1860.6695	0.955	-0.011	-0.052	-0.0040	-0.0090	0.0010
lm0223m14105	85.57337	-68.2356	1.929876	15.54	15.34	1064.8019	0.949	-0.027	-0.064	-0.0090	-0.026	0.0010
lm0213m21940*	83.98845	-68.12432	1.929908	17.30	17.06	1470.6691	0.93	-0.0040	-0.105	-0.0030	-0.071	0.0090
lm0333k3930	81.89461	-66.62161	1.931105	16.77	16.61	1424.8853	0.968	-0.015	-0.023	-0.0020	-0.0020	-0.0010
lm0193k25506	79.7946	-68.14185	1.931244	17.31	17.34	2202.6715	0.968	-0.021	-0.036	-0.0050	-0.013	0.0010
lm0612110791	87.82247	-71.03349	1.931428	16.87	16.73	1935.7651	0.963	-0.031	-0.052	-0.0080	-0.022	0.0020
lm0040110857	85.85925	-69.2738	1.93296	15.71	15.73	1870.7164	0.954	-0.011	-0.066	-0.0030	-0.041	0.0010
lm0436m10069*	76.66067	-65.98062	1.9334	16.63	16.42	1577.6794	0.943	0.0020	-0.107	0.0010	-0.067	-0.0030
lm0593k19127*	84.89216	-70.90414	1.933712	17.28	17.24	2187.8067	0.992	0.0	-0.028	-0.0020	-0.012	-0.0020
lm0324n9405	79.59524	-67.1628	1.93932	16.36	16.23	510.5997	0.894	-0.064	-0.157	-0.031	-0.082	0.0050
lm0214124228	82.46417	-68.66476	1.940698	16.11	15.92	1643.5361	0.983	-0.0070	-0.023	-0.0050	-0.011	0.0030
lm0175m19864	76.65556	-68.46029	1.946591	16.35	16.01	361.8658	0.982	-0.016	-0.035	-0.0080	-0.022	-0.0
lm0184k17599	76.65575	-68.46017	1.946593	16.43	16.19	2185.8582	0.976	-0.023	-0.037	-0.01	-0.024	0.0
lm0287k5453*	73.26482	-67.33714	1.946622	16.78	16.55	1851.5814	0.927	-0.0080	-0.095	-0.0010	-0.035	0.0020
lm0345k11158	83.68483	-67.02755	1.946912	15.29	15.06	398.7737	0.872	-0.049	-0.173	-0.019	-0.076	0.0
lm0362n18001*	86.56198	-66.88331	1.950688	17.32	17.31	1125.6826	0.978	-0.0040	-0.023	-0.0020	-0.0010	-0.0
lm0331119382	81.99602	-66.52695	1.951358	15.87	15.63	837.7715	0.904	-0.052	-0.139	-0.02	-0.059	0.0010



APPENDIX A. PROPERTIES OF THE “HOT” ECLIPSING BINARIES IN THE LMC

lm0107m20535	77.44138	-70.40098	1.953697	17.26	17.07	1442.7940	0.959	-0.012	-0.029	-0.0080	-0.016	0.0050
lm0033m22177	85.45951	-69.53269	1.954291	15.67	15.66	1079.8238	0.939	-0.030	-0.074	-0.0010	-0.041	-0.0010
lm0314n5827*	77.88079	-67.1447	1.955694	16.99	16.78	1898.5986	0.967	-0.070	-0.05	-0.0020	-0.033	0.0
lm0032i12916	83.94649	-69.64218	1.960459	15.77	15.66	2026.5388	0.98	-0.015	-0.038	-0.0050	-0.027	0.0020
lm0191m9387*	80.29841	-67.92636	1.96275	16.74	16.44	799.8349	0.957	0.011	-0.097	-0.0040	-0.079	0.0010
lm0030k12130*	84.07157	-69.13973	1.96284	17.08	17.00	2063.4914	0.959	-0.020	-0.076	-0.0020	-0.055	-0.0010
lm0024m7851	82.3537	-69.80221	1.966268	17.28	17.23	2243.6361	0.899	0.060	-0.153	0.0030	-0.102	0.0
lm0170i14651	74.94912	-67.89419	1.967818	17.60	17.50	2334.5736	0.935	-0.019	-0.101	-0.0090	-0.027	-0.0040
lm0294m6230*	74.46889	-67.14491	1.9694	17.02	16.85	1527.5936	0.993	-0.010	-0.019	-0.0040	-0.016	0.0030
lm0123k12359	73.01024	-69.47138	1.969574	15.85	15.69	2251.7679	0.977	-0.050	-0.018	-0.0020	-0.0040	0.0020
lm0165i18886*	74.26136	-68.61124	1.974794	17.35	17.34	1532.5938	0.894	-0.030	-0.145	-0.0030	-0.057	0.0010
lm0091m30316	79.3163	-69.222	1.978761	16.83	16.78	530.5569	0.928	-0.042	-0.105	-0.021	-0.052	0.0010
lm0090i12995*	78.06702	-69.29122	1.982342	16.86	16.78	1755.8747	0.932	0.070	-0.053	0.0030	-0.015	0.0030
lm0320i22546*	79.32981	-66.55835	1.9847915	16.37	16.13	2183.7525	0.926	-0.066	-0.116	-0.025	-0.067	-0.0090
lm0020k12115*	81.98923	-69.14169	1.9894755	14.40	14.14	506.5490	0.972	-0.013	-0.027	-0.0020	-0.0090	0.0030
lm0101m23916*	77.41695	-69.34105	1.99006	14.62	14.32	1154.8129	0.863	-0.019	-0.184	-0.0030	-0.072	0.0070
lm0025m1533*	83.66955	-69.98922	1.990814	16.63	16.40	1916.5944	0.972	-0.014	-0.029	-0.0030	-0.0	0.0010
lm0031m23092*	85.49733	-69.34815	2.018832	17.28	17.17	1375.9103	0.961	0.050	-0.046	0.0010	-0.015	0.0010
lm0015m10153*	81.44854	-69.95987	2.020196	17.24	17.20	1396.9036	0.987	0.0	-0.018	0.0	-0.01	0.0010
lm0344i25518	82.61061	-70.28287	2.023458	16.58	16.42	2027.5739	0.915	-0.066	-0.125	-0.027	-0.074	-0.0050
lm0583k6016	82.49748	-70.84832	2.024389	16.20	15.99	1475.7354	0.975	-0.012	-0.036	-0.0080	-0.024	-0.0010
lm0306i8041*	75.77498	-67.50262	2.0253776	17.60	17.43	1821.7503	0.972	-0.0	-0.04	0.0030	-0.03	0.0030
lm0283n24858	73.36237	-66.90843	2.026102	16.43	16.27	1819.6920	0.976	-0.021	-0.047	-0.01	-0.032	0.0020
lm0561i15749	78.07403	-70.69122	2.028764	17.39	17.28	1854.6210	0.946	0.060	-0.058	0.0030	-0.0	-0.0010
lm0366i15212	86.18124	-67.5631	2.029431	15.72	15.48	2033.5447	0.973	-0.014	-0.034	-0.0030	-0.0010	0.0030
lm0551m10503	76.50545	-70.66306	2.03144	15.85	15.58	1881.6171	0.991	-0.011	-0.012	0.0	-0.0010	0.0030
lm0323i28741	79.89295	-66.92704	2.032993	17.50	17.45	2344.6129	1.003	-0.02	-0.034	-0.0020	-0.025	-0.0
lm0632i14637	92.27526	-71.08018	2.033454	16.50	16.67	384.7207	0.965	-0.021	-0.042	-0.0090	-0.014	0.0020
lm0307i17542	76.7601	-67.58324	2.034164	15.64	15.33	1628.5280	0.99	-0.01	-0.017	-0.0	-0.0	-0.0
lm0386i17576*	89.92579	-67.63681	2.04171	17.96	17.78	1568.7252	0.916	0.011	-0.133	0.0010	-0.103	-0.01
lm0121i22166	72.95621	-69.38456	2.042442	14.94	14.97	2130.7894	0.986	-0.0020	-0.016	-0.0020	-0.01	-0.0
lm0310m18574	78.05985	-66.5498	2.043743	16.92	16.79	1129.6499	0.986	-0.019	-0.017	-0.0010	-0.0010	0.0020
lm0033k11169	85.0617	-69.46637	2.043963	15.32	15.14	1381.9065	0.872	-0.038	-0.179	-0.013	-0.078	0.0010
lm0296m14458	74.2611	-67.39555	2.044072	15.50	15.30	2198.6280	0.923	-0.03	-0.091	-0.0060	-0.026	0.0050
lm0323k3395	80.02339	-66.61923	2.046694	17.04	17.12	2224.7712	0.931	-0.049	-0.123	-0.027	-0.075	-0.0010
lm0394m9536*	92.04965	-67.01563	2.048044	16.82	16.61	2140.8873	0.94	0.030	-0.119	0.0040	-0.096	-0.0010
lm0427m12788*	76.05393	-66.15369	2.048492	17.77	17.66	1764.8415	0.95	-0.030	-0.061	-0.0010	-0.037	0.0040
lm0184m11334	77.18704	-68.57391	2.048845	17.19	17.03	1892.8390	0.934	0.010	-0.098	-0.0090	-0.066	-0.0020
lm0181i15831	77.97285	-67.89126	2.049965	16.44	16.25	1091.7610	0.938	-0.026	-0.063	-0.0050	-0.012	0.0030
lm0177i22821	76.20412	-69.01093	2.050346	16.38	16.07	403.7508	0.958	-0.013	-0.053	-0.012	-0.032	0.0030
lm0323k16171	80.11238	-66.69728	2.050964	17.04	16.96	434.7552	0.903	-0.102	-0.141	-0.04	-0.076	0.0030

lm0207k27793*	81.77397	-68.8758	2.054994	17.11	16.94	1955.6861	0.937	-0.013	-0.059	-0.0020	-0.012	0.0010
lm0214i23257	82.60628	-68.6583	2.056505	17.55	17.42	2130.8364	0.965	-0.023	-0.04	-0.0090	-0.034	0.0060
lm0454i24956	79.67753	-65.88205	2.057119	16.46	16.26	1109.8177	0.985	-0.014	-0.026	-0.01	-0.019	0.0010
lm0467m13027*	82.43788	-65.99099	2.0578661	16.36	16.13	1977.6446	0.925	0.0030	-0.089	-0.0020	-0.032	-0.0020
lm0030i12866	84.00575	-69.29671	2.058756	15.69	15.62	2223.6288	0.948	-0.027	-0.065	-0.0070	-0.02	-0.0010
lm0010m21049	77.61272	-69.17686	2.059198	15.91	15.75	2093.9045	0.925	-0.014	-0.087	-0.0050	-0.014	-0.0050
lm0217n11196	83.9752	-68.93308	2.059265	16.00	15.78	1197.6663	0.992	-0.0070	-0.014	-0.0010	-0.0050	0.0010
lm0031i26732	85.00806	-69.36966	2.060787	17.38	17.35	1581.6987	0.977	-0.0070	-0.081	-0.0020	-0.069	-0.0090
lm0346m26007*	83.19507	-67.4804	2.0627301	16.92	16.75	1952.6230	0.909	-0.010	-0.138	-0.0090	-0.082	0.0
lm0347m24253	84.12629	-67.4671	2.062809	16.84	16.64	1618.6821	0.984	-0.01	-0.045	-0.0090	-0.025	0.0030
lm0015m33370*	81.49503	-69.92983	2.064046	16.71	16.46	775.8333	0.873	-0.0040	-0.166	0.0010	-0.058	0.0010
lm0581i21536*	82.62171	-70.72562	2.064116	17.37	17.22	1901.8440	0.96	-0.023	-0.096	-0.0080	-0.081	-0.0030
lm0021i6609	83.01333	-69.24357	2.064204	15.80	15.57	384.7892	0.877	-0.058	-0.156	-0.022	-0.076	0.0060
lm0103n19330*	77.57442	-69.65899	2.064678	16.78	16.51	2185.6532	0.981	0.013	-0.051	0.0050	-0.038	-0.0010
lm0182k16150*	76.83647	-68.12493	2.065838	16.31	16.18	2227.6109	0.991	-0.0020	-0.038	0.0070	-0.0090	-0.0020
lm0340m15950	82.98613	-66.35673	2.066753	15.78	15.54	402.6230	0.989	-0.0090	-0.021	-0.0050	-0.0070	-0.0
lm0294k30560	73.85571	-67.06038	2.066959	16.48	16.40	1150.6036	0.982	0.0020	-0.054	-0.0020	-0.039	-0.013
lm0606m11871	86.44399	-71.57547	2.071847	17.05	16.96	1752.8762	0.974	-0.025	-0.03	0.0	0.0030	0.0
lm0013k30220*	81.04465	-69.56256	2.072228	17.14	17.15	2218.8452	0.972	0.0040	-0.071	-0.0050	-0.059	-0.0010
lm0030k16342	84.14584	-67.02705	2.077371	15.94	16.14	2225.7022	0.963	-0.021	-0.077	-0.0070	-0.06	-0.0060
lm0030m20233	84.228	-69.38287	2.077922	15.91	15.78	2141.8535	0.98	-0.0060	-0.021	0.0	-0.0070	0.0020
lm0587i18183*	82.60552	-71.78322	2.077996	16.70	16.59	1277.5481	0.972	0.0030	-0.029	0.0020	-0.0060	-0.0
lm0364n12802	86.75311	-67.19625	2.078818	16.84	16.67	1336.4763	0.909	0.0040	-0.14	0.0010	-0.077	-0.0020
lm0120n28365	72.66602	-69.37864	2.079315	16.75	16.61	1090.6622	0.971	-0.060	-0.027	-0.0050	-0.014	0.0060
lm0320m11672	79.71178	-66.47893	2.082247	17.40	17.27	1834.7450	0.979	-0.003	-0.023	-0.0030	0.0010	-0.0040
lm0376m19861	88.63075	-67.48616	2.082899	16.84	16.59	1910.8389	0.985	0.0060	-0.042	0.0020	-0.025	-0.0030
lm0135k22834	71.14445	-69.89752	2.086075	16.83	16.77	1404.7858	0.955	-0.0030	-0.072	-0.0030	-0.037	-0.0040
lm0216i17602	82.58384	-68.98538	2.088156	16.09	15.90	2155.8047	0.94	-0.0080	-0.107	-0.0040	-0.079	0.0030
lm0283i8947	73.24627	-66.80928	2.088225	16.07	15.90	2575.5757	0.941	-0.0030	-0.085	-0.0030	-0.056	0.0030
lm0353k13716	85.43765	-66.68657	2.0904	17.15	17.04	2183.8061	0.982	0.0	-0.037	-0.011	-0.019	0.0090
lm0374i15319	87.98088	-67.22025	2.090547	16.63	16.44	1630.5740	0.904	-0.055	-0.107	-0.024	-0.033	0.01
lm0120n11810	72.36481	-69.27577	2.090994	16.69	16.56	1867.5646	0.984	-0.01	-0.021	-0.0030	-0.0070	0.0
lm0021n14065	83.69031	-69.28125	2.091973	17.16	17.01	818.8144	0.963	-0.012	-0.077	-0.0010	-0.053	-0.0070
lm0017k18680*	80.84479	-70.22322	2.094048	17.30	17.36	2535.8269	0.961	0.0	-0.055	0.0040	-0.025	-0.0010
lm0426m23242*	75.02346	-66.21718	2.09473	16.67	16.37	1987.5435	0.944	-0.0030	-0.08	0.0020	-0.056	0.0
lm0311k11634	78.2451	-66.33708	2.095304	16.98	16.74	1997.5510	0.987	-0.0090	-0.019	-0.0010	-0.0040	0.0010
lm0543m11267*	74.62118	-70.85887	2.09621	16.89	16.78	1291.4889	0.876	-0.0040	-0.17	-0.0010	-0.077	0.0020
lm0284n24091	72.42796	-67.28827	2.098031	17.23	17.15	1546.7474	0.976	-0.029	-0.024	0.0020	0.0010	0.0080
lm0120n12064	72.71161	-69.27655	2.099324	17.07	16.96	2344.5253	0.928	-0.012	-0.067	-0.0050	-0.0030	-0.0010
lm0020k18818	81.9151	-69.18844	2.101491	15.79	15.57	1555.6796	0.964	-0.020	-0.044	-0.0020	-0.022	-0.0

APPENDIX A. PROPERTIES OF THE “HOT” ECLIPSING BINARIES IN THE LMC

lm0184k7714	76.91956	2.102557	15.41	15.21	1842.8236	0.977	-0.011	-0.021	0.0010	-0.0020	-0.0030
lm0211k22900*	83.56939	2.103998	17.58	17.43	1945.7784	0.981	-0.090	-0.039	-0.0040	-0.033	0.0010
lm0346m11026	83.27558	2.108278	15.35	15.09	2053.5015	0.974	-0.080	-0.046	-0.0020	-0.035	0.0
lm0121m19697	73.2997	2.108675	17.23	17.13	871.5515	0.96	-0.090	-0.052	-0.0010	-0.03	0.0010
lm0090m28977	78.40084	2.108725	16.45	16.36	455.8341	0.942	-0.026	-0.111	-0.014	-0.084	0.0020
lm0210m24868	82.9734	2.111375	16.60	16.40	1470.6691	0.936	-0.012	-0.088	0.0030	-0.039	-0.0040
lm0585k2867	82.67001	2.113799	17.33	17.26	1566.6288	0.945	-0.01	-0.058	-0.011	-0.016	0.0030
lm0014116806	80.07167	2.116274	17.35	17.19	1442.8081	0.915	0.090	-0.128	-0.060	-0.086	-0.0040
lm0184k27793*	76.91822	2.116352	17.47	17.45	1749.9270	0.948	-0.080	-0.065	-0.0040	-0.013	-0.0020
lm034018015	82.7471	2.117866	15.86	15.65	1075.7470	0.957	-0.019	-0.052	0.0	-0.0090	0.01
lm0447m16378	79.09147	2.119938	16.71	16.49	1153.6390	0.978	-0.011	-0.037	-0.01	-0.02	-0.0030
lm0285k4193	73.28319	2.12335	15.59	15.46	1867.5702	0.984	-0.016	-0.012	-0.0040	-0.0050	0.0010
lm0345k7628	83.43781	2.123454	15.37	15.18	1169.7965	0.965	-0.050	-0.044	-0.0020	-0.017	0.0010
lm0111k6722	74.88413	2.124105	17.05	16.86	1374.8887	0.953	-0.030	-0.063	0.0020	-0.033	0.0020
lm0131m13819*	71.70255	2.124143	17.22	17.08	2195.6001	0.914	0.020	-0.114	-0.0020	-0.038	0.0060
lm002019163	82.07743	2.127403	16.22	15.96	1164.7212	0.981	-0.021	-0.021	-0.0	-0.0010	-0.0010
lm016418885	73.08891	2.129469	17.09	16.96	2245.7783	0.976	-0.013	-0.037	-0.0040	-0.013	0.0010
lm0831m8738	86.43787	2.132923	17.35	17.38	1920.7865	0.931	-0.050	-0.101	-0.0040	-0.051	0.0030
lm0214k13590	82.3609	2.133649	17.21	17.14	950.4813	0.965	-0.023	-0.025	0.0020	0.0030	-0.0
lm0164m11674	73.64248	2.13616	17.16	17.06	2214.6954	0.943	-0.050	-0.07	0.0010	-0.025	0.0020
lm0327m5562	80.56402	2.137046	16.20	15.94	1423.8485	0.97	-0.016	-0.026	-0.0	-0.0010	0.0020
lm0557m5208	76.48716	2.137119	15.53	15.16	2251.6337	0.949	-0.020	-0.068	-0.0020	-0.028	0.0010
lm0335m14542	82.3786	2.139656	17.21	16.97	1751.8582	0.946	-0.090	-0.094	-0.0070	-0.071	-0.0090
lm0093m22090*	79.41649	2.140468	17.55	17.57	1622.5442	0.975	-0.040	-0.04	0.0080	-0.035	-0.0
lm0574m16657	79.94568	2.140756	15.98	15.82	1930.6592	0.939	-0.02	-0.095	-0.011	-0.07	0.0
lm0157m11115	72.8539	2.14176	17.16	16.99	2330.5523	0.948	-0.026	-0.052	-0.0060	-0.012	-0.0020
lm0115k23126	74.89513	2.142218	17.25	17.22	1381.9210	0.982	-0.030	-0.05	0.0020	-0.038	-0.0030
lm0364k5553	86.23784	2.143821	16.65	16.49	2245.8514	0.989	-0.016	-0.014	0.0010	0.0	-0.0010
lm0317k3682	78.43808	2.145239	16.24	15.97	2257.6240	0.956	-0.011	-0.063	-0.0070	-0.041	0.0070
lm0013132365	80.91383	2.145755	16.15	16.18	380.7020	1.025	-0.020	-0.028	-0.0010	-0.026	-0.0020
lm0280m23309	72.78232	2.146408	16.90	16.74	1768.7941	0.944	-0.035	-0.059	-0.0080	-0.017	0.0020
lm003119480*	84.97111	2.149394	17.10	17.26	2206.6565	0.97	-0.010	-0.063	-0.0060	-0.022	-0.0050
lm036519532	87.07831	2.149591	17.37	17.26	1076.8497	0.914	-0.098	-0.131	-0.046	-0.087	0.0010
lm035417923	84.42679	2.149846	17.23	17.07	1078.8711	0.998	-0.032	-0.024	-0.021	-0.017	0.0040
lm0331m11496	82.35971	2.151473	15.98	15.67	947.5096	0.967	-0.015	-0.026	0.0010	-0.010	0.0040
lm0184k12216	76.64318	2.154475	15.51	15.19	1281.5396	0.942	0.020	-0.09	-0.0060	-0.054	-0.0010
lm0175m14310	76.64287	2.154499	15.19	14.95	351.8527	0.971	-0.030	-0.08	0.0040	-0.064	-0.0080
lm0285m20817	73.35147	2.155777	16.24	16.18	1619.5305	0.986	-0.090	-0.027	-0.0050	-0.022	-0.0020
lm0112m20997	74.43411	2.156503	16.45	16.32	428.6244	0.942	-0.025	-0.068	-0.0060	-0.019	0.0030
lm0204k11078*	80.58988	2.15745	16.91	16.90	327.8730	0.981	-0.040	-0.026	-0.0030	-0.011	0.0010
lm0025m22937	83.35719	2.157874	15.35	15.19	2233.5777	0.995	-0.013	-0.0070	-0.0010	-0.0010	-0.0

lm0375k19793	88.82509	-67.09479	2.158691	16.43	16.30	1641.5539	0.931	-0.0050	-0.078	-0.0030	-0.018	-0.0020
lm0016m21306*	80.61341	-70.3948	2.159334	17.00	16.83	1763.8058	0.883	-0.081	-0.172	-0.043	-0.092	-0.0020
lm0377m4439	89.34411	-67.33731	2.160335	17.52	17.28	2198.7009	0.964	-0.043	-0.052	-0.0030	-0.013	-0.0020
lm0014m16700	80.30362	-69.84745	2.160507	17.34	17.26	1771.8841	0.945	-0.0080	-0.087	-0.012	-0.067	-0.0030
lm0344k16854	82.61313	-67.06915	2.164252	16.00	15.81	533.5582	0.966	-0.0090	-0.077	-0.0030	-0.058	0.0030
lm0031m19001	85.26359	-69.17275	2.165249	17.19	17.32	1150.7403	0.954	-0.034	-0.08	-0.0080	-0.026	-0.01
lm0321m8452	80.60069	-66.29375	2.168221	16.88	16.55	819.8227	0.974	-0.017	-0.027	0.0	-0.0010	-0.0010
lm0317k5360	78.51571	-67.34183	2.169716	15.68	15.45	786.8320	0.984	-0.0090	-0.016	-0.0030	-0.0070	0.0040
lm0122m5050*	72.74168	-69.43543	2.169742	16.36	16.15	2172.6922	0.966	-0.016	-0.067	-0.01	-0.047	-0.0010
lm0476m8386*	83.50353	-66.10806	2.1700301	17.21	17.07	2236.6030	0.886	-0.0070	-0.149	0.0040	-0.064	0.0060
lm0214m10775*	82.998	-68.57209	2.175728	17.39	17.23	1166.6841	0.982	-0.015	-0.028	-0.01	-0.023	0.0020
lm0104k10462	76.16645	-69.81477	2.178028	16.43	16.22	1367.8576	0.882	-0.016	-0.17	-0.0030	-0.088	-0.0040
lm0012m16798	80.64725	-69.52878	2.183354	15.84	15.48	697.8926	0.936	-0.02	-0.095	-0.015	-0.059	-0.0020
lm0205m25742	82.16942	-68.69351	2.184881	15.35	14.97	1136.8511	0.964	-0.0050	-0.057	-0.011	-0.027	-0.0
lm0294n13388	74.43611	-67.18884	2.188141	15.69	15.44	1858.8282	0.983	-0.0	-0.021	-0.012	-0.0080	-0.0070
lm0366k6375*	86.15242	-67.49247	2.1890061	17.15	17.00	2155.8487	0.974	-0.0070	-0.038	-0.0060	-0.019	-0.0030
lm0543m9484*	74.37811	-70.85007	2.1894	17.29	17.13	864.6909	0.975	-0.0	-0.046	0.0010	-0.038	-0.0010
lm0315m20618*	78.86678	-67.06945	2.19195	17.34	17.15	1389.8800	0.97	-0.0060	-0.027	-0.0030	-0.0090	0.0010
lm0113m6637*	75.31889	-69.43376	2.19245	17.00	16.88	1830.7101	0.971	-0.0040	-0.026	-0.0010	-0.0090	-0.0030
lm0461n15640	82.5222	-65.1763	2.192546	17.34	17.12	1445.8946	0.974	-0.0070	-0.031	-0.0030	-0.012	0.0020
lm0191m2265	79.9646	-67.83491	2.193241	17.04	16.90	1900.7488	0.953	-0.015	-0.066	-0.0080	-0.041	0.0020
lm0013m20283	81.51292	-69.5146	2.193383	15.39	15.13	2255.6523	0.969	-0.015	-0.034	0.0	0.0	0.0
lm0123k15744	72.81945	-69.49155	2.195774	16.50	16.34	1090.6622	0.989	-0.031	-0.016	-0.0090	-0.016	0.0010
lm0541n4981	74.66565	-70.64066	2.195876	16.83	16.48	1775.7720	0.984	-0.016	-0.022	-0.0070	-0.013	0.0020
lm0044n5926	86.59323	-69.94393	2.195876	16.92	16.91	2017.5920	0.886	-0.098	-0.157	-0.044	-0.082	0.0070
lm0281n14618	73.56365	-66.49116	2.199786	17.07	16.87	1526.5916	0.889	-0.087	-0.181	-0.048	-0.108	0.0060
lm0300m25571	76.14499	-66.41666	2.200747	15.94	15.64	1825.7028	0.94	-0.021	-0.059	-0.0020	-0.0090	0.0030
lm0340m19568	83.17912	-66.38233	2.202876	17.49	17.25	1803.8692	0.968	-0.017	-0.042	-0.011	-0.024	0.0
lm0290m12262	74.359	-66.48642	2.203112	16.37	16.21	1181.6470	0.948	-0.0090	-0.099	-0.0090	-0.075	0.0040
lm0370k17512	87.81232	-66.37514	2.203777	17.07	16.89	1524.6881	0.887	-0.074	-0.145	-0.031	-0.065	0.0040
lm0107k22985	77.27191	-70.24754	2.207411	17.32	17.09	435.7162	0.98	0.0050	-0.036	0.0010	-0.024	-0.0020
lm0290l21965	73.96035	-66.57577	2.211292	15.93	15.85	317.8596	0.989	-0.0040	-0.012	-0.0010	-0.0060	-0.0030
lm0241l25390	89.18869	-67.97323	2.214714	17.44	17.34	365.7348	0.978	-0.0060	-0.03	-0.0050	-0.021	0.0010
lm0610k4113	87.85881	-70.5359	2.214823	17.15	16.98	1244.6823	0.975	0.0020	-0.039	-0.0010	-0.029	-0.0
lm0591n25314	85.29076	-70.7462	2.216887	16.04	15.84	1167.8282	0.929	-0.03	-0.081	-0.0090	-0.022	0.0020
lm0020k119961	84.45912	-67.79554	2.21799	17.00	16.84	2297.7697	0.905	-0.069	-0.133	-0.028	-0.069	-0.0040
lm0020k11440	82.0627	-69.13661	2.220169	15.22	14.93	1869.6092	0.975	-0.0090	-0.063	-0.0070	-0.046	-0.0020
lm0203n15393	81.84417	-68.23549	2.225954	15.52	15.28	394.7756	0.973	-0.012	-0.025	0.0010	0.0	0.0030
lm0581k6931	82.64645	-70.48988	2.227595	17.07	16.87	1879.6402	0.978	-0.02	-0.019	-0.0010	-0.0020	0.0060
lm0230m4155	86.84193	-67.67424	2.229129	17.16	16.89	2019.5821	0.974	-0.0030	-0.052	-0.013	-0.027	-0.013
lm0033m24762	85.32805	-69.54912	2.230059	16.31	16.16	837.7160	0.986	-0.0060	-0.029	-0.0020	-0.021	-0.0010

APPENDIX A. PROPERTIES OF THE "HOT" ECLIPSING BINARIES IN THE LMC

Im0285n4645	73.58179	-67.1328	2.230755	17.20	16.98	2225.5834	0.981	-0.012	-0.024	-0.0050	-0.015	0.0010
Im0303n12403	76.83486	-66.82148	2.234478	16.69	16.53	1860.5816	0.944	-0.0070	-0.085	-0.0030	-0.052	0.0010
Im0335k26760	81.73943	-67.11696	2.234913	16.22	16.09	1117.6933	0.887	-0.065	-0.149	-0.026	-0.068	0.0010
Im0103l11316	77.23053	-69.61654	2.235387	16.87	16.78	1272.5541	0.976	-0.014	-0.032	-0.0060	-0.014	-0.0040
Im0175k25724	75.99716	-68.49432	2.241225	17.26	17.22	1153.6015	0.932	-0.037	-0.1	-0.016	-0.041	-0.0020
Im0301m9832	76.87818	-66.45832	2.242879	16.16	15.99	1895.7454	0.984	-0.012	-0.018	-0.0060	-0.011	-0.0
Im0127n21487	73.64413	-70.40732	2.244659	17.11	16.88	1341.9223	0.965	0.020	-0.056	-0.0010	-0.041	-0.0020
Im0200k25034	80.53284	-67.81569	2.244789	16.65	16.21	1788.8132	0.947	-0.019	-0.079	-0.01	-0.056	0.0040
Im0193m14935	79.97507	-68.08203	2.249797	15.10	14.89	1570.5930	0.967	-0.017	-0.038	-0.0010	-0.0050	0.0020
Im0020k24295	82.1302	-69.22794	2.250701	16.27	16.05	1916.5944	0.979	0.010	-0.027	0.0010	-0.013	0.0010
Im0331l17455	81.99669	-66.51466	2.254984	16.95	16.93	1934.7177	0.963	-0.010	-0.053	-0.0	-0.034	-0.0
Im0466l15239	81.32446	-66.16268	2.25864	16.22	15.99	2211.7638	0.931	-0.016	-0.115	-0.01	-0.078	0.0040
Im0021l32791	83.07767	-69.38839	2.25996	16.94	16.78	1644.5527	0.962	-0.0040	-0.072	0.0010	-0.047	0.0010
Im0033l8128*	85.00657	-69.60188	2.2622781	16.06	16.26	1838.8431	0.927	-0.016	-0.122	-0.0080	-0.093	-0.0040
Im0355k3317	85.17943	-66.97744	2.265278	17.38	17.32	1850.8182	1.004	-0.021	-0.012	0.0040	-0.0030	-0.01
Im0117m10584	75.35456	-70.17046	2.26826	15.61	15.36	1139.8417	0.973	-0.014	-0.023	0.0	-0.0	-0.0010
Im0551n13003	76.55602	-70.6779	2.270432	15.45	15.11	1861.6594	0.991	0.0040	-0.025	-0.0020	-0.02	0.0
Im0294m26342	74.56661	-67.1114	2.271254	17.11	16.95	1867.5915	0.992	-0.02	-0.014	-0.018	-0.0080	-0.0010
Im0100m5690	76.65727	-69.2394	2.27321	16.90	16.75	2009.5280	0.907	-0.0090	-0.117	-0.0020	-0.056	-0.0010
Im0030n18202	84.49421	-70.32818	2.273798	16.13	15.97	1873.7450	0.988	-0.018	-0.014	-0.0040	-0.011	0.0010
Im0551k22031	75.9421	-70.61975	2.27601	17.29	17.17	2014.5141	0.958	-0.011	-0.048	-0.018	-0.03	-0.0020
Im0093m18940	79.41344	-69.50216	2.277221	16.57	16.39	1272.5694	0.986	-0.012	-0.024	-0.0060	-0.014	-0.0
Im0123m12046	73.51901	-69.46607	2.278014	16.05	15.96	2172.6922	0.913	-0.045	-0.106	-0.013	-0.04	0.0050
Im0173l13985	75.92725	-68.23103	2.27859	16.21	16.06	2208.5925	0.968	-0.019	-0.025	0.0	0.0010	0.0030
Im0092m20117*	78.50788	-69.55312	2.27942	16.91	16.83	2390.5244	0.973	-0.0080	-0.026	-0.0030	-0.012	-0.0020
Im0354m18367	84.90615	-67.07169	2.279477	16.84	16.74	1952.6459	0.962	-0.070	-0.048	-0.0050	-0.0080	0.0
Im0161m20878	74.58093	-67.77289	2.27958	16.52	16.30	879.5520	0.968	-0.0020	-0.055	-0.0	-0.034	-0.0010
Im0681m16073	77.63693	-71.94809	2.280521	17.39	17.16	1503.6392	0.945	0.060	-0.092	-0.0020	-0.066	-0.0
Im0037m13144*	85.36341	-70.19321	2.280632	17.45	17.31	1071.8607	0.974	0.0030	-0.06	0.0010	-0.042	-0.0010
Im0211m23264	83.98286	-67.78861	2.280982	16.35	16.11	1150.7130	0.89	-0.056	-0.146	-0.026	-0.067	0.0020
Im0117m15641	75.59811	-70.20151	2.2838	16.30	16.10	442.7809	0.987	-0.0080	-0.017	0.0	-0.01	0.0030
Im0175n31573*	76.57935	-68.67835	2.286902	15.93	15.87	2030.4981	0.993	-0.0020	-0.013	-0.0020	-0.0080	-0.0010
Im0543n27195	74.72801	-71.10363	2.293317	17.25	17.06	1289.5076	0.962	-0.031	-0.038	0.0	0.0010	0.0010
Im0184k13561*	76.85596	-68.43673	2.294172	16.58	16.53	418.8373	0.988	-0.011	-0.017	-0.0050	-0.01	-0.0020
Im0294n10273	74.31829	-67.16995	2.298904	15.77	15.56	1739.7894	0.931	-0.039	-0.09	-0.019	-0.042	0.0070
Im0337k20128	81.91348	-67.44235	2.300298	15.54	15.28	1794.8525	0.945	-0.014	-0.099	-0.0060	-0.066	0.0
Im0090l13156	78.15229	-69.29216	2.301266	16.70	16.50	2184.7283	0.879	-0.017	-0.153	-0.0050	-0.072	-0.0010
Im0355n12209	85.75128	-67.18314	2.303794	17.25	17.15	1383.8643	0.927	-0.063	-0.108	-0.022	-0.042	0.0040
Im0313m21348	78.79807	-66.72394	2.304919	15.63	15.32	2545.7533	0.958	-0.017	-0.043	-0.0010	-0.0040	-0.0010
Im0343l17247	83.79672	-66.86069	2.308411	17.37	17.28	1090.6924	0.96	0.0	-0.062	-0.0010	-0.039	-0.0010
Im0322k20845	79.31416	-66.77314	2.311547	15.93	15.75	892.6213	0.918	-0.04	-0.097	-0.013	-0.033	0.0030

lm0586k16977	81.53131	-71.60798	2.316108	15.24	14.99	1556.7363	0.979	0.0030	-0.035	0.0	-0.024	0.0020
lm0166k8280*	73.30392	-68.75893	2.32533	16.88	16.77	2229.7862	0.946	-0.0050	-0.064	-0.0010	-0.02	0.0010
lm0563m21591*	78.91696	-70.91882	2.327632	17.31	17.19	2003.5423	0.978	0.0070	-0.037	-0.0030	-0.016	-0.0060
lm0366l21345	86.19773	-67.6337	2.328524	16.73	16.52	1908.8216	0.985	-0.026	-0.02	-0.0020	-0.0070	0.0
lm0001l9491	80.48924	-67.9369	2.329272	15.93	15.86	1993.5747	0.938	-0.029	-0.058	-0.0020	-0.0040	0.0090
lm0592n11646*	84.18167	-71.11731	2.329534	17.04	16.97	1775.7456	0.973	0.0010	-0.03	0.0040	-0.01	-0.0020
lm0096m21147	78.54099	-70.38856	2.332835	17.15	16.98	1914.6271	0.922	0.0030	-0.119	-0.0	-0.078	0.0070
lm0186m14790	77.10658	-68.95847	2.333025	17.11	17.16	538.5531	0.947	-0.037	-0.058	-0.01	-0.019	0.0010
lm0030m4163	84.37804	-69.08817	2.333416	15.30	15.31	388.8496	0.899	0.0020	-0.118	-0.0010	-0.027	0.0060
lm0121112322	73.16189	-69.3917	2.334903	16.82	16.64	1482.5760	0.971	-0.0090	-0.042	-0.0090	-0.017	-0.0010
lm0020k2403*	82.1265	-69.07292	2.335872	17.85	17.70	537.5088	0.874	-0.0060	-0.177	0.0030	-0.108	0.01
lm0033n25448	85.4593	-69.70678	2.340327	16.26	15.99	1771.8981	0.987	0.0	-0.06	-0.0010	-0.044	-0.0010
lm0115k28730*	75.13218	-69.91555	2.341022	16.80	16.76	1246.5952	0.991	-0.0050	-0.035	-0.0010	-0.025	0.0030
lm0211k9308*	83.44762	-67.70132	2.341696	17.22	17.12	1289.5751	0.956	-0.011	-0.039	-0.0030	-0.013	0.0020
lm0186k5622	76.9543	-68.74386	2.341898	16.62	16.35	2047.4882	0.968	-0.0090	-0.042	-0.0050	-0.022	-0.0020
lm0033l8978	84.97257	-69.60731	2.344895	15.75	15.85	2173.6941	0.996	-0.0010	-0.01	-0.0020	-0.0030	-0.0
lm0103k4043	77.1157	-69.42463	2.345441	15.89	15.84	1224.6130	0.974	-0.016	-0.038	-0.012	-0.019	0.0070
lm0426m23482	75.07795	-66.06284	2.345573	15.15	14.83	1447.7508	0.95	-0.015	-0.042	-0.0020	0.0030	0.0010
lm01212127892	73.21002	-69.36678	2.34604	17.10	16.97	1755.8861	0.925	-0.0040	-0.12	0.0010	-0.07	-0.0040
lm012129182	74.13397	-69.73558	2.347385	15.57	15.38	2574.6019	0.952	0.0040	-0.067	-0.0	-0.02	0.0
lm0111n16405	75.47253	-69.29324	2.347974	16.90	16.77	1539.6904	0.966	-0.018	-0.026	-0.0020	0.0010	0.0010
lm0364n5901	86.49151	-67.14732	2.347977	16.56	16.51	374.8669	0.913	-0.0040	-0.101	0.0020	-0.027	0.0010
lm0437n8267*	77.38103	-66.11499	2.353292	17.49	17.33	2082.9236	0.937	-0.0030	-0.068	-0.0020	-0.027	0.0
lm0287n14280*	73.57127	-67.55517	2.353686	17.40	17.15	1550.6252	0.977	-0.0030	-0.065	-0.0030	-0.046	-0.0010
lm0223n30265	85.87513	-68.33033	2.355531	15.64	15.40	1477.7595	0.894	-0.035	-0.151	-0.0050	-0.067	0.0
lm0091n16520	79.31001	-69.29892	2.361363	16.11	15.91	1894.6111	0.943	-0.03	-0.065	-0.0010	-0.013	0.0080
lm0031m19305	85.28377	-69.17464	2.361448	16.81	16.83	1079.8238	0.882	-0.067	-0.16	-0.033	-0.077	-0.0
lm0294n9088	74.43098	-67.16268	2.365682	16.87	16.75	1273.4985	0.88	-0.071	-0.161	-0.036	-0.079	0.0020
lm0033m29238*	85.53677	-69.57492	2.369442	17.11	17.03	1255.6286	0.981	-0.0040	-0.02	0.0010	-0.015	-0.0030
lm0355n19896*	85.67514	-67.23285	2.37175	17.39	17.38	2239.8177	0.98	0.0	-0.024	0.0	-0.019	0.0020
lm0363m3939*	87.71331	-66.62361	2.373044	17.97	17.80	2317.7067	0.969	-0.0020	-0.04	-0.0030	-0.025	-0.0030
lm0314n10346	77.74369	-67.1175	2.375213	15.35	15.12	948.4991	0.993	-0.0040	-0.014	-0.0040	-0.01	0.0
lm0205l5928	81.64704	-68.53675	2.37907	17.00	17.00	1823.8086	0.97	-0.014	-0.024	-0.0010	0.0	-0.0010
lm0012124572*	79.93726	-69.70587	2.3808	17.70	17.55	2184.7521	0.941	-0.0080	-0.089	-0.0050	-0.047	0.0050
lm0120112772	72.0101	-69.28588	2.381339	16.75	16.58	2186.6509	0.983	-0.01	-0.022	0.0060	-0.012	-0.0010
lm0367m17417*	87.39254	-67.42827	2.381462	16.60	16.46	1581.7108	0.977	0.0060	-0.041	0.0060	-0.039	0.0010
lm0541m17201	74.39101	-70.55125	2.381813	16.34	16.07	1924.6018	0.92	-0.05	-0.115	-0.017	-0.044	0.0010
lm0427m16915	76.0344	-66.02195	2.382868	17.37	17.06	2191.6631	0.97	-0.0090	-0.049	-0.016	-0.026	0.0070
lm0355m8399	85.75041	-67.0058	2.38434	16.70	16.54	1271.6074	0.997	-0.01	-0.0060	0.0010	-0.0010	-0.0
lm0035n29174	85.2573	-70.08448	2.385178	15.84	15.75	2225.7022	0.944	-0.0020	-0.114	-0.0010	-0.078	-0.0010
lm0290m16993	74.30885	-66.42699	2.386669	15.96	15.78	2161.7323	0.993	-0.0090	-0.012	-0.0030	-0.0080	-0.0010

APPENDIX A. PROPERTIES OF THE “HOT” ECLIPSING BINARIES IN THE LMC

lm0346n10735	83.11024	-67.53125	2.387713	15.28	15.06	1953.7492	0.873	-0.036	-0.153	-0.019	-0.058	0.0050
lm0354l9263	84.53328	-67.16815	2.388225	16.91	16.78	1192.7386	0.971	-0.027	-0.034	0.0010	0.0030	0.0020
lm0557l10945	76.16366	-71.7335	2.388866	17.07	16.83	1547.5995	0.972	0.0010	-0.064	-0.0050	-0.045	0.0070
lm0590m3501	83.99441	-70.50731	2.389369	16.33	16.09	2322.6754	0.961	-0.019	-0.035	0.0	-0.0020	-0.0
lm0187l17648	78.0774	-68.97554	2.390532	17.15	17.08	1774.8356	0.956	0.0020	-0.068	-0.0020	-0.045	-0.0
lm0165l9604	74.07694	-68.56038	2.390599	17.02	16.96	1497.5988	0.99	-0.02	-0.013	-0.0010	-0.0010	-0.0030
lm0297k16068	74.94967	-67.40864	2.394267	15.34	15.08	1927.6449	0.983	-0.0060	-0.014	-0.0010	0.0010	0.0010
lm0015m12964*	81.58582	-69.82269	2.394782	17.38	17.14	1198.6598	0.964	-0.0080	-0.049	0.0040	-0.033	0.0030
lm0556k7966	75.02718	-71.54348	2.398208	16.40	16.27	490.6397	0.984	-0.015	-0.011	-0.0020	0.0030	0.0010
lm0230l15982	86.08001	-67.91372	2.398351	16.89	16.74	1316.5454	0.97	0.0030	-0.035	-0.0050	-0.015	-0.0030
lm0305n13969	76.92468	-67.22035	2.399246	15.96	15.75	2183.7002	0.982	-0.0090	-0.017	-0.0010	-0.0010	0.0010
lm0093m6482	79.31403	-69.43746	2.400068	17.32	17.18	1511.6682	0.965	0.0010	-0.058	-0.0060	-0.039	0.0040
lm0030k7421	84.0848	-69.1045	2.403842	16.77	16.65	414.7142	0.963	-0.022	-0.05	-0.031	-0.02	-0.01
lm0344n9069	83.37507	-67.16455	2.40841	17.05	16.89	1500.7083	0.917	0.0030	-0.127	-0.0070	-0.083	-0.0020
lm0323n20798*	80.66736	-66.87361	2.408672	17.43	17.24	1619.5834	0.956	0.0010	-0.076	-0.0020	-0.06	0.0060
lm0033m27772	85.38415	-69.56713	2.411216	16.64	16.55	2239.6372	0.987	-0.0080	-0.017	-0.0030	-0.011	0.0010
lm0290n7998	74.37665	-66.45622	2.413031	15.78	15.90	792.7880	0.95	-0.02	-0.074	-0.014	-0.057	0.0
lm0037l4563	84.78055	-70.29163	2.413848	17.29	17.29	1186.7208	0.972	-0.0010	-0.05	-0.0010	-0.032	0.0010
lm0294k28142*	73.97016	-67.13081	2.418202	16.92	16.81	1237.6064	0.922	0.0050	-0.129	0.0030	-0.092	0.0030
lm0346k17136	82.6852	-67.42661	2.418824	15.97	15.28	809.6945	0.931	0.0010	-0.102	-0.0020	-0.057	0.0010
lm0030l15810	84.01883	-69.31956	2.419399	15.97	15.99	1510.6986	0.958	-0.012	-0.055	-0.0080	-0.029	0.0010
lm0056l25826	87.95228	-70.43383	2.419986	17.17	16.94	1917.8619	0.908	0.0010	-0.142	-0.0060	-0.089	-0.0040
lm0157n15497*	72.71625	-68.96325	2.427398	17.17	17.13	1792.7476	0.985	0.0010	-0.024	0.0	-0.015	0.0
lm0015n17499	81.72312	-69.99707	2.431098	16.87	16.74	1530.6941	0.931	-0.0020	-0.103	-0.0020	-0.066	-0.0010
lm0325m19625*	80.36654	-67.07111	2.431928	15.94	15.71	800.6959	0.989	-0.0030	-0.02	-0.0010	-0.018	-0.0010
lm0105l16640	76.99286	-70.07014	2.433279	17.10	16.98	1212.6100	0.986	0.0	-0.025	0.0010	-0.014	-0.0030
lm0345m8490	83.84136	-67.00352	2.434907	15.70	15.41	1815.8120	0.943	-0.0050	-0.1	-0.0050	-0.066	-0.0010
lm0325n9718	80.64354	-67.15893	2.436797	16.72	16.55	1858.6030	0.989	-0.0040	-0.019	-0.0060	-0.011	-0.0010
lm0013n22558	81.2643	-69.67498	2.437445	16.01	16.14	857.7605	0.941	-0.036	-0.066	-0.0050	-0.060	0.0030
lm0344l18357	82.70144	-67.23384	2.442181	16.60	16.41	1940.7662	0.98	-0.02	-0.035	-0.02	-0.026	-0.0020
lm0550m23266	75.58039	-70.6071	2.443675	15.44	15.11	835.6237	0.947	0.0060	-0.066	0.0020	-0.02	0.0
lm0340l22963	82.77249	-66.57868	2.447199	15.95	15.74	1148.8286	0.931	-0.0	-0.102	-0.0050	-0.061	-0.0
lm0331n5533	82.11053	-66.48606	2.44858	15.95	15.64	701.7900	0.989	-0.0090	-0.090	-0.018	-0.0070	-0.0050
lm0035k5826	85.17619	-69.79019	2.457281	16.15	16.08	1483.7020	0.972	-0.017	-0.041	-0.016	-0.024	-0.0030
lm0551n5128*	76.70335	-70.74281	2.457712	17.69	17.45	842.6809	0.963	-0.0050	-0.059	-0.011	-0.022	0.0020
lm0165l14067	74.19318	-68.58468	2.457888	16.57	16.43	2263.6042	0.946	-0.035	-0.067	-0.0060	-0.019	0.0020
lm0374n6499	88.47515	-67.14809	2.459114	17.11	16.93	2057.5077	0.984	-0.0080	-0.028	-0.013	-0.021	0.0
lm0345m13290	84.10019	-67.03212	2.46055	16.11	15.78	1077.8037	0.969	-0.013	-0.043	-0.01	-0.026	0.0
lm0120l22437	72.16619	-69.3588	2.465148	16.56	16.43	2191.6165	0.963	-0.0080	-0.04	-0.0040	-0.0090	0.0010
lm0344k5068	82.7452	-66.9896	2.465608	16.30	16.14	1618.6821	0.981	-0.0030	-0.04	-0.014	-0.02	0.0080
lm0343l28019	83.61952	-66.937	2.467596	16.55	16.37	1254.6180	0.986	-0.014	-0.024	-0.0060	-0.017	0.0040

lm0285125392*	73.30353	-67.2703	2.468374	16.33	16.06	1546.7474	0.978	-0.0040	-0.022	-0.0030	-0.017	0.0020
lm0213k24315	83.4129	-68.13946	2.469496	16.87	16.81	1883.6801	0.95	0.0020	-0.082	-0.0010	-0.05	0.0040
lm0093m4296	79.48343	-69.42473	2.469981	16.33	16.13	574.5017	0.888	-0.064	-0.153	-0.031	-0.075	0.0010
lm0545m6699	74.75974	-71.18265	2.471238	16.90	16.71	1775.7720	0.904	-0.013	-0.125	-0.0030	-0.039	-0.0010
lm002415083	82.0993	-69.94233	2.471267	16.33	16.44	2225.8015	0.917	-0.063	-0.125	-0.022	-0.055	0.0030
lm0406l944*	93.19933	-67.49614	2.473836	17.35	17.26	1641.5820	0.916	-0.0050	-0.102	-0.0070	-0.035	0.0030
lm0095m32814	79.49724	-69.92743	2.474934	17.16	17.06	532.5152	0.948	-0.0030	-0.083	-0.0020	-0.033	-0.0020
lm0121120722	73.05065	-69.32508	2.476666	16.50	16.41	864.6842	0.998	-0.023	-0.090	-0.0050	-0.090	0.0020
lm0321m17018*	80.38102	-66.35411	2.48037	16.18	15.84	1955.6702	0.929	0.0010	-0.132	0.0020	-0.099	-0.0070
lm0317k7278	78.45743	-67.35601	2.480964	15.37	15.13	420.7769	0.975	-0.0060	-0.031	-0.0040	-0.021	0.0010
lm0344k24636	82.91964	-67.12202	2.483249	15.52	15.32	1091.8088	0.961	-0.023	-0.053	-0.0020	-0.040	0.0020
lm0284n19951	72.80519	-67.24532	2.483961	16.07	15.80	1546.7474	0.961	-0.0050	-0.065	-0.0070	-0.045	0.0050
lm016711590*	74.25992	-68.93697	2.484712	16.77	16.58	434.7245	0.967	0.0020	-0.043	0.0010	-0.02	0.0
lm0106k14838	76.23628	-70.19882	2.485333	15.62	15.55	2250.5739	0.935	-0.0090	-0.119	-0.0040	-0.083	-0.0020
lm0550m14903	75.48979	-70.7021	2.487136	16.15	15.88	1243.5615	0.999	-0.047	-0.0040	-0.0040	-0.090	0.0030
lm0427110110	75.28292	-66.13402	2.489254	16.72	16.48	1927.6506	0.944	-0.014	-0.073	-0.0080	-0.043	0.0
lm0331k10198	81.90125	-66.31168	2.490214	16.51	16.33	1455.7731	0.983	-0.021	-0.02	-0.0010	0.0010	0.0020
lm001017439*	79.98371	-69.32095	2.493082	15.73	15.50	1396.9036	0.97	-0.0060	-0.019	-0.0030	-0.040	0.0030
lm0307k13715	76.50485	-67.3919	2.495074	16.66	16.46	845.7351	0.979	-0.049	-0.06	-0.014	-0.029	-0.0010
lm0542117356	72.97089	-71.06788	2.495564	16.59	16.54	1811.7353	0.987	-0.016	-0.012	0.0020	-0.0010	0.0
lm0457n6420	80.83767	-66.09135	2.495654	15.64	15.41	1951.7180	0.897	-0.046	-0.118	-0.016	-0.045	0.012
lm0572k3238*	79.50726	-70.81947	2.495964	17.66	17.58	1126.6354	0.946	0.0070	-0.086	0.0050	-0.041	-0.0060
lm0040k11551*	86.09652	-69.12661	2.499232	16.99	16.78	1634.5805	0.971	-0.0	-0.031	0.0	-0.018	-0.0010
lm0032120643	84.01087	-69.69192	2.499392	15.45	15.24	1148.5930	0.984	-0.0070	-0.016	-0.0	-0.0080	0.0020
lm012118367*	73.15498	-69.25074	2.500777	16.28	16.07	1306.4884	0.973	-0.034	-0.03	-0.02	-0.017	0.0020
lm0015m19643	81.65213	-69.857	2.50362	16.82	16.66	387.7572	0.981	0.0030	-0.04	-0.0050	-0.031	-0.0
lm0045k19706	86.9848	-69.86957	2.505617	15.05	14.88	1589.7317	0.988	-0.027	-0.024	-0.01	-0.017	-0.0030
lm0010m6843	80.31027	-69.09451	2.505974	15.92	15.57	438.7844	0.946	0.0020	-0.095	-0.01	-0.061	0.0080
lm0303m21604	76.8608	-66.72639	2.50701	16.29	16.05	1191.6543	0.98	-0.035	-0.037	-0.0010	-0.0010	0.0020
lm0346m16504	82.99672	-67.41379	2.508841	15.91	15.71	2234.8536	0.982	-0.0010	-0.019	-0.0020	-0.012	0.0020
lm0216121415	82.66991	-69.01434	2.509407	15.99	15.81	2190.7652	0.985	-0.0040	-0.037	0.0010	-0.021	0.0
lm0021132167	82.79402	-69.38642	2.512288	16.64	16.74	748.7738	0.96	-0.04	-0.067	-0.018	-0.03	-0.0020
lm0540n13869	73.49776	-70.6908	2.512757	16.07	15.89	1833.6867	0.935	-0.0	-0.084	0.0	-0.028	-0.0
lm0256m23734*	90.21733	-68.88663	2.513574	17.77	17.53	2030.5829	0.966	-0.0060	-0.047	0.0010	-0.03	0.0
lm0596119261	83.43063	-71.81285	2.515392	17.38	17.17	1617.6885	0.939	-0.038	-0.049	-0.0010	-0.060	0.0040
lm0020126644	81.8095	-69.38345	2.516899	16.72	16.56	2025.5258	0.897	-0.08	-0.144	-0.037	-0.07	0.0030
lm018016512	77.02743	-67.84095	2.516909	15.79	15.54	1172.8434	0.93	-0.035	-0.092	-0.015	-0.04	0.0050
lm0567k6881	78.04749	-71.54482	2.520574	17.25	17.11	2343.5725	0.958	-0.034	-0.04	0.0	-0.0030	-0.0050
lm0040m27318	86.37798	-69.2243	2.522133	15.72	15.60	1941.6268	0.868	-0.061	-0.182	-0.033	-0.088	0.0020
lm0343122832	83.59525	-66.89561	2.527193	15.04	14.83	1893.7021	0.917	-0.0060	-0.102	-0.0030	-0.025	0.0010
lm0186m5534	77.24272	-68.89526	2.529495	16.16	16.04	477.7326	0.951	-0.049	-0.087	-0.025	-0.049	-0.0090



APPENDIX A. PROPERTIES OF THE “HOT” ECLIPSING BINARIES IN THE LMC

Im0206m28489	16.81	16.72	1435.7606	0.956	-0.0090	-0.052	-0.0080	-0.036	0.0070
Im00097m15434	16.27	16.06	1957.6478	0.906	-0.0070	-0.116	-0.0040	-0.043	0.0010
Im00015m13576	16.77	16.72	1367.8727	0.946	-0.036	-0.067	-0.019	-0.032	-0.0030
Im00023k3564	17.13	17.07	507.5296	0.978	0.0070	-0.06	-0.0010	-0.047	-0.0020
Im0190m11239*	17.27	17.10	1766.9130	0.944	0.0090	-0.081	-0.0020	-0.065	-0.0020
Im0294l11216	17.00	16.40	2256.5844	0.962	-0.0050	-0.054	-0.018	-0.025	-0.0090
Im00104l210	16.60	16.86	588.5004	0.943	-0.072	-0.104	-0.035	-0.063	-0.0070
Im0466m15347	16.68	16.62	795.7699	0.978	-0.019	-0.023	-0.0020	0.0	-0.0020
Im0212m18380	17.21	17.23	1530.7138	0.955	0.01	-0.087	-0.0030	-0.056	-0.012
Im0347m14660	16.36	16.10	1364.9387	0.959	-0.012	-0.058	-0.017	-0.032	-0.0060
Im0010k17235	16.21	15.94	1959.6465	0.943	-0.010	-0.057	-0.0010	-0.017	0.0010
Im0333k24619	15.71	15.51	1977.6400	0.98	-0.012	-0.02	-0.0040	-0.0090	0.0010
Im0105m14713*	16.83	16.68	1496.6366	0.979	0.020	-0.029	-0.0010	-0.011	0.0
Im0581m21519	17.10	16.95	1901.8440	0.949	-0.063	-0.076	-0.028	-0.05	-0.0050
Im0155n22259	17.14	17.02	1523.6658	0.947	-0.051	-0.084	-0.02	-0.04	-0.0020
Im0457k24667	16.76	16.59	1786.7633	0.98	-0.0080	-0.03	-0.0050	-0.016	-0.0010
Im0100m16266	16.74	16.46	2303.6323	0.937	-0.034	-0.074	-0.0080	-0.018	0.0010
Im0170m4805	16.19	15.86	334.9063	0.909	-0.049	-0.108	-0.021	-0.045	-0.0040
Im0307m15491	16.78	16.63	1589.6733	0.887	-0.01	-0.153	-0.012	-0.076	0.0010
Im0292m23708	16.08	15.84	1463.6953	0.916	0.020	-0.151	-0.010	-0.08	-0.0070
Im0586l13797	16.37	16.18	2389.5114	0.954	-0.0060	-0.084	-0.0020	-0.058	0.0
Im0112l18575	16.56	16.36	1603.6181	0.911	-0.057	-0.125	-0.025	-0.056	-0.0030
Im0177k17667	16.51	16.28	1711.9094	0.963	-0.015	-0.026	-0.0020	0.0020	-0.0
Im0020k24655	15.95	15.73	1096.6711	0.915	-0.013	-0.129	-0.0	-0.074	0.0050
Im0602l6118	15.61	15.68	1266.6051	0.972	0.050	-0.084	0.0010	-0.061	0.0
Im0211ms293	15.95	15.70	390.7804	0.972	-0.01	-0.035	-0.0010	-0.015	0.0
Im0054m17797	16.09	15.98	1833.8282	0.982	-0.013	-0.063	-0.0040	-0.048	0.0010
Im0343l25613	15.68	15.49	1538.7375	0.951	-0.014	-0.049	-0.0040	-0.01	0.0010
Im0341n5260	14.90	14.61	2579.7163	0.964	-0.0080	-0.059	-0.0060	-0.04	-0.0040
Im0355n26448	15.07	14.76	405.8522	0.974	-0.015	-0.024	0.0030	-0.0	0.0030
Im0331k18134	16.69	16.50	1120.7651	0.939	0.0040	-0.089	0.0030	-0.048	0.0
Im0041k21578	17.03	16.89	1620.6137	0.991	-0.0070	-0.02	-0.0040	-0.014	-0.0
Im0012m2814	16.84	16.59	812.7853	0.965	-0.046	-0.044	-0.0040	-0.0090	-0.0020
Im0366m14428	16.80	17.02	1899.8172	0.98	0.0030	-0.048	0.0030	-0.035	0.0010
Im0427m16528	16.28	15.99	1899.8172	0.962	-0.028	-0.03	0.0010	0.0010	0.0020
Im0340n5836	15.75	15.47	517.5934	0.967	-0.012	-0.056	-0.0080	-0.037	0.0020
Im0040k23476	15.90	15.70	1463.7628	0.935	-0.0080	-0.105	-0.0080	-0.07	-0.0010
Im0116l19585*	16.72	16.52	1901.7951	0.975	-0.019	-0.053	-0.016	-0.032	0.0050
Im0212m20099*	16.92	16.86	1447.7468	0.975	-0.010	-0.043	-0.0050	-0.039	0.0080
82.87114	2.621128		2343.5959	0.968	-0.0060	-0.039	-0.0010	-0.021	-0.0010
81.03877	2.531791								
79.41568	2.532518								
81.38394	2.534117								
82.85258	2.536665								
78.96418	2.538094								
74.07755	2.546991								
79.84039	2.551967								
81.479	2.552722								
82.72618	2.553893								
84.04889	2.554528								
80.18843	2.556111								
82.01793	2.556706								
77.47108	2.55891								
82.77934	2.559421								
72.62359	2.560105								
80.38014	2.561858								
83.54977	2.561989								
76.62051	2.565832								
75.23106	2.566232								
77.24938	2.569726								
77.24916	2.56975								
74.27014	2.569894								
81.46549	2.574108								
74.15131	2.574239								
75.82558	2.577507								
82.13845	2.579334								
85.65851	2.580945								
83.8299	2.58613								
88.22564	2.586745								
83.61661	2.589002								
83.86604	2.58955								
85.90168	2.592722								
81.88285	2.592838								
87.06688	2.595648								
80.39538	2.595659								
86.8028	2.601096								
75.77647	2.608226								
83.1235	2.614459								
85.916	2.615418								
74.01844	2.61797								
82.87114	2.621128								

lm0303n16128	76.82415	-66.84364	2.62196	17.01	16.86	2535.7713	0.947	-0.014	-0.091	-0.011	-0.068	-0.0090
lm0551m7343	76.66848	-70.49136	2.622983	17.33	17.03	1126.6152	0.912	-0.072	-0.116	-0.027	-0.049	-0.0010
lm0377l5586	89.15001	-67.60273	2.628894	16.59	16.31	1861.7884	0.93	-0.047	-0.105	-0.015	-0.042	-0.0010
lm0020l9813	81.92152	-69.27233	2.631352	15.84	15.58	434.6709	0.942	-0.0090	-0.087	-0.0050	-0.061	-0.0020
lm0345k13606	83.55195	-67.04492	2.631534	14.90	14.71	395.6878	0.929	-0.027	-0.109	-0.011	-0.057	-0.0
lm0316l17312	77.64399	-67.57343	2.631631	16.53	16.34	1906.8206	0.981	-0.0040	-0.026	-0.0020	-0.017	-0.0010
lm0183l17185	77.70033	-68.24991	2.634221	17.10	17.01	2517.7988	0.982	-0.015	-0.026	-0.0060	-0.015	0.0010
lm0090n29324	78.34942	-69.3802	2.636584	15.96	15.97	2009.5215	0.952	0.0	-0.119	-0.01	-0.078	0.011
lm0543n18447*	74.71233	-71.0528	2.63776	16.73	16.51	2198.7862	0.96	-0.0030	-0.068	-0.0010	-0.054	0.0010
lm0220n19791*	84.80013	-67.93172	2.641188	16.70	16.51	2305.7351	0.972	-0.0050	-0.038	-0.0060	-0.028	0.0010
lm0335n24071	82.45012	-67.24932	2.641403	16.14	15.91	1463.7486	0.99	-0.0090	-0.017	0.0020	-0.0	-0.0030
lm0294l21960	73.98799	-67.24958	2.641427	15.39	15.17	1575.6394	0.963	-0.019	-0.031	-0.0010	-0.0020	0.0040
lm0200l6405	80.58213	-67.84146	2.649042	15.77	15.58	2329.6599	0.987	-0.0090	-0.022	-0.0050	-0.014	0.0010
lm0130m14780*	70.56684	-69.1412	2.650674	17.75	17.56	1838.6513	0.945	0.0050	-0.06	-0.0050	-0.041	0.0050
lm0465l26736	82.04834	-65.88179	2.654428	15.86	15.63	1761.8323	0.92	-0.034	-0.09	-0.01	-0.025	0.0080
lm0184k17447	76.9537	-68.45944	2.656173	16.54	16.41	1374.9038	0.885	-0.088	-0.179	-0.043	-0.095	0.0010
lm0216l17243	82.53308	-68.98278	2.657392	15.88	15.74	1424.8947	0.924	-0.045	-0.106	-0.018	-0.036	0.0010
lm0013l21404	81.15178	-69.66975	2.658097	16.67	16.58	1866.6505	0.992	-0.019	-0.018	-0.0	-0.0030	0.0
lm0037n10595*	85.59315	-70.32818	2.658698	16.45	16.33	2323.6869	0.985	-0.030	-0.032	-0.0020	-0.014	-0.0
lm0124m15092	72.48036	-69.84957	2.659129	16.47	16.38	2231.5516	0.968	-0.03	-0.036	-0.0	-0.0	-0.0010
lm0173m21250*	76.52163	-68.11563	2.661334	16.02	15.71	1139.7472	0.976	-0.014	-0.049	-0.0090	-0.039	0.0
lm0230l9562	86.31025	-67.86845	2.662658	17.05	16.89	1775.9264	0.896	-0.046	-0.138	-0.022	-0.059	0.0020
lm0173n13333	76.4494	-68.2276	2.665684	17.29	17.14	1468.6078	1.003	-0.014	-0.023	-0.0050	-0.02	0.0020
lm0115k4086	74.91607	-69.77763	2.666177	15.36	15.24	2280.5789	0.983	-0.025	-0.028	-0.0020	0.0	-0.0040
lm0195m16673*	80.27267	-68.44344	2.666476	16.11	15.91	1136.8411	0.963	-0.0040	-0.047	-0.0040	-0.019	0.0020
lm0155m28483	72.70091	-68.52691	2.667227	16.84	16.58	1833.6610	0.976	0.0060	-0.044	-0.0020	-0.029	-0.0020
lm0344m24630	83.25301	-67.11572	2.667896	15.46	15.23	1256.5883	0.985	-0.0060	-0.028	-0.0050	-0.02	0.0
lm0127l9642	73.14306	-70.31871	2.669394	16.88	16.63	2471.8652	0.975	-0.038	-0.035	-0.018	-0.033	0.0010
lm0285m10287	73.37918	-67.01608	2.669725	15.30	15.12	2199.7855	0.96	-0.0040	-0.039	-0.0060	-0.015	0.0040
lm0045k10445*	87.16535	-69.8126	2.669896	15.78	15.66	2269.7456	0.95	0.0	-0.086	0.0010	-0.063	0.0
lm0011m22713	81.37201	-69.18227	2.674348	16.13	15.86	1711.9362	0.98	0.0030	-0.034	-0.0030	-0.019	0.0010
lm0125m5589	73.74855	-69.77929	2.676261	15.04	14.77	1076.6950	0.957	-0.0010	-0.069	-0.0020	-0.036	-0.0010
lm0174l12903*	74.82639	-68.60046	2.676506	17.53	17.43	1848.6318	0.92	0.0010	-0.045	-0.0020	-0.015	0.0040
lm0330n19300*	81.32542	-66.53023	2.677262	17.72	17.76	1968.6406	0.976	0.0030	-0.048	-0.0050	-0.035	0.0020
lm0685n23191	77.55507	-72.85828	2.678273	17.25	17.13	2214.7789	0.926	-0.0	-0.12	-0.0010	-0.068	-0.0020
lm0186m8773	77.37151	-68.91724	2.678832	15.08	14.81	496.6719	0.947	-0.025	-0.076	-0.015	-0.051	0.0060
lm0022k3890*	82.1389	-69.43238	2.680612	16.57	16.48	1941.6202	0.98	-0.0	-0.036	-0.0010	-0.023	0.0020
lm0092m3797*	78.43077	-69.43449	2.683288	17.36	17.31	1096.6877	0.97	-0.0040	-0.062	-0.0010	-0.039	-0.0040
lm0093m11981	79.42347	-69.46606	2.68737	16.31	16.17	1771.8776	0.932	-0.046	-0.082	-0.019	-0.042	0.0040
lm0571n26162	80.64243	-70.75	2.68743	16.07	15.84	351.8187	0.972	-0.0080	-0.04	-0.0060	-0.023	-0.0
lm0177l21797	75.94157	-69.00561	2.687489	16.96	16.73	2307.6238	0.983	-0.025	-0.038	0.0020	-0.0010	-0.0030

APPENDIX A. PROPERTIES OF THE “HOT” ECLIPSING BINARIES IN THE LMC

lm0530m21215	71.54592	2.687638	16.26	16.02	2305.6051	0.954	-0.026	-0.071	-0.0070	-0.015	-0.0010
lm0165k28784	73.92743	2.691754	16.85	16.83	1107.8097	0.887	-0.05	-0.16	-0.036	-0.082	0.014
lm0564k4754	77.14207	2.692888	16.11	15.95	1070.8255	0.983	-0.0040	-0.023	-0.0040	-0.014	0.0010
lm0241k13248*	88.96394	2.695078	16.93	16.73	2143.8261	0.945	-0.0010	-0.067	-0.0020	-0.022	0.0030
lm0165k13612	74.30469	2.696423	15.14	14.93	1928.5757	0.967	-0.0060	-0.05	-0.0030	-0.034	-0.0030
lm0213k23159*	83.44848	2.700634	16.94	16.82	1906.8448	0.984	-0.0030	-0.034	-0.0060	-0.013	-0.0060
lm0215m2414	83.66528	2.701612	16.01	15.79	1483.6936	0.971	-0.01	-0.011	-0.055	-0.017	0.023
lm029115438	74.86958	2.70368	15.88	15.74	1809.7745	0.909	-0.048	-0.137	-0.02	-0.055	0.0020
lm0213n30527*	83.70361	2.703828	17.15	17.03	858.6189	0.952	-0.0030	-0.091	-0.0060	-0.085	0.0020
lm0115k17125	75.08609	2.707842	16.52	16.43	1154.8513	0.891	-0.061	-0.14	-0.028	-0.06	0.0060
lm0164m26844	73.45852	2.709069	17.23	17.16	1898.7369	0.959	-0.016	-0.062	-0.025	-0.032	0.013
lm0015m15054	81.70531	2.709872	17.03	16.99	1224.5329	0.969	-0.0020	-0.025	-0.01	-0.0070	0.0070
lm0012n14828	80.45366	2.71287	16.09	15.93	1878.6691	0.971	-0.026	-0.042	-0.01	-0.022	-0.0020
lm0103k10582	76.95848	2.713007	16.09	16.03	414.7172	0.914	-0.055	-0.111	-0.025	-0.047	0.0060
lm0431n15433	77.305	2.714038	16.93	16.76	2096.8743	0.932	-0.053	-0.064	-0.011	-0.021	0.0090
lm0311n21352	78.7045	2.715097	16.44	16.26	1463.7082	0.932	-0.059	-0.104	-0.026	-0.053	0.0010
lm0185n22544*	78.19087	2.7182	17.35	17.22	1851.6120	0.963	-0.015	-0.064	-0.017	-0.051	-0.0010
lm0333m22120*	82.20273	2.720332	15.92	15.66	1184.6748	0.978	-0.0070	-0.031	-0.0020	-0.0090	0.0020
lm0325k28914*	80.03764	2.72169	16.63	16.52	1493.7102	0.932	-0.0090	-0.063	-0.0040	-0.0040	0.0010
lm0172n6253	75.27408	2.727663	15.53	15.29	775.8599	0.956	-0.016	-0.075	-0.0050	-0.052	0.0010
lm0206k25944	80.81531	2.73146	16.21	16.03	1730.9271	0.981	-0.027	-0.035	-0.0010	-0.030	0.0030
lm0294l8864	73.76054	2.740388	15.14	14.77	1253.5437	0.945	-0.0090	-0.087	-0.0060	-0.063	0.0
lm0091m28603*	79.70007	2.74089	16.96	16.81	1193.6169	0.952	0.0020	-0.053	-0.0020	-0.029	-0.0030
lm0123k17044	73.229	2.744816	15.52	15.42	1581.5896	0.963	-0.019	-0.033	0.0010	0.0020	0.0030
lm0027119420	83.10967	2.745088	16.89	16.82	1435.7638	0.931	-0.061	-0.085	-0.018	-0.038	0.013
lm0020k16826	81.94932	2.747223	15.35	15.17	569.5124	0.917	-0.043	-0.111	-0.022	-0.049	0.0030
lm0205m4021	81.99126	2.749866	17.02	16.85	1082.8700	1.007	-0.027	-0.015	-0.0070	-0.0090	-0.0030
lm0294n7479	74.52813	2.75026	16.19	15.97	2192.6865	0.962	-0.026	-0.036	0.0020	0.0	0.0030
lm0204118900	80.53603	2.754503	17.23	17.05	2198.6817	0.918	0.0070	-0.084	0.0090	-0.055	-0.0090
lm0231112015*	87.04159	2.754824	16.67	16.49	1879.6968	0.992	0.0050	-0.025	-0.0020	-0.021	-0.0010
lm0036m17521	84.42606	2.755856	16.42	16.26	491.5981	0.956	-0.015	-0.067	-0.0070	-0.041	0.0040
lm0556m17386*	75.7215	2.755996	17.85	17.67	2200.7675	0.968	-0.011	-0.045	-0.0060	-0.033	0.0070
lm0417n17063	74.21734	2.760288	16.55	16.39	1820.6634	0.96	-0.010	-0.05	-0.0010	-0.026	0.0010
lm0091n21452	79.64253	2.765244	16.95	16.84	2161.7543	0.947	-0.077	-0.093	-0.028	-0.06	-0.0040
lm0611m4959	89.1808	2.767514	16.87	16.61	2237.6572	0.936	-0.0040	-0.115	-0.0020	-0.079	-0.0020
lm0541k20099*	73.74083	2.768156	17.12	17.02	2258.7505	0.972	-0.0080	-0.05	-0.0030	-0.017	-0.0020
lm0093l26030	79.19029	2.772257	16.76	16.77	2349.5849	0.975	-0.03	-0.023	-0.0020	-0.0020	-0.0040
lm0025k17489	82.89583	2.773556	16.95	16.90	1480.8463	0.937	-0.0070	-0.094	-0.0010	-0.046	-0.0020
lm0176k25619	75.07291	2.774489	15.73	15.50	1884.6086	0.925	-0.027	-0.077	-0.0080	-0.015	0.011
lm0346n23003	83.1751	2.777051	15.29	14.97	1258.5926	0.942	-0.0010	-0.088	-0.0050	-0.052	-0.0020
lm0177n10023	76.25629	2.777775	16.35	16.20	361.8658	0.962	-0.037	-0.053	-0.012	-0.022	-0.0020

lm0033k11425	84.84785	-69.46915	2.780835	15.79	15.73	365.7526	0.951	-0.02	-0.039	0.0010	0.0020	0.0070
lm0604l25268	85.55837	-71.47772	2.781504	16.29	16.13	1819.8138	0.955	-0.016	-0.03	0.0030	-0.0010	-0.0
lm0427k15685	75.52656	-66.07629	2.791595	15.83	15.53	1946.6815	0.963	-0.022	-0.038	0.0	0.0010	0.0040
lm0337k18241	81.96413	-67.42895	2.793995	15.50	15.31	2207.6279	0.988	0.0040	-0.027	-0.0010	-0.019	-0.0030
lm0580m16604*	81.83325	-70.55214	2.796134	16.68	16.51	1894.7423	0.964	-0.0020	-0.046	-0.0010	-0.036	0.0020
lm0156m2401	71.936	-68.79046	2.797172	16.26	16.13	1830.6572	0.964	-0.02	-0.031	0.0010	0.0	-0.0010
lm0344m16200*	83.14781	-67.06121	2.798582	16.26	16.06	1820.7202	0.989	-0.0060	-0.03	-0.0040	-0.023	-0.0010
lm0294l8466	73.94168	-67.16181	2.801658	16.87	16.67	835.6182	0.991	-0.013	-0.022	-0.013	-0.011	0.0010
lm0343k4683	83.41175	-66.62775	2.805072	15.25	15.01	2580.7284	0.91	-0.041	-0.13	-0.016	-0.061	0.0060
lm0162m24878*	73.48437	-68.178	2.808848	16.31	16.28	2294.6311	0.946	0.0010	-0.074	-0.0030	-0.029	0.0010
lm0466l16461*	81.34921	-66.23447	2.81516	15.73	15.70	2021.5871	0.973	-0.0040	-0.021	-0.0030	-0.0030	0.0010
lm0214n17417*	82.91098	-68.61314	2.816108	17.67	17.60	1839.7094	0.971	-0.011	-0.034	-0.0040	-0.021	-0.0040
lm0336k7065	80.85757	-67.34331	2.821258	16.06	15.96	1447.8177	0.957	-0.02	-0.04	0.0010	0.0010	0.0050
lm0191n4635	80.21988	-67.86435	2.822611	17.01	16.88	2031.5042	0.908	-0.08	-0.143	-0.033	-0.066	-0.0040
lm0351n10267*	85.72673	-66.58611	2.8255601	17.13	17.00	1189.7100	0.977	-0.0050	-0.023	-0.0010	-0.0040	0.0010
lm0106l11713	75.91194	-70.33262	2.827501	15.85	15.62	1755.8780	0.962	-0.011	-0.061	-0.0080	-0.047	-0.0
lm0014m9900*	80.38968	-69.81157	2.83114	17.62	17.60	1442.8081	0.971	-0.0070	-0.045	-0.0030	-0.041	-0.0050
lm0204k9178*	80.62568	-68.40605	2.839278	16.25	16.21	1927.7495	0.965	0.0	-0.038	-0.0020	-0.070	0.0010
lm0032k15660	84.04461	-69.53401	2.841496	14.72	14.52	1449.7822	0.965	-0.0050	-0.059	-0.0040	-0.038	-0.01
lm0195n5472	79.95177	-68.53449	2.841972	16.87	16.85	759.8540	0.892	-0.083	-0.149	-0.039	-0.084	-0.0050
lm0581l29010	82.62001	-70.76699	2.843662	16.73	16.71	2008.5601	0.943	-0.05	-0.081	-0.02	-0.032	0.0050
lm0020m12840*	82.38831	-69.28667	2.851276	16.98	16.73	2345.5803	0.954	-0.0090	-0.053	-0.0070	-0.014	0.0030
lm0034k12920*	84.06626	-69.83668	2.8522141	16.30	16.17	1997.5843	0.928	-0.0050	-0.095	0.0030	-0.035	0.0020
lm0021k13770	82.91711	-69.13302	2.853292	15.33	15.09	797.5801	0.88	-0.068	-0.171	-0.031	-0.086	0.0010
lm0541m10971	74.48554	-70.50982	2.861934	16.96	16.77	2188.6643	0.952	-0.052	-0.068	-0.013	-0.029	0.0010
lm0031k19705	85.2061	-69.21836	2.867536	14.91	14.97	1977.6787	0.916	-0.02	-0.086	-0.0060	-0.024	0.0030
lm0011n10445*	81.2678	-69.2638	2.867908	16.16	16.07	727.8740	0.97	-0.0040	-0.036	-0.0040	-0.013	0.0
lm0424n23353	75.09632	-65.86689	2.869312	15.03	14.68	332.8429	0.948	-0.0070	-0.085	-0.0050	-0.051	0.0020
lm0314m22740	77.72598	-67.0924	2.871881	16.77	16.81	1128.6838	0.89	-0.076	-0.149	-0.038	-0.066	0.0040
lm0165k19767*	74.30445	-68.46583	2.87351	16.99	16.92	1407.9117	0.97	-0.016	-0.051	-0.011	-0.047	0.0010
lm0321k15088*	80.21354	-66.42353	2.876456	17.00	16.83	1122.6202	0.995	-0.0030	-0.016	-0.0010	-0.0060	0.0010
lm0013k29788	81.08815	-69.56005	2.882388	15.93	15.95	2329.6567	0.974	-0.029	-0.028	0.0030	-0.0020	0.0010
lm0031l21280	85.01322	-69.33192	2.882489	16.08	15.99	2257.6709	0.979	-0.0020	-0.023	-0.011	-0.011	0.0050
lm0285m24289	73.57847	-67.10683	2.883361	16.38	16.15	1838.6761	0.977	-0.0020	-0.032	-0.0040	-0.017	0.0
lm0417m19623	74.2255	-66.07416	2.88552	15.85	15.57	1886.5721	0.957	-0.029	-0.047	-0.0050	-0.0080	0.0040
lm0105k31240	77.04771	-69.92838	2.887854	17.14	17.06	1503.6434	0.939	-0.042	-0.062	0.0010	-0.0040	0.0090
lm0541l17906	73.85615	-70.78171	2.895575	16.81	16.74	1835.6883	0.921	-0.069	-0.129	-0.031	-0.07	-0.0010
lm0331m17723	82.18919	-66.36106	2.896212	16.92	16.65	792.7472	0.976	-0.0040	-0.03	-0.0070	-0.018	-0.0010
lm0110l20525	74.09064	-69.34248	2.89896	16.46	16.28	1881.6086	0.95	0.0060	-0.094	-0.0020	-0.065	0.0090
lm0103k15198	77.065	-69.4846	2.899283	15.80	15.96	2270.7371	0.973	-0.0	-0.04	-0.0	-0.034	0.0010
lm0364k6997	86.16238	-67.00003	2.900784	17.02	16.87	456.7497	0.958	0.0010	-0.059	0.0020	-0.029	0.0010

APPENDIX A. PROPERTIES OF THE “HOT” ECLIPSING BINARIES IN THE LMC

Im0166118511	73.07786	68.98609	2.9026	15.65	15.42	426.7382	0.962	-0.024	-0.036	0.0030	0.0	0.0040
Im0120m24579*	72.50389	-69.35576	2.907138	15.87	15.82	1083.8175	0.976	-0.070	-0.029	-0.0040	-0.0050	-0.0
Im0345k23310	83.8351	-67.10524	2.908255	15.89	15.65	1994.5888	0.966	-0.030	-0.046	-0.027	-0.0080	0.015
Im0327m5927	80.55827	-67.33953	2.911755	15.88	15.61	1290.5196	0.918	-0.0030	-0.138	-0.0020	-0.081	-0.0010
Im0285m6767	73.5462	-67.14954	2.91176	17.23	17.00	1922.6488	0.978	-0.011	-0.045	-0.0060	-0.038	0.0020
Im0701l6892*	81.73971	-72.03964	2.912402	17.02	16.89	1528.6720	0.968	-0.0040	-0.038	-0.0040	-0.0080	0.0010
Im0216m15995	83.13799	-68.96256	2.913514	14.86	14.74	2056.4677	0.875	-0.056	-0.176	-0.024	-0.075	0.0
Im0614l19970*	87.57282	-71.44319	2.916522	17.16	17.34	2204.8174	0.958	-0.020	-0.046	0.0020	-0.027	-0.0030
Im0323m7828	80.33908	-66.79742	2.916801	16.43	16.24	405.8007	0.945	-0.0030	-0.084	-0.0010	-0.042	-0.0020
Im0024m7552	82.69505	-69.80001	2.917208	16.12	16.00	1480.8463	0.887	-0.084	-0.159	-0.039	-0.079	0.012
Im0120m11973	72.67068	-69.12053	2.917753	15.92	15.72	1766.8815	0.919	-0.046	-0.104	-0.014	-0.042	0.01
Im0025k31765	82.9931	-69.92558	2.918039	16.62	16.56	1480.8463	0.949	0.0020	-0.08	-0.0090	-0.05	-0.0080
Im0300k8884	75.75457	-66.30696	2.921834	16.91	16.64	1463.6953	0.969	-0.0090	-0.054	-0.0020	-0.042	0.0050
Im0294m28623	74.27429	-67.12564	2.922208	16.12	15.98	1472.6386	0.978	-0.0010	-0.044	0.0040	-0.028	0.0
Im0426m17949	75.10564	-66.17679	2.924628	16.47	16.18	2187.6958	0.982	-0.01	-0.024	-0.0060	-0.012	0.0020
Im0296m23406	74.18081	-67.4537	2.924942	16.77	16.59	845.7283	0.979	-0.011	-0.032	-0.0080	-0.023	0.0010
Im0303m5318	76.92088	-66.62704	2.926082	17.10	16.93	819.7995	0.957	-0.0030	-0.073	0.0	-0.045	-0.0010
Im0021k24967	83.20222	-69.20132	2.9261	15.43	15.19	1259.6007	0.945	0.0060	-0.082	0.0010	-0.051	-0.0010
Im0110l21211*	73.9183	-69.34737	2.926536	16.89	16.70	1771.8649	0.961	-0.0080	-0.069	-0.011	-0.054	0.0010
Im0335l8729	81.83248	-70.15958	2.931618	16.39	16.27	809.6847	0.909	-0.011	-0.123	-0.0050	-0.042	0.0
Im0560m7493	77.45808	-69.49391	2.934794	16.11	16.17	1140.5975	0.954	-0.043	-0.061	-0.012	-0.032	0.0040
Im0312m15741*	77.94811	-66.8564	2.935118	16.86	16.55	2131.8057	0.979	-0.0080	-0.028	-0.0040	-0.015	-0.0020
Im0112n21013	74.45324	-69.67947	2.938561	15.11	14.93	2315.6271	0.976	-0.013	-0.029	-0.0020	-0.0070	0.0020
Im0340k22602*	82.8816	-66.42372	2.940286	17.72	17.52	1941.7750	0.968	0.0010	-0.057	-0.0010	-0.017	0.0010
Im0041n7760*	87.2648	-69.26173	2.945402	17.39	17.02	1272.6320	0.969	-0.01	-0.039	-0.0040	-0.011	0.0010
Im0326l11003	79.35985	-67.52361	2.94932	17.22	17.02	1855.7875	0.962	-0.0080	-0.055	-0.0090	-0.027	-0.01
Im0051n15468	89.46855	-69.30452	2.949872	17.05	16.86	1883.7779	0.952	-0.036	-0.049	-0.0	-0.0060	0.0030
Im0344k13297	82.77059	-67.04496	2.950326	15.65	15.44	2265.8050	0.985	0.0040	-0.015	-0.0030	-0.0050	-0.0010
Im0114k26929	74.05413	-69.92131	2.950903	15.96	15.80	1137.8006	0.966	-0.0010	-0.044	-0.0060	-0.022	-0.0030
Im0230l9767*	86.11941	-67.86997	2.953796	17.28	17.09	384.8400	0.962	-0.0080	-0.054	-0.0060	-0.043	-0.0
Im0207m16357	82.0992	-68.80512	2.956567	15.30	15.04	1759.8484	0.908	-0.011	-0.131	-0.0060	-0.076	-0.0020
Im0101k24223*	76.99818	-69.20334	2.95906	16.39	16.30	1905.7517	0.913	-0.01	-0.116	-0.0010	-0.05	0.0
Im0122m2614*	72.71173	-69.41842	2.963894	16.04	15.83	2172.6922	0.969	0.0040	-0.038	-0.0010	-0.028	0.0
Im0112k21024	74.26042	-69.5569	2.966307	15.44	15.26	428.6244	0.985	-0.019	-0.024	-0.0010	0.0010	-0.0010
Im0347m23821	83.95327	-67.46569	2.970994	15.77	15.52	1190.7742	0.98	-0.01	-0.025	-0.0080	-0.013	0.0
Im0032n10570	84.62591	-69.62399	2.971654	15.73	15.57	403.6255	0.988	-0.021	-0.018	-0.0010	-0.020	-0.0020
Im0090k3504	78.10337	-69.07876	2.972621	15.73	15.61	380.7049	0.984	-0.012	-0.044	-0.0060	-0.026	0.0010
Im0335k26756	82.00323	-67.11539	2.97543	16.36	16.32	1964.6408	0.895	-0.079	-0.168	-0.045	-0.085	-0.01
Im0444n15607	78.12441	-65.80446	2.977039	17.03	16.94	1793.7590	0.948	-0.026	-0.037	0.0030	0.0020	0.0010
Im0294m4825	74.53203	-66.98277	2.97779	15.18	14.95	1306.4950	0.959	-0.03	-0.058	-0.0090	-0.02	0.0010
Im0331k23717*	81.79068	-66.42442	2.9901454	16.42	16.30	1660.5094	0.961	-0.014	-0.035	0.0030	-0.0010	0.0080

lm0093m17914*	79.46277	-69.49655	3.011341	16.08	15.96	361.7824	0.886	-0.075	-0.159	-0.044	-0.083	0.0060
lm0224m10741*	84.80999	-68.41814	3.023257	16.33	16.23	1059.9217	0.926	0.0010	-0.083	0.0	-0.017	-0.0
lm0017m23847	81.51398	-70.25371	3.024535	17.02	16.89	511.5374	0.992	0.0	-0.036	-0.0030	-0.018	-0.0010
lm0033k17847*	85.0648	-69.50791	3.0259981	15.54	15.42	1997.5843	0.976	-0.0070	-0.042	-0.0080	-0.025	0.0040
lm0541m15871	74.38819	-70.73805	3.02721	16.46	16.25	1077.7004	0.983	-0.0030	-0.016	-0.0020	-0.0060	-0.0020
lm0021m5306	83.41862	-69.23153	3.039916	14.86	14.71	2007.5547	0.988	-0.01	-0.02	-0.0	-0.0010	-0.0010
lm0133n11237*	71.46663	-69.61311	3.042348	17.05	16.94	1478.5739	0.948	-0.0020	-0.074	-0.0010	-0.037	-0.01
lm0551m22887	76.6378	-70.59362	3.044929	15.41	15.09	1094.7740	0.935	-0.034	-0.089	-0.012	-0.026	0.0020
lm0313m12666*	78.79619	-66.67068	3.04777	17.48	17.32	2298.6856	0.938	0.0050	-0.102	-0.0070	-0.075	-0.0040
lm0191m3743	80.03616	-67.85401	3.053936	16.37	16.27	1162.6817	0.942	-0.016	-0.056	-0.0010	-0.020	0.0040
lm0333k29474	81.85984	-66.77636	3.057151	15.51	15.33	1961.7493	0.97	-0.015	-0.029	0.0010	-0.0010	0.0040
lm0426m22620*	75.0737	-66.21255	3.058626	16.37	16.08	1593.6165	0.983	-0.0080	-0.028	-0.0060	-0.016	0.0010
lm0330m5632	81.49411	-66.2831	3.061442	15.64	15.36	1277.5437	0.978	-0.0090	-0.036	-0.015	-0.027	0.0
lm0045k15007	86.91472	-69.84105	3.063892	16.64	16.78	327.8286	0.914	-0.065	-0.113	-0.025	-0.071	0.0080
lm0033i24296	85.10421	-69.69974	3.066509	15.45	15.43	1579.7131	0.909	-0.014	-0.081	-0.0	-0.0060	0.016
lm0105l13533	77.02341	-70.03877	3.066536	16.06	15.88	1854.6134	0.976	-0.019	-0.026	0.0020	-0.0020	0.0030
lm0022n14480	82.56715	-69.64186	3.068277	16.11	15.95	2516.8652	0.982	-0.0040	-0.035	-0.0050	-0.027	-0.0030
lm0564k20997	77.44903	-71.28016	3.074219	15.10	14.89	1572.7651	0.982	-0.0050	-0.023	-0.0020	-0.0020	0.0010
lm0020k18927*	82.06909	-69.18918	3.081764	15.73	15.56	878.6014	0.937	-0.0040	-0.076	-0.0010	-0.017	-0.0
lm0547l6434	74.17473	-71.69228	3.081798	15.87	15.69	1620.5483	0.986	-0.015	-0.013	-0.0	0.0	0.0030
lm0125l25666	73.1602	-70.0558	3.088091	14.98	14.72	1976.5606	0.954	-0.016	-0.043	-0.0010	-0.0010	0.0030
lm0454k24315	79.70137	-65.71829	3.096796	15.71	15.50	1615.5724	0.972	-0.012	-0.038	-0.0080	-0.017	-0.0010
lm0172n24468	75.39748	-68.30194	3.102677	16.43	16.19	808.8476	0.898	-0.055	-0.118	-0.024	-0.043	0.0040
lm0113n24057	75.47999	-69.68381	3.106244	16.80	16.67	1591.6232	0.924	0.0020	-0.129	-0.0020	-0.089	-0.0070
lm0095m9501	79.51951	-69.80527	3.107019	14.94	14.68	1818.7747	0.96	-0.020	-0.065	-0.0060	-0.044	0.0060
lm0346m3392	83.10783	-67.32369	3.113759	15.83	15.67	1273.5625	0.952	-0.028	-0.046	-0.0	-0.0010	0.0080
lm0026m14151	82.68247	-70.19015	3.115609	16.86	16.90	1771.8904	0.905	-0.034	-0.072	-0.0030	-0.0010	0.016
lm0334n23519	81.4573	-67.25705	3.119701	15.80	15.55	1116.8374	0.957	-0.0070	-0.067	-0.018	-0.032	-0.0070
lm0340m20801	83.06523	-66.39168	3.120686	16.88	16.66	1592.6396	0.958	0.0010	-0.046	0.0010	-0.017	0.0010
lm0033m3196	85.32926	-69.41801	3.122574	15.29	15.12	2047.4882	0.945	-0.0060	-0.088	-0.0010	-0.057	-0.0
lm0207m27588	81.91838	-68.87609	3.12647	15.81	15.55	1059.8723	0.952	0.0020	-0.062	-0.011	-0.038	-0.0080
lm0112m21875	74.51557	-69.55377	3.130149	16.11	15.97	436.8064	0.918	-0.017	-0.087	-0.0010	-0.013	0.0040
lm0034m1263	84.64997	-69.77342	3.134554	16.18	16.19	1235.6455	0.976	-0.017	-0.023	-0.0010	-0.0	0.0010
lm0202l15311	80.82547	-68.25012	3.139857	15.63	15.43	2264.6298	0.89	-0.044	-0.16	-0.029	-0.074	0.0020
lm0045m12168	87.51845	-69.87298	3.140267	15.89	15.63	1822.7635	0.979	-0.017	-0.021	0.0040	0.0060	0.0020
lm0364k3633	86.17755	-66.9754	3.141938	16.07	15.91	1266.6517	0.944	-0.045	-0.065	-0.013	-0.026	0.0040
lm0024m24264	82.5705	-69.88751	3.144057	16.03	15.96	1916.5944	0.983	-0.014	-0.018	-0.0010	-0.0	0.0010
lm0580m20047	82.12091	-70.57273	3.145045	16.11	15.82	1300.5510	0.888	-0.06	-0.134	-0.028	-0.062	0.0020
lm0345k4036	83.5982	-66.9814	3.153308	15.89	15.70	1317.5216	0.988	-0.0060	-0.018	0.0	-0.0090	-0.0010
lm0037k8689	84.95645	-70.16619	3.154552	16.28	16.17	2404.5534	0.953	-0.077	-0.087	-0.03	-0.065	-0.0060
lm0333n16489	82.41114	-66.84767	3.16106	15.07	14.73	2335.6579	0.937	-0.037	-0.081	-0.0090	-0.021	0.0010

APPENDIX A. PROPERTIES OF THE “HOT” ECLIPSING BINARIES IN THE LMC

lm0106m9917	76.2925	-70.16055	3.16128	15.02	14.83	2169.7551	0.918	-0.033	-0.099	-0.011	-0.033	-0.0
lm0333n10485	82.21101	-66.81298	3.162796	14.75	14.46	809.6847	0.979	-0.016	-0.026	-0.0010	-0.0010	-0.0020
lm0331n13474	82.46639	-66.58544	3.163636	16.21	15.99	2204.6430	0.892	-0.062	-0.142	-0.029	-0.063	0.0020
lm0214n27117	82.69834	-68.67364	3.17278	15.00	14.85	1532.6636	0.989	-0.016	-0.017	0.0	-0.0	-0.0010
lm0397l9693	92.42364	-67.5322	3.177116	16.71	16.55	396.8372	0.991	-0.028	-0.019	-0.0020	0.0010	-0.0060
lm0092k17584*	78.14727	-69.54077	3.192096	16.21	16.16	2294.6856	0.984	-0.020	-0.033	-0.0010	-0.0080	-0.0
lm0543m30093	74.33289	-70.97212	3.193725	15.85	15.74	1467.6623	0.968	-0.026	-0.037	-0.0040	-0.0060	0.0010
lm0090l7215*	78.07533	-69.25455	3.19449	16.66	16.70	2184.7283	0.979	-0.030	-0.041	-0.0050	0.03	-0.0010
lm0223k6698*	85.20794	-68.03923	3.205024	16.35	16.20	2396.5282	0.982	-0.050	-0.017	-0.0020	-0.0080	0.0030
lm0240m16931	88.32281	-67.76502	3.209594	15.86	15.81	1594.7469	0.964	0.060	-0.048	-0.026	-0.0090	-0.015
lm0287m4239	73.69951	-67.32634	3.213864	16.24	15.98	2298.6313	0.979	0.020	-0.027	-0.0010	-0.014	-0.0020
lm0093k23075	79.06935	-69.52412	3.214621	15.86	15.72	1503.6563	0.926	-0.051	-0.093	-0.015	-0.033	0.0050
lm0092m16608	78.47966	-69.53371	3.219523	14.56	14.29	1766.8702	0.859	-0.056	-0.166	-0.033	-0.082	-0.0050
lm0583l28540	82.667	-71.11311	3.22106	15.63	15.80	1257.5922	0.994	-0.060	-0.090	-0.013	-0.020	0.0020
lm0123l25563	73.2624	-69.69687	3.222946	15.30	15.10	1071.7427	0.937	-0.090	-0.046	0.0060	-0.0010	0.0050
lm0012k23809	80.14888	-69.57091	3.224639	16.54	16.24	2178.7047	0.929	-0.048	-0.087	-0.015	-0.03	-0.0030
lm0290l18998	73.88709	-66.54208	3.224805	15.32	15.15	1193.5685	0.934	-0.021	-0.066	-0.0020	-0.0070	0.0080
lm0115n13901	75.4074	-69.98117	3.224925	14.83	14.60	2265.6246	0.898	-0.026	-0.123	-0.011	-0.028	0.0010
lm0396m17800	92.06155	-67.5855	3.230491	17.16	16.98	1982.6641	0.96	-0.056	-0.036	-0.0030	-0.020	-0.0040
lm0455k23532	80.43622	-65.71217	3.233372	15.88	15.80	1823.8001	1.005	-0.080	-0.017	-0.060	-0.015	-0.0020
lm0285l15911	73.19292	-67.2065	3.23396	16.09	15.90	2257.5727	0.904	-0.073	-0.147	-0.036	-0.085	-0.0090
lm0221m22693	85.6782	-67.94212	3.234518	16.25	16.09	1496.7246	0.969	-0.024	-0.032	-0.0010	-0.0030	-0.0020
lm0305k4072*	76.49398	-66.97811	3.239846	17.33	17.22	2081.9115	0.995	0.0	-0.016	-0.0010	-0.0070	-0.0010
lm0326k22117	79.36645	-67.44853	3.240622	16.42	16.19	1254.5989	0.966	0.030	-0.061	0.0030	-0.042	0.0010
lm0344k19755	82.8889	-67.08871	3.240951	14.51	14.30	1941.7750	0.958	-0.016	-0.05	-0.0040	-0.012	-0.0020
lm0123m18261	73.35284	-69.50294	3.250247	16.99	16.95	2545.6634	0.934	-0.016	-0.05	-0.012	-0.094	0.011
lm0214n12207	82.93724	-68.58121	3.252969	16.15	16.04	425.6291	0.977	-0.05	-0.034	-0.019	-0.03	0.0020
lm0207m8280	82.00201	-68.75682	3.256904	17.13	16.71	1805.8790	0.926	-0.055	-0.094	-0.01	-0.023	0.0080
lm0566l18883	77.01925	-71.84052	3.256957	16.88	16.64	2258.7599	0.956	-0.036	-0.058	0.0020	-0.0090	-0.0040
lm0106k14921	75.85521	-70.19912	3.261387	15.92	15.76	491.5882	0.968	-0.025	-0.037	0.0030	-0.0030	0.0080
lm0207n22625	81.9823	-69.01378	3.264492	15.85	15.63	2314.7037	0.944	-0.010	-0.073	0.0030	-0.046	-0.0040
lm0353l18484	85.17781	-66.87581	3.269629	16.92	16.96	1196.6902	0.936	-0.053	-0.08	-0.029	-0.042	-0.0030
lm0435k20023	77.25556	-65.68476	3.281595	16.90	16.68	2217.8281	0.992	-0.011	-0.032	-0.0080	-0.03	-0.0010
lm0013m14520*	81.31911	-69.48442	3.288232	16.30	16.07	1296.5242	0.973	0.0010	-0.032	-0.0020	-0.029	0.0010
lm0090n12880*	78.26413	-69.28665	3.289332	16.92	16.93	1887.6347	0.971	-0.020	-0.035	0.0	-0.029	0.0020
lm0114n17444	74.33831	-70.00589	3.296076	16.11	15.92	1374.8887	0.99	-0.050	-0.064	-0.0010	-0.053	-0.0010
lm0200l18257	80.50925	-67.9272	3.296949	14.59	14.40	1147.8162	0.891	-0.028	-0.13	-0.015	-0.043	0.0080
lm0366n9903	86.80193	-67.52169	3.300117	16.39	16.21	1978.6227	0.97	-0.032	-0.026	-0.0020	0.0010	-0.0020
lm0436l19007	76.28093	-66.19386	3.301123	15.18	14.87	1945.6937	0.98	-0.012	-0.017	-0.0	0.0	-0.0
lm0093n28064*	79.27002	-69.70178	3.3058419	17.47	17.54	1347.9240	0.977	-0.012	-0.042	0.0020	-0.041	0.0040
lm0091n23508	79.27861	-69.33696	3.308983	15.79	15.62	2208.6229	0.94	-0.017	-0.064	0.0	-0.0020	0.0020

lm0157m5026	72.80917	-68.88096	3.311319	16.72	16.58	1859.5651	0.959	-0.026	-0.036	-0.0060	-0.0070	0.0080
lm0335m11683	82.15568	-67.02177	3.311557	15.54	15.32	2001.5948	0.981	-0.011	-0.014	-0.0020	-0.0010	0.0070
lm0113k24074	75.00863	-69.53223	3.317551	16.47	16.39	1945.6583	0.936	-0.014	-0.081	-0.038	-0.02	-0.024
lm0193n14440*	80.28239	-68.23227	3.318844	16.71	16.60	2554.7174	0.973	0.020	-0.032	-0.0020	-0.011	0.0010
lm0343i22239	83.74418	-66.9411	3.321188	15.91	15.70	2238.6138	0.96	-0.0020	-0.05	-0.0050	-0.027	-0.0040
lm0360k14673	86.17458	-66.35411	3.326186	15.94	15.76	1273.6097	0.98	-0.024	-0.024	-0.058	-0.016	0.021
lm0353i25823	85.54038	-66.92105	3.326584	16.83	16.73	1960.7184	0.975	-0.004	-0.034	-0.0040	-0.017	-0.0
lm0551k13555	76.3388	-70.55255	3.334194	16.01	15.75	705.7491	0.989	-0.0030	-0.015	-0.0	-0.0090	0.0010
lm0126m15554	72.52938	-70.20161	3.350086	15.56	15.42	2198.7800	0.9	-0.011	-0.157	-0.0070	-0.094	-0.0090
lm0317n15681	78.69001	-67.56308	3.359371	15.13	14.98	2031.4960	0.891	-0.018	-0.131	-0.01	-0.034	0.0080
lm0296m11158	74.30055	-67.52851	3.359377	16.37	16.18	1629.5409	0.947	-0.017	-0.097	-0.018	-0.064	-0.01
lm0335n9834*	82.48561	-67.16005	3.362948	16.85	16.57	1654.5282	0.979	-0.01	-0.037	-0.0060	-0.031	-0.0
lm0541n13040	74.59473	-70.71196	3.36718	16.78	16.53	1259.5290	0.986	-0.0060	-0.022	-0.0060	-0.016	-0.0010
lm0157n6157	72.81882	-68.8896	3.370074	15.17	15.03	1529.5687	0.959	-0.019	-0.044	-0.0020	-0.013	0.0020
lm0023k4265	83.10466	-69.42709	3.37023	15.66	15.44	1538.6523	0.917	-0.0080	-0.144	-0.0050	-0.086	-0.0040
lm0216m26624*	82.80184	-68.87256	3.371126	17.31	17.25	1659.5486	0.949	-0.0060	-0.085	-0.0060	-0.066	-0.0040
lm0366m8525*	86.6264	-67.35921	3.371884	16.93	16.81	2000.5921	0.957	-0.0020	-0.066	-0.0010	-0.051	0.0020
lm0342k17321	82.66393	-66.74441	3.373808	15.43	15.23	1468.6747	0.959	-0.0040	-0.05	-0.0050	-0.021	0.0030
lm0184i24349	76.66006	-68.65452	3.375765	15.57	15.44	1247.5587	0.977	-0.041	-0.031	-0.041	-0.019	0.0060
lm0345k15489	83.54525	-67.05712	3.378755	17.31	15.13	1968.6547	0.98	-0.0060	-0.024	-0.0040	-0.010	0.0010
lm0036m19194*	84.50262	-70.22628	3.381742	15.26	17.21	1454.7138	0.963	0.010	-0.031	-0.0010	-0.017	-0.0010
lm0466k20008	77.87865	-66.04859	3.382065	16.67	16.54	2183.7359	0.991	-0.027	-0.015	0.0	0.0	-0.0050
lm0180i20443*	77.089	-67.9353	3.383502	16.75	16.60	1198.6496	0.973	-0.0010	-0.039	-0.0020	-0.016	0.0010
lm0595k6058*	84.56346	-71.19237	3.38627	17.22	17.18	1281.6027	0.978	-0.0040	-0.037	-0.0020	-0.021	0.0020
lm0093n33808*	79.33719	-69.73054	3.390984	17.05	16.98	1078.7844	1.002	-0.0	-0.03	-0.0010	-0.018	0.0030
lm0365n23864	87.63119	-67.26356	3.400307	16.92	16.69	1657.5424	0.94	-0.037	-0.069	-0.0070	-0.016	0.0030
lm0022k4406	81.91673	-69.43566	3.403997	15.00	14.78	1653.5704	0.89	-0.035	-0.135	-0.023	-0.057	0.0080
lm0333n18392	82.35435	-66.85994	3.404099	16.75	16.59	2511.8285	0.882	-0.055	-0.147	-0.029	-0.06	0.0060
lm0030i13351	83.91936	-69.30042	3.408736	14.56	14.40	1763.8154	0.9	-0.024	-0.121	-0.0090	-0.032	0.0030
lm0331m23548	82.12763	-66.40021	3.412884	15.34	15.08	2249.8462	0.971	-0.024	-0.03	0.0	-0.0010	0.0030
lm0030i4784	84.1129	-69.2377	3.413421	15.79	15.86	1879.6639	0.981	-0.0010	-0.031	-0.0020	-0.022	-0.0030
lm0115k10662	75.0248	-69.81396	3.416375	16.49	16.43	1122.7615	0.914	-0.053	-0.094	-0.018	-0.031	0.0040
lm0294m14933	74.25877	-67.0444	3.420709	16.74	16.68	1947.6718	0.96	-0.017	-0.035	0.0020	-0.0010	0.0040
lm0584n18193	82.08746	-71.41213	3.426518	15.10	14.94	1528.6761	0.866	-0.054	-0.169	-0.027	-0.086	0.0020
lm0466n13702	81.53741	-66.14992	3.432734	14.40	14.60	1790.8409	0.922	-0.017	-0.081	-0.011	-0.0020	-0.0
lm0285m13349	73.53375	-67.03497	3.438956	16.30	16.12	782.6400	0.935	-0.0090	-0.104	-0.0060	-0.062	-0.0020
lm0175k30401	75.83732	-68.52178	3.440068	15.87	15.79	1200.6503	0.974	-0.023	-0.025	-0.0020	0.0	0.0010
lm0105i7047	77.00614	-69.97644	3.442404	16.92	16.76	762.6691	0.98	-0.0030	-0.03	-0.022	-0.012	-0.0070
lm0466i18501	81.25829	-66.18943	3.445012	15.87	15.85	2132.8315	0.927	-0.026	-0.072	-0.0010	-0.0070	0.0060
lm0187i13941*	77.99728	-68.95024	3.447762	17.36	17.49	496.6719	0.963	0.0070	-0.04	-0.0010	-0.019	0.0020
lm0225k26953	85.28308	-68.51655	3.452879	16.43	16.40	1883.7115	0.896	-0.06	-0.13	-0.027	-0.053	0.0040



APPENDIX A. PROPERTIES OF THE “HOT” ECLIPSING BINARIES IN THE LMC

Im0541m18320	74.75107	-70.75661	3.459966	16.70	16.47	1067.7413	0.932	-0.047	-0.089	-0.016	-0.035	-0.0020
Im0175n21939*	76.4601	-68.62454	3.462514	16.25	16.08	1453.8443	0.968	0.0010	-0.034	0.0	-0.0040	0.0030
Im0343k22299	83.82234	-66.73423	3.466279	15.52	15.28	933.5105	0.987	-0.0030	-0.023	-0.0020	-0.0080	-0.0020
Im0033k4809	84.89519	-69.4277	3.468732	16.77	16.76	1970.6225	0.973	-0.015	-0.019	-0.0030	0.0010	0.0030
Im0166l12483	73.08311	-68.94035	3.468778	15.42	15.25	2198.6216	0.977	-0.018	-0.024	0.0020	0.0040	0.0040
Im0221m7928	85.89611	-67.84467	3.468802	15.24	14.94	2192.8314	0.995	-0.0050	-0.02	-0.011	-0.014	-0.0
Im0321m6695	80.51609	-66.28211	3.46972	16.11	15.70	776.7560	0.979	-0.020	-0.037	-0.0050	-0.02	-0.0040
Im020212407	80.65683	-68.30712	3.472186	16.85	16.75	1819.7651	0.964	-0.026	-0.033	-0.0010	0.0030	0.0030
Im0105n27365	77.64679	-70.05544	3.476907	16.47	16.26	1992.5496	0.96	-0.028	-0.031	0.0	0.0010	0.0050
Im0681m21371	77.62627	-71.98581	3.486964	16.07	15.81	1591.6457	0.98	-0.018	-0.021	-0.0010	0.0010	0.0010
Im0177l9536	76.03674	-68.91984	3.491026	16.79	16.60	390.7627	0.975	-0.080	-0.026	-0.0020	-0.014	-0.0030
Im0157n20802	72.50246	-69.00251	3.491766	16.24	16.06	1494.5699	0.968	-0.023	-0.039	-0.0030	0.0020	-0.0030
Im0344m8000	83.13842	-67.00822	3.496288	15.36	15.14	2251.6815	0.956	0.070	-0.065	0.0010	-0.04	-0.0060
Im0195m24877	80.04894	-68.49353	3.508008	16.80	16.75	741.7994	0.974	-0.034	-0.043	-0.0060	-0.0	-0.0020
Im0184l15997	77.03259	-68.60547	3.509246	15.72	15.53	1388.8150	0.973	-0.0080	-0.031	-0.0030	-0.014	-0.0
Im0180l24836	76.77216	-67.96542	3.513017	15.37	15.17	1555.6224	0.972	-0.014	-0.022	0.0020	0.0010	0.0060
Im0024k23511*	81.607	-69.77156	3.522356	16.28	16.16	523.6086	0.987	-0.0050	-0.015	-0.0020	-0.01	0.0020
Im0091k14479	78.9015	-69.13946	3.524759	16.67	16.47	1844.7458	0.971	-0.086	-0.104	-0.025	-0.059	-0.0030
Im0021n29435	83.65434	-69.36785	3.531735	15.52	15.24	2144.8051	0.989	-0.080	-0.014	-0.0060	-0.0090	-0.0010
Im0013n30008	81.28676	-67.71265	3.538905	15.87	15.70	1467.7256	0.974	-0.022	-0.022	0.0010	0.0010	0.0030
Im0037k23342	81.89047	-67.46495	3.543441	14.98	14.73	1442.8167	0.985	-0.043	-0.03	-0.016	-0.028	-0.0040
Im0305m27052	76.82996	-67.11363	3.545493	15.98	15.75	1082.8328	0.925	-0.046	-0.092	-0.016	-0.035	0.0010
Im0303k13861*	76.76351	-66.67879	3.54569	17.20	17.11	2187.7137	0.98	-0.010	-0.028	0.0010	-0.012	-0.0010
Im0095n30847	79.72056	-70.07168	3.546722	16.91	16.72	325.8327	0.911	-0.094	-0.142	-0.047	-0.079	0.0040
Im0343k13626	83.68195	-66.68211	3.549134	15.99	15.80	1463.7628	0.931	-0.039	-0.081	-0.070	-0.021	0.0030
Im0182n12429*	77.41051	-68.22771	3.551178	17.52	17.43	1088.7063	0.97	-0.030	-0.044	-0.020	-0.027	-0.0040
Im0556k5652	75.15243	-71.52508	3.553122	16.62	16.52	1265.5806	0.958	-0.03	-0.054	-0.0	-0.0050	0.0030
Im0344n24008*	83.25517	-67.2601	3.555342	15.85	15.62	1764.8820	0.979	-0.010	-0.022	-0.0030	-0.0050	0.0010
Im0090m4479	78.38006	-69.08046	3.558236	16.65	16.46	1342.9334	0.968	-0.029	-0.04	-0.0060	-0.011	0.0010
Im0230k5872*	86.05593	-67.82598	3.561718	16.97	16.93	539.5715	0.956	-0.020	-0.042	-0.0010	-0.014	0.0020
Im0344l21596	82.79621	-67.25583	3.584081	16.96	16.82	1067.8030	0.978	-0.028	-0.025	-0.0	0.0020	0.0070
Im0341l21911	83.41158	-66.57944	3.584716	16.17	16.14	1937.7144	0.923	-0.065	-0.104	-0.029	-0.053	-0.0010
Im0343n20447	83.99897	-66.93869	3.585424	15.49	15.20	507.5786	0.987	-0.080	-0.019	-0.0050	-0.0090	-0.0010
Im0287m15070	73.36558	-67.40108	3.586708	16.88	16.78	2262.8470	0.966	-0.031	-0.019	-0.0030	0.0040	0.0090
Im0374m16724*	88.40874	-67.07084	3.593318	16.80	16.65	1784.8338	0.978	-0.040	-0.029	-0.0060	-0.018	-0.0030
Im0121l22345	73.04166	-69.33462	3.595392	16.67	16.52	1424.7830	0.94	-0.038	-0.062	-0.0060	-0.015	0.0030
Im0325n11823*	80.60303	-66.81992	3.599714	16.69	16.47	2025.5114	0.982	-0.070	-0.019	-0.0030	-0.0070	-0.0
Im0110l21613	74.04657	-69.35041	3.606183	15.58	15.34	708.8980	0.967	0.030	-0.064	0.0030	-0.036	-0.0020
Im0343l15840	83.65609	-66.85268	3.609432	14.85	14.61	540.5105	0.924	-0.022	-0.067	0.0	-0.0040	0.01
Im0340l6791	82.66304	-66.45076	3.612113	16.87	16.78	1267.5930	0.875	-0.107	-0.158	-0.05	-0.079	0.0090
Im0366l7734	86.22426	-67.50409	3.613542	16.61	16.45	1824.7695	0.956	-0.012	-0.075	-0.0060	-0.049	-0.0

lm0163i24856	74.13186	-68.29759	3.618347	16.37	16.29	2389.5005	0.984	-0.0010	-0.015	-0.0060	-0.0030	-0.0010
lm0015m30492	81.28868	-70.07286	3.625513	16.49	16.35	1532.6440	0.971	-0.0080	-0.06	-0.0070	-0.042	0.0040
lm0093k27461	79.20581	-69.54608	3.628299	15.62	15.43	931.4989	0.96	-0.0050	-0.051	-0.0050	-0.026	-0.0010
lm0091i25158	79.11048	-69.34246	3.634311	15.28	15.24	1441.7489	0.927	-0.03	-0.077	-0.015	-0.03	0.0040
lm0560m17742	77.72478	-70.55739	3.640989	16.33	16.13	788.7677	0.956	-0.029	-0.042	0.0010	-0.0010	0.0040
lm0013m22363	81.34314	-69.52733	3.646111	16.74	16.73	1784.7748	0.948	-0.015	-0.015	-0.0	0.0040	0.0040
lm0225n7592	85.63734	-68.54787	3.652101	15.74	15.52	1108.8501	0.98	-0.0080	-0.086	-0.0080	-0.063	0.0060
lm0184i4957*	76.90969	-68.53939	3.65273	16.53	16.62	1059.8512	0.989	-0.0020	-0.027	0.0	-0.014	0.0010
lm0303n17856*	76.9238	-66.85285	3.65542	16.54	16.32	1201.5979	0.983	-0.0030	-0.026	-0.0030	-0.019	0.0010
lm0343i16325	83.40523	-66.85714	3.655533	15.13	14.89	2344.6483	0.959	-0.0020	-0.058	-0.014	-0.038	0.0070
lm0184k13409	76.68995	-68.43575	3.659249	16.16	16.04	2057.4846	0.969	-0.028	-0.032	-0.0020	-0.0090	0.0020
lm0343k22859	83.58619	-66.73907	3.664324	15.30	15.07	1901.8483	0.847	-0.038	-0.18	-0.021	-0.057	0.025
lm0207m6963*	81.84109	-68.75027	3.677332	15.35	15.12	1374.9246	0.94	-0.0020	-0.08	-0.0	-0.023	-0.0
lm0100i22336*	76.0634	-69.35643	3.679464	16.82	16.85	2294.6647	0.985	-0.0010	-0.026	-0.0010	-0.018	0.0
lm0565k6340	78.48164	-71.1866	3.690546	14.79	14.60	1142.6656	0.97	-0.019	-0.03	-0.0	-0.0010	0.0030
lm0033n18886	85.43758	-69.6679	3.694692	14.70	14.44	1950.6193	0.987	-0.0010	-0.015	-0.0030	-0.0030	0.0010
lm0344i19313	82.71621	-67.24027	3.695935	15.18	14.96	2017.5704	0.967	0.0020	-0.051	-0.02	-0.02	-0.012
lm0013m8661	81.31174	-69.60346	3.714526	16.00	15.92	532.5185	0.971	-0.0	-0.037	-0.0020	-0.02	0.0
lm0033m17063	85.30712	-69.50278	3.718525	14.84	14.67	388.8496	0.984	-0.01	-0.013	-0.0020	-0.0010	0.0010
lm0331n1614	82.1504	-66.42878	3.72069	16.76	16.59	1442.8167	0.992	-0.018	-0.011	-0.013	-0.01	0.0020
lm0125n23449	73.42151	-70.04054	3.738714	15.31	15.11	1976.5606	0.881	-0.06	-0.151	-0.027	-0.07	0.0030
lm0551m20681*	76.8773	-70.57786	3.740874	17.61	17.43	1838.7292	0.961	0.0060	-0.063	0.0020	-0.047	0.0
lm0283n15751	73.62331	-66.8483	3.742176	16.62	16.38	2255.5680	0.961	-0.02	-0.065	-0.019	-0.044	-0.0070
lm0424n5194	74.80668	-65.73664	3.744226	14.62	14.42	1183.6480	0.897	-0.018	-0.118	-0.018	-0.046	0.0080
lm0013n32504	81.27858	-69.72549	3.745008	16.28	16.17	1266.5735	0.987	-0.01	-0.013	-0.0020	0.0010	0.0040
lm0291i4891	75.00036	-66.42614	3.751829	15.47	15.14	2257.8605	0.913	-0.041	-0.109	-0.015	-0.036	0.0070
lm0027k3823*	82.86165	-70.13678	3.761414	16.19	16.10	511.5406	0.958	-0.014	-0.039	-0.0030	-0.0050	0.0030
lm0101n25168	77.61906	-69.34659	3.773408	15.86	15.56	508.5718	0.977	0.012	-0.044	-0.011	-0.02	-0.014
lm0207k16837	81.73428	-68.80786	3.775084	15.76	15.48	428.6362	1.0	-0.02	-0.003	0.00010	-0.0060	-0.0010
lm0092m24157	78.27531	-69.57623	3.779528	15.91	15.76	2460.9331	0.993	-0.036	-0.013	-0.01	-0.016	0.0010
lm0214n8614	82.96898	-68.55869	3.785845	16.52	16.44	2242.6112	0.974	-0.0090	-0.012	-0.051	-0.014	-0.021
lm0333k4914	81.80424	-66.6282	3.790269	15.57	15.38	1895.6174	0.985	-0.0060	-0.011	-0.018	-0.0030	-0.0090
lm0266m8808	92.49346	-69.05534	3.791436	16.61	16.37	503.7005	0.933	-0.053	-0.069	-0.0090	-0.018	0.011
lm020m22505	82.62036	-69.19407	3.791691	15.68	15.55	2297.7436	0.921	-0.029	-0.07	-0.0	-0.0090	0.012
lm0285k22500	73.2004	-67.10051	3.79278	15.83	15.70	2258.7408	0.958	-0.018	-0.041	0.0010	-0.0030	0.0050
lm0030i15904	84.16062	-69.32033	3.797121	15.21	15.21	2312.7491	0.977	-0.011	-0.017	-0.0	0.0	0.0060
lm0555m16884	76.54721	-71.27836	3.800767	16.44	16.30	1987.5504	0.907	-0.04	-0.115	-0.018	-0.039	-0.0010
lm0550m5212	75.62754	-70.48438	3.801039	15.88	15.55	2204.6021	0.974	-0.0040	-0.035	-0.0060	-0.017	0.0010
lm0257i8931	91.10599	-68.92443	3.810748	15.53	15.19	2264.8051	0.933	0.01	-0.106	-0.0040	-0.074	0.01
lm0583i28572	82.36022	-71.11471	3.822895	16.57	16.55	1266.6017	0.984	-0.0020	-0.024	-0.0	-0.014	-0.0
lm0050m16262*	88.34579	-69.30547	3.8284881	16.85	16.71	390.7966	0.951	0.018	-0.094	0.0090	-0.084	0.0010

APPENDIX A. PROPERTIES OF THE “HOT” ECLIPSING BINARIES IN THE LMC

lm0125k8106	72.82349	-69.80212	3.843898	15.86	15.80	1888.5707	0.961	-0.027	-0.053	-0.0080	-0.018	-0.0010
lm0367l13331	87.24167	-67.55966	3.846704	16.49	16.28	1804.8601	0.953	-0.049	-0.057	-0.0080	-0.014	0.0050
lm0112i222418*	74.07703	-69.69282	3.851004	17.18	17.04	1804.7621	0.957	-0.0010	-0.072	0.0020	-0.066	0.011
lm0090n30909	78.32119	-69.38894	3.852097	15.73	15.64	1711.9284	0.988	-0.01	-0.018	-0.0050	-0.013	-0.0
lm0030l11056	84.20283	-69.28329	3.853558	15.33	15.14	433.6799	0.95	-0.016	-0.037	-0.0056	-0.020	-0.021
lm0090k10170*	78.12455	-69.12116	3.854796	16.56	16.50	2202.6635	0.982	-0.0040	-0.028	-0.0040	-0.0080	0.0010
lm0175n28869	76.49599	-68.66344	3.855031	16.37	16.03	381.8370	0.934	-0.039	-0.085	-0.011	-0.031	0.0
lm0020k15581	82.06669	-69.16523	3.863955	14.97	14.77	1076.8903	0.966	-0.0030	-0.049	0.0	-0.022	-0.0010
lm0026m7027	82.35945	-70.30285	3.870485	16.17	16.28	665.8444	0.936	-0.044	-0.091	-0.028	-0.046	0.0050
lm0024k6529	81.83158	-69.68507	3.872692	16.35	16.17	931.4717	0.949	-0.049	-0.065	-0.0090	-0.02	-0.0020
lm0117m12730	75.62958	-70.18216	3.873811	16.34	16.22	2208.7498	0.912	-0.1	-0.131	-0.05	-0.084	-0.0040
lm0177l9754	75.87027	-68.92221	3.890098	15.48	14.96	2300.6332	0.917	-0.057	-0.12	-0.02	-0.058	0.0060
lm0362n5182	86.7338	-66.78992	3.891688	16.16	15.96	892.6980	0.928	-0.0090	-0.114	-0.0080	-0.086	-0.01
lm0112m21394	74.53396	-69.55076	3.895853	15.35	15.21	2389.5164	0.96	-0.021	-0.036	-0.0010	0.0	0.0010
lm0010i23506	80.08352	-69.36236	3.904077	16.22	16.12	1492.6657	0.953	-0.023	-0.029	-0.0010	0.0030	0.0030
lm0121i27208	73.12209	-69.36341	3.907531	15.75	15.63	1821.7064	0.967	-0.015	-0.024	-0.045	-0.0070	0.019
lm0354i23952	84.27038	-67.27003	3.909404	15.83	15.54	1290.5659	0.904	-0.078	-0.124	-0.041	-0.072	0.0060
lm0345n27198	84.27032	-67.27011	3.909474	15.70	15.46	1059.9019	0.896	-0.073	-0.124	-0.034	-0.055	0.0050
lm0055k6835	88.97061	-69.7922	3.915014	16.45	16.36	510.6379	0.959	-0.034	-0.034	0.0	0.0010	0.0030
lm0165n5928	74.56977	-68.53736	3.926326	15.02	14.82	1093.7740	0.899	-0.035	-0.13	-0.014	-0.04	0.0030
lm0120m20609	72.73139	-69.17757	3.931665	16.82	16.66	2241.5917	0.871	-0.053	-0.187	-0.035	-0.07	0.0010
lm0287m22036	73.60184	-67.44495	3.945121	16.20	16.03	2074.9341	0.896	-0.081	-0.158	-0.041	-0.092	-0.0050
lm0187m9985	78.16571	-68.76748	3.945319	16.76	16.59	842.6535	0.931	-0.077	-0.106	-0.03	-0.055	-0.0040
lm0345k9648	83.73768	-67.01699	3.948231	15.44	15.24	1955.7165	0.966	-0.012	-0.032	0.0010	0.0030	0.0010
lm0443i6372	78.81883	-65.52974	3.949185	16.65	16.47	1267.5402	0.962	-0.048	-0.052	-0.0090	-0.017	-0.0020
lm0200l6074	80.57817	-67.83901	3.950478	15.89	15.65	1273.5276	0.985	-0.020	-0.029	-0.0010	-0.02	-0.0030
lm0377l5481	89.05696	-67.562	3.951541	16.72	16.49	1572.8209	0.933	-0.041	-0.065	-0.0080	-0.014	0.0070
lm0091m3797*	79.44924	-69.07108	3.9545	17.13	16.93	490.7461	0.94	-0.0010	-0.137	-0.0060	-0.095	-0.0030
lm031k21866	81.85552	-66.39288	3.959113	16.76	16.53	1531.6643	0.982	-0.015	-0.012	-0.041	-0.0080	-0.019
lm0015k8658	80.91297	-69.80448	3.959962	16.17	16.32	521.5561	0.987	-0.011	-0.016	-0.010	0.0010	0.0010
lm0364l14193	86.15885	-67.20871	3.959976	16.53	16.39	2018.5846	0.937	-0.052	-0.066	-0.012	-0.032	0.0030
lm0331i26042	81.98427	-66.57005	3.969029	15.95	15.81	1805.8877	0.871	-0.059	-0.153	-0.038	-0.062	0.013
lm0300m22019	75.95469	-66.39246	3.986529	16.62	16.36	1549.6231	0.973	-0.0030	-0.0090	-0.056	-0.02	-0.029
lm0317k7631	78.33439	-67.35943	3.990126	15.61	15.33	2141.8302	0.99	-0.0	-0.022	-0.025	-0.0050	0.02
lm0184n26760	77.48968	-68.65823	4.022428	15.38	15.20	1547.6132	0.877	-0.058	-0.168	-0.024	-0.071	0.0080
lm0012n4832	80.28006	-69.5904	4.027903	16.65	16.30	2162.7516	0.977	-0.049	-0.045	-0.0040	-0.0030	0.0090
lm0021i4530*	82.86946	-69.23199	4.0375387	15.06	14.80	1621.5653	0.917	-0.0080	-0.11	-0.0030	-0.037	0.0020
lm0600k25018	85.58539	-70.62667	4.046607	14.85	14.75	2056.4893	0.967	-0.019	-0.033	0.0010	-0.0	0.0040
lm0317k22978	78.15681	-67.4726	4.051916	14.67	14.41	1145.6945	0.97	-0.023	-0.027	0.0010	-0.0	0.0050
lm0022k4055	81.96774	-69.43346	4.054951	16.23	16.09	1934.7295	0.89	-0.058	-0.124	-0.025	-0.046	0.0080
lm0224m12405	84.68721	-68.42851	4.061928	16.41	16.32	1453.8637	0.92	-0.034	-0.091	-0.01	-0.023	0.0050

lm038718658	90.6794	-67.52584	4.064731	16.82	16.62	1654.5882	0.983	-0.021	-0.02	0.0010	0.0	0.0020
lm0101k23784	77.11118	-69.20004	4.069483	15.66	15.48	491.5882	0.97	-0.021	-0.012	-0.0040	0.0020	0.012
lm0223n19693	85.5091	-68.27015	4.075455	15.32	15.14	1661.5381	0.939	-0.047	-0.096	-0.022	-0.044	0.0030
lm0174k16339	75.13969	-68.45168	4.080948	15.44	15.28	1212.6916	0.947	-0.01	-0.039	0.0010	0.0010	0.015
lm0243m4872	89.41949	-68.078	4.081141	15.22	14.96	950.4929	0.999	-0.012	-0.003	0	-0.0010	-0.0040
lm0343k21737	83.98722	-66.88599	4.086492	14.66	14.36	947.5193	0.988	-0.0090	-0.014	-0.0020	-0.0050	-0.0010
lm0357k7500	85.56595	-67.35875	4.094591	15.02	14.77	1263.6234	0.923	-0.025	-0.072	-0.0030	-0.0060	0.013
lm0691m10693	79.56567	-71.91106	4.097389	16.28	16.03	1827.7694	0.92	-0.048	-0.086	-0.011	-0.021	0.0070
lm0337k10847	82.01922	-67.37806	4.115728	14.85	14.60	1875.6678	0.889	-0.05	-0.165	-0.026	-0.07	0.0070
lm0170m12305	75.52214	-67.88198	4.116486	15.80	15.58	1962.6911	0.92	-0.011	-0.122	-0.0050	-0.071	-0.0030
lm0585m13419	82.98242	-71.22553	4.118108	16.85	16.53	759.8288	0.986	-0.062	-0.032	-0.026	-0.036	0.0010
lm0206m26379	80.97014	-69.02722	4.127665	14.78	14.45	1788.8132	0.912	-0.033	-0.113	-0.0080	-0.04	0
lm0343k21879	83.58343	-66.73332	4.163179	15.89	15.68	1850.6457	0.991	-0.0040	-0.019	-0.0040	-0.012	-0.0010
lm0344i21656	82.78869	-67.25619	4.164156	15.51	15.30	1604.6224	0.989	-0.0050	-0.023	-0.0090	-0.013	0.0020
lm0101k17968	76.82463	-69.16519	4.176462	15.33	15.19	1792.7984	0.868	-0.069	-0.173	-0.036	-0.079	0.0070
lm0466116077	81.34282	-66.16931	4.179091	14.14	14.13	1547.6825	0.956	-0.0050	-0.018	0.0030	-0.0060	0.0040
lm0020k8691	82.09951	-69.11761	4.1797	14.77	14.55	947.4796	0.966	-0.0050	-0.037	-0.0030	-0.015	0.0020
lm0344m20206	82.94425	-67.08835	4.181412	15.24	15.07	1567.7128	0.932	-0.016	-0.055	0.0020	0.0010	0.013
lm0125m6068	73.33501	-69.93669	4.187756	15.92	15.79	2225.5710	0.93	-0.033	-0.076	-0.01	-0.02	0.0070
lm0110m10393	74.42887	-69.11062	4.192625	16.24	16.08	1269.5361	0.93	-0.074	-0.096	-0.027	-0.049	0.0020
lm0103k26311	77.04234	-69.54322	4.203111	16.30	16.26	1891.6261	0.9	-0.057	-0.116	-0.034	-0.051	0.013
lm0347m6886*	84.05524	-67.49722	4.210858	16.07	15.97	1291.5689	0.984	-0.01	-0.04	-0.0070	-0.034	-0.0040
lm0366116862	86.21569	-67.57577	4.232527	15.74	15.55	1760.8354	0.986	-0.015	-0.014	-0.0010	-0.0010	-0.0010
lm0346k23825	82.78651	-67.48403	4.249299	14.90	14.67	385.6731	0.955	-0.014	-0.066	-0.034	-0.029	-0.019
lm0177116525	76.18763	-68.96767	4.253577	16.56	16.40	1274.5110	0.96	-0.0050	-0.045	-0.0010	-0.02	0.0020
lm0313m25631	78.76599	-66.75024	4.263934	16.40	16.12	755.7254	0.983	-0.0080	-0.014	-0.0040	-0.01	0.0020
lm0466m21959	81.51327	-66.21313	4.273267	16.24	16.04	1262.5227	0.971	-0.024	-0.038	0.0010	-0.0010	0.0030
lm0094i25321	78.01319	-70.05957	4.274982	16.48	16.51	1891.6482	0.971	-0.016	-0.033	0.0010	0.0030	-0.0010
lm0122115581	72.06089	-69.66111	4.284122	15.70	15.51	2257.5669	0.984	-0.0050	-0.02	-0.0050	-0.0040	0.0010
lm011328118*	75.28282	-69.70783	4.30563	16.26	16.21	2516.7654	0.973	-0.0060	-0.026	-0.0050	-0.0020	0
lm0376m4773	88.48133	-67.33126	4.306026	15.91	15.74	512.7044	0.986	-0.018	-0.090	0.0010	0	0.0020
lm012516652	73.10946	-69.94208	4.313464	15.72	15.54	2140.8024	0.952	-0.013	-0.04	0.0010	0.0020	0.0090
lm0297m14819	75.21066	-67.5588	4.318638	15.55	15.26	1934.6377	0.989	-0.021	-0.014	-0.0010	-0	-0.0030
lm0467k18222	82.14873	-66.03215	4.320224	15.97	15.79	416.6277	0.97	-0.0090	-0.031	0	-0	0.0010
lm0187m17967	78.38296	-68.8134	4.323013	16.27	16.00	1579.6813	0.97	-0.012	-0.04	-0.024	-0.014	-0.0080
lm0467n17850	82.43197	-66.19001	4.324035	15.94	15.68	2309.7130	0.968	0	-0.061	-0.0010	-0.04	-0
lm0205n17550	81.93375	-68.60016	4.332041	16.77	16.52	1455.7692	0.942	-0.0040	-0.092	-0.0070	-0.061	-0.0060
lm0344n9074	83.1502	-67.16532	4.334821	14.78	14.54	825.8571	0.921	-0.011	-0.104	-0.0050	-0.044	-0.0010
lm0577k22178	80.32518	-71.684	4.336319	16.18	15.97	2161.7718	0.927	-0.024	-0.068	0.0010	-0.0030	0.0060
lm0331k22811	81.80895	-66.3997	4.337633	15.09	14.91	1355.9273	0.926	-0.032	-0.085	-0.0050	-0.021	0.0050
lm0091n32274	79.32109	-69.38282	4.339628	15.92	15.88	931.4989	0.967	-0.015	-0.032	0.0010	-0	0.0020

APPENDIX A. PROPERTIES OF THE “HOT” ECLIPSING BINARIES IN THE LMC

lm0211k23803	83.5757	-67.79595	4.341552	15.72	15.53	1116.8420	0.973	-0.022	-0.018	0.0	0.0020	0.0060
lm0317k21886	78.25325	-67.4642	4.359786	14.84	14.76	1935.6599	0.929	-0.025	-0.086	-0.0080	-0.022	0.0050
lm0344n11851	83.19611	-67.18331	4.402585	15.60	15.37	845.6938	0.99	-0.0030	-0.012	0.0	-0.0040	-0.0010
lm0337k25005	81.75818	-67.47718	4.408822	15.00	14.76	1906.8403	0.953	0.0050	-0.067	-0.01	-0.039	0.012
lm0093m11955	79.37473	-69.46628	4.422796	16.03	15.87	1451.7376	0.963	0.0020	-0.057	-0.0050	-0.033	-0.0020
lm0292i5541*	74.12264	-66.79039	4.442046	16.76	16.58	2245.6216	0.967	0.0010	-0.05	-0.0010	-0.032	0.0020
lm0034m4602*	84.66394	-69.80398	4.454894	16.73	16.80	2223.6288	0.983	0.0020	-0.022	-0.0010	-0.016	-0.0010
lm0290m4510	74.26176	-66.27256	4.45663	15.72	15.58	382.7421	0.873	-0.052	-0.141	-0.025	-0.052	0.017
lm0197m20835	79.94283	-68.83562	4.488418	15.99	15.78	397.8481	0.994	-0.0040	-0.012	-0.011	0.0	0.0040
lm0090m20034	78.25898	-69.32768	4.502363	15.79	15.78	590.4779	0.978	0.0010	-0.033	-0.022	-0.014	0.0090
lm0021i15985	82.86938	-69.29774	4.502779	14.83	14.59	1082.8784	0.867	-0.033	-0.175	-0.021	-0.057	0.0060
lm0551i21419	76.05641	-70.73615	4.503208	15.74	15.52	837.7661	0.98	-0.01	-0.019	-0.012	-0.0060	-0.0010
lm0243m4824	89.25168	-68.07858	4.517961	15.84	15.64	1987.6340	0.964	-0.0050	-0.046	-0.0030	-0.027	-0.0050
lm0030i9014	83.85675	-69.26823	4.523622	15.20	15.09	440.7544	0.967	-0.0010	-0.039	-0.0010	-0.019	-0.0010
lm0207m11446	82.14797	-68.77459	4.526578	14.31	14.03	741.8064	0.867	0.0010	-0.158	-0.0070	-0.038	0.0060
lm0182m15099	77.35368	-68.24348	4.535109	15.59	15.41	2263.6346	0.983	-0.0010	-0.017	-0.0050	-0.0030	-0.0
lm0283m15233	73.4938	-66.70205	4.540844	15.45	15.15	1783.7591	0.933	-0.075	-0.115	-0.041	-0.075	0.0020
lm0021i15606	82.80078	-69.29588	4.557581	15.11	14.88	1492.6909	0.992	-0.0040	-0.018	-0.0040	-0.012	0.0010
lm0091i14577	78.91731	-69.28719	4.566657	16.40	16.59	1791.7729	0.963	-0.049	-0.067	-0.028	-0.043	-0.0010
lm0027n9856*	83.4818	-70.31804	4.56889	17.29	17.21	1883.6761	0.947	-0.0040	-0.086	0.0020	-0.057	-0.0030
lm0190m21869	79.39204	-67.93565	4.571853	15.25	15.04	2172.7658	0.967	0.0030	-0.043	-0.0010	-0.024	0.0020
lm0114k19051	73.96926	-69.86952	4.577471	15.33	15.13	532.5305	0.873	-0.038	-0.152	-0.025	-0.054	0.0010
lm0020n19615	82.67397	-69.32445	4.585353	14.10	13.94	754.7607	0.909	-0.034	-0.092	-0.01	-0.080	-0.0020
lm0187m11496	78.38739	-68.77464	4.591479	16.31	16.07	1892.8390	0.903	-0.09	-0.144	-0.042	-0.074	-0.0020
lm0033m21700	85.42329	-69.53002	4.613339	15.19	15.07	799.8171	0.984	-0.0050	-0.019	-0.0050	-0.0050	0.0030
lm0133n16000	71.60732	-69.64112	4.613573	16.42	16.26	2305.6006	0.994	-0.035	-0.018	0.0010	-0.0020	-0.0040
lm0025m30936	83.32691	-69.91737	4.636845	16.37	16.35	1092.6860	0.891	-0.088	-0.139	-0.039	-0.068	0.0080
lm0211m18859*	83.90938	-67.76044	4.6432219	16.65	16.53	2171.7647	0.927	-0.011	-0.076	0.0020	-0.080	-0.0
lm0550k11523	75.25322	-70.52935	4.658797	16.63	16.49	1811.7418	0.985	0.0020	-0.023	-0.0080	-0.015	0.0060
lm0185n11636	78.27415	-68.8445	4.66509	16.29	16.02	1278.5415	0.984	-0.0060	-0.025	-0.0060	-0.013	0.0010
lm0135k14008	70.90269	-68.56689	4.673342	16.37	16.18	1255.5650	0.946	-0.046	-0.068	-0.014	-0.031	0.0020
lm0350i4429	84.46882	-69.83939	4.674718	16.40	16.38	737.8651	0.977	-0.02	-0.02	0.0020	0.0010	0.0010
lm0135k9012	71.2563	-69.8038	4.708726	16.22	16.16	2254.5578	0.992	-0.021	-0.011	-0.0	0.0010	-0.0020
lm0093m30768	79.33994	-69.56467	4.721156	16.56	16.42	1440.8605	0.909	-0.12	-0.135	-0.061	-0.088	0.0060
lm0225k18526	85.5041	-68.46532	4.750699	16.19	16.01	1547.7200	0.976	-0.0020	-0.01	-0.046	-0.0060	-0.024
lm0356m19146	84.7948	-67.43387	4.755264	15.43	15.22	2224.7903	0.951	-0.0020	-0.067	-0.046	-0.0060	0.0080
lm0177m19148	76.59168	-68.82087	4.760853	16.67	16.48	802.7677	0.981	-0.013	-0.025	-0.0010	0.0010	-0.0010
lm0551i20848*	76.23095	-70.73175	4.7619636	15.03	14.79	731.8206	0.986	-0.0040	-0.016	-0.0010	-0.0040	0.0
lm0333n6568	82.25158	-66.78851	4.770854	15.11	14.84	1791.7908	0.953	-0.022	-0.042	-0.0010	0.0020	0.0050
lm0543m8169	74.54655	-70.84114	4.777862	16.01	15.76	1926.6584	0.949	-0.0070	-0.078	-0.019	-0.044	0.0090

lm0180k16760	76.81278	-67.75484	4.784288	15.54	15.26	1927.6826	0.976	0.0	-0.044	-0.0070	-0.018	-0.0040
lm0567k23259	78.47329	-71.64955	4.803925	16.56	16.38	1312.5079	0.977	-0.027	-0.026	0.0	0.020	-0.0040
lm0427l12767	75.272	-66.15544	4.805932	16.12	15.86	1124.7340	0.981	-0.0060	-0.028	-0.0010	-0.016	0.0030
lm0031n6676	85.46572	-69.23969	4.853431	15.58	15.51	828.6578	0.954	0.0050	-0.04	-0.014	-0.014	-0.0070
lm0294l25574	73.8772	-67.27274	4.855458	15.50	15.32	1947.6718	0.971	-0.033	-0.037	0.0030	0.0	-0.0030
lm0375l14140	89.03712	-67.20525	4.870657	16.50	16.36	806.7311	0.902	-0.087	-0.133	-0.049	-0.07	0.0010
lm0311n13108	78.6852	-66.48576	4.876315	15.63	15.35	1569.6472	0.962	-0.017	-0.068	-0.016	-0.055	-0.0060
lm0127k13132	73.14424	-70.1884	4.892616	16.08	15.96	1830.6673	0.893	-0.061	-0.141	-0.038	-0.065	0.0020
lm0216l16590	82.6847	-68.97782	4.943171	15.93	15.76	2263.7731	0.981	-0.0050	-0.025	-0.0070	-0.015	-0.0010
lm0192n26066*	79.02275	-68.31199	4.9456601	15.38	15.31	397.8481	0.992	-0.0060	-0.018	0.0010	-0.0090	-0.0010
lm0326m17046*	79.46031	-67.56801	4.951432	17.29	17.07	1266.5563	0.984	-0.0050	-0.027	0.0060	-0.014	0.0020
lm0476k5610	82.74342	-65.94116	4.951673	16.20	16.09	1615.5919	0.897	-0.012	-0.125	-0.01	-0.034	0.0050
lm0344l12773	82.6699	-67.19545	4.952487	15.43	15.23	2095.9139	0.98	0.0050	-0.036	-0.0040	-0.023	0.0020
lm0185l23772	77.78312	-68.63659	4.970047	15.73	15.55	496.6719	0.976	-0.023	-0.019	0.0020	0.020	-0.0010
lm0015m26793	81.58538	-69.89497	4.970604	16.08	15.84	1193.6422	0.968	-0.036	-0.017	0.0020	0.020	0.0020
lm0121m11642	73.60162	-69.11359	4.995179	15.46	15.31	1153.5648	0.877	-0.088	-0.171	-0.049	-0.079	0.017
lm0343n25745	83.9537	-66.91106	4.99707	14.69	14.42	459.7833	0.856	-0.033	-0.152	-0.017	-0.041	0.014
lm0112k22638	74.22448	-69.56688	4.999207	14.56	14.44	2448.9162	0.906	0.0090	-0.043	0.011	-0.025	-0.011
lm0427k13855	75.55629	-66.00605	5.016469	15.86	15.62	2210.7725	0.91	-0.038	-0.088	-0.0080	-0.025	0.0060
lm0345k8617	83.80798	-67.00978	5.019559	16.20	15.94	2085.9135	0.996	-0.012	-0.050	-0.0030	-0.040	0.0040
lm0585n19126*	83.19272	-71.41206	5.021392	17.37	17.17	2085.9098	0.984	-0.0	-0.047	-0.0060	-0.042	0.0010
lm051m13870*	76.50467	-70.53596	5.023262	16.27	15.91	1477.6548	0.981	-0.0080	-0.035	-0.0080	-0.032	0.0010
lm024k24487	84.35433	-68.5083	5.049097	15.93	15.76	2279.5966	1.002	-0.0080	-0.021	-0.0040	-0.01	-0.0
lm0011k23633	81.12698	-69.18929	5.083128	16.32	16.37	2174.7794	0.879	-0.066	-0.154	-0.036	-0.068	0.0040
lm0093k30805	79.18672	-69.56374	5.085768	16.39	16.34	1900.7455	0.9	-0.076	-0.146	-0.04	-0.073	0.0070
lm0012n22151	80.39573	-69.68261	5.111026	16.64	16.33	1082.8546	0.966	-0.018	-0.03	0.0010	0.0030	0.0040
lm0540m13587	73.46764	-70.53421	5.118075	16.11	15.80	1942.6161	0.983	-0.0060	-0.024	-0.0030	-0.017	0.0
lm0355l4619	85.47574	-67.13673	5.132899	15.70	15.53	1845.8486	0.976	-0.03	-0.019	0.0010	0.0	0.0060
lm0123k2357	72.82093	-69.4152	5.156041	16.33	16.32	2303.6038	0.899	-0.076	-0.137	-0.042	-0.08	0.0080
lm0191l25589	79.64754	-67.98489	5.159253	15.67	15.58	1745.8712	0.886	-0.025	-0.12	-0.011	-0.03	0.0090
lm0021l30770	83.06041	-69.37757	5.171793	15.58	15.37	1082.8784	0.965	-0.016	-0.013	-0.076	-0.026	-0.034
lm0701m12218	81.93523	-71.94132	5.172023	16.45	16.45	1624.5706	1.004	-0.011	-0.0060	0.0010	0.0010	-0.0070
lm0216k9627	82.60651	-68.76948	5.203106	14.13	13.95	1823.8298	0.984	-0.014	-0.021	-0.0	-0.0020	-0.0010
lm0024k27974	81.69832	-69.80184	5.204477	15.44	15.32	1582.6441	0.983	-0.017	-0.014	0.0	0.0010	0.0060
lm0052n19538	88.26495	-69.68688	5.22544	15.58	15.38	2347.6571	0.964	-0.019	-0.042	0.0020	-0.0020	0.0020
lm0111m9175	75.64376	-69.09596	5.255775	15.39	14.99	1865.5941	0.995	-0.0070	-0.04	-0.0020	-0.034	0.0020
lm0100m12334	76.38395	-69.12991	5.262912	16.19	16.03	468.7993	0.896	-0.077	-0.141	-0.036	-0.072	0.0080
lm0033k7569	85.20626	-69.44349	5.2691	15.30	15.16	2225.7022	0.989	-0.0040	-0.011	-0.0040	-0.0020	0.0030
lm0333l15404	81.89971	-66.84652	5.27222	15.55	15.42	2202.7808	0.955	-0.019	-0.042	0.0010	0.0020	0.0040
lm0612l10194	87.80168	-71.02961	5.279445	16.45	16.33	1547.7661	0.991	-0.023	-0.012	-0.0010	0.0020	-0.0010
lm0330k4290	80.97198	-66.27295	5.28192	16.57	16.43	1089.8193	0.907	-0.098	-0.136	-0.049	-0.085	-0.0020

APPENDIX A. PROPERTIES OF THE “HOT” ECLIPSING BINARIES IN THE LMC

lm0587118507	82.38394	-71.78632	5.282775	15.96	15.80	383.7489	0.913	-0.085	-0.133	-0.035	-0.077	-0.0010
lm022316459	85.37276	-68.18986	5.299378	15.34	15.20	845.6984	0.922	-0.023	-0.074	-0.0020	-0.0080	0.0080
lm0116k21077	74.17121	-70.24412	5.30968	15.40	15.19	2250.5707	0.972	-0.028	-0.028	-0.0010	0.0010	0.0020
lm0207k17059	81.64794	-68.80979	5.311128	16.22	16.14	851.7868	1.011	-0.064	-0.034	-0.027	-0.039	0.0020
lm0121m28673	73.65569	-69.36974	5.327283	16.05	15.94	1610.5479	0.895	-0.032	-0.118	-0.015	-0.036	0.0090
lm0020m16359	82.46783	-69.15634	5.335197	14.99	14.76	1794.8611	0.933	-0.026	-0.105	-0.035	-0.053	-0.013
lm0224m12591*	84.97701	-68.42867	5.34493	14.79	14.59	1289.6036	0.984	0.0010	-0.032	-0.020	-0.029	-0.0
lm0033m6304	85.23578	-69.43834	5.369545	15.48	15.29	2226.8657	0.981	-0.060	-0.03	-0.050	-0.02	-0.0010
lm0245k7095*	89.09202	-68.39552	5.377706	16.86	16.74	1773.8788	0.978	-0.020	-0.035	-0.020	-0.01	0.0010
lm0031122987	85.19681	-69.34126	5.413977	14.20	14.06	1786.7890	0.93	-0.070	-0.111	-0.050	-0.061	-0.0010
lm00216m10589	82.75361	-68.92483	5.44858	14.84	14.64	1255.6141	0.977	-0.015	-0.026	-0.020	0.0	-0.0020
lm0092m18774	78.42181	-69.54597	5.457309	15.73	15.55	378.7175	0.942	-0.080	-0.073	0.0020	-0.048	0.0040
lm029413818	74.12505	-67.19756	5.471904	15.72	15.55	1277.4981	0.987	-0.01	-0.013	-0.010	0.0010	0.0010
lm0114k21690	74.05789	-69.88678	5.507995	15.32	15.14	555.5532	0.947	0.0030	-0.097	-0.028	-0.058	0.017
lm0223k27353	85.28551	-68.16349	5.529928	16.20	16.11	1191.7629	0.991	-0.012	-0.060	-0.0	0.0	-0.0
lm0186m23446	77.18403	-68.85675	5.534274	16.50	16.37	1827.7468	0.966	-0.026	-0.037	-0.030	-0.0080	-0.0020
lm0346113438	82.81742	-67.54852	5.570352	14.39	14.16	837.7814	0.91	-0.034	-0.078	-0.050	-0.01	0.019
lm0207n15251	81.93445	-68.96115	5.598846	15.47	15.20	1252.5839	0.99	-0.030	-0.013	-0.030	-0.0080	0.0
lm0093k26732	79.18502	-69.54251	5.603447	15.88	15.79	821.7920	0.967	0.0080	-0.059	0.0020	-0.049	-0.0080
lm0357k24043*	85.56601	-67.47813	5.629336	16.74	16.66	384.8700	0.922	-0.015	-0.085	-0.050	-0.016	0.0070
lm0024k16099	81.77809	-69.73688	5.638806	15.78	15.68	361.8543	0.926	-0.077	-0.105	-0.034	-0.063	-0.0010
lm0021k21280	82.75955	-69.18045	5.671847	15.60	15.65	1628.5730	0.949	-0.010	-0.051	-0.01	-0.016	-0.0020
lm0021m26411*	83.24668	-69.20468	5.708342	15.11	14.95	1195.7057	0.968	-0.010	-0.056	-0.010	-0.045	-0.0010
lm0185k15339	77.97996	-68.43905	5.726627	16.31	16.27	367.7268	0.898	-0.071	-0.133	-0.036	-0.062	0.0050
lm0543128153	73.87045	-71.11878	5.736595	15.91	15.88	556.5493	0.979	-0.025	-0.016	0.0010	-0.0010	0.0060
lm0127110608	73.20634	-70.32542	5.78278	16.11	16.00	1896.7349	0.925	-0.013	-0.086	-0.020	-0.022	-0.0010
lm010515842	76.97995	-69.9654	5.78581	16.12	16.00	2230.8260	0.976	0.0020	-0.018	-0.048	0.0030	0.03
lm0091m26247	79.40242	-69.3506	5.813256	15.41	15.30	518.5181	0.983	-0.018	-0.013	0.0	0.0	0.0030
lm0466m11710	81.64273	-66.13484	5.822653	15.27	15.05	1910.7258	0.97	-0.016	-0.071	-0.015	-0.034	0.0020
lm010511377*	76.82283	-70.01872	5.8361182	15.37	15.19	1416.8380	0.983	-0.060	-0.022	-0.030	-0.0060	0.0
lm0013m20776	81.44272	-69.51774	5.874426	16.29	16.35	1114.7395	0.942	-0.083	-0.095	-0.051	-0.065	0.0010
lm0010124242	79.89864	-69.36666	5.941613	15.38	15.20	1367.8727	0.968	-0.012	-0.034	0.0	-0.0010	0.0040
lm0021k14832	83.10998	-69.1388	5.973243	15.36	15.16	411.8004	0.991	-0.040	-0.015	-0.070	-0.0080	0.0010
lm0427n16272*	76.03168	-66.18205	6.00374	15.24	14.95	1208.6509	0.963	-0.023	-0.042	0.0010	0.0	-0.0030
lm0355m22531	85.62223	-67.10039	6.053452	15.49	15.33	1845.8486	0.982	-0.017	-0.01	-0.010	0.0020	0.0040
lm0220119368	84.44876	-67.94483	6.055055	16.07	15.95	1560.7753	0.935	-0.038	-0.076	-0.0080	-0.016	-0.0010
lm0171m5451	76.17842	-67.84531	6.065706	14.96	14.77	1929.6359	0.898	-0.054	-0.147	-0.036	-0.082	-0.0010
lm0356115776	84.5512	-67.5715	6.072745	15.89	15.79	809.7491	0.987	-0.013	-0.0080	0.0020	0.0	0.0030
lm0120k21262*	72.10659	-69.19104	6.127084	16.50	16.42	1468.5778	0.971	-0.050	-0.052	-0.0060	-0.039	-0.0
lm021116920	83.30612	-67.84072	6.19121	16.22	16.13	1883.6801	0.973	-0.018	-0.018	-0.0	-0.0010	0.0020
lm0560m18929	77.53186	-70.71221	6.192697	16.23	16.02	2028.5055	0.979	-0.070	-0.024	-0.01	-0.016	-0.0020

lm0101k22147	76.88401	-69.19093	6.208241	14.74	14.53	1442.7940	0.974	-0.027	-0.026	-0.0010	-0.0010	0.0030
lm0020m6294*	82.59216	-69.24788	6.2292581	14.76	14.42	875.5657	0.955	0.0050	-0.084	0.0020	0.0020	-0.014
lm0020m21732*	82.66334	-69.33662	6.271038	16.69	16.52	596.4752	0.989	0.0010	-0.02	0.0020	0.0020	0.0010
lm0564k21288	77.28653	-71.28191	6.306663	15.53	15.41	792.7147	0.89	-0.075	-0.142	-0.038	-0.038	0.012
lm0466m6181	81.56648	-66.09182	6.332723	15.64	15.55	363.8197	0.91	-0.069	-0.11	-0.025	-0.025	0.013
lm0173n16894	76.40417	-68.24821	6.347941	14.97	14.70	538.5495	0.98	-0.0020	-0.016	-0.015	-0.015	0.0050
lm0540k16892*	72.73725	-70.56097	6.37983	16.60	16.55	1117.7763	0.982	-0.0010	-0.03	-0.0	-0.0	-0.0
lm0344k22660	82.63513	-67.10897	6.434828	15.04	14.84	1193.6830	0.969	-0.022	-0.027	0.0010	0.0010	-0.0
lm0124k25126	72.188	-69.91293	6.438358	15.64	15.58	864.6842	0.982	-0.016	-0.014	-0.0010	-0.0010	-0.0
lm0303k23599	76.57203	-66.73731	6.463085	15.59	15.46	445.7635	0.916	-0.041	-0.099	-0.013	-0.013	0.0020
lm0194m25484	79.01997	-68.65582	6.473465	15.36	15.22	1098.6948	0.953	-0.0070	-0.053	-0.0060	-0.0060	0.0070
lm0090k15089*	78.00357	-69.15152	6.5169401	16.53	16.39	583.4991	0.987	-0.0	-0.029	0.0030	0.0030	-0.0030
lm0091n31944*	79.41439	-69.38044	6.51753	16.79	16.75	727.8706	0.96	-0.012	-0.05	-0.0060	-0.0060	-0.0
lm0346m17567	82.98578	-67.58377	6.532332	14.09	13.85	1582.6577	0.957	0.0020	-0.052	-0.0050	-0.0050	-0.0030
lm0035m23079	85.5935	-69.88483	6.569401	15.66	15.50	862.7340	0.961	-0.017	-0.041	0.0020	0.0020	-0.0010
lm0690k9526	78.10279	-71.90847	6.596262	15.73	15.50	508.6562	0.977	-0.017	-0.021	-0.0020	-0.0020	-0.0010
lm0457l13469	80.52857	-66.1587	6.640871	15.17	14.96	2263.6549	0.905	-0.06	-0.131	-0.03	-0.03	-0.0030
lm0335n23069	82.48431	-67.2425	6.898566	16.26	16.07	1768.8468	0.973	-0.043	-0.03	-0.0020	-0.0020	-0.0020
lm0180m27164*	77.51915	-67.81345	6.9137979	15.45	15.10	2294.6680	0.982	-0.0080	-0.028	0.0010	0.0010	0.0030
lm0364k12751	86.12186	-67.04148	6.977975	15.92	15.78	705.8406	0.953	-0.048	-0.041	-0.0060	-0.0060	0.0050
lm0294l4906*	73.84732	-67.13827	7.096154	15.37	15.17	1782.7369	0.989	0.0	-0.013	-0.0010	-0.0010	0.0010
lm0335n25477*	82.28467	-67.28841	7.1173239	14.93	14.70	1834.7677	0.91	-0.0030	-0.093	-0.0030	-0.0030	0.0020
lm0214m14689*	82.89389	-68.59669	7.150098	15.07	15.16	2270.6509	0.991	-0.0030	-0.0090	-0.015	-0.015	0.0030
lm0367m14504*	87.60799	-67.4051	7.177252	16.90	16.79	2338.6533	0.995	0.0010	-0.017	0.0010	0.0010	-0.0
lm0427n12122	75.86553	-66.14977	7.194033	15.73	15.45	1942.6265	0.984	-0.0080	-0.022	-0.03	-0.03	-0.012
lm0241n18960	89.43426	-67.93432	7.227958	15.87	15.72	402.6331	0.978	-0.033	-0.022	0.0010	0.0010	-0.0020
lm0246k6595	88.14596	-68.74102	7.284157	15.60	15.50	2028.5439	0.942	-0.078	-0.092	-0.029	-0.029	-0.0020
lm0093k5253*	78.97127	-69.43271	7.284388	15.71	15.74	1835.7526	0.925	-0.039	-0.136	-0.02	-0.02	-0.0020
lm0585l5842	82.78241	-71.33556	7.286296	14.95	14.74	1102.7832	0.967	-0.016	-0.026	0.0	0.0	0.0080
lm0033m20529	85.47251	-69.52251	7.464778	14.26	14.07	1818.8043	0.962	-0.0020	-0.052	-0.0030	-0.0030	0.0050
lm0014k7299	80.17669	-69.79884	7.536747	15.88	15.79	2259.5285	0.974	-0.022	-0.024	0.0	0.0	0.0010
lm0427k7505*	75.42766	-65.95939	7.684446	15.40	15.15	2192.6953	0.981	-0.0060	-0.015	-0.03	-0.03	-0.0090
lm0435m12381	77.55651	-65.62774	7.696551	16.04	15.88	1886.6258	0.89	-0.018	-0.138	0.0060	0.0060	0.018
lm0180n9316	77.12842	-67.92971	7.754096	15.40	15.22	1589.6684	0.972	-0.029	-0.028	0.0010	0.0010	-0.0
lm0356m11102	84.74967	-67.37777	7.78835	15.73	15.66	2053.5103	0.99	-0.026	-0.011	0.0010	0.0010	-0.0030
lm0033n12413	85.26999	-69.63026	7.942126	15.02	14.92	315.8958	0.974	0.0070	-0.051	-0.01	-0.01	-0.011
lm0326m7743	79.81672	-67.49871	8.015506	15.69	15.55	1896.7593	0.929	-0.038	-0.116	-0.028	-0.028	0.0050
lm0156m3536*	71.65461	-68.83272	8.278086	16.51	16.51	2155.7386	0.909	-0.013	-0.129	-0.0060	-0.0060	0.0050
lm0157m4689*	72.58175	-68.73229	8.402946	16.44	16.40	411.7114	0.972	0.0010	-0.021	-0.0020	-0.0020	-0.0010
lm0354n16185*	84.83711	-67.21527	8.4584	16.06	15.95	1497.7810	0.972	-0.0030	-0.03	-0.0080	-0.0080	-0.0020
lm0020k10287	81.94049	-69.1285	8.463039	14.74	14.56	1566.6321	0.923	-0.032	-0.101	-0.021	-0.021	0.0010



APPENDIX A. PROPERTIES OF THE “HOT” ECLIPSING BINARIES IN THE LMC

lm0467k11917*	82.09084	-65.9874	8.4646063	15.03	14.81	1538.6456	0.983	-0.0050	-0.017	-0.0050	-0.0090	0.0010
lm0024m1498	82.29974	-69.76834	8.485941	15.07	14.98	1447.8263	0.915	-0.09	-0.145	-0.053	-0.099	0.0030
lm0033m5960	85.30216	-69.43568	8.583074	13.83	13.63	2263.7846	0.984	-0.0030	-0.02	-0.017	-0.0030	0.0060
lm0356l21486	84.35704	-67.61704	8.816562	15.69	15.54	1657.5337	0.887	-0.025	-0.122	-0.012	-0.035	0.014
lm0541l9275*	73.90085	-70.67855	8.850098	16.55	16.45	1926.6584	0.98	0.0010	-0.021	0.0	-0.0080	0.0
lm0173m17717	76.54398	-68.09531	8.856537	13.59	13.39	1918.6627	0.976	-0.0040	-0.027	-0.015	-0.0070	0.0030
lm0191n3246*	80.12526	-67.84655	14.645028	15.45	15.39	1150.6566	0.986	-0.0010	-0.017	-0.0010	-0.0030	0.0010
lm0173n32162*	76.48671	-68.33424	21.041492	14.93	15.11	759.8432	0.957	-0.0090	-0.086	-0.011	-0.016	-0.01

Table A.1: Identification, main properties and Fourier parameters for 1768 HEBs in the LMC (Column 1: EROS-2 identification of the star; Column 2: Right ascension from the EROS-2 catalogue; Column 3: Declination from the EROS-2 catalogue; Column 4: Period (\*). Stars for which a new period was derived in this study. See text for the details.); Column 5: Mean magnitude in the  $R_{EROS}$  passband; Column 6: Mean magnitude in the  $B_{EROS}$  passband; Column 7: Epoch of the primary minimum; Column 8-Column 14: Fourier parameters of the light curves).

EROS-2 id	VMC id	Period (day)	$K_{s,max}$ (mag)	$R_{EROS,max}$ (mag)
lm0323n20546	VMC J052140.98-665227.93	0.900708	17.116	17.057
lm0344m26510	VMC J053208.76-670741.80	0.912445	17.260	17.161
lm0023n11843	VMC J053319.72-693719.70	0.912568	17.314	17.143
lm0030n21391	VMC J053717.63-692254.37	0.922672	16.754	16.644
lm0226n20767	VMC J053825.02-690004.55	0.923941	17.497	17.560
lm0231k9063	VMC J054830.84-674223.25	0.927999	16.992	16.883
lm0214n10459	VMC J053127.29-683413.65	0.938971	17.652	17.635
lm0171m16733*	VMC J050444.08-674447.89	0.939001	15.982	15.748
lm0127k12134	VMC J045304.25-701051.19	0.939454	16.700	17.384
lm0342k18196	VMC J053134.88-664500.10	0.941447	17.195	16.915
lm0346l14981	VMC J053111.35-673339.52	0.941548	16.370	17.043
lm0466k23468	VMC J052536.95-660416.63	0.943032	17.170	17.085
lm0436n21036	VMC J050715.90-661216.34	0.944593	17.196	17.059
lm0217m19208	VMC J053621.59-684929.14	0.954486	16.093	16.951
lm0030n19548	VMC J053752.94-692013.54	0.955261	16.975	16.924
lm0090n16243	VMC J051340.27-691821.72	0.956439	16.777	16.634
lm0340m15852	VMC J053216.72-662120.52	0.958465	17.381	17.349
lm0015k6383	VMC J052344.20-694735.21	0.964159	17.116	16.780
lm0542k20454	VMC J045137.03-705752.57	0.965838	17.335	17.277
lm0034k10238	VMC J053511.80-694913.60	0.968988	16.425	17.019
lm0355n11866	VMC J054408.49-671042.57	0.969348	17.292	17.052
lm0093k16356	VMC J051623.46-692920.82	0.977186	16.810	16.706
lm0321l27158	VMC J052054.57-663434.22	0.977509	17.104	17.065
lm0223n26953	VMC J054244.88-681844.65	0.979034	17.558	17.662
lm0023k20021	VMC J053227.77-693037.28	1.011662	17.128	16.700
lm0033m10429	VMC J054125.68-692745.13	1.019232	17.774	17.693
lm0117l9906	VMC J050011.97-701923.12	1.020034	17.152	17.105
lm0030n22649	VMC J053721.60-692128.37	1.026528	16.532	16.624
lm0025n17091	VMC J053414.41-695957.92	1.028086	16.682	17.315
lm0091m27064	VMC J051718.22-691213.89	1.041214	17.253	16.755
lm0093n5032	VMC J051820.70-693454.13	1.042603	16.634	16.539
lm0173m9757	VMC J050455.74-680305.15	1.046688	16.610	16.680
lm0424n14561	VMC J045939.22-654819.86	1.047235	16.853	16.677
lm0493n18692	VMC J054907.59-652842.80	1.050931	16.819	17.488
lm0031m9651	VMC J054224.86-690610.38	1.051009	16.408	16.838
lm0011l5712	VMC J052349.29-691422.12	1.051238	16.539	16.607
lm0244k10748	VMC J055158.84-682518.50	1.051608	17.509	17.600
lm0540l15552	VMC J045139.44-704222.55	1.052165	17.312	17.474
lm0020l8553	VMC J052721.55-691551.08	1.054358	17.103	16.790

APPENDIX A. PROPERTIES OF THE “HOT” ECLIPSING BINARIES IN THE LMC

lm0367n18805	VMC J054943.82-673602.65	1.055955	17.576	17.578
lm0184n14844	VMC J050834.41-683353.52	1.067386	16.868	16.903
lm0570m20301	VMC J051907.13-703420.27	1.070216	16.315	16.109
lm0336i21294	VMC J052426.44-673557.02	1.070847	17.879	17.697
lm0334i20690	VMC J052330.93-671420.32	1.071333	16.975	16.920
lm0116m17752	VMC J045716.76-701251.26	1.071932	16.860	16.684
lm0335i16808	VMC J052714.45-671241.07	1.073703	16.377	16.092
lm0337k16442	VMC J052714.12-672502.96	1.07405	17.683	17.526
lm0295i19334	VMC J045943.51-671309.04	1.074702	17.050	16.855
lm0207n19761	VMC J052855.52-685929.93	1.074897	17.305	17.066
lm0335n6422	VMC J052954.30-670819.99	1.076161	17.361	17.193
lm0184k20015	VMC J050709.23-682830.38	1.079741	17.332	17.328
lm0040k16225	VMC J054335.85-690932.27	1.087516	17.347	17.281
lm0374n6047	VMC J055318.81-670841.54	1.090677	17.550	17.490
lm0301m26336	VMC J050730.31-662441.93	1.090782	17.581	17.622
lm0425n26027	VMC J050257.84-655243.78	1.090849	17.718	17.760
lm0584i11571	VMC J052643.38-712231.69	1.091989	17.231	17.632
lm0466m12019	VMC J052701.89-655854.05	1.092537	16.964	16.977
lm0207i9965	VMC J052651.53-685529.03	1.094904	16.933	16.739
lm0207i11656	VMC J052624.11-685614.69	1.095419	17.498	17.608
lm0093n12350	VMC J051847.36-693705.07	1.100478	18.407	17.412
lm0550k13137	VMC J050109.34-703227.41	1.10302	16.570	16.997
lm0366k17409	VMC J054412.68-672537.21	1.105186	16.330	16.498
lm0364i13690	VMC J054451.36-671217.70	1.105617	17.282	17.056
lm0346i8111	VMC J053107.21-673023.70	1.112761	17.417	17.115
lm0243i16058	VMC J055515.72-681548.49	1.112807	17.310	17.421
lm0232i17259	VMC J054515.80-681626.21	1.120751	17.271	17.205
lm0457k18380	VMC J052226.94-660141.91	1.127347	17.341	17.357
lm0172i6626	VMC J050054.84-681414.07	1.13021	17.132	16.869
lm0310k15114	VMC J051006.33-662105.59	1.132918	17.648	17.631
lm0325i27285	VMC J052041.48-671625.15	1.135758	16.563	16.402
lm0010k15429	VMC J051905.15-690917.93	1.136931	16.852	16.585
lm0556m19867	VMC J050310.90-713801.60	1.139527	17.425	17.469
lm0214n9616	VMC J053143.12-683354.22	1.143016	17.175	17.346
lm0245k7908	VMC J055523.86-682408.62	1.143467	17.459	17.426
lm0455i5567	VMC J052215.63-654416.74	1.143775	16.647	16.352
lm0217n14277*	VMC J053610.78-685726.49	1.147572	16.327	16.312
lm0467m6802	VMC J053019.84-655639.46	1.147802	16.211	16.033
lm0571i24463	VMC J052213.31-704439.71	1.148628	17.603	17.538
lm0031n17224	VMC J054205.62-692226.65	1.14893	16.641	16.318
lm0033m26708	VMC J054125.66-693338.54	1.158284	17.164	17.041

lm0575n11053	VMC J052322.45-712622.63	1.16016	17.267	17.216
lm0014i20054	VMC J052019.46-700156.85	1.160262	17.829	17.524
lm0466i19242	VMC J052538.13-661143.48	1.163589	17.652	17.487
lm0535n11277	VMC J044942.73-712822.25	1.168449	16.767	16.958
lm0103i13951	VMC J050851.76-693748.69	1.174507	16.745	16.544
lm0226n24168	VMC J053839.17-690140.79	1.176008	16.273	16.196
lm0457i19060	VMC J052113.24-661252.39	1.176108	17.248	17.301
lm0214m29033	VMC J053122.05-683134.08	1.178663	16.065	16.422
lm0540i22424	VMC J045123.99-704536.93	1.181881	16.845	16.945
lm0303i23428	VMC J050712.25-665310.23	1.183669	17.587	17.510
lm0021k22831	VMC J053134.92-691121.79	1.184539	16.742	16.755
lm0201k10778	VMC J052621.83-674226.98	1.187596	16.769	17.553
lm0312k15523	VMC J050955.28-664355.14	1.188117	17.292	17.443
lm0114m27899	VMC J045712.52-695443.81	1.191167	16.922	16.774
lm0200k19885	VMC J052142.45-674951.21	1.191483	17.020	17.205
lm0366k10436	VMC J054457.24-672229.27	1.193346	16.695	16.447
lm0044k3974	VMC J054428.89-694644.07	1.193368	16.255	16.133
lm0344m1850	VMC J053215.41-665803.46	1.193709	16.554	16.219
lm0214n25393	VMC J053111.12-683947.01	1.205505	16.994	17.335
lm0115n14463	VMC J050256.10-695854.83	1.2068	17.187	16.952
lm0373m20395	VMC J055711.53-664418.59	1.207672	17.585	17.780
lm0230m9259	VMC J054543.42-674247.82	1.207767	17.290	17.471
lm0193n5944	VMC J052101.69-681058.62	1.207775	17.370	17.314
lm0540k22686	VMC J045150.15-703608.59	1.210708	17.806	17.667
lm0302n12595	VMC J050518.64-664956.27	1.213151	17.168	17.091
lm0030n6815	VMC J053752.89-692349.91	1.213239	16.376	16.212
lm0255m21132	VMC J060440.97-683057.48	1.213994	17.600	17.565
lm0033i8069	VMC J053955.35-693606.14	1.215039	16.603	16.692
lm0423m21313	VMC J050306.73-652030.78	1.21574	17.503	17.227
lm0240i13940	VMC J055157.14-675351.67	1.22005	17.249	17.318
lm0552n28102	VMC J050138.11-710745.89	1.224882	17.587	17.468
lm0025i19940	VMC J053232.13-700056.63	1.225202	17.368	17.387
lm0346i13640	VMC J053015.09-673259.82	1.225316	16.563	16.362
lm0200i20561	VMC J052200.96-675643.02	1.225852	16.214	15.884
lm0184n22563	VMC J050841.72-683809.04	1.226475	17.163	17.279
lm0304n29842	VMC J050439.61-671727.85	1.229024	16.720	16.475
lm0090m26466	VMC J051432.59-691226.75	1.232396	17.092	16.816
lm0336m21470	VMC J052622.67-672644.90	1.236096	17.527	17.393
lm0344i5959	VMC J053028.46-670858.59	1.240057	17.045	17.179
lm0090m13647	VMC J051308.32-690801.68	1.240532	16.511	16.523
lm0175m17458	VMC J050608.86-682652.63	1.244897	16.650	16.337

APPENDIX A. PROPERTIES OF THE “HOT” ECLIPSING BINARIES IN THE LMC

lm0303n10523	VMC J050848.42-664825.91	1.246321	17.550	17.673
lm0342n24002	VMC J053158.91-665526.33	1.24847	17.472	17.409
lm0304n24921	VMC J050357.90-671538.31	1.24985	16.697	16.477
lm0214n7884	VMC J053112.15-683316.02	1.250305	17.020	16.925
lm0044i24715	VMC J054356.05-700343.04	1.251463	17.393	17.590
lm0020m14007	VMC J052946.13-690828.40	1.256518	15.781	16.643
lm0182i13191	VMC J050756.93-681406.12	1.256523	17.041	16.896
lm0325m15768	VMC J052300.57-670238.00	1.260551	16.881	16.770
lm0671i5056	VMC J045819.25-720727.05	1.271916	17.580	17.682
lm0436k8952	VMC J050527.83-655803.42	1.275596	17.600	17.725
lm0214m29858	VMC J053110.13-683153.59	1.279218	17.294	17.298
lm0583m25712	VMC J053144.06-705623.79	1.280423	16.441	16.934
lm0012m20602	VMC J052233.82-693255.68	1.284101	16.667	17.289
lm0197n19534	VMC J052043.69-685923.38	1.284845	17.209	17.331
lm0017m17883	VMC J052701.41-701252.43	1.289967	15.915	16.975
lm0293i14089	VMC J045959.15-665005.45	1.29204	17.617	17.642
lm0030k6634	VMC J053607.01-690554.27	1.293848	15.904	15.966
lm0366k19655	VMC J054434.04-672637.09	1.295471	16.897	16.791
lm0184k11257	VMC J050750.94-682524.40	1.297875	17.064	16.852
lm0207i9702	VMC J052630.11-685524.08	1.302753	15.797	16.319
lm0200i20952	VMC J052204.85-675654.07	1.304803	16.366	16.250
lm0033k16643	VMC J053920.50-693006.88	1.305743	15.700	15.671
lm0033k28357	VMC J053941.71-693424.83	1.306841	15.684	15.661
lm0344k4525	VMC J053112.67-665909.15	1.310804	16.848	16.612
lm0323i7738	VMC J052102.34-664749.90	1.315224	16.912	16.910
lm0321m13358	VMC J052123.12-661945.79	1.31821	17.192	17.273
lm0551k19078	VMC J050403.86-703547.38	1.318882	17.501	17.209
lm0466m23585	VMC J052547.02-660437.18	1.318958	16.578	16.576
lm0340n22383	VMC J053222.31-663309.62	1.319689	17.673	17.616
lm0366n14593	VMC J054735.62-673323.51	1.321337	17.842	17.693
lm0032k20313	VMC J053634.89-693349.73	1.323792	16.681	16.990
lm0012i17935	VMC J051951.14-694002.58	1.323984	16.143	16.314
lm0033m6850	VMC J054129.05-692626.67	1.32799	17.168	17.058
lm0330i18021	VMC J052419.71-663140.41	1.330011	16.530	16.447
lm0210k24451	VMC J052920.91-674917.62	1.337468	16.762	16.565
lm0587n19385	VMC J053143.62-714716.42	1.339509	16.050	16.605
lm0056n22735	VMC J055425.98-702434.41	1.341028	16.992	16.802
lm0012i19396	VMC J052042.63-694032.82	1.342001	16.545	16.324
lm0045n27451	VMC J054956.22-700341.04	1.34273	16.393	16.104
lm0125m17447	VMC J045457.57-695049.69	1.343061	17.287	17.580
lm0032m19079	VMC J053656.06-693308.54	1.344214	16.557	16.284

lm0090k15522	VMC_J051120.53-690915.24	1.345239	15.618	16.817
lm0091l113141	VMC_J051644.35-691641.14	1.347207	16.474	16.586
lm0040k25840	VMC_J054332.02-691340.55	1.352819	17.495	17.527
lm0095n21786	VMC_J051726.24-700127.78	1.355226	17.252	17.009
lm0033l12538	VMC_J054043.71-693742.60	1.356261	16.456	16.932
lm0020m2675	VMC_J052939.57-690409.01	1.356457	17.073	16.855
lm0541n10909	VMC_J045739.17-704139.45	1.357818	17.792	17.700
lm0033i20481	VMC_J054028.88-694038.49	1.359961	16.665	16.988
lm0225m4465	VMC_J054343.80-682229.25	1.360634	16.321	16.243
lm0325k8184	VMC_J052039.10-670006.14	1.361238	16.312	16.152
lm0306m11218	VMC_J050438.55-672209.43	1.36289	16.935	16.811
lm0331n11495	VMC_J052921.37-663345.53	1.363165	15.899	15.578
lm0055m20627	VMC_J055754.45-695256.64	1.365312	17.322	17.350
lm0610k1228	VMC_J055210.93-702924.54	1.36879	17.032	17.379
lm0216l7335	VMC_J053031.40-685436.11	1.370367	17.322	17.227
lm0331l12991	VMC_J052647.95-662913.64	1.370492	17.419	17.302
lm0587k6387	VMC_J052936.28-713235.42	1.372249	17.065	16.936
lm0584k14035	VMC_J052515.64-711408.45	1.372777	16.387	16.326
lm0426m6757	VMC_J050026.30-655633.63	1.372785	16.716	16.530
lm0194l20512	VMC_J051413.51-683800.65	1.373732	17.084	16.806
lm0031n12282	VMC_J054102.99-692257.92	1.375196	16.183	15.935
lm0575n3947	VMC_J052251.87-712123.87	1.375523	16.533	16.188
lm0186n25699	VMC_J050951.73-690204.06	1.376787	16.632	16.733
lm0601l27234	VMC_J054650.69-704549.22	1.378285	17.573	17.545
lm0010n9981	VMC_J052232.91-691615.75	1.379098	16.694	16.594
lm0010k3563	VMC_J051933.33-690437.18	1.380453	16.989	17.031
lm0161l22253	VMC_J045633.71-675601.33	1.380684	17.113	17.060
lm0033k16425	VMC_J053914.93-693002.10	1.381841	15.582	15.813
lm0187k25395	VMC_J051114.93-685136.09	1.384476	15.549	16.740
lm0033i8982	VMC_J054038.40-693622.56	1.384664	17.428	17.215
lm0337k24187	VMC_J052709.25-672817.38	1.397227	16.701	16.545
lm0217n12376	VMC_J053551.97-685634.41	1.398198	16.504	16.326
lm0127l20498	VMC_J045252.28-702354.70	1.398538	16.717	16.686
lm0040l12070	VMC_J054401.24-691656.11	1.399558	16.249	16.703
lm0597l19272	VMC_J053907.04-714720.39	1.402455	15.955	15.822
lm0200k21051	VMC_J052214.89-674716.67	1.403365	17.845	17.654
lm0457k24395	VMC_J052109.04-660423.06	1.40671	17.511	17.647
lm0306l18659	VMC_J050320.07-673444.75	1.407038	17.572	17.512
lm0433m7146	VMC_J050956.35-651412.85	1.413646	15.385	16.225
lm0332l24989	VMC_J052344.17-665522.22	1.415919	17.596	17.426
lm0332n21956	VMC_J052558.72-665357.58	1.416264	17.047	16.944

APPENDIX A. PROPERTIES OF THE “HOT” ECLIPSING BINARIES IN THE LMC

lm0226k21375	VMC J053725.81-685140.49	1.418055	17.423	17.401
lm0033m14746	VMC J054115.56-692919.24	1.420343	15.708	15.632
lm0186n6732	VMC J050951.23-685411.92	1.420433	16.113	16.122
lm0331k22319	VMC J052711.08-662347.02	1.421485	16.231	16.034
lm0427k7569	VMC J050156.00-655734.94	1.423526	16.515	16.392
lm0090l7821	VMC J051253.37-691529.98	1.425433	17.493	17.180
lm0021n5140	VMC J053402.01-691347.18	1.429287	15.900	15.945
lm0467l1196	VMC J052833.77-660844.17	1.429906	16.507	16.287
lm0030m9744	VMC J053752.85-690945.80	1.434738	15.812	16.142
lm0216m6805	VMC J053051.59-684443.33	1.436319	16.212	16.068
lm0336n6255	VMC J052604.45-672915.15	1.438008	16.188	16.230
lm0030n5266	VMC J053708.54-691427.21	1.438845	15.913	16.142
lm0327m23717	VMC J052207.69-672725.27	1.439496	16.034	15.954
lm0030n19275	VMC J053741.57-692007.66	1.441502	17.476	17.578
lm0101l4898	VMC J050710.82-691411.34	1.447797	17.164	17.072
lm0105l4144	VMC J050740.85-695658.02	1.44808	16.157	15.918
lm0023m4635*	VMC J053429.30-692530.24	1.450334	16.983	16.871
lm0030k13920	VMC J053613.98-690911.12	1.450827	15.604	16.053
lm0040k25978	VMC J054356.21-691331.32	1.451215	16.289	16.235
lm0440l7192	VMC J051140.79-650649.80	1.453087	17.505	17.525
lm0337k19646	VMC J052755.58-672619.02	1.453921	17.518	17.490
lm0095m18525	VMC J051743.89-695109.36	1.454941	16.437	16.996
lm0090k11333	VMC J051156.28-690742.90	1.456551	16.587	17.136
lm0335m23184	VMC J052858.68-670529.33	1.457715	16.770	16.521
lm0605n23731	VMC J055017.48-712635.54	1.458149	15.959	16.904
lm0021l14650	VMC J053247.63-691717.60	1.462272	15.758	15.511
lm0344m20086	VMC J053207.14-670514.52	1.462707	17.377	17.157
lm0034k9201	VMC J053634.21-694851.86	1.463902	16.764	16.455
lm0335k26831	VMC J052648.70-670703.57	1.464774	17.563	17.317
lm0033k9023	VMC J054006.19-692712.40	1.469976	16.428	16.252
lm0092n16033	VMC J051433.63-693919.03	1.47342	16.066	15.612
lm0214k25540	VMC J053014.20-683054.97	1.476843	17.558	17.544
lm0364n9855	VMC J054558.79-671034.27	1.477007	17.734	17.622
lm0020m14812	VMC J053006.95-690845.62	1.478725	16.200	15.924
lm0173m22752	VMC J050528.36-680732.55	1.479232	16.945	16.668
lm0173l29233	VMC J050335.63-681853.85	1.480115	17.028	16.790
lm0300k22331	VMC J050335.08-662402.09	1.48138	17.958	17.738
lm0346k12896	VMC J053144.92-672341.69	1.481784	16.295	16.902
lm0333m10861	VMC J052818.84-663945.55	1.482148	16.212	15.990
lm0556m6525*	VMC J050244.20-713208.39	1.493494	16.116	16.067
lm0030n12500*	VMC J053711.38-692325.86	1.499784	15.983	15.744

lm0346m23398	VMC J053218.78-672742.65	1.519681	16.517	16.428
lm0056k8196	VMC J055220.90-700913.42	1.523926	17.006	16.952
lm0125i9302	VMC J045306.88-695724.58	1.526312	16.051	16.893
lm0103m23150	VMC J050908.75-693135.47	1.527199	17.356	17.050
lm0184i11316	VMC J050720.38-683440.28	1.529922	17.556	17.339
lm0040i13585	VMC J054401.94-691733.61	1.534167	16.797	17.140
lm0020k13620	VMC J052733.57-690908.23	1.534702	16.587	16.235
lm0196k26764	VMC J051520.48-685250.05	1.538051	16.684	16.519
lm0090m4818	VMC J051359.87-690455.71	1.541924	16.336	16.224
lm0016m17269	VMC J052204.48-701232.45	1.542338	17.270	17.100
lm0573n13173	VMC J052259.87-710126.56	1.545989	17.373	17.321
lm0340i8577	VMC J053050.61-662750.56	1.546361	16.794	16.551
lm0427m21459	VMC J050309.74-660353.59	1.546547	17.025	16.890
lm0026k10665	VMC J052718.12-701020.06	1.548267	17.038	16.819
lm0214k24604	VMC J053012.25-683032.63	1.548706	15.709	15.853
lm0090n11730	VMC J051344.44-691647.91	1.554973	16.861	16.668
lm0114i6671	VMC J045608.39-695634.46	1.555878	16.077	16.464
lm0184i9660	VMC J050732.58-683404.62	1.568984	16.244	16.099
lm0214i25109	VMC J052930.93-684012.84	1.575578	16.596	17.391
lm0032i22874	VMC J053529.76-694222.65	1.576927	15.759	15.406
lm0337k23492	VMC J052720.43-672758.77	1.578628	17.247	17.209
lm0207k15472	VMC J052636.95-684801.13	1.579423	15.392	15.651
lm0023m7584	VMC J053421.06-692631.39	1.579887	16.008	15.714
lm0434m21038	VMC J050610.75-654136.07	1.585547	16.551	16.249
lm0172i15709	VMC J050022.92-682014.39	1.588034	17.465	17.348
lm0540k9199	VMC J045226.26-703024.46	1.588396	16.217	16.298
lm0335n5747	VMC J052859.28-670811.51	1.588518	17.243	17.077
lm0376m12338	VMC J055408.79-672316.93	1.591615	16.815	16.898
lm0330n10876	VMC J052503.26-662825.24	1.593612	16.191	16.684
lm0210i20271	VMC J052945.11-675617.49	1.594599	16.650	16.466
lm0550n7880	VMC J050312.39-703915.87	1.596858	17.242	17.010
lm0435i5752	VMC J050905.46-654412.60	1.597033	17.588	17.604
lm0344m8291	VMC J053223.60-670037.00	1.597243	16.603	16.441
lm0031m7414	VMC J054227.01-690514.40	1.605989	15.345	15.399
lm0175k18167	VMC J050416.00-682709.19	1.606206	16.581	16.329
lm0044i23659	VMC J054320.00-700319.30	1.607072	16.329	16.238
lm0197k23467	VMC J051922.30-685056.34	1.608347	16.394	16.280
lm0325n23385	VMC J052144.24-671456.26	1.60901	17.111	16.982
lm0161n24107	VMC J045802.92-675630.70	1.611475	17.580	17.523
lm0367n6835	VMC J054949.23-673014.98	1.61154	17.699	17.638
lm0603i24970	VMC J054716.29-710559.59	1.614227	17.190	17.066



APPENDIX A. PROPERTIES OF THE “HOT” ECLIPSING BINARIES IN THE LMC

lm0030k13205	VMC J053555.53-690851.07	1.615205	15.621	15.905
lm0550m20196	VMC J050212.68-703511.11	1.616823	17.337	17.137
lm0425n15511	VMC J050237.74-654810.17	1.623384	17.744	17.596
lm0210l18828	VMC J053006.02-675536.00	1.625897	17.474	17.450
lm0710k10285	VMC J053143.64-715525.17	1.627842	17.415	17.553
lm0090n29958	VMC J051408.45-692300.22	1.628407	17.485	17.095
lm0344k10601	VMC J053012.11-670137.35	1.628604	16.646	16.535
lm0711m4218	VMC J053809.16-715152.38	1.630559	16.150	17.089
lm0584l6042	VMC J052642.20-712027.14	1.632344	16.404	16.932
lm0424n10133	VMC J045954.71-654621.02	1.63539	15.761	16.247
lm0093n24281	VMC J051706.36-694056.92	1.635799	17.515	17.113
lm0204m18679	VMC J052437.28-682732.49	1.636472	17.411	17.329
lm0201n26407	VMC J052835.82-675713.84	1.63867	17.453	17.510
lm0333k9915	VMC J052647.20-663933.45	1.639068	16.656	16.488
lm0090m4321	VMC J051424.31-690444.21	1.641272	17.013	16.842
lm0032m22261	VMC J053724.44-693419.40	1.644146	15.963	15.623
lm0551l21081	VMC J050341.36-704404.32	1.645211	15.833	15.561
lm0101l22900	VMC J050740.89-692031.03	1.653449	16.196	15.963
lm0304n25535	VMC J050416.28-671551.76	1.657245	15.798	15.707
lm0033k15395	VMC J054014.74-692935.55	1.65801	15.856	15.767
lm0030l4662	VMC J053622.07-691412.04	1.660651	16.302	16.800
lm0344l24076	VMC J053034.04-671622.54	1.662852	16.353	16.213
lm0325k9805	VMC J052116.52-670037.65	1.664351	16.290	16.079
lm0207n18537	VMC J052805.77-685905.10	1.664777	15.689	15.555
lm0583l22712	VMC J052924.87-710456.80	1.665565	15.818	15.514
lm0212n20573	VMC J053207.19-681706.13	1.668092	16.687	16.830
lm0216l8793	VMC J053018.27-685515.64	1.669043	15.814	15.798
lm0127n6455	VMC J045414.43-701741.35	1.669262	16.325	16.148
lm0184k22807	VMC J050724.58-682932.36	1.672505	16.419	16.708
lm0030m3468	VMC J053740.88-690441.50	1.674098	15.877	15.992
lm0127m8589	VMC J045503.04-700917.18	1.676613	17.068	17.080
lm0035m23233	VMC J054247.23-695305.28	1.677625	15.456	15.442
lm0344l13598	VMC J053031.13-671203.93	1.685395	16.556	16.262
lm0376n11230	VMC J055309.98-673210.21	1.686368	17.761	17.568
lm0340n5950	VMC J053209.76-662627.63	1.692577	15.539	15.507
lm0021m15207	VMC J053320.13-690812.64	1.695205	17.134	17.141
lm0186m18764	VMC J050929.29-684935.24	1.697031	15.772	15.672
lm0344k4409	VMC J053006.15-665906.66	1.697053	16.337	16.183
lm0221n12398	VMC J054311.88-675229.02	1.700592	17.248	17.199
lm0214n4693	VMC J053137.55-683202.08	1.702754	17.039	17.366
lm0207m26339	VMC J052722.36-685208.12	1.715015	16.191	15.956

lm0344n5050	VMC J053201.43-670825.85	1.71895	16.739	16.594
lm0117k26536	VMC J050018.07-701648.93	1.725788	16.977	16.787
lm0366m3543	VMC J054555.72-671923.24	1.727942	17.109	17.010
lm0333k27925	VMC J052737.68-664600.67	1.731749	17.433	17.357
lm0125k22446	VMC J045157.79-695306.67	1.735186	16.405	16.476
lm0710k7222	VMC J053027.87-715408.47	1.746476	17.088	17.134
lm0127l6731	VMC J045251.09-701741.33	1.748158	15.547	15.305
lm0127m9330	VMC J045433.62-700938.70	1.751161	15.774	15.864
lm0205n15591	VMC J052720.98-683522.88	1.753697	16.514	16.225
lm0436l14585	VMC J050541.42-660933.77	1.756971	15.897	15.963
lm0184n9824	VMC J051000.53-683353.20	1.757143	15.694	16.037
lm0020m10621	VMC J052956.91-690712.60	1.758876	15.247	15.236
lm0223m18449	VMC J054305.08-680646.09	1.759816	16.880	16.834
lm0090l2236	VMC J051151.43-692049.38	1.7601	17.343	17.015
lm0030n22278	VMC J053726.68-692119.34	1.760563	16.731	16.629
lm0217n24885	VMC J053609.55-685527.46	1.762408	16.294	16.096
lm0045n24754	VMC J054937.26-700545.14	1.76449	16.992	16.694
lm0206k18004	VMC J052208.75-684900.57	1.765559	16.694	16.708
lm0304n29084	VMC J050357.90-671712.57	1.772755	15.962	15.743
lm0550k19577	VMC J050110.29-703512.78	1.774651	16.258	15.952
lm0291m21869	VMC J050018.99-662301.69	1.774816	17.366	17.200
lm0101k8669	VMC J050818.75-690618.00	1.775599	16.458	16.273
lm0012l16381	VMC J051939.82-693930.37	1.77902	15.982	15.706
lm0031m22434	VMC J054226.89-691140.76	1.779049	16.929	17.087
lm0543k12503	VMC J045641.13-705208.24	1.780468	17.025	17.055
lm0217l17550	VMC J053332.41-685854.05	1.784201	16.738	16.760
lm0014m14940*	VMC J052149.02-695017.37	1.785634	16.944	16.897
lm0031m11024	VMC J054230.15-691313.22	1.788741	17.159	17.290
lm0344l16103	VMC J053031.34-671306.04	1.79294	15.569	15.568
lm0053k11941	VMC J055635.72-692821.72	1.799736	17.231	17.449
lm0300k5450	VMC J050322.38-661656.91	1.801747	16.115	15.966
lm0467k11376	VMC J052819.72-655900.26	1.802175	15.677	15.518
lm0173m15001	VMC J050535.16-680448.15	1.803035	17.718	17.393
lm0010l24269	VMC J052025.52-692200.41	1.803838	16.113	15.775
lm0455n9465	VMC J052332.51-654530.84	1.804726	17.457	17.195
lm0336l20011	VMC J052440.50-673820.51	1.807377	17.056	17.057
lm0342k4708	VMC J053131.23-663804.45	1.807389	17.023	16.875
lm0340l19594	VMC J053113.33-663506.98	1.809525	15.661	15.398
lm0334l20839	VMC J052347.23-671749.01	1.813255	16.114	15.944
lm0323m29284	VMC J052121.36-664637.35	1.814879	17.290	17.429
lm0046k17569	VMC J054438.66-701413.83	1.815216	16.826	16.822

APPENDIX A. PROPERTIES OF THE “HOT” ECLIPSING BINARIES IN THE LMC

lm0257m20281*	VMC J060505.88-685110.75	1.821306	17.269	17.250
lm0583l19373	VMC J052949.18-710347.39	1.822309	16.253	15.965
lm0340m6792	VMC J053211.55-661728.73	1.825479	16.564	16.454
lm0186n11896	VMC J050927.62-685619.21	1.82799	17.335	16.997
lm0231l24501	VMC J054817.13-675727.75	1.833426	16.737	16.601
lm0305l17796	VMC J050708.80-671231.16	1.833544	17.249	17.275
lm0193n13361	VMC J052119.22-681332.15	1.834589	17.570	17.430
lm0114k17880	VMC J045620.59-695144.31	1.842075	17.206	16.931
lm0033k2872	VMC J053952.21-692452.91	1.842642	17.165	17.043
lm0195m11246	VMC J051956.85-682450.96	1.853886	17.483	17.344
lm0095m2603*	VMC J051849.48-694604.15	1.859576	17.454	17.365
lm0424m15104	VMC J050030.23-653854.61	1.861021	16.284	16.079
lm0022l3631	VMC J052739.83-693833.90	1.863346	16.396	16.553
lm0455l17462	VMC J052129.04-654936.53	1.866168	16.837	16.866
lm0115l9321	VMC J050027.66-695724.94	1.867104	17.029	16.888
lm0291l25349	VMC J045900.43-663317.11	1.874248	16.856	16.852
lm0173m20587	VMC J050500.89-680650.97	1.874478	17.235	16.959
lm0540m22710	VMC J045348.79-703544.28	1.876681	16.531	16.618
lm0171n18834	VMC J050559.23-675737.97	1.877095	16.545	17.043
lm0226k6378	VMC J053747.98-684446.10	1.877873	16.651	16.888
lm0550k19385	VMC J050014.84-703507.65	1.878439	16.130	16.021
lm0195m9279	VMC J052114.37-682400.27	1.880086	16.651	16.491
lm0125m29599	VMC J045343.29-695513.53	1.881055	17.522	17.562
lm0335l22611	VMC J052655.66-671500.28	1.886389	16.026	15.793
lm0015l24985	VMC J052327.72-700253.32	1.886947	16.222	15.901
lm0012n19000	VMC J052214.30-693955.73	1.887943	15.930	15.775
lm0545n19142	VMC J045801.37-712450.17	1.888095	16.876	16.713
lm0184n18118	VMC J050941.57-683638.07	1.890723	16.570	16.467
lm0030l10277	VMC J053643.01-691639.57	1.890838	17.177	17.133
lm0011n17783	VMC J052630.09-691811.54	1.90002	17.322	17.273
lm0212m19169	VMC J053100.08-680903.95	1.900405	15.593	15.575
lm0466n20073	VMC J052619.77-661153.80	1.900502	17.029	17.101
lm0013m7466	VMC J052603.43-692637.05	1.903719	15.779	15.369
lm0217n17433	VMC J053541.09-685857.90	1.906896	16.026	16.209
lm0093m28032	VMC J051811.10-693255.61	1.908406	16.792	16.924
lm0455l8958	VMC J052203.66-654549.37	1.909773	16.911	16.732
lm0355n17331	VMC J054355.71-671728.72	1.914858	17.286	17.325
lm0424n24516	VMC J050012.68-655258.00	1.915386	15.845	15.628
lm0333n16187	VMC J052849.50-665051.91	1.91737	16.075	15.899
lm0014k22435	VMC J052036.79-695302.65	1.918806	16.751	16.491
lm0091l5423	VMC J051612.97-691412.15	1.923877	16.246	16.617

lm0301122532	VMC J050551.70-663237.27	1.925101	16.176	15.993
lm0187k17340	VMC J051133.78-684840.14	1.925776	16.813	16.835
lm0306m3943	VMC J050346.96-671920.36	1.927241	16.452	16.700
lm0333k3930	VMC J052734.68-663717.69	1.931105	16.800	16.721
lm0612110791	VMC J055117.34-710200.47	1.931428	16.789	16.800
lm0040110857	VMC J054326.23-691625.48	1.93296	15.315	15.609
lm0436m10069*	VMC J050638.56-655850.58	1.9334	16.791	16.616
lm0214124228	VMC J052951.41-683953.31	1.940698	16.247	16.101
lm0175m19864	VMC J050637.38-682737.16	1.946591	16.498	16.217
lm0331119382	VMC J052759.07-663137.08	1.951358	15.888	15.661
lm0033m22177	VMC J054150.32-693157.75	1.954291	15.544	15.567
lm0032112916	VMC J053547.17-693831.87	1.960459	15.800	15.698
lm0191n9387*	VMC J052111.63-675534.67	1.96275	16.791	16.570
lm0030k12130*	VMC J053617.19-690822.45	1.96284	16.938	16.887
lm0024m7851	VMC J052924.86-694808.06	1.966268	17.345	17.033
lm0170114651	VMC J045947.76-675339.11	1.967818	17.381	17.392
lm0294n6230*	VMC J045752.57-670841.93	1.9694	16.963	16.944
lm0091m30316	VMC J051715.96-691319.62	1.978761	16.717	16.390
lm0090112995*	VMC J051216.17-691728.32	1.982342	15.283	16.495
lm0020k12115*	VMC J052757.42-690830.00	1.989476	14.578	14.221
lm0101n23916*	VMC J050940.09-692027.99	1.99006	14.679	14.256
lm0025n15353*	VMC J053440.77-695921.45	1.990814	16.523	16.435
lm0031n23092*	VMC J054159.42-692053.14	2.018832	17.297	17.068
lm0015n10153*	VMC J052547.65-695735.20	2.020196	16.519	16.982
lm0344125518	VMC J053026.56-671658.34	2.023458	16.576	16.471
lm0583k6016	VMC J052959.41-705054.11	2.024389	16.299	16.121
lm030618041*	VMC J050306.00-673009.81	2.025378	17.645	17.533
lm0366115212	VMC J054443.45-673347.50	2.029431	15.879	15.761
lm0307117542	VMC J050702.43-673500.13	2.034164	15.785	15.612
lm0033k11169	VMC J054014.85-692758.72	2.043963	15.281	15.116
lm0296m14458	VMC J045702.64-672344.42	2.044072	15.662	15.464
lm0427n12788*	VMC J050412.98-660913.59	2.048492	17.539	17.649
lm0184n11334	VMC J050844.93-683426.34	2.048845	17.068	17.031
lm0323k16171	VMC J052026.98-664150.18	2.050964	16.971	16.933
lm0207k27793*	VMC J052705.79-685233.29	2.054994	16.884	16.954
lm0214123257	VMC J053025.55-683929.91	2.056505	17.448	17.489
lm0467m13027*	VMC J052945.12-655928.13	2.057866	16.502	16.296
lm0030112866	VMC J053601.42-691748.25	2.058756	15.503	15.529
lm0101m21049	VMC J051027.09-691036.55	2.059198	15.558	15.662
lm0217n11196	VMC J053554.09-685559.45	2.059265	16.209	16.038
lm0031126732	VMC J054002.00-692210.74	2.060787	17.366	17.128

APPENDIX A. PROPERTIES OF THE “HOT” ECLIPSING BINARIES IN THE LMC

lm0015m33370*	VMC J052558.88-695547.52	2.064046	16.518	16.345
lm0581l21536*	VMC J053029.23-704332.07	2.064116	17.366	17.171
lm0021l6609	VMC J053203.23-691436.59	2.064204	15.685	15.455
lm0103n19330*	VMC J051017.91-693932.44	2.064678	16.912	16.612
lm0182k16150*	VMC J050720.77-680729.73	2.065838	16.222	16.175
lm0340m15950	VMC J053156.66-662124.11	2.066753	15.843	15.751
lm0013k30220*	VMC J052410.69-693345.42	2.072228	15.679	16.779
lm0030k16342	VMC J053635.07-691028.12	2.072852	16.113	16.073
lm0030n20233	VMC J053654.77-692258.32	2.077922	16.050	15.832
lm0587l18183*	VMC J053025.40-714659.83	2.077996	16.398	16.632
lm0364n12802	VMC J054700.75-671146.56	2.078818	16.716	16.739
lm0376m19861	VMC J055431.36-672910.33	2.082899	16.815	16.852
lm0216l17602	VMC J053020.11-685907.74	2.088156	16.275	16.076
lm0374l15319	VMC J055155.42-671312.72	2.090547	16.607	16.521
lm0021n14065	VMC J053445.71-691652.11	2.091973	16.977	16.816
lm0017k18680*	VMC J052322.73-701324.01	2.094048	16.757	17.051
lm0426n23242*	VMC J050005.65-661302.21	2.09473	16.710	16.582
lm0543m11267*	VMC J045829.12-705131.81	2.09621	16.410	16.645
lm0020k18818	VMC J052739.64-691118.35	2.101491	15.917	15.596
lm0184k7714	VMC J050740.70-682408.60	2.102557	15.557	15.333
lm0090n28977	VMC J051336.22-692241.42	2.108725	16.542	16.176
lm0210n24868	VMC J053153.66-675738.38	2.11375	16.626	16.497
lm0585k2867	VMC J053040.80-711011.10	2.113799	17.228	17.199
lm0184k27793*	VMC J050740.40-683120.02	2.116352	17.237	17.301
lm0340l8015	VMC J053059.30-662735.08	2.117866	15.923	15.787
lm0020l9163	VMC J052818.55-691605.47	2.127403	16.139	16.034
lm0214k13590	VMC J052926.63-682615.25	2.133649	17.111	17.140
lm0327m5562	VMC J052215.41-672012.93	2.137046	16.306	16.170
lm0335n14542	VMC J052930.89-671123.90	2.139656	17.298	17.110
lm0093n22090*	VMC J051739.94-694012.33	2.140468	16.625	17.282
lm0574m16657	VMC J051947.00-711454.76	2.140756	16.084	15.889
lm0115k23126	VMC J045934.87-695305.66	2.142218	17.251	17.100
lm0013l32365	VMC J052339.33-694334.38	2.145755	15.844	15.965
lm0031l9480*	VMC J053953.09-691530.24	2.149394	17.356	16.815
lm0365l9532	VMC J054818.80-671009.18	2.149591	17.330	17.263
lm0331m11496	VMC J052926.30-661900.38	2.151473	16.025	15.877
lm0175m14310	VMC J050634.35-682544.08	2.154499	15.450	14.998
lm0204k11078*	VMC J052221.57-682503.49	2.15745	16.809	16.852
lm0375k19793	VMC J055518.04-670541.26	2.158691	16.387	16.341
lm0016n21306*	VMC J052227.26-702341.90	2.159334	16.965	16.721
lm0344k16854	VMC J053027.16-670409.15	2.164252	16.142	15.939

lm003lm19001	VMC J054103.31-691021.77	2.165249	16.669	16.969
lm032lm8452	VMC J052224.18-661737.44	2.168221	16.724	16.744
lm0214n10775*	VMC J053159.53-683419.68	2.175728	17.488	17.345
lm0012m16798	VMC J052235.33-693143.32	2.183354	16.043	15.624
lm0205n25742	VMC J052840.72-684136.80	2.184881	15.444	15.233
lm0294n13388	VMC J045744.69-671120.12	2.188141	15.849	15.679
lm0366l6375*	VMC J054436.51-672932.75	2.189006	17.287	17.147
lm0543m9484*	VMC J045730.80-705100.20	2.1894	17.229	17.224
lm019ln2265	VMC J051951.52-675005.72	2.193241	16.914	16.868
lm0013m20283	VMC J052603.17-693052.56	2.193383	15.455	15.219
lm054ln4981	VMC J045839.79-703826.47	2.195876	16.891	16.715
lm0300m25571	VMC J050434.81-662559.99	2.200747	15.958	15.809
lm0610k4113	VMC J055126.09-703208.81	2.214823	17.077	17.076
lm020k11440	VMC J052815.05-690811.69	2.220169	15.109	14.963
lm0203n15393	VMC J052722.65-681407.98	2.225954	15.679	15.476
lm058lk6931	VMC J053035.14-702923.35	2.227595	16.830	16.939
lm0230m4155	VMC J054722.01-674027.42	2.229129	17.047	17.026
lm0033m24762	VMC J054118.77-693256.97	2.230059	16.471	16.208
lm0303n12403	VMC J050720.40-664917.75	2.234478	16.658	15.593
lm0335k26760	VMC J052657.47-670701.31	2.234913	16.149	15.925
lm0103l11316	VMC J050855.37-693659.62	2.235387	16.967	16.717
lm0301n9832	VMC J050730.80-662729.86	2.242879	15.986	16.055
lm0127n21487	VMC J045434.59-702425.97	2.244659	16.931	16.980
lm0200k25034	VMC J052207.88-674856.17	2.244789	16.586	16.515
lm0193m14935	VMC J051954.07-680455.35	2.249797	15.149	15.035
lm0020k24295	VMC J052831.27-691340.71	2.250701	16.443	16.038
lm0331117455	VMC J052759.22-663052.92	2.254984	16.256	16.820
lm0466l15239	VMC J052517.86-660946.10	2.25864	16.430	16.221
lm0021132791	VMC J053218.71-692318.54	2.25996	17.020	16.683
lm003318128*	VMC J054001.58-693606.81	2.262278	15.604	15.875
lm0117m10584	VMC J050125.12-701013.80	2.26826	15.645	15.572
lm0294m26342	VMC J045816.03-670641.29	2.271254	17.272	17.062
lm0100n5690	VMC J050637.75-691421.91	2.27321	16.640	16.639
lm0030n18202	VMC J053758.63-691941.38	2.273798	16.169	16.036
lm055lk22031	VMC J050346.11-703711.18	2.27601	17.479	17.092
lm0093m18940	VMC J051739.28-693007.67	2.277221	16.561	16.373
lm0173l13985	VMC J050342.58-681351.74	2.27859	16.326	16.128
lm0092m20117*	VMC J051401.93-693311.09	2.27942	16.821	16.673
lm0161m20878	VMC J045819.44-674622.35	2.27958	16.318	16.316
lm0117m15641	VMC J050223.60-701205.80	2.2838	16.501	16.233
lm0543n27195	VMC J045854.80-710613.14	2.293317	17.055	17.155

APPENDIX A. PROPERTIES OF THE “HOT” ECLIPSING BINARIES IN THE LMC

lm0184k13561*	VMC J050725.44-682612.68	2.294172	16.195	16.477
lm0337k20128	VMC J052739.26-672632.76	2.300298	15.789	15.461
lm0090l13156	VMC J051236.57-691731.71	2.301266	16.375	16.334
lm0355n12209	VMC J054300.35-671059.52	2.303794	17.156	17.063
lm0366l21345	VMC J054447.47-673801.43	2.328524	16.527	16.707
lm0200l19491	VMC J052157.43-675612.75	2.329272	15.825	15.825
lm0186n14790	VMC J050825.60-685731.18	2.333025	16.949	16.978
lm0030m4163	VMC J053730.75-690517.52	2.333416	14.774	15.119
lm020k2403*	VMC J052830.37-690422.92	2.335872	17.161	17.182
lm0033n25448	VMC J054150.30-694224.53	2.340327	16.466	16.151
lm0115k28730*	VMC J050031.77-695456.05	2.341022	16.346	16.606
lm0186k5622	VMC J050749.03-684438.35	2.341898	16.765	16.544
lm0033l8978	VMC J053953.42-693626.39	2.344895	15.566	15.693
lm0103k4043	VMC J050827.80-692528.63	2.345441	15.660	15.707
lm0426m23482	VMC J050018.72-660346.73	2.345573	15.291	15.129
lm0437n8267*	VMC J050931.45-660654.35	2.353292	17.350	17.419
lm0223n30265	VMC J054330.07-681949.07	2.355531	15.590	15.516
lm0091n16520	VMC J051714.46-691756.24	2.361363	15.996	15.783
lm0031m19305	VMC J054108.15-691028.57	2.361448	16.437	16.551
lm0294n9088	VMC J045743.46-670945.93	2.365682	16.854	16.745
lm0033m29238*	VMC J054208.84-693429.71	2.369442	16.885	17.010
lm0355n19896*	VMC J054242.12-671358.55	2.37175	16.901	17.333
lm0205l5928	VMC J052635.34-683212.58	2.37907	16.675	16.898
lm0012l24572*	VMC J051944.94-694221.32	2.3808	17.663	17.208
lm0367m17417*	VMC J054934.20-672541.73	2.381462	16.588	16.583
lm0541m17201	VMC J045733.88-703304.22	2.381813	16.262	16.138
lm0427m16915	VMC J050408.27-660119.21	2.382868	17.446	17.299
lm0035n29174	VMC J054101.78-700504.83	2.385178	15.644	15.633
lm0187l17648	VMC J051218.60-685832.42	2.390532	17.122	16.992
lm0297k16068	VMC J045947.96-672431.53	2.394267	15.423	15.329
lm0015m12964*	VMC J052620.61-694921.75	2.394782	17.070	17.013
lm0556k7966	VMC J050006.52-713236.56	2.398208	16.372	16.393
lm0230l15982	VMC J054419.25-675449.55	2.398351	16.930	16.847
lm0305n13969	VMC J050741.97-671313.43	2.399246	15.987	15.884
lm0093m6482	VMC J051715.38-692614.89	2.400068	17.317	17.044
lm0030k7421	VMC J053620.35-690615.75	2.403842	16.625	16.637
lm0323n20798*	VMC J052240.22-665225.02	2.408672	17.196	17.308
lm0033m27772	VMC J054132.23-693401.79	2.411216	16.610	16.573
lm0346k17136	VMC J053044.42-672536.18	2.418824	15.681	15.447
lm0030l15810	VMC J053604.55-691910.42	2.419399	15.816	15.855
lm0056l25826	VMC J055148.54-702602.02	2.419986	16.905	17.063

lm0015n17499	VMC J052653.58-695949.42	2.431098	16.613	16.556
lm0325m19625*	VMC J052128.05-670416.10	2.431928	16.048	15.860
lm0325n9718	VMC J052234.47-670932.29	2.436797	16.580	16.635
lm0013n22558	VMC J052503.44-694030.01	2.437445	15.196	15.773
lm0344l18357	VMC J053048.33-671401.96	2.442181	16.878	16.549
lm0550m23266	VMC J050219.33-703625.59	2.443675	15.378	15.331
lm0340229663	VMC J053105.42-663443.42	2.447199	16.090	15.843
lm0331n5533	VMC J052826.55-662909.99	2.44858	16.232	15.864
lm0035k5826	VMC J054042.32-694724.78	2.457281	16.051	16.031
lm0374n6499	VMC J055354.03-670852.89	2.459114	17.093	17.072
lm0344k5068	VMC J053058.85-665922.68	2.465608	16.514	16.281
lm0093m4296	VMC J051756.07-692528.88	2.469981	16.262	15.990
lm0545m6699	VMC J045902.42-711057.71	2.471238	16.576	16.692
lm0024i5083	VMC J052823.84-695632.32	2.471267	16.332	16.272
lm0095m32814	VMC J051759.42-695538.84	2.474934	16.922	16.816
lm0321m17018*	VMC J052131.47-662114.59	2.48037	16.194	15.982
lm0344k24636	VMC J053140.72-670719.32	2.483249	15.696	15.475
lm0550n14903	VMC J050157.58-704207.47	2.487136	16.275	16.052
lm0427l10110	VMC J050107.92-660803.00	2.489254	16.778	16.626
lm0331k10198	VMC J052736.30-661841.88	2.490214	16.494	16.416
lm0010l17439*	VMC J051956.06-691915.10	2.493082	15.868	15.516
lm0307k13715	VMC J050601.20-672331.32	2.495074	16.354	16.495
lm0542l17356	VMC J045153.01-710404.47	2.495564	16.443	16.536
lm0457n6420	VMC J052321.04-660529.14	2.495654	15.752	15.515
lm0572k3238*	VMC J051801.78-704910.02	2.495964	17.428	17.426
lm0040k11551*	VMC J054423.15-690735.61	2.499232	16.890	16.878
lm0032i20643	VMC J053602.65-694130.94	2.499392	15.790	15.380
lm0015m19643	VMC J052636.54-695125.31	2.50362	16.890	16.569
lm0010m6843	VMC J052114.52-690540.53	2.505974	15.990	15.665
lm0303m21604	VMC J050726.63-664335.17	2.50701	16.343	16.219
lm0346m16504	VMC J053159.21-672449.84	2.508841	16.122	15.965
lm0216i21415	VMC J053040.80-690051.78	2.509407	16.145	15.990
lm0540n13869	VMC J045359.49-704126.63	2.512757	16.049	15.954
lm0256m23734*	VMC J060052.16-685311.89	2.513574	17.531	17.743
lm0596l19261	VMC J053343.35-714846.38	2.515392	17.026	17.290
lm0020i26644	VMC J052714.33-692300.29	2.516899	16.758	16.369
lm0180l6512	VMC J050806.56-675027.24	2.516909	15.788	15.598
lm0186n5534	VMC J050858.28-685343.40	2.529495	16.218	16.106
lm0206m28489	VMC J052409.32-685226.75	2.531791	16.963	16.764
lm0097n15434	VMC J051739.82-702127.55	2.532518	16.240	16.023
lm0015m13576	VMC J052532.18-694939.02	2.534117	16.534	16.479



APPENDIX A. PROPERTIES OF THE “HOT” ECLIPSING BINARIES IN THE LMC

lm0023k3564	VMC J053124.61-692528.08	2.536665	17.051	16.915
lm00104210	VMC J051921.83-691410.07	2.551967	16.991	16.586
lm0466n15347	VMC J052554.98-660944.34	2.552722	16.482	16.734
lm0212n18380	VMC J053054.27-681617.55	2.553893	17.090	17.125
lm0010k17235	VMC J052045.22-691001.22	2.556111	16.174	15.967
lm0353i24619	VMC J052804.34-665405.97	2.556706	15.857	15.688
lm0105m14713*	VMC J050953.12-694956.11	2.55891	16.742	16.609
lm0581m21519	VMC J053107.06-703435.43	2.559421	16.895	16.873
lm0457k24667	VMC J052131.27-660427.77	2.561858	16.586	16.504
lm0100m16266	VMC J050628.93-690917.59	2.565832	16.589	16.501
lm0170m4805	VMC J050055.48-674051.34	2.566232	16.082	15.975
lm0307m15491	VMC J050859.82-672351.19	2.56975	16.613	16.558
lm0020k24655	VMC J052833.25-691349.10	2.579334	16.127	15.693
lm0602i6118	VMC J054238.05-705955.39	2.580945	15.454	15.524
lm0355n26448	VMC J054336.43-671621.64	2.592838	15.181	14.955
lm0331k18134	VMC J052731.92-662201.92	2.595648	16.818	16.568
lm0012m2814	VMC J052134.84-692534.58	2.5989	16.955	15.615
lm0366n14428	VMC J054712.66-673320.55	2.601096	17.256	17.158
lm0427m16528	VMC J050306.40-660118.95	2.608226	16.396	16.229
lm0340n5836	VMC J053229.63-662624.02	2.614459	15.861	15.618
lm0040k23476	VMC J054339.83-691229.04	2.615418	15.921	15.801
lm0116i19585*	VMC J045604.34-702310.12	2.61797	16.779	16.656
lm0212m20099*	VMC J053129.10-680923.84	2.621128	16.888	16.860
lm0303n16128	VMC J050717.83-665037.51	2.621196	17.007	16.874
lm0020i9813	VMC J052741.15-691620.23	2.631352	15.931	15.630
lm0090n29324	VMC J051323.89-692249.10	2.636584	15.338	15.640
lm0543n18447*	VMC J045851.03-710310.07	2.63776	16.640	16.631
lm0355n24071	VMC J052948.04-671457.62	2.641403	16.082	16.054
lm0200i6405	VMC J052219.71-675029.29	2.649042	15.819	15.713
lm0465i26736	VMC J052811.63-655254.69	2.654428	15.906	15.748
lm0184k17447	VMC J050748.91-682734.19	2.656173	16.474	16.348
lm0216i17243	VMC J053007.92-685858.46	2.657392	15.759	15.857
lm0013i21404	VMC J052436.47-694011.32	2.658097	16.763	16.465
lm0037n10599*	VMC J054222.44-701941.93	2.658698	16.342	16.373
lm0173m21250*	VMC J050605.24-680656.43	2.661334	16.156	15.896
lm0230i9562	VMC J054514.46-675206.17	2.662658	17.007	16.937
lm0173n13333	VMC J050547.84-681339.33	2.665684	16.898	17.169
lm0195m16675*	VMC J052105.51-682636.76	2.666476	16.093	16.001
lm0127i9642	VMC J045234.39-701907.80	2.669394	17.000	16.824
lm0011m22713	VMC J052529.30-691055.92	2.674348	16.162	15.892
lm0330n19300*	VMC J052518.11-663148.77	2.677262	17.278	17.587

lm0186n8773	VMC J050929.22-685502.67	2.678832	15.329	14.992
lm0092m3797*	VMC J051343.39-692603.75	2.683288	17.152	17.036
lm0093m11981	VMC J051741.69-692757.61	2.68737	16.196	16.051
lm0571n26162	VMC J052234.21-704500.11	2.68743	16.210	15.959
lm029115438	VMC J045928.72-662549.78	2.70368	15.546	15.671
lm0015m15054	VMC J052649.31-694957.17	2.709872	16.265	16.754
lm0012n14828	VMC J052148.91-693835.05	2.71287	15.567	15.834
lm0103k10582	VMC J050750.07-692737.89	2.713007	15.903	15.876
lm0431n15433	VMC J050913.18-651027.16	2.714038	16.805	16.792
lm0185n22544*	VMC J051245.86-684150.78	2.7182	17.001	17.162
lm0333m22120*	VMC J052848.66-664355.07	2.720332	16.086	15.881
lm0172n6253	VMC J050105.81-681132.55	2.727663	15.612	15.428
lm0206k25944	VMC J052315.68-685211.41	2.73146	15.972	16.199
lm0091m28603*	VMC J051848.11-691234.85	2.74089	16.697	16.628
lm0020k16826	VMC J052747.85-691026.64	2.747223	15.486	15.124
lm0205m4021	VMC J045806.79-670908.39	2.75026	16.235	16.142
lm0294n7479	VMC J052208.66-683715.49	2.754503	16.978	17.082
lm0204118900	VMC J054809.96-675243.96	2.754824	16.644	16.620
lm0231112015*	VMC J050253.20-714733.12	2.755996	17.677	17.753
lm0556n17386*	VMC J051834.35-692335.98	2.765244	16.854	16.585
lm0091n21452	VMC J045457.81-703446.63	2.768156	16.998	16.966
lm0541k20099*	VMC J051645.73-694131.53	2.772257	16.614	16.536
lm0093126030	VMC J053135.02-695108.99	2.773556	16.896	16.657
lm0025k17489	VMC J053923.48-692808.77	2.780835	15.803	15.684
lm0033k11425	VMC J050206.39-660434.80	2.791595	15.866	15.789
lm0427k15685	VMC J052751.41-672544.08	2.793995	15.692	15.486
lm0337k18241	VMC J052719.98-703307.27	2.796134	16.590	16.580
lm0580m16604*	VMC J052523.82-661403.99	2.81516	15.526	15.800
lm0466116461*	VMC J053138.66-683647.52	2.816108	17.576	17.560
lm0214n17417*	VMC J052325.82-672036.30	2.821258	16.332	16.027
lm0336k7065	VMC J052052.76-675151.43	2.822611	16.741	16.811
lm0191n4635	VMC J050338.84-701957.81	2.827501	16.216	15.736
lm0106117113	VMC J052133.54-694842.47	2.83114	16.872	17.343
lm0014m9900*	VMC J052230.17-682421.93	2.839278	16.141	16.187
lm0204k9178*	VMC J053610.74-693202.25	2.841496	14.906	14.629
lm0032k15660	VMC J051948.46-683204.41	2.841972	16.635	16.681
lm0195n5472	VMC J053028.83-704601.15	2.843662	16.103	16.567
lm0581129010	VMC J052933.20-691711.93	2.851276	16.796	16.744
lm0020n12840*	VMC J053615.92-695012.08	2.852214	16.361	16.118
lm0034k12920*	VMC J053140.14-690758.94	2.853292	15.365	15.022
lm0021k13770				

APPENDIX A. PROPERTIES OF THE “HOT” ECLIPSING BINARIES IN THE LMC

lm0541m10971	VMC J045756.56-703035.19	2.861934	16.639	16.788
lm0031k19705	VMC J054049.55-691305.78	2.867536	14.554	14.699
lm0011m10445*	VMC J052504.33-691549.51	2.867908	15.999	15.903
lm0424n23353	VMC J050023.14-655201.05	2.869312	15.226	14.945
lm0321k15088*	VMC J052051.31-662524.78	2.876456	16.913	16.883
lm0013k29788	VMC J052421.11-693336.19	2.882388	15.318	15.740
lm0031l21280	VMC J054003.22-691954.74	2.882489	16.016	15.954
lm0105k31240	VMC J050811.48-695542.47	2.887854	16.930	16.912
lm0541l17906	VMC J045525.52-704654.22	2.895575	16.706	16.654
lm0331m17723	VMC J052845.42-662139.94	2.896212	16.971	16.817
lm0103k15198	VMC J050815.66-692904.84	2.899283	14.516	15.669
lm0327m5927	VMC J052214.03-672022.41	2.911755	15.845	15.750
lm0216n15995	VMC J053233.12-685745.57	2.913514	14.737	14.755
lm0323n7828	VMC J052135.79-664750.80	2.916801	16.353	16.322
lm0024m7552	VMC J053046.75-694759.25	2.917208	16.033	15.910
lm0025k31765	VMC J053158.40-695532.19	2.918039	16.607	16.402
lm0300k8884	VMC J050301.07-661824.94	2.921834	16.986	16.773
lm0426n17949	VMC J050025.36-661036.89	2.924628	16.640	16.493
lm0303m5318	VMC J050741.04-663737.41	2.926082	16.904	17.004
lm0021k24967	VMC J053248.62-691204.11	2.9261	15.568	15.169
lm0335l8729	VMC J052719.81-670934.72	2.931618	16.321	16.233
lm0340k22602*	VMC J053131.67-662525.78	2.940286	17.639	17.566
lm0051m15468	VMC J055752.51-691816.23	2.949872	16.912	16.939
lm0344k13297	VMC J053104.94-670241.96	2.950326	15.950	15.644
lm0114k26929	VMC J045613.03-695516.83	2.950903	16.028	15.847
lm0230l9767*	VMC J054428.71-675211.90	2.953796	17.370	17.204
lm0207m16357	VMC J052823.83-684818.76	2.956567	15.388	15.138
lm0101k24223*	VMC J050759.60-691211.86	2.95906	16.432	16.086
lm0032n10570	VMC J053830.23-693726.24	2.971654	15.656	15.666
lm0090k3504	VMC J051224.83-690443.59	2.972621	15.425	15.490
lm0335k26756	VMC J052800.78-670655.56	2.97543	16.348	16.169
lm0294m4825	VMC J045807.70-665858.21	2.97779	15.299	15.118
lm0331k23717*	VMC J052709.79-662528.28	2.990145	16.373	16.256
lm0093m17914*	VMC J051751.12-692947.46	3.011134	15.903	15.781
lm0017m23847	VMC J052603.40-701513.52	3.024535	16.977	16.808
lm0033k17847*	VMC J054015.61-693028.35	3.025998	15.641	15.479
lm0541m15871	VMC J045733.22-704416.94	3.02721	16.596	16.370
lm0021m5306	VMC J053340.51-691353.32	3.039916	14.750	14.673
lm0191m3743	VMC J052008.69-675114.37	3.053936	16.099	16.219
lm0333k29474	VMC J052726.38-664635.10	3.057151	15.673	15.480
lm0426n22620*	VMC J050017.70-661245.51	3.058626	16.521	16.389

lm0330m5632	VMC J052558.56-661659.31	3.061442	15.631	15.578
lm0033i24296	VMC J054025.06-694159.18	3.066509	15.270	15.317
lm0022n14480	VMC J053016.06-693830.08	3.068277	15.906	15.936
lm0020k18927*	VMC J052816.59-691120.99	3.081764	15.820	15.523
lm0547i6434	VMC J045641.99-714132.41	3.081798	15.864	15.847
lm0125i25666	VMC J045238.51-700320.93	3.088091	14.810	14.879
lm0172n24468	VMC J050135.42-681807.15	3.102677	16.283	16.284
lm0095m9501	VMC J051804.70-694818.92	3.107019	14.833	14.706
lm0346m3392	VMC J053225.87-671925.35	3.113759	15.885	15.830
lm0026m14151	VMC J053043.79-701124.46	3.115609	16.105	16.685
lm0334n23519	VMC J052549.78-671525.64	3.119701	15.945	15.728
lm0340m20801	VMC J053215.66-662329.93	3.120686	16.735	16.775
lm0033m3196	VMC J054119.07-692505.08	3.122574	15.339	15.190
lm0207m27588	VMC J052740.43-685234.40	3.12647	15.949	15.757
lm0034m1263	VMC J053836.03-694624.12	3.134554	15.950	16.101
lm0202i15311	VMC J052318.13-681500.47	3.139857	15.709	15.474
lm0024m24264	VMC J053016.91-695314.69	3.144057	15.815	15.893
lm0580m20047	VMC J052829.08-703421.01	3.145045	15.987	15.912
lm0333n16489	VMC J052938.72-665051.63	3.16106	15.112	14.987
lm0333n10485	VMC J052850.66-664846.84	3.162796	14.935	14.720
lm0331n13474	VMC J052951.96-663507.50	3.163636	16.222	16.038
lm0214n27117	VMC J053047.68-684025.42	3.17278	15.037	14.983
lm0092k17584*	VMC J051235.40-693226.84	3.192096	16.155	16.001
lm0543m30093	VMC J045719.93-705819.96	3.193725	15.729	15.769
lm0090i7215*	VMC J051218.08-691516.42	3.19449	17.271	16.360
lm0240m16931	VMC J055317.48-674553.67	3.209594	15.041	15.811
lm0093k23075	VMC J051616.67-693126.91	3.214621	15.778	15.580
lm0092m16608	VMC J051355.15-693201.13	3.219523	14.429	14.199
lm0583i28540	VMC J053040.13-710647.28	3.22106	15.039	15.596
lm0012k23809	VMC J052035.75-693415.24	3.224639	16.622	16.254
lm0115n13901	VMC J050137.80-695852.43	3.224925	14.790	14.650
lm0455k23532	VMC J052144.72-654243.91	3.233372	15.921	15.826
lm0221n22693	VMC J054242.79-675631.74	3.234518	16.252	16.185
lm0305k4072*	VMC J050558.59-665841.61	3.239846	17.331	17.221
lm0344k19755	VMC J053133.34-670519.39	3.240951	14.726	14.467
lm0214n12207	VMC J053144.95-683452.55	3.252969	16.116	16.131
lm0207m8280	VMC J052800.48-684524.60	3.256904	16.553	16.988
lm0106k14921	VMC J050325.22-701157.08	3.261387	15.958	15.829
lm0207n22625	VMC J052755.80-690049.78	3.264492	15.554	15.764
lm0435k20023	VMC J050901.35-654105.20	3.281595	16.985	16.844
lm0013m14520*	VMC J052516.61-692903.95	3.288232	16.534	16.120

APPENDIX A. PROPERTIES OF THE “HOT” ECLIPSING BINARIES IN THE LMC

lm0090n12880*	VMC J051303.43-691712.00	3.289332	16.954	16.687
lm0114n17444	VMC J045721.21-700021.41	3.296076	16.048	16.019
lm0200l18257	VMC J052202.22-675537.82	3.296949	14.592	14.418
lm0366n9903	VMC J054712.45-673118.21	3.300117	16.496	16.406
lm0436l19007	VMC J050507.38-661138.42	3.301123	15.346	15.206
lm0091n23508	VMC J051706.93-692013.17	3.308983	15.675	15.489
lm0335m11683	VMC J052837.35-670118.46	3.311557	15.689	15.450
lm0193n14440*	VMC J052107.83-681356.02	3.318844	16.472	16.612
lm0296n11158	VMC J045712.12-673143.07	3.359377	16.442	16.302
lm0335n9834*	VMC J052956.56-670936.23	3.362948	17.011	16.766
lm0541n13040	VMC J045822.81-704242.90	3.36718	16.654	16.684
lm0023k4265	VMC J053225.15-692537.33	3.37023	15.618	15.399
lm0216m26624*	VMC J053112.47-685221.51	3.371126	17.170	17.271
lm0366m8525*	VMC J054630.32-672133.22	3.371884	16.983	16.919
lm0342k17321	VMC J053039.31-664439.86	3.373808	15.640	15.398
lm0180l20443*	VMC J050821.43-675607.12	3.383502	16.780	16.599
lm0093n33808*	VMC J051720.98-694350.27	3.390984	16.918	16.835
lm0365n23864	VMC J055031.50-671548.89	3.400307	16.768	16.732
lm0333n18392	VMC J052925.08-665135.83	3.404099	16.590	16.628
lm0030l13351	VMC J053540.66-691801.62	3.408736	14.545	14.374
lm0331m23548	VMC J052830.64-662400.92	3.412884	15.441	15.211
lm0030k4784	VMC J053627.18-691415.46	3.413421	15.279	15.649
lm0584n18193	VMC J052821.01-712443.87	3.426518	14.976	14.891
lm0466n13702	VMC J052608.98-660900.11	3.432734	13.797	14.397
lm0105l7047	VMC J050801.50-695835.42	3.442404	16.942	16.749
lm0466l18501	VMC J052501.99-661122.28	3.445012	15.658	15.886
lm0187l13941*	VMC J051159.43-685701.73	3.447762	16.611	17.179
lm0541n18320	VMC J045900.32-704523.67	3.459966	16.666	16.520
lm0033k4809	VMC J053934.84-692539.50	3.468732	16.467	16.671
lm0221n7928	VMC J054335.09-675041.08	3.468802	15.322	15.206
lm0321m6695	VMC J052203.88-661655.51	3.46972	16.019	15.966
lm0202l24207	VMC J052237.66-681825.71	3.472186	16.766	16.764
lm0344m8000	VMC J053233.23-670029.72	3.496288	15.544	15.325
lm0195m24877	VMC J052011.82-682937.05	3.508008	16.524	16.670
lm0184l15997	VMC J050807.87-683619.94	3.509246	15.762	15.635
lm0180l24836	VMC J050705.32-675755.64	3.513017	15.436	15.247
lm0024k23511*	VMC J052625.67-694617.08	3.522356	17.061	16.123
lm0091k14479	VMC J051536.44-690821.97	3.524759	16.068	16.214
lm0021n29435	VMC J053437.12-692204.36	3.531735	15.672	15.327
lm0013n30008	VMC J052508.84-694245.66	3.538905	15.963	15.695
lm0337k23342	VMC J052733.73-672754.18	3.543441	15.154	14.960

lm0305m27052	VMC J050719.25-670649.37	3.545493	15.991	15.820
lm0303k13861*	VMC J050703.27-664043.72	3.54569	16.986	17.131
lm0095n30847	VMC J051852.99-700418.30	3.546722	16.410	16.556
lm0556k5652	VMC J050036.62-713130.23	3.553122	16.575	16.575
lm0090m4479	VMC J051331.24-690449.80	3.558236	16.448	16.360
lm0230k5872*	VMC J054413.46-674933.88	3.561718	16.794	16.898
lm0344i21596	VMC J053111.09-671521.00	3.584081	16.846	16.902
lm0323n11823*	VMC J052224.77-664911.74	3.599714	16.607	16.646
lm0340i6791	VMC J053039.12-662702.79	3.612113	16.724	16.687
lm0366i7734	VMC J054453.76-673014.68	3.613542	16.574	16.612
lm0163i24856	VMC J045631.69-681751.39	3.618347	16.339	16.260
lm0015n30492	VMC J052509.30-700422.45	3.625513	16.099	16.242
lm0093k27461	VMC J051649.40-693246.00	3.628299	15.706	15.420
lm0091i25158	VMC J051626.57-692032.77	3.634311	15.230	14.984
lm0013m22363	VMC J052522.38-693138.53	3.646111	16.116	16.530
lm0184i4957*	VMC J050738.34-683221.67	3.65273	15.597	16.379
lm0303n17856*	VMC J050741.74-665110.66	3.65542	16.550	16.482
lm0184k13409	VMC J050645.59-682609.23	3.659249	16.052	16.011
lm0207m6963*	VMC J052721.82-684500.86	3.677332	15.420	15.266
lm0033n18886	VMC J054145.08-694004.48	3.694692	14.935	14.661
lm0344i19313	VMC J053051.88-671425.06	3.695935	15.400	15.145
lm0013n8661	VMC J052514.83-693612.54	3.714526	16.149	15.821
lm0033m17063	VMC J054113.76-693010.14	3.718525	14.909	14.781
lm0331n1614	VMC J052836.11-662543.99	3.72069	16.695	16.651
lm0125n23449	VMC J045341.21-700226.31	3.738714	15.249	15.100
lm0013n32504	VMC J052506.88-694331.87	3.745008	16.173	16.101
lm0291i4891	VMC J050000.09-662534.19	3.751829	15.450	15.303
lm0027k3823*	VMC J053126.76-700813.18	3.761414	16.125	16.018
lm0101n25168	VMC J051028.64-692047.85	3.773408	15.992	15.667
lm0207k16837	VMC J052656.27-684828.76	3.775084	16.072	15.741
lm0092m24157	VMC J051306.10-693434.50	3.779528	15.978	15.715
lm0214n8614	VMC J053152.56-683331.43	3.785845	16.516	16.487
lm0333k4914	VMC J052712.99-663741.46	3.790269	15.647	15.505
lm0020m22505	VMC J053028.96-691138.42	3.791691	15.516	15.447
lm0030i15904	VMC J053638.60-691913.02	3.797121	14.969	15.126
lm0550m5212	VMC J050230.64-702903.58	3.801039	15.647	15.798
lm0257i8931	VMC J060425.47-685528.09	3.810748	15.631	15.492
lm0583i28572	VMC J052926.46-710653.28	3.822895	16.581	16.515
lm0125k8106	VMC J045117.66-694808.09	3.843898	15.811	15.761
lm0367i13331	VMC J054858.00-673334.62	3.846704	16.475	16.475
lm0090n30909	VMC J051317.10-692320.48	3.852097	15.923	15.519

APPENDIX A. PROPERTIES OF THE “HOT” ECLIPSING BINARIES IN THE LMC

lm0030111056	VMC J053648.74-691659.46	3.853558	15.477	15.185
lm0090k10170*	VMC J051229.86-690716.00	3.854796	16.026	16.316
lm0020k15581	VMC J052816.01-690954.65	3.863955	15.043	14.791
lm0026m7027	VMC J052926.19-701810.40	3.870485	15.213	16.019
lm0117m12730	VMC J050231.16-701056.10	3.873811	16.241	16.249
lm0010123506	VMC J052020.04-692144.27	3.904077	15.990	15.994
lm0187m9985	VMC J051239.82-684603.34	3.945319	16.588	16.573
lm0200i6074	VMC J052218.76-675020.51	3.950478	16.068	15.823
lm0091m3797*	VMC J051747.87-690416.05	3.9545	16.699	16.741
lm0331k21866	VMC J052725.35-662334.39	3.959113	16.789	16.634
lm0015k8658	VMC J052339.15-694816.29	3.959962	15.523	15.966
lm0364i14193	VMC J054438.11-671231.41	3.959976	16.415	16.462
lm0331i26042	VMC J052756.25-663412.32	3.969029	15.894	15.772
lm0300m22019	VMC J050349.13-662332.69	3.986529	16.662	16.518
lm0184n26760	VMC J050957.57-683929.83	4.022428	15.046	15.160
lm0012n4832	VMC J052107.20-693525.30	4.027903	16.477	16.378
lm0021i4530*	VMC J053128.69-691354.95	4.037539	14.860	14.766
lm0600k25018	VMC J054220.50-703736.59	4.046607	14.797	14.770
lm0101k23784	VMC J050826.75-691200.02	4.069483	15.601	15.468
lm0337k10847	VMC J052804.62-672241.05	4.115728	14.832	14.687
lm0170n12305	VMC J050205.40-675254.89	4.116486	15.697	15.663
lm0206m26379	VMC J052352.88-690138.35	4.127665	14.561	14.682
lm0344i21656	VMC J053109.29-671522.29	4.164156	15.602	15.487
lm0101k17968	VMC J050717.92-690954.16	4.176462	15.313	15.063
lm0466i16077	VMC J052522.27-661009.94	4.179091	14.002	14.164
lm0020k8691	VMC J052823.88-690703.31	4.1797	14.826	14.603
lm0344m20206	VMC J053146.63-670518.41	4.181412	15.354	15.162
lm0125n6068	VMC J045320.39-695612.33	4.187756	15.892	15.792
lm0103k26311	VMC J050810.19-693235.80	4.203111	16.204	16.097
lm0366i16862	VMC J054451.73-673433.15	4.232527	15.758	15.798
lm0346k23825	VMC J053108.79-672902.67	4.249299	15.143	14.894
lm0466m21959	VMC J052603.19-661247.50	4.273267	16.158	16.274
lm0376m4773	VMC J055355.50-671952.50	4.306026	15.938	15.961
lm0125i6652	VMC J045226.31-695631.61	4.313464	15.644	15.630
lm0297n14819	VMC J050050.61-673332.28	4.318638	15.615	15.555
lm0467k18222	VMC J052835.72-660155.83	4.320224	16.027	16.003
lm0187m17967	VMC J051332.00-684848.77	4.323013	16.255	16.175
lm0467n17850	VMC J052943.72-661124.34	4.324035	16.022	15.924
lm0205n17550	VMC J052744.16-683601.02	4.332041	16.604	16.557
lm0331k22811	VMC J052714.17-662358.98	4.337633	15.095	14.917
lm0091n32274	VMC J051717.14-692258.26	4.339628	15.674	15.644

lm0337k25005	VMC J052701.99-672838.24	4.408822	15.134	14.949
lm0093m11955	VMC J051729.97-692758.49	4.422796	15.980	15.827
lm0034m4602*	VMC J053839.39-694814.13	4.454894	16.415	16.644
lm0197m20835	VMC J051946.37-685008.91	4.488418	15.997	15.968
lm0090m20034	VMC J051302.18-691939.75	4.502363	15.705	15.567
lm0021115985	VMC J053128.68-691751.77	4.502779	14.658	14.462
lm00309014	VMC J053525.69-691605.91	4.523622	15.165	15.075
lm0207m11446	VMC J052835.52-684628.74	4.526578	14.245	14.121
lm0021115606	VMC J053112.20-691745.07	4.557581	15.246	14.922
lm0091114577	VMC J051540.18-691714.02	4.566657	15.523	16.114
lm0114k19051	VMC J045552.65-695210.47	4.577471	15.389	15.117
lm0020n19615	VMC J053041.78-691928.06	4.585353	13.955	13.838
lm0187m11496	VMC J051333.04-684629.11	4.591479	16.156	16.186
lm0033m21700	VMC J054141.63-693148.16	4.613339	15.172	15.123
lm0025m30936	VMC J053318.56-695502.89	4.636845	15.999	16.114
lm0550k11523	VMC J050100.77-703145.34	4.66509	16.117	16.213
lm0185n11636	VMC J051305.86-683401.04	4.673342	16.099	16.201
lm0093m30768	VMC J051721.64-693352.95	4.721156	16.435	16.301
lm0333n6568	VMC J052900.40-664718.78	4.770854	15.162	15.057
lm0543m8169	VMC J045811.23-705028.09	4.777862	15.832	15.888
lm0180k16760	VMC J050715.05-674517.10	4.784288	15.624	15.370
lm0427112767	VMC J050105.30-660920.15	4.805932	16.195	16.063
lm0031n6676	VMC J054151.77-691422.82	4.853431	15.530	15.414
lm0127k13132	VMC J045234.68-701118.42	4.892616	15.968	15.920
lm0216l16590	VMC J053044.33-685840.57	4.943171	16.073	15.981
lm0476k5610	VMC J053058.40-655628.62	4.951673	16.003	16.098
lm0344112773	VMC J053040.75-671143.77	4.952487	15.649	15.417
lm0185l23772	VMC J051108.01-683812.13	4.970047	15.765	15.602
lm0015m26793	VMC J052620.48-695341.86	4.970604	16.083	15.836
lm0427k13855	VMC J050213.54-660022.15	5.016469	15.733	15.772
lm0011k23633	VMC J052430.51-691121.03	5.083128	15.642	15.955
lm0093k30805	VMC J051644.81-693349.66	5.085768	16.052	16.090
lm0012n22151	VMC J052134.93-694057.58	5.111026	16.505	16.414
lm0540m13587	VMC J045352.25-703202.59	5.118075	16.155	16.058
lm0021130770	VMC J053214.56-692239.46	5.171793	15.758	15.342
lm0216k9627	VMC J053025.55-684610.42	5.203106	14.352	14.173
lm0033k7569	VMC J054049.56-692636.29	5.2691	15.324	15.254
lm0333l15404	VMC J052735.95-665047.68	5.27222	15.500	15.482
lm0612l10194	VMC J055112.35-710146.54	5.279445	16.302	16.442
lm0330k4290	VMC J052353.25-661622.88	5.28192	16.228	16.248
lm0116k21077	VMC J045641.08-701439.31	5.30968	15.502	15.397



APPENDIX A. PROPERTIES OF THE “HOT” ECLIPSING BINARIES IN THE LMC

lm0207k17059	VMC J052635.55-684835.76	5.311128	15.961	16.102
lm0020m16359	VMC J052952.31-690922.56	5.335197	15.066	14.762
lm0033m6304	VMC J054056.63-692618.25	5.369545	15.562	15.429
lm0031l22987	VMC J054047.30-692028.25	5.413977	14.157	14.029
lm0216n10589	VMC J053100.88-685529.85	5.44858	15.022	14.866
lm0092m18774	VMC J051341.27-693245.36	5.457309	15.767	15.517
lm0114k21690	VMC J045613.93-695312.52	5.507995	15.371	15.193
lm0186m23446	VMC J050844.21-685124.83	5.534274	16.436	16.435
lm0346l13438	VMC J053116.19-673254.59	5.570352	14.541	14.355
lm0207n15251	VMC J052744.32-685740.53	5.598846	15.658	15.461
lm0093k26732	VMC J051644.41-693233.12	5.603447	15.713	15.684
lm0021k21280	VMC J053102.31-691049.89	5.671847	14.824	15.352
lm0021m26411*	VMC J053259.22-691216.78	5.708342	15.201	14.868
lm0543i28153	VMC J045528.97-710707.80	5.736595	15.668	15.866
lm0127l10608	VMC J045249.58-701931.94	5.78278	15.788	16.007
lm0105l5842	VMC J050755.21-695755.57	5.78581	16.274	15.934
lm0091n26247	VMC J051736.67-692102.17	5.813256	15.303	15.194
lm0466n11710	VMC J052634.25-660805.77	5.822653	15.351	15.274
lm0013m20776	VMC J052546.29-693104.04	5.874426	15.564	16.089
lm0010i24242	VMC J051935.67-692159.86	5.941613	15.325	15.144
lm0021k14832	VMC J053226.44-690819.30	5.973243	15.421	15.177
lm0427n16272*	VMC J050407.60-661055.51	6.00374	15.241	15.155
lm0171n5451	VMC J050442.87-675043.17	6.065706	14.831	14.727
lm0101k22147	VMC J050732.18-691127.03	6.208241	14.721	14.542
lm0020n6294*	VMC J053022.13-691452.06	6.229258	14.812	14.546
lm0020n21732*	VMC J053039.25-692012.07	6.271038	16.528	16.509
lm0466n6181	VMC J052615.95-660530.75	6.332723	15.585	15.601
lm0173n16894	VMC J050537.05-681453.66	6.347941	15.020	14.901
lm0540k16892*	VMC J045056.98-703339.68	6.37983	16.352	16.485
lm0344k22660	VMC J053032.44-670632.49	6.434828	15.086	15.007
lm0303k23599	VMC J050617.31-664414.50	6.463085	15.460	15.470
lm0194n25484	VMC J051604.83-683921.27	6.473465	15.244	15.272
lm0090k15089*	VMC J051200.84-690905.16	6.51694	16.594	16.293
lm0091n31944*	VMC J051739.56-692249.57	6.51753	16.252	16.447
lm0346n17567	VMC J053156.59-673501.72	6.532332	14.212	14.094
lm0035m23079	VMC J054222.53-695305.37	6.569401	15.578	15.541
lm0457l13469	VMC J052206.87-660931.67	6.640871	15.167	15.066
lm0335n23069	VMC J052956.24-671433.05	6.898566	16.010	16.148
lm0335n25477*	VMC J052908.36-671718.38	7.117324	14.695	14.756
lm0214n14689*	VMC J053134.55-683548.30	7.150098	14.566	15.083
lm0367m14504*	VMC J055025.93-672418.38	7.177252	16.809	16.904

lm0427n12122	VMC J050327.76-660859.75	7.194033	15.733	15.711
lm0093k5253*	VMC J051553.21-692557.89	7.284388	15.199	15.312
lm0585l5842	VMC J053107.72-712008.04	7.286296	14.828	14.861
lm0033m20529	VMC J054153.44-693121.05	7.464778	14.263	14.185
lm0014k7299	VMC J052042.42-694755.97	7.536747	15.678	15.706
lm0427k7505*	VMC J050142.67-655734.13	7.684446	15.468	15.373
lm0435m12381	VMC J051013.60-653740.01	7.696551	15.718	15.874
lm0180n9316	VMC J050830.82-675546.93	7.754096	15.342	15.292
lm0033n12413	VMC J054104.81-693749.22	7.942126	14.854	14.963
lm0020k10287	VMC J052745.76-690742.63	8.463039	14.678	14.503
lm0467k11917*	VMC J052821.82-655914.77	8.464606	15.188	15.062
lm0024m1498	VMC J052911.89-694606.17	8.485941	14.973	14.883
lm0033m5960	VMC J054112.57-692608.68	8.583074	13.862	13.746
lm054119275*	VMC J045536.25-704042.58	8.850098	16.362	16.462
lm0173m17717	VMC J050610.62-680543.31	8.856537	13.349	13.492
lm0191n3246*	VMC J052030.06-675047.48	14.645028	14.983	15.339
lm0173n32162*	VMC J050556.86-682003.38	21.041492	12.734	14.658

Table A.2: Properties of 999 HEBs in the LMC, which have a counterpart in the VMC catalogue (Column 1: EROS-2 identification of the star; Column 2: VMC identification; Column 3: Period from the EROS-2 catalogue (\*- Stars for which a new period was derived in this study. See text for the details.); Column 4:  $K_s$  magnitude at maximum light; Column 5:  $R_{\text{EROS}}$  magnitude at maximum light).

# Bibliography

- Alcock, C., Allsman, R. A., Alves, D., et al. 1997, AJ, 114, 326
- Alibert, Y., Baraffe, I., Hauschildt, P., & Allard, F. 1999, A&A, 344, 551
- Alves D. R., 2005, Highlights in astronomy, IAU, O. Engvold, San Francisco, CA, Astronomical Society of the Pacific, Vol. 13, 1448
- Andersen, J. 1991, A&AR, 3, 91
- Baldacci, L., Rizzi, L., Clementini, G., & Held, E. V. 2005, A&A, 431, 1189
- Beaulieu, J. P., Krockenberger, M., Sasselov, D. D., et al. 1997, A&A, 321, L5
- Benedict, G. F., McArthur, B. E., Fredrick, L. W., et al. 2002, AJ, 123, 473
- Benedict, G. F., McArthur, B. E., Feast, M. W., et al. 2007, AJ, 133, 1810
- Benedict, G. F., McArthur, B. E., Feast, M. W., et al. 2011, AJ, 142, 187
- Besla, G., Kallivayalil, N., Hernquist, L., et al. 2010, ApJ, 721, L97
- Besla, G., Kallivayalil, N., Hernquist, L., et al. 2012, MNRAS, 421, 2109
- Blazko, S. 1907, AN, 175, 325
- Bonanos, A. Z., Castro, N., Macri, L. M, Kudritzki, R.-P. 2011, ApJ, 729, L6
- Bono, G., Caputo, F., Castellani, V., & Marconi, M. 1996, ApJL, 471, L33
- Bono, G., Marconi, M., & Stellingwerf, R. F. 1999, ApJS, 122, 167
- Bono, G., Caputo, F., Castellani, V., Marconi, M., Storm, J., & Degl'Innocenti, S. 2003, MNRAS, 344, 1097
- Bono, G., Caputo, F., Marconi, M., & Musella I. 2008, ApJ, 684, 102

- Borissova, J., Rejkuba, M., Minniti, D., Catelan, M. & Ivanov, V. D. 2009, *A&A*, 502, 505
- Bragaglia, A., Gratton, R. G., Carretta, E., et al. 2001, *AJ*, 122, 207
- Braun, R., & Thilker, D. A. 2004, *A&A*, 417, 421
- Brown, A. G. A., 2013, ArXiv e-prints: 1310.3485
- Brüns, C., Kerp, J., Staveley-Smith, L., et al. 2005, *A&A*, 432, 45
- Butler, D., Carbon, D., & Kraft, R. P. 1976, *ApJ*, 210, 120
- Butler, D., Kraft, R. P., & Kinman, T. D. 1979, *AJ*, 84, 993
- Cacciari, C., Corwin, T. M., & Carney, B. W. 2005, *AJ*, 129, 267
- Caputo, F., Marconi, M., & Musella, I. 2000, *A&A*, 354, 610
- Cardelli, J. A., Clayton, G. C., & Mathis, J. S. 1989, *ApJ*, 345, 245
- Cardwell, J. A. R., & Coulson, I. M. 1986, *MNRAS*, 218, 223
- Carney, B. W. 1996, *PASP*, 108, 900
- Carretta, E., & Gratton, R. G. 1997, *A&A Supp.*, 121, 95
- Carretta, E., Bragaglia, A., Gratton, R. G., et al. 2009, *A&A*, 505, 117
- Catelan, M., Pritzl, B. J., & Smith, H. A. 2004, *ApJS*, 154, 633
- Catelan, M., & Cortes, C. 2008, *ApJ*, 676, L135
- Chiosi, C., Wood, P. R., & Capitanio, N. 1993, *ApJS*, 86, 541
- Cioni, M.-R. L., van der Marel, R. P., Loup, C., & Habing, H. J. 2000, *A&A*, 359, 601
- Cioni, M.-R. L., Clementini, G., Girardi, L., et al. 2011, *A&A*, 527, A116
- Clementini, G., Carretta, E., Gratton, R., et al. 1995, *AJ*, 110, 2319
- Clementini, G., Di Tomaso, S., Di Fabrizio, L., et al. 2000, *AJ*, 120, 2054
- Clementini, G., Gratton, R. G., Bragaglia, A., et al. 2003, *AJ*, 125, 1309
- Clementini, G. 2009, in the *Magellanic System: Stars, Gas and Galaxies*, IAU Sym., 256, 373

## *BIBLIOGRAPHY*

---

- Connors, T. W., Kawata, D., & Gibson, B. K. 2006, *MNRAS*, 371, 108
- Cox, J. P., & Whitney, C. 1958, *ApJ*, 127, 561
- Cross, N. J. G., Collins, R. S., Mann, R. G., et al. 2012, *A&A*, 548, A119
- Cutri, R., Skrutskie, M. F., van Dyk, S., et al. 2003, University of Massachusetts and Infrared Processing and Analysis Centre (IPAC/California Institute of Technology)
- Dall’Ora, M., Storm, J., Bono, G., et al. 2004, *ApJ*, 610, 269
- De Grijs, R., Wicker J. E., & Bono, G., 2014, *AJ*, 147, 122
- Del Principe, M., Piersimoni, A. M., Storm, J., et al. 2006, *ApJ*, 652, 362
- Derekas A., Kiss L. L., Bedding T. R., Kjeldsen H., Lah P., Szabó Gy. M., 2006, *ApJ*, 650, L55
- Derekas, A., Kiss, L.L., & Bedding T.R. 2007, *ApJ*, 663, 249
- Di Criscienzo, M., Greco, C., Ripepi, V., et al. 2011, *AJ*, 141, 81
- Di Fabrizio, L., Clementini, G., Maio, M., et al. 2005, *A&A*, 430, 603
- Dolphin, A. E. & Hunter, D. A. 1998, *AJ*, 116, 1275
- Eddington, A. S. 1926, *The Observatory*, 49, 88
- Evans, C. J., Lennon, D. J., Smartt, S. J., Trundle, C. 2006, *A&A*, 456, 623
- Evans, C. J., Taylor, W., Sana, H. et al., 2011, *A&A*, 530, A108
- Eyer, L., & Cuypers, J., 2000, in *The Impact of Large-Scale on Pulsating Star Research*, ed. L. Szabados, & D. W. Kurtz, ASP Conf. Ser. 203, Astronomical Society of Pacific, San Francisco, 71
- Faccioli, L., Alcock, C., Cook, K., Prochter, G. E., Protopapas, P., Syphers, D. 2007, *AJ*, 134, 1963
- Feast, M. W., Clifton, D. L., Kinman, T. D., van Leeuwen, F. & Whitelock, P. A. 2008, *MNRAS*, 386, 2115
- Fernley, J. A., Skillen, I. & Burki, G. 1993, *A&AS*, 97, 815

- Fernley, J., Skillen, I., Carney, B. W., Cacciari, C., & Janes, K. 1998, MNRAS, 293, L61
- Fernley, J., Barnes, T. G., Skillen, I., et al. 1998, A&A, 330, 515
- Fiorentino, G., Caputo, F., Marconi, M., & Musella, I. 2002, ApJ, 576, 402
- Fitzpatrick, E. L., Ribas, I., Guinan, E. F., et al. 2002, ApJ, 564, 260
- Fitzpatrick, E. L., Ribas, I., Guinan, E. F., Maloney, F. P., & Claret, A. 2003, ApJ, 587, 685
- For, B-Q., Sneden, C., Preston, G. 2011, ApJS, 197, 29
- Fouqu e, P., Strom, J., & Gieren, W. 2003, in D. Allon & W. Gieren (eds), Lecture Notes in Physics, 6
- Freedman, W. J., Madore, B. F., Gibson, B. K., et al. 2001, ApJ, 553, 47
- Gardiner, L. T., & Noguchi, M. 1996, MNRAS , 278, 191
- Gautschy, A. 1987, Vistas in Astron., 30, 197
- Gibson, B. K. 2000, MmSAI, 71, 693
- Govea, J., Gomez, T., Preston, & G. W., Sneden, C. 2014, ApJ, 782, 59
- Graczyk, D. & Eyer, L. 2010, Acta Astron., 60, 109
- Graczyk, D., Soszyński, I., Poleski, R., et al., 2011, Acta Astron., 61, 103
- Gratton, R. G., Bragaglia, A., Clementini, G., et al. 2004, A&A, 421, 937
- Grison, P. Beaulieu, J. P., Pritchard, J. D., et al. 1995, A&AS, 109, 447
- Groenewegen, M. A. T., & Oudmaijer, R. D. 2000, A& A, 356, 849
- Groenewegen, M. A. T. 2005, A&A, 439, 559
- Guinan, E. F., Fitzpatrick, E. L., Dewarf, L. E., et al. 1998, ApJ, 509, L21
- Guhathakurta, P., & Reitzel, D. B. 1998, Galactic Halos, 136, 22
- Hanson, R. B. 1979, MNRAS, 186, 875
- Harris, J., & Zaritsky, D. 2009, AJ, 138, 1243

## *BIBLIOGRAPHY*

---

- Haschke, R., Grebel, E. K., & Duffau, S. 2011, *AJ*, 141, 158
- Hunter, I., Lennon, D. J., Dufton, P. L., et al. 2008, *A&A*, 479, 541
- Hunter, I., Brott, I., Langer, N., et al. 2009, *A&A*, 496, 841
- Jenkins, L. F., *Yale Parallax Catalogue*, Yale University Press, 1952
- Jones, R. V., Carney, B. W., & Fulbright, J. P. 1996, *PASP*, 108, 877
- Jordi, C., Gebran, M., Carrasco, J. M., et al. 2010, *A&A*, 523, A48
- Jurcsik, J. 1995, *Acta Astron.*, 45, 653
- Jurcsik, J., & Kovacs, G. 1996, *A&A*, 312, 111
- Kallivayalil, N., van der Marel, R. P., & Alcock, C. 2006, *ApJ*, 652, 1213
- Kallivayalil, N., van der Marel, R. P., Alcock, C., et al. 2006, *ApJ*, 638, 772
- Kanbur, S., & Ngeow, C. 2004, *MNRAS*, 350, 962
- Kapakos, E., Hatzidimitriou, D., & Soszyński, I. 2011, *MNRAS*, 415, 1366
- Kim, S., Staveley-Smith, L., Dopita, M. A., et al. 1998, *ApJ*, 503, 674
- King, D. S., & Cox, J. P. 1968, *PASP*, 80, 365
- Kinman, T. D., Aoki, W., Beers, T. C., Brown, W. R. 2012, *ApJ*, 755, L18
- Kim, D.-W., Protopapas, P., Bailer-Jones, C. A. L., et al. 2014, *A&A*, 566, A43
- Koerwer, J. F. 2009, *AJ*, 138, 1
- Kolenberg, K., Fossati, L., Shulyak D., et al. 2010, *A&A*, 519, A64
- Lah, P., Kiss, L. L. & Bedding, T. R. 2005, *MNRAS*, 359, L42
- Lambert, D. L., Heath, J. E., Lemke, M., & Drake J. 1996, *ApJS*, 103, 183
- Layden, A. C. 1994, *AJ*, 108, 1016
- Leavitt, H. S., & Pickering, E. C. 1912, *Harvard College Observatory Circular*, 173, 1
- Lee, Y.-W., Demarque, P., & Zinn, R. 1994, *ApJ*, 423, 248

- Lewis, J. R., Irwin, M., & Bunclark, P. 2010, in Yoshihiko M., Koh-Ichirp M., Masatoshi O., eds, ASP Conf. Ser. Vol. 434, *Astronomical Data Analysis Software and Systems XIX*. Astron. Soc. Pac., San Francisco, p. 91
- Liu, T., & Janes, K. A. 1990, *ApJ*, 354, 273
- Longmore, A. J., Fernley, J. A., & Jameson, R. F. 1986, *MNRAS*, 220, 279
- Luri, X., Palmer, M., Arenou, F., et al. 2014, *A&A*, 566, A119
- Lutz, T. E. & Kelker, D. H. 1973, *PASP*, 85, 573
- Maceroni, C. & Rucinski, S. M. 1999, *AJ*, 118, 1819
- Madore, B. F., & Freedman, W. L. 1991, *PASP*, 103, 933
- Madore, B. F., & Freedman, W. L. 2012, *ApJ*, 744, 132
- Marconi, M., Musella, I., & Fiorentino, G. 2005, *ApJ*, 632, 590
- Marconi, M. 2009, in *AIP Conf. Proc. 1170, Stellar Pulsation: Challenges for Theory and Observation*, ed. J. A. Guzik & P. A. Bradley (Melville, NY: AIP), 223
- Marconi, M., Musella, I., Fiorentino, G., et al. 2010, *ApJ*, 713, 615
- Marquette, J. B., Beaulieu, J. P., Buchler, J. R., et al. 2009, *A&A*, 495, 249
- Mastropietro, C., Moore, B., Mayer, L., Wadsley, J., & Stadel, J. 2005, *MNRAS*, 363, 509
- McGonegal, R., McAlary, C. W., Madore, B. F., & McLaren, R. A. 1982, *ApJL*, 257, L33
- Mignard, F., 1998, *Proceedings of the 179th Symposium of the International Astronomical Union*, edited by Brian J. McLean, Daniel A. Golombek, Jeffrey J. E. Hayes, and Harry E. Payne, p. 399.
- Moretti, M. I., Clementini, G., Muraveva, T., et al. 2014, *MNRAS*, 437, 2702
- Morgan, S. M., Wahl, J. N., & Wieckhorst, R. M. 2007, *MNRAS*, 374, 1421
- Muraveva, T., Clementini, G., Maceroni, C., et al. 2014, *MNRAS*, 443, 432
- Nelan, E. P., 2010, *Fine Guidance Sensor Instrument Handbook* (17th ed.; Baltimore, MD: STScI)



## *BIBLIOGRAPHY*

---

- Nemec, J. M., Nemec, A. F. L., & Lutz, T. E. 1994, *AJ*, 108, 222
- Nemec, J. M., Cohen J. G., Ripepi V., et al. 2013, *ApJ*, 773, 181
- Ngeow, C.-C., Kanbur, S. M., & Nanthakumar, A. 2008, *A&A*, 447, 621
- Nikolaev, S., Drake, A. J., Keller, S. C. et al. 2004, *ApJ*, 601, 260
- Nidever, D. L., Majewski, S. R., Butler Burton, W., & Nigra, L. 2010, *ApJ*, 723, 1618
- Olsen, K. A. G. & Salyk, C. 2002, *AJ*, 124, 2045
- Paczynski, B. 1986, *ApJ*, 304, 1
- Paczynski, B. 1997, in *Proc.12th IAP Astrophysics Coll. 1996: Variable Stars and Astrophysical Returns from Microlensing Surveys*, ed. R. Ferlet, J. P. Maillard, & B. Raban (Éditions Frontières), 357
- Pawlak, M., Graczyk, D., Soszyński, I., et al. 2013, *Acta Astron.*, 63, 323
- Perryman, M. A. C., de Boer, K. S., Gilmore, G., et al. 2001, *A&A*, 369, 339
- ed. Perryman, M. A. C. and ESA, 1997, *ESA Special Publication*, 1200
- Persson, S. E., Madore, B. F., Krzemiński, W., et al. 2004, *AJ*, 128, 2239
- Petersen, J. O. 1973, *A&A*, 27, 89
- Pietrzyński, G., Graczyk, D., Gieren, W., et al. 2013, *Nat*, 495, 76
- Preston, G. W. 1959, *ApJ*, 130, 507
- Putman, M. E., Staveley-Smith, L., Freeman, K. C., Gibson, B. K., & Barnes, D. G. 2003, *ApJ*, 586, 170
- Ribas, I., Fitzpatrick, E. L., Maloney, F. P., Guinan, E. F., & Udalski, A. 2002, *ApJ*, 574, 771
- Rich, M. R., Corsi, C. E., Cacciari, C., et al. 2005, *AJ*, 129, 2670
- Ripepi, V., Moretti, M. I., Marconi, M., et al. 2012, *MNRAS*, 424, 1807
- Ripepi, V., Marconi, M., Moretti, M. I., et al. 2014, *MNRAS*, 437, 2307

- Ritchie, B. W., Stroud, V. E., Evans, C. J., et al. 2012, *A&A*, 537, A29
- Romaniello, M., Primas, F., Mottini, M., et al. 2005, *A&A*, 429, 37
- Romaniello, M., Primas, F., Mottini, M., et al. 2008, *A&A*, 488, 731
- Rowan-Robinson, M., 1985, *The cosmological distance ladder* (Freeman and Company)
- Rubele, S., Kerber, L., Girardi, L., et al. 2012, *A&A*, 537, A106
- Rucinski, S. M. 1993, *PASP*, 105, 1433
- Rucinski, S. M. 1997, *AJ*, 113, 407
- Rucinski, S. M. 1998, *AJ*, 115, 1135
- Rucinski, S. M. 1999, *Acta Astron.*, 49, 341
- Saha, A., Sandage, A., Tammann, G. A. 1999, *ApJ*, 522, 802
- Saha, A., Sandage, A., Tammann, G. A. 2001, *ApJ*, 562, 314
- Saio, H., & Gautschy, A. 1998, *ApJ*, 498, 360
- Sandage, A. *ApJ*, 244, L23
- Sandage, A. *ApJ*, 248, 161
- Sandage, A., Bell, R. A., & Tripicco, M. J. 1999, *ApJ*, 522, 250
- Sandage, A., Tammann, G. A., & Reindl, B. 2004, *A&A*, 424, 43
- Schaefer, B. E. 2008, *AJ*, 135, 112
- Schaefer, B. E. 2013, *Nat*, 495, 51
- Schlegel, D. J., Finkbeiner, D.P., & Davis, M. 1998, *ApJ*, 500, 525
- Schwarzenberg-Czerny, A. 2003, *Interplay of Periodic, Cyclic and Stochastic Variability in Selected Areas of the H-R Diagram*, 292, 383
- Simon, N. R., & Teays, T. J. 1982, *ApJ*, 261, 586
- Skillen, I., Fernley, J. A., Stobie, R. S., & Jameson, R. F. 1993, *MNRAS*, 265, 301

## *BIBLIOGRAPHY*

---

- Smith, H. A. 1995, RR Lyrae stars (Cambridge University Press)
- Sollima, A., Cacciari, C. & Valenti, E., 2006, MNRAS, 372, 1675
- Sollima, A., Cacciari, C., Arkharov, A. A. H., et al. 2008, MNRAS, 384, 1583
- Soszyński, I., Udalski, A., Kubiak, M., et al. 2004, Acta Astron., 54, 347
- Soszyński, I., Poleski, R., Udalski, A., et al. 2008, Acta Astron., 58, 163
- Soszyński, I., Udalski, A., Szymański, M. K., et al. 2009, Acta Astron., 59, 1
- Soszyński, I., Poleski, R., Udalski, A., et al. 2010, Acta Astron., 60, 17
- Soszyński, I., Udalski, A., Szymański, M. K., et al. 2010, Acta Astron., 60, 165
- Soszyński, I., Udalski, A., Poleski, R. et al., 2012, Acta Astron., 62, 219
- Spano, M., Mowlavi, N., Eyer, L., et al. 2011, A&A, 536, A60
- Stetson, P. B., Davis, L. E., & Crabtree, D. R. 1990, in Jacoby G. H., ed., ASP Conf. Ser. Vol. 8, CCDs in Astronomy. Astron. Soc. Pac., San Francisco, p. 289
- Sturch, C. 1966, ApJ, 143, 774
- Subramaniam, A. 2003, ApJ, 598, L19
- Szewczyk, O., Pietrzyński, G., Gieren, W., et al. 2008, AJ, 136, 272
- Szymański, M. K. 2005, Acta Astron., 55, 43
- Tammann, G. A., & Reindl, B. 2002, ApSS, 280, 165
- Tammann, G. A., Reindl, B., Thim, F., Saha, A., & Sandage, A. 2002, in N. Metcalfe & T. Shanks (eds.), A New Era in Cosmology, ASPC 283,(San Fransisco: ASP), p. 258
- Tisserand, P., Le Guillou, L., Afonso, C., et al. 2007, A&A, 469, 387
- Torres, G., Andersen, J. & Giménez, A., 2010, A&AR, 18, 67
- Udalski, A., Szymanski, M., Kaluzny, J., Kubiak, M., & Mateo, M. 1992, Acta Astron., 42, 253
- Udalski, A., Szymanski, M., Kaluzny, J., et al. 1993, Acta Astron., 43, 289

- Udalski, A., Kubiak, M., & Szymanski, M. 1997, *Acta Astron.*, 47, 319
- Udalski, A., Szymański, M., Kubiak, M., et al. 1999, *Acta Astron.*, 49, 201
- Udalski, A. 2003, *Acta Astron.*, 53, 291
- van der Marel, R. P. & Cioni, M.-R. 2001, *AJ*, 122, 1807
- van Leeuwen, F., 2007, *Hipparcos*, the New Reductions of the Raw Data, *Astrophys. Space Sci. Lib.* (Berlin: Springer) 350
- Walborn, N. R., Sana, H., Simón-Díaz, S., et al. 2014, *A&A*, 564, A40
- Walker, A. R. 2003, *Stellar Candles for the Extragalactic Distance Scale*, *Lecture Notes in Physics*, D. Alloin & W. Gieren, 635, 265
- Walker, A. R. 2012, *Ap&SS*, 341, 43
- Wood, P. R., Alcock, C., Allsman, R. A., et al., 1999, in *IAU Symp. 191, Asymptotic Giant Branch Stars*, ed. T. Le Bertre, A. Lébre, & C. Waelkens (San Francisco: ASP), 151
- Wyrzykowski, L. A., Udalski, A., Kubiak, M. et al., 2003, *Acta Astron.*, 53,1
- Zaritsky, D., Harris, J., Grebel, E. K., & Thompson, I. B. 2000, *ApJL* , 534, L53
- Zaritsky, D. 2004, *ApJ*, 614, L37
- Zhevakin, S. A. 1953, *Astr. Zh.* 30, 161
- Zinn, R., & West, M. J. 1984, *Astrop. J. Supp.*, 55, 45